A 2D-Difference Gel Electrophoresis Strategy For Redox Proteomics

Hong-Lin CHAN

DEPARTMENT OF BIOCHEMISTRY AND MOLECULAR BIOLOGY
UNIVERSITY COLLEGE LONDON
GOWER STREET, LONDON

THIS THESIS IS SUBMITTED IN PARTIAL FULFILMENT OF THE REQUIREMENTS FOR THE DEGREE OF DOCTOR OF PHILOSOPHY FROM THE UNIVERSITY OF LONDON

ProQuest LLC
789 East Eisenhower Parkway
P.O. Box 1346
Ann Arbor, MI 48106-1346

ABSTRACT

Post-genomic biomedical science requires quantitative proteomics. In most cases this involves differential protein expression analysis using matched pairs of simultaneously detectable labelling reagents for specific protein amino acids. In this thesis the development and optimisation of a novel cysteine labelling strategy, that is based on the use of iodoacetyl derivatives of Cy3 and Cy5 (ICy3/5) and 2D-difference gel electrophoresis (2D-DIGE) is described. The differentially labelled samples are separated on a single 2D gel and detected by multi-wavelength fluorescence scanning. The method is used to analyse standard proteins and then cell lysates to define the stoichiometry, sensitivity and specificity of this labelling technique. A comparative study of this new proteomic ICy dye protocol with the current NHS-Cy dye labelling system and methods that employ commonly used protein staining methods is described. The method is then used for cysteine labelling of proteins in non-reduced, denatured biological samples allowing accurate monitoring and sensitive detection of redox-dependent thiol modifications and expression level changes. The method is shown to be compatible with the use of MALDI mass spectrometry to identify proteins by analysis of trypsinised ICy labelled peptide digests. Using parallel sample analysis within single gels, the ICy-dye reagents were used to detect redox-, ErbB-2- and growth factor-dependent changes in a human mammary luminal epithelial cell system which was exposed to hydrogen peroxide or to growth factor stimulation. The conventional lysine labelling 2D-DIGE technique was also used in parallel to assess the new ICy labelling strategy for determination of the effects of oxidative stress on protein isoform levels. This study has revealed the identity of proteins involved in the response to oxidative stress and growth factor stimulation in the context of ErbB-2 growth factor receptor over-expression. In addition, this labelling strategy was also used to detect changes in thiol reactivity that follow the UV irradiation of plasma proteins as part of a study designed to evaluate the effect of UV disinfection on plasma product safety for clinical use.

Acknowledgements

I wish to dedicate this thesis to my family, friends, colleagues and supervisors for their continuous encouragement and support.

Firstly, I sincerely thank my two supervisors: Professor Michael Waterfield FRS, for his inspirational guidance during my PhD and for giving me the opportunity to broaden my learning in the world of proteomics; Dr. John Timms, for his daily excellent supervision throughout the course of my research, for teaching me a number of experimental techniques in the field of proteomics and for his support during the writting of this thesis.

In addition, I am grateful to Dr. Rainer Cramer and his bioanalytical chemistry group for their instruction and expertise in mass spectrometry. I also want to thank Dr. Piers Gaffney (Imperial College London) who syntheses the protein labelling dyes for my research. To my colleagues and friends: Severine, Akunna, Mariana, Bertran, Eleonora, Musarat, Mark, John, Yuqin, Carmen, Richard and Denis and all those at the Ludwig Institute UCL branch, for their friendship, expertise, unconditional help and patience. Especially for all of you have taken time to read sections of this thesis and help me to prepare my oral examination.

The funding for my PhD study was provided by the Graduate School Research Scholarship and Overseas Research Scholarship. I would like to express my gratitude to both UCL Graduate School and University UK.

Finally, I want to thank my father (Yi-Tien Chan), my mother (Pao-Hsiu Chen), my sister (Ho-Ling Chan), my brother-in-law (Sheng-Ling Wu) and the other family members in Taiwan for their love, understanding, encouragement, unconditional support and in particular my wife Hsiu-Chuan Chou, who has supported me in every possible way during my study in higher education and is currently finishing her PhD thesis in King's College London.

感謝

我希望將此博士論文獻給我親愛的家人，朋友，實驗室伙伴以及我的指導教授。

首先，要感謝我的兩位指導教授: Michael Waterfield 教授，感謝他對我的啟迪與帶領我進入蛋白質體學領域。 另外，我要感謝 John Timms 博士，感激他時時刻刻的指導，並不厭其煩地與我討論研究課題。 此外，也感激他在我論文寫作期間之悉心協助。

除此之外，還要感謝 Rainer Cramer 博士，感激他及他的小組成員在質譜技術的協助指導。 還要感謝 Piers Gaffney 博士合成蛋白質標定劑，做為我實驗之材料。 另外，要感謝實驗伙伴們 Severine, Akunna, Mariana, Bertran, Eleonora, Musarat, Mark, John, Denis, Carmen, Richard 及 瑜琴，感謝你們提供我愉快的研究時光，特別是在我論文寫作及準備口試期間，給我建議及幫忙。

我也要感謝倫敦大學大學學院和英國高等教育聯盟，提供我攻讀博士期間的獎學金。

最後，我要感謝我的父親詹益田先生及母親陳寶秀女士，感謝他們的多年栽培，才會有我今日成就，感謝他們多年如一日對我生活的關心與照顧。 另外，我要感謝姊姊鶴齡及姊夫昇凌的關心與照顧。 此外，我要感激每天照顧我起居，與我分憂解愁，同甘共苦，同時，也即將獲得博士學位的太太秀專。

TABLE OF CONTENTS

LIST OF FIGURES AND TABLES

Chapter 1

Chapter 2

Chapter 3

Chapter 4

Chapter 5

Chapter 6

Chapter 7

Appendix

(Appendix A) Synthesis and structure of the iodoacetyl cyanine dyes.

(Figure Appendix B1) Quantitative determination of free thiol content in standard proteins (BSA, OVA and α-Crys).

(Figure Appendix B2) Quantitative determination of free thiols (Ellman test).

ABBREVIATIONS

Chemicals and reagents

CCB	colloidal coomassie blue
CHAPS	(3-[(3-cholamidopropyl)dimethylammonio]-1-propanesulfonate)
CHCA	α-cyano-4-hydroxycinnamic acid
Cy2	3-(4-carboxymethyl)phenylmethyl)-3'-ethyloxacarbocyanine halide *N*-hydroxy-succinimidyl ester
Cy3	1-(5-carboxypentyl)-1'-propylindocarbocyanine halide *N*-hydroxysuccinimidyl ester
Cy5	1-(5-carboxypentyl)-1'-methylindodicarbocyanine halide *N*-hydroxysuccinimidyl
ddH_2O	double deionised water
DCF	dichlorofluorescein
DCFH	dichlorofluorescin
DHB	2, 5-dihydroxybenzoic acid
DMSO	dimethyl sulfoxide
DTNB	5, 5'-dithiobis (2-nitrobenzoic acid)
DTT	dithiothreitol
EDTA	ethylenediaminetetraacetic acid
FCS	foetal calf serum
H_2O_2	hydrogen peroxide
HEPES	N-[2-hydroxyethyl]piperazine-N'[2-ethanesulphonic acid]
IAM	iodoacetamide
ICy3	N-(6-iodoacetamidohexyl)-N'-propyl Cy3 iodide
ICy5	N-(6-iodoacetamidohexyl)-N'-methyl Cy5 iodide
NaCl	sodium chloride
NHS	N-hydroxy succinimidyl
NP-40	Nonidet P-40
PBS	phosphate-buffered saline
SDS	sodium dodecyl sulphate

TBS	tris buffered saline
TCEP	tris-carboxy ethyl phosphine
TFA	trifluoroacetic acid
TNB^{2-}	2-nitro-5-thiobenzoate
Tris	tris-(hydroxymethyl)aminomethane

Software and instrumentation

BVA	biological variation analysis
CCD	charge-coupled device
CID	collision-induced dissociation
DIA	difference in-gel analysis
ESI	electrospray ionisation mass spectrometry
MS	mass spectrometry
MS/MS	tandem mass spectrometry
MALDI	matrix assisted laser desorption/ionisation
PMF	peptide mass fingerprinting
PMT	photomultiplier tube
PSD	post source decay
TOF	time of flight

General

1DE	one-dimensional gel electrophoresis
2DE	two-dimensional gel electrophoresis
Ab	antibody (mAb: monoclonal Ab; pAb: polyclonal Ab)
CDK	cyclin dependent kinase
DIGE	difference gel electrophoresis
DNA	deoxyribonucleic acid
ECL	enhanced chemiluminescence
FACS	fluorescence activated cell sorting
FRET	fluorescence resonance energy transfer
HMLEC	human mammary luminal epithelial cell

HRP	horseradish peroxidase
ICAT	isotope coded affinity tags
IEF	isoelectrofocusing
IP	immunoprecipitation
IPG	immobilised pH gradient
kDa	kilodalton
kVh	kilovolt hours
m/z	mass-to-charge ratio
MD-LC	multi-dimensional liquid chromatograpy
PAGE	polyacrylamide gel electrophoresis
PEM	protein expression map
ppm	parts per million
PVDF	polyvinylidene fluoride
RNA	ribonucleic acid
SD	standard deviation
Vhr	volt hours

Protein, enzymes, growth factors and inhibitors

APC	amyloid P component
AR	amphiregulin
ATM	ataxia telangiectasia mutated protein
BpVphen	potassium bisperoxo(1, 10-phenanthroline)oxovanadate
BSA	bovine serum albumin
BTC	betacellulin
CK	cytokeratin
α -Crys	bovine α-rystallin
EGF	epidermal growth factor
EGFR	epidermal growth factor receptor
EPR	epiregulin
ErbB-2	erythroblastosis B-2
ErbB-3	erythroblastosis B-3

ErbB-4	erythroblastosis B-4
G3PDH	glyceraldehyde 3-phosphate dehydrogenase
GAP	GTPase activating protein
GEP	GDP/GTP exchange protein
GLUT1	glucose transporter 1
GSSG	glutathione disulphide
GST	*S. japonicum* glutathione S-transferase
HB-EGF	heparin-binding EGF
HIF-1α	hypoxia-inducible transcription factor-1α
JAK	Janus kinase
LPS	lipopolysaccharide
LT	SV40 large T antigen
MAPK	mitogen activated protein kinase
MxA	interferon induced resistance protein
Myo	horse myoglobin
NADPH	5,10-methylenetetrahydrofolate reductase
NRG-1	neuregulin-1
NRG-2	neuregulin-2
NRG-3	neuregulin-3
NRG-4	neuregulin-4
Ova	chicken ovalbumin
Pak1	p21-activated kinase
PI3K	phosphatidylinositol 3-kinase
PTB	protein tyrosine binding domain
PTP	protein tyrosine phosphatase
PTK	protein tyrosine kinase
Prxn	peroxiredoxin
Ras	retrovirus-associated DNA sequence
Rb	retinoblastoma protein
RBP	retinol binding protein
RhoGDI	rho-GDP-dissociation inhibitor

RNS	reactive nitrogen species
ROS	reactive oxygen species
SAP	serum amyloid P component
SH2	src homology-2 domain
SH3	src homology-3 domain
STAT	signal transducers and activators of transcription
SV40	simian virus 40
TGFα	transforming growth factor-α
TPI	triosephosphate isomerase
VEGF	vascular endothelial growth factor

Chapter 1 INTRODUCTION

1.1 Overview on proteomics

After the human genome was sequenced, the understanding of protein function has become the most important issue in the post-genomic era and proteomics is the field uses protein analysis tools to globally study the behaviours of gene products. Proteomics has benefited from the development of accurate high-throughput technologies allowing global protein analysis. Despite the fact that the main techniques used in proteomic analysis were developed in the early 1970s (Kenrick and Margolis, 1970), this new terminology, proteomics, was first mentioned in 1994 at a "2-D Electrophoresis" Symposium held in Siena, Italy. The study of the proteome represents the large-scale analysis of proteins expressed in a genome. Differential proteome analysis is the comparison of protein expression profiles between two or more samples on a large scale. It was mainly in the 1990s, with the emergence of high-sensitivity analytical chemistry for protein identification using mass spectrometry, that the field of proteomics really became useful for biological studies. Major improvements in mass spectrometry have replaced the former method of choice for protein identification by Edman degradation, an approach which although powerful, was time consuming and required larger amounts of sample. The field of proteomics has rapidly developed and the study of the proteome now includes methods that evaluate not only changes in protein expression between biological samples, but also the examination of protein-protein interactions, activity status, post-translational modifications and protein sub-cellular localization on a large scale.

1.1.1 Principles of two-dimensional gel electrophoresis

The most commonly used approach for the study of proteomics is a combination of two-dimensional gel electrophoresis (2DE) for protein separation with detection by staining or protein labelling and mass spectrometry for protein identification. Two-dimensional polyacrylamide gel electrophoresis (2D-PAGE) was first developed in the early 1970s (Kenrick *et al.*, 1970) and was optimised using denaturing isoelectrofocusing (Klose and

Spielmann, 1975;O'Farrell, 1975;Scheele, 1975). The technique was greatly improved with the development of immobilised pH gradient (IPG) gels, which gave increased protein resolution in the first dimension (Bjellqvist et al., 1982). Subsequently, pre-cast IPG strips were made commercially available, making 2D-PAGE a more reproducible technique which could be easily applied by many users. Moreover, with the application of highly sensitive mass spectrometry techniques, 2D-PAGE became even more widely used for proteomic analysis.

The main challenge of 2D-PAGE is to achieve high-resolution protein separation and detection in order to provide pure samples for mass spectrometric analysis and for high-sensitively differential protein expression analysis. In principle, 2DE relies on the separation of proteins in the first dimension according to their charge and then in the second dimension according to their relative molecular weight (Figure 1-1). In the first dimension, denatured proteins are separated by isoelectrofocusing (IEF) in a pH gradient and focus when they acquire a zero net charge at their isoelectric point (pI). Proteins are then separated in the second dimension according to their mass by conventional SDS-PAGE. Full descriptions of current methodologies and optimised techniques have been reported (Rabilloud et al., 1994a;Gorg et al., 1999;Gorg et al., 2000a). In order to reduce the complexity in protein samples and the problem of multiple proteins migrating at the same coordinates, the use of narrow range IPG strips (Gorg *et al.*, 1999;Westbrook et al., 2001a) and large format gels (Klose, 1999) are utilised for improved separation of larger amounts of protein sample. In addition, improvements have been made in the solubilisation of proteins using detergents that are compatible with isoelectrofocusing and gel electrophoresis, thereby, providing a means to increase sample loading and improve the resolution of membrane proteins (Rabilloud *et al.*, 1994a;Rabilloud, 1998;Rabilloud et al., 1999;Herbert, 1999). Different sample application methods can also be performed to improve the entry of proteins into the first dimension. For example, cup-loading has made possible the analysis of up to 1 mg of proteins loaded on to an IPG-strip (Hanash et al., 1991).

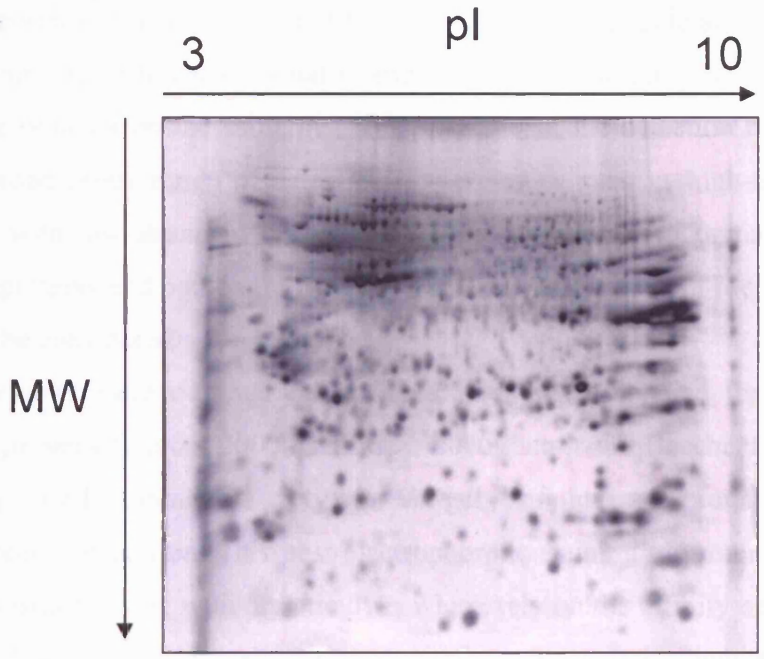

(Figure 1-1) Two-dimensional electrophoresis. Protein samples (epithelial cell lysates) are separated by isoelectric focusing (IEF) electrophoresis according to the isoelectric point of the proteins and then separated by SDS-polyacrylamide gel electrophoresis according to their molecular weight.

Despite the benefits of 2DE for global protein expression analysis, the technique suffers from several drawbacks. Most notable is the poor resolution of basic proteins (Figure 1-1). These proteins represent a large fraction of the proteome and include membrane, nuclear proteins and other positively charged proteins that are poorly resolved due to the inadequate buffering by ampholytes at basic pHs and also because of a loss of reductive capacity and concentration (electro-endo-osmosis) resulting in spurious disulphide bond reformation and protein precipitation. This can be partially remedied by using stronger detergents, high pH range IPG strips, and additives such as isopropanol and DTT to improve protein solubility. Thus, for maximal resolution several different 2DE gels must be run to separate the acidic and basic fractions of the proteome, although this is often not a practical solution.

After electrophoretic separation, it is necessary to detect and quantitate proteins in order to select proteins of interest for identification. The challenge is to achieve the detection of the complete proteome and to visualise and accurately quantitate the low- as well as high-abundance proteins on the same gel. This means that the detection method used has to cover a broad linear range of detection. Other issues such as high-abundant spots co-migrating with low-abundant ones masking the detection of potentially regulated low-abundant proteins and compatibility of the stain with downstream identification methods must also be considered.

Several reviews have outlined the different methods of choice for detection of gel-separated proteins (Patton, 2000;Rabilloud, 2000;Patton and Beechem, 2002). The most commonly used approaches rely on in-gel staining of proteins subsequent to electrophoretic separation. This post-electrophoretic staining of proteins can be achieved by noncovalent staining with organic dyes which rely on the affinity between the dye and proteins. For instance, protein staining with a coomassie brilliant blue (CCB R-250) solution in methanol and acetic acid is commonly used. Although this method is rapid and provides a uniform staining of proteins across gels, it is relatively insensitive with a detection limit of 100-200 ng. In addition, the method requires the extensive destaining of gels, which can create variations in background staining from gel-to-gel. This method has been further improved with the use of colloidal coomassie blue G-250 (CCB G-250), a dimethylated form of CCB used in an acidic solution containing ammonium sulphate (Neuhoff et al., 1988). The limit of detection of colloidal CCB G-250 staining is around 10-20 ng. Another advantage of colloidal coomassie blue staining is that it does not require de-staining of the gels compared to conventional CCB staining, providing increased reproducibility in protein detection from gel-to-gel. Both CCB R-250 and colloidal CCB G-250 are commonly used for the analysis of abundant proteins or those that have been overexpressed for post-translational modification analysis, since these dyes are compatible with downstream mass spectrometric analysis as they can be easily removed (Scheler et al., 1998).

The most commonly used high sensitivity detection method relies on the precipitation of silver with proteins under acidic or alkaline conditions, a method that can show up to 50-fold higher sensitivity compared with conventional CCB R-250 staining. With such

approaches, gels are usually fixed and washed in order to remove excess SDS or salts which can react with silver and produce a high background. Numerous silver staining protocols have been described, although the most sensitive approach uses aldehyde-based fixatives which interfere with subsequent protein identification by mass spectrometry or Edman sequencing due to covalent cross-linking of proteins to the gel preventing efficient elution and due to heterogeneous protein modification by the aldehyde. Other silver staining methods have been developed to overcome these problems which do not use such harsh fixatives (Shevchenko et al., 1996;Yan et al., 2000). However, these methods provide less sensitivity in protein detection as only surface staining of gels is achieved. A major problem with these silver staining methods is that staining from gel-to-gel tends to be variable since it is not an end-point staining method. In addition, some proteins show a higher affinity for silver staining than others, making it a poor quantitative approach (Rabilloud et al., 1994b;Lopez et al., 2000). Thus, although silver staining is a sensitive method, it is not really suitable for accurate differential expression analysis by gel-to-gel comparison.

So-called reverse staining has also been applied for protein visualisation, using potassium chloride, zinc chloride or copper chloride. These methods rely on the precipitation of salts, which occurs faster in the gel areas with no proteins. Therefore this method stains the gel only, leaving proteins as transparent spots which can be viewed with appropriate back illumination. The most sensitive reverse staining uses zinc chloride-imidazole where 10 to 20 ng of protein has been detected (Ortiz et al., 1992;Castellanos-Serra et al., 1999). Although this method is rapid, the extent of reverse staining is not fixed and the reverse image tends to fade quickly. In addition, the linear range of detection is limited (Castellanos-Serra *et al.*, 1999) and so zinc chloride-imidazole staining is also unsuitable for quantitative proteomic analyses.

The most promising protein visualisation methods use fluorescent dyes which can be detected under a standard 300 nm UV light or using an imaging device equipped with the appropriate lasers and wavelength filters. The main advantage in the use of fluorescent stains is that fluorescence gives a very broad and linear dynamic range of detection. This greatly enhances protein quantitation of biological samples where protein abundance can range over seven or eight orders of magnitude. Hydrophobic dyes such as 1, 8-ANS (1-

anilinonaphthalene 8-sulfonate) and bis-ANS (bis (8-p-toluidino-1-naphthalenesulfonate)) have been used and display a sensitivity level similar to conventional CCB R-250 (Hartman and Udenfriend, 1969;Pina et al., 1985;Horowitz and Bowman, 1987). Nile red staining was more recently described as a hydrophobic probe interacting with SDS-protein complexes in the gel (Daban et al., 1991;Daban, 2001). Consequently, this method requires the use of low concentrations of SDS for the gel electrophoresis to avoid increased fluorescent background. The method shows good sensitivity and detection of as little as 10 ng of protein has been reported. However, the stain is relatively insoluble in water (Daban, 2001).

More recently, Molecular Probes developed a panel of fluorescent dyes, the SYPRO®dyes (Steinberg et al., 1996;Steinberg et al., 2000;Berggren et al., 2002). The SYPRO Orange, Red and Tangerine dyes also interact with SDS-protein complexes similarly to Nile red dye and the sensitivity reported was similar, although these dyes are more water-soluble. Two transition metal chelate stains have also been developed, SYPRO Ruby and SYPRO Rose stains. The most attractive for use in quantitative proteomics is SYPRO Ruby, a ruthenium-based metal chelate stain showing high sensitivity down to 1 ng of protein (Lopez *et al.*, 2000;Berggren *et al.*, 2002). The fluorophore reacts directly with proteins via lysine, arginine and histidine residues, enabling the sensitive and specific detection of all gel-separated proteins (Patton, 2000). Importantly, this method was shown to be compatible with downstream mass spectrometric analysis (Steinberg *et al.*, 2000;Gharbi et al., 2002). SYPRO Ruby staining is also rapid and is performed in a single step followed by minimal washing to remove excess dye, and is an end-point stain allowing consistent staining from gel-to-gel. Consequently, SYPRO Ruby staining represents a considerable improvement in the detection of gel-separated proteins for proteomic analysis, although gel-to-gel variation still remains an obstacle for both statistical and accurate differential analysis.

Amongst all the detection methods described, fluorescence labelling appears to be the best method due to its high sensitivity and wide linear dynamic range. Historically, the main method for visualisation of fluorescently labelled proteins required the use of UV trans-illumination and direct visual detection. However, many fluorphores are excited optimally outside the UV range and detection systems have been developed which use

specific lasers for excitation. A single laser source cannot provide the appropriate excitation over the entire wavelength range of different fluorophores and so some devices use a broadband visible light source in combination with narrow band filters enabling the selection of a specific wavelength adequate for each fluorophore of interest. Similarly, the detection device can be equipped with a selection of emission filters, allowing the detection of fluorescence emission for a range of different fluorophores. Several types of detectors can be used, such as a cooled charged-coupled device (CCD) or photomultiplier tube (PMT), as exemplified by the 2920 2D-MasterImager and Typhoon 9400, respectively. These devices, commercialised by GE Healthcare (U.K.), enable optimal excitation and detection of a broad range of fluorescent dyes and were used in the work presented in this thesis. The 2920 2D-MasterImager fluoroimager has a high intensity xenon arc lamp source equipped with filter wheels enabling the selection of narrow range wavelengths and is combined with a cooled CCD camera providing sensitive detection of fluorescent signals. Using this device, the gel is scanned directly between glass plates using edge illumination. The Typhoon 9400 relies on a multiple laser source and photomultiplier detection device providing improved fluorescent detection and high image resolution.

Protein detection can also be achieved by covalent labelling pre- or post-electrophoretic separation. Perhaps the most sensitive covalent labelling method used prior to electrophoresis is radioactive labelling which provides the widest linear dynamic range of detection. Radiolabelling is mainly accomplished by incorporation of radioactive metabolites during the growth of cells. For instance, ^{3}H, ^{35}S, ^{32}P or ^{33}P can be incorporated into proteins by addition of growth media containing isotopically labelled nutrients. Proteins can also be radiolabelled post-lysis for example by *in vitro* kinase assay or through the use of radiolabelled protein tags, such as alkylating agents. Radiolabelled proteins are then detected in-gel by exposure to film (autoradiography) or using a phosphorimager. The latter imaging method provides a wider dynamic range than autoradiography enabling better quantitative analysis. However, concerns remain as to the effects of addition of radioactive compounds to cells. Indeed, DNA damage can occur, as well as elevation of p53 levels leading to cell cycle arrest and apoptosis. Another important issue and drawback in the use of radioactive compounds is their

hazardous nature and their higher cost. Limitations in the use of radioactive compounds now represents a high priority for many laboratories and finding alternative methods is favoured.

Fluorescent tags have also been used to covalently label proteins. Most covalent labelling has been performed on gel-separated proteins, and several fluorophores, such as fluorescamine, fluorescein isocyanate, N-(7-di-methylamino-4-methylcoumarinyl) maleimide and dansyl chloride, have been used for this purpose. Dyes such as 5-(4, 6-dichlorotriazin) aminofluorescein, monobromobimane, 2-methoxy-2, 4-diphenyl-3 (2H) furanone (MDPF) and dansyl chloride have also been used for covalent labelling prior to gel electrophoresis, although low sensitivity and poor resolution on 2DE gels was reported (as reviewed in (Patton, 2000;Rabilloud, 2000)). Indeed, the major problem faced was that most of the dyes possess a charge which affects the electrophoretic properties of proteins. In addition, covalent protein modification can also dramatically affect the ability to subsequently identify the proteins by mass spectrometry.

Unlu *et al.* recently described a new covalent lysine labelling approach for differential protein detection, known as difference gel electrophoresis (DIGE) (Unlu et al., 1997b). A combination of two fluorescent cyanine protein tags, were used together enabling differential labelling of two samples prior to their electrophoretic separation on the same 2D gel. Cyanine dyes were first described by Mujumdar *et al.* (Mujumdar et al., 1989;Mujumdar et al., 1993). These fluorophors have a structure which can be modified to create a panel of reactive fluorescent tags. The dyes developed by Unlu *et al.* are N-hydroxy-succinimidyl (NHS)-ester derivatives of the fluorescent cyanines 3 and 5 (NHS-propyl-Cy3, NHS-methyl-Cy5) (Figure 1-2A). A third cyanine dye, NHS-Cy2 is now commercially available and all three dyes have distinct and non-overlapping excitation and emission spectra (Figure 1-2B) enabling their specific detection with a multi-wavelength fluorescent detection device. Using these dyes, proteins are covalently labelled on lysine ε-amino groups (ε-NH_2-lys) by nucleophilic attack resulting in the loss of the NHS group (Figure 1-2C). The advantage of using lysine labelling is that almost all proteins contain at least one lysine residue and so most proteins can be labelled. The labelling reaction appears to be specific for ε-NH_2-lys lysine groups, although the NHS-ester could also react with the N-terminal α-amino groups of proteins (α-NH_2-Nterm).

Conceptually, the dyes should be mass and charge matched and the dye modification should not perturb the electrophoretic mobility of labelled proteins. For this reason, the size of the aliphatic chain (Figure 1-2A) was originally modulated to maintain a similar molecular weight between each dye and the dyes possess a positive charge which matches the positively charged amino groups they modify. Low stoichiometry labelling conditions were established for covalent labelling without adversely affecting protein mobility, but keeping the sensitivity of detection high and linear over a wide dynamic range. This approach was then further optimised and commercialised by GE Healthcare and the method was originally evaluated and applied by Tonge et al. and Gharbi et al. (Tonge et al., 2001;Gharbi *et al.*, 2002). Tonge et al. used the NHS-cyanine dyes Cy2, Cy3 and Cy5 to label liver homogenates from pools of untreated and paracetamol-treated mice and separated these labelled liver proteins by 2DE. After normalisation of the individual fluorescent images, quantitative protein differences were determined between the samples from replicate gels. A number of the significantly changing features was identified by mass spectrometry and some of these identified proteins could be rationalised based on available information on the mechanism of paracetamol hepatotoxicity. Gharbi et al. also evaluated this technique using a model cell system to study the effects of ErbB-2 overexpression, an oncogenic receptor tyrosine kinase implicated in breast cancer progression. A Cy2-labelled pool of samples was used as a standard and run on all gels for comparison with the Cy3- and Cy5- labelled sample pairs for improved cross-gel quantitative analysis (Figure 1-3). Decyder software (GE HealthCare) was used to distinguish clear statistical differences in protein expression over time and between the cell lines. This internal standard method was also subsequently described by Alban et al. (Alban et al., 2003).

1.1.2 Problems and limitations of current two-dimensional gel based proteomics

As mentioned previously, 2DE-based proteomic studies are somewhat limited since only a fraction of the proteome can be visualised (Corthals et al., 2000). One of the limitations is in protein separation due to the physico-chemical properties of proteins. Very basic or hydrophobic proteins, such as membrane proteins, are not well separated in the first

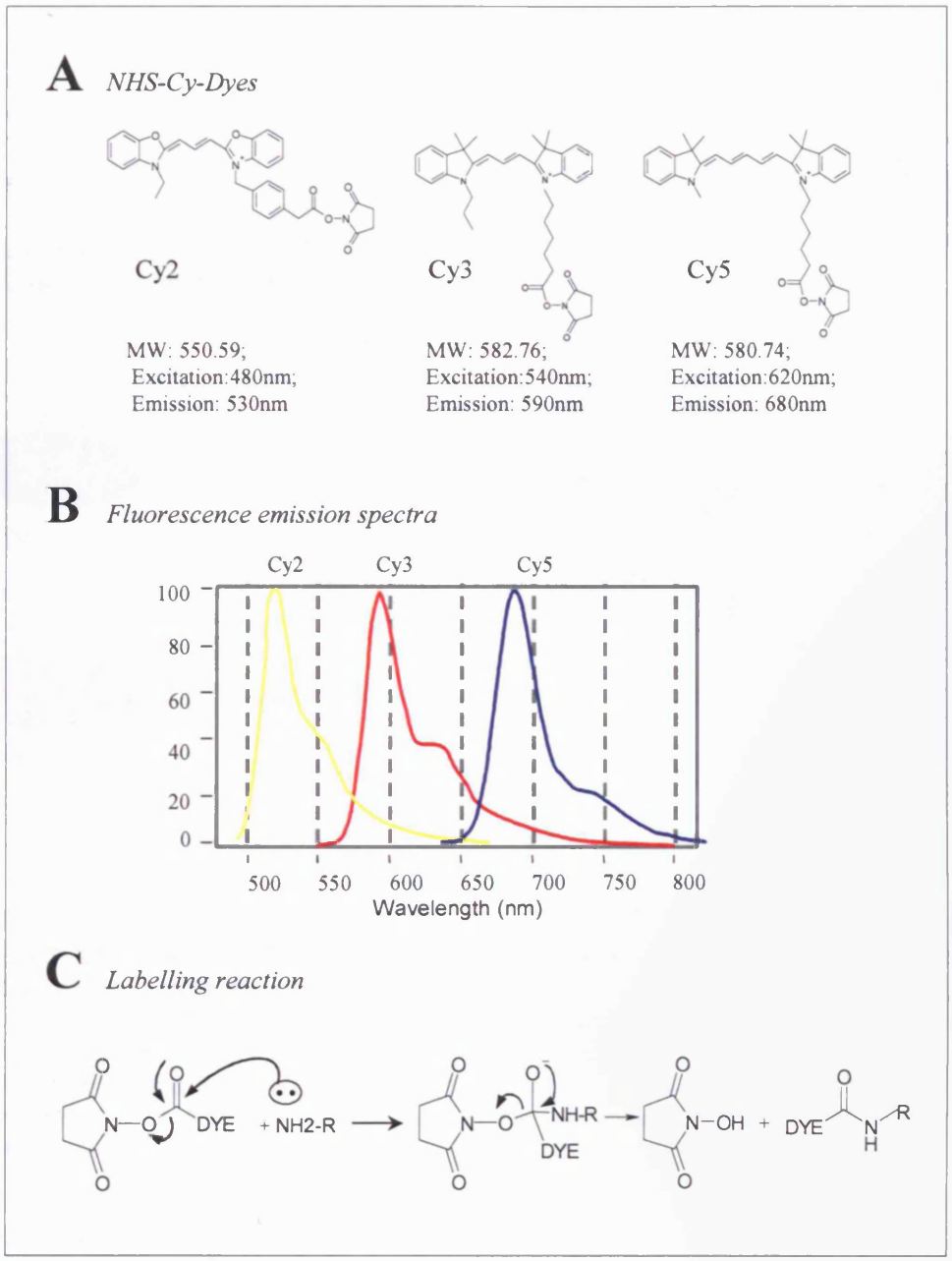

(Figure 1-2) Characteristics of the NHS-Cy-dyes. **(A)** Structure of the NHS-Cyanine dyes. Cy2,3-(4-carboxymethyl)phenylmethyl)-3'-ethyloxacarbocyanine halide *N*-hydroxy-succinimidyl ester; Cy3, 1-(5-carboxypentyl)-1'-propylindocarbocyanine halide *N*-hydroxysuccinimidyl ester, Cy5; 1-(5-carboxypentyl)-1'-methylindodicarbocyanine halide *N*-hydroxysuccinimidyl. Each dye has a similar molecular weight and single positive charge matching the charge of the modified primary amino group. **(B)** Each dye displays a distinct emission spectra enabling the individual detection of differentially labelled proteins at the appropriate wavelength without overlap of signals. **(C)** The dyes have an *N*-hydroxysuccinimidyl ester reactive group triggering covalent interaction with the primary amine groups of lysine residues or the N-terminus.

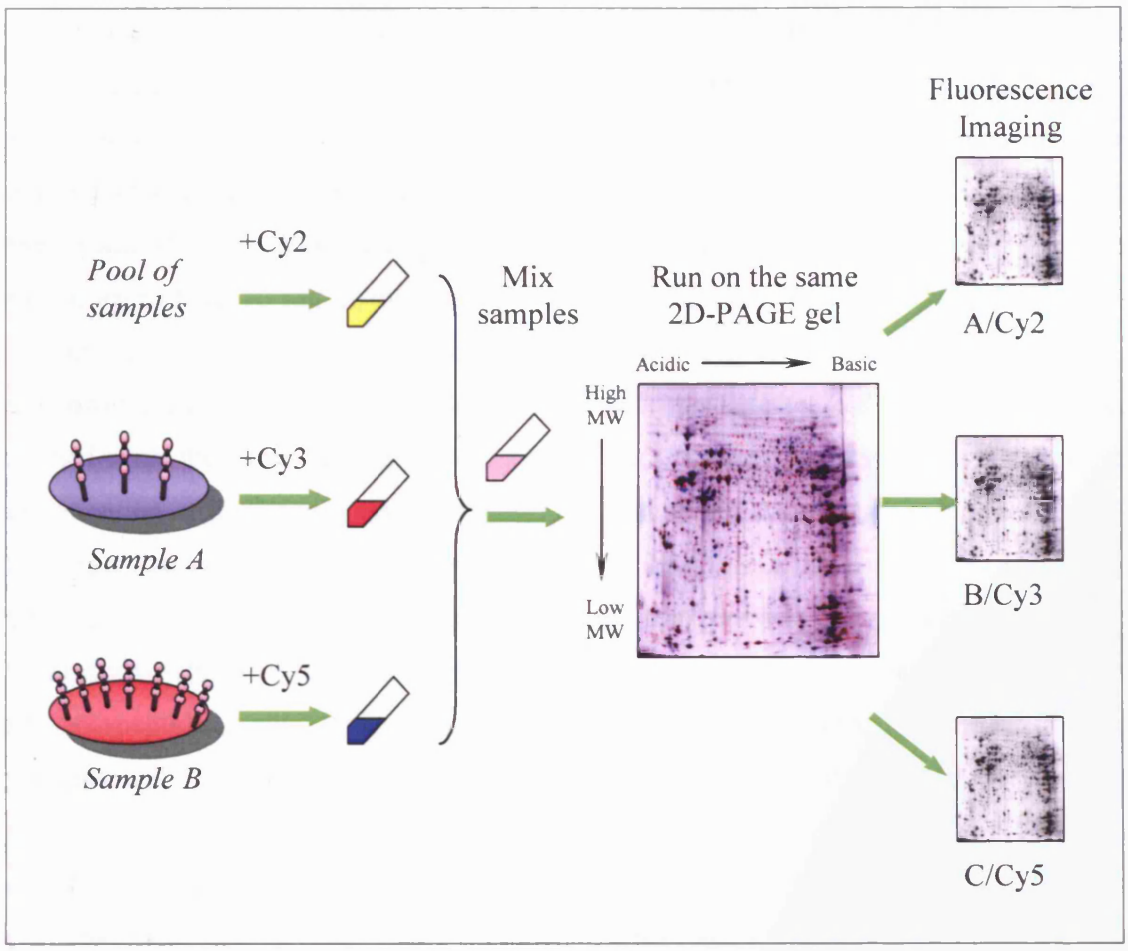

(Figure 1-3) The principle of NHS-CyDye Lysine-labelling 2D-difference gel electrophoresis (2D-DIGE). Up to three samples can be covalently labelled with a distinct fluorescent cyanine dye (Cy2, Cy3 or Cy5) which are mixed prior to protein separation by 2DE. Proteins are visualised by fluorescence imaging using a multi-wavelength fluorescence detection device generating three single, but directly super-imposable images of the three samples analysed. In this scheme, Cy2 is used to label a pool of all samples and used as an internal standard on every gel to aid spot matching and provide more accuracy in quantitation.

dimension or are poorly transferred to the second dimension. It may also be difficult to detect low molecular weight proteins as they are more difficult to stain. It is estimated that of the tens of thousands of genes expressed in a human cell, only a small fraction can be routinely resolved and visualised on a 2DE gel. This subset of proteins represents the most highly abundant and soluble proteins. Moreover, each protein expressed may have different splice variants, proteolysis products or be post-translationally modified, therefore increasing the number of protein features which are resolved. Thus the number

of different gene products is much higher than the ~3 thousand protein products that are routinely detected by 2DE. The dynamic range of expression of proteins is also very high in biological samples, extending over seven or eight orders of magnitude, with a small proportion of the most abundant proteins making up a high percentage of the total mass, and potentially masking the low abundance proteins (Wilkins et al., 1996). According to theoretical studies, to analyse a protein expressed at 1000 copies/cell, it would be necessary to load 10 mg of total lysate, assuming that proteins can be visualised at the low nanogram level on a gel. Since high loading precludes high-resolution separation, the lower copy number proteins will be masked or not detected on an average 2DE gel stained with the most sensitive stain. Gygi *et al.* showed in previous work that the combination of 2DE and mass spectrometry only detected the most abundant proteins in the yeast *Saccharomyces cerevisiae* (Gygi et al., 2000). In a small genome such as the yeast genome, it is possible to estimate the level of expression of a protein according to its propensity to use only one of several codons to incorporate a specific amino acid into the polypeptide chain. This is known as codon bias. According to this estimation, proteins which are largely expressed appear to have a higher codon bias (>0.2). The authors evaluated the protein abundance based on codon bias and showed that the majority of proteins visualised on a 2DE and identified by MALDI-TOF-MS, were proteins expressed at high copy number. This study inferred the need for the development of different techniques which could make possible the detection of low-abundance proteins, for instance using pre-gel enrichment techniques such as sub-cellular fractionation or using liquid-chromatography fractionation for enrichment. Thus, the most important issue in the use of 2D-DIGE, and other 2DE-based separation methods, remains the limitations in proteome coverage. Due to the wide dynamic range in protein expression of biological samples, proteomic analyses favour the characterisation of highly abundant proteins with masking of potentially important changes in low-abundant proteins. Therefore, highly abundant proteins such as heat shock proteins or cytokeratins are often cited as targets of differential protein expression, although these proteins may still represent important markers in biological processes and disease. Improvements in 2DE analysis have enabled increased sample loads, protein solubility and separation through the use of narrow-range pH strips (Gorg et al., 2000b;Westbrook et al., 2001b),

whilst sample pre-fractionation via liquid chromatography (Cooper et al., 2004), or the isolation of organelles and sub-proteomes can increase detection and sensitivity of a subset of proteins when combined with conventional gel-based methods (Bardel et al., 2002;Schirmer and Gerace, 2002). Protein separation and analysis have also been improved using non-gel based methods such as chromatographic separation coupled to mass spectrometric analysis. For instance, multi-dimensional protein identification technology (MudPIT) (Washburn et al., 2001), which can be coupled to differential isotope tagging methods such as SILAC (Ong et al., 2002;Blagoev et al., 2003) for quantitation have received a lot of attention lately and appear to be applicable for in vivo incorporation of specific amino acids into all mammalian proteins and capable of using as quantitative proteomic analysis of different cell culture systems.

A further disadvantage of conventional 2DE-based analysis of differential protein expression is its variability and hence only semi-quantitative nature. Indeed, even minor variations in temperature, polymerization, current, or batch-to-batch variation in the IPG strips used can cause variations between and within multiple gel runs. Although various proteomic studies have shown successful results in the comparison of multiple samples and enabled the identification of various protein targets (Lewis et al., 2000;Benvenuti et al., 2002;Chen et al., 2002), these kind of studies are labour intensive as many replicate gels need to be run, and complex and time consuming image analysis is required for statistical validity. In addition, commonly used staining methods such as silver stain are non-end point methods and protein detection is somewhat variable from gel-to-gel, obligating the need for comparison of many replicate gels.

The ability to run different samples on the same gel such as in 2D-DIGE, so that proteins are subjected to the same physical microenvironments during gel electrophoresis is therefore a huge technical advance. Covalent labelling with the set of fluorescent Cy dye tags described by Unlu et al. (Unlu *et al.*, 1997b) and further developed and evaluated by Tonge et al. and Gharbi et al. (Tonge *et al.*, 2001;Gharbi *et al.*, 2002), therefore represents an attractive tool for improved reproducibility for the comparison of multiple samples. Moreover, fluorescence detection using this method offers a high sensitivity and broader linear dynamic range for improved quantitation of biological samples.

1.1.3 Mass spectrometry in proteomics

Mass spectrometry is an analytical tool allowing the determination of the mass of a molecule with high accuracy. Mass spectrometers are composed of an ion source where the sample is applied, a mass analyser which measures the mass-to-charge ratio (m/z) of ionised particles and a detector. The two major types of approach used in the study of proteins and peptides are matrix-assisted laser-desorption/ionisation mass spectrometry (MALDI-TOF-MS) (Karas and Hillenkamp, 1988) and electrospray ionisation mass spectrometry (ESI-MS) (Whitehouse et al., 1985;Fenn et al., 1989) which rely on distinct methods of ionisation (Figure 1-4). MALDI-TOF-MS relies on ions generated from a solid phase using laser pulses. The sample is usually applied in a matrix solution that facilitates the ion formation by absorption of photon energy from a laser source (Figure 1-4A, left). The most commonly used matrices for protein/peptide analysis are 2, 5-dihydroxybenzoic acid (DHB) and α-cyano-4-hydroxycinnamic acid (CHCA). ESI-MS generates ions from a liquid phase. The sample, in a solvent mixture is directly sprayed into the mass spectrometer where an electrostatic field is formed between the capillary and the walls of the mass spectrometer. As the droplets form and travel, they evaporate and the resulting charged particles enter into the gas phase (Figure 1-4A, right). Both ionisation methods can be performed either in the positive or negative ion mode, although typically for peptide mass analysis, ionisation scans are performed in the positive ion mode. Each ion is separated in the mass spectrometer according to its m/z ratio and several mass analysers have been developed for improved ion separation, resolution and mass accuracy. For protein/peptide sample analysis, these include single time-of-flight (TOF) methods (Figure 1-4B, left) and tandem-mass spectrometers such as TOF-TOF, triple quadrupole, or quadrupole-TOF (Figure 1-4B, right).

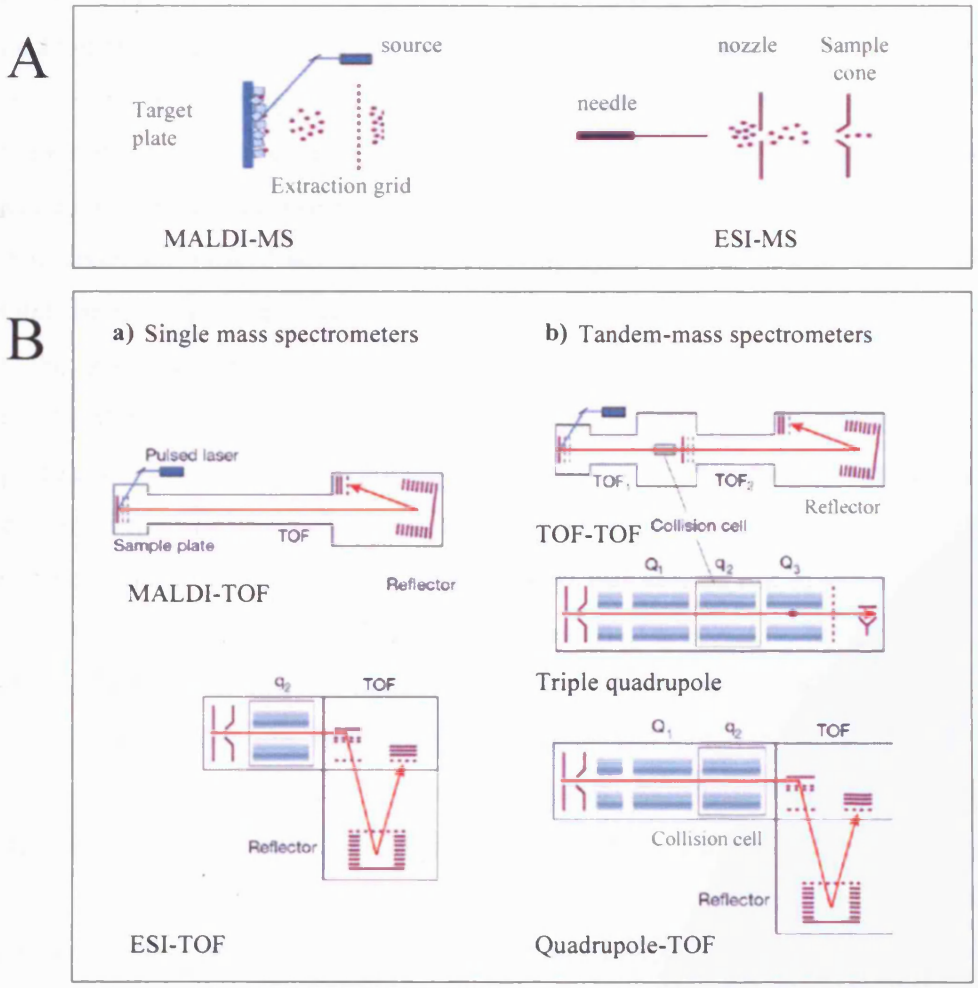

(Figure 1-4) Principles of mass spectrometry and instrumentation (adapted from(Aebersold *et al.*, 2003). (A) Two main ionisation methods can be applied for protein identification and characterisation. These are matrix assisted laser desorption/ionisation mass spectrometry (MALDI-TOF-MS) and electrospray ionisation mass spectrometry (ESI-MS). (B) Several mass analysers have been developed and they can be combined for improved mass resolution and sensitivity.

Protein identification by mass spectrometry can be carried out by peptide mass mapping using MALDI-TOF MS or by further peptide fragmentation to generate sequence data using tandem mass spectrometry (MS/MS). Peptide mass mapping, also called peptide mass fingerprinting (PMF), has been the common method of choice for proteomic analysis (Henzel et al., 1993;James et al., 1993;Mann et al., 1993;Yates, III et al., 1993). A protein of interest usually separated by methods such as 2DE is first picked from gels and then proteolysed using a specific protease to generate a peptide mixture.

Subsequently, the masses of the peptides in the mixture are accurately measured in a mass spectrometer. The list of peptide masses is then matched against theoretical masses for all known proteins using a database search. Several databases can be used which contain theoretical protein cleavages according to the enzyme of choice and possible post-translational modifications and known chemical modifications. A list of potential matches is given and ranked according to a scoring system depending on the probability of a match being real. Confidence in the identification then depends on the species studied, the mass and p*I* of the protein observed on a gel, the number of peptides matching the theoretical masses, the mass accuracy of detection, the protein sequence coverage reached, the number of missed cleavages during the proteolysis process and also the type of modifications observed, which reflects the process of sample handling. Protein identification by peptide mass fingerprinting was carried out in this study and its application is further described in Chapters 2, 4, 5 and 6.

The MALDI-TOF-MS ionisation method generates predominantly singly charged ions $[M+H]^+$ and mass spectra are therefore easier to interpret in terms of the peptide mass profile. The other method of choice for protein/peptide analysis is peptide fragmentation by tandem mass spectrometry (MS/MS). In addition to accurate information on the sequence of a peptide and thus the identification of a protein, tandem mass spectrometry is also an important tool for the analysis of post-translational modifications, such as glycosylation, phosphorylation or acetylation. In tandem mass spectrometry, selected parent peptide ions are selected and fragmented in the mass spectrometer to generate daughter ions with the loss of amino acids (Biemann and Scoble, 1987;Hunt et al., 1987;Wilm et al., 1996). Two main approaches have been used for this fragmentation, post source decay (PSD) in a MALDI-TOF-MS instrument, and collision-induced dissociation (CID) in an ESI-MS/MS instrument. The common principle of these methods is that peptide ions will fragment along the peptide backbone of the molecule at high energy, inducing the formation of a series of smaller daughter ions. According to the bond fragmented, the ions are given an annotation as shown in Figure 1-5. Generally, the ions most likely to be generated are the "b" and "y" ion series, which represent fragmentations at the amino bond from the N- and C- terminus, respectively (Figure 1-5). In MS/MS, peptide mixtures are first analysed in the mass analyser and selected parent

ions of interest are focused and fragmented in a collision cell, where the necessary energy is provided through collision with inert gas molecules. The resulting daughter ions are subsequently analysed in a second mass analyser with the sequence of "b" and "y" ions resulting from the loss of a single amino acid per peptide backbone allowing partial sequence to be deduced by comparison of masses in the series. Again, the list of fragments is matched against a database of theoretical fragmentation pattens, although manual interpretation of data is often needed for improved confidence in the analysis.

Tremendous progress has been made in recent years in the development of optimised instrumentation for increased mass accuracy, sensitivity, yield of detection and automation. The size of instruments has also decreased and several mass analysers have been combined, providing elaborate and compact analytical instruments for high sensitivity and high-resolution biological mass spectrometry. In addition, high-throughput automation is constantly pushing the detection and identification limits further, allowing a promising future for global proteomic analyses.

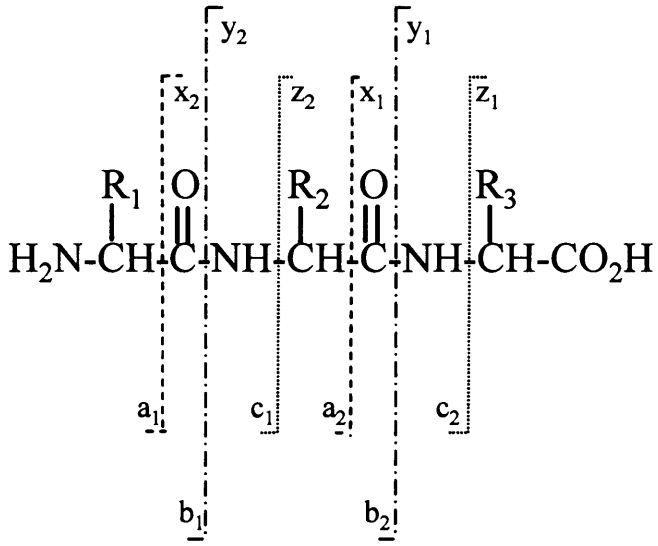

(Figure 1-5) Representation of the fragment ions generated from a peptide by MS/MS (from (Biemann, 1990)). A series of daughter ions is generated upon fragmentation at high collision energy. According to the ionisation method applied, the fragment ion pattern will vary. Commonly, in a collision-induced dissociation, the bond most likely to fragment will be the amino bond, therefore generating mainly b and y ions. On the other hand, in post-source decay (PSD), other ions are observed such as a and x ions.

1.2 Cell signalling and cancer

In multi-cellular organisms, cells have to communicate with each other in order to control their proliferation, differentiation, survival and to perform diverse physiological functions. Cells release and receive signals to induce these different states of growth either by direct cell-to-cell interaction or via secreted molecules. This communication is elicited through so-called signalling molecules such as transmembrane receptors that are embedded in the cell membrane and which can activate intracellular signal transduction cascades which ultimately lead to gene activation or repression and a cellular response. According to the specificity, strength and duration of the signal received, the cell will proliferate, differentiate, change shape, migrate, enter into growth arrest or undergo apoptosis. Signalling pathways are of great complexity and although major routes have been elucidated, the spatio-temporal organisation and components of intracellular machinery are still poorly understood (reviewed in (Hunter, 2000)). Although a large number of proteins are involved in specific signalling event, this can be simplified somewhat by their classification according to their protein structure or functional domain content. Indeed, the major events dominating signal transduction involve cascades of protein-protein or protein-lipid interactions that occur through specific domains, although these interactions can be regulated by post-translational modifications such as phosphorylation. Many protein interaction domains have been classified such as the SH2, PTB, SH3, LIM and PDZ domains, and have been shown to play a central role in many diverse signalling pathways (Pawson, 1995).

These complex signalling networks are highly regulated and alterations of the normal intracellular signals can lead to the development of diseases such as cancer. It is now known that a series of genetic mutations is required for the progressive conversion of normal human cells into cancerous cells. Hanahan and Weinberg have proposed a model of tumourigenesis, whereby several physiological conditions are required by cells before they become tumourigenic (Hanahan and Weinberg, 2000). These are self-sufficiency in growth signals, insensitivity to growth-inhibitory signals, evasion of programmed cell death (apoptosis), limitless replicative potential, sustained angiogenesis, and tissue invasion and metastasis. In proliferative signalling pathways for example, numerous

proto-oncogenes or tumour suppressors have been identified, the mutation of which cause amplification of signalling or loss of negative regulation resulting in over-proliferation and eventual tumour formation. Unlike normal cells, which tightly regulate extracellular ligand levels, receptor expression and secondary signalling molecules, cancer cells often lose the ability to regulate these signalling events. For example, overexpression of RTKs (Libermann et al., 1985), mutation of Ras (Marshall, 1996) or the overexpression of PI3K (phosphatidylinositol 3-kinase) (Sulis and Parsons, 2003) are thought to lead to cell transformation.

RTKs (receptor tyrosine kinases) are able to bind extracellular mitogenic growth factors and transduce these growth signals to intracellular second messengers to directly regulate specific gene expression. Many different RTKs can activate common pathways such as the Ras/Raf/MAPK (mitogen activated protein kinase) signalling pathway, the PI3K/Akt signalling pathway and the Jak/STAT (Janus kinase/ signal transducers and activators of transcription) signalling pathways that lead to increased E2F and Myc mediated transcription and subsequent proliferation (Bell and Ryan, 2005).

In contrast to the highly complex signalling molecular network, most mitogenic signals converge on a small number of nuclear proteins that regulate cell-cycle progression and gene expression. One of these proteins is the retinoblastoma protein (pRb), which inhibits cell cycle progression in resting cells, but following mitogen stimulation is phosphorylated by cyclin/CDK (cyclin dependent kinase) complexes, releasing its inhibition of the E2F family of transcription factors to induce the expression of genes involved in traversing the G1 to S phase transition of the cell cycle (Sherr and McCormick, 2002;Bell and Ryan, 2004). Many intracellular factors can regulate the function of pRb which is inactivated in the vast majority of human cancers (Sherr *et al.*, 2002). In addition, viral oncoproteins such as the E7 protein of human papilloma viruse (Dyson et al., 1989) or SV40 large T antigen (Jha et al., 1998) can inhibit pRb function and lead to cellular immortalisation and tumour formation.

Another well characterised tumour suppressor is p53, the most frequently mutated and inactivated gene in human cancer (Ryan et al., 2001). p53 exists at low levels in normal cells, but when stabilised and activated by various forms of cellular stress or DNA damage, it can activate genes such as p21, inducing cell cycle arrest and

Bax/PUMA/NOXA to induce apoptosis. In addition, Mdm2, a negative regulator of p53, mediates the degradation of p53 via ubiquination (Kubbutat et al., 1997) and the E6 protein of human papilloma virus also binds to and induces ubiquitin-mediated proteolysis of p53 (Scheffner et al., 1990). Thus, inactivation of p53 is a major determinant of cellular transformation.

Tumour cells also need to overcome a hypoxic environment in order to survive and hypoxia-inducible factor 1α (HIF-1α) is a major factor that activates a wide variety of genes responsible for angiogenesis and glucose metabolism (Bardos and Ashcroft, 2004). HIF-1α has been observed to be upregulated in many human cancers including breast cancer and is closely correlated with patient mortality (Harris, 2002). Indeed, many signalling defects associated with cancer have been shown to increase HIF-1α activity, including aberrant signalling by ErbB-2 overexpression (Laughner et al., 2001), PI3K & MAPK (Fukuda et al., 2002), Src (Jiang et al., 1997) and loss of p53 function (Ravi et al., 2000).

Although several markers of cancer progression are already well characterised, there is still a need to better understand the function of these molecules and their relationship with other cellular components. Indeed, attempting to target one signalling molecule of a pathway needs to be done with caution as such an approach often neglects other signalling processes which may be affected. Therefore, in order to better understand the molecular mechanisms associated with tumourigenesis, it is necessary to identify all affected components and to characterise the changes in as much detail as possible. This is one of the aims of proteomics and other global screening methods.

1.2.1 The ErbB receptor tyrosine kinase family

As previously mentioned, one of the major mechanisms used to mediate transmembrane signalling is the ligand induced tyrosine phosphorylation of receptors that generate intracellular binding motifs for interaction with downstream signalling molecules. A large family of receptor tyrosine kinases (RTK) have been identified and characterised (Schlessinger, 2000). These receptors can be classified into 14 different sub-groups according to their structural organisation. They generally share a single transmembrane hydrophobic domain that connects an extracellular ligand binding domain and an

intracellular kinase domain. Signal transfer requires the binding of specific ligands to the extracellular domain, which induces preferential dimerisation of receptor molecules and activation of the tyrosine kinase activity. This results in auto-phosphorylation and cross-phosphorylation of specific tyrosine residues in the cytoplasmic domains and tyrosine phosphorylation of specific signalling molecules that induce a complex series of downstream signalling events, ultimately resulting in the regulation of diverse cellular processes such as proliferation, differentiation and cell motility through regulated gene expression, protein turnover, localisation and changes in enzyme activity status. RTKs also play an important role in development as shown by gene knock-out studies (Lee et al., 1995;Chan et al., 2002) and are known to play a role in the progression of major diseases particularly cancers (Schlessinger, 2000;Zwick et al., 2002).

One of the best-studied sub-families of RTKs is the epidermal growth factor receptor (EGFR) family. The ErbB receptor tyrosine kinase family is composed of four members: ErbB1/HER1 (EGF receptor), ErbB-2/HER2, ErbB3/HER3 and ErbB4/HER4. Each of these receptors can bind a specific subset of ligands (Peles and Yarden, 1993;Riese and Stern, 1998;Olayioye et al., 2000b;Yarden *et al.*, 2001). These ligands are the epidermal growth factor (EGF)-related peptides, which fall into three main groups according to receptor specificity: EGF, amphiregulin (AR) and transforming growth factor-α, which specifically bind to EGFR (ErbB-1); betacellulin, epiregulin and heparin binding EGF-like growth factor which bind to both the EGFR and ErbB-4 receptors, and the Neu differentiation factors or heregulins (Hrg) which are specific ligands for the ErbB-3 and ErbB-4 receptors. The ErbB-2 receptor has no known ligands (Figure 1-6).

Each receptor of the EGFR family has the ability to be activated by homodimerisation upon ligand binding, but heterodimers with other members of the ErbB family appear to be preferred. Several studies have shown that the way in which the receptors dimerise within a particular cell type, determines the specificity of downstream signalling events (Riese *et al.*, 1998). Importantly, although the ErbB-2 receptor does not itself have a specific ligand, it is the preferred heterodimerisation partner for the other ErbB family members (Tzahar et al., 1996;Graus-Porta et al., 1997). It has also been reported to form homodimers in ErbB-2 overexpressing cell systems, and could therefore lead to constitutive, ligand-independent signalling (Lindberg et al., 2002). In addition, ErbB-2

heterodimerisation with ErbB-3 is required for signalling, since ErbB-3 receptors lack intrinsic tyrosine kinase activity (Guy et al., 1994;Kim et al., 1998) (Figure 1-7). Thus, the specificity of signalling in a particular cell type is determined by a combination of factors: the presence of a specific ligand, the availability of co-receptors for dimerisation and the surface expression level of the dimerisation partners.

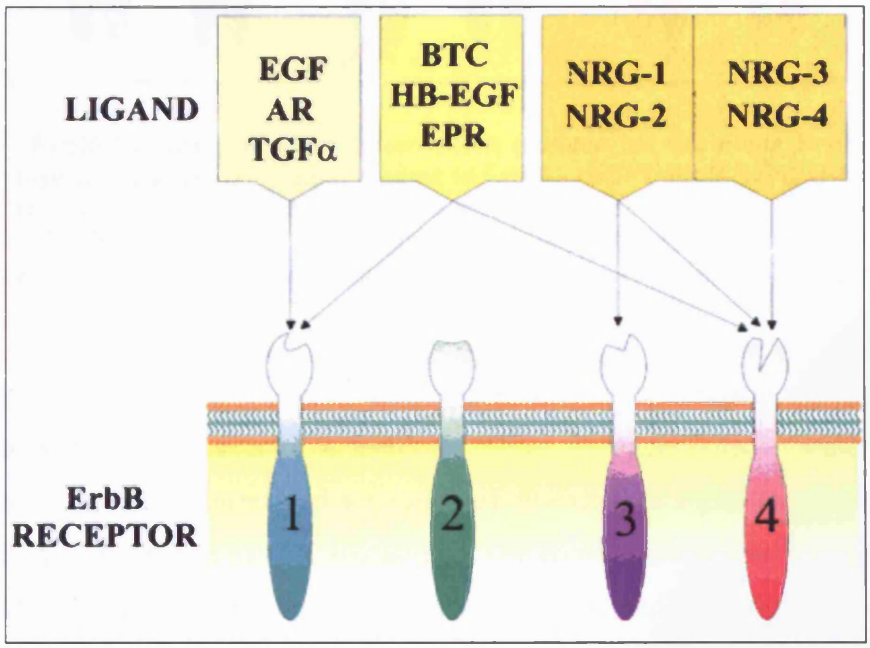

(Figure 1-6) Binding specificities of the EGF-related peptide growth factors (from (Olayioye *et al.*, 2000a)). There are four types of ligands that bind ErbB family receptors. EGF, amphiregulin (AR) and transforming growth factor-α (TGF-α) bind ErbB1; betacellulin (BTC), heparin-binding EGF (HB-EGF) and epiregulin (EPR) bind ErbB1 and ErbB4; neuregulin-1 (NRG-1) and neuregulin-2 (NRG-2) bind ErbB3 and ErbB4; and neuregulin-3 (NRG-3) and neuregulin-4 (NRG-4) bind ErbB4.

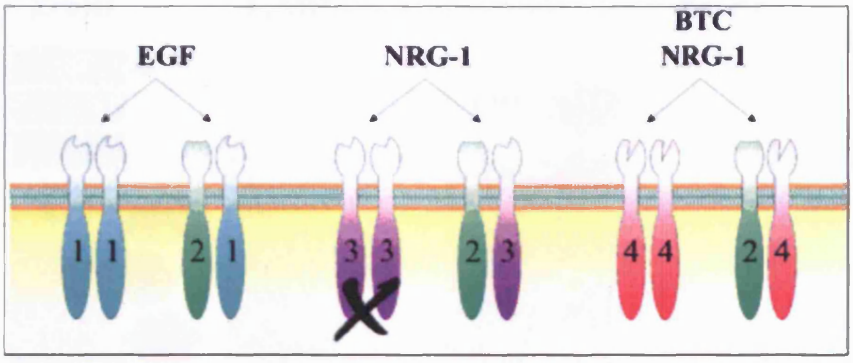

(Figure 1-7) ErbB-2 is the preferred dimerization partner for the other ErbB receptors (from (Olayioye *et al.*, 2000a)). Ligand binding to ErbB-1 (EGF), ErbB-3 (NRG-1) or ErbB-4 (NRG-1, BTC) induces the formation of receptor homodimers and ErbB-2-containing heterodimers. ErbB-3 homodimers do not signal (indicated by the X), since the receptor has impaired kinase activity. Only some of the possible ligand–receptor-induced combinations are indicated.

Each receptor possesses a number of shared and distinct phosphorylation sites which are phosphorylated following receptor activation. These phosphorylated tyrosine residues are essential for the recruitment and activation of downstream signal molecules such as those involved in PI3K and MAPK signalling. The consensus tyrosine phosphorylation sites of each ErbB family members has been determined and the substrates which are recruited to these specific sites identified (reviewed by (Weiss and Schlessinger, 1998;Olayioye *et al.*, 2000b;Yarden *et al.*, 2001) (Figure 1-8). Three main classes of substrates are recruited by activated ErbB receptors (Figure 1-8): adaptor proteins, including Shc, Grb2, Grb7 and Gab1; kinases, such as phosphatidylinositol 3-kinase (PI3K) through its p85 subunit, Src and Chk and tyrosine phosphatases, such as Shp1 and Shp2. All ErbB receptors possess at least one docking site for the recruitment of Shc, which binds via its protein tyrosine binding (PTB) domain or its src homology-2 (SH2) domain and which is additionally able to recruit the adaptor Grb2 (Shoelson, 1997). However, other effector proteins are more specific, and for instance EGFR is the only ErbB member able to recruit the E3 ubiquitin ligase c-Cbl or Shp1. In addition, ErbB-3 possesses six known phosphorylation sites able to recruit the regulatory subunit of PI3K, p85, via its SH2 domains and is therefore thought to be the most potent activator of downstream PI3K signalling (Cantley et al., 1991;Songyang et al., 1993).

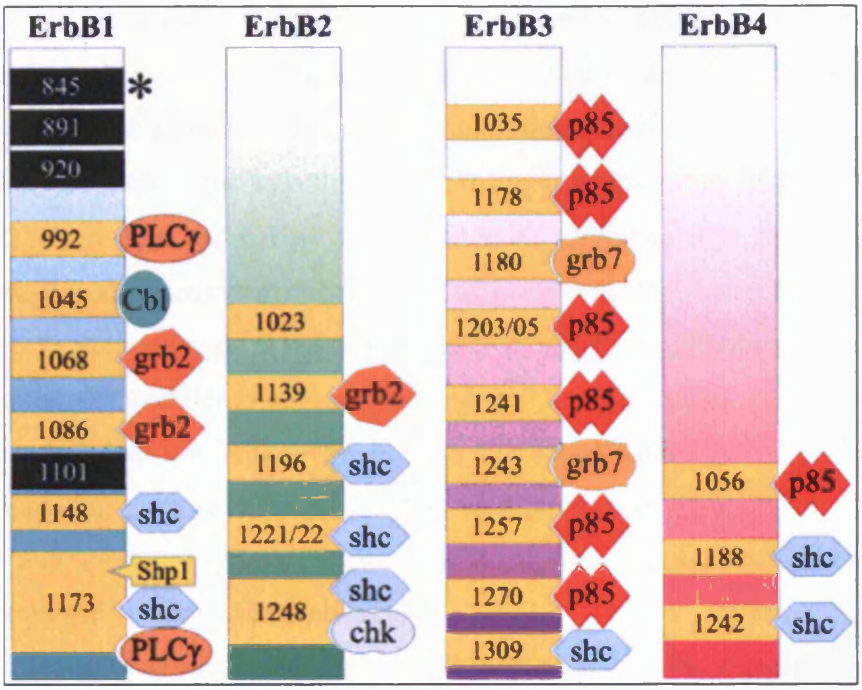

(Figure 1-8) Summary of known ErbB family consensus phophotyrosine residues and reported recruitment of signalling molecules (from (Olayioye *et al.*, 2000a)). Autophosphorylation sites are shown in yellow and Src kinase phosphorylation sites are shown in black.

This diversity in recruitment, together with preferential heterodimerisation reveals the complexity of the signalling that can be generated through the activation of this family of receptor tyrosine kinases. As shown in Figure 1-9, many of the recruited molecules are also receptor substrates and/or substrates for recruited kinases such as Src. The recruitment and activation of effector proteins is an important step in the initiation of various downstream signalling cascades. For example, two of these signal cascades include the mitogen-activated protein kinase (MAPK) and the PI3K pathways (Neve et al., 2002). Both of them display distinct activation profiles in response to growth factor treatment (such as HRG or EGF), with obvious differences in both the intensity and duration of signal output. Through inhibition of each of these pathways it is apparent that each pathway is necessary, yet insufficient alone, to stimulate proliferation. Each pathway regulates distinct subsets of essential cell cycle regulators and integration of these signal networks is required for the timely expression of these components, which culminates in cell cycle progression. The MAPK pathway is activated downstream of the

ErbB family members via the recruitment of Shc, Grb2 and SOS (an exchange factor required for the activation of the small GTPase Ras). In turn, activated Ras at the plasma membrane can recruit and activate a kinase signalling cascade consisting of Raf, MEK, ERK and Rsk that leads to the activation of downstream transcription factors such as AP-1, Elk-1/p62TCF, c-Myc and C/EBPβ (Johnson et al., 1996;Olayioye et al., 2001). The PI3K pathway is also activated downstream of ErbB-3/ErbB-2 heterodimer formation thus leading to activation of Akt/PKB dependent signalling (Vanhaesebroeck et al., 1997), required for proliferation, survival and cellular migration. Furthermore, each signalling cascade does not work alone, but can interact with other pathways (such as the cytokine signalling pathway) to affect the amplitude and duration of the signals transmitted and therefore determine the quality of the output signal and hence the biological response of a particular cell type.

Importantly, ErbB signalling is rapidly down-regulated and so the signals they generate are transient. This has been shown to involve the recruitment of protein phosphatases such as PTP-1B resulting in receptor dephosphorylation and so inhibition or knock-out of PTP-1B leads to the sustained activation of RTKs such as EGFR and PDGFR (Ostman and Bohmer, 2001;Haj et al., 2003). In addition, receptor down-regulation occurs by rapid endocytosis via clathrin coated-pits and subsequent intracellular degradation (Sorkin and Waters, 1993;Sorkina et al., 2002). This process appears to be tightly controlled and varies for each ErbB receptor. For example, EGFR is rapidly endocytosed and degraded via the ubiquitin-proteasome pathway, due to its ability to recruit c-Cbl, a ubiquitin E3 ligase (Levkowitz et al., 1998;Levkowitz et al., 1999), whilst ErbB-2 appears to have impaired ligand-mediated endocytosis (Sorkin *et al.*, 1993;Baulida et al., 1996;Levkowitz *et al.*, 1999).

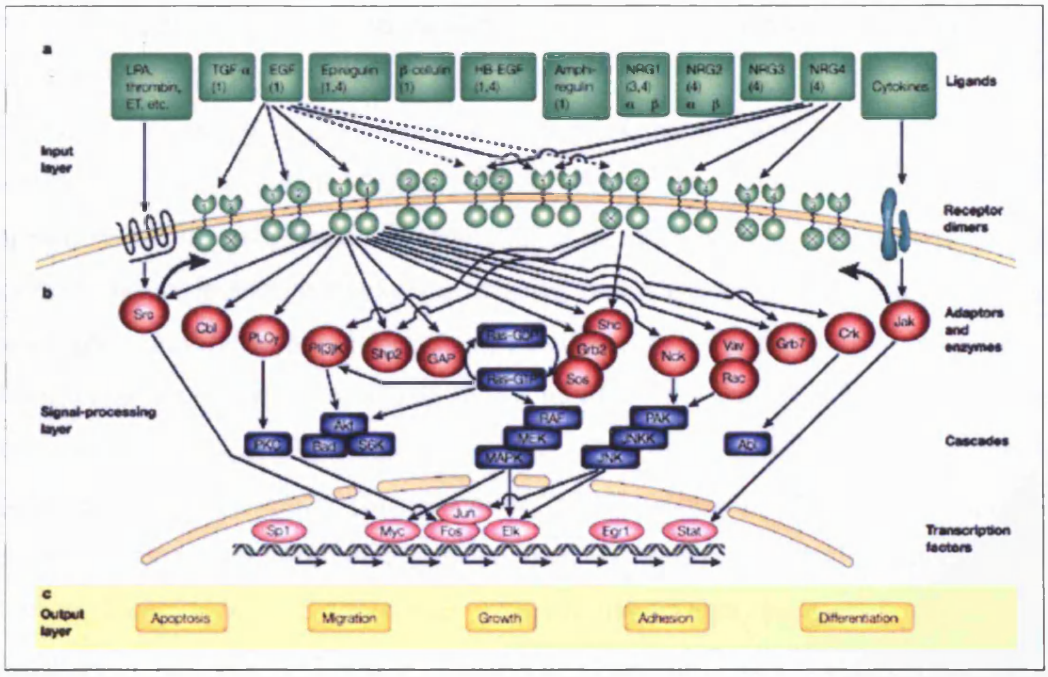

(Figure 1-9) The ErbB signalling network (from (Yarden *et al.*, 2001)). This figure summarises the complexity of the ErbB signalling network. It can be described as several layers of activation. From an array of specific ligands, ErbB receptors are activated in combinations of dimers subsequently leading to the recruitment of various specific and overlapping effector proteins. Kinase activation enables further cascade activation of signalling molecules. Amongst those, the best studied pathways activated downstream of the ErbB family members are the mitogen-activated protein kinase (MAPK) pathway via the recruitment of Shc, Grb2 and Sos and the phosphatidylinositol 3-kinase (PI3K) pathway leading to the activation of Akt and S6Kinase. The next layer of this cascade activation results in the activation of specific transcription factors such as Myc, activated protein-1 (AP-1) (consisting of Jun, Fos), and Elk leading to gene expression and ultimately the alteration of cellular phenotype.

1.2.2 Role of ErbB receptor expression in cancer

EGFR was the first ErbB receptor to be cloned (Ullrich et al., 1984), has been found to be overexpressed in several different types of human cancer such as non-small cell lung carcinoma, bladder, cervical and ovarian cancers and in squamous cell carcinomas of the head and neck (Nicholson et al., 2001). Increased EGFR signalling due to overexpression is thought to play a critical role in tumourigenesis. Several tyrosine kinase inhibitors have been developed in order to specifically target this receptor for prospective therapies, such as the compound ZD1839 (Iressa) (Ciardiello, 2000), or the monoclonal antibody directed against EGFR, cetuximab (C225) (Baselga, 2001). These

EGFR targeted therapies were both designed for preventing the activation of the receptor (Overholser et al., 2000).

ErbB-2 is known to be a potent activator of downstream signalling in response to a variety of EGF family ligands (Wang and Hung, 2001). Moreover, ErbB-2 also plays an important role in the progression of some human cancers. Specifically, ErbB-2 has been reported to be an important marker in invasive breast cancer (Bange et al., 2001) and through gene amplification and its protein overexpression has been observed in 10% to 30% of invasive breast cancers and in 40 to 60% of intraductal breast carcinomas (Slamon et al., 1987). ErbB-2 overexpression is also correlated with the reduced survival of patients with breast cancer (Slamon *et al.*, 1987). Thus, ErbB-2 protein expression level can therefore be a useful diagnostic marker. For this reason, breast cancer research has been focused on the molecular and cellular events associated with ErbB-2 overexpression and in determining its role in cancer progression.

1.2.3 Cellular model of ErbB-2 dependent breast cancer

In the study for new-targeted therapies against cancers, the use of cancer cell models can be advantageous as it enables the accurate and reproducible study of the various properties of human cancer mechanisms. Despite clinical cancer biopsies obtained from patients more accurately reflecting the real state of the illness, these samples are usually very heterogeneous, difficult to purify and often cannot be obtained in sufficient quantities for study. The prerequisite for a good cancer cell model is that it should mimic to the best extent the biological behaviour of an *in situ* cancer. However, this criterion is not always evident as model cancer cell systems are prone to genetic instability during culture, and lack the appropriate cellular or tissue environment. For a single disease, multiple models can be used, however, there is no perfect model and the most appropriate way to choose the model for study is carefully matching it to the experimental question that is being asked.

Many breast cancer cell lines such as SKBr3 BT474 and the SUM cell lines have been derived from pleural effusions of patients with metastatic disease, therefore they represent more the final stages of the tumour and thus little is known about the earlier stages of tumour formation. In contrast, cell lines can be derived from the modification

of normal cells allowing the study of early events in cancer development. It is now well understood that for a normal cell to be transformed into a cancerous cell, several genetic events need to occur (Hanahan *et al.*, 2000). Thus, to efficiently convert normal primary cells into tumourigenic cells, the alteration of several oncogenes or tumour suppressors needs to be carried out (Land et al., 1983). For example, the expression of the simian virus 40 (SV40) large T antigen (LT) can be used to immortalised primary human epithelial or fibroblast cells, which can then be transformed in conjunction with ectopic activation of the telomerase catalytic subunit (*hTERT*) and an oncogenic allele of H-*ras* (Hahn *et al.* 1999).

In the present study, a cellular model of breast cancer was chosen to investigate the role of ErbB-2 overexpression in cellular transformation and signalling. Stamps et al. developed an immortalised luminal epithelial cell line, HB4a, derived from reduction mammoplasty tissue of a normal subject by flow-sorting (Stamps et al., 1994). As most breast cancers arise from the luminal epithelium of the mammary gland (Bartek et al., 1991), this cell type is ideal for the study of the early stages of breast cancer. Indeed, the cells display several markers of the luminal epithelial cell type and have a characteristic luminal epithelial cellular morphology in culture. These cells were immortalised with a temperature-sensitive mutant of SV40 large T antigen (ts A58-U19) (Jat and Sharp, 1989). This process of immortalisation involves the sequestration and inactivation of the tumour suppressor proteins pRb and p53 by the SV40 large T antigen. These proteins normally block the cell cycle, and also act as sensors of cell damage inducing cell cycle arrest and apoptosis, given the appropriate stimuli.

In order to better understand the role of ErbB-2 overexpression in transformation, this model human mammary luminal epithelial cell system was engineered to stably overexpress ErbB-2 (Harris et al., 1999). In detail, HB4a cell lines were stably transfected with a human ErbB-2 cDNA construct and clones were selected by fluorescence activated cell sorting (FACS) based on the level of surface ErbB-2 expression they showed. A panel of cell lines was generated which overexpressed various levels of ErbB-2 (Harris *et al.*, 1999). In this thesis, the parental cell line, HB4a and one of the ErbB-2 overexpressing clones, C3.6, were used to establish the differential protein expression profile relating to ErbB-2 overexpression. The C3.6 clone has been

shown to overexpress surface levels of ErbB-2 similar to those observed in breast cancers (Harris *et al.*, 1999). The C3.6 cells display an altered morphology compared to HB4a indicating a loss of cell-to-cell contact inhibition. In addition, the ErbB-2 overexpressing cell lines were shown to display an increased proliferative capacity and showed enhanced growth responsiveness to EGF and Hrgβ1, growth factors that are specific for EGFR and ErbB-3, respectively. The C3.6 cells were also found to display an increase in anchorage-independent growth, as measured by their ability to form colonies on soft agar. However, these cells can not form tumours after inoculation into nude or SCID mice, showing that they do not display the phenotype of a fully transformed cell line (Harris *et al.*, 1999). This system is currently being used in our laboratory for biochemical, proteomic and microarray analyses in an attempt to establish the cellular defects associated with ErbB-2 overexpression.

This model cell system was also used to study the effect of ErbB-2 overexpression on mitogenic signalling and cell cycle progression (Timms et al., 2002). This work showed that the C3.6 and HB4a cells were able to activate downstream signalling via the MAPK and the PI3K signalling pathways in response to EGF and Hrgβ1 treatment and that the ErbB-2 overexpressing cells had enhanced MAPK signalling, but not PI3K signalling. In addition, both EGF and Hrgβ1 could induce myc, cyclin D1, cdk6 and cyclin E, known activators of the cell cycle, and this effect was more prominent in the ErbB-2 overexpressing cells. The cell cycle inhibitor $p27^{kip}$ was also suppressed in the C3.6 cells, which has been previously shown in other models of ErbB-2 overexpression (Lane et al., 2000;Lenferink et al., 2001). These combined changes induced an increase in cdk2 activity that promotes more rapid progression through the cell cycle. Together, this prior work showed that this cellular model is a valid system for the study of breast cancer and was therefore used here to examine the effects of ErbB-2 overexpression on overall protein expression and on the response of luminal epithelial cells to oxidative stress.

1.3 Stress Signalling, ROS and redox regulation

Originally, reactive oxygen species (ROS) were recognised as products of the mammalian host defence mechanism, and early studies focused on the characterisation of the so-called respiratory burst in neutrophils (SBARRA and KARNOVSKY, 1959) and

the role of the NADPH oxidase complex, which is now recognised as a primary source of intracellular ROS (Babior, 1999). Apart from this defensive role in phagocytic cells, ROS have also been shown to play a role in cell signalling in many diverse biological systems. Indeed, ROS can induce programmed cell death (apoptosis) or necrosis, induce or suppress the expression of many genes and activate/inactivate cell signalling cascades, such as the mitogen-activated protein kinase pathways (Torres and Forman, 2003). Moreover, ROS are believed to play a pivotal role in aging, degenerative diseases, immuno-defence and cancer. Based on these reasons, it is important to study the roles and mechanisms of cellular ROS.

1.3.1 Formation of cellular Reactive Oxygen Species (ROS)

ROS are species of oxygen which are in a more reactive state than molecular oxygen, and in which the oxygen is reduced to varying degrees. ROS comprise several species such as hydrogen peroxide (H_2O_2), the hydroxyl radical ($^{\cdot}OH$), superoxide ($^{\cdot}O_2^-$) and singlet oxygen ($^{\cdot}O$). $^{\cdot}O_2^-$ can be generated by the action of such enzymes as NADPH oxidase, lipoxygenase, cyclooxygenase, cytochrome P450 or through UV irradiation and can be converted into H_2O_2 and O_2 by the action of superoxide dismutases (SOD) (Figure 1-10). H_2O_2 can be also further converted to $^{\cdot}OH$ (a very reactive ROS) in the presence of Fe^{2+}. ROS have been widely reported to play an important role in promoting apoptosis and tumourigenesis. For example, ROS have been shown to induce apoptotic proteins, whereas antioxidants inhibited this apoptotic effect (Rollet-Labelle et al., 1998;Tanaka et al., 1998). However, ROS-induced tumourgenesis has been linked to oxidative DNA damage through the generation of the DNA oxidative product 8-oxo-deoxyguanosine, a highly mutagenic agent (Floyd, 1990). ROS are also thought to contribute to cancer through interference with various signal cascade systems including pathways involving nuclear transcription factor kappa B (NFκB), activated protein-1 (AP-1), phospholipase A2 (PLA2), mitogen-activated protein kinases (MAPKs), Akt and Jun kinase (Guyton et al., 1996a;Bae et al., 1997;Musonda and Chipman, 1998;Manna et al., 1998) (see 1.3.3).

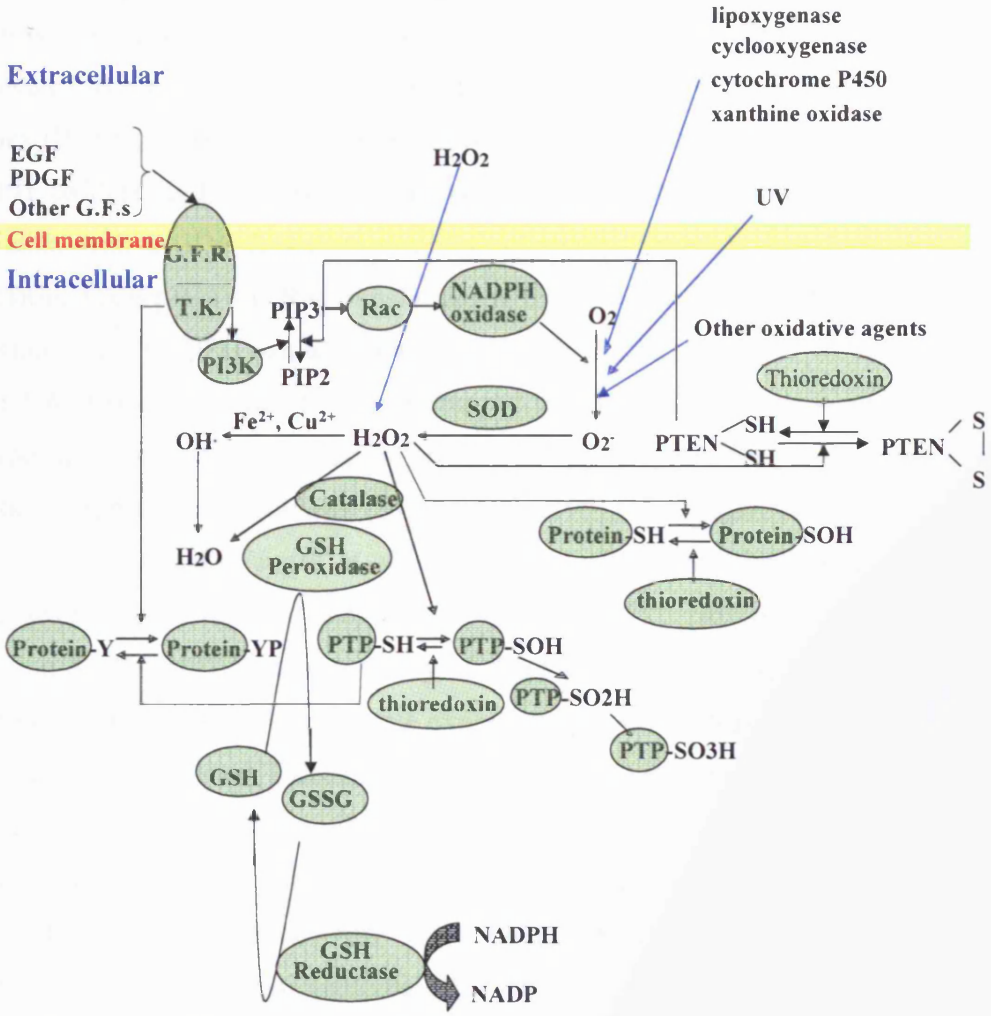

(Figure 1-10) Metabolic pathways and mechanisms of cellular ROS production and its effect on cellular proteins.

Several enzymes are able to produce ROS; the most important of these is NADPH oxidase. NADPH oxidase was first discovered in neutrophils, which following stimulation with microorganisms undergo a respiratory burst, with the release of superoxide ions into the phagosome (Babior, 1999). In resting cells, NADPH oxidase is a heterodimeric plasma membrane-associated protein complex consisting of two polypeptides, p22-phox and gp91-phox, which together make up the flavocytochrome b_{558}. gp91-phox contains a FAD group and two haem groups, which together comprise an electron transfer module which enables the transfer of electrons from cytosolic NADPH to molecular oxygen. However, no NADPH oxidase activity is seen in resting cells and

other components of the enzyme must be recruited. These cytoplasmic components are p47-phox, p67-phox and p40-phox. Upon stimulation, these polypeptides are translocated to the inner surface of the plasma membrane to form a fully active enzyme complex (Babior, 1999). Two small GTPases, Rap and Rac/p21, are also associated with NADPH oxidase and are involved in its activation. Rac in the resting state is in association with a GDP-dissociation inhibition factor, Rho-GDI, but upon stimulation, dissociation takes place and Rac translocates to the plasma membrane where it aids in the activation of the NADPH oxidase complex (Bokoch, 2000).

Whilst NADPH oxidase was first characterized in neutrophils, it is also present in other cell types that have no role in host defence. For example, NADPH oxidase components have been reported in fibroblasts (Meier et al., 1991), mesangial cells (Radeke et al., 1991), endothelial cells (Jones et al., 1996), osteoclasts (Steinbeck et al., 1994) and chondrocytes (Hiran et al., 1997;Moulton et al., 1997). However, the rate of ROS generation by NADPH oxidase in many of these cell types is very low compared with that in neutrophils, but such a disparate expression pattern for this enzyme implies a role other than in host defence. Indeed, recent work suggests it may play a more general role in signal transduction (Torres *et al.*, 2003).

Another source of ROS is xanthine oxidoreductase or xanthine oxidase (Harrison, 2002) (Figure 1-10). This molybdenum- and iron-containing flavoprotein catalyses the oxidation of hypoxanthine to xanthine and then to uric acid. Molecular oxygen is the oxidant, and products include superoxide and H_2O_2. This enzyme can also produce $NO^{\bullet}$, suggesting that it might have a dual role in cellular signalling.

The electron transport system of mitochondria also produce ROS. Electron transport through the mitochondrial respiratory chain is extraordinarily efficient, and normally the vast majority of O_2 is consumed. However, 1–2% of electrons are leaked to generate $^{\bullet}O_2^-$ in reactions mediated by coenzyme Q and ubiquinone and its complexes. Thus, mitochondria are believed to be a major site of ROS production *in vivo* (Boveris and Chance, 1973). Similarly electron transport in the endoplasmic reticulum generates $^{\bullet}O_2^-$ by the leakage of electrons from NADPH cytochrome P450 reductase (Cross and Jones, 1991). Finally, $^{\bullet}O_2^-$ is also generated by lipoxygenase, cyclooxygenase and UV

irradiation of molecular O_2, whilst cells may also be exposed to extracellular sources of ROS (Figure 1-10).

1.3.2 ROS-dependent protein modifications

Several chemical moieties have been found to be potential regulators of cellular redox status. One of these, the free thiol group (RSH) of cysteine residues is a potent nucleophilic agent and can undergo a number of redox-induced modifications under physiological conditions. Oxidative modifications of RSH groups other than disulphide formation include the formation of the sulfenic acid (RSOH), sulfinic acid (RSO_2H) and sulfonic acid (RSO_3H) depending upon the oxidative capacity of the oxidant ((Schafer and Buettner, 2001) and see Figure 1-10). Oxidation of RSH groups to sulfinic and sulfonic acids is irreversible under physiologic conditions, whilst sulfenic acids were thought to exist only as transient intermediates (Hamann et al., 2002). Recently however, it has been shown that the formation of relatively stable protein sulfenates can occur, and that these intermediates may play a role in the regulation of biochemical pathways and in cellular physiology (Willett and Copley, 1996). For example, the crystal structure of the flavoprotein NADH peroxidase revealed that the protein possesses an active site cysteine in the form of a sulfenic acid (Yeh et al., 1996). It was proposed that stabilization of the active site Cys-SOH was derived from electronic interaction with the flavin moiety, coupled with weak interactions with other active site proximal residues. In another example, the protein tyrosine phosphatase (PTP-1B) was shown to be inhibited by exposure to relatively low concentration of hydrogen peroxide, and that this inhibition was due to formation of Cys-SOH at the catalytic Cys residue ((Denu and Tanner, 1998) and (Figure 1-10)). Moreover, this Cys-SOH could be shown *in vitro* to be subject to glutathionylation, which protected the Cys-SOH from further oxidation to sulfinic or sulfonic acids (Lee et al., 1998) (Figure 1-11).

The cellular redox buffer glutathione (GSH) is present within most cells at a millimolar concentration and acts as a first line of defense to detoxify ROS (Kosower and Kosower, 1978). Glutathione peroxidase catalyzes the reduction of ROS via the oxidation of the GSH thiol to glutathione disulphide (GSSG) and then the GSSG is restored to GSH by GSH reductase, an enzyme which uses NADPH for reducing potential (Meister, 1994)

and (Figure 1-10). In addition, glutathione peroxidase can reduce ROS via the oxidation of the reduced cysteine on various proteins to form mixed disulphides (RSSG) and RSSG is restored to RSH by protein disulphide isomerase, glutaredoxin or thioredoxin (Arscott et al., 2000) (Figure 1-11). The antioxidative molecule, thioredoxin, is a small multifunctional protein that has a redox active disulphide within the conserved active site sequence (Holmgren, 1989a;Nakamura et al., 1997). Thioredoxin is capable of reducing some ROS, including H_2O_2, as well as reducing oxidized proteins (Mitsui et al., 1992). Oxidized thioredoxin is in turn restored to its reduced form by thioredoxin reductase which uses NADPH as a source of electrons. In addition, all cells possess the protective enzymes, catalase which can degrade H_2O_2 to O_2 plus H_2O. Another family of enzymes, the peroxiredoxins (Prxns) are required to reduce intracellular peroxides and have been shown to suppress tumour formation (Neumann et al., 2003). In humans, the family consists of 6 members, comprising the classical cytosolic 2-Cys peroxiredoxins (Prxns 1-5) and the 1-Cys, Prxn-6. The 2-Cys Prxns contain a redox-sensitive cysteine at the active site (Choi et al., 1998) and another conserved cysteine (Hirotsu et al., 1999;Declercq et al., 2001). The active site cysteine is oxidized to cysteine sulfenic acid (Choi *et al.*, 1998) or to a disulphide with the other conserved cysteine (Chae et al., 1994) when peroxide levels are reduced. In order to complete the enzymic catalytic cycle, the peroxiredoxins are reduced back to their active thiol form via the thioredoxin/thioredoxin reductase system (Chae *et al.*, 1994). Very recently, 2-Cys Prxn has been found to play a signalling related role in yeast where it regulates the peroxide induced oxidation and activation of a stress-activated MAP kinase (Sty1) by forming an intermolecular disulphide bridge (Veal et al., 2004).

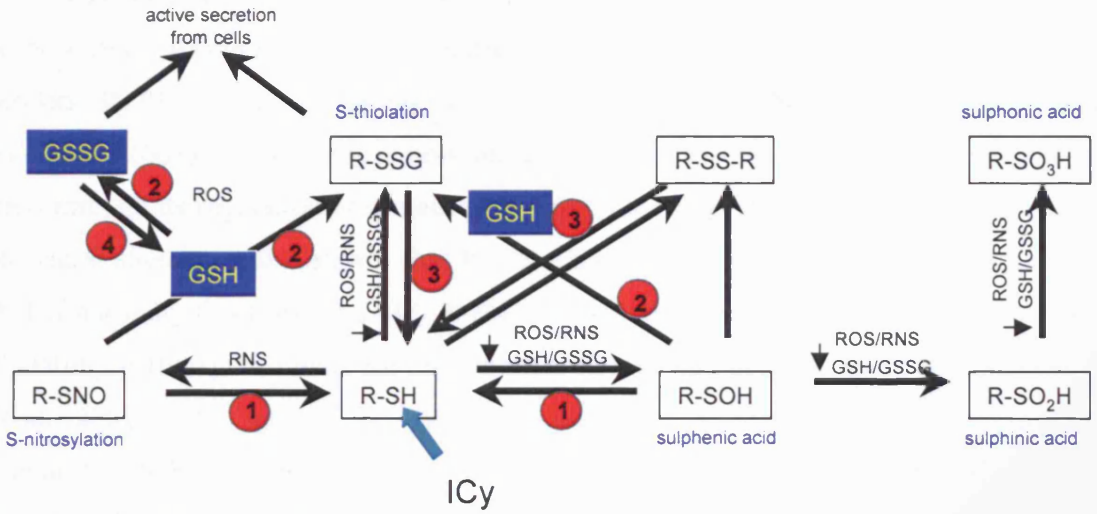

(Figure 1-11) Thiol-dependent redox modifications. Cellular thiol containing proteins can be modified to different oxidative states which can be revesible or irreversible reactions. The reversible redox regulations are always enzyme-dependent. These redox regulatory reactions involve the following catalytic enzymes: peroxiredoxins/thioredoxin, glutathione peroxidase/glutathione S-transferase, protein disulphide isomerase/glutaredoxin/thioredoxin and glutathione reductase which are responsible for catalysing the indicated reactions 1, 2, 3 and 4, respectively.

1.3.3 Redox regulation of cellular signalling

ROS are ideally suited to be signalling molecules as they are small and can diffuse quickly through cells. Moreover, there are a number of mechanisms for ROS production, some of which are rapid and controllable. In addition, ROS can be also rapidly removed through various mechanisms. Many studies have indicated a role for ROS in the induction or inhibition of cell proliferation, in the activation or inhibition of apoptosis and in the induction of necrosis at high concentrations (Gamaley and Klyubin, 1999).

Reversible protein phosphorylation is a key biochemical event in many cell signalling pathways and numerous studies have shown that ROS can significantly affect this protein phosphorylation process. For example, several reports have shown that the proteins Erk1/2, Akt , p38 and JNK are activated by H_2O_2 in animal cells (Fialkow et al., 1994;Guyton et al., 1996b;Blanc et al., 2003;Ruffels et al., 2004), leading to the modulation of gene expression. Importantly, H_2O_2 has been shown to inhibit phosphatases by the direct oxidation of the active site cysteine in these molecules

(Sullivan et al., 1994;Wu et al., 1998). For example, the protein-tyrosine phosphatase 1B (PTP-1B) which can regulate the phosphorylation state of signalling proteins was found to be a target of H_2O_2 in cells. Modification of the catalytic cysteine residue by H_2O_2 renders PTP1B inactive leading to increased tyrosine phosphorylation (Lee and Esselman, 2002). Thus, H_2O_2 is now recognized as a secondary signalling molecule in cells through its regulation of protein phosphorylation (Barrett et al., 1999;Finkel, 2000). Recent studies have also shown that PTEN plays an important role in redox signalling. PTEN normally functions as a PIP_3 3'-phosphatase which negatively modulates the PI3K signalling pathway to inhibit the proliferation of cells and promote apoptosis (Maehama et al., 2001) and (Figure 1-10). It was shown that cysteine-124 in the active site of human PTEN is a target for exogenous oxidants (such as H_2O_2) and forms a disulphide bridge with Cys-71 (Lee et al., 2002). Moreover, when cells are stimulated with peptide growth factors (such as EGF or PDGF), part of the cellular pool of PTEN was found to be transiently oxidised to the inactive form (Kwon et al., 2004). It was suggested that this was due to the generation of endogenous H_2O_2 through the activation of the PI3K pathway and subsequent NADPH oxidase via Rac1 activation. Thus, activation of PI3K by growth factors might not be sufficient to accumulate enough PIP_3 for downstream signalling due to the antagonistic activity of PTEN and H_2O_2 might be needed to inhibit PTEN activity to permit PIP_3 accumulation. Since PTEN is a known tumour suppressor, the modulation of PTEN by ROS could be one mechanism by which ROS promotes survival and proliferation of cancer cells (Figure 1-10).

ROS can induce gene expression, and many studies have shown that the expression of a wide range of genes is regulated by oxidative stress (Allen and Tresini, 2000). For example, addition of H_2O_2 to cells stimulates expression of transcription factors such as c-fos, c-jun (AP-1), c-myc, myb and Ets (Amstad et al., 1990;Nose et al., 1991;Myrset et al., 1993;Wasylyk and Wasylyk, 1993;Rao et al., 1996) and results in activation of NF-κB through dissociation of the factor from its inhibitor Iκ-B (Schreck et al., 1991). Thus, by activating various transcription factors, ROS have the potential to affect the expression of many genes. This response, at least in part, appears to play a cytoprotective role since many ROS induced genes are redox protective enzymes such as GST, catalase and thioredoxin reductase. Whilst these transcription factor activation events are likely to

be due to activation of upstream signalling pathways, perhaps due to protein and lipid phosphatase inhibition, some mechanisms of transcription factor activation by ROS appear to be more direct. For example, STAT pathways in animal cells are activated by H_2O_2 (Simon et al., 1998), showing how H_2O_2 can transduce its message directly into the nuclei of cells. In yeast, the peroxidatic cysteine of Gpx3 was found to directly induce the activation of the transcriptional factor Yap1 in response to H_2O_2 through the transient formation of an intermolecular disulphide bond with Yap1 (Delaunay et al., 2002). Also, 2-Cys Prxn regulates the peroxide induced oxidation and activation of a stress-activated MAP kinase (Sty1) by forming an intermolecular disulphide bridge in yeast (Veal et al., 2004).

Extracellular growth factors can transduce signals into cells through different signalling pathways using RTKs, serine/threonine kinases, phospholipases, Ca^{2+} and other mechanisms (see Section 1.1). Similarly, when cells are exposed to ROS, signals are transferred through many of the same signalling pathways (Kamata and Hirata, 1999). Oxidants can activate RTKs (Aslan and Ozben, 2003) and downstream signalling molecules such as MAP kinases (Torres *et al.*, 2003), Ras (Lander et al., 1995), PI-3 kinase and Akt (Park et al., 2004), protein kinase C (PKC) (Inoguchi et al., 2003), phospholipase C (Gonzalez-Pacheco et al., 2002) and molecules involved in Ca^{2+} signalling (Mikoshiba, 1997). The activation of phospholipase-γ by oxidative stress increases the cytosolic Ca^{2+} levels by altering the flux from intracellular Ca^{2+} pools, such as the ER or the extracellular space (Poli et al., 2004). In turn a number of transcription factors become activated, thereby affecting gene expression (Rahman et al., 2004).

It is through their effects on signalling that ROS molecules appear to play the roles of secondary messenagers. Indeed cells activated by extracellular stimuli, are known to produce ROS, which in turn modulate diverse signalling pathways. Thus, there is a cross-talk between signalling systems and the cellular redox state (Poli *et al.*, 2004). The current model for ROS production as secondary messengers is that receptor tyrosine kinases activated by growth factors cause the activation of PI3K, the product of which, namely PtdIns(3,4,5)P_3, then bind to the PH domain of guanine nucleotide exchange factors (GEFs) (e.g. Sos, Vav1 and βPix) and stimulate the GDP-GTP exchange activity of GEFs. The activated GEF can convert Rac1-GDP to Rac1-GTP, which binds directly

to and recruit components of membrane-bound NADPH oxidase. Thus, the activated NADPH oxidase can promote the electron transfer from NADPH to molecular oxygen and subsequently mediate the production of superoxide anions (O_2^-) (Bae *et al.*, 1997;Bae et al., 2000;Di-Poi et al., 2001;Price et al., 2002;Park *et al.*, 2004). These superoxide anions (O_2^-), or H_2O_2 produced by superoxide dismutase, can then activate signalling kinases through unknown mechanisms, possibly through phosphatase inhibition or direct activation by peroxidases, leading to the activation of downstream transcription factors which then regulate gene expression to promote cell survival and proliferation (Guyton *et al.*, 1996b). Conversely, other studies have shown that oxidative stress promotes apoptosis (Curtin et al., 2002) and can occur through the production of ceramide (Verheij et al., 1996) that can activate JNK (Ishikawa et al., 1997) and p53 (Yin et al., 1998). Thus, the role of ROS in inducing cell death or survival is uncertain and the end effects rely on the cross-talk and balanced regulation of many signalling pathways.

With regard to tumour development, ROS have been considered as DNA-damaging agents that increase the mutational rate and promote oncogenic transformation (Jackson and Loeb, 2001). In addition, an elevated oxidative status has been found in many types of cancer cells, with ROS activating signalling cascades that induce and maintain the oncogenic phenotype (Behrend et al., 2003). ROS may also lead to the stabilisation and activation of HIF-1α, a transcription factor controlling tumour angiogenesis under normoxic or hypoxic conditions via the p42/p44 MAPK pathway (Richard et al., 1999). Interestingly, the elimination of excessive ROS by chemical (Mukhopadhyay-Sardar et al., 2000) or enzymatic (Lam and Reprecht, 1994) antioxidants decreases the tumourigenicity of various types of cancer cells, possibly offering new strategies for cancer therapy. One of the antioxidant enzymes with anti-tumour activity is the mitochondrial protein, MnSOD, which has been shown to retard the growth of tumours when overexpressed in rat glioma cells and human oral carcinoma cells (Zhong et al., 1996;Liu et al., 1997). Moreover, MnSOD expression is found to be lowered in cancer cells compared with normal control cells (Oberley and Oberley, 1988). This infers that tumour cells have the capacity to produce more superoxide radical, the substrate for MnSOD and this may be a general characteristic of tumour cells.

1.4 Redox proteomics

A wealth of knowledge exists, which indicates that ROS play critical roles in regulating cell behavior through the modification of protein molecules (Moran et al., 2001). However, compared with the knowledge accumulated from extensive proteomic studies on phosphorylation, relatively little is known about the extent of redox modifications of proteins. As outlined above, reactive oxygen species (ROS) and reactive nitrogen species (RNS) cause various types of chemical modifications to proteins. Such modifications are often irreversible (sulphonation, carbonylation, nitration or protein-protein cross-linking), are associated with permanent loss of protein function and may lead to the accumulation, degradation or aggregation of the damaged or modified proteins. Some modifications are reversible (S-nitrosylation or glutathionylation), and appear to play a role in protecting cysteines from irreversible oxidation and in regulating the redox status of cells (Ghezzi and Bonetto, 2003). In the following paragraphs, the techniques available for identifying proteins based on their redox status is described, in particular methods for identifying changes in the thiol-disulphide chemistry of cysteine residues and for identifying protein glutathionylation.

Most redox studies have made use of maleimide or iodoacetyl derivatives of fluorescent or biotinylated reagents which react with free thiol groups to covalently tag the protein. Such reagents include: monobromobimane (Berggren et al., 2001), (4-iodobutyl) triphenyl-phosphonium (Lin et al., 2002), maleimidobutyrylbiocytin (Garant et al., 1999), Oregon green maleimide (Essex et al., 2001), N-biotinoylaminoethyl methanethiosulfonate (Ennion and Evans, 2002), N-biotinoyl-N-(maleimidihexanoyl) hydrazine (Hare and Lee, 1989), fluorescein-5-maleimide (Birge et al., 1991), N-(biotinoyl)-N-(iodoacetyl) ethylendiamine (Kim et al., 2000), NEM-biotin (Lind et al., 2002) and N-(6-(biotinamido)hexyl)-39-(29-pyridyldithio) propionamide (Jaffrey et al., 2001a) and maleimide derivates (Yamamoto and Sekine, 1978;Jaffrey et al., 2001b). Since oxidation of a thiol would prevent its labelling by these reagents, they can be used in comparative 2DE studies to detect loss of free thiols due to oxidation. To detect disulphides, one approach has been to block all free thiols with iodoacetamide or NEM, then to reduce the disulphides and detect the new free thiols with the thiol reactive reagents described above. In addition, by using different reductants, the specific form of

oxidation (thiolation, S-nitrosylation or glutathionylation) has been inferred. For example, ascorbate can reduce S-NO (Jaffrey *et al.*, 2001a), whilst thioredoxin can be used to reduce protein disulphide bonds (Yano et al., 2001).

Formation of mixed disulphides in cell systems can occur by sulfhydryl oxidation or by thiol-disulphide exchange (e.g. glutathionylation). The reactions below show the formation of a mixed disulphide:

$$\text{Protein-SH} + \text{GSH} + H_2O_2 \text{ (or NO)} \rightarrow \text{Protein-S-S-G} + H_2O$$

$$\text{Protein-SH} + \text{GSSG} \rightarrow \text{Protein-S-S-G} + \text{GSH}$$

Whilst intra- or intermolecular disulphides can be reduced by thioredoxin, the glutathionylated disulphide complexes (Protein-S-S-G) are reduced by glutaredoxins (Holmgren, 1989b). Many proteins including enzymes, transcription factors and cytoskeletal proteins have been identified as glutathionylated proteins and the activity of some of these appears to be regulated by glutathionylation (Cotgreave and Gerdes, 1998;Klatt and Lamas, 2000). Although glutathionylation often occurs during oxidative stress, many proteins may be glutathionylated under normal physiological conditions. In fact, the amount of glutathione present as a mixed disulphide with proteins is 20-30 nmol/g in liver tissue (approximately 4-6% of total protein) (Brigelius et al., 1983). Several methods have been used to identify glutationylated proteins in living cell systems. One method involves metabolically labelling cells with ^{35}S-cysteine in the presence of high concentrations of cycloheximide (Rokutan et al., 1991). This technique allows labelling of the intracellular GSH pool, but avoids the incorporation ^{35}S-cysteine into newly synthesized proteins. Labelled cell lysates can then be resolved by 2DE for further analysis. Another method to analyse glutathionylated proteins is by alkylation of free thiols with NEM, specific reduction of protein-glutathione mixed disulphides by glutaredoxin and then labelling the newly formed thiols with NEM-biotin. Proteins can then be enriched by affinity purification and analysed by 2DE (Lind *et al.*, 2002). Glutathionylated proteins have also been enriched on GSH or GSNO-sepharose columns (Klatt et al., 2000) and have been detected by immunostaining with specific antibodies (Wang et al., 2001).

S-nitrosylation of proteins is also an important mechanism of redox regulation and is a means by which NO can modulate the activity of proteins (Jaffrey *et al.*, 2001a). This modification is reversible and can be reduced *in vitro* by ascorbic acid, GSH (Kashiba-Iwatsuki et al., 1997) or thioredoxin (Nikitovic and Holmgren, 1996). S-nitrosylation of proteins has been detected by blocking free thiols with methanethiosulfonate, which cannot react with nitrosothiols; then nitrosothiols are reduced to thiols with ascorbate and the newly formed thiols are derivatized with a biotinylated thiol reagent for detection by immunoblotting of 2D gels (Jaffrey *et al.*, 2001a).

ROS-mediated protein carbonylation is an important marker of oxidative damage. Carbonyl groups may be introduced into a protein at different sites and its extent has been correlated with neurodegenerative diseases and aging (Stadtman and Berlett, 1997;Butterfield and Kanski, 2001). Protein carbonylation occurs via direct oxidation of the protein backbone leading to fragmentation producing polypeptides with an N-terminal alpha-ketoacyl amino acid residue (Stadtman *et al.*, 1997) which can be detected in a colorimetric assay using 2, 4-dinitrophenylhydrazine (DNPH) (Levine et al., 1990).

The nitration of tyrosine residues to form 3-nitrotyrosine (3-NT) is the most studied case of protein nitration and is considered as a marker of irreversible protein modification by peroxynitrite (Beckman, 1996). Increased levels of 3-NT have been shown in various diseases such as Alzheimer's disease, Parkinson's disease and atherosclerosis and can be detected by immunoblotting with specific anti-3-NT antibodies (Ye et al., 1996).

1. 5 Aims of this study

The aim of this study was to develop a method to detect cysteine-labelling changes for use in protein expression profiling and to apply 2D-DIGE to study redox regulation of proteins. In order to apply the cysteine specific ICy dye technique to 2D-DIGE, it was first necessary to establish the optimal labelling conditions (temperature, denaturant, reductant and so on) using standard proteins and total cell lysate samples. After optimising these labelling conditions, the cysteine labelling strategy would then used to probe for targets of cellular oxidative stress (H_2O_2 treatment) in human luminal epithelial cells expressing normal levels of the receptor tyrosine kinase ErbB-2 and a derivative overexpressing this receptor. These experiments would therefore test the effects of

overexpression of an oncogenic RTK on redox stress responses which may be linked to tumour progression. It is expected that any changes in labelling are caused either by differential protein expression or from the exchange of reactive thiol groups into higher oxidative states that prevent reactivity with the ICy dyes. Proteins displaying differential labelling would then be picked from 2D gels for identified by MALDI-TOF-MS with further validation of changes, carried out by 1-D and 2-D immunoblotting. In addition, identification of labelled peptides by MS would be used to identify sites of modifications. Finally, the cysteine labelling 2D-DIGE strategy will be applied to the study of EGF induced alteration in thiol reactivity and to study the effects of UV on thiol reactivity in purified human serum samples.

Chapter 2: MATERIALS AND METHODS

All chemicals, solvent and reagents were purchased from Sigma-Aldrich Company Ltd., UK, unless otherwise stated.

2.1 Cy dyes

The NHS-Cyanine dyes (Cy2, Cy3, Cy5) were purchased from GE Healthcare. Subsequently NHS-Cy3/Cy5 and ICy3/ICy5 were synthesised "in-house" by Dr. P. Gaffney (Appendix A). Cyanine dye stock solutions of 1 mM in dimethyl formamide (DMF) could be kept at -20°C for at least 4 months without loss of labelling efficiency. Cyanine dye dilutions for labelling were made fresh in DMF and kept in the dark and on ice prior to use.

2.2 Tissue Culture

2.2.1 Cell Growth

HB4a, C3.6 and other clones derived from the HB4a cell line, were obtained from Dr. M. O'Hare as described (Harris *et al.*, 1999). They were maintained in 1640 RPMI media containing 10% (v/v) foetal calf serum (FCS), supplemented with L-glutamine (2 mM), streptomycin (100 μg/ml), penicillin (100 IU/ml) (all purchased from Gibco-Invitrogen Corp. , UK), insulin (5 μg/ml) and hydrocortisone (5 μg/ml) in tissue culture dishes at 37°C in a 10% CO_2 humidified incubator. Cells were passaged when they reached 70 to 80% confluence by trypsinisation according to standard procedures.

Stocks of luminal epithelial cells were stored in liquid nitrogen and new batches of low passage cells were used after 25 passages in order to avoid potential genetic drift, which can occur during prolonged passaging of cells. For freezing, trypsinised cells were pelleted and resuspended in 10% (v/v) DMSO in 90% (v/v) FCS. Cells were slowly taken to –70°C in a propanol container and then transferred to liquid nitrogen for long-term storage. Rapid thawing was carried out in a 37°C water bath and excess DMSO was removed by centrifugation prior to plating. Cells were allowed to recover for three passages prior to sampling.

2.2.2 Cell treatment with EGF and hydrogen peroxide

For EGF treatment, cells were first serum-starved in 0.1% (v/v) FCS in 1640 RPMI media supplemented with L-glutamine (2 mM), hydrocortisone (5 μg/ml) and antibiotics for 48 hours. They were then treated with 1 nM (6 ng/ml) of EGF (R&D system) for 15 min.

For hydrogen peroxide treatment, cells in 10 cm dishes at ~80% confluence were treated with hydrogen peroxide (H_2O_2) at 0.5 mM final concentration by addition to the growth media. Cells were harvested after the indicated times.

2.3Sample preparation

2.3.1 Labelling of standard proteins

Standard proteins used in this study were: bovine serum albumin (BSA); chicken ovalbumin (Ova); *S. japonicum* glutathione S-transferase (GST); bovine α-crystallin (α - Crys) A and B chains; and horse myoglobin (Myo). All proteins were from Sigma except GST, which a gift from Dr. Ivan Gout (LICR). It was expressed in *E. coli* and purified on glutathione sepharose beads according to standard procedures. Standard proteins were solubilised in denaturing ICy 2D lysis buffer (4% (w/v) CHAPS, 8 M urea, 10 mM Tris-HCl, pH 8.3, 1 mM EDTA) as an equimolar mixture containing 2 pmol of each protein. Labelling with ICy3/5 was carried out at the indicated dye to protein ratios for 1 h on ice in the dark, after which the samples were reduced with dithiothreitol (DTT) at 65 mM prior to gel analysis. In some cases, samples were first reduced with DTT, acetone precipitated and resolubilised in 2D lysis buffer prior to ICy labelling. For NHS-Cy dye labelling, routinely, standard proteins prepared in denaturing NHS-Cy dye 2D lysis buffer (8 M urea, 2 M thiourea, 4% (w/v) CHAPS, 0.5% NP-40 (w/v), 10 mM Tris-HCl pH 8.3) were "minimally" labelled with dye to protein ratios of normally 4 pmol of dye/μg of protein unless otherwise stated. Labelling was performed on ice in the dark for 1 h and reactions were quenched with a 20-fold molar excess of free lysine to dye for 10 min on ice in the dark.

2.3.2 Labelling of total cell lysates

Cells were washed twice in 0.5X PBS (Invitrogen), drained well and lysed in ICy 2D lysis buffer (see above) without reductant. Samples were homogenized by passage through a 25-gauge needle (6 times) and insoluble material removed by centrifugation (13, 000 rpm/10 min/4°C). Protein concentration was determined using the Coomassie Protein Assay Reagent (Pierce). Typically, 2 µl of protein sample is mixed in 200 µl of the assay reagent, followed by measuring the absorbance at 595 nm. The sample concentation is further calculated by comparing the values from standard proteins. For labelling, extracts were labelled with 80 pmol/µg of ICy3/5 on ice in the dark for 1 h and reactions quenched with DTT at a final concentration of 65 mM. For NHS-Cy labelling, 4 pmol/µg of dye were used, and reactions were quenched with a 20-fold molar excess of lysine to dye, prior to addition of DTT. For 2D-DIGE redox experiments, cells were lysed in the presence of ICy dye for rapid labelling and to limit post-lysis thiol modification. Since ICy dye interferes with the protein assay, protein concentrations were determined on replica lysates not containing dye. Test samples (control or H_2O_2 treated) were labelled with ICy5 and mixed with an equal amount of ICy3-labelled standard pool, prepared by mixing equal amounts of protein from all samples. Experiments were also performed where the dye labelling was swapped. Volumes were adjusted to 350 µl with lysis buffer containing DTT (65 mM final) and carrier Ampholines/Pharmalytes (50/50 V/V) (GE HealthCare) (pH 3-10) added to a final concentration of 2%. Labelled samples were mixed prior to protein separation by gel electrophoresis. All gels were cast and run at the same time.

2.4 One- and Two-dimensional Gel Electrophoresis

Cy dye-labelled proteins in Laemmli sample buffer (50 mM Tris pH 6.8, 10% (v/v) glycerol, 2% SDS (w/v), 0.1% (w/v) bromophenol blue) were separated by 1DE according to standard procedures, except that samples in urea-containing buffer were not boiled and low-fluorescence glass plates were used. For 2D SDS-PAGE, 18 cm, non-linear pH 3-10 Immobilised pH gradient (IPG) strips (GE HealthCare) were rehydrated with Cy-labelled samples in the dark at room temperature overnight, in a reswelling tray according to the manufacturer's guidelines. Isoelectric focusing was performed on a

Multiphor II (GE HealthCare) apparatus for a total of 80 kVh at 20 °C. Strips were equilibrated for 10 min in 50 mM Tris-HCl pH 6.8, 6M urea, 30% (v/v) glycerol and 2 % (w/v) SDS containing 65 mM DTT and then for 10 min in the same buffer containing 240 mM iodoacetamide (IAM). Equilibrated IPG strips were then transferred onto 1.5 mm thick 18 X 20 cm 12% polyacrylamide gels cast between low-fluorescence glass plates. In some experiments, gels were bonded to the inner surface of one plate at casting by pre-treatment with bind-silane solution (80% ethanol, 2% acetic acid, 0.08% Plus One Bind-Silane (GE HealthCare)) according to the manufacturer's protocol. Strips were overlaid with 0.5% (w/v) low-melting point agarose in running buffer with bromophenol blue. Gels were run in Protean II tanks (BioRad) at 10 mA per gel at 10°C until the dye front had run off the bottom. All steps were carried out in a dedicated clean room.

2.5 Detection of Dye-labelled Proteins

1DE and 2DE were scanned between low-fluorescence glass plates using either a CCD-based 2920 2DMaster Imager with PixCel software or a Typhoon™ 9400 multicolour fluorescence scanner using ImageQuant software (both (GE HealthCare)). Excitation and emission wavelengths used are shown in Table 2.1. The exposure time (2DMasterImager™) or photomultiplier tube voltage (Typhoon™) was adjusted on each channel (Cy2, Cy3 and Cy5) for preliminary low-resolution scans (1000 μm) to give maximum pixel values within 10% for each Cy image but below the saturation level. These settings were then used for high-resolution (100 μm) scans. Images were exported as tif files for image analysis.

2.6 Image analysis

Images were curated and analysed using Melanie IV (Swiss Institution of Bioinformatics) or DeCyder™ software (GE Healthcare). Differences were also detected by overlaying psedo-coloured images in Adobe Photoshop (Adobe Systems Inc.) which were used for display purposes only. For DeCyder analysis, the DIA module was first used to define spot boundaries and to measure normalised spot volumes of ICy3- and ICy5-labelled features for calculation of difference ratios for samples run on the same gel. Features resulting from non-protein sources (e.g. dust particles and scratches) were filtered out as

much as possible using the exclusive filter based on low-area, volume and shape. The BVA mode of DeCyder was then used to match all pair-wise image comparisons from DIA for comparative cross-gel statistical analysis. User intervention was required at this stage to set landmarks on gels for accurate cross-gel matching and to match as many spots as possible. Comparison of test spot volumes with the corresponding standard spot volumes gave a standardised abundance for each matched spot and values were averaged across triplicates for each experimental condition and data plotted graphically within BVA. Stastical analysis was performed and spots displaying a ≥ 1.5 average-fold increase or decrease in abundance and with p values <0.05 from a student T-test were selected for analysis.

	Excitation (nm)	Emission (nm)
Cy2	480	530
Cy3/ICy3	540	590
Cy5/ICy5	620	680
CCB	620	680

(Table 2-1) Excitation and emission wavelengths used for the detection of each cyanine dye and Colloidal Commassie blue stain.

2.7 Protein-staining

Silver staining and colloidal Coomassie blue G-250 staining (CCB) were used to visualise gel separated Cy dye-labelled proteins. For silver staining of non-bonded gels, a mass spectrometry-compatible method was used (Shevchenko *et al.*, 1996). Briefly, gels were fixed for >3 h in fix solution (40 % methanol, 7.5 % (v/v) acetic acid) and washed twice for 15 min each in ddH_2O. Gels were sensitised in 0.02% (w/v) sodium thiosulphate for 1 min and washed twice in ddH_2O for 1 min each. Gels were then incubated for 30 min in 0.15% (w/v) silver nitrate at 4°C and washed twice in ddH_2O for 1 min each before developing in 2% (w/v) sodium carbonate with 0.02% (v/v)

formaldehyde. Staining was quenched with 5% (v/v) acetic acid and gels were stored in 1% (v/v) acetic acid at 4°C for spot picking and MS.

For CCB staining, a modified version of the protocol by (Neuhoff *et al.*, 1988) was used. Bonded gels were fixed in 35% (v/v) ethanol with 2% (v/v) phosphoric acid for >3 h on a shaking platform and washed three times for 30 min each in ddH_2O. They were then incubated in 34% (v/v) methanol, 17% (w/v) ammonium sulphate and 3% (v/v) phosphoric acid for 1 h prior to the addition of 0.5 g/L Coomassie G-250 (Merck) and left to stain for 2-3 days. No destaining step was required. Post-stained gels were imaged on a BioRad GS-800 calibrated densitometer (silver and CCB) or Typhoon™ 9400 scanner using the red laser and no emission filters (CCB).

2.8 Spot Picking and In-gel Digestion

Post-stained images were matched with Cy dye images using DeCyder or Melanie IV software and a pick list of coordinates created for spots of interest relative to a pair of reference markers fixed to the glass plates at casting. Spots were excised using an Ettan automated spot picker (GE HealthCare) with a 2 mm picking head from gels submerged under 1-2 mm of ddH_2O. Spots were collected in 96-well plates, drained and stored at -20°C prior to MS analysis. In some experiments, spots were picked without post-staining using coordinates from the ICy-labelled image.

For in-gel digestion, gel pieces were washed three times in 50% acetonitrile, dried in a SpeedVac for 10 min, reduced with 10 mM DTT in 5 mM ammonium bicarbonate pH 8. 0 (AmBic) for 45 min at 50°C and then alkylated with 50 mM IAM in 5 mM AmBic for 1 h at room temperature in the dark. Gel pieces were then washed three times in 50% acetonitrile and vacuum-dried before reswelling with 50 ng of modified trypsin (Promega) in 5 mM AmBic. The pieces were then overlaid with 10 µl of 5 mM AmBic and trypsinised for 16 h at 37°C. Supernatant was collected and peptides were further extracted twice with 5% trifluoroacetic acid in 50% acetonitrile and the supernatants pooled. Peptide extracts were vacuum-dried and resuspended in 5 µL ddH_2O and stored at -20°C prior to MS analysis.

2.9 Protein Identification by MALDI-TOF-MS

Matrix-assisted laser desorption/ionization (MALDI) MS with peptide mass mapping was used for protein identification. Typically, 0.5 μl of the tryptic digest was mixed with 1 μl of matrix solution (saturated aqueous 2, 5-dihydroxybenzoic acid) and spotted onto a sample target plate and dried. MALDI mass spectra were acquired using an Ultraflex TOF/TOF mass spectrometer (Bruker Daltonics) in the reflector mode. The mass spectrometer was calibrated using a standard mixture of peptides (calibration mixture 2 from the Sequazyme kit, Applied Biosystems). Internal calibration of each spectrum was carried out using the trypsin autolysis peaks at m/z 842.51 and m/z 2211.10. Prominent peaks in the mass range m/z 500-5000 were used to generate a peptide mass fingerprint which was matched against the updated NCBI database using Protein Prospector version 3.4.1 MS-Fit (University of California, San Francisco, USA) and Mascot (Matrix Sciences Ltd.). A positive identification was accepted when a MOWSE score value of a protein is higher than the threshold MOWSE value ($p<0.05$) with mass error of ±50 ppm allowing 1 missed cleavage and a minimum of 6 peptide masses matched to a particular protein. The protein hit also had to be in agreement with the molecular weight of the detected gel spot and the searched masses of Cy dye labelled motifs and be the human sequence.

2.10 Immunoblotting

Immunoblotting was used to validate expression differences and protein identities where antibodies were available. Briefly, cell extracts were separated by 1DE or 2DE and electro-blotted onto polyvinylidene fluoride membrane (Immobilon P, Millipore) in a transfer tank using transfer buffer (195 mM glycine, 25 mM Tris, 20% (v/v) methanol). Membranes were blocked for 1h with 5% (w/v) low fat milk in Tris buffered saline (50 mM Tris pH 8, 150 mM NaCl) with 0.1% Tween-20 (TBS-T). Membranes were incubated for ≥ 1 h in primary antibody solution in TBS-T. All of antibodies used in this thesis listed in Table 2-2. Membranes were washed in TBS-T (3X 10 min) and then probed with the appropriate horseradish peroxidase-coupled secondary antibody (GE HealthCare). After further washes in TBS-T, immunoprobed proteins were visualised using enhanced chemiluminescence (PerkinElmer Life Sciences Inc). Films were

scanned on a BioRad GS-800 densitometer and matched to ICy dye images using Adobe Photoshop.

Primary antibody	molecular weights (rainbow markers)	company	monoclonal/poly clonal	working conc. for WB
14-3-3 σ (Ab-1)	28	Oncogene	rab pAb	1:2000
Akt	60	CST/NEB	rab pAb	1:2000
Akt anti-phospho(Ser473)	60	Cell Signaling Technology	mo mAb	1:2000
Cyclophilin A	19	Upstate	rab pAb	1:5000
Cytokeratin 10	59	Progen	mo mAb	1:2000
Cytokeratin 6	53	Sunhil Lakhani	mo mAb	1:10000
Cytokeratin 7	51	Progen	mo mAb	1:10000
GST (B-14) sc-138	26	St Cruz	mo mAb	1:2000
HSP-27	27	Stressgen Biotech.	mo mAb	1:3000
HSP-60	60	Stressgen Biotech.	mo mAb	1:10000
HSP-70	70	sigma	mo mAb	1:10000
Ly-Rho GDI	28	St Cruz	goat pAb	1:1000
MEK1/2	45	CST/NEB	rab pAb	1:2000
MEK1/2 (anti-phospho Ser217/221)	45	CST/NEB	rab pAb	1:2000
Mn SOD	20	Upsate	rab pAb	1:2000
p38 MAPK	38	CST/NEB	rab pAb	1:2000
p38 MAPK (anti-phosphoT180/Y182)	38	CST/NEB	rab pAb	1:1000
PDI	57	Stressgen Biotech.	rab pAb	1:5000
Peroxiredoxin 2	29	Ewald Schroder	rab pAb	1:5000
Peroxiredoxin 6	25	Ewald Schroder	rab pAb	1:5000
Peroxiredoxin Kit (I-VI)	17-27	Lab Frontier	rab pAb	all 1:2000
Phospho-tyrosine, clone 4G10	N/A	UBI	mo mAb	1:5000
Prohibitin	30	LAB VISION	mo mAb	1:5000
Ran (Gor)	24	Gorlich Lab	rab pAb	1:20000
SAPK/JNK	54	CST/NEB	rab pAb	1:2000
SAPK/JNK(anti-phosphoT183/Y185)	54	CST/NEB	rab pAb	1:1000
TCP-1 beta	57	Stressgen Biotech.	rat mAb	1:5000

(Table 2-2) List of antibodies used in this thesis for the validation of differential protein expression analysis.

2.11 Quantitative determination of free thiols (Ellman's test)

Measurement of free thiols was determined using the Ellman test (Riddles et al., 1979) with minor modifications. Briefly, DTNB buffer was prepared by dissolving 40 mg of DTNB (5, 5'-dithiobis-2-nitrobenzoate) in 10 ml of 0. 1 M sodium phosphate buffer (pH 8.0) i.e. 10 mM final concentration. 100 µl of each freshly prepared sample were diluted with 2800 µl of 0. 1 M sodium phosphate buffer (pH 8.0) and 100 µl of 10mM DTNB reagent added and left to incubate at RT in the dark for 15 min and then the absorbance

measured at 412 nm using a 1 cm cuvette in spectrophotometer CE-2041 (CECIL Co.). For preparing a reference solution, 100 µl of DTNB buffer was added to 2900 µl of 0.1 M sodium phosphate buffer (pH 8.0) and the absorbance measured. The concentration of sulfhyalryl groups was calculated using the following equation; [SH] = [A412 (sample)-A412 (reference)] / 13650.

2.12 Cell proliferation assay (MTT assay)

HB4a and C3.6 cells growing exponentially were chosen for trypsinisation and counted using a heamocytometer. Cells (200 µl/well) were seeded into 96-well plates at 2.5×10^4 and 1×10^4 cells/ml for HB4a and C3.6, respectively, to control for the faster growth of the C3.6. The cultures were then incubated for 24 h before treated with 0.5 mM H_2O_2 for 20, 60, 240, 480 and 720 min or left untreated. After removal of the medium, 50 µl of MTT working solution (1 mg/ml) (Sigma) was added to the cells in each well, followed by a further incubation at 37 °C for 4 h. The supernatant was carefully removed, 100 µL of DMSO was added to each well and the plates vibrated for 20 min. The absorbance of samples was then measured at a wavelength of 540 nm in multiplate reader (Molecular Devices) and data ploted using Excel (Microsoft Co.).

Chapter 3 OPTIMISATION AND CHARACTERISATION OF CYSTEINE LABELLING 2D-DIGE

3.1 Introduction

Global differential protein expression analysis is a powerful tool for defining protein changes between two or more cellular states and has been used to identify proteins involved in various diseases and cellular functions. Traditionally, 2DE has been used for large-scale protein separation and comparison of protein expression across different biological samples. In conventional 2DE, gel-separated features are visualised mainly using post-electrophoretic staining methods such as silver staining, coomassie blue staining or non-covalent fluorescent staining. However, many protein detection methods have problems such as poor linear dynamic range of detection (silver staining and coomassie blue staining), variable staining from gel to gel (silver stain) or are hazardous to use (metabolic radio isotope labelling). To overcome these problems, Unlu and co-workers described a novel strategy for differential protein expression analysis using covalent modification of protein lysine residues with fluorescent tags (Unlu *et al.*, 1997b). In their original study, this new approach allowed the direct comparison of two samples on the same 2D gel through differential labelling with spectrally distinct fluorescent dyes. This strategy produced directly superimposable images to facilitate comparison of spot intensities and eliminate gel-to-gel variation. Another advantage of this strategy was that these fluorescent tags have a broader linear dynamic range of detection that is superior to non-fluorescent protein detection methods such as silver staining or coomassie blue staining (Patton, 2000). Therefore, the use of these covalent fluorescent dyes should increase the sensitivity of detection, as well as allowing accurate quantification of low-abundance and high-abundance proteins in the same gel. This methodology was later commercialised by GE Healthcare as difference gel electrophoresis (DIGE) which was evaluated in two published studies (Tonge *et al.*, 2001;Gharbi *et al.*, 2002). This lysine labelling strategy uses three fluorescent dyes (NHS-Cy3, -Cy5 and -Cy2) to label experimental samples. A Cy2-labelled pool of all samples is typically used as an internal standard which is run on all gels for comparison with Cy3- and Cy5-labelled test sample pairs to facilitate cross-gel quantitative analysis.

This labelling strategy uses a low dye to protein stoichiometry (4 pmol dye/μg protein) to reduce alterations in electrophoretic mobility and to prevent losses due to sample insolubility. Figure 3-1 shows the heterogeneous labelling of standard proteins using NHS Cy dye lysine labelling at increasing dye to protein ratio. As more protein is labelled, multiple molecular weight isoforms appear, which would complicate 2D spot patterns. Thus, the sensitivity of the minimal labelling method is limited and has been reported to be lower than conventional silver staining (Tonge *et al.*, 2001;Patton *et al.*, 2002). Furthermore, as only approximately 4% of protein is labelled, the other 96% runs with a slightly higher mobility during SDS-PAGE (~500 Da). For low molecular weight proteins, this creates a problem for spot excision for MS analysis; therefore, post-staining and further spot matching between the fluorescent image and the post-stained image are required. To facilitate direct spot picking and to improve sensitivity, it would be preferable to label an alternative, less prevalent amino acid residue at higher stoichiometry. One such amino acid is cysteine, which has the chemistry amenable to chemical modification through reaction with its thiol group. Although fluorescent biotinylated or radiolabelled thiol alkylating reagents have been used in various studies, their potential as DIGE reagents had not yet been realized and so the primary goal of this project was to develop a 2D-DIGE strategy for optimal labelling of free thiol groups. Toward this goal, Dr. Piers Gaffney (Imperial College London) synthesized a pair of iodoacetylated derivates of the fluorescent cyanine dyes, termed ICy3 and ICy5 (Figure 3-2 and see Appendix A). These dyes are spectrally distinct, but charge and size matched allowing specific fluorescence detection of differentially labelled, but co-migrating proteins on the same 2DE. Since the target of the ICy dyes is the thiol group of cysteine residues and because these alkylating reagents should not be able to label oxidized forms of the thiol group, these dyes also have potential use as probes to monitor changes in cysteine thiol oxidation in response to oxidative stress or growth factor induced ROS production. In this chapter, a description of the optimisation and characterisation of ICy cysteine labelling is presented. A workflow is established for further application in the examination of proteomic changes in a model system of ErbB-2 dependent breast cancer.

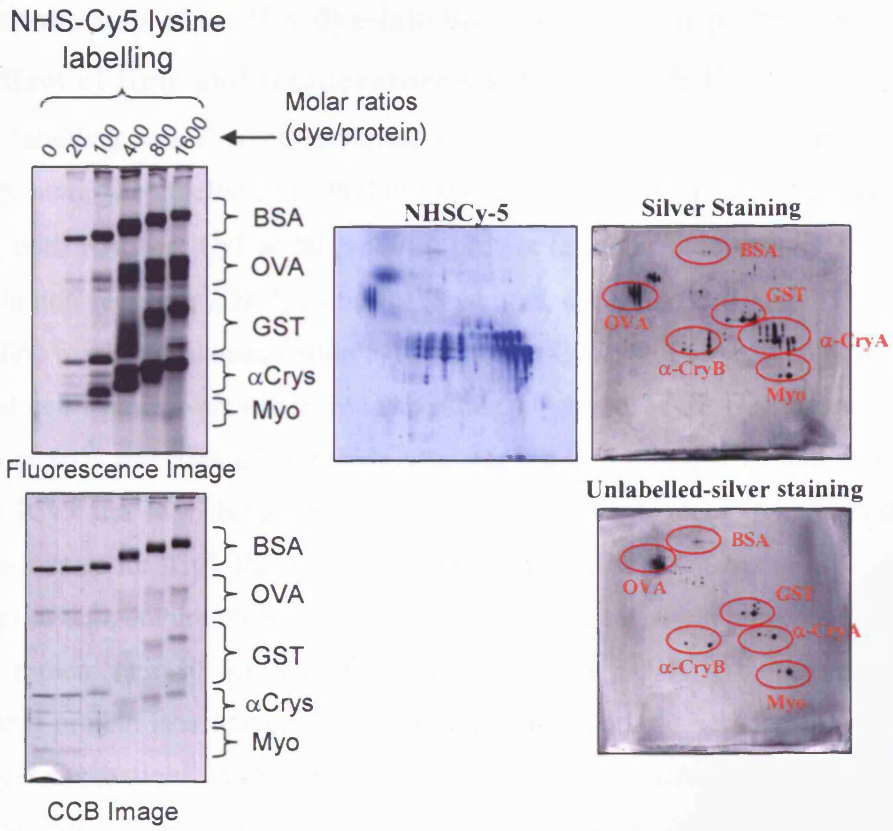

(Figure 3-1) NHS-Cy dye labelling at increasing dye to protein ratios. Labelling of a standard mixture of proteins at increasing molar ratios of NHS-Cy5 dye to standard proteins. An equimolar mixture (2 pmol each for 1DE; 200 pmol each for 2DE (dye to protein ratio 5 : 1)) of BSA, Ova, GST, α-Crys A/B and Myo in 2D lysis buffer was labelled at the indicated molar ratios for 1 h on ice. Reactions were quenched with free lysine and proteins resolved by 12% 1DE (left panels) and 2DE (middle and right panels). Also the corresponding coomassie blue stained 1DE and the silver stained 2DE are shown in the bottom left and right panels, respectively.

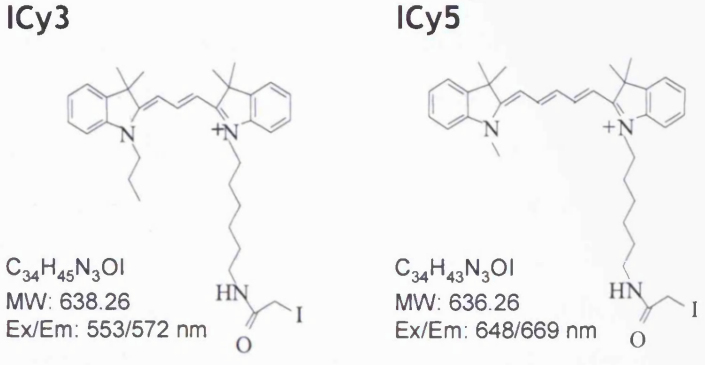

(Figure 3-2) Structure of the matched ICy3 and ICy5 iodoacetylated cyanine dyes. Chemical formulas, molecular weights and excitation/emission wavelengths are shown. (The synthesis of these reagent is outlined in Appendix A).

3.2 Optimisation of an ICy dye-labelling strategy for proteomics

3.2.1 Effect of time and temperature on ICy dye-labelling

ICy dye labelling was first characterised on standard proteins and total lysates from mammary luminal epithelial cells. Preliminary 1D-SDS-PAGE experiments revealed that labelling with ICy3 or ICy5 at 80 pmol/μg protein (a molar ratio of ~5:1 for a 60 kDa protein) in non-reducing 2DE lysis buffer (8 M urea, 4% CHAPS, 10 mM Tris pH 8.3, 1 mM EDTA) reached a plateau within 5-10 min at 0 °C. Two of the ICy3/5 labelled bands from total cell lysates were quantified using ImageQuant 5.2 (GE Healthcare) (Figure 3-3A). About 80% and 95% of saturation was reached in 5 min and 10 min, respectively, and both ICy3 and ICy5 behaved with the same labelling kinetics. Although the signal was more intense for ICy5, these images were not normalised.

The effect of temperature on ICy dye labelling was investigated in total cell lysates using a dye to protein ratio of 5:1 over a timecourse (Figure 3-3B). This experiment again showed that protein labelling occurred within minutes, and did not increase significantly with longer incubations. Although incubation at 30°C did increase the overall labelling slightly, temperature appears not to be a major factor that can improve of labelling. Since lower temperatures are preferable to reduce potential side reactions (eg. carbamylation from the breakdown products of urea in the buffer), a temperature of 0°C was chosen for all future ICy-dye labelling experiments.

3.2.2 Effect of denaturants and reductants on ICy dye-labelling

Denaturants are reagents that alter proteins by unfolding their tertiary structure. In an ICy dye labelling experiment, it is expected that overall labelling will be increased if proteins are first denatured. To test this, labelling was compared using 8 M urea/4% CHAPS as a denaturant versus 1% CHAPS alone (native) (Figure 3-3C). The result indicated that more intense labelling was achieved in buffers containing urea. In addition, a different pattern of bands was observed in the two conditions with fewer bands in the native labelling conditions. This experiment also shows that significant numbers of cellular proteins possess reduced thiols which can be detected under denatured and native conditions. This raises the possibility that the dyes could be used to probe for changes in thiol accessibility due to protein association and dissociation following a test stimulus in

addition to monitoring protein level or thiol oxidation. Thiourea, another denaturant that has been used to improve protein solubility in 2DE experiments, significantly interfered with labelling efficiency (right panel of Figure 3-3C). This is likely to result from reaction of the ICy dye with thiourea, as reported for other alkylating agents (Galvani et al., 2001) and would decrease the amount of reactive ICy dye available for protein labelling.

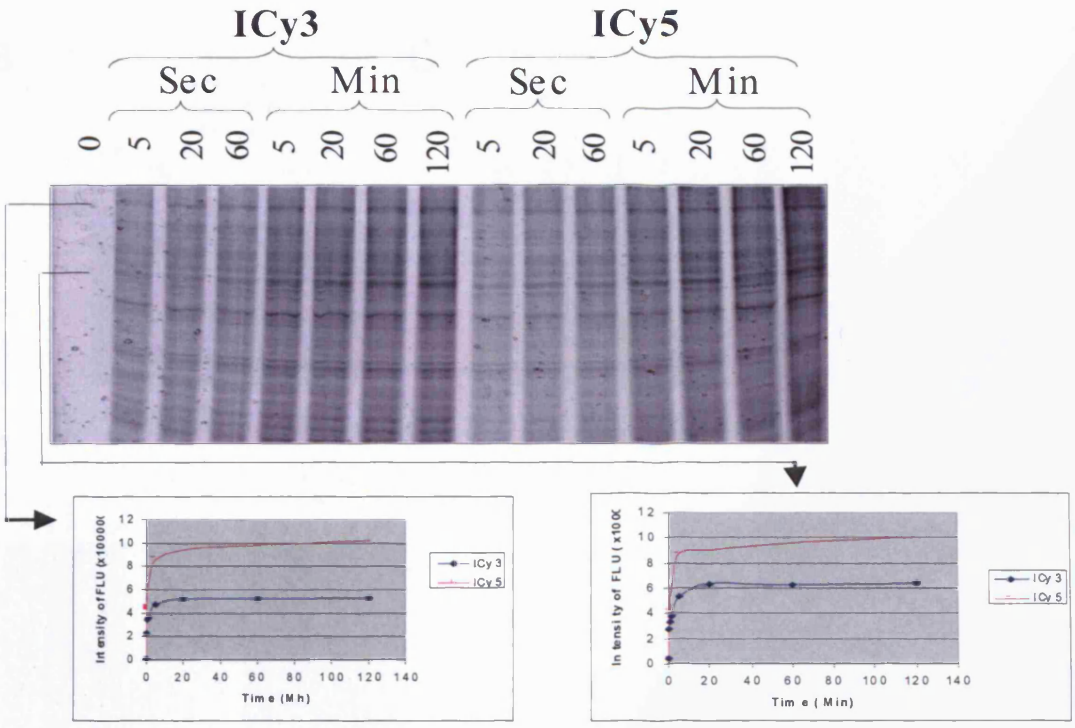

(Figure 3-3A) Optimisation of ICy dye protein labelling. The kinetics of ICy dye labelling. HB4a cells were lysed in 4%CHAPS/10mM Tris(pH 8.3)/ 8M urea and then labelled with 80 pmol of ICy dye per μg of protein on ice for the indicated times. After quenching with 65mM DTT, 10 μg of each ICy dye labelled lysate was loaded and analysed by 1DE and fluorescence imaging.

The effect of commonly used reductants on labelling was also investigated. The addition of reductants in 2DE samples is used to reduce disulphide bonds between peptide chains enabling the analysis of single peptide, but also to prevent the formation of mixed disulphide induced precipitation. However, the reductant will also compete with protein for ICy dye alkylation prior to labelling. Therefore, finding an optimal concentration of reductant is important in determining optimal labelling conditions. In the case of adding

DTT to the labelling buffer, as expected the higher the concentration of DTT the lower the labelling efficiency between protein and ICy dye (Figure 3-3D). This phenomenon was found to be even worse in labelling buffer containing tris-carboxy ethyl phosphine (TCEP) and may be due to TCEP dramatically lowering the pH of the buffer thus inhibiting the labelling reaction. It is important to note that concentrations of reductants that do not significantly inhibit labelling are unlikely to fully reduce proteins in a cell lysate.

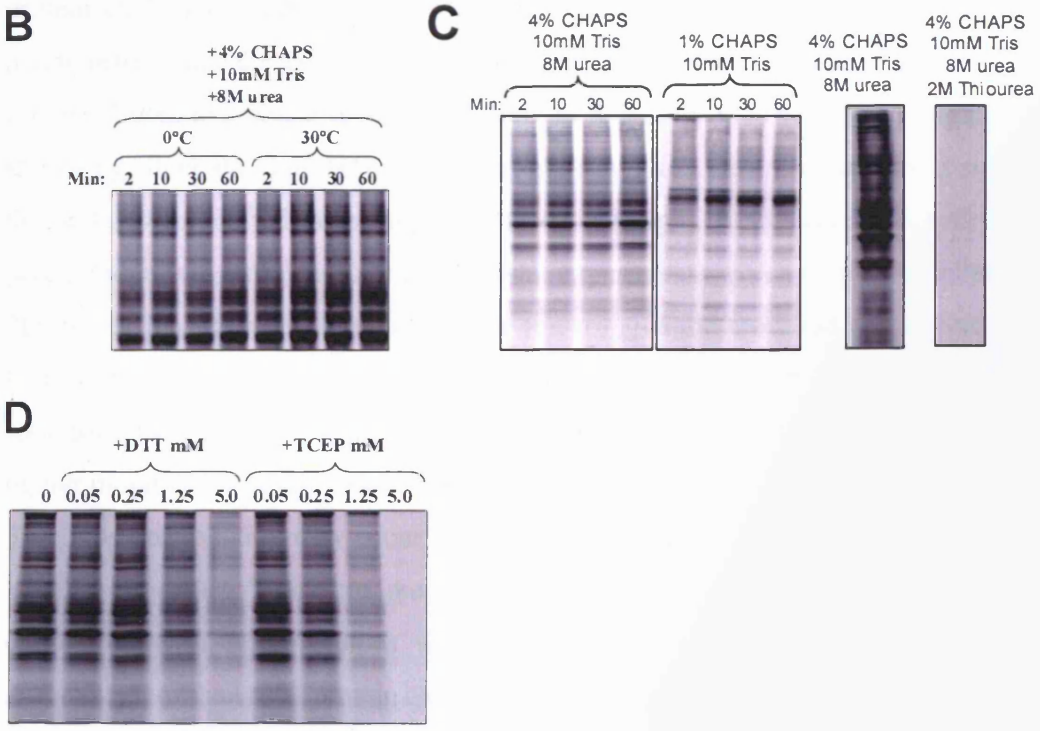

(Figure 3-3B, C and D) Optimisation of ICy dye protein labelling. (B) Effect of temperature on ICy dye labelling. Total cell lysates were prepared in 4%CHAPS/10mM Tris buffer (pH 8.3) containing 8M urea. An estimated dye to protein molar ratio of 5:1 (80 pmol dye/μg protein) was used for labelling at 0°C and 30°C over a time course. Proteins (10 μg) were resolved by 12% 1DE and fluorescent images captured. **(C)** Comparison of denatured versus native labelling. HB4a cell lysates in 2D lysis buffer (left panel) with or without 2M thiourea (right panel) or in 1% CHAPS/10 mM Tris pH 8.3 (middle panel) were labelled with ICy3 at 80 pmol/μg for the indicated times, and quenched by addition of Laemmli sample buffer. Proteins (10 μg) were resolved by 12% 1DE and fluorescent images captured. **(D)** Effect of reductants on ICy dye labelling. Total cell lysates in 4%CHAPS/10mM Tris (pH 8.3)/8M urea buffer were labelled with 80 pmol dye/μg protein for 1 hr at 0°C in the presence of the indicated concentrations of DTT or TCEP. Protein (10 μg) was resolved by SDS-PAGE and labelling monitored by fluorescent imaging.

3.2.3 Effect of pre-reduction on ICy dye-labelling

A previous study showed that saturated labelling of thiols with an alkylating reagent could be achieved by first reducing samples, and then removing the reductant prior to labelling (Smolka et al., 2001). Briefly, DTT was applied to reduce disulphide bonds and then the reduced protein was precipitated with cold ethanol, acetone and acetic acid to remove DTT prior to ICy dye labelling. This modified method was applied to a standard protein, BSA, which has one free thiol and 17 disulphides (Figure 3-3E). Reduced BSA protein could be highly labelled with dye even at low dye to cysteine ratios (1:1) and much better than the control without DTT at higher dye to cysteine ratios. The BSA protein shifted to a higher molecular weight as dye molecules became conjugated to it, as shown by silver staining. However, complete saturation was never achieved since not all the protein was shifted to the highest molecular weight. Also, protein recovery from the precipitation was variable among individual experiments which would be undesirable for 2D expression profiling. In addition, the smearing of the modified protein indicates that there is a heterogeneous mixture of dye-labelled species which would over-complicate spot patterns. Furthermore, precipitation of protein-dye complexes was also apparent at higher molar ratios of dye to cysteine which resulted in a loss of protein (lane 8, Figure 3-3E). This precipitation may occur as a result of the increased hydrophobicity of multiply labelled molecules. Therefore, pre-reduction of samples for ICy-dye labelling was not the chosen route in future studies where the dyes were optimized for redox proteomic analysis rather than total protein expression.

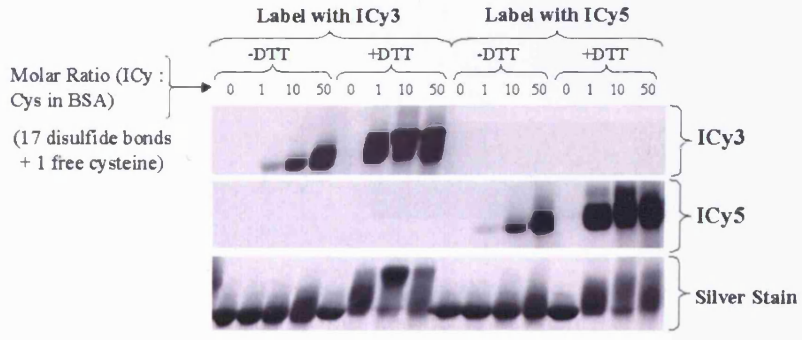

(Figure 3-3E) Optimisation of ICy dye protein labelling. Effect of pre-reduction on ICy3 and ICy5 dye labelling. The BSA standard was reduced with 65mM DTT, precipitated with EtOH/Acetone to remove DTT then resuspended in 4%CHAPS/10mM Tris (pH 8.3)/8M urea buffer and labelled with ICy dye at the indicated molar ratios of ICy3 or ICy5 to the number of cysteines in BSA, of which there are 35.

3.2.4 Optimisation of the dye to protein ratio for ICy dye-labelling

In order to apply the ICy dye technique in labelling, establishing an optimal molar ratio of dye to protein is crucial. To assess this, different molar ratios of ICy dye to BSA were used for the labelling reaction. The results (Figure 3-3F) together with previous data indicate that a molar ratio of dye to protein between 5:1 and 10:1 is optimal for "saturation" labelling of non-reduced BSA with either ICy3 or ICy5. As estimation of the free thiol content of cell lysates made using Ellman's reagent (see Appendix B) showed that there were ~6 mol/mol of free thiol/ protein in total cell lysates, a result made using the average molecular weight of a human protein which was then calculated to be 48 kDa, by averaging the predicted molecular weights of all known human sequences in the SwissProt/ TrEMBL & NCBI databases accessed using the international protein index (IPI) (calculated by Richard Jacob, LICR, UCL)(http://www.ebi.ac.uk/IPI). Thus, the ratio of dye to thiol used is roughly equal to 1. However, higher dye to protein ratios resulted in significant precipitation of labelled proteins. Therefore, a 5:1 ratio (i.e. ~80 pmol dye per μg of protein) was chosen for future labelling experiments.

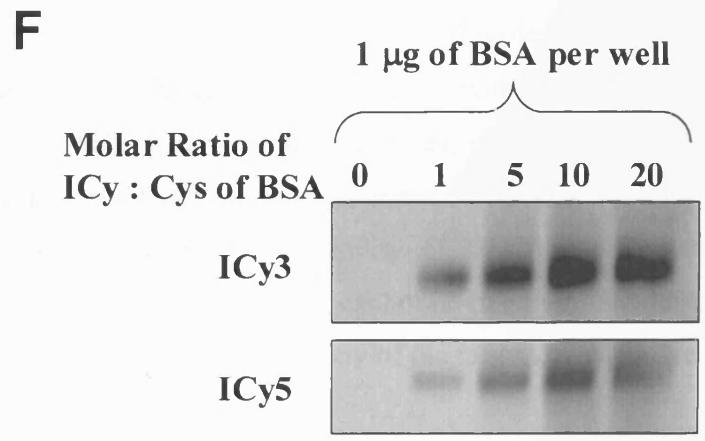

(Figure 3-3F) Optimisation of ICy dye protein labelling. Saturation test of ICy3 and ICy5. Different molar ratios of ICy dyes to the number of cysteines on BSA were applied for the labelling reaction. A mixture of equal amounts of ICy3 and ICy5 labelled BSA (1 μg) of each was resolved by SDS-PAGE and fluorescence images captured.

3.3 Characterisation of ICy dye-labelling

3.3.1 Comparison of cysteine- and lysine-labelling of standard proteins

Following the previous study to determine the optimal molar ratio of dye to protein for ICy dye labelling, additional standard proteins with different number of free cysteines and different molecular weights were selected to examine the efficiency of labelling and to compare this with the lysine labelling method using the NHS-Cy dyes. An equimolar mixture of standard proteins was prepared containing: BSA - 1 free thiol/17 disulphides; Ova - 4 free thiols/1 disulphide; GST - 4 free thiols; α-Crys A chain - 1 free thiol; α-Crys B chain - no thiols; and Myo - no thiols. The protein mixture was labelled at increasing dye to protein ratios in a non-reducing, 2DE ICy lysis buffer. Proteins containing free thiols were labelled with ICy dye, although α-Crys A chain could only be seen at extended scan time (Figure 3-4A). However, the fluorescence intensities varied between proteins. For example, GST with 4 free thiols was detected at higher intensity than Ova, also with 4 free thiols, whilst BSA with one free thiol was labelled to the greatest extent. Since these samples were denatured in 8 M urea, this data suggests that free cysteine thiols have variable reactivity for the dyes or that these samples are already partially oxidised. In support of this, an Ellman's test was performed (see Apendix B), which indicated that BSA contains 0.61 mol/mol free thiol/protein, ovalbumin 1.67 mol/mol and α–Cryst 0.53 mol/mol. Although this does suggest partial oxidation, it cannot account for the differences in labelling between the standards, indicating that free cysteine thiols do indeed have variable reactivity for the dyes even in 8 M urea. Although alkylation should be specific for thiol groups, the possibility of labelling on reactive lysine groups, particularly at higher dye concentrations, cannot be ruled out. In addition, it appeared that saturation labelling was not reached for any of the targets, even at dye to protein ratios of 1600:1 (Figure 3-4B).

Under these non-reduced conditions, lysine labelling was more sensitive than cysteine labelling, but resulted in significant and heterogeneous molecular weight increases to all proteins (at ratios >5:1), presumably as more dye molecules react with the greater number of lysines on each protein (Figure 3-4A and B). 2DE gel analysis of the samples labelled at ratios of 5:1 generated a higher isoform complexity of lysine- versus cysteine-labelled proteins (Figure 3-4C). For example, unlabelled and cysteine-labelled α-Crys A chain

ran as 3 isoforms on 2DEs, whereas at least 12 lysine-labelled isoforms were detected. These results obviously reflect the relative numbers of lysine and cysteine residues in target proteins, but indicate the advantage of stoichiometric cysteine labelling, which for most proteins would generate only a minimal number of labelled isoforms. Despite the charge on ICy dyes, there was no apparent shift in pI when comparing dye-labelled and unlabelled standards. Importantly, there was significant protein precipitation at higher dye to protein ratios using both labelling strategies, evidenced by higher MW precipitation in the gels. For this reason, an optimal dye to protein ratio of 5 to1 was used for further 2D-DIGE optimisation to avoid unwanted protein loss, but to still provide a reasonable level of sensitivity for the detection of free thiol-containing proteins.

Labelling was also examined after pre-reduction of disulphide bonds with DTT, which was removed by acetone precipitation and resuspesion of proteins prior to labelling. For these reduced samples, ICy labelling became more extensive as free thiols were made available for labelling and as expected these alternations did not affect lysine-labelling (Figure 3-4D). The data also indicated that GST and α-Crys A chain may indeed be partially oxidised, since they were detected at higher sensitivity after reduction, despite containing free thiols only. Heterogeneous labelling was apparent and protein recovery from the precipitation was variable, and so only the analysis of free thiol-containing proteins was pursued.

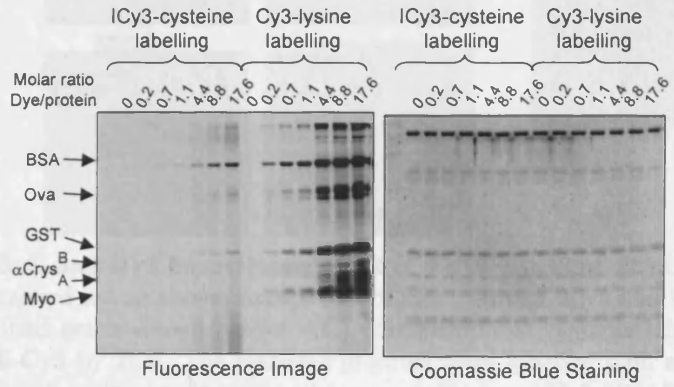

(Figure 3-4A) Characterisation of ICy dye labelling. Labelling of a standard mixture of proteins at increasing molar ratios of ICy3 or NHS-Cy3 to protein. An equimolar mixture (2 pmol each) of BSA, Ova, GST, α-Crys A/B and Myo in 2D lysis buffer was labelled at the indicated molar ratios for 1 h on ice. Reactions were quenched with DTT for ICy dye or free lysine for NHS-Cy dye and proteins resolved by 12% 1DE after addition of Laemmli sample buffer containing β-mercaptoethanol. The resulting fluorescent image is shown in the left panel and the corresponding colloidal coomassie blue stained gel is shown in right panel.

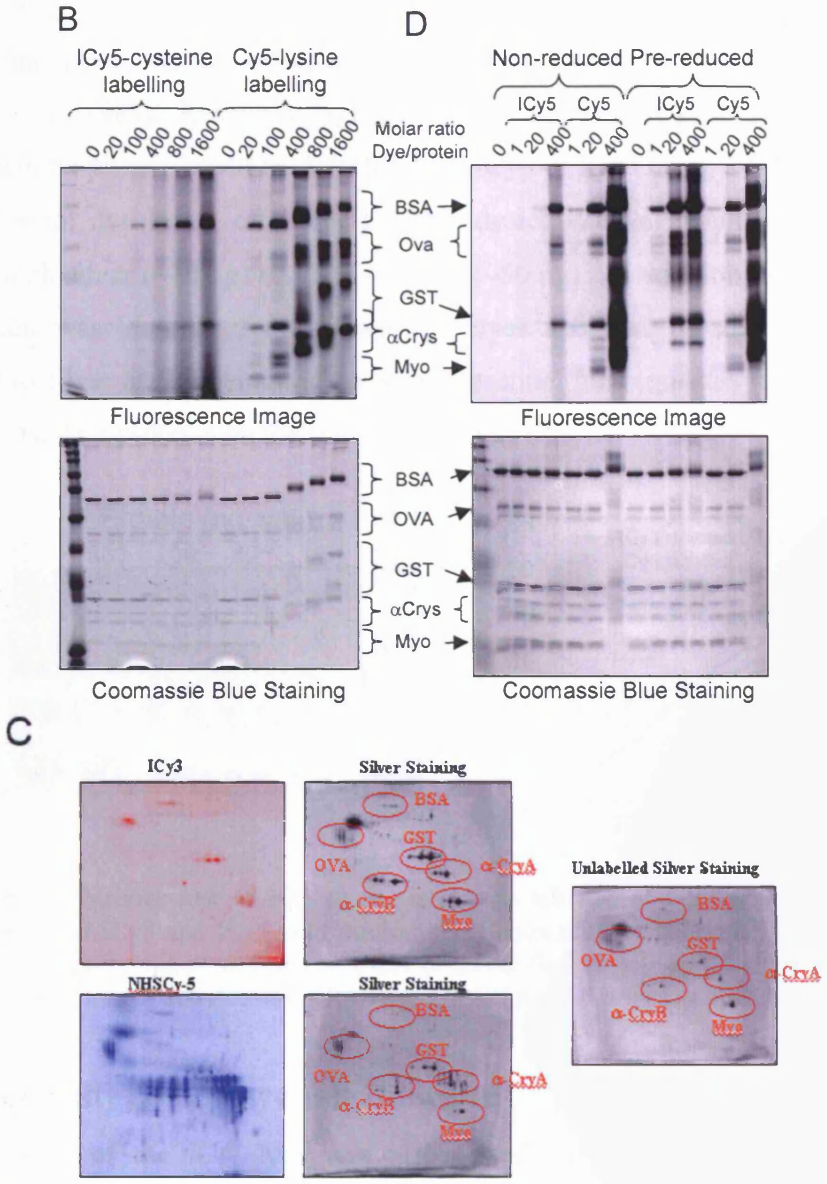

(Figure 3-4 B, C and D) Characterisation of ICy dye labelling. (B) Labelling of the standard mixture was carried out as above, except that higher ratios of ICy5 and NHS-Cy5 were used. A CCB post-stained gel is shown below. **(C)** Comparison of cysteine labelling ICy-3 and lysine labelling NHS-Cy5 by 2DE. The standard proteins were labelled with a 5-fold molar excess of ICy3 or NHS-Cy5 without reductant and were resolved on pH 3-10, 12% 2D gels. Unlabelled sample was also run for comparison, and gels were post-stained with silver to visualise proteins. **(D)** Effect of pre-reduction on ICy and NHS-Cy dye labelling. The standards were labelled with ICy5 or NHS-Cy5 at the indicated dye:protein ratios without reductant, or after reduction with 65 mM DTT. DTT was removed prior to labelling by acetone precipitation of proteins and resuspend in 2D lysis buffer. A CCB post-stained gel is shown below.

3.3.2 Sensitivity of ICy dye-labelling

The sensitivity of ICy labelling of BSA was next compared with MS-compatible silver staining (Shevchenko *et al.*, 1996) and colloidal Coomassie blue G-250 (CCB) staining (Neuhoff *et al.*, 1988). Results in Figure 3-5 show that as little as 2 ng of this single free thiol-containing protein could be detected with ICy3 or ICy5 using a 5:1 molar excess of dye (~80 pmol dye to μg of protein). This detection level result is better than that achieved with silver (~10 ng) or CCB staining (~50 ng). In addition, the dynamic range of detection was identical for the two ICy dyes and was broader and more linear compared to silver or CCB staining; these are essential pre-requisites for quantifying low and high abundant proteins on the same 2D-DIGE gels.

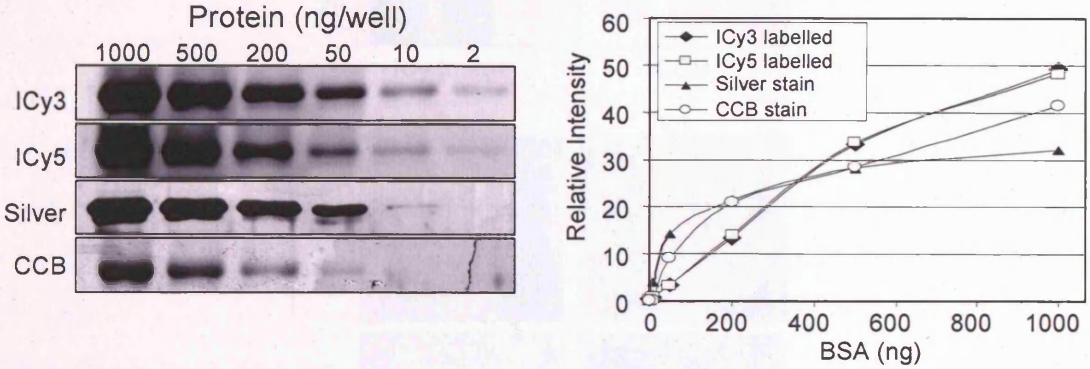

(Figure 3-5) Sensitivity test of ICy dyes. BSA was labelled at a 5:1 molar ratio (~80 pmol dye/μg protein) of ICy3 and ICy5, and the indicated amounts of labelled BSA resolved on a 1D gel. Gels were post-stained with either CCB or silver (left panel) and relative band intensities from fluorescent images and densitometry were plotted against protein amounts (right panel).

3.3.3 Specificity of ICy dye-labelling

The specificity of the ICy dyes was also tested by competition experiments using iodoacetamide (IAM). Non-reduced lysates from a human epithelial cell line were treated with 80 and 400 pmol IAM per μg protein or left untreated, and then labelled with ICy dye at 80 pmols/μg protein. Proteins were resolved by 1DE and 2DE and fluorescence images compared (Figure 3-6). As expected, the results show that IAM is an effective competitor for reagent in ICy-labelling, since no protein labelling could be detected when a 5-fold molar excess of IAM was used. Given the known reactivity of IAM for thiol groups, this shows that the ICy dyes specifically react with reduced protein

thiols. Moreover, this is supported by the previous data showing that DTT effectively inhibits protein labelling when present in the labelling mixture.

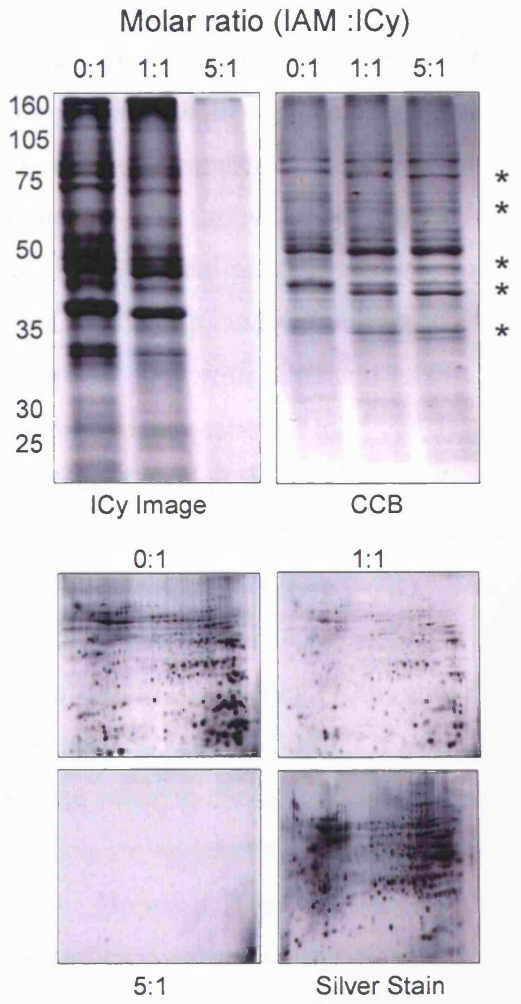

(Figure 3-6) Specificity of labelling assessed by competition with IAM. Total cell lysate (HB4a) was pre-treated with IAM at 0, 80 and 400 pmol/μg, and then labelled with 80 pmol/μg of ICy3 or ICy5. Samples were separated by 1DE (10 μg; upper panel) and 2DE (50 μg; lower panel), and fluorescent images captured at the same PMT voltage. Gels were post-stained with CCB and silver, respectively. The "*" symbols indicate significant shifts in protein mobility after ICy dye labelling.

3.3.4 Co-migration of ICy dye-labelled proteins with NHS dye-labelled, colloidal coomassie blue and silver-stained proteins in 2D gels

Comparison of 2-D ICy images of cell lysates with the composite silver-stained images showed that a significant number of protein features were detected at a higher sensitivity with fluorescence ICy-labelling than with silver staining (Figure 3-7A). Whilst the total number of spots detected was similar, a number of spots labelled with the dye pair did not comigrate. To explore this phenomenon further and to test the labelling properties of the ICy dyes for 2D-DIGE application, a detailed 2DE analysis was carried out comparing ICy dye labelling with NHS-Cy labelling, and with silver, CCB and Sypro Ruby post-staining. Total cell lysates were labelled with ICy3 and NHS-Cy5 and separated on the same 2D gel. In addition, replicated ICy-labelled total cell lysate samples were run on gels and post-stained with silver, CCB or Sypro Ruby. Spots were matched across images using Melanie software. The matched spots were marked with green tags and the unmatched ones were labelled with red tags (figure 3-7B). This analysis revealed that similar numbers of protein features could be detected with ICy dyes (903-1034 spots) as with NHS lysine labelling (956) and CCB-staining (900); with silver staining performing slightly better (1205 ± 78). Interestingly, only ~50% of ICy-labelled features co-migrated with features detected using the other methods. This difference is partly attributed to proteins lacking free thiols which are revealed by the other staining/labelling methods or proteins that silver-stain poorly. However, since the total number of detected spots was similar, it is likely that a significant subset of proteins with reactive thiols are only detectable by ICy labelling (as implied from Figure 3-7A) which indicates an important advantage in sensitivity for detection of free thiol containing proteins by this method. However, there is a further level of complexity in that the ICy dyes are positively charged, such that labelled proteins may shift to more basic pIs. In contrast, if saturation labelling could be reached, all of the labelled protein should shift to their maximum p*I*s without heterogenous charge chains but this is probably not the case. It is noteworthy that SyproRuby post-staining yielded poor images and intense ICy-labelled features appeared as 'inverse spots' on a high background (Figure 3-7C). Thus, ICy dye labelling appears to interfere with SyproRuby staining, despite the fact that these reagents interact with different protein residues (cysteine residues in the case of the ICy dyes, but lysine and

arginine residues in the case of SyproRuby). A possible explanation for this interference may be that the ICy dye fluorescence may quench the SyproRuby signal.

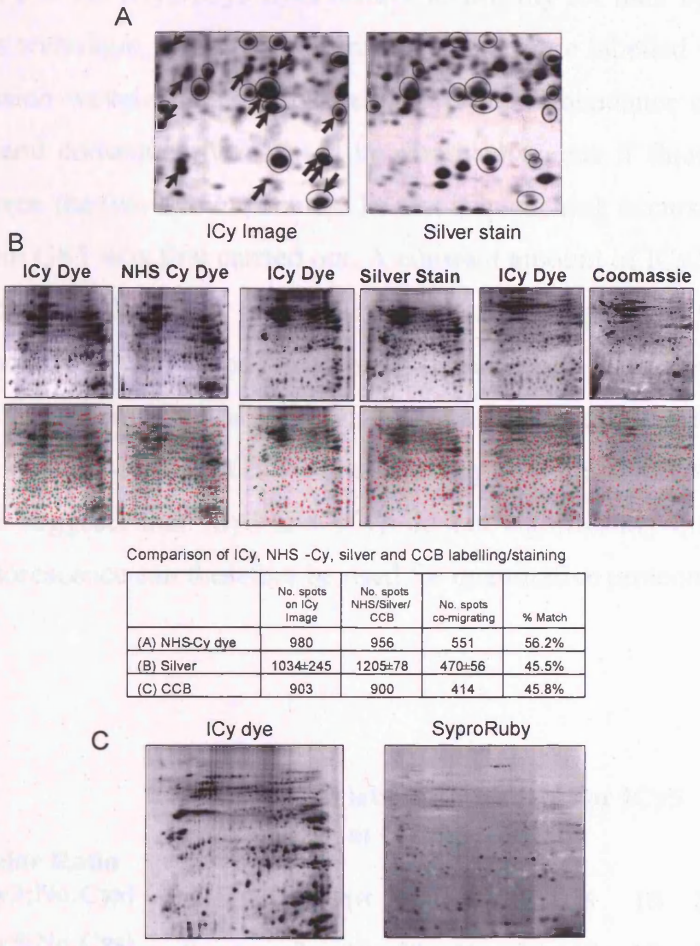

Comparison of ICy, NHS -Cy, silver and CCB labelling/staining

	No. spots on ICy Image	No. spots NHS/Silver/ CCB	No. spots co-migrating	% Match
(A) NHS-Cy dye	980	956	551	56.2%
(B) Silver	1034±245	1205±78	470±56	45.5%
(C) CCB	903	900	414	45.8%

(Figure 3-7) Comparison of co-migrating spot-intensities. (A) HB4a cell lysate (200 μg) was labelled with 16 nmol of ICy3 (80 pmol/μg) and separated by 2DE and the gel post-stained with silver for comparison of spot migration. 'Landmark' features are circled and arrows indicate features detected with higher intensity by ICy labelling. (B) Comparative 2DE analysis of ICy and NHS-Cy labelling, silver and CCB. HB4a cell lysates (200 μg) were labelled with ICy3 and NHS-Cy5 in the ratios of 80 pmol/μg and 4 pmol/μg respectively, and then separated on the same 2D gel. Replicate ICy-labelled samples were also resolved by 2DE and subsequently post-stained with silver or CCB. Images were analysed with Melanie IV software and gel spots matched to the corresponding NHS-Cy-labelled or silver-stained or CCB-stained spots on each gel (marked with green tags). In contrast, the unmatched ones were marked with red tags. Total numbers of spots were taken for each detection method, and the number of co-migrating spots and the % match calculated. The ICy3-silver stained pair was repeated three times and average spot numbers ± the standard deviations are shown. All of the "thumbnail" images in (B) are presented in Appendix H as enlarged images. (C) Images of the ICy dye and SyproRuby post-stained gel are shown.

3.3.5 Examination of differential labelling and dye bias

It is important that the ICy3/ICy5 dyes behave identically for their optimised use in 2D-DIGE. In this technique, two different protein samples are labelled with dyes that have different emission wavelengths, so that relative protein abundance can be compared in the same gel and consequently it would be disadvantageous if fluorescence quenching occurred between the two dye molecules. To test if quenching occurs, dual labelling of a standard protein GST was first carried out. A constant amount of ICy3 labelled GST (dye to protein ratio of 10:1) was mixed with the same amount of GST labelled with increasing amounts of ICy5 and *vice versa* (Figure 3-8). The results show that the fluorescence signal from ICy3 labelled GST was not significantly affected by increasing the proportion of ICy5-labelled GST in the labelling mixture. The reverse was also true. This data thus suggests that ICy3 and ICy5 do not significantly quench one another's signals and fluorescence can therefore be used for quantitative proteomic analysis.

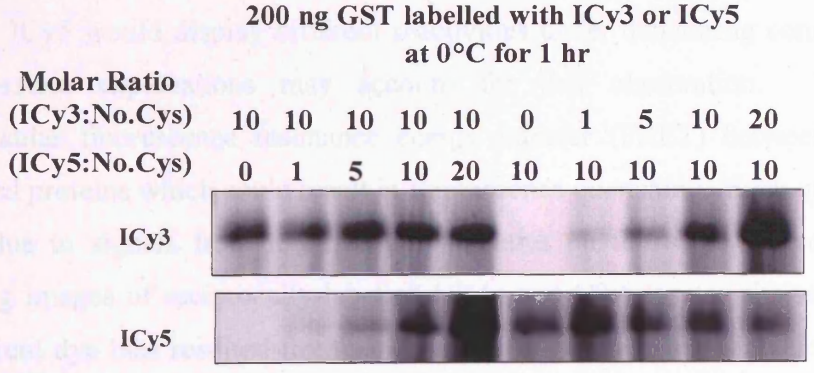

(Figure 3-8) Quench test between ICy3 and ICy5. A constant amount of ICy3 labelled GST (dye to protein ratio of 10:1) was mixed with the same amount of GST labelled with increasing amounts of ICy5. The reciprocal labelling experiment was also performed

3.3.6 Preferential labelling by ICy3 and ICy5

Having established conditions for 2DE labelling, the performance of the ICy dyes for 2D-DIGE experiments was next assessed. Initially, a comparison was made of ICy3-labelled lysates of HB4a, an immortalised human mammary luminal epithelial cell line, with ICy5-labelled lysates from the C3.6 cell line, which in an ErbB-2 overexpressing derivative of HB4a (Figure 3-9A). Many high-intensity ICy-labelled protein features were detected (700-800 spots) indicating that a significant number of cellular proteins and isoforms possess reduced, reactive thiols in these exponentially growing epithelial cells. Some charge trains were also observed at higher MWs. Since the ICy dyes are positively charged, these basic shift charge trains may reflect partial labelling of proteins with multiple reactive thiols. Importantly, clear differences in the expression of some proteins indicating ErbB-2 dependent expression changes were apparent between the cell lines (see Chapter 4). To test and control for differences in labelling by ICy3 and ICy5, lysate from the same cells (HB4a) was labelled with ICy3 and ICy5 and the mixed samples separated by 2DE. Image comparison, using DeCyder software, suggested that a small subset of proteins (8% over a 1.5-fold threshold; 1% over a 2-fold threshold) were preferentially labelled by one dye over the other (Figure 3-9B). Since it is unlikely that ICy3 and ICy5 would display different reactivities under denaturing conditions, several other possible explanations may account for this observation. These include intermolecular fluorescence resonance energy transfer (FRET) between the dyes on colocalised proteins which could result in fluorescence quenching. Such quenching could also be due to signals from multiple dye moieties on the same molecule. However, overlaying images of reciprocally-labelled HB4a and C3.6 lysates showed that most of this apparent dye bias resulted from separation of ICy3- and ICy5-labelled proteins into doublets (specifically in the 25-30 kDa range), with the ICy3-labelled proteins migrating faster than those labelled with ICy5 (Figure 3-9C). Although this apparent dye bias would be problematic for 2D-DIGE analysis, it is important to note that in further 2D-DIGE experiments (Chapters 4, 5 and 6), these "false" differences will be automatically filtered out by labelling test samples with the same ICy dye and running them against a standard pool of all samples labelled with the other dye, as used for the NHS-Cy dyes (Gharbi *et al.*, 2002;Alban *et al.*, 2003).

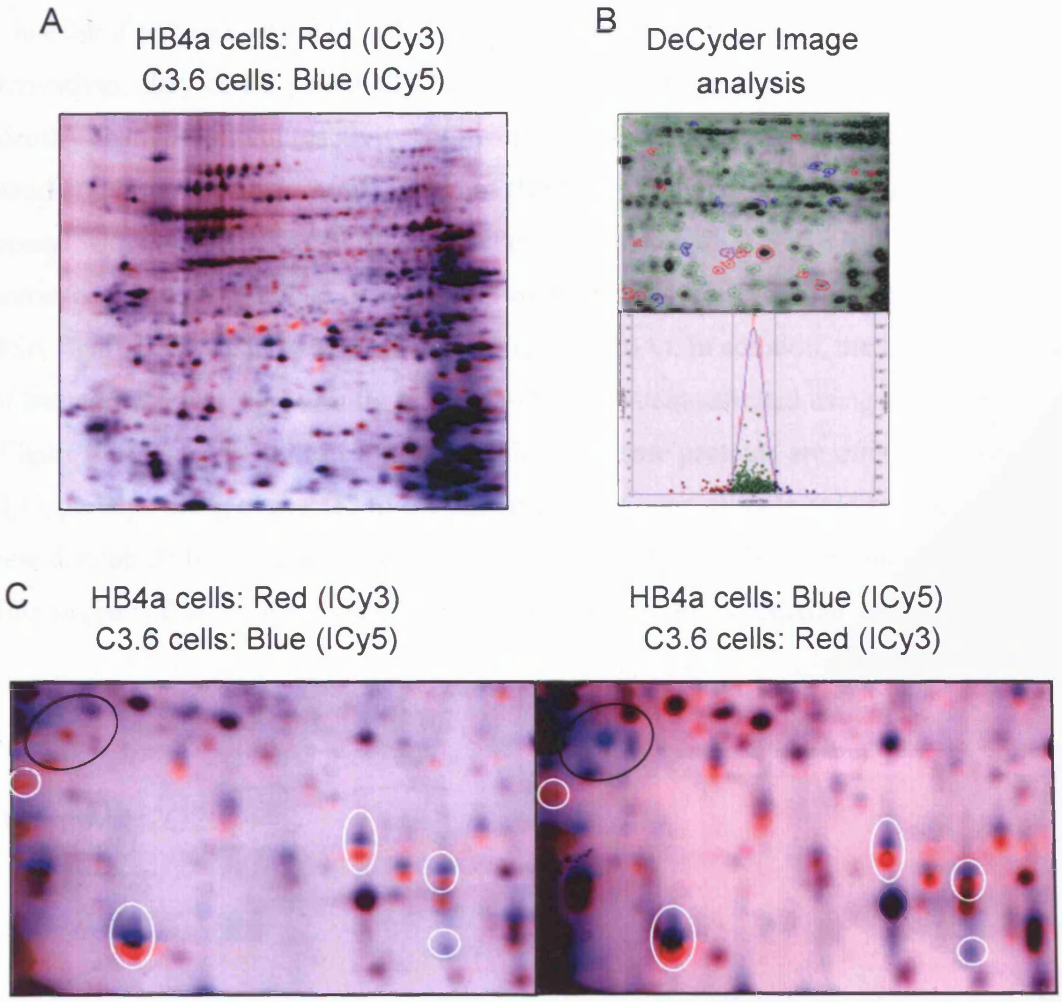

(Figure 3-9) Differential ICy3 and ICy5 labelling. (A) HB4a and C3.6 cell lysates were labelled with ICy3 and ICy5, respectively. The samples were mixed and resolved by 2DE. Images were captured at the appropriate excitation and emission wavelengths and pseudo-coloured (HB4a in red; C3.6 in blue) and overlaid in Adobe Photoshop. **(B)** Analysis of preferential ICy dye labelling. The same lysate was labelled with ICy3 and ICy5 and the sample were mixed and resolved by 2DE and analysed using DeCyder DIA software with a 1.5 fold cut-off applied for changes in abundance. A section of the image and spot statistics are shown. Green denotes no significant difference between co-migrating spots, whilst blue and red denote increased and decreased intensity, respectively, above the threshold. **(C)** Dye bias and spot splitting revealed by reciprocal labelling. HB4a and C3.6 lysates were reciprocally labelled with ICy3 and ICy5, mixed appropriately and resolved by 2DE. Images were captured, pseudo-coloured and overlaid in Adobe Photoshop for comparison. Black-circled spots represent real differences between HB4a and C3.6 cells whilst white-circled spots indicate dye bias and spot splitting in the 25-30 kDa range of the gels.

3.3.7 Initial investigation of the effects of oxidation on ICy dye labelling

Since the ICy dyes specifically label reduced cysteinyl thiol groups and not their oxidised derivatives, they could potentially be used in redox proteomic studies, for example to identify changes in thiol reactivity following oxidative stress. To test this application, the standard proteins, human serum albumin (HSA) and bovine serum albumin (BSA) were treated with 0.5 mM H_2O_2 for 20 min and then labelled with ICy dye and compared to the untreated labelled proteins. The results demonstrated that H_2O_2 treatment of HSA or BSA significantly reduces ICy labelling (Figure 3-10A). In addition, the free thiol content of treated BSA was significantly reduced (~50%) as demonstrated using the Ellman's test (Figure 3-10B). This indicates that free thiols on these proteins are directly modified by H_2O_2 perhaps being converted to the sulfenic, sulfinic or sulfonic acid forms, or forming new disulphide bonds that prevent efficient reaction of ICy dye with the target proteins. This suggests that the ICy dyes can be used to monitor thiol-oxidation status.

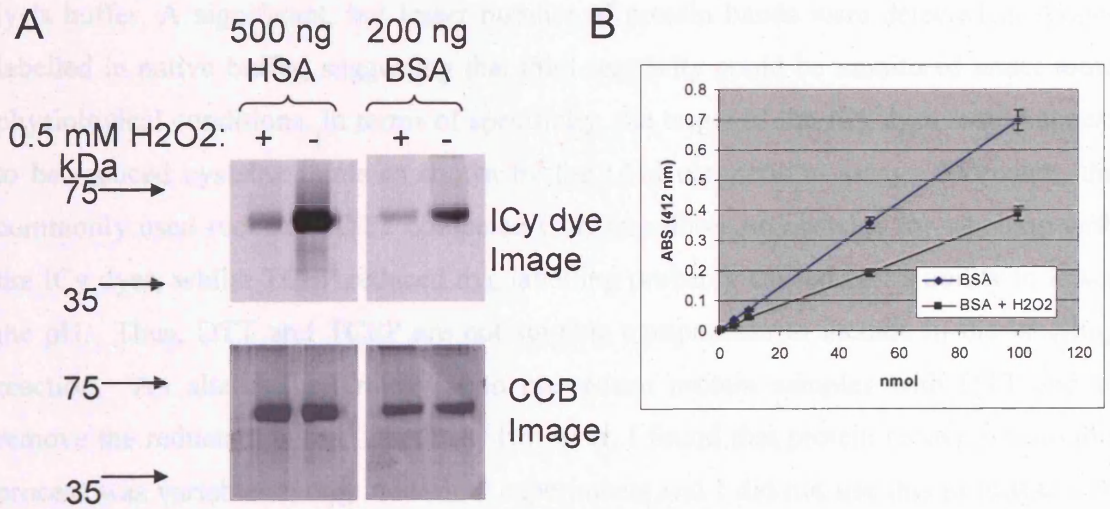

(Figure 3-10) Effect of H_2O_2 on thiol reactivity of standard proteins. (A) The indicated amount of standard proteins (HSA and BSA) in urea lysis buffer were treated with 0.5mM H_2O_2 for 20 min or left untreated. Samples were labelled with ICy dye, resolved by 1DE, detected by fluorescence scanning and post-stained with CCB. **(B)** Ellman's test of thiol content. The indicated amounts of BSA or 0.5mM H_2O_2-treated BSA in 2.9 ml of 0.1 M sodium phosphate buffer (pH 8.0) were prepared and 100 µl of 0.01 M DTNB (Ellman's reagent) in sodium phosphate buffer added. The mixture were left to stand in the dark for 15 min and then the absorbance measured at 412 nm

3.4 Conclusions

The goal of this project was to develop an alternative fluorescent labelling strategy to improve on the existing 2D-DIGE expression profiling technology. Thus instead of labelling lysine residues at low stoichiometry, the target was to label cysteine thiols at higher stoichiometry to improve sensitivity without adversely affecting protein solubility or migration behaviour in 2DEs. In addition, it was assessed whether these dyes could be used to probe for inducible changes in the reactivity of protein thiols, allowing one to monitor redox modification events such as disulphide bond formation/breakage, glutathionylation, S-nitrosylation or oxidation to the sulphenic (RSOH), sulphinic (RSO_2H) and sulphonic (RSO_3H) acids and to investigate changes in thiol accessibility in native samples caused by protein association or dissociation.

In this chapter, I present a description of the optimisation and characterisation of cysteine labelling using the ICy dyes. It was shown that ICy3/5 labelling of protein lysate was rapid and that saturation was reached within 5-10 min in non-reducing, denaturing 2DE lysis buffer. A significant, but lesser number of protein bands were detected in lysates labelled in native buffer, suggesting that thiol reactivity could be monitored under more physiological conditions. In terms of specificity, the target of the ICy dyes would appear to be reduced cysteine thiols as shown by the IAM competition assay. Moreover, the commonly used reductant DTT competed with free thiols on proteins for labelling with the ICy dyes, whilst TCEP reduced dye labelling probably caused by its ability to lower the pH. Thus, DTT and TCEP are not suitable components to include in the labelling reaction. An alternative strategy is to pre-reduce protein samples with DTT and to remove the reductant before labelling. However, I found that protein recovery from this process was variable among individual experiments and I did not use this in further 2D-DIGE experiments. I found that ICy dye labelling could detect as low as 2 ng or less of BSA protein using a 5:1 molar excess of dye to protein which was better than the silver (~10 ng) or CCB (~20 ng) detection methods. In addition, the dynamic range of detection of the ICy dyes was broader and more linear compared to silver and CCB staining and was identical for the two ICy dyes; these were essential pre-requisites for quantifying low and high abundant proteins on the same 2DE. As for dye to protein ratio in labelling, 80 pmol of dye per μg of total cell lysate which was chosen for 2D-DIGE

experiments gave a reasonably high sensitivity of labelling without compromising sample solubility or resulting in heterogeneous labelling and formation of over-complex spot patterns.

Comparison of 2DE ICy images of cell lysates with the composite silver-stained images also revealed that a significant number of protein features could be detected with higher sensitivity using ICy-labelling. Co-migration of ICy labelled spots with silver-stained or CCB-stained spots were 45.5% and 45.8%, respectively. Although some proteins may not stain well with silver or CCB and some proteins do not contain free thiols, the data suggest detect thiol-containing proteins at higher sensitivity than with silver and CCB stains. In addition, I showed that many cellular proteins in epithelial cells possess reduced thiols under exponential growth conditions. My study of the reproducibility of labelling with ICy3 versus ICy5 showed that a small percentage of protein features displayed apparent dye bias when the same sample was labelled with ICy3 and ICy5. This was mostly due to splitting of some spots in the 25-30 kDa region, with the ICy3-labelled pool migrating faster in the pair (Figure 3-9C). This effect could be caused by slightly different affinities of SDS for the Cy3 and Cy5 labelled moieties on the protein, thereby affecting their migration in gels. Although a potential problem, this apparent dye bias was overcome when test samples were labelled with one dye and compared to a reference sample labelled with the other dye as in the procedure used for the NHS Cy dyes (Gharbi *et al.*, 2002;Alban *et al.*, 2003).

In summary, the results in this chapter demonstrate the conditions and the properties of using ICy dyes for protein labelling and expression profiling in 2D-DIGE. The application of the cysteine labelling 2D-DIGE technique for analysis of redox regulation and growth factor stimulation of HB4a and C3.6 cells and UV irradiation-induced thiol changes in plasma samples are discussed in the following Chapters.

Chapter 4 CYSTEINE LABELLING 2D-DIGE TO PROBE FOR CELLULAR TARGETS OF OXIDATION

4.1 Introduction

The iodoacetylated Cy dyes whose utility for 2D-DIGE was described in the previous chapters react with the reduced thiol groups on proteins which can be the targets for oxidation by ROS. These modifications have been shown to be biologically important (see introduction) and their study is relevant to current proteomics in biomedical research. Since the ICy dyes do not react with the oxidised forms of the thiol groups, these reagents should be useful as probes for experiments designed to accurately monitor changes in cysteine oxidation and for the identification of cellular targets of oxidation in response to oxidative stress or growth factor-induced ROS production. This use of the ICy dye 2D-DIGE strategy to study this area of biology is a major aim of this thesis.

In the previous Chapter, the characterisation and optimisation of cysteine labelling using ICy3/5 dyes was reported (Chapter 3). However, its real usefulness as a proteomic technique needed to be tested in a biological context. Thus, ICy dye 2D-DIGE cysteine labelling was used to probe protein targets of oxidative stress following H_2O_2 treatment of human mammary luminal epithelial cells. This study was also designed to investigate the effects of overexpression of the oncogenic receptor tyrosine kinase ErbB-2 on the stress response, and also to allow the simultaneous assessment of basal proteomic changes which are caused by ErbB-2 overexpression. This analysis was carried out by 2D-DIGE comparison of a parental breast luminal epithelial cell line HB4a and an ErbB-2 overexpressing derivative, C3.6 (detailed in Chapter 1) in the absence and prescence of exogenous H_2O_2. It was expected that changes in labelling would be caused either by differential protein expression or from the conversion of reactive thiol groups to higher oxidative states that cannot react with the ICy dyes. The identities of differentially labelled proteins were then determined by MALDI-TOF-MS and peptide mass fingerprinting of excised and trypsinised gel pieces. Furthermore, the biochemical changes of some of the identified proteins were validated by 1D and 2D immunoblotting.

4.2 The effect of H_2O_2 treatment on HB4a and C3.6 cells

As H_2O_2 is a major form of ROS in cells (Rhee et al., 2003), it was chosen here as a model ROS to treat HB4a and C3.6 cells and to investigate changes in protein expression, thiol oxidation and intracellular signalling. First of all, treatment conditions were determined that would induce an oxidative stress response in HB4a and C3.6 cells following hydrogen peroxide treatment. According to some signalling studies which have used H_2O_2 treatment of human or epithelial cells, a concentration range between 0.1 mM and 1 mM H_2O_2 was used to elicit a cellular response (Nishida et al., 2000;Kim et al., 2002;Fratelli et al., 2002;Barnouin et al., 2002;Zhang et al., 2003;Garg and Chang, 2003;Kim et al., 2003a;Kim et al., 2003b;Pelaia et al., 2004;Young et al., 2004). Initially, HB4a or C3.6 cells were treated with high concentrations of hydrogen peroxide (10 mM) which lead to rapid cell death with most the cells detaching from the substratum after 20 minutes. In contrast, low concentrations of hydrogen peroxide (10 μM) did not stimulate a significant cellular response (such as Akt, p38, JNK stimulations) for the phosphorylated and activated forms of these signalling kinases (data not shown). A concentration of 0.5 mM H_2O_2 was therefore chosen and was found to stimulate cellular signalling without causing immediate cell death.

Immunoblotting was used to monitor protein tyrosine phosphorylation, since this protein modification has been reported to be affected by ROS due to inhibition of phosphotyrosine phoshatases. In agreement with previous work in other cell systems, H_2O_2 produced a robust, but transient increase in total tyrosine phosphorylation (Figure 4-1). Interestingly, more proteins were tyrosine phosphorylated to a greater degree in the HB4a cells than in C3.6 cells, suggesting that ErbB-2 can affect this response. The stress-activated protein kinase, p38, was found to be more rapidly activated after hydrogen peroxide treatment of HB4a cells than of C3.6 cells, whilst H_2O_2-induced JNK activation was only apparent in the C3.6 cells at longer times. In addition, both the ERK and PI3K pathways were activated, with ERK1/2 activation being more intense in the HB4a cells and Akt activation similar in both cell types (Figure 4-1). Interestingly, MnSOD, which generates cellular hydrogen peroxide from superperoxide, exhibited lower expression in the C3.6 cells. Together these observations indicate that ErbB-2

overexpression affects proliferative and survival signalling in response to oxidative stress, although the details of this mechanism are unclear.

The effects of H_2O_2 on cell proliferation were next examined using an MTT assay (Figure 4-2). This assay is a quantitative colorimetric method for determining cell number and viability. It utilises the yellow tetrazolium salt MTT as a substrate, which is metabolised by the mitochondrial respiratory chain enzyme, succinate dehydrogenase, to yield a purple formazan reaction product in actively proliferating cells. Comparison of the value to control cells provides a relative increase in cellular proliferative activity. Conversely, in cells that were undergoing apoptosis or necrosis, MTT conversion was decreased, reflecting the loss of cell proliferation. Using this assay, the proliferation of both the HB4a and C3.6 cells was decreased following hydrogen peroxide treatment. The results (Figure 4-2) show that approximately 80%, 50% and 30% of proliferative activity was maintained after treatment with 0.5 mM of H_2O_2 for 20, 60 and 240 min, respectively. Interestingly, the C3.6 cells retained their proliferative capacity better than HB4a at longer timepoints suggesting that ErbB-2 dependent signalling plays a role in providing cellular resistance to redox stress. This may be linked to the previously observed delayed activation of p38 or JNK in C3.6 cells (Figure 4-1).

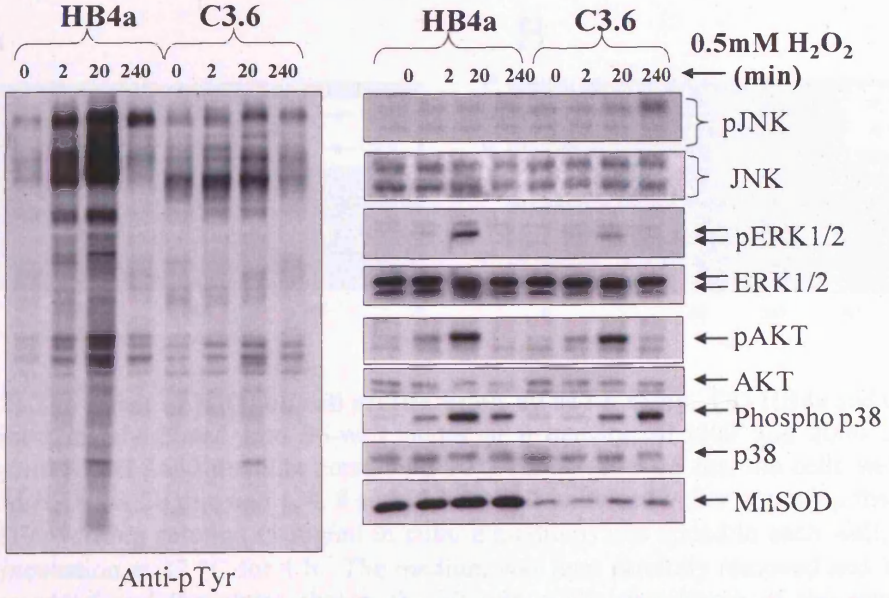

(Figure 4-1) Effect of hydrogen peroxide treatment on signalling events in HB4a and C3.6 cells. Total cell lysates were prepared from HB4a and C3.6 cells treated with 0.5 mM hydrogen peroxide for the indicated times. Total proteins (30 μg) were separated by SDS-PAGE, electrophoretically transferred to Immobilon P membrane (Millipore) and probed with specific antibodies to the indicated proteins and phosphorylation motifs.

On a gross scale, the free thiol content of the HB4a and C3.6 cells prior to H_2O_2 treatment was similar with approximately 6 moles of free thiols per mole of protein as measured using Ellman's reagent (Appendix B). Hydrogen peroxide has found to induce a significant drop in the cellular free thiol content of both cell types; the free thiol content dropping by 45% and 23% in HB4a cells and C3.6 cells, respectively, within 2 min of treatment (Figure 4-3). Following this drop, the free thiol content recovered to approximately 80% in both cell lines after 20 min. This result likely indicates a loss of reduced glutathione (GSH) in the cells which acts as a "buffer" to neutralise the influx of H_2O_2, but also presents the oxidation of free thiols on proteins. The recovery may be due to the regeneration of GSH by glutaredoxin or reduction of oxidised protein thiols by peroxiredoxins. Importantly, these results show that ErbB-2 affects the cellular response to H_2O_2, seemingly providing more resistance through the provision of greater anti-oxidant activity. This may explain the overall higher survival rate of C3.6 cells (Figure 4-2) and the delayed activation of the ERK and p38 MAPK pathways (Figure 4-1). To explore these differences further, and to identify cellular targets of oxidative stress, ICy dye 2D-DIGE was used to study H_2O_2 treated HB4a and C3.6 cells.

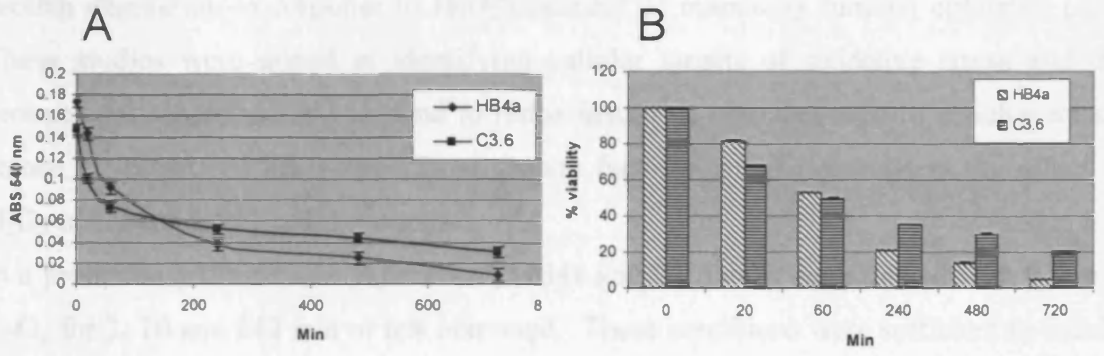

(Figure 4-2) The effect of H_2O_2 on cell proliferation by MTT assay. (A) HB4a and C3.6 cells were inquintriplicately plated into 96-well plates at a density of 5000 and 2000 cells/well, respectively, in RPMI 1640 medium containing 10% FBS. After 36 hrs, the cells were treated with 0.5 mM H_2O_2 for 20 min and 1, 4, 8 and 12 hr or left untreated. After removing the medium, 50 µl of MTT working solution (1 mg/ml in culture medium) was added to each well, followed by further incubation at 37 °C for 4 h. The medium was then carefully removed and 100 µL of DMSO was added and the plates shaken for 20 min. The absorbance of the samples was measured at a wavelength of 540 nm in a multiplate reader and values plotted against time. **(B)** Plot of % viability versus time. % viability was calculated as the ratio of the absorbance at each timepoint versus the untreated sample.

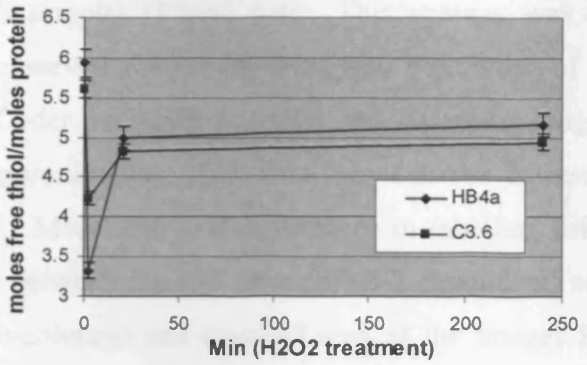

(Figure 4-3) Quantitative determination of free thiols (Ellman test). Lysates from untreated and H_2O_2 treated HB4a and C3.6 cells for the indicated times were freshly prepared and 200 μg of total protein assayed for thiol content as described above.

4.3 Differential protein expression and thiol-reactivity analysis using ICy 2D-DIGE

The cysteine labelling strategy outlined in Chapter 3 was applied in a detailed 2D-DIGE and MALDI-TOF-MS analysis to accurately identify changes in thiol reactivity and protein expression in response to H_2O_2 treatment of mammary luminal epithelial cells. These studies were aimed at identifying cellular targets of oxidative stress and the protective mechanisms that respond to redox insult. It was also used to simultaneously screen for targets of ErbB-2-mediated growth factor signalling and assess the effect of H_2O_2 treatment on the redox response.

In a preliminary timecourse experiment, HB4a and C3.6 cells were treated with 0.5 mM H_2O_2 for 2, 20 and 240 min or left untreated. These conditions were sufficient to induce an increase in total cellular tyrosine phosphorylation (likely through inhibition of protein tyrosine phosphatases), and trigger activation of the p38 stress-activated protein kinase, ERK1/2 and Akt signalling pathways (Figure 4-1). Duplicate cultures of treated cells were lysed under non-reducing, denaturing conditions in the presence of ICy3 and ICy5 (80 pmol/μg protein) to rapidly label proteins and limit post-lysis redox modifications. Samples were then reduced with DTT prior to 2DE separation. Individual ICy5-labelled samples were run with an equal load of an ICy3-labelled standard pool consisting of an

equal mixture of all samples (Figure 4-4). This strategy was used to control for the apparent dye bias observed for the labelling and separation of some proteins. Image analysis using DeCyder software revealed the dynamic range of detection of the experiments was approximately 1000 fold between the lowest and highest-abundant proteins in the gels. More than 100 differences in labelling using a ≥1.5-fold cut off, were observed both between the cell lines (ErbB-2 dependent) and in response to H_2O_2 treatment. A pseudo-coloured and overlaid area of the images for the C3.6 samples is shown for each timepoint in Figure 4-5. Of particular note, H_2O_2 treatment for only 2 min reduced the labelling of a number of proteins, suggestive of rapid thiol modifications that block ICy-dye-labelling (eg. Spots 24 and 27 in Figure 4-5), rather than changes in protein expression *per se*. Such modifications could include disulphide bond formation, modification by glutathionylation or oxidation to the sulphenic (R-SOH) acid. Since the latter modification is generally unstable, a disulphide may be formed with a nearby thiol or the RSOH may be further oxidized to the sulphinic ($R\text{-}SO_2H$) or sulphonic ($R\text{-}SO_3H$) acid forms of the thiol. In some cases, the change in ICy dye labelling recovered over time, indicating reversible modification, perhaps through the activation of redox defence mechanisms. A number of proteins also showed rapid increases in labelling (eg. Spots 25 and 26 in Figure 4-5), suggesting generation of new thiol groups, for example through scission of disulphide bonds, or through labelling of isoforms generated after redox-dependent shifts in p*I*, as reported for the peroxiredoxins (Wagner et al., 2002;Rabilloud et al., 2002a). Some of these observations may explain the dramatic changes in free thiol content that occur within 2 min of hydrogen peroxide treatment (Figure 4-3) and the activation of cellular signal pathway (Figure 4-1).

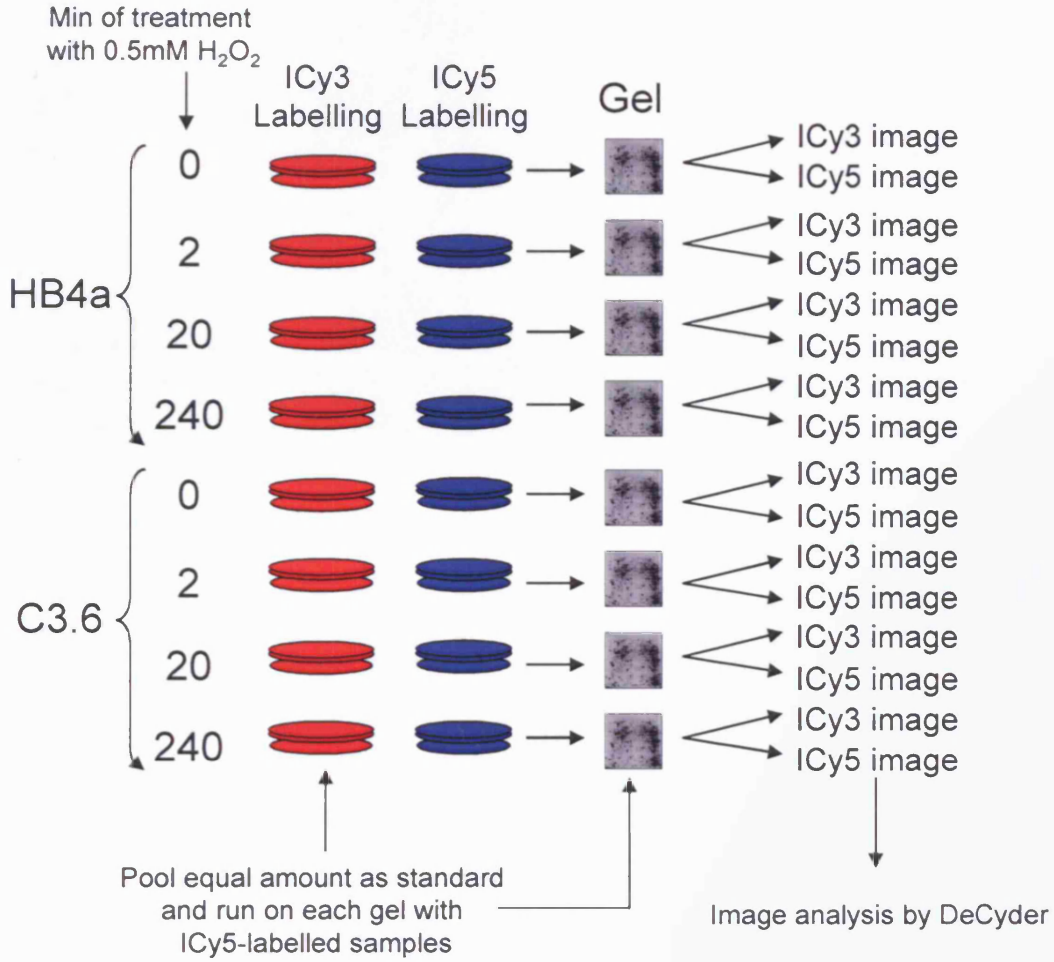

(Figure 4-4) Strategy for ICy3/5 cysteine-labelling 2D-DIGE to monitor oxidant-dependent and ErbB-2 dependent thiol reactivity changes. Duplicate samples of untreated and H_2O_2 treated cells were lysed in the presence of ICy3 and ICy5. A standard pool was made from the ICy3-labelled samples by mixing equal amounts of all eight samples. 150 μg of this was run against 150 μg of each ICy5-labelled sample on each gel, generating 16 images for DeCyder image analysis.

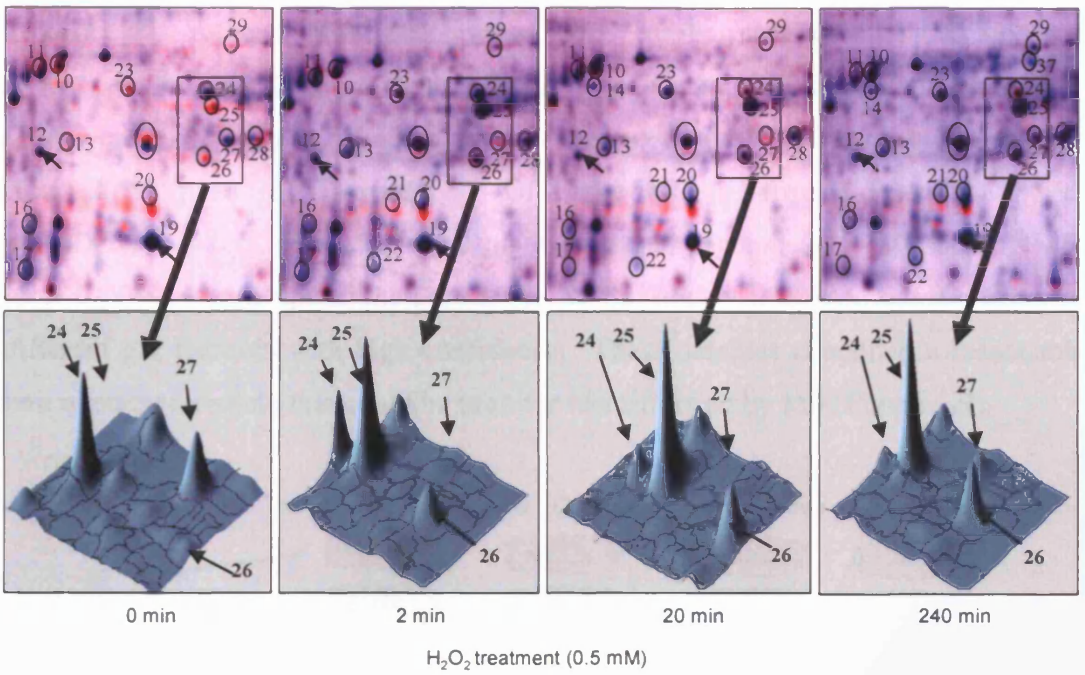

(Figure 4-5) Use of ICy3/5 cysteine-labelling 2D-DIGE to monitor thiol reactivity in response to H_2O_2 treatment of mammary luminal epithelial cells. The top images indicate merged 2D fluorescence images of standard pool (red/ICy3/mixture of all samples) vs. H_2O_2-treated samples (blue/ICy5) showing differential labelling with time. The lower images show enlarged 3D fluorescence profiles of the boxed areas showing some of the changes in detail.

4.4 Application of cysteine-labelling 2D-DIGE to study peroxide-dependent and ErbB-2-dependent changes in thiol-reactivity

The experiment in the previous section (section 4.3) was performed on single samples of cultured cells for each peroxide treatment condition. However, for statistical validation, analysis of multiple samples for each experimental condition is essential. Thus, the 0 min and 20 min timepoints were chosen for a more detailed statistical analysis of thiol labelling in human mammary luminal epithelial cells (HB4a) and ErbB-2 overexpressing partners (C3.6). Each condition was run in triplicate and 2-D gels were analysed using DeCyder software. Gels were then post-stained with silver-stained or CCB stained. Protein features of interest were picked for identification using MALDI-MS. The labelling strategy is outlined in Figure 4-6 and the 24 fluorescent images obtained are shown in Figure 4-7. This experiment was repeated twice. In one of these experiment the ICy3/5 labelling was reversed, and CCB used as a post-stain instead of silver. In the

other, spots of interest were excised from unstained gels, using the coordinates of the fluorescent spots, rather than the post-stained spots. Similar changes in ICy3/5 labelling were observed in these 3 experiments. In one experiment, 126 significant changes in labelling were identified (>1.5-fold up or down regulated; $p < 0.05$; the statistics used here is discussed in Appendix J) (Figure 4-8). Of these, 51 were peroxide-dependent and 90 were ErbB-2 dependent, with 15 changes displaying dual dependency. Post-staining with silver or CCB and matching to the corresponding fluorescent images allowed picking of 89 different gel features with high confidence. These samples contained a reasonable amount of stained protein that could be used for identification by MS (Figure 4-9).

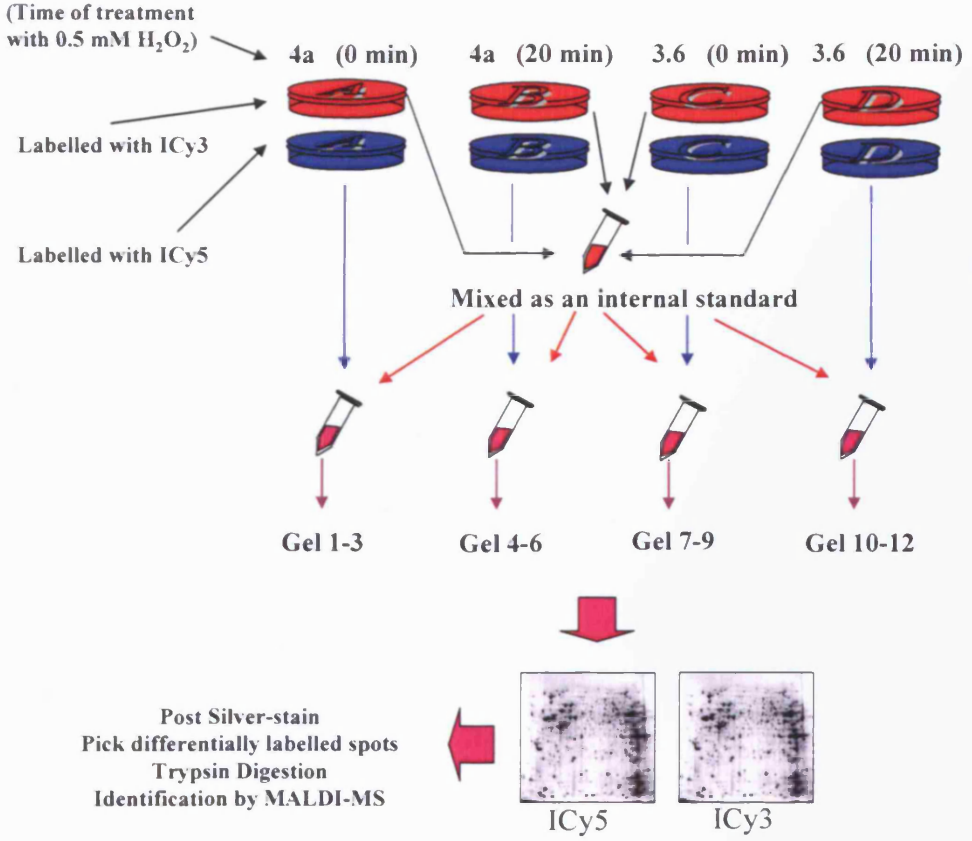

(Figure 4-6) Strategy for ICy3/5 cysteine-labelling 2D-DIGE to monitor oxidant-dependent and ErbB-2 dependent thiol reactivity changes in HB4a and C3.6 cells. Untreated HB4a and C3.6 cells or cells treated with 0.5 mM for 20 min were lysed in the presence of ICy3 and ICy5 and incubated for labelling. Equal amount of the ICy3 labelled samples were mixed as an internal standard and run against the individual untreated or hydrogen peroxide treated samples. Each individual sample was run triplicate against the standard pool and a statistical analysis performed using Decyder BVA software. Gels were post-stained with silver or CCB and the spots of interest were excised for in-gel digestion and subsequent MALDI-TOF-MS analysis.

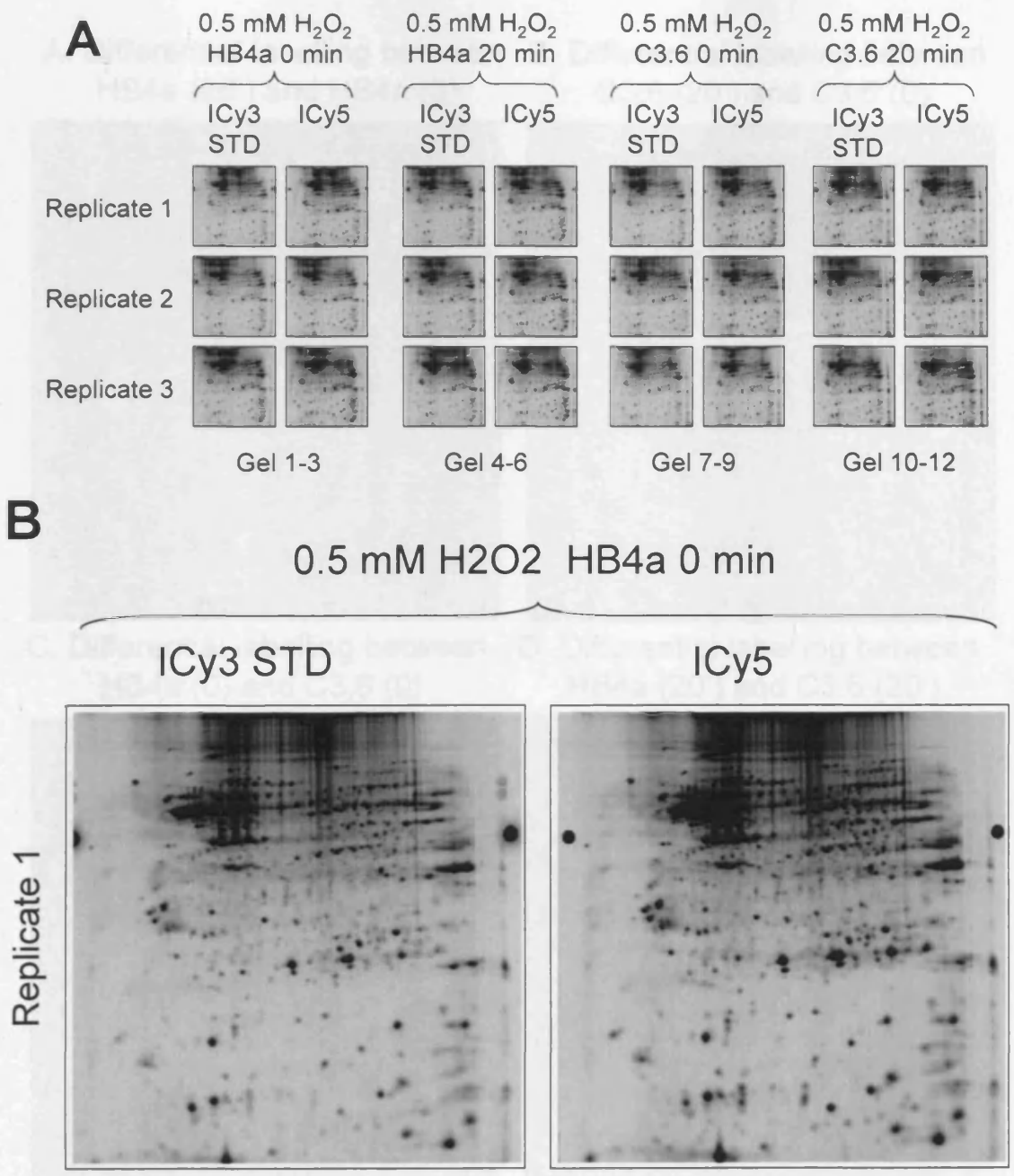

(Figure 4-7) Representation of the experimental design and images obtained in the study of thiol reactivity in HB4a and C3.6 cells in response to 0.5 mM H_2O_2 treatment. (A) Randomly growing HB4a and C3.6 cells were treated with 0.5 mM H_2O_2 for 20 min and compared to untreated samples. Equal amounts of ICy3 labelled lysates were mixed as an internal standard pool and run against ICy5 labelled hydrogen peroxide-treated or untreated samples. Samples were run in triplicate to assess reproducibility and for statistical analysis of changes. This represents 12 gels with 24 images generated. Gel images were processed using the BVA module of DeCyder software. 2 representative enlarged images are shown in **(B).**

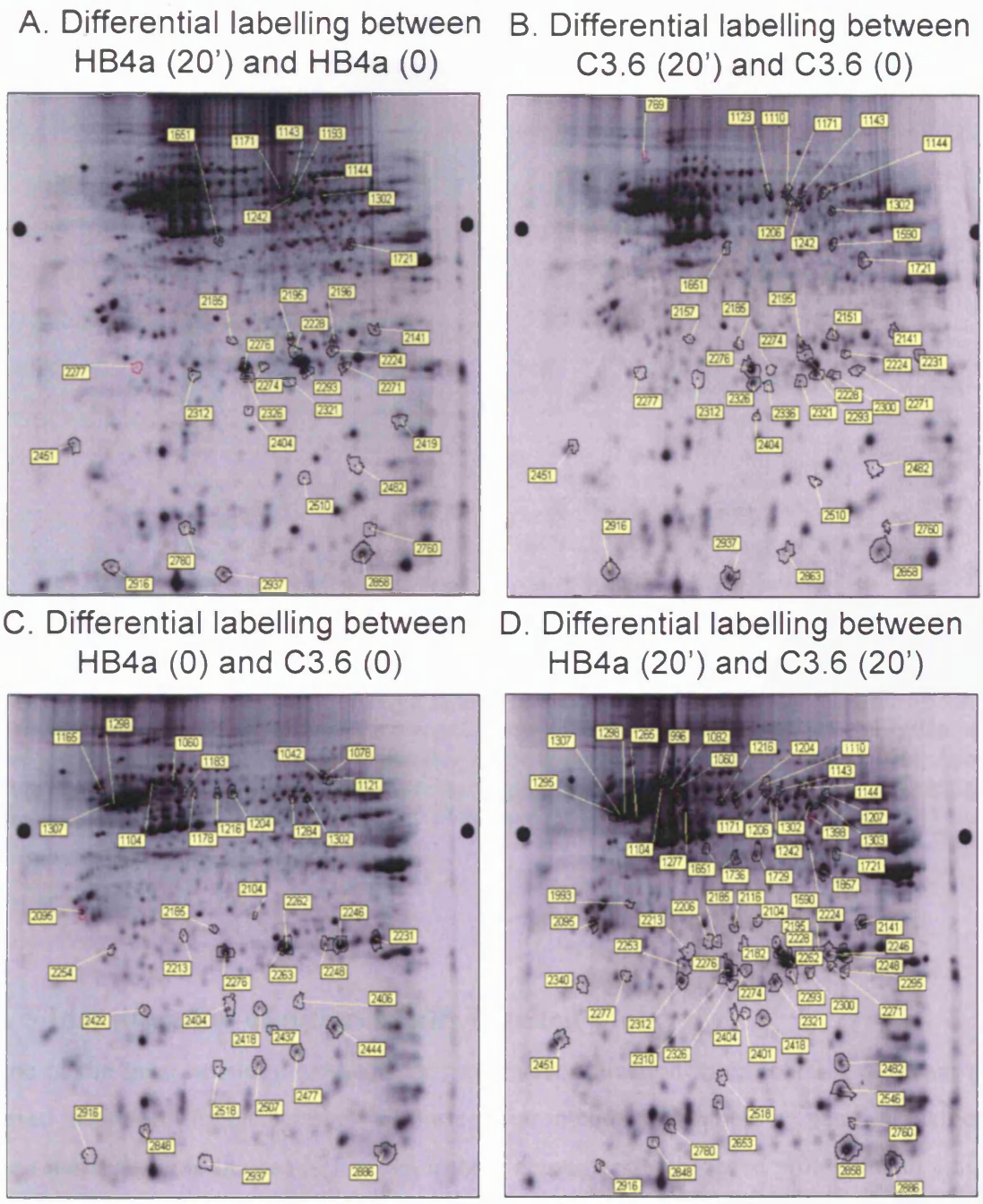

(Figure 4-8) Visualisation of spots that display changes in cysteine thiol labelling with H_2O_2 treatment and between HB4a vs. C3.6 cells. Representative ICy dye images of H_2O_2 treated/untreated HB4a and C3.6 cells are shown. Protein features with altered ICy-labelling are labelled with a spot identity number.

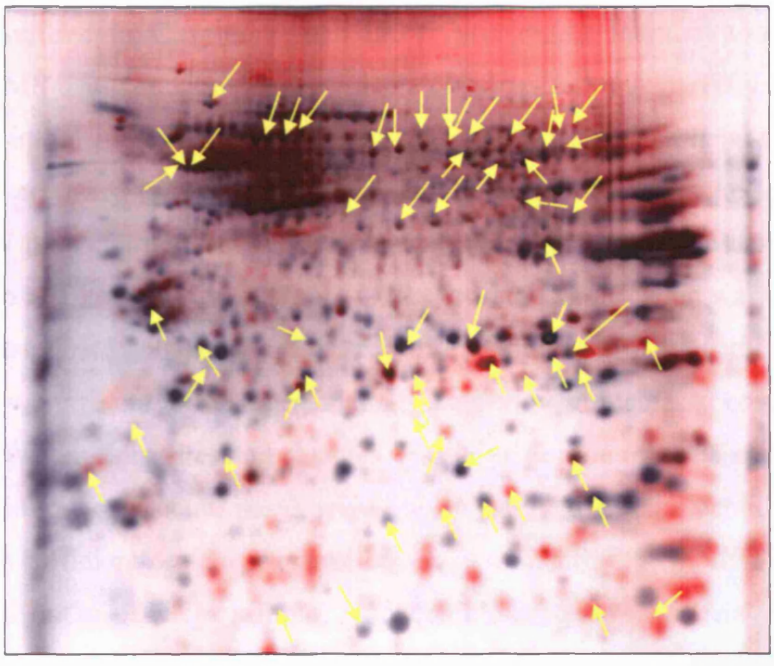

(Figure 4-9) Master gel image of ICy3 labelled standard pool and its corresponding silver stained image. The image shown is a merged image of ICy3 labelled HB4a/C3.6 cell lysate pool (red spots) and the image of its corresponding silver stained gel (black spots) created using Adobe Photoshop software. The arrows indicate the aligned features between significant differentially labelled spots and the silver-stained spots. These spots (89) were picked for identification.

4. 5 Identification of differentially labelled spots

One of the most sensitive methods for protein identification in proteomics relies on gel based mass spectrometry. Improved mass spectrometers and sample preparation methods now make possible the use of low femtomole amounts of gel-loaded proteins with a high probability of successful identification. Several approaches are used for protein MS-identification, with the most commonly used method being peptide mass mapping using matrix assisted-laser desorption/ionisation-mass spectrometry (MALDI-TOF-MS) and database searching (Chapters 1 and 2).

In this work, a modified porcine trypsin was used to generate tryptic peptides from gel-

separated proteins. This enzyme efficiently cleaves at the C-terminal side of lysine and arginine residues without giving rise to any autolysis peaks. Proteins were digested (procedure described in Chapter 2) and the tryptic digest mixture was analysed by MALDI-TOF-MS using an Ultraflex instrument (Bruker Daltronics). Fifty one out of the 89 proteins of interest (57%) gave well resolved spectra with high signal-to-noise ratios and high mass accuracy (within +/- 50 ppm) and consequently the picked proteins were identified with high confidence. A typical example of a peptide mass spectrum with database search results is shown in Figure 4-10. Protein identification was carried out on samples from triplicate gels and from the repeat experiments. Many of the same protein identifications were found in the repeated analysis, giving an increased confidence in the validity of the protein identities and changes. However, for the other 38 spots of interest, the signals were low or spectral peaks were poorly resolved and the peptide fingerprints did not provide sufficient protein sequence coverage to identify the protein. This problem may be caused by insufficient sample, inadequate extraction of special peptides (e.g. hydrophobic peptides), the lack of tryptic sites, or post-translational modification of the proteins. In these cases the proteins could not be identified, despite repeat picking, digestion and peptide mass fingerprinting.

Identification of differentially labelled features from unstained gels was also attempted using automated picking methos based on coordinates derived from the fluorescent images alone. Although the picking accuracy was good (confirmed by re-scanning of gels), only ~40% of the features could be identified with confidence. Of the samples that could not be identification, they generally generated low intensity spectra, implying that there was insufficient material in these spots. Thus, whilst detection of these low-abundance thiol-containing proteins was possible using the ICy dyes, the steps in the processing for MALDI-TOF analysis were insufficiently sensitive to detect the digested proteins. This would be due to the labelling of very reactive thiols on protein species expressed at low levels and affinity purification strategies could be used to enrich them.

A

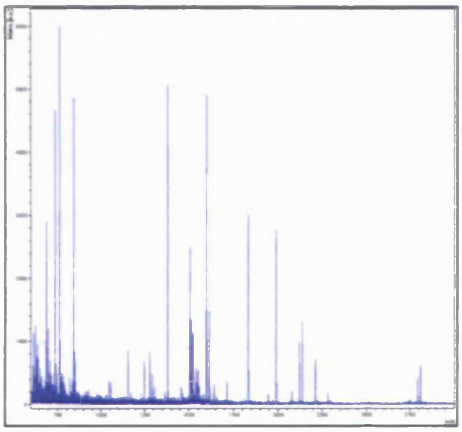

B

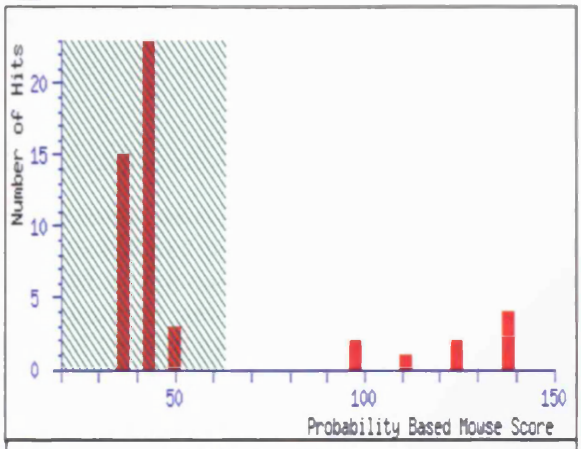

CSHEA Mass: 18229 Score: 135 Expect: 3.9e-09 Queries matched: 20

peptidylprolyl isomerase (EC 5.2.1.8) A - human

Observed	Mr(expt)	Mr(calc)	Delta	Start	End	Miss	Peptide
696.32	695.31	695.35	-0.04	77 -	82	0	SIYGEK
705.33	704.33	704.37	-0.04	38 -	44	0	ALSTGEK
737.34	736.33	736.35	-0.02	32 -	37	0	TAENFR
763.33	762.32	762.32	-0.00	50 -	55	0	GSCFHR
913.49	912.48	912.55	-0.07	126 -	133	1	EVVFGKVK
1055.60	1054.59	1054.53	0.06	20 -	28	0	VSFELFADK
1154.61	1153.60	1153.57	0.04	83 -	91	0	FEDENFILK
1247.64	1246.63	1246.62	0.01	155 -	165	1	KITIADCGQLK
1278.64	1277.63	1277.57	0.05	134 -	144	0	EGMNIVEAMER
1294.58	1293.57	1293.57	0.00	134 -	144	0	EGMNIVEAMER + Oxidation (M)
1310.54	1309.54	1309.56	-0.03	134 -	144	0	EGMNIVEAMER + 2 Oxidation (M)
1379.81	1378.80	1378.75	0.05	20 -	31	1	VSFELFADKVPK
1505.79	1504.79	1504.74	0.05	132 -	144	1	VKEGMNIVEAMER
1515.84	1514.83	1514.79	0.04	119 -	131	1	TEWLDGKHVVFGK
1521.76	1520.75	1520.73	0.02	132 -	144	1	VKEGMNIVEAMER + Oxidation (M)
1537.74	1536.73	1536.73	0.00	132 -	144	1	VKEGMNIVEAMER + 2 Oxidation (M)
1598.83	1597.83	1597.74	0.09	56 -	69	0	IIPGFMCQGGDFTR
1614.82	1613.81	1613.73	0.08	56 -	69	0	IIPGFMCQGGDFTR + Oxidation (M)
1831.96	1830.95	1830.90	0.05	77 -	91	1	SIYGEKFEDENFILK
1946.06	1945.05	1944.99	0.06	2 -	19	0	VNPTVFFDIAVDGEPLGR

C

Acc. #: IPI:IPI00419585.3 Species: TREMBL:Q71V99 Name: SWISS-PROT:P62937
Acc. #: REFSEQ_NP:NP_066953 Species: ENSEMBL:ENSP00000335257;ENSP00000284889 TAX_ID=9606 CYCLOPHILIN
Index: 38871 MW: 17972 Da pI: 7.7

m/z Submitted	MH+ Matched	Delta ppm	Modifications	Start	End	Missed Cleavages	Database Sequence
737.3382	737.3582	-27		32	37	0	(K)TAENFR (A)
1154.6106	1154.5734	32		83	91	0	(K)FEDENFILK (H)
1278.6359	1278.5822	42		134	144	0	(K)EGMNIVEAMER (F)
1294.5775	1294.5771	0.27	1Met-ox	134	144	0	(K)EGMNIVEAMER(F)
1310.5429	1310.5721	-22	2Met-ox	134	144	0	(K)EGMNIVEAMER(F)
1379.8057	1379.7575	35		20	31	1	(R)VSFELFADKVPK (T)
1505.7938	1505.7456	32		132	144	1	(K)VKEGMNIVEAMER (F)
1515.8377	1515.7960	28		119	131	1	(K)TEWLDGKHVVFGK (V)
1521.7580	1521.7405	11	1Met-ox	132	144	1	(K)VKEGMNIVEAMER(F)
1537.7373	1537.7354	1.2	2Met-ox	132	144	1	(K)VKEGMNIVEAMER(F)
1614.8188	1614.7409	48	1Met-ox	56	69	0	(R)IIPGFMCQGGDFTR(H)
1831.9612	1831.9118	27		77	91	1	(R)SIYGEKFEDENFILK (H)

The matched peptides cover 44% (73/164AA's) of the protein.
Coverage Map for This Hit (MS-Digest index #): 38871

D

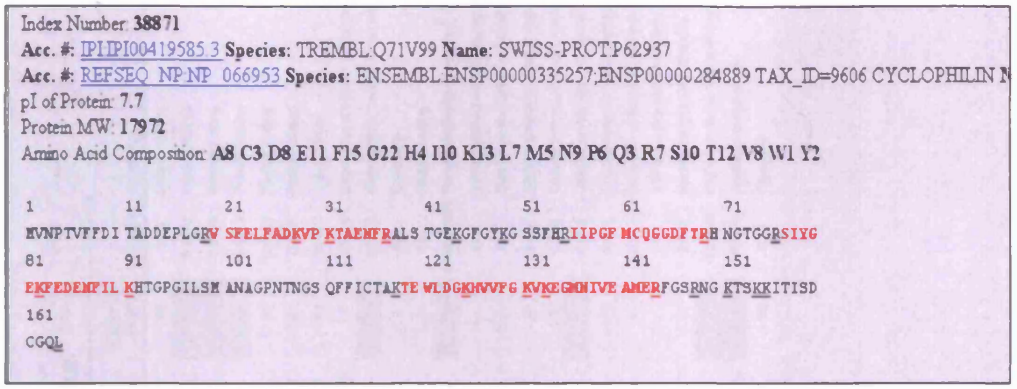

(Figure 4-10) Typical mass spectra and database searching for protein identification by peptide mass fingerprinting. Proteins were picked and proteolysed with trypsin (Chapter 2). The peptide mixture generated was then analysed by matrix-assisted laser-desorption/ionisation-MS (MALDI-TOF-MS). **(A)** A typical mass spectrum was acquired on an Ultraflex TOF/TOF mass spectrometer (Bruker Daltonics). The list of peptide masses was searched against the NCBI theoretical peptide fragment database (updated NCBInr. 3.24.2003 or Swiss-prot) using Mascot and Protein Prospector. **(B)** Peptide mass mapping was performed by database searching using Mascot (Matrix Science) with a probability score higher than the threshold value (62 in this case) meaning the hit is highly significant. **(C)** Protein Prospector (version 3.4.1) MS-Fit search tool (UCSF, USA). The search criteria allowed a +/- 50 ppm mass error and up to 1 missed cleavage. Identical search parameters were used for all MS searches. **(D)** Representation of protein coverage, where in the case analysed (Cyclophilin A), the matched peptides represent 44% of the sequence of the protein.

Table 4-1A shows the 25 of the 51 identified proteins which displayed peroxide-dependent changes in ICy labelling and includes 10 isoforms which also showed some ErbB-2 dependency at the fold cut-offs used. Table 4-1B shows the 26 identified proteins displaying ErbB-2-dependent differences alone (i.e. C3.6 vs. HB4a). Some isoforms (such as chaperonin containing TCP1-β and cytokeratin 13) formed charge trains that could be induced by labelling of a number of thiols and implying that saturation labelling was not achieved in this experiment. The migration of all of the identified features are shown in a master gel in Figure 4-11A. Proteins located in the high molecular weight, acidic region of the gel are shown in a zoomed-in area of the figure (Figure 4-11B). Examples of some these changes are represented graphically in Figure 4-12. It is important to note that all proteins identified contain at least one free cysteine thiol, which helps to validate the specificity of this labelling technique.

A

Spot No.	Protein Name	% Cov	Mowse Score	Est. mass	Est. pI	Pred. Mass	Pred. pI	Accession No.	Average fold-difference † and *p*-value: 4a(20') to 4a(0)	*P*-value	3.6(20') to 3.6(0)	*P*-value	3.6(0') to 4a(0)	*P*-value	3.6(20') to 4a(20')	*P*-value	Function
769	BiP protein[a]	35	105/64	72000	5.1	70932	5.2	6470150	1.49	0.18	1.71	0.0051	-1.08	0.69	1.06	0.63	Protein folding
1123	Chaperonin containing TCP1-α	27	72/64	60000	6.7	60344	5.8	135538	-1.6	0.004	-1.09	0.45	1.12	0.59	1.65	0.0082	Protein folding
1242	Chaperonin containing TCP1-β[a]	50	123/64	55000	6.8	57489	6	5453603	-1.88	0.0012	-1.06	0.52	1	0.96	1.77	0.0026	Protein folding
1206	Chaperonin containing TCP1-β[a]	50	127/64	55000	6.7	57489	6	5453603	N.A.	N.A.	1.55	0.0056	N.A.	N.A.	1.55	0.0082	Protein folding
1110	Chaperonin containing TCP1-γ	36	88/64	57000	6.6	60403	6.1	20455521	-1.5	0.013	-1.1	0.31	1.09	0.73	1.48	0.0035	Protein folding
1144	Chaperonin containing TCP1-ζ	43	124/64	56000	7.2	58025	6.2	730922	-1.91	0.0000016	1.01	1	-1.31	0.0018	1.47	0.013	Protein folding
1143	Cytokeratin 10	28	69/64	58000	6.9	58827	5.1	4557697	-1.74	0.013	-1.34	0.029	1.1	0.0048	1.43	0.0077	Cytoskeleton
2276	Glutathione S-transferase π	55	68/64	25000	6.4	24678	5.7	121746	-1.61	0.00052	-1.27	0.011	-1.78	0.00043	-1.4	0.0018	Regulation of cellular redox state
2253	Glutathione S-transferase π chain A	54	71/64	25000	5.7	23225	5.4	494066	-1.55	0.031	-1.45	0.015	-1.7	0.023	-1.59	0.0074	Regulation of cellular redox state
2049	Glyceraldehyde-3-phosphate DH[a]	42	124/64	35000	9	36054	8.6	120649	1.53	0.0038	N.A.	N.A.	N.A.	N.A.	N.A.	N.A.	Glycolysis
1088	HSP-73[a]	46	88/64	70000	6	70898	5.4	123648	-1.84	0.0056	N.A.	N.A.	N.A.	N.A.	N.A.	N.A.	Protein folding
2482	Peptidyl-prolyl cis-trans isomerase A[a]	65	94/64	15000	8	17881	7.8	13937981	16.19	5.4E-08	7.36	0.00003	1.09	0.046	-2.01	0.00000048	Protein folding/conformation
1536	Peroxiredoxin 1[a]	34	68/64	23000	8.6	22111	8.3	548453	4.82	0.0039	N.A.	N.A.	N.A.	N.A.	N.A.	N.A.	Cellular protection from oxidative stress
1603	Peroxiredoxin 2[a]	33	107/64	20000	6	21892	5.7	2507169	14.67	0.000089	N.A.	N.A.	N.A.	N.A.	N.A.	N.A.	Cellular protection from oxidative stress
2274	Peroxiredoxin 3 (antioxidant protein 1)	33	138/64	26000	6.4	27693	7.7	2507171	2.76	0.016	7.37	0.000013	-2.13	0.047	1.25	0.009	Cellular protection from oxidative stress
2510	Peroxiredoxin 5, chain A[a]	44	138/64	17000	7.2	16900	7	15826629	3.42	0.0011	2.15	0.00052	1.32	0.039	-1.21	0.032	Cellular protection from oxidative stress
2195	Peroxiredoxin 6 (antioxidant protein 2)	68	113/64	26000	6.9	25035	6	1718024	-2.74	0.016	-2.19	0.011	1.35	0.008	1.69	0.026	Cellular protection from oxidative stress
2228	Peroxiredoxin 6 (antioxidant protein 2)	59	98/64	27000	7	25035	6	1718024	3.69	0.0004	4.58	0.0000005	-1.43	0.046	-1.15	0.011	Cellular protection from oxidative stress
2157	Prohibitin	44	68/64	30000	5.6	29804	5.6	4505773	2.69	0.0062	2.95	0.0012	-1.1	0.039	1	0.012	Growth/proliferation suppresion
1563	Proteasome β 2 subunit[a]	38	71/64	22000	7.5	22836	6.5	1709762	-2.27	0.0000093	N.A.	N.A.	N.A.	N.A.	N.A.	N.A.	ATP/ubiquitin-dep. proteolysis
2271	RAN small GTPase	57	104/64	25000	7.6	24423	7	5453555	-5.55	0.0059	-3.97	0.013	-1.3	0.026	1.07	0.032	Nucleo-cytoplasmic transport
2141	Signal recognition particle receptor β subunit	33	66/64	29000	8.1	29651	9.2	20141812	2.88	0.00016	1.68	0.00064	-1.05	0.55	-1.81	0.00045	SRP-association with membrane
1302	Splice isoform of Glutaryl-Co A DH	36	87/64	50000	7.3	47356	8.6	2492631	-1.54	0.00026	-1.35	0.048	-6.43	0.000042	-5.63	0.000006	Oxidative metabolism
2224	Triosephosphate isomerase[a]	51	80/64	28000	7.4	26539	6.5	136060	-2.85	0.014	-3.68	0.0037	1.37	0.069	1.06	0.83	Glycolysis

B

Spot No.	Protein Name	% Cov	Mowse Score	Est. mass	Est. pI	Pred. Mass	Pred. pI	Accession No.	Average fold-difference † and *p*-value: 4a(20') to 4a(0)	*P*-value	3.6(20') to 3.6(0)	*P*-value	3.6(0') to 4a(0)	*P*-value	3.6(20') to 4a(20')	*P*-value	Function
2095	14-3-3 protein σ	31	91/65	30000	4.6	27774	4.7	5454052	1.01	0.85	-1.15	0.11	-1.71	0.00014	-2	0.00087	Growth regulation
1207	Aldehyde dehydrogenase 6	25	76/64	54000	7.4	56010	6.6	4502041	-1.41	0.0008	-1.12	0.18	1.43	0.0013	1.81	0.0026	Detox. of aldehydes
1183	Cytokeratin 6	53	100/64	55000	6.1	53501	5.4	14318422	1.04	0.76	1.11	0.35	1.6	0.014	1.72	0.036	Cytoskeleton
1277	Cytokeratin 7[a]	54	98/64	55000	6.1	51335	5.4	20178293	-1.25	0.01	-1.16	0.00012	1.45	0.000065	1.67	0.00058	Cytoskeleton
1307	Cytokeratin 13	48	137/64	50000	4.9	49587	4.9	24234696	-1.05	0.01	-1.13	0.01	4.15	0.0000039	3.67	0.000098	Cytoskeleton
1298	Cytokeratin 13	45	221/64	50000	4.8	49587	4.9	24234696	-1.01	0.93	-1.11	0.21	3.17	0.000069	2.88	0.00031	Cytoskeleton
1295	Cytokeratin 13	31	102/64	50000	4.9	49587	4.9	24234696	1.3	0.016	-1.06	0.016	5.54	0.0001	4.03	0.00073	Cytoskeleton
1165	Cytokeratin 13	39	116/64	55000	4.9	49587	4.9	24234696	1.05	0.012	1.04	0.012	2.29	0.024	2.28	0.0064	Cytoskeleton
1303	Dihydrolipoamide dehydrogenase	42	110/64	54000	7.5	54151	7.6	118674	-1.04	0.77	1.18	0.22	-1.84	0.000044	-1.51	0.018	Regulation of cellular redox state
2262	Glutathione S-transferase π	67	74/64	26000	7.2	24678	5.7	121746	-1.47	0.0034	-1.12	0.00078	-2.36	0.00000085	-1.8	0.00065	Regulation of cellular redox state
2182	HSP-27[a]	46	115/64	27000	6.6	22783	6	4504517	-1.31	0.0043	-1.46	0.0011	2.51	0.0023	2.25	0.0082	Protein folding
2213	HSP-27[a]	25	67/60	27000	6.1	22783	6	4504517	1.37	0.0038	-1.12	0.009	6.42	0.000091	4.2	0.029	Protein folding
1104	HSP-60	32	140/64	60000	5.4	61055	5.7	129379	-1.26	0.09	-1.05	0.45	-1.89	0.000019	-1.58	0.023	Protein folding
1060	HSP-60, mitochondrial precusor[a]	26	81/64	57000	5.7	61213	5.7	129379	1.11	0.0034	-1.07	0.009	-1.53	0.00046	-1.82	0.00008	Protein folding
1082	HSP-60, mitochondrial precusor[a]	40	127/63	57000	5.4	61213	5.7	4504521	-1.03	0.037	-1.04	0.037	-1.77	0.000016	-1.78	0.0012	Protein folding
996	HSP-70[a]	44	160/64	71000	5.4	70899	5.4	5729877	1.1	0.55	-1.13	0.33	-1.44	0.00015	-1.79	0.028	Protein folding
1736	Maspin precusor (protease inhibitor 5)	41	67/64	41000	6.6	42229	5.8	453368	-1.28	0.0008	1.08	0.18	1.48	0.0014	2.04	0.0000041	Growth/Proliferation suppresion
1729	Maspin precusor (protease inhibitor 5)	56	75/64	41000	6.7	42229	5.8	547892	-1.07	0.053	1.09	0.12	1.4	0.003	1.64	0.00003	Growth/Proliferation suppresion
2507	Nucleoside diphosphate kinase A	44	77/64	16000	6.6	17149	5.8	127981	1.27	0.1	-1.05	0.15	1.89	0.0049	1.42	0.00078	Nucleotide metabolism
2248	Proteasome alpha 2 subunit	32	63/60	26000	7.4	25899	6.9	4506181	1.13	0.069	1.07	0.68	-2	0.00013	-2.12	0.0033	ATP/ubiquitin-dep. Proteolysis
1204	Protein disulfide-isomerase A3 precursor[a]	37	261/64	55000	6.5	56783	6	2507461	-1.28	0.00038	-1.23	0.00062	1.57	0.000032	1.64	0.000002	Disulfide bond formation/protein folding
1216	Protein disulfide-isomerase A3 precursor[a]	34	79/64	56000	6.3	56783	6	2507461	-1.09	0.013	-1.02	0.0094	1.56	0.00012	1.66	0.000028	Disulfide bond formation/protein folding
1178	Protein disulfide-isomerase ER60 precusor	25	78/64	56000	6.2	56680	6.1	1085373	1.12	0.0021	-1.04	0.0031	1.57	0.0013	1.34	0.0018	Disulfide bond formation/protein folding
2254	Rho-GDP-dissociation inhibitor 1	31	86/64	27000	5	23207	5	4757768	1.33	0.019	-1.07	0.028	2.01	0.011	1.41	0.017	Inact. of NADPH oxidase/small GTPases
2518	Ubiquitin-conjugating enzyme E2N	55	114/64	16000	6.4	17138	6.1	2501432	1.01	0.00018	1.13	0.0046	1.74	0.0023	1.94	0.00046	Ubiquitin conjugation

(Table 4-1) Identification of differentially labelled/expressed proteins. (A) Proteins displaying H_2O_2-induced differential labelling in normal (HB4a) and ErbB-2-overexpressing (C3.6) human mammary luminal epithelial cells. **(B)** Proteins displaying differential labelling between HB4a and C3.6 luminal epithelial cells. Proteins were identified by MALDI-TOF peptide mass mapping (see Materials and Methods (Chapter 2)). [a]Proteins identified in two or more independent experiments. Proteins appearing more than once in the tables were identified as isoforms with different p*I*s. The % coverage of analysed peptides, the MOWSE score from Mascot searches and the significance threshold score, the estimated mass and p*I* (from gels), the predicted mass and p*I* (from the database) and the NCBI gene identifier (Accession Number) are shown for each protein. MS spectra, MOWSE score histograms, matching peptides and sequence coverage for all proteins are shown in Appendix C. [†]Average fold-differences from DeCyder analysis show abundance ratios for treated HB4a cells versus untreated (4a(20') to 4a(0)), treated C3.6 cells versus untreated (3.6(20') to 3. 6(0)), untreated C3.6 versus untreated HB4a (3.6(0) to 4a(0)) and treated C3.6 versus treated HB4a (3. 6(20') to 4a(20')). Proteins displaying an average fold-difference of $\geq$ 1.5-fold up (+) or down (-) regulation between pairs of conditions where $p<0.05$ and spots matched in all images are shaded grey. N. A. not analysed. Functions were ascribed from the NCBInr database and literature searches.

A

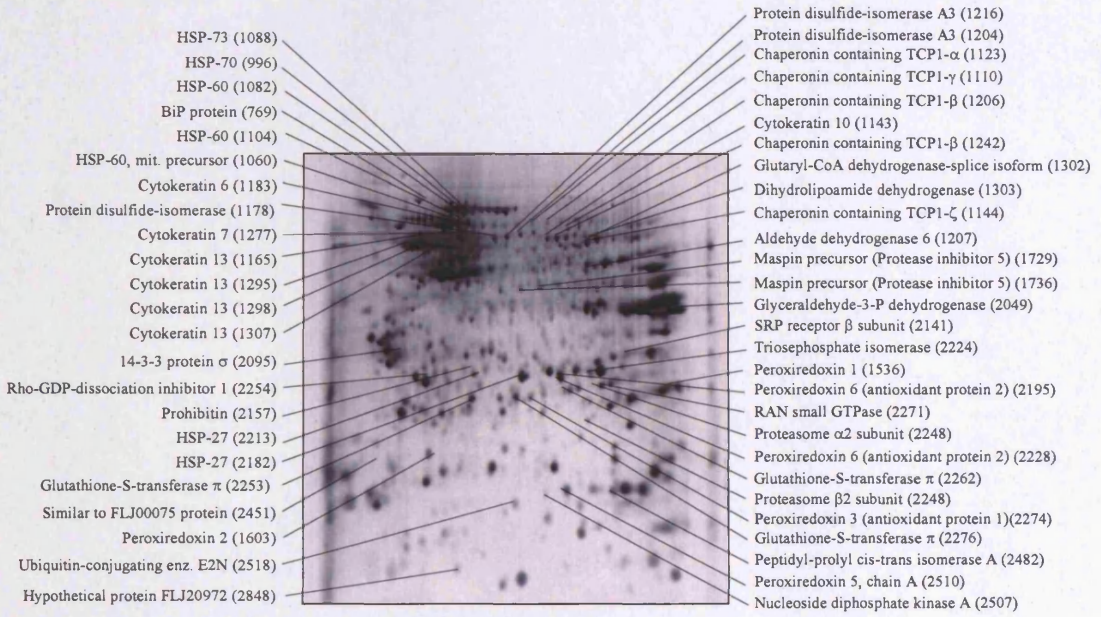

B

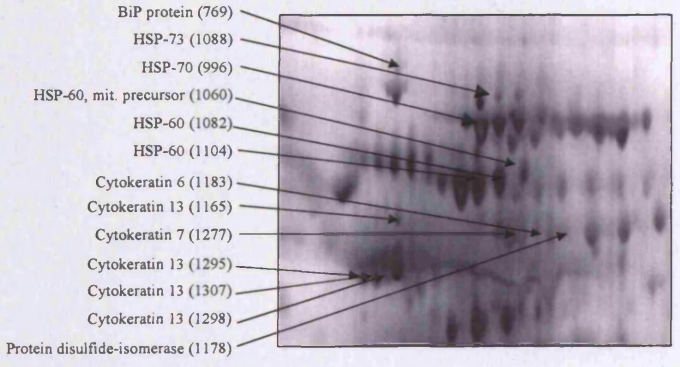

(Figure 4-11) 2DE migration of proteins identified by MALDI-TOF-MS displaying H_2O_2-induced differential labelling and/or ErbB-2 dependent differential expression (see Table 4-1). **(A)** A silver-stained image of a representative gel is shown. **(B)** An enlarged image of the high molecular weight acidic region is shown.

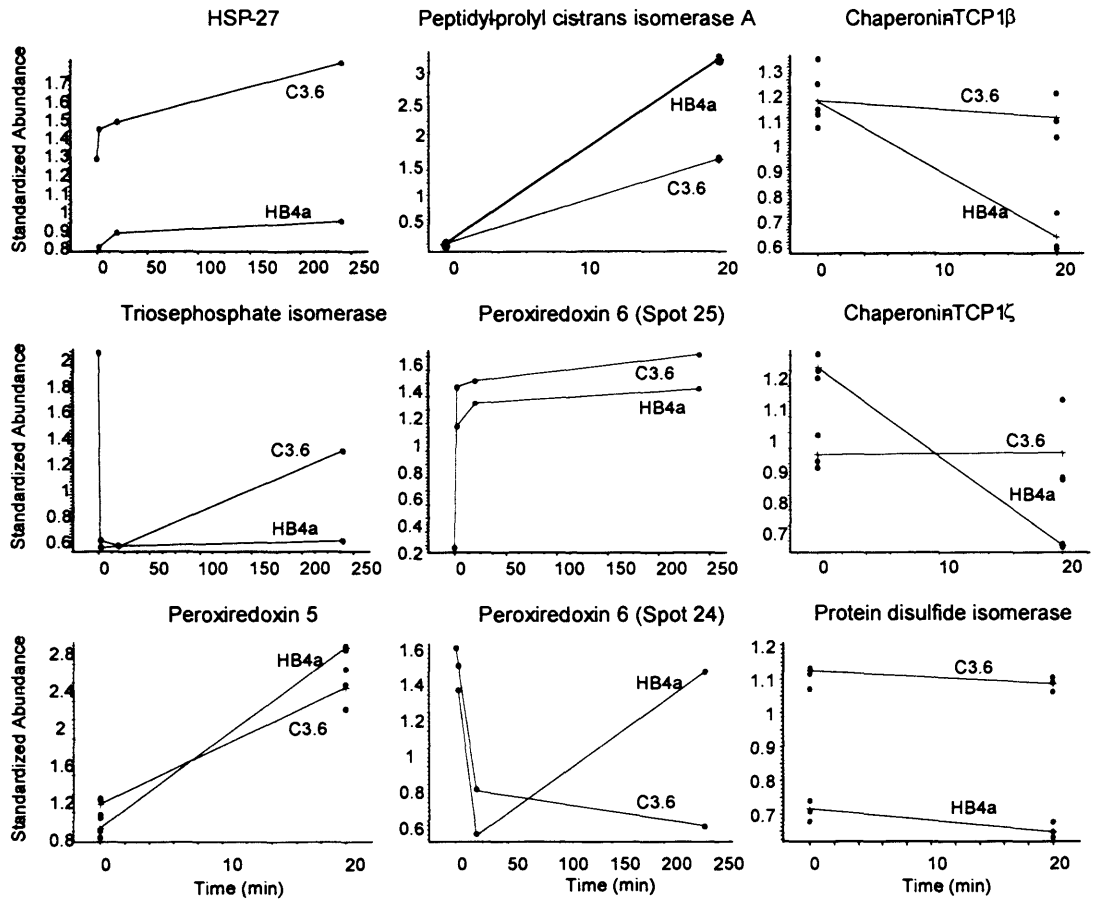

(Figure 4-12) Examples of proteins displaying altered labelling following H_2O_2 treatment and/or differential expression between normal (HB4a) and ErbB-2 overexpressing (C3.6) cell lines. Proteins were identified from gels by MALDI-TOF-MS as described in Materials and Methods (Chapter 2). Graphs were derived from DeCyder image analysis where the standardised abundance is the ratio of the volume of a test gel feature versus the volume of the corresponding internal standard gel feature. Triplicate data points are shown for the 0 and 20 min experiments with lines joining the average values, whilst single data points are shown from the preliminary timecourse experiment.

Proteins differentially labelled or expressed in response to H_2O_2 fell into several functional groups. Firstly, molecular chaperones were highly representative. Heat shock protein 73/hsc70, the ER chaperone BiP/Grp78, peptidyl-prolyl cis-trans isomerase A (cyclophilin A/CypA), signal recognition particle receptor β subunit (SRβ) and the chaperonin-containing T-complex protein 1 (TCP1) subunits α, β, γ and ζ, are all known

to be involved in processes such as ATP-dependent protein folding, protein transport, degradation of incorrectly folded polypeptides and prevention of aggregation of newly synthesised polypeptides. ICy labelling of these individual proteins were both increased and reduced by H_2O_2 treatment depending on the particular protein (Table 4-1A). CypA showed the greatest increase in labelling in response to H_2O_2. Immunoblotting was used to reveal that this was not due to altered protein expression, although the differential labelling between cell lines did appear to result from a change in protein expression (Figure 4-13A and Figure 4-14).

Reassuringly, a number of the identified proteins have known roles as cellular redox regulators. This includes two isoforms of glutathione S-transferase π, in which labelling was both reduced after H_2O_2 treatment and in the C3.6 cells. Again, no significant changes in protein expression level were detected by 1D immunoblotting (Figure 4-14), which was suggestive of a mechanism involving direct oxidative modification. In support of this, a reduction in ICy labelling of recombinant GST protein was observed after treatment with H_2O_2, although a specific site of modification could not be identified by MS (Figure 4-15 and see later). There also appeared to be a shift in the molecular weight of the H_2O_2-treated sample that might be due to oxidation changing the charge and therefore the mobility of the protein. Five of the six known mammalian peroxiredoxin (Prxn) family members were also identified as targets of H_2O_2-induced redox stress in the human luminal epithelial cell system. The Prxns are antioxidant enzymes that function by reducing hydroperoxides that have been implicated in redox-regulation of cell signalling (Wood et al., 2003). ICy dye labelling of 2DE isoforms which corresponded to Prxn1, 2, 3, 5 and 6 was increased after H_2O_2 treatment, whilst the level of another isoform of Prxn6 was reduced (Table 4-1A and Figure 4-12). 1D immunoblotting showed that overall, Prxn expression did not correlate well with ICy labelling; Prxn1 and 3 levels were increased slightly by H_2O_2 treatment in HB4a cells in agreement with the ICy dye labelling results; whereas Prxn2 decreased in HB4a cells and Prxn5 and 6 levels were unaffected (Figure 4-14). These results infer that the labelling changes are not only due to changes in protein level, but also due to changes in the reactivity of thiols within these proteins.

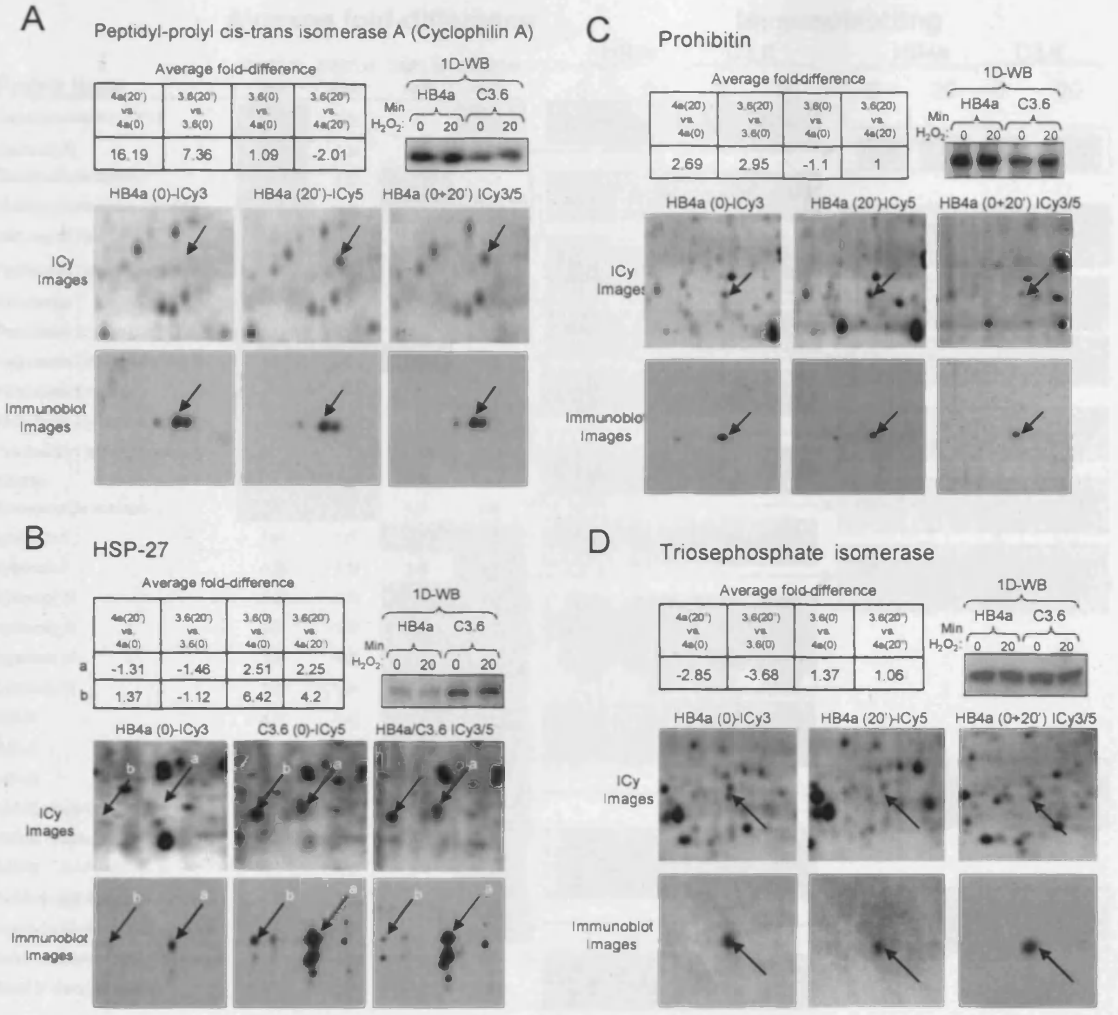

(Figure 4-13) Validation of differential labelling/expression by 1D and 2D immunoblotting. Expression of selected targets was analysed by 1D and 2D immunoblotting using specific antibodies. 2D blots of lysates from untreated and H_2O_2-treated HB4a cells and a mixed lysate are shown aligned with the corresponding ICy dye fluorescence images. Average-fold differences are taken from Table 4-1A. Results are shown for **(A)** Peptidyl-prolyl cis-trans isomerase A (CypA) **(B)** Hsp27 **(C)** Prohibitin **(D)** Triosephosphate isomerase (TPI).

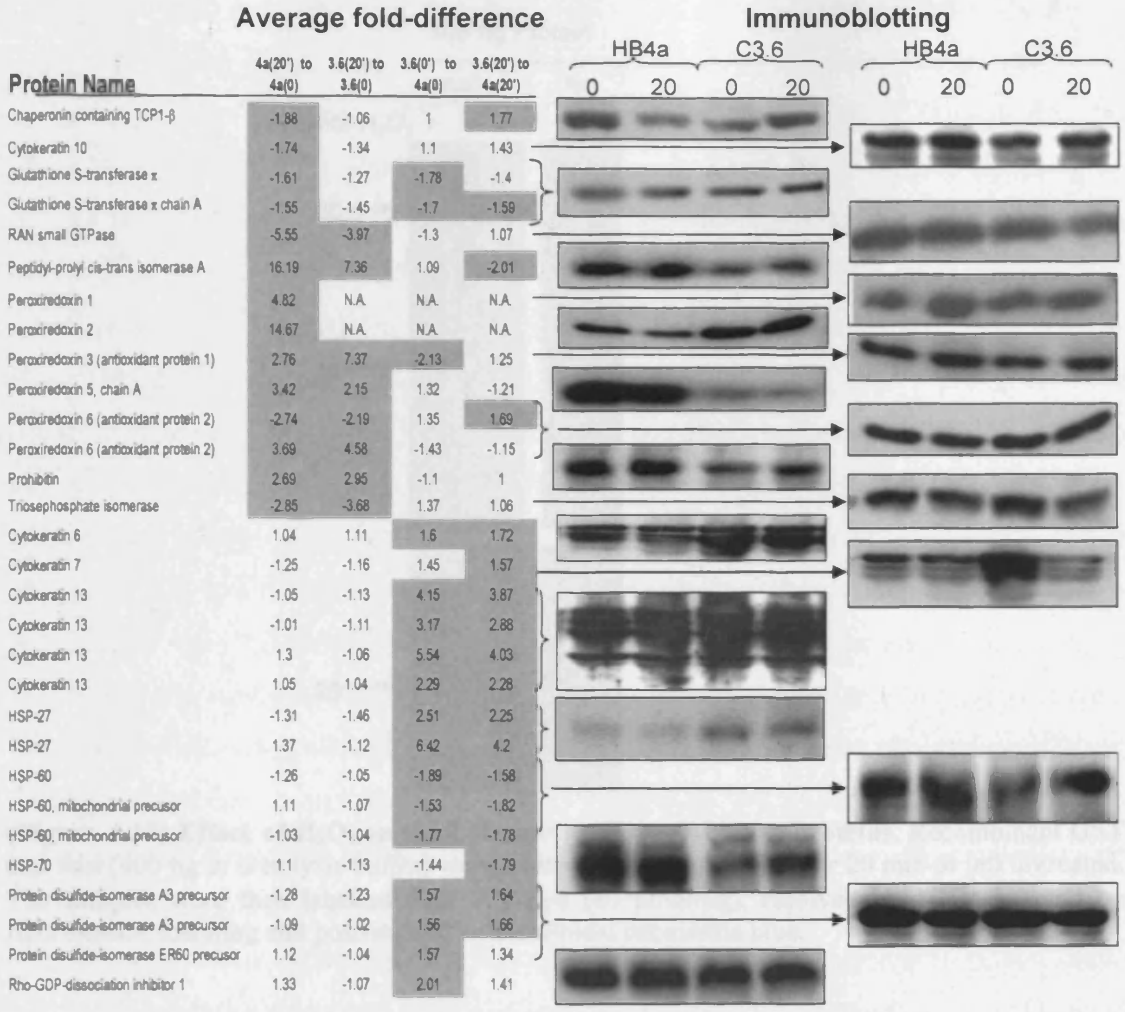

Protein Name	4a(20') to 4a(0)	3.6(20') to 3.6(0)	3.6(0') to 4a(0)	3.6(20') to 4a(20')
Chaperonin containing TCP1-β	-1.88	-1.06	1	1.77
Cytokeratin 10	-1.74	-1.34	1.1	1.43
Glutathione S-transferase π	-1.61	-1.27	-1.78	-1.4
Glutathione S-transferase π chain A	-1.55	-1.45	-1.7	-1.59
RAN small GTPase	-5.55	-3.97	-1.3	1.07
Peptidyl-prolyl cis-trans isomerase A	16.19	7.36	1.09	-2.01
Peroxiredoxin 1	4.82	N.A.	N.A.	N.A.
Peroxiredoxin 2	14.67	N.A.	N.A.	N.A.
Peroxiredoxin 3 (antioxidant protein 1)	2.76	7.37	-2.13	1.25
Peroxiredoxin 5, chain A	3.42	2.15	1.32	-1.21
Peroxiredoxin 6 (antioxidant protein 2)	-2.74	-2.19	1.35	1.69
Peroxiredoxin 6 (antioxidant protein 2)	3.69	4.58	-1.43	-1.15
Prohibitin	2.69	2.95	-1.1	1
Triosephosphate isomerase	-2.85	-3.68	1.37	1.06
Cytokeratin 6	1.04	1.11	1.6	1.72
Cytokeratin 7	-1.25	-1.16	1.45	1.57
Cytokeratin 13	-1.05	-1.13	4.15	3.87
Cytokeratin 13	-1.01	-1.11	3.17	2.88
Cytokeratin 13	1.3	-1.06	5.54	4.03
Cytokeratin 13	1.05	1.04	2.29	2.28
HSP-27	-1.31	-1.46	2.51	2.25
HSP-27	1.37	-1.12	6.42	4.2
HSP-60	-1.26	-1.05	-1.89	-1.58
HSP-60, mitochondrial precusor	1.11	-1.07	-1.53	-1.82
HSP-60, mitochondrial precusor	-1.03	-1.04	-1.77	-1.78
HSP-70	1.1	-1.13	-1.44	-1.79
Protein disulfide-isomerase A3 precursor	-1.28	-1.23	1.57	1.64
Protein disulfide-isomerase A3 precursor	-1.09	-1.02	1.56	1.66
Protein disulfide-isomerase ER60 precusor	1.12	-1.04	1.57	1.34
Rho-GDP-dissociation inhibitor 1	1.33	-1.07	2.01	1.41

(Figure 4-14) Validation of differential labelling/expression by 1D-immunoblotting. Protein expression in total cell lysates from H_2O_2-treated/untreated HB4a and C3.6 cells is compared by 1D-SDS-PAGE and immunoblotting with specific antibodies. The protein expression profiles are compared with the ICy dye labelling ratios from the 2D-DIGE experiment.

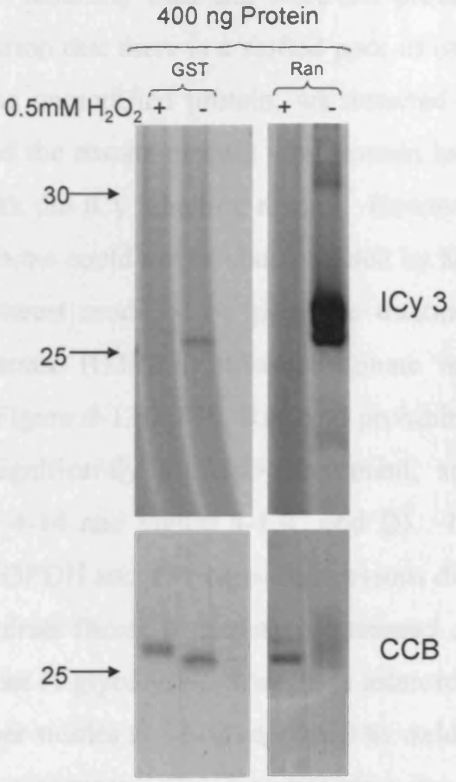

(Figure 4-15) Effect of H_2O_2 on thiol reactivity of recombinant proteins. Recombinant GST and Ran (400 ng in urea lysis buffer) were treated with 0.5mM H_2O_2 for 20 min or left untreated. The samples were then labelled with ICy dye (80 pmol/μg), resolved by 1DE, detected by fluorescence scanning and post-stained with colloidal coomassie blue.

All Prxns contain an active-site cysteine which is oxidized to a sulfenic acid by the peroxide substrate which is then converted back to the free thiol via various mechanisms include intra- and inter-molecular disulphide bond formation and reduction by the thioredoxin system. Previous data have shown that Prxn cysteines can be over-oxidised to sulphinic or sulphonic acids, resulting in their detection as proteins with an acidic shift on 2D gels (Wagner *et al.*, 2002;Rabilloud *et al.*, 2002a). Whilst it is expected that H_2O_2-dependent oxidation of Prxn active-site cysteines would block ICy labelling, we hypothesise that the increased labelling observed may occur as a result of labelling of other free thiols (present in all Prxns) on a p*I*-shifted pool of oxidised protein. However, one could also envisage that Prxns may be partially oxidised in resting cells, and that activation of cellular antioxidant mechanisms leads to their complete reduction and the

creation of additional labelling sites that were not present prior to oxidative insult. In support of the suggestion that there is a shifted pool of oxidised peroxiredoxin which can be separated from the unmodified protein, we detected 2 isoforms of peroxiredoxin 6. These hypotheses and the results explain why protein levels seen in immunoblotting do not correlate well with the ICy labelling results. However, the nature of the differences between the two isoforms could not be characterised by MALDI-TOF-MS.

Other proteins of interest modified by peroxide treatment included glyceraldehyde 3-phosphate dehydrogenase (G3PDH), triosephosphate isomerase (TPI), prohibitin, and Ran (Table 4-1 and Figure 4-13). TPI, Ran and prohibitin expression levels were found not to be altered significantly by H_2O_2 treatment, suggesting that direct oxidative modification (Figure 4-14 and Figure 4-13C and D). The observed modulation of the glycolytic enzymes G3PDH and TPI supports previous data showing that oxidative stress can redirect carbohydrate fluxes to generate increased reducing power in the form of NADPH at the expense of glycolysis. Thus, it is interesting that these two proteins have been identified in other studies as being regulated by oxidative stress (Shenton and Grant, 2003). Prohibitin can prevent cellular proliferation by binding to the Rb protein thus promoting suppression of E2F-mediated transcription, and it has been implicated in cell cycle regulation, senescence, immortalization and tumourigenesis (reviewed in (McClung et al., 1995)). Its oxidative modification may therefore have profound effects on cellular proliferation, which was found to be reduced in these cells by H_2O_2 treatment. The small GTPase Ran is known to play a critical role in active nuclear transport (Quimby and Dasso, 2003), and its modification may adversely affect protein localisation or be part of a redox protective mechanism. In support of the concept that direct oxidative modification of Ran take place, reduced ICy dye labelling of recombinant Ran protein was observed after treatment with H_2O_2 (Figure 4-15) which was in agreement with the observed 2D-DIGE results. SRβ is also a small GTPase involved in targeting of nascent polypeptides to the endoplasmic reticulum translocation machinery (Connolly and Gilmore, 1989). Thus, my results suggest that GTPases could be novel targets of oxidative stress and the impact of redox modification of these enzymes on protein localisation and processing merits further analysis.

The experimental strategy used here also allowed simultaneous comparison of the effects of ErbB-2 overexpression on the proteome of luminal epithelial cells exposed to oxidative stress. In my experiment, 26 gene products were identified (representing 36 isoforms) that were significantly up- or down-regulated (>1.5-fold; p <0.05) in untreated or H_2O_2-treated normal versus ErbB-2 overexpressing cells (Table 4-1B). The differential modulation of several molecular chaperones was observed, suggesting that ErbB-2 overexpression may alter protein folding/processing and influence the stress response. For example, multiple isoforms of Hsp27 and PDI/ERp60 were up-regulated in the C3.6 cells and these were found to be moderately affected (1.2-1.5-fold) by H_2O_2. Hsp60 and Hsp70 were down-regulated but unaffected by H_2O_2 and TCP1-α, TCP1-β, SRβ and CypA showed both robust ErbB-2- and H_2O_2-dependent regulation (Table 4-1, Figures 4-12 and 4-13 and 4-14). Although the functional consequences of these changes are unclear, several of these stress-response proteins have been shown to be dysregulated in human cancer and appear to alter the response of tumour cells to immune surveillance, anticancer drugs and oxidative stress (reviewed in (Sarto et al., 2000b)). In support of our data, Hsp27 is overexpressed in invasive ductal carcinomas of the breast (Sarto *et al.*, 2000b) and protects cells against oxidative stress through p38-dependent phosphorylation and cytoskeletal modulation (Dalle-Donne et al., 2001).

Interestingly, CypA contains only free thiols, and so the increased labelling observed suggests that a more complex mechanism of redox modulation. One possibility is that H_2O_2 may cleave a disulphide bond between CypA and another protein. In support of this, CypA has been shown to bind to and promote the antioxidant activity of the peroxiredoxins (Lee, 2001). The modulation of these molecular chaperones by H_2O_2 is likely to affect protein folding and may trigger the unfolded protein response (UPR) that modulates expression of ER chaperones such as BiP/Grp78 and the protein disulphide isomerase PDI/ERp60. Thus H_2O_2 may allow cells to tolerate the accumulation of unfolded proteins (Lee, 2001). It is of interest that BiP/GRP78 has been shown to play an important role in the UPR by providing cytoprotection from H_2O_2 in a mechanism involving activation of ERK1/2 signalling (Hung et al., 2003). In correlating with previous blotting results, H_2O_2 was found to activate the ERK 1/2 signalling in the HB4a and C3.6 cell system.

Isoforms of several redox regulatory proteins (GSTπ, Prxn3, Prxn6, Rho-GDP-dissociation inhibitor 1 (RhoGDI1) and dihydrolipoamide dehydrogenase) were also altered by ErbB-2 overexpression, although data from 1D immunoblotting of total protein expression did not particularly agree with that from ICy labelling data. Again, this indicates that direct oxidative modification which does not alter protein abundance. However, the prescence of differentially labelled multiple isoforms cannot be resolved by 1DE so the effect on isoform distribution could not be observed. Dysregulated expression (mostly up-regulation) of Prxns has been observed in human cancers, including breast cancer. Such changes have been connected with a protective role against anti-tumour agents and oxidants, and have even been reported to promote cell proliferation and tumour progression (Noh et al., 2001;Shen and Nathan, 2002). Whilst changes in Prxn expression and redox signalling may contribute to the hyperproliferative phenotype observed in the C3.6 cells (Timms *et al.*, 2002), down-regulation of 14-3-3σ, a negative regulator of cell proliferation (Table 4-1B) could also have an important effect. Indeed, and in agreement with our findings, 14-3-3σ expression has been shown to be down-regulated in a significant proportion of primary breast carcinomas examined (Vercoutter-Edouart et al., 2001), and it is tempting to speculate that ErbB-2 overexpression may directly cause this down regulation.

RhoGDI functions to inhibit the activity of the Rho-family of small GTPases by directly preventing the exchange of GDP for GTP by guanine exchange factors (GEFs), by preventing intrinsic and RhoGAP mediated GTP hydrolysis and by keeping Rho/Rac in the cytoplasma (Adra et al., 1997). Thus, RhoGDI can inhibit cell motility by inhibiting the activity of Rho proteins. RhoGDI overexpression has been shown to increase the estrogen receptor transcription level (Su et al., 2001) and the expression of the estrogen receptor directly inhibits breast cancer cell motility and invasion (Lazennec et al., 2001). These studies suggest that RhoGDIs play an important role in cancer cell motility. The data here in (Table 4-1) show that the observed increased labelling of RhoGDI in the HB4a cells with no significant difference in protein level measured by immunoblotting (Figure 4-14). Thus, ErbB-2 signalling could control cell motility via a mechanism involving the altered thiol accessibility of RhoGDI.

4.6 Identification of ICy dye labelled residues by MALDI-TOF-MS

It was reasoned that it would be possible to identify the specific sites of cysteine redox modification by identifying peptides that were labelled with ICy dye. Therefore all MS database searches were conducted with the inclusion of the ICy3 (510 Da) and ICy5 (508 Da) modification. However, this search revealed only a few modified peptides with high confidence. Two of the examples were Prxn6 and GAPDH, which were labelled at Cys90 and Cys246, respectively (Figure 4-16). Whilst these are not the active site cysteines of these redox-sensitive enzymes (Lind *et al.*, 2002;Wood *et al.*, 2003), they are accessible to labelling, corroborating our theory of how the labelling of some protein isoforms can be increased (i.e. an oxidation-dependent shift in p*I* with labelling of the shifted form at additional sites). It is important to note that the unlabelled forms of these peptides were also identified, suggesting that labelling is sub-stoichiometric or that the dye moiety was lost during ionisation. The poor recovery of labelled peptides in general may possibly be due to their lowered solubility and hence inefficient extraction of peptides from gel pieces. In support of this, other work in the laboratory showed that model peptides labelled in solution performed well in MALDI-TOF MS. Further refinements to the extraction procedures were carried out including extraction of peptides from gel pieces using higher percentages of acetonitrile (50% or 70%), and trifluoroacetic acid (5% or 10%), with or without sonication. However, these different extraction strategies did not improve the ability to identify dye-labelled peptides.

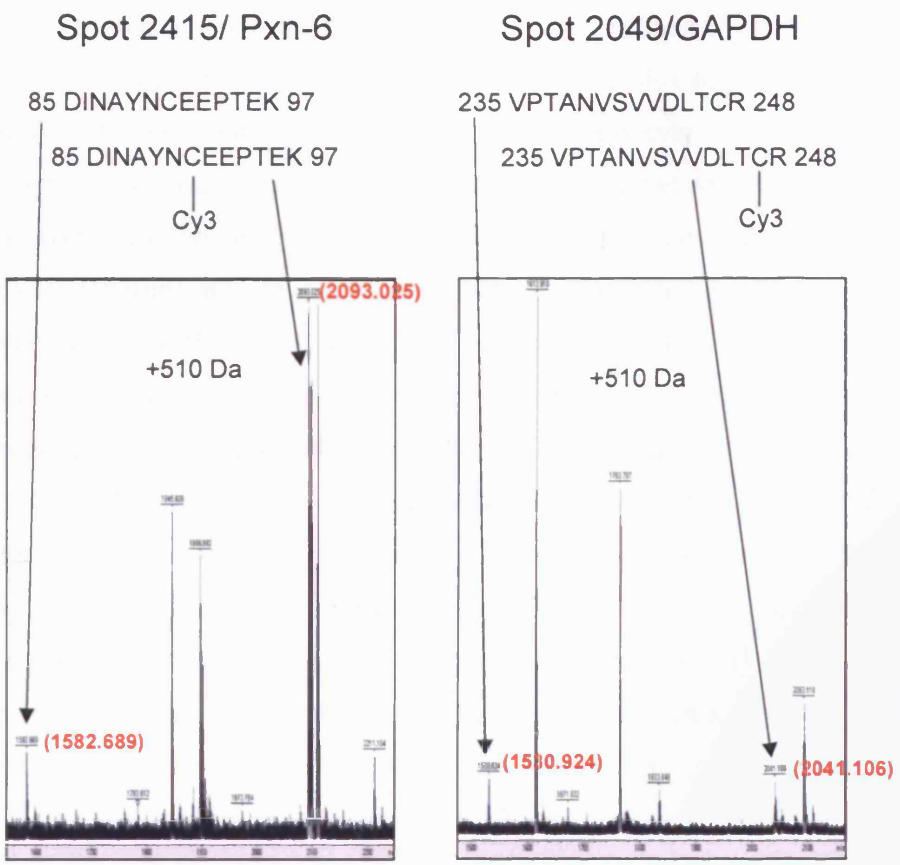

(Figure 4-16) Identification of ICy-modified cysteine residues by MALDI-TOF-MS. MALDI-TOF-MS spectra are shown for ICy-modified peptides of Prxn6 and GAPDH from the ICy 2D-DIGE analysis. The molecular weights of ICy3-modified peptides are 510 Da higher than the corresponding unmodified peptides.

4.7 Effect of H_2O_2 on dye integrity

As part of the 2D-DIGE analytical strategy, gels were post-stained with silver, which was subsequently removed prior to in-gel digestion and MS analysis using 1% H_2O_2 treatment (approximately 300 mM) (Gharahdaghi et al., 1999). However, 1% H_2O_2 (300 mM) treatment might also oxidise and damage the dyes on labelled proteins leading to problems in identifying labelled peptides by MS. Based on this hypothesis, the effect of H_2O_2 on ICy3/5 labelling was investigated. Firstly, the indicated concentration of ICy3 and ICy5 were treated with 1% H_2O_2 at room temperature for 10 min, the duration used for removing silver stain prior to in-gel digestion. Subsequently, the absorbance at 553 and 648 nm were recorded for the ICy3 samples and ICy5 samples, respectively (Figure 4-17A). Similarly, the fluorescence excitation/emission wavelengths of 532/580 nm and 633/680 nm were used to detect fluorescence from the ICy3 and ICy5 samples, respectively. Both measurements indicated that 1% H_2O_2 caused damage to ICy3, reducing its absorbance and fluorescence emission by approximately 40%. ICy5 was more severely affected and only 10-20% of the ICy5 signal remained after treatment. MALDI-TOF-MS analysis of the H_2O_2-treated dyes indicated that the 636 Da ICy5 signal nearly disappears, whilst the 638 Da signal of ICy3 was no significant change after H_2O_2 treatment (Figure 4-17B). According to these observations, the process of silver destaining to improve MALDI-TOF-MS identifications of proteins damages the ICy molecules, presumably through oxidation and breakage of the ring structure of these dyes and would lead to loss of observable dye-modified peptides. For this reason, this step was omitted in subsequent analyses or CCB post-staining was used instead. It is important to note that the concentration of H_2O_2 used for destaining is >600 times higher than that used for induction of oxidative stress in cells, such that damage to the dyes in lysates would not occur.

A

ICy3

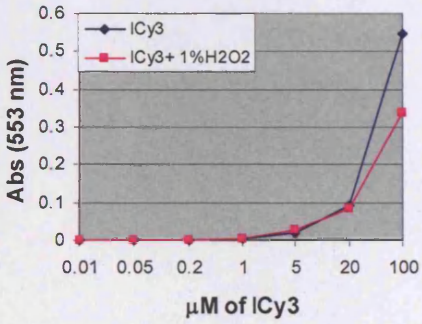
ICy3
ICy3+ 1%H2O2
Abs (553 nm)
0.6
0.5
0.4
0.3
0.2
0.1
0
0.01 0.05 0.2 1 5 20 100
µM of ICy3

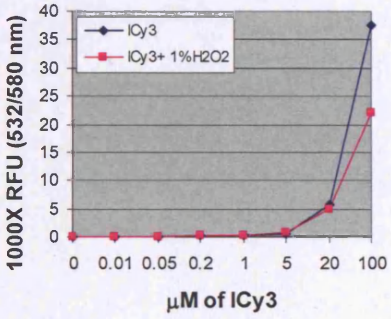
ICy3
ICy3+ 1%H2O2
1000X RFU (532/580 nm)
40
35
30
25
20
15
10
5
0
0 0.01 0.05 0.2 1 5 20 100
µM of ICy3

ICy5

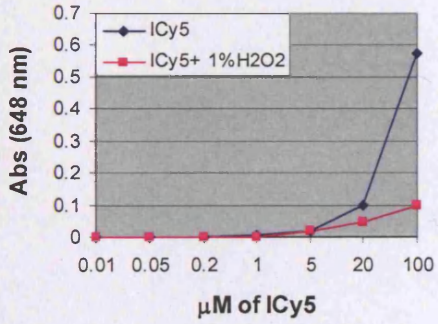
ICy5
ICy5+ 1%H2O2
Abs (648 nm)
0.7
0.6
0.5
0.4
0.3
0.2
0.1
0
0.01 0.05 0.2 1 5 20 100
µM of ICy5

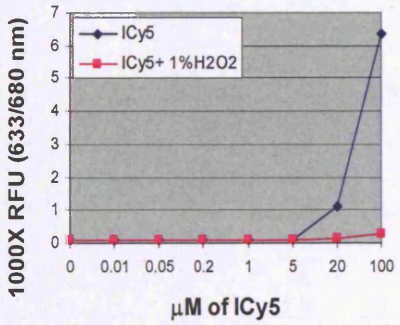
ICy5
ICy5+ 1%H2O2
1000X RFU (633/680 nm)
7
6
5
4
3
2
1
0
0 0.01 0.05 0.2 1 5 20 100
µM of ICy5

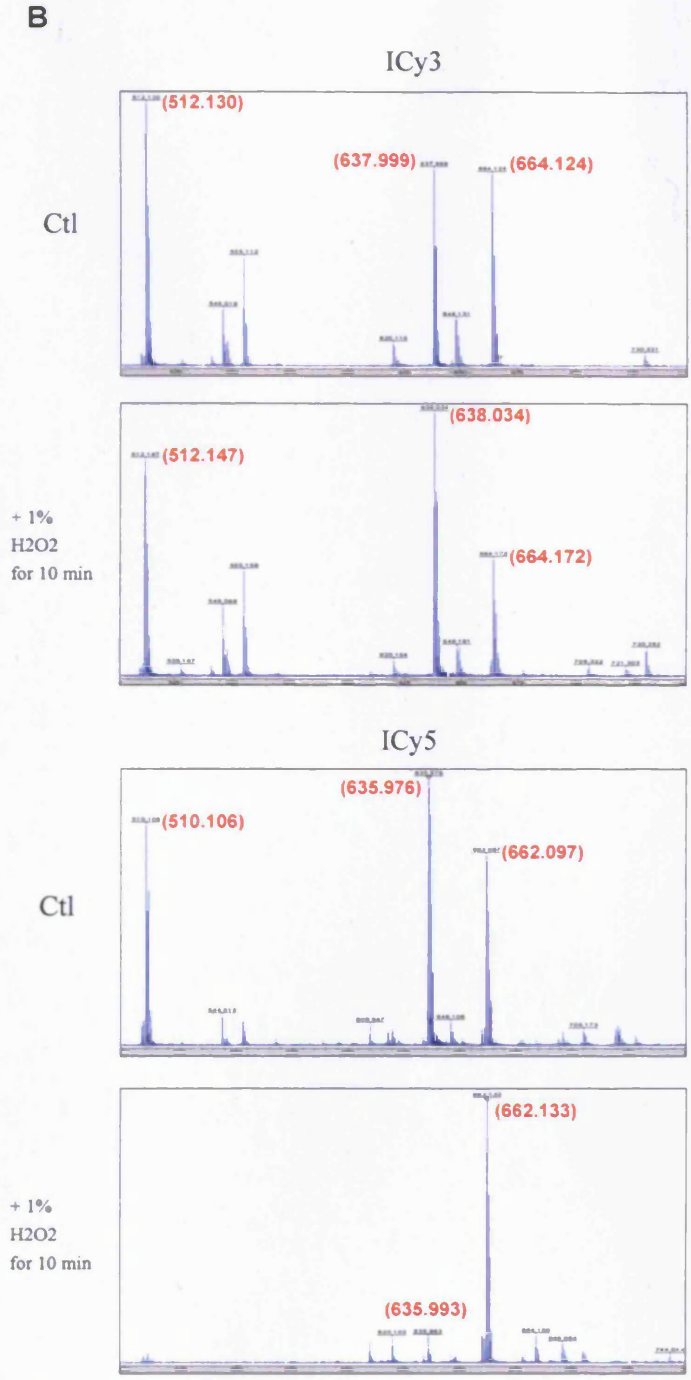

(Figure 4-17) The Effect of H_2O_2 on ICy3 and ICy5 integrity. **(A)** 60 µl of the indicated concentrations of ICy3 and ICy5 were treated with 1% H_2O_2 at room temperature for 10 min or left untreated. The absorbance at 553 and 648 nm were recorded for ICy3 and ICy5 samples, respectively. The fluorescence of the H_2O_2–treated and untreated dyes were measured at excitation/emission wavelengths of 532/580 nm and 633/680 nm for ICy3 and ICy5, respectively. **(B)** 1 pmol of ICy3 and ICy5 were treated with 1% H_2O_2 at room temperature for 10 min. After mixing with 1 µl of DHB matrix, spectra were acquired by MALDI-TOF-MS on an Ultraflex instrument calibrated with Calmix 2.

4.8 Analysis of H_2O_2-induced and ErbB-2 dependent protein changes by NHS-lysine labelling 2D-DIGE.

According to the previous cysteine 2D-DIGE analysis (Table 4-1), two differentially labelled isoforms of peroxiredoxin 6 were observed that are likely to represent different oxidative states; one reduced form and one oxidized (sulfenic/sulfinic/sulfonic) form. In order to corroborate this and other findings, lysine 2D-DIGE was applied to analyses changes in protein level due to oxidative stress.

Thus, a minimal-NHS-Cy dye lysine labelling 2D-DIGE experiment was performed where triplicate cultures of HB4a and C3.6 cells were treated with 0.5 mM H_2O_2 for 20 and 240 minutes or left untreated. This experimental design would allow the simultaneous examination of significant changes due to ErbB-2 overexpression and H_2O_2 treatment, and provide gels for the excision of protein spots for MS identification. Three biological triplicate sets of samples were run on 9 gels using a Cy2-labelled standard consisting of a mixture of all samples, and 27 fluorescent images were captured (Figure 4-18). DeCyder BVA analysis showed 138 significant changes in labelling across the different conditions (>1.5-fold up or down regulated; $p<0.05$) (Figure 4-19). Of these, 117 could be aligned to corresponding CCB stained spots (Figure 4-20) and 53 (45%) of them were identified by MALDI-TOF-MS representing 38 gene products (Table 4-2). The other 64 (55%) could not be identified due to low sequence coverage or low MS signals. Comparison between the ICy and NHS-Cy dye-labelling approaches revealed 18 common identities, representing isoforms of 11 individual gene products. In most cases, these displayed the same direction of altered expression, indicating that the ICy dyes were detecting changes in abundance for these proteins.

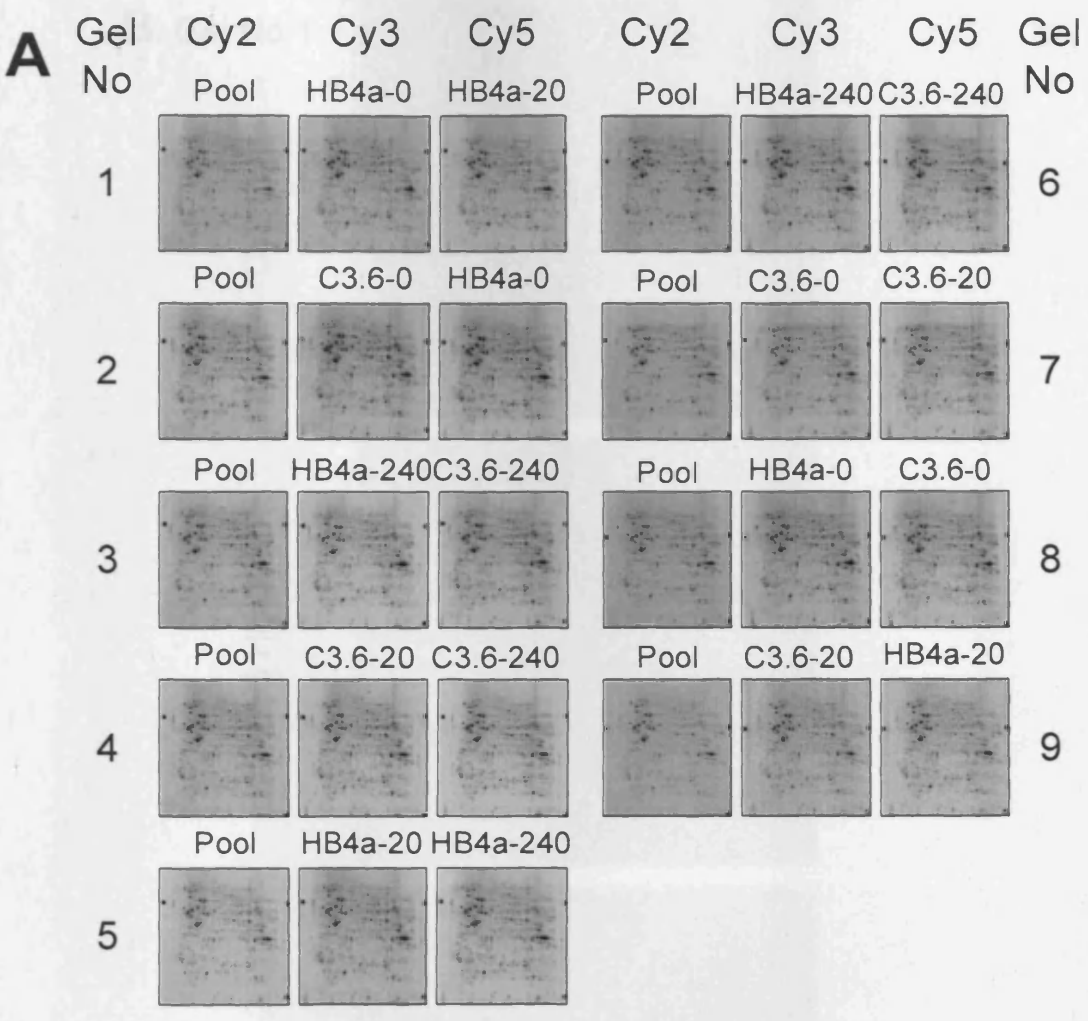
A
Gel No
Cy2
Cy3
Cy5
Cy2
Cy3
Cy5
Gel No
Pool
HB4a-0
HB4a-20
Pool
HB4a-240
C3.6-240
1
6
Pool
C3.6-0
HB4a-0
Pool
C3.6-0
C3.6-20
2
7
Pool
HB4a-240
C3.6-240
Pool
HB4a-0
C3.6-0
3
8
Pool
C3.6-20
C3.6-240
Pool
C3.6-20
HB4a-20
4
9
Pool
HB4a-20
HB4a-240
5

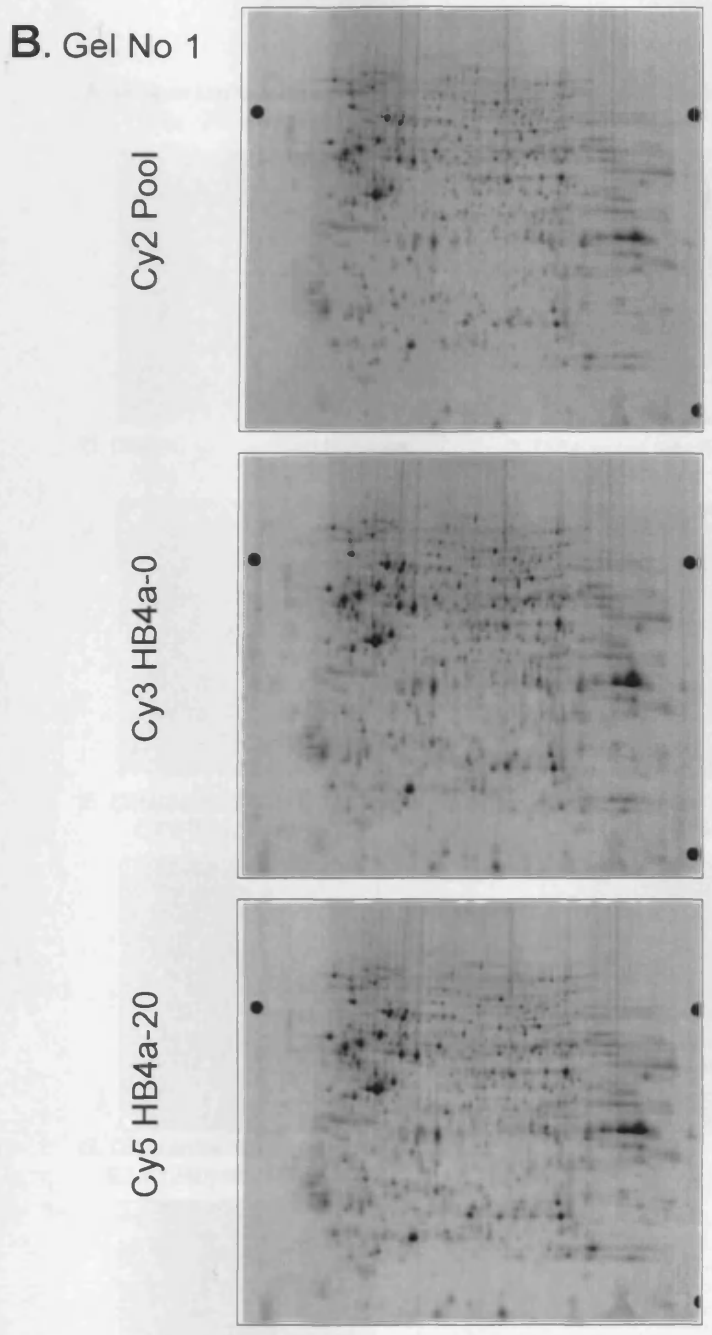

(Figure 4-18) Representation of the experimental design and images obtained in the analysis of the proteomic response to H_2O_2 treatment in HB4a and C3.6 cells using NHS-Cy 2D-DIGE. (A) Randomly growing HB4a and C3.6 cells were treated with 0.5 mM H_2O_2 for 20 and 240 min and compared to the untreated samples. Lysates were prepared and labelled with NHS-Cy3 or NHS-Cy5 and compared to an internal standard representing pooled aliquots of each sample labelled with NHS-Cy2. Samples were run in triplicate for statistical analysis and to assess reproducibility. This represents 9 gels with 27 images generated. Gel images were processed using the BVA module of DeCyder software. One of the image sets in **(A)** are shown in **(B)** with representative enlarged images.

A. Differential labelling between HB4a (20) and HB4a (0)

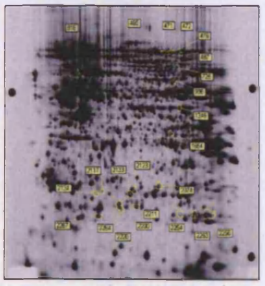

B. Differential labelling between HB4a (240) and HB4a (0)

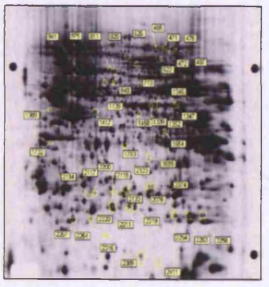

C. Differential labelling between C3.6 (20) and C3.6 (0)

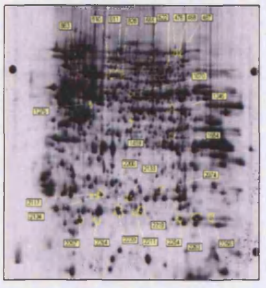

D. Differential labelling between C3.6 (240) and C3.6 (0)

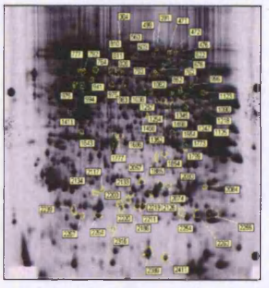

E. Differential labelling between C3.6 (0) and HB4a (0)

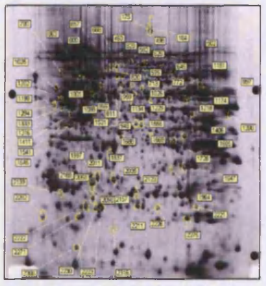

F. Differential labelling between C3.6 (20) and HB4a (20)

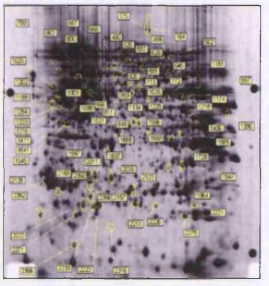

G. Differential labelling between C3.6 (240) and HB4a (240)

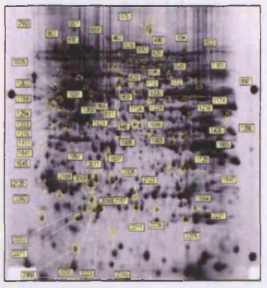

(Figure 4-19) Differential protein expression in HB4a vs. C3.6 cells and H_2O_2-induced differences. Representative Cy dye images of H_2O_2 treated/non-treated HB4a and C3.6 cells are shown. Protein features with altered expression across the time course or between cell lines are labelled with the master spot identity numbers. All of the images in this figure are presented in Appendix I with representative enlarged images.

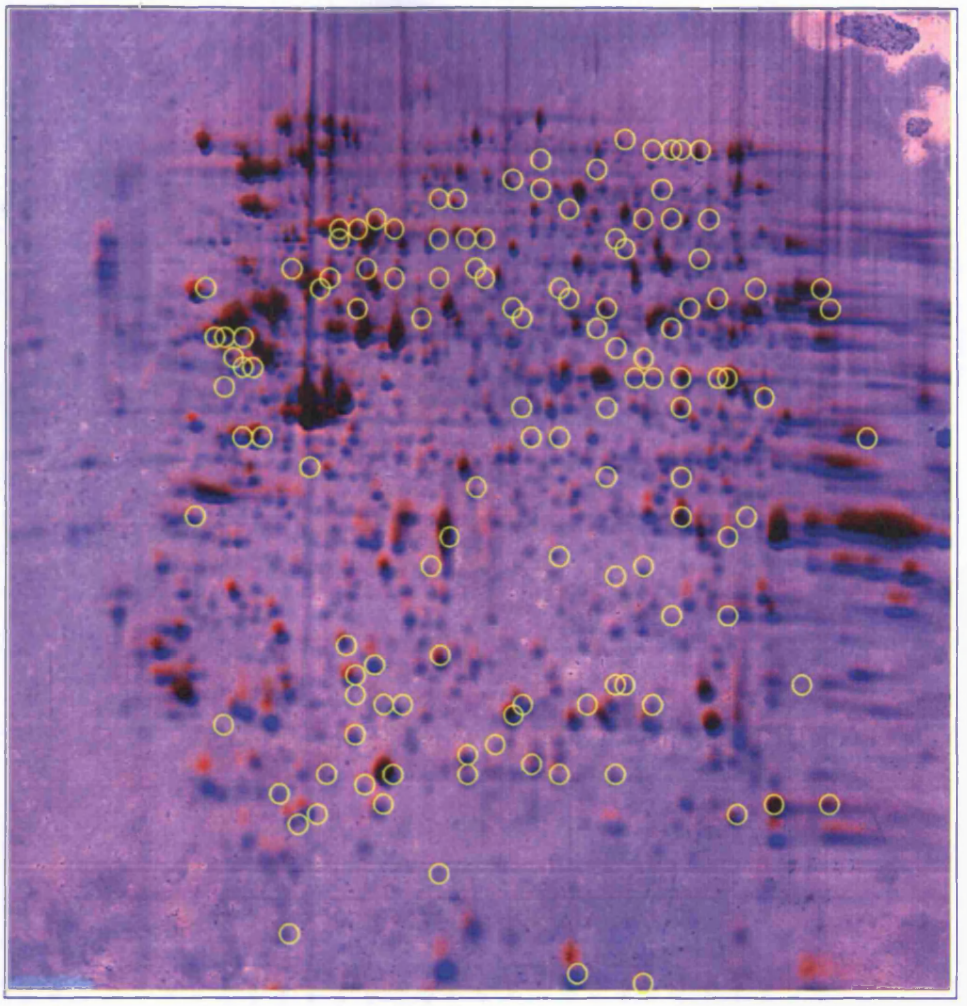

(Figure 4-20) Master gel image of NHS-Cy2 labelled standard pool and its corresponding colloidal coomassie blue stained image. The image shown is a merged image of the NHS-Cy2 labelled HB4a/C3.6 cell lysate pool (red) and the corresponding colloidal coomassie blue stained gel (blue) created using Adobe Photoshop software. The yellow circled spots indicate aligned differentially labelled spots that were excised for further identification.

A

Spot No.	Protein Name	% Cov	Mowse Score	Est. mass	Est. pI	Pred. Mass	Pred. pI	Accession No.	Average fold-difference † and *p*-value: 4a(20') to 4a(0)	*P*-value	4a(240') to 4a(0)	*P*-value	3.6(20') to 3.6(0)	*P*-value	3.6(240') to 3.6(0')	*P*-value	Function
391	2-OGDH	27	104/64	110000	7.2	114601	8	1352618	-1.03	0.79	-1.15	0.17	1	0.98	-1.52	0.0015	TCA cycle enzyme/Oxidative metabolism
1123	Cytokeratin 8A	30	104/64	60000	8	59914	8.1	46812692	1.13	0.014	1.53	0.0011	1.07	0.0081	1.66	0.00021	Cytoskeleton
1090	Dihydrolipoyl dehydrogenase	35	100/64	55000	7.8	54713	7.6	51095146	-1.09	0.2	-1.35	0.038	-1.11	0.12	-1.67	0.0017	Component of pyruvate dehydrogenase
471	Elongation factor 2[a]	13	67/64	95000	7.1	96246	6.4	119172	5.09	0.021	4.39	0.00013	5.55	0.00002	3.53	0.000096	Protein synthesis
472	Elongation factor 2[a]	21	75/66	95000	7.2	96246	6.4	119172	3.19	0.0089	2.53	0.000026	3.12	0.0011	2.7	0.0018	Protein synthesis
476	Elongation factor 2[a]	37	157/64	95000	7.3	96246	6.4	119172	2.24	0.031	1.67	0.0007	2.23	0.00036	1.62	0.0023	Protein synthesis
468	Elongation factor 2[a]	27	83/64	95000	7.4	96246	6.4	119172	-1.34	0.028	-1.25	0.01	-1.5	0.011	-1.28	0.025	Protein synthesis
487	Elongation factor 2[a]	39	169/64	95000	7.5	96246	6.4	119172	-2.48	0.00085	-2.25	0.00013	-3.27	0.000059	-2.93	0.000056	Protein synthesis
1345	Enolase alpha[a]	41	125/64	47000	7.3	47481	7	29792061	1.34	0.033	1.46	0.0042	1.52	0.0062	1.94	0.0016	Glycolysis
1347	Enolase alpha[a]	76	228/64	47000	7.5	47481	7	29792061	-1.15	0.028	-1.59	0.0012	-1.26	0.014	-1.82	0.00099	Glycolysis
994	HSP-60	57	247/64	60000	5.5	61187	5.7	31542947	1.07	0.48	-1.07	0.5	-1.1	0.36	-1.89	0.0012	Protein folding
764	HSP-70 protein 9B[a]	66	317/64	70000	6	73920	5.9	24234688	-1.09	0.015	-1.22	0.015	-1.11	0.021	-1.78	0.00018	Protein folding
777	HSP-70 protein 9B[a]	31	118/64	70000	5.6	73920	5.6	24234688	1.06	0.71	1.38	0.07	-1.01	0.92	1.7	0.0018	Protein folding
713	HSP-71	55	204/64	70000	6.5	71082	5.7	16741727	1.19	0.063	1.57	0.0038	-1.15	0.0036	-1.2	0.007	Protein folding
1777	Lactate dehydrogenase B[a]	56	236/64	37000	6	36801	5.7	49259212	-1.04	0.0047	-1.4	0.005	-1.1	0.0017	-1.74	0.00085	Glycolysis (regeneration of NADH)
725	Lamin A/Ca	57	206/24	70000	6	70903	6.6	27436948	-1.58	0.017	-1.28	0.15	-1.43	0.0027	-1.44	0.00078	Nuclear protein for mitosis
863	L-plastin[a]	56	245/64	70000	5.5	70815	5.2	4504965	-1.43	0.000045	-1.34	0.011	-2.64	0.0001	-1.4	0.0038	Actin binding protein
503	NRAS-related protein	32	115/64	85000	6.5	80046	6.2	16356661	-1.03	0.62	-1.21	0.025	-1.03	0.8	-1.54	0.0051	Ras oncoprotein
2256	Peroxiredoxin 1[a]	75	183/64	23000	8.5	22324	8.3	32455266	-4.91	0.027	-5.83	0.00034	-6.54	0.000072	-9.83	0.00000026	Cellular protection from oxidative stress
2263	Peroxiredoxin 1[a]	74	157/64	23000	8.3	22324	8.3	32455266	5.17	0.014	4.77	0.00019	5.64	0.000077	6.17	0.000059	Cellular protection from oxidative stress
2267	Peroxiredoxin 2 isoform b	37	73/64	20000	5.5	16036	6.1	33188452	11.71	0.0058	9.38	0.000026	8.57	0.00032	8.8	0.00032	Cellular protection from oxidative stress
2264	Peroxiredoxin 2[a]	58	190/64	22000	5.8	21892	5.7	2507169	-9	0.0014	-4.14	0.0001	-8.15	0.00015	-7.39	0.0000044	Cellular protection from oxidative stress
2211	Peroxiredoxin 3 isoform b	28	84/64	26000	7	25839	7	32483377	-4.03	0.00056	-4.11	0.00012	-3.04	0.0000037	-3.83	0.000000088	Cellular protection from oxidative stress
2123	Peroxiredoxin 6[a]	82	160/64	27000	6.2	25035	6	1718024	-1.85	0.0073	-1.74	0.0011	-1.41	0.0017	-1.01	0.0048	Cellular protection from oxidative stress
2133	Peroxiredoxin 6[a]	47	87/64	27000	6	25035	6	1718024	9.54	0.0082	9.19	0.000063	12.42	0.00005	13.9	0.000036	Cellular protection from oxidative stress
2074	Phosphoglycerate mutase 1	53	102/64	28000	7	28931	6.8	49456447	-1.82	0.00021	-1.73	0.00056	-3.77	0.000021	-3.97	0.00005	Glycolysis
2076	Phosphomannomutase 2	35	71/64	28000	6.5	28406	6.4	4557839	-1.48	0.012	-1.51	0.0089	-1.42	0.0052	-1.55	0.018	Protein glycosylation
1352	Sorting nexin 5	43	100/64	47000	6.8	47072	6.3	23111047	1.19	0.0018	2.08	0.000027	1.26	0.017	2.5	0.000063	intracellular trafficking
762	TNFR 1 asso. proteina	43	162/64	70000	8.3	70618	8	1082886	-1.13	0.0099	-1.33	0.0093	1.04	0.012	-2.11	0.0014	Cytokine involved inflammatory

B

Spot No.	Protein Name	% Cov	Mowse Score	Est. mass	Est. pI	Pred. Mass	Pred. pI	Accession No.	Average fold-difference † and *p*-value: 3.6 (0') to 4a(0')	*P*-value	3.6 (20') to 4a(20')	*P*-value	3.6 (240') to 4a(240')	*P*-value	Function
1202	Cytokeratin 13A	45	161/64	50000	5	49898	4.9	24234696	1.63	0.000071	1.54	0.0016	1.79	0.0000079	Cytoskeleton
1316	Cytokeratin 17[a]	54	219/64	40000	5	40520	4.9	47939651	2.36	0.0038	2.05	0.019	2.37	0.00095	Cytoskeleton
1541	Cytokeratin 19	44	161/64	45000	4.8	44079	5	417200	-1.56	0.0062	-1.6	0.0041	-1.43	0.008	Cytoskeleton
1545	Cytokeratin 19[a]	82	325/64	45000	4.9	44079	5	417200	-1.61	0.00089	-1.82	0.0001	-1.61	0.001	Cytoskeleton
1088	FK506-binding protein 4	35	65/64	52000	5.8	52057	5.4	4503729	-1.65	0.00067	-1.51	0.047	-1.89	0.0017	Immuno-regulation/protein folding (PPIase)
2221	Flavin reductase (NADPH)	55	65/64	24000	8	22219	7.1	32891807	-1.57	0.0095	-1.29	0.19	-1.32	0.009	Protection from oxidative stress/iron metabolism
1406	Fumarate hydratase	43	114/64	50000	8.5	54773	8.8	32880021	1.63	0.0028	1.63	0.0005	1.5	0.0027	TCA cycle enzyme
1294	Rb-binding protein p46[a]	44	142/64	50000	5	48132	5.2	4506439	-1.73	0.00095	-2.35	0.011	-3.41	0.023	Suppression of proliferation
2223	Glutathione S-transferase pi	69	179/64	25000	5.5	24678	5.7	121746	-1.94	0.00054	-2.05	0.00033	-1.84	0.00014	Regulation of cellular redox state
800	HSP-70	52	136/64	70000	6	70263	5.6	32879973	-1.57	0.0018	-1.77	0.00044	-1.92	0.0015	Protein folding
713	HSP-71	55	204/64	70000	6.5	71082	5.7	16741727	2.07	0.00032	1.51	0.00039	1.1	0.16	Protein folding
2366	Human eIF1[a]	50	75/60	16000	5.5	16433	5.1	7546515	1.51	0.013	1.62	0.00071	1.67	0.00079	Protein synthesis
1688	Isocitrate dehydrogenase 3	30	78/64	40000	6.5	40022	6.5	5031777	1.67	0.0013	1.63	0.0062	1.31	0.0051	TCA cycle enzyme
863	L-plastin[a]	60	260/64	70000	5.5	70815	5.2	4504965	3.32	0.000038	1.79	0.00024	3.19	0.00045	Actin bundling protein
592	Mito. Inner memb. Protein[a]	29	84/64	85000	7	84026	6.1	12803209	1.5	0.0074	1.47	0.00049	1.33	0.0017	Unknown
657	Myxovirus resistance protein 1	39	122/64	75000	6	75886	5.6	21619147	-4.88	0.0078	-7.99	0.00041	-6.86	0.0066	Anti-viral protein/IFN-induced
668	Myxovirus resistance protein 1	55	222/64	75000	6.3	75886	5.6	21619147	-10.01	0.000026	-6.7	0.00055	-12.92	0.000024	Anti-viral protein/IFN-induced
2211	Peroxiredoxin 3 isoform b	28	84/64	26000	7	25839	7	32483377	1.74	0.0017	2.3	0.0021	1.67	0.00056	Cellular protection from oxidative stress
2123	Peroxiredoxin 6	82	160/64	27000	6.2	25035	6	1718024	-1.99	0.0035	-1.51	0.00017	-1.16	0.073	Cellular protection from oxidative stress
1025	Protein disulfide-isomerase	63	236/64	57000	4.8	57117	4.8	1085373	-1.51	0.0078	-1.58	0.00053	-1.41	0.0072	Disulfide bond formation/protein folding
1411	Thioredoxin domain containing 4	32	87/64	45000	5	47297	5	37183214	-1.73	0.0042	-2.21	0.00037	-2.06	0.0021	Protection from oxidative stress/protein folding
1134	Trp-tRNA synthetase isoform b	26	67/64	50000	6.3	48852	6	47419920	-1.67	0.0012	-1.59	0.0002	-1.7	0.0021	Protein synthesis
1001	Ub-specific protease 14	37	123/64	60000	5.6	61317	5.6	30583205	-1.59	0.00028	-1.68	0.0026	-1.54	0.0059	Unknown

(Table 4-2) Identification of H_2O_2- and ErbB-2-dependent differentially expressed proteins. **(A)** Proteins displaying H_2O_2-induced differential labelling in normal (HB4a) and ErbB-2-overexpressing (C3.6) human mammary luminal epithelial cells. **(B)** Proteins displaying differential labelling between HB4a and C3.6 luminal epithelial cells. Proteins were identified by MALDI-TOF peptide mass mapping (see Materials and Methods (Chapter 2)). [a]Proteins identified in two or more independent experiments. Proteins appearing more than once in the tables were identified as isoforms with different p*I*s. The % coverage of analysed peptides, the MOWSE score from Mascot searches and the significance threshold score, the estimated mass and p*I* (from gels), the predicted mass and p*I* (from the database) and the NCBI gene identifier (Accession Number) are shown for each protein. MS spectra, MOWSE score histograms, matching peptides and sequence coverage for all proteins are shown in Appendix D. [†]Average fold-differences from DeCyder analysis show abundance ratios for treated HB4a cells versus untreated (4a(240') and 4a(20') versus 4a(0)), treated C3.6 cells versus untreated (3.6(240') and 3.6(20') versus 3.6(0)) and C3.6 versus HB4a at each timepoint(3.6(0') to 4a(0'), 3.6(20') to 4a(20') and 3.6(240') to 4a(240')). Proteins displaying an average fold-difference of $\geq$ 1.5-fold up (+) or down (-) regulation between pairs of conditions where $p<0.05$ and spots matched in all images are shaded grey. N. A. not analysed. Functions were ascribed from the NCBInr database and literature searches.

The lysine labelling results showed that 30 of the 53 identified proteins displayed peroxide-dependent changes (Table 4-2A) and the other 23 ErbB-2-correlated changes (Table 4-2B). All of the identified features are shown in Figure 4-21. As expected, 7 of the 23 ErbB-2- correlated proteins were matched with those from a previous analysis of these cell lines from our laboratory (Gharbi *et al.*, 2002) where a similar lysine labelling 2D-DIGE and MALDI-TOF-MS was used to identify ErbB-2 correlated differential expression. These proteins include myxovirus resistance protein 1, HSP-70, L-plastin, ubiquintin carboxyl hydrolase 14, FK506-binding protein 4 and cytokeratin 17. Whilst a higher overlap of identifications might be expected from these two studies, differences in gel resolution, the fact that not all differentially expressed features were identified and the way the cells were grown (serum-starved in the previous study versus grown in the presence of serum in this study) may account for the low overlap.

The differentially expressed proteins identified by NHS-Cy labelling and MS were again involved in redox regulation, protein folding, proliferative suppression, glycolysis and the cytoskeleton, suggesting that these cellular functions are the major targets of redox stress and ErbB-2 overexpression. In addition, four citrate (TCA) cycle enzymes were modulated, including dihydrolipoamide dehydrogenase, which possesses a redox-active disulphide bond at its active site, and four proteins involved in protein synthesis. Importantly, Prxns 1, 2, 3 and 6 were again identified and three (Prxn-1, Prxn-2 and Prxn-6) were identified in doublet spots (Figure 4-21 and Table 4-2A). Interestingly, all of the basic spots of the doublets became less intense and the acidic spots more intense after hydrogen peroxide treatment. Since MALDI-TOF-MS and database searching gave high confidence hits for both proteins in the spot pairs, this shows that the difference in intensity between the two spots is due to a post-translational modification. The study of Wagner et al. and Rabilloud et al. (Wagner *et al.*, 2002;Rabilloud et al., 2002b) also found doublets for the Prxns by 2DE and MALDI-TOF-MS which changed in a similar manner to that observed here following oxidative stress. Further analysis showed that the bacic spot is the native Prxn while the acidic spot corresponded to the sulfinic or sulfonic form of each Prxn. Thus, we can infer that the basic spots in the doublet of Prxn-1, Prxn-2 and Prxn-6 are the native forms of the enzymes and that the acidic spots in the doublet correspond to the sulfenic, sulfinic or sulfonic forms. In addition, elongation factor 2 and

enolase alpha also existed as multiple isoforms, where the more acidic isoforms were up-regulated by H_2O_2 treatment, suggesting that both of them may be oxidized and shifted in p*I*. It is likely that such modifications would affect protein translation and glycolysis, respectively. Differences were also detected in the response of several proteins isoforms to H_2O_2 in the two cell lines. These included Hsp73/71, Prxn-6 and L-plastin (Table 4-2A); differences which are likely to reflect their altered abundance in the ErbB-2 overexpressing cells (Table 4-2B). In summary, these data show the complexity of the response of epithelial cells to redox stress and the effect that ErbB-2 overexpression has on these responses.

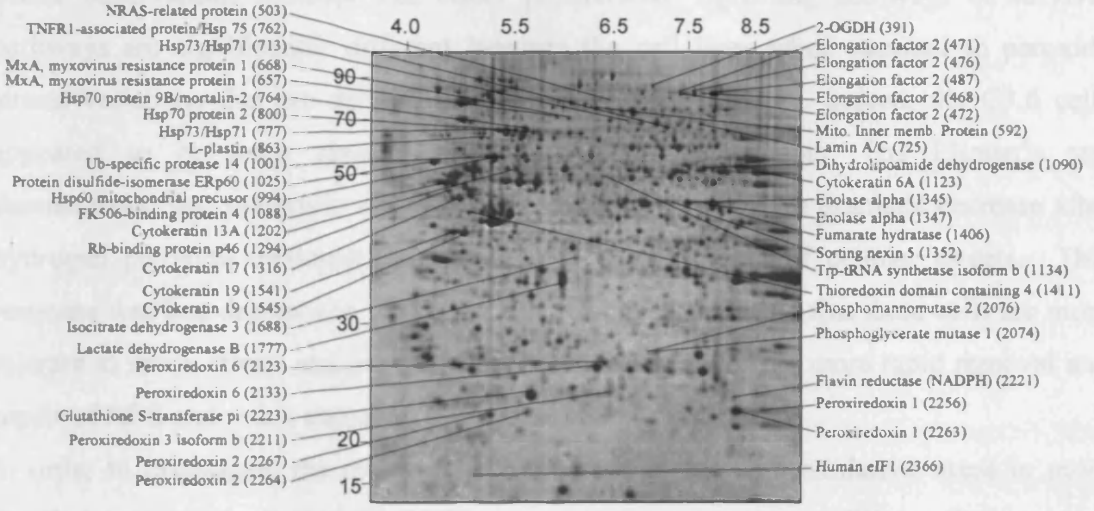

(Figure 4-21) 2DE migration of proteins identified by MALDI-TOF-MS displaying H_2O_2-induced and/or ErbB-2 dependent differential expression (see Table 4-2). An NHS-Cy-dye image is shown with the identified proteins.

4.9 Conclusions

In experiments to assess the response of epithelial cells to oxidative stress and ErbB-2 overexpression, the activation of certain signalling molecules was firstly examined. The results demonstrated that the responses between HB4a and C3.6 cells to hydrogen peroxide were significantly different. More proteins and a greater degree of tyrosine phosphorylation were observed in the HB4a versus C3.6 cells. Moreover, the stress protein kinase, p38, was fully activated in 5 minutes after H_2O_2 treatment in HB4a, but not until 20 minutes in C3.6 cells. Both the MAP kinase and PI3Kinase pathways were activated after H_2O_2 treatment in both cell lines. Interestingly, MnSOD, which generates cellular hydrogen peroxide from superoxide, exhibited lower expression in the C3.6 cells. These observations indicate that either proliferative signalling pathways or survival pathways are significantly different between the cell lines when exposed to peroxide stress, variations that are derived from ErbB-2 overexpression. Indeed, the C3.6 cells appeared to be more resistant to H_2O_2–induced cell death. The Ellman's test demonstrated that the levels of total free thiols in cells display a dramatic decrease after hydrogen peroxide treatment, consistant with the oxidation of cellular targets. This response was less dramatic in the C3.6 cells, which may indicate that these cells are more tolerant to redox stress, and have developed mechanisms for the more rapid removal and repair of ROS and redox damage.

In order to investigate the molecular changes associated with oxidative stress in more detailed, lysine and cysteine 2D-DIGE were used for expression profiling and to examine changes in thiol reactivity. This work showed that DIGE analysis could provide a sensitive, accurate and quantitative analysis of differential protein regulation in this model cell system. Reproducible and significant differences were detected both between the parental and ErbB-2 overexpressing cell lines and in responses to hydrogen peroxide treatment.

Cysteine labelling 2D-DIGE using iodoacetylated versions of the Cy dyes (ICy dyes) under non-reduced conditions, was employed to probe for targets of cellular oxidative stress (H_2O_2 treatment) in HB4a and C3.6 cells. Firstly, a timecourse of H_2O_2 treatment was carried out in the two cell lines revealing multiple differential ICy labelling between cell lines and with H_2O_2 treatment. Notably, very rapid (within 2 minutes) changes in

labelling were observed, indicative of thiol oxidation rather than changes in protein expression. A more detailed study using a 20 minute exposure to hydrogen peroxide was then carried out and proteins identified by MALDI-TOF-MS. In this study, the number of spots that could be matched between all gels was high, showing the reproducibility of the 2D-DIGE method. These experiments also showed the compatibility of ICy dye covalent labelling with subsequent identification by MALDI-TOF-MS, although some proteins could not be identified in most cases due to low protein abundance. Thus, whilst changes in thiol reactivity could be detected at a high level of sensitivity, the proteins could not be identified because of limitations in the sample preparation steps for MS. In one of three repeat experiments, the results showed that 126 gel features were significantly differentially labelled with a > 1.5 fold-increases or decreases in labelling ($P<0.05$) between the cell lines or in response to H_2O_2 treatment. 89 of these changes could be matched to their corresponding silver stained spots and these were picked from gels for MS identification. So far, 51 proteins have been identified using MALDI-TOF-MS. These identified proteins have functions in protein folding, redox regulation, cytoskeleton, proliferation and nuclear transport. In addition, 26 of these identified proteins were ErbB-2-dependent, such as Hsp-27, and some of them are related to the biological functions in cancer cell such as maspin precursor (protease inhibitor 5).

To validate the changes observed by DIGE, some of the proteins of interest were further investigated by 1-D and 2-D immunoblotting. The levels of many of the identified proteins did not correlate with the changes seen for ICy dye labelling, supporting the notion that H_2O_2 was acting by inducing changes in thiol reactivity instead of altering the protein level. However, the limited dynamic range of ECL used for immundetection and the lack of resolution of differentially charged isoforms by 1DE; made it difficult to correlate the data well. All of the proteins identified contain at least 1 free cysteinyl thiol group, demonstrating the specificity of labelling. However, very few ICy labelled peptides could be identified by MALDI-TOF-MS. This is possibly caused by the low solubility of dye-labelled peptides, the low efficiency of peptide extraction or the loss of the ICy dye label during ionization.

Modifications of cysteine residues can induce an increase or decrease in ICy dye labelling. The absence or reduction in labelling could be caused by glutathionylation or

oxidise cysteines to sulfenic, sulfinic or sulfonic forms/ the form of disulphides. In contrast, the gain or increase in labelling could have been induced by breakage of disulphides or by peroxide-induced shifts in p*I* and labelling of non-oxidised thiols on the p*I* shifted proteins. Support for the latter was seen in results from the lysine-labelling 2D-DIGE experiments where doublet spots for peroxiredoxins/ elongation factor 2/ enolase were found with the sulfinic/sulfonic acid forms of the proteins migrating to more acidic *p*I but still amenable to ICy dye labelling on additional sites. Finally, the identification of unique and shared gene products using both lysine labelling and cysteine labelling strategies helps to better define the biological changes associated with H_2O_2 stress and ErbB-2 overexpression and demonstrates the usefulness of 2D-DIGE for the study of post-translational modifications. However, in the absence of a 100% hit rate for MS protein identifications, it is still difficult to compare the relative contributions of changes in abundance versus changes in thiol reactivity using these methods.

Chapter 5 APPLICATION OF CYSTEINE-LABELLING 2D-DIGE AS A PROBE FOR GROWTH FACTOR DEPENDENT CHANGES IN THIOL ACCESSIBILITY AND OXIDATION

5.1 Introduction

In the previous chapter, the potential of the cysteine-labelling 2D-DIGE method was shown in an analysis the cellular targets of oxidative stress and ErbB-2 overexpression. In this chapter, the utility of the 2D-DIGE strategy for the analysis of EGF-induced changes in thiol reactivity and accessibility is assessed. As previously described, the ErbB receptor family of receptor tyrosine kinases is responsible for transferring extracellular stimuli in the form of growth factors to downstream intracellular signalling events.

The recruitment and activation of effector proteins to the receptor is an important step in the initiation of various downstream signalling cascades. This process involves a series of protein-protein interactions which include hydrophobic interactions, ionic interactions, covalent bond formation/breakage and hydrogen bond formation/breakage. It is possible that thiol accessibility could change during the process of signal transduction if specific thiol groups are located at the interface between interacting proteins. Thus, by labelling cysteinyl thiols with the ICy dye reagents under native conditions, it may be possible to monitor the dissociation and association of protein complexes, for example, in response to mitogen treatment. Thus, the work in this chapter was aimed at testing whether this strategy was feasible. It has also been shown that cysteinyl thiol groups play important roles in signal transduction through covalent changes in their oxidative status (Chapter 1). Indeed, a growing body of evidence suggests that endogenously generated H_2O_2 is required for growth factor signalling (see Introduction) (Lee et al., 2000;Park *et al.*, 2004;Kwon *et al.*, 2004). Thus, the second aim of this work was to establish whether mitogen stimulation produces changes in the redox status of proteins and to identify these targets using ICy dye 2D-DIGE and MS.

5.2 ICy dye differential labelling under native conditions and identification of EGF-induced changes

In order to apply cysteine labelling 2D-DIGE to study potential changes in thiol accessibility, native protein labelling conditions were developed. The normally used urea ICy dye labelling buffer replaced by a Nonidet P-40 (NP-40) lysis and labelling buffer (1% NP-40/10mM Tris pH 8.0/1 mM EDTA), which contains a mild non-ionic detergent that has minimal effect in the conformation of proteins. Experiments were performed to compare serum-starved HB4a cells with EGF-stimulated cells. A timepoint of 10 min was chosen to examine immediate growth factor signalling events and 1 nM EGF was used. This concentration is known to robustly stimulate mitogenic signalling events in these cells (Timms *et al.*, 2002). Cells were grown and treated in triplicate and lysed in the presence of ICy dye. ICy3- labelled individual samples were run against an equal load of ICy5-labelled standard pool consisting of an equal mixture of all 6 samples. Subsequently, urea-containing buffer was added and the samples reduced to improve sample solubility prior to 2DE. Although the resulting 2D images could still be scanned and analysed by DeCyder, there appeared to be an appreciable level of precipitation and aggregation of proteins/dyes particularly across the gel in the 50-60 kDa region and fewer spots could be resolved by this native 2D-DIGE labelling compare with denaturing 2D-DIGE (Figure 5-1). Two independent experiments were run with 6 gels and 12 fluorescent images were captured in each. In one of these experiments, 10 significant changes in labelling were identified (>1.3 fold up or down regulated; $p<0.05$) (Figure 5-2A and B). Post-staining with colloidal coomassie blue or silver and matching of the patterns to the corresponding fluorescent images allowed the picking of 6 gel features with confidence (Figure 5-2C), and 3 proteins were identified by MALDI-TOF peptide mass mapping with a mass accuracy set at +/-50 ppm (Figure 5-3). These 3 proteins were aldehyde reductase, annexin IV and peroxiredoxin 6. All of these proteins contained at least one cysteine in their protein sequence and displayed reduced ICy dye labelling following EGF treatment. This may suggest that these proteins are interacting with other proteins to protect their free thiols or are the targets of EGF-induced generation of oxidants.

Of note, the post-staining did not produce the apparent precipitation or aggregation in the 50-60 kDa region (Figure 5-2C), therefore, it must be a dye labelling phenomena and possibly due to the aggregation of dyes induced by NP-40 buffer.

This significant precipitation/dye aggregation problem resulted in the loss of some labelled features from the DeCyder analysis. Therefore, an extension of this study was performed using ICy labelling buffer with urea instead of NP-40 to compare EGF treated versus untreated HB4a total cell lysates. Under these denaturing conditions, potential EGF- induced changes in intermolecular accessibility would no longer be observed, however, EGF-induced thiol oxidative changes can still be investigated. The experimental design was the same as the previous experiment and ICy3-labelled EGF treated/untreated samples were run with against an equal load of ICy5-labelled standard pool consisting of an equal mixture of all samples. The precipitation problem was significantly improved and seven changes in labelling were determined by DeCyder analysis with the criteria of >1.3 fold up or down regulation with $p<0.05$ (Figure 5-4). Only two changes were found with a 1.5 fold cut-off (data not shown). Post-staining with colloidal coomassie blue stain and matching to the corresponding fluorescent images allowed picking of three gel features with confidence (Figure 5-4B), and two proteins were identified by MALDI-TOF peptide mass mapping (Figure 5-4). These two proteins were Rho-GDP dissociation inhibitor (GDI) and peroxiredoxin 6. Both of them displayed reduced ICy dye labelling after EGF treatment.

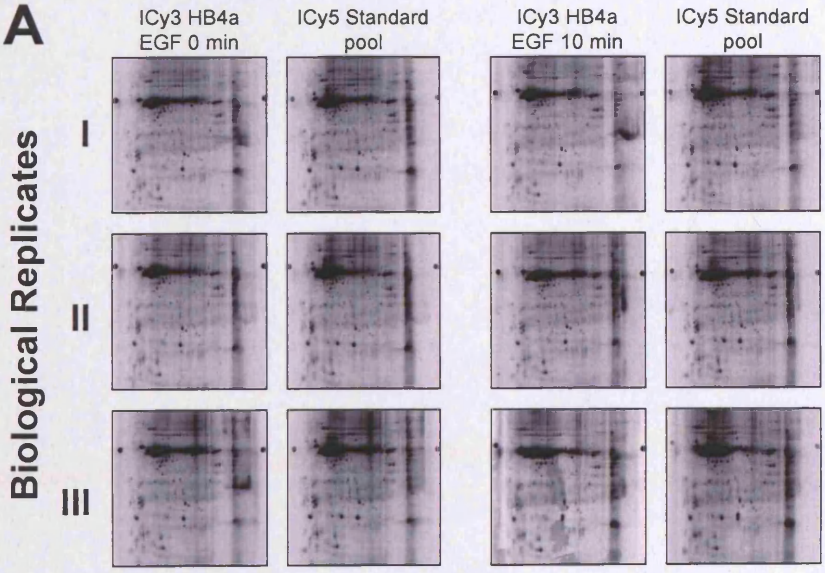

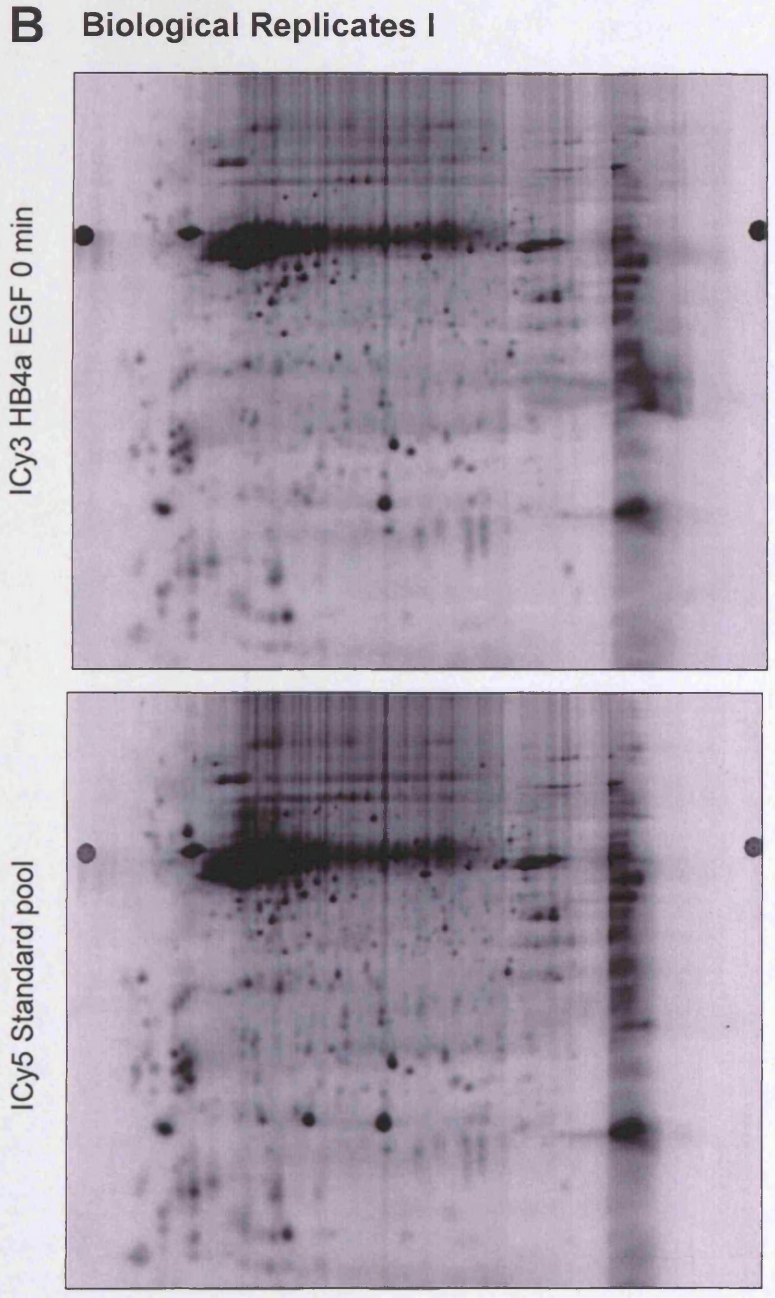

(Figure 5-1) Representation of the experimental design in the study of the thiol reactivity in HB4a cells in response to 1 nM EGF treatment using ICy dye labelling under native conditions. (A) Serum-starved HB4a cells were treated with 1nM EGF for 10 min or left untreated. Equal amounts of ICy5 labelled cell lysates (in 1% NP-40 native buffer) were mixed as an internal standard pool and run against ICy3-labelled lysates from untreated and EGF treated cells. Samples were run in triplicate as biological replicates for statistical analysis and to assess reproducibility. This represents 6 gels with 12 images generated. Gel images were processed using the BVA module of DeCyder software. All of the images in this figure are also presented in Appendix L with representative enlarged images. One of the image sets in (A) is shown in (B) as representative enlarged images.

A

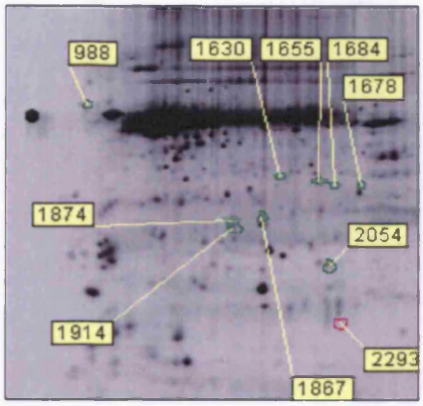

C

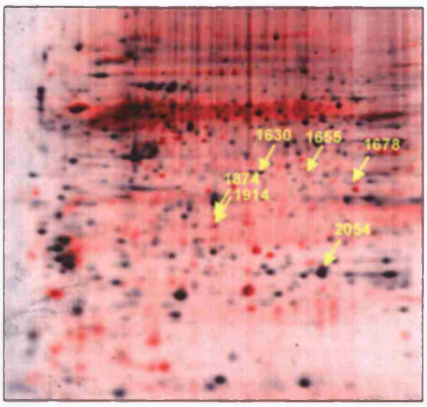

B

Protein Table T-test and Av.Ratio: 4a (EGF) / 4a (0)

Pos.	Master No.	Protein ID	Appearance	T-test	Av. Ratio
1	988		12 (12) A, M	0.0068	1.42
2	1630		12 (12) A, M	0.0055	1.30
3	1655		12 (12) A, M	0.00010	1.51
4	1678		12 (12) A, M	0.00049	-1.39
5	1684		12 (12) A, M	0.011	-1.53
6	1867		12 (12) A, M	0.023	-1.32
7	1874		12 (12) A, M	0.00027	-1.37
8	1914		12 (12) A, M	0.018	-1.36
9	2054		12 (12) A, M	0.0048	-1.34
10	2293		12 (12) A, M	0.00080	1.39

(Figure 5-2) Visualisation of differential thiol reactivity in EGF treated versus untreated HB4a cells labelled under native conditions. **(A)** Representative ICy dye image of EGF treated treated samples. Protein features displaying altered expression levels (> 1.3 fold) after EGF-treatment are labelled with a spot identity number. **(B)** Table showing the 10 differentially labelled protein spots with average fold change and T-test *p*-values. **(C)** The image is a merged image of the ICy5-labelled standard pool (red spots) with the image of its corresponding silver stained gel (black spots). The arrows indicate the aligned features between differentially labelled spots and the corresponding silver-stained spots. These spots were picked for identification by MALDI-TOF MS.

A

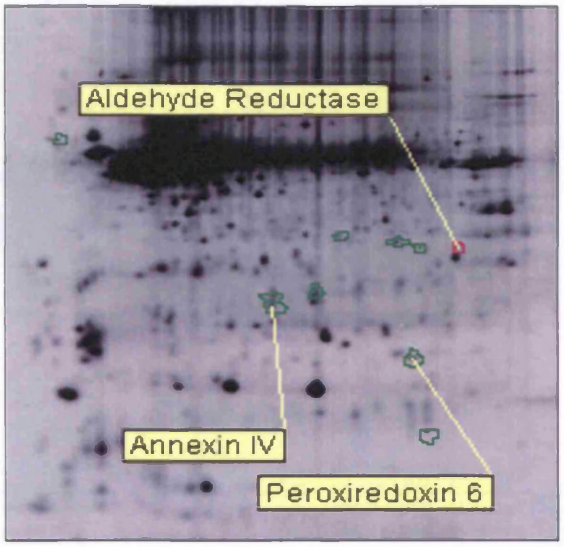

B

I. 1678 Aldehyde Reductase

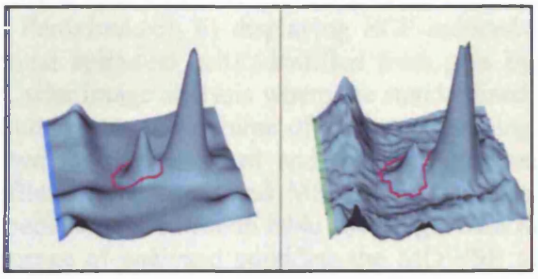

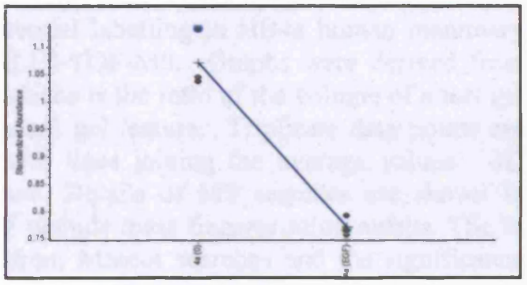

EGF 0 min EGF 10 min

II. 1914 Annexin IV

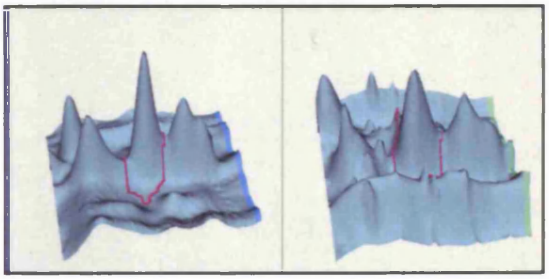

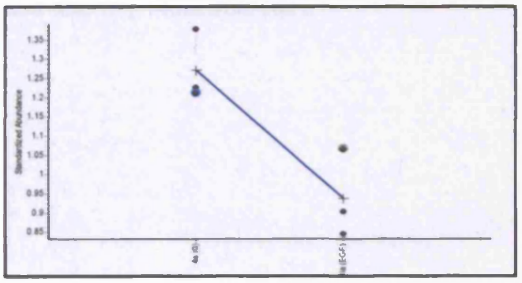

EGF 0 min EGF 10 min

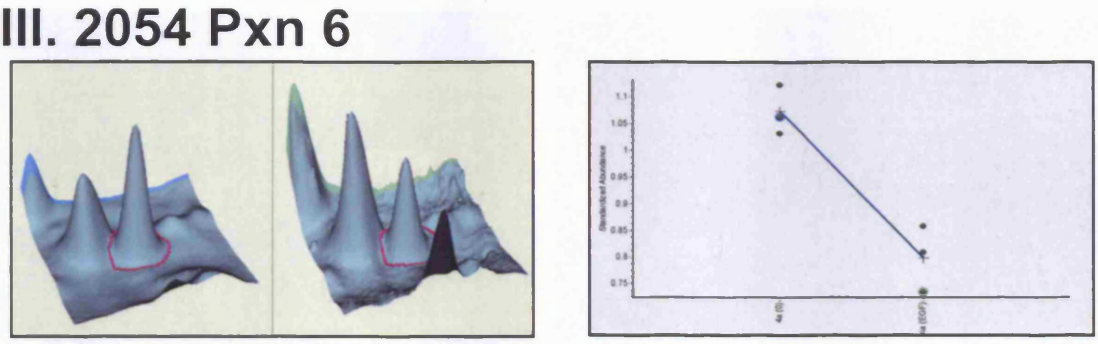

C

Spot No.	Protein Name	% Cov	Mowse Score	Est. mass	Est. pI	Pred. Mass	Pred. pI	Accession No.	Average fold-difference † and *p*-value HB4a EGF(10'-0')	*P*-value	Function
1678	Aldehyde Reductase	47	138/64	36000	7.5	36573	6.3	113600	-1.39	0.00049	NADPH-dependent reduction of a variety of aldehydes
1914	Annexin IV	71	285/64	32000	5.6	36085	5.8	1703319	-1.36	0.018	Ca/phospholipid binding; membrane fusion; exocytosis
2054	Peroxiredoxin 6 (antioxidant protein 2)	79	160/64	25000	7	25035	6	1718024	-1.34	0.0048	Cellular protection from oxidative stress

(Figure 5-3) 2DE migration and identification of proteins displaying EGF-induced differential labelling. **(A)** An ICy-dye image of a representative gel shows the positions of aldehyde reductase, annexin IV and peroxiredoxin 6. **(B)** Proteins (aldehyde reductase, annexin IV, Peroxiredoxin 6) displaying EGF-induced differential labelling in HB4a human mammary luminal epithelial cells identified from gels by MALDI-TOF-MS. Graphs were derived from DeCyder image analysis where the standardised abundance is the ratio of the volume of a test gel feature versus the volume of the corresponding standard gel feature. Triplicate data points are shown for the untreated and treated experiments with lines joining the average values. 3D profiles of the spots and MS spectra are also shown. Details of MS searches are shown in Appendix E. **(C)** Protein table showing MALDI-TOF peptide mass fingerprinting results. The % coverage of analysed peptides, the MOWSE score from Mascot searches and the significance threshold score, the estimated mass and p*I* (from gels), the predicted mass and p*I* (from the database) and the NCBI gene identifier (Accession Number) are shown for each protein. †Average fold-differences from DeCyder analysis show abundance ratios for EGF treated HB4a cells versus untreated (4a(10') versus 4a(0)). Proteins displaying an average fold-difference of ≥ 1.3-fold up (+) or down (-) regulation where $p<0.05$ and spots matched in all images are shaded grey. Functions were ascribed from the NCBInr database and literature searches.

A

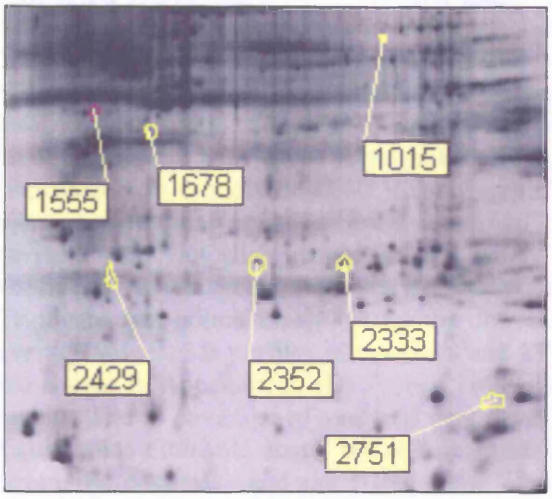

B

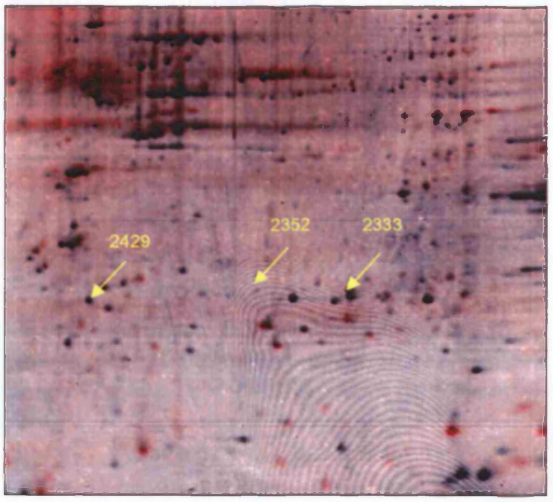

C **Spot 2333 Pxn 6**

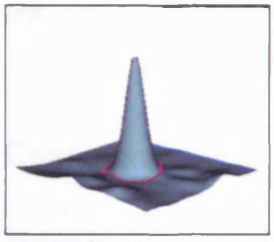

EGF 0 min

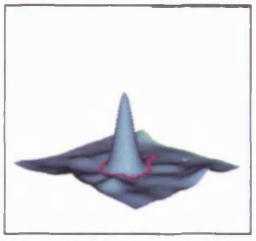

EGF 10 min

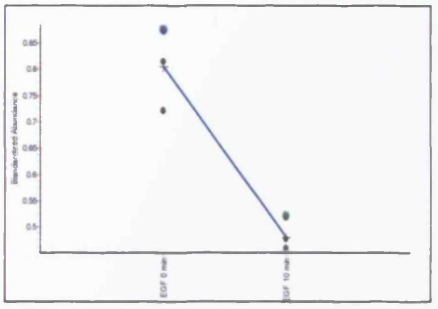

Spot 2429 Rho-GDI

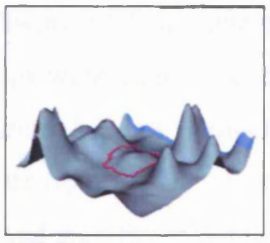

EGF 0 min

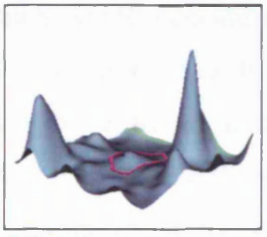

EGF 10 min

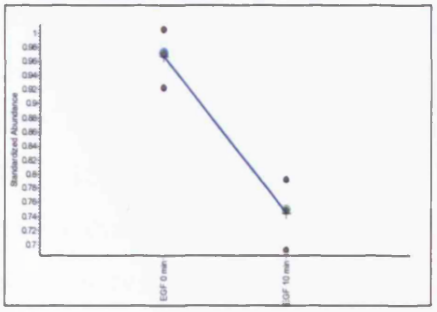

D

Spot No.	Protein Name	% Cov	Mowse Score	Est. mass	Est. pI	Pred. Mass	Pred. pI	Accession No.	Average fold-difference † and p-value: HB4a EGF(10'-0')	P-value	Function
2333	Peroxiredoxin 6 (antioxidant protein 2	65	127/64	25000	7	25035	6	1718024	-1.65	0.0017	Cellular protection from oxidative stress
2429	Rho-GDP dissociation inhibitor (GDI)	41	77/64	24000	5.5	23207	6	4757768	-1.3	0.0049	Inactivation of NADPH oxidase/small GTPase

(Figure 5-4) Visualisation and identification of differential thiol reactivity in EGF treated or untreated HB4a cell lysates labelled under denaturing conditions. **(A)** Representative ICy dye image of EGF-treated HB4a cell lysate. Protein features with altered expression levels (>+/-1.3 folds; $p<0.05$) are indicated. **(B)** Merged image of ICy5 labelled EGF treated and untreated HB4a cell standard pool (red spots) and the corresponding colloidal coomassie blue stained gel image (black spots). The arrows indicate the aligned features of the significantly differentially labelled spots. These spots were picked for identification by MALDI-TOF-MS. **(C)** Proteins (Peroxiredoxin 6 and Rho-GDI) displaying EGF-induced differential labelling in HB4a human mammary luminal epithelial cells identified from gels by MALDI-TOF-MS. Graphs were derived from DeCyder image analysis where the standardised abundance is the ratio of the volume of a test gel feature versus the volume of the corresponding standard gel feature. Triplicate data points are shown for the untreated and treated experiments with lines joining the average values. 3D profiles of the spots and MS spectra are also shown. Details of MS searches are shown in Appendix F. **(D)** Protein table showing MALDI-TOF peptide mass fingerprinting results. The % coverage of analysed peptides, the MOWSE score from Mascot searches and the significance threshold score, the estimated mass and p*I* (from gels), the predicted mass and p*I* (from the database) and the NCBI gene identifier (Accession Number) are shown for each protein. †Average fold-differences from DeCyder analysis show abundance ratios for EGF treated HB4a cells versus untreated (4a(10') versus 4a(0)). Proteins displaying an average fold-difference of ≥ 1.3-fold up (+) or down (-) regulation where $p<0.05$ and spots matched in all images are shaded grey. Functions were ascribed from the NCBInr database and literature searches.

5.3 Conclusions

In this chapter, peroxiredoxin 6, aldehyde reductase and annexin IV were identified as proteins that display reduced thiol accessibility or reactivity after EGF treatment. This may be due to changes in its association of the proteins with other intracellular molecules following EGF treatment, which would occlude reactive thiol groups or because these groups were directly oxidised in response to EGF. However, it is also possible that these proteins become degraded or move to an insouluble compartment following EGF stimulation. Under denaturing labelling conditions, Rho-GDI and peroxiredoxin 6 also showed significant reductions in thiol reactivity, suggesting that cysteine residues in both of these proteins are covalently modified via an EGF receptor-dependent pathway.

Aldehyde reductase is an NADP(H)-dependent oxidoreductase implicated in the pathogenesis of various diabetic complications (Yabe-Nishimura, 1998). The enzyme is rate limiting in the polyol pathway, where glucose is converted to sorbitol by aldehyde reductase, followed by NAD^+ dependent conversion to fructose by sorbitol dehydrogenase. Under conditions of hyperglycemia, the stimulation of the polyol

pathway leads to an overflow of the products and the depletion of $NADP^+$ and NAD^+ in cells. The resulting increase in the $NADH/NAD^+$ ratio in these cells leads to a condition similar to hypoxia (Williamson et al., 1993). Thus, numerous aldehyde reductase inhibitors are being developed as possible agents for diabetic complications. A study from Nishinaka and Yabe-Nishimura showed that intracellular hydrogen peroxide can up-regulate the gene expression of aldehyde reductase (Nishinaka and Yabe-Nishimura, 2001) and it is known that hydrogen peroxide can be induced by EGF stimulation via Rac and Rho dependent pathways (Lee *et al.*, 2000). These findings imply that aldehyde reductase could be regulated by EGF at the transcription level via generation of endogenous H_2O_2 and could also be modified to a higher oxidative status by hydrogen peroxide at the post-translational level. Indeed, Cys-298 of aldehyde reductase has been reported as a potential redox-sensitive active site cysteine (Srivastava et al., 2003). Both of these may explain the decrease in ICy dye labelling of aldehyde reductase after EGF treatment. This finding warrants further investigation, particularly the effect of EGF on the polyol pathway, although this work is beyond the scope of this thesis.

The annexins are a family of closely related calcium- and membrane-binding proteins expressed in most eukaryotic cell types. Twelve annexin subfamilies have been identified in vertebrates which all have similar biochemical functions. The annexins participate in the regulation of membrane organisation and membrane traffic and the regulation of ion (Ca^{2+}) passage across membranes and hence Ca^{2+} concentrations within cells (Hayes and Moss, 2004;Moss and Morgan, 2004). AnnexinVI has been shown to specifically inhibit EGF-dependent Ca^{2+} influx through the plasma membrane and Ca^{2+} release from intracellular stores (Fleet et al., 1999). Annexins I & II have been identified as major substrates for the tyrosine kinase activity associated with the EGF receptor and their reactivity appears to be controlled by phosphorylation following growth factor stimulation (Rothhut, 1997). In addition, annexin II was recently identified as an oxidant-sensitive protein in HeLa cells. This study showed that oxidants from exogenous H_2O_2 or generated in response to extracellular growth stimuli increased the incorporation of a glutathione into a reactive cysteine of annexin II (Sullivan et al., 2000). A more recent study demonstrated that reversible glutathionylation could regulate annexin phospholipid and F-actin binding activity (Caplan et al., 2004). Taken together, these studies suggest

that the annexins are subject to complex regulation and modification by receptor tyrosine kinases, such as the EGF receptor, and oxidants such as EGF-induced hydrogen peroxide and could have play an important role in cross-talk between growth factor and Ca^{2+} signalling. Using cysteine labelling 2D-DIGE, it was demonstrated that there was a EGF induced decrease in ICy labelling of annexin IV. By analogy to Annexin II, this is likely to be as a result of glutathionylation of the active site cysteines in response to EGF-induced oxidant production, which would block ICy dye labelling.

Rho-GTPases regulate many cellular processes including growth and differentiation, vesicular transport, reactive oxygen species production, apoptosis, cytoskeletal dynamics and cellular motility (Bishop and Hall, 2000). The regulators for these Rho-GTPases can mainly be classified into three groups:GDP/GTP exchange factors (GEFs) which stimulate the conversion of Rho proteins from the GDP-bound form to the activated GTP-bound form; GTPase activating proteins (GAPs) which stimulate the conversion GTP to GDP conversion to inactive Rho-proteins and Rho GDP dissociation inhibitors (RhoGDIs) which bind to the GDP-bound forms of Rho proteins (Rho, Rac and Cdc42) and inhibits GDP dissociation (Van Aelst and D'Souza-Schorey, 1997). Rho-GDI is also involved in the translocation of Rho, Rac and Cdc42 between the cytosol and the membrane (Takai et al., 1993). In addition, recent studies indicate that phosphorylation of Rho-GDI by p21-activated kinase (Pak1) mediates its dissociation from Rac (DerMardirossian et al., 2004) and the Pak1 can interact with the Grb2 adapter protein coupling Rac activation with EGF signalling (Puto et al., 2003). In the work presented here, Rho-GDI displayed reduced labelling following EGF treatment, suggesting that the single cysteine in Rho-GDI is oxidised by indirect signalling from EGFR. This oxidation may occur via EGF-induced hydrogen peroxide in a feedback loop and the oxidation event could be one mechanism by which Rho-GDI function is regulated.

Peroxiredoxin 6, which is involved in the defence against cellular oxidative stress, can scavenge peroxides and can also reduce peroxidised membrane phospholipids. Thus, peroxiredoxin 6 can protect cells against oxidant-induced plasma membrane damage, thereby playing an important role in cellular defense against oxidant stress (Manevich et al., 2002). From the data in this chapter (Figure 5-3 and Figure 5-4), peroxiredoxin 6 was identified as being differentially labelled under both native and denaturing (urea)

conditions inferring that the changes in thiol reactivity of the Prxn-6 are derived from covalent modification (such as forming the sulfenic, sulfinic or sulfonic acid) rather than the changes in non-covalent association of cysteine accessibility. This is highly likely, since Prxn-6 was also identified as a proximal target of H_2O_2-elicited redox stress in the previous chapter and has been reported to become oxidised following oxidant treatment (Wagner *et al.*, 2002). In addition, the study of Bae et al. indicated that EGF can induce the generation of H_2O_2 (Bae *et al.*, 1997) This infers that the reduced labelling of Prxn-6 following EGF treatment is likely to occur as a result of oxidation of the thiol group. Importantly, the preferred hypothesis for EGF dependent modification of Prxn-6 is that EGF stimulates the generation of low concentrations of hydrogen peroxide which oxidises the active site cysteine in Prxn-6.

In this chapter, native denatured labelling of the cysteine thiol in proteins was used for studying thiol accessibility and cellular redox regulation following EGF stimulation. In two independent experiments using triplicate samples, only a small number features were detected that displayed significant changes. One possible reason for this observation could be the use of a sub-optimal labelling buffer that leads to the aggregation of dyes which generate a strong background and mask a subset of labelled features for analysis. Another possible reason could be that the modifications that occur on proteins of lower abundance cannot be detected by this method. It must be considered also that EGF induced H_2O_2 production will be much lower than exogenously added H_2O_2 as 0.5 mM, this would induce less proteins labelling by ICy dye because only a subset of the protein was modified by oxidation.

Chapter 6 Application of cysteine labelling 2D-DIGE to analyse changes in plasma fractions following UV irradiation

6.1 Introduction

In the previous chapters, the potential utility of cysteine labelling 2D-DIGE for the identification of cellular targets of oxidative stress and EGF-induced changes in thiol accessibility and modification has clearly demonstrated. In this chapter, the utility of this technique for studying the effects of UV irradiation on cysteine thiol modifications in purified human plasma fractions is presented. Transmission of viruses in human sera represents a considerable risk for humans, particularly when the serum is used for the production of pharmaceutical products such as vaccines and blood clotting agents. Therefore, procedures for inactivating different viruses or bacteria in these products are mandatory. Conventional disinfection techniques that have been used for pathogen inactivation include solvent-detergent treatment (Wainwright, 2002b) and ultra-violet irradiation (Wainwright, 2002a). However, it is possible that such treatments may also damage the protein components of these blood products affecting their potency.

In this work, a human plasma fraction developed by Baxter Healthcare (Vienna, Austria) was used to evaluate the potential of cysteine labelling 2D-DIGE on detecting UV irradiation induced changes. This chromatographically-purified fraction known as FIBA is being developed for use as a blood clotting agent for heamophilics and for use after serious injury. Baxter Healthcare developed a large-scale UV-C irradiation strategy to disinfect any pathogen in these preparations since this method has been shown to remove various viruses with high clearance rates (Kurth et al., 1999). However, some reports indicate that UV treatment can modify the thiol groups of proteins. For example, UV irradiation induces a change of thiol reactivity of crystallin and the cleavage of heavy chain subfragment 1 of myosin (Grammer et al., 1988;El'chaninov and Fedorovich, 1990). These thiols are all related to protein activity. The aim of the work presented here was to determine if thiol reactivity is altered in the purified plasma fraction following

exposure to different doses of UV-C treatment. In addition, we wanted to identify which plasma proteins are the targets of UV irradiation induced damage.

6.2 Identification of differentially expressed/labelled plasma proteins following UV-irradiation

Cysteine labelling 2D-DIGE was applied to study the effect of UV irradiation on thiol reactivity in a purified fraction of human plasma. Labelling with ICy dyes was carried out on denatured, non-reduced samples prepared in ICy urea labelling buffer. Experiments were performed on samples subjected to UV irradiation doses of 0 mJ/cm^2, 20 mJ/cm^2, 40 mJ/cm^2 and 80 mJ/cm^2, in triplicate (Figure 6-1). ICy3 labelled individual samples were run on 2D gels with an equal load of ICy5-labelled standard pool, consisting of an equal mixture of all samples. Although hundreds of protein features can be separated well by 2D-DIGE, poor focusing of some abundant proteins was observed in this experiment (Figure 6-1 and 6-2). This might be caused by the plasma samples containing buffer components ($NaHCO_3$ + NaCl) which interfere with the isoelectric focusing.

Twenty-nine protein spots displaying significant changes in labelling between the treated and untreated samples were identified (>1.5 fold up or down regulated; $p<0.05$) with a large degree of overlap in their regulation at the different UV doses (Figure 6-2). Post-staining with colloidal coomassie blue and matching to the corresponding fluorescent images allowed picking of 17 gel features with confidence (Figure 6-3). The fewer number of post-stainable matching spots might be caused by low abundance proteins that cannot be detected by CCB staining but which contain reactive thiol groups. In addition, the positively charged ICy dye may induce p*I* shift in dye-labelled proteins which would dilute the signal if labelling is sub-stoichiometric (see discussion in Chapters 3 and 4). 13 of these 17 proteins were identified by MALDI-TOF peptide mass mapping using a mass accuracy of +/- 50 ppm (Figure 6-4). These 13 protein isoforms represented 7 different gene products. These gene products were actin, ALB protein (a human albumin fragment in serum with a molecular weight of 48 kDa), complement component C4, kininogen precursor, prethrombin 2, retinol-binding protein and serum amyloid P component. The 3-D spot images, the standardised protein levels and the MALDI-TOF-MS spectra of

these proteins are shown in Figure 6-5. Of these proteins, kininogen precursor, multiple isoforms of serum amyloid P component and retinol binding protein displayed an increase in labelling in response to UV irradiation; conversely, actin, ALB protein, complement component C4 and prethrombin 2 showed a decrease in labelling in response to UV irradiation (Figure 6-5). Interestingly, several of the proteins showed dose-dependent changes. These data suggest that the blockage of free thiols due to disulphide bond formation/oxidation and the breakage of disulphide bonds/reduction may occur as a result of UV-C irradiation.

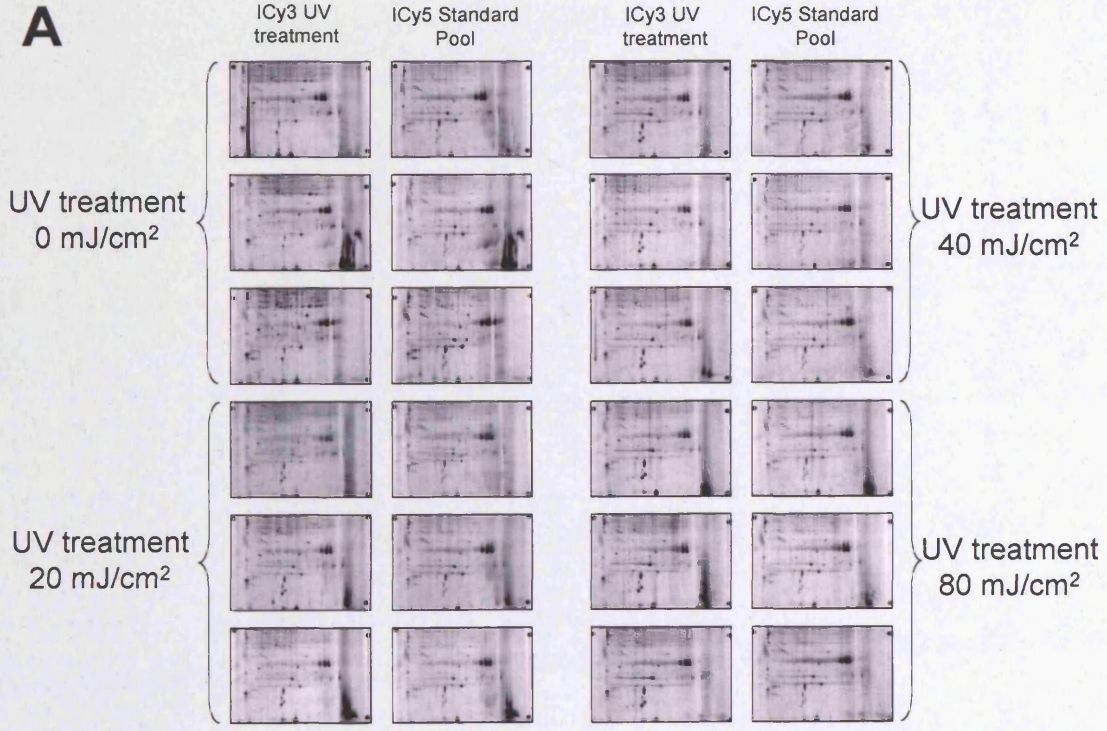

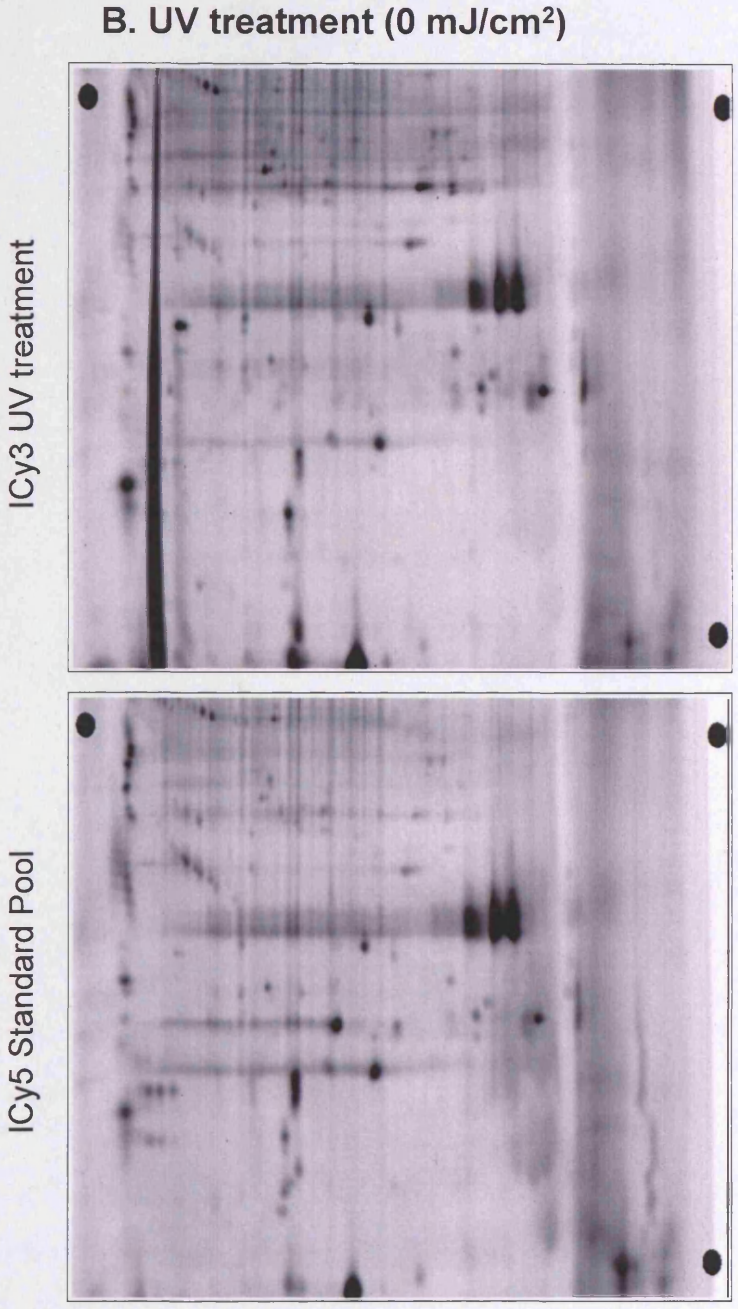

(Figure 6-1) Representation of the experimental design in the study of the thiol reactivity of plasma fractions in response to different doses of UV-C irradiation. (A) Plasma fractions were treated with 20, 40 and 80 mJ/cm^2 of UV-C irradiation and compared to the untreated samples. Equal amounts of ICy5 labelled plasma samples were mixed as an internal standard pool and run against the untreated and UV-treated samples labelled with ICy3. Samples were run in triplicate for statistical analysis to assess reproducibility. Thus 12 gels were run with 24 images generated. Gel images were processed using the BVA module of DeCyder software to identify significant changes in protein isoform abundance/ ICy labelling. One of the image sets in **(A)** are shown in **(B)** with representative enlarged images.

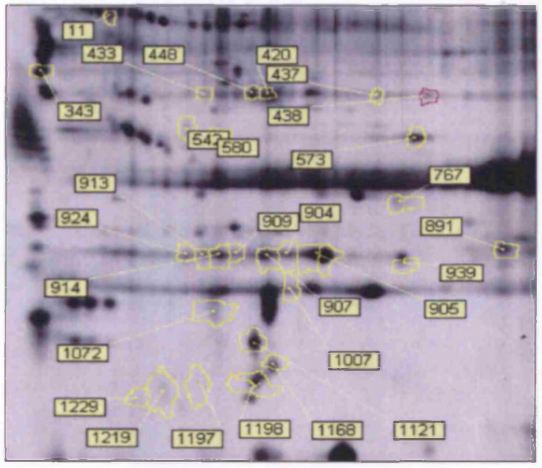

P<0.05; Spot Volumes>50000
Average fold difference >1.5 or <-1.5 fold

Master No.	(20/0)	*p*-value	(40/0)	*p*-value	(80/0)	*p*-value
1168	14.33	0.0048	22.61	0.0028	25.56	0.0026
1198	15.89	8.8E-07	22.82	3.4E-05	23.82	4.00E-06
905	7.47	1.2E-05	10.49	4.1E-05	15.24	1.80E-05
904	4.31	0.0053	8.26	0.0012	15.13	0.00048
1197	8.43	0.0016	11.33	0.00015	14.39	0.00049
909	4.4	0.018	6.58	0.0068	13.41	0.0025
924	3.87	0.0024	6.2	0.00075	9.8	0.00031
914	3.26	0.0047	5.96	0.00067	9.5	0.00031
1219	2.03	0.011	2.74	0.04	9.08	0.0024
907	2.58	0.0058	3.86	0.0013	5.89	0.00049
1005	2.23	0.0092	3.35	0.0019	4.79	0.00063
1072	1.87	0.0015	2.26	0.0006	4.09	8.90E-05
939	2.13	0.035	2.81	0.017	3.98	0.0056
913	1.67	0.007	2.02	0.021	2.75	0.0067
343	2.21	0.00034	2.01	0.0011	2.32	0.00024
11	1.61	0.0059	1.75	0.003	2.13	0.0013
580	1.52	0.0025	1.38	0.0024	1.67	0.0016
542	1.39	0.02	1.2	0.059	1.62	0.0054
1007	1.28	0.09	1.4	0.014	1.57	0.0047
891	-1.13	0.34	-1.25	0.048	-1.57	0.0025
1121	1.26	0.59	1.05	0.69	-1.63	0.0049
573	-1.15	0.0047	-1.5	0.00075	-1.74	3.50E-05
433	-1.7	0.0059	-1.81	0.003	-1.78	0.0069
767	-1.42	0.019	-1.53	0.011	-1.79	0.0033
420	-1.33	0.038	-1.57	0.0012	-1.86	0.00026
448	-1.2	0.0051	-1.49	0.0009	-1.88	0.0002
1229	-1.21	0.48	-1.96	0.0082	-2.03	0.023
437	-3.99	0.0036	-3.47	0.0051	-3.55	0.0043
438	-7.11	0.00048	-5.65	0.00087	-6.22	0.00082

(Figure 6-2) Visualisation of differential thiol labelling in UV-treated versus untreated plasma fractions. A representative ICy dye image of a UV treated plasma fraction is shown. Protein features with altered labelling (>+/- 1.5 fold up or down) across the time course are labelled with their spot identity number (top left). The table shows the average fold difference in labelling intensity between the treated samples and the untreated sample for 29 spots matched across all gels with *p*-values from the applied T-test. Green shaded values are >1.5 fold up or down regulated. The Venn diagram shows the number of spots and their co-regulation between each exposure and the untreated sample.

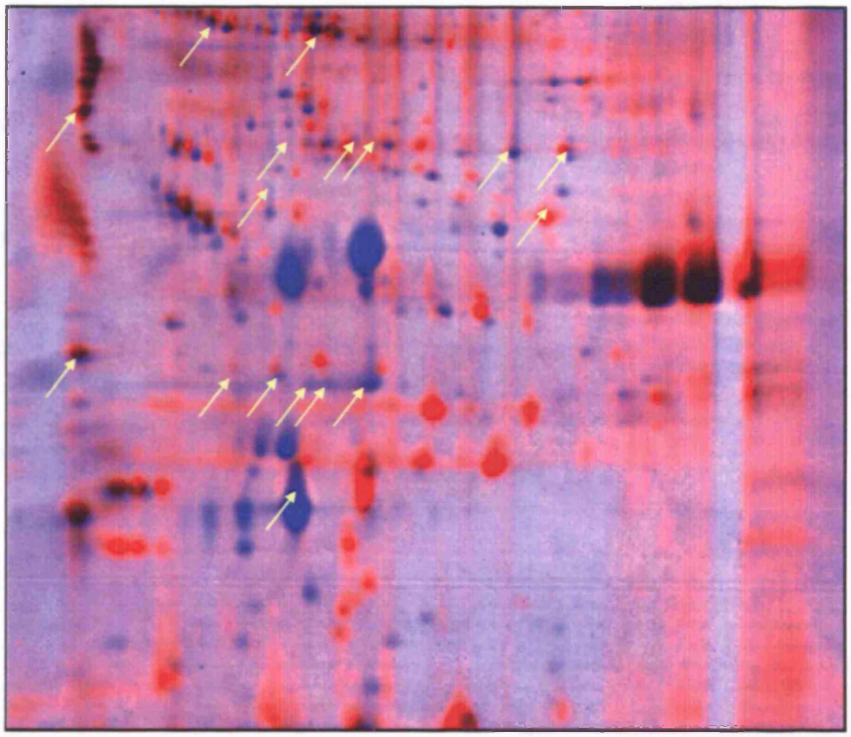

(Figure 6-3) Master gel image of ICy5 labelled standard pool and its corresponding colloidal coomassie blue stained image. The image shown is an aligned image of the internal standard pool labelled with ICy5 (red spots) and the image of its corresponding colloidal coomassie blue stained gel (blue spots). The arrows indicate the aligned features of significant differentially labelled spots and the corresponding colloidal coomassie blue-stained spots. These spots were picked from gels for identification by MALDI-TOF-MS.

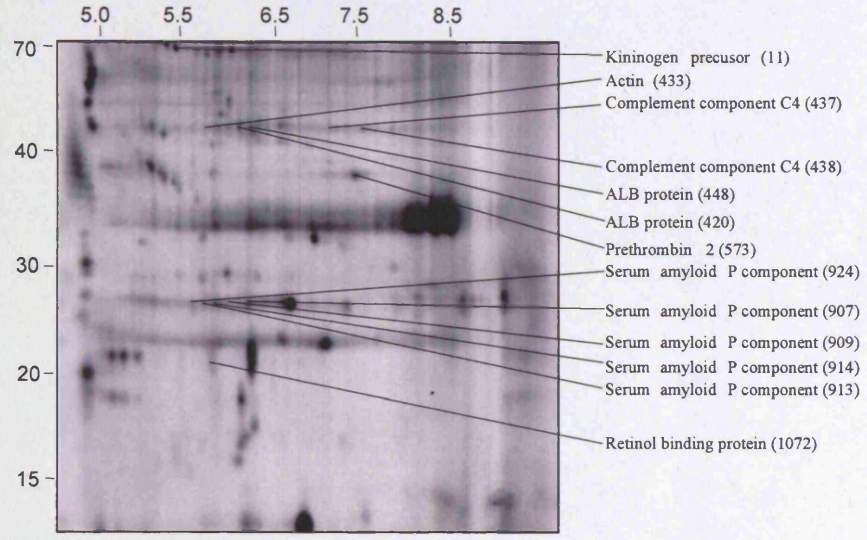

									Average fold-difference † and *p*-value						
Spot No.	Protein Name	% Cov	Mowse Score	Est. mass	Est. pI	Pred. Mass	Pred. pI	Accession No.	UV (20/0 mJ/cm²)	*P*-value	UV (40/0 mJ/cm²)	*P*-value	UV (80/0 mJ/cm²)	*P*-value	Function
433	Actin	42	92/64	43000	5.5	42188	5.4	156759	-1.7	0.0059	-1.81	0.003	-1.78	0.0069	cytoskeleton protein
420	ALB protein	53	181/64	45000	6	47361	6	27692693	-1.33	0.038	-1.57	0.0012	-1.86	0.00026	similar to human serum albumin
448	ALB protein	31	90/64	45000	5.9	48664	6	27692693	-1.2	0.0051	-1.49	0.0009	-1.88	0.0002	similar to human serum albumin
437	Complement component C4	35	90/64	46000	7	48037	5.8	40737308	-3.99	0.0036	-3.47	0.0051	-3.55	0.0043	complement protein
438	Complement component C4	39	113/64	46000	7.5	48037	5.8	40737308	-7.11	0.00046	-5.65	0.00067	-6.22	0.00082	complement protein
11	Kininogen precursor	35	81/64	70000	5.5	71945	6.3	125507	1.61	0.0059	1.75	0.003	2.13	0.0013	Blood coagulation
573	Prethrombin 2	46	94/64	35000	7.5	34245	8.3	809450	-1.15	0.0047	-1.5	0.00075	-1.74	0.000035	Blood coagulation
1072	Retinol binding protein	75	103/64	21000	5.5	20959	5.3	230284	1.87	0.0015	2.26	0.0006	4.09	0.000089	Transporting vitamin A from liver to vitamin A dependent tissu
907	Serum Amyloid P component, chain A	39	90/64	24000	6	23358	6.1	576259	2.58	0.0058	3.86	0.0013	5.89	0.00049	chaperone; chromatin degradation control
909	Serum Amyloid P component, chain A	39	107/64	24000	5.8	23358	6.1	576259	4.4	0.018	6.58	0.0068	13.41	0.00025	chaperone; chromatin degradation control
913	Serum Amyloid P component, chain A	39	112/64	24000	5.6	23358	6.1	576259	1.67	0.007	2.02	0.021	2.75	0.0067	chaperone; chromatin degradation control
914	Serum Amyloid P component, chain A	33	70/64	24000	5.7	23358	6.1	576259	3.26	0.0047	5.96	0.00067	9.5	0.00031	chaperone; chromatin degradation control
924	Serum Amyloid P component, chain A	39	78/64	24000	5.5	23358	6.1	576259	3.87	0.0024	6.2	0.00075	9.8	0.00031	chaperone; chromatin degradation control

(Figure 6-4) 2DE migration of proteins identified by MALDI-TOF-MS displaying UV-induced changes in thiol labelling. A representative ICy-dye image is shown displaying proteins with UV-induced differential labelling. UV-induced differentially labelled proteins were identified from gels by MALDI-TOF-MS as described in Materials and Methods. Protein table showing MALDI-TOF peptide mass fingerprinting results. The % coverage of analysed peptides, the MOWSE score from Mascot searches and the significance threshold score, the estimated mass and p*I* (from gels), the predicted mass and p*I* (from the database) and the NCBI gene identifier (Accession Number) are shown for each protein. MS spectra, MOWSE score histograms, matching peptides and sequence coverage for all proteins are shown in Appendix G. The criteria for inclusion was an average fold-difference of ≥ 1.5-fold up (+) or down (-) regulation where $p<0.05$ and spots were matched across all 12 images.

A. Kininogen precursor (11)

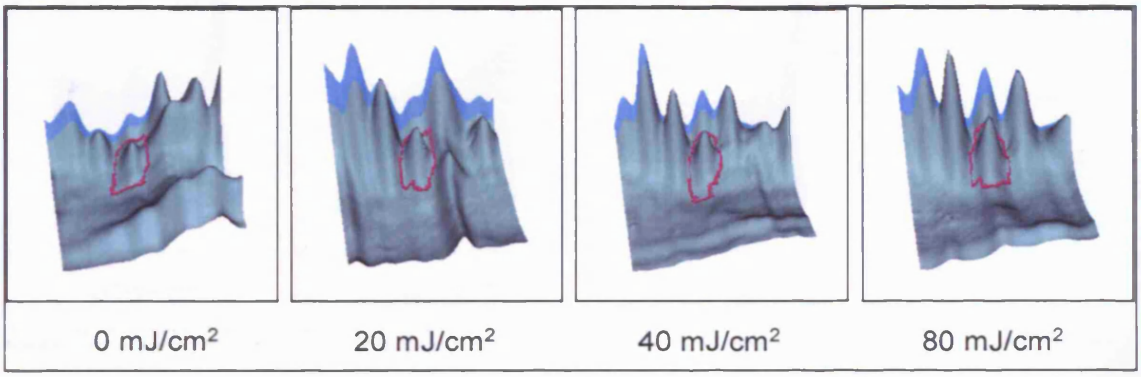

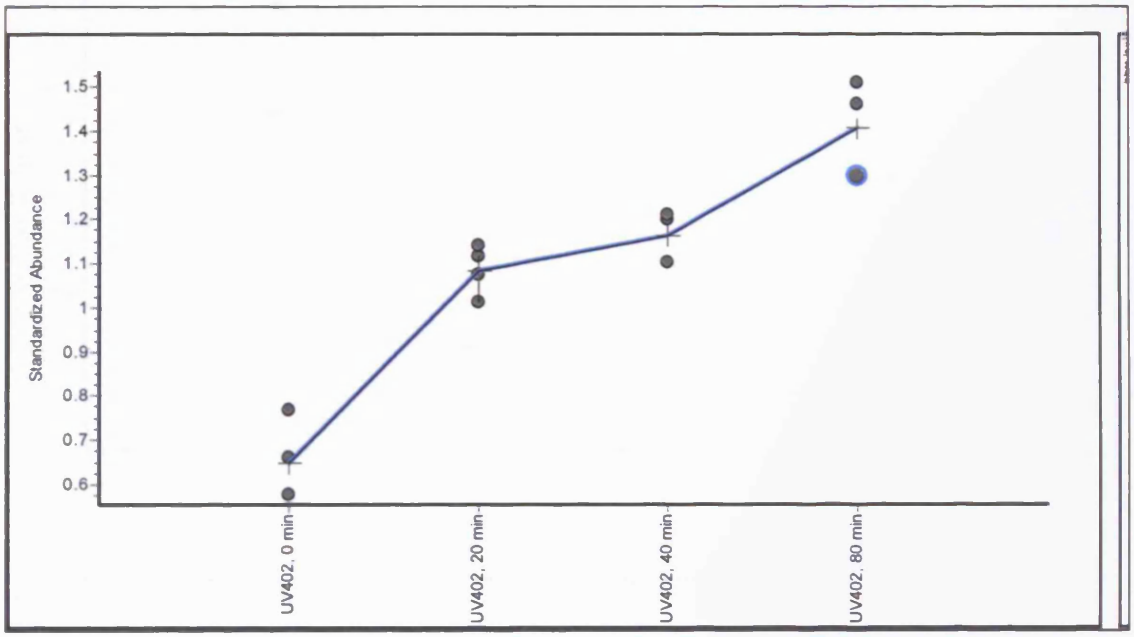

B. Actin (433)

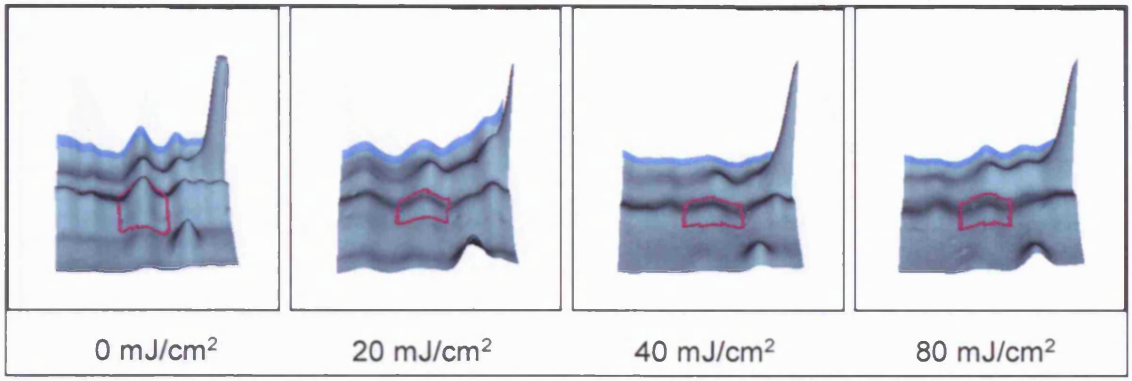
0 mJ/cm²
20 mJ/cm²
40 mJ/cm²
80 mJ/cm²

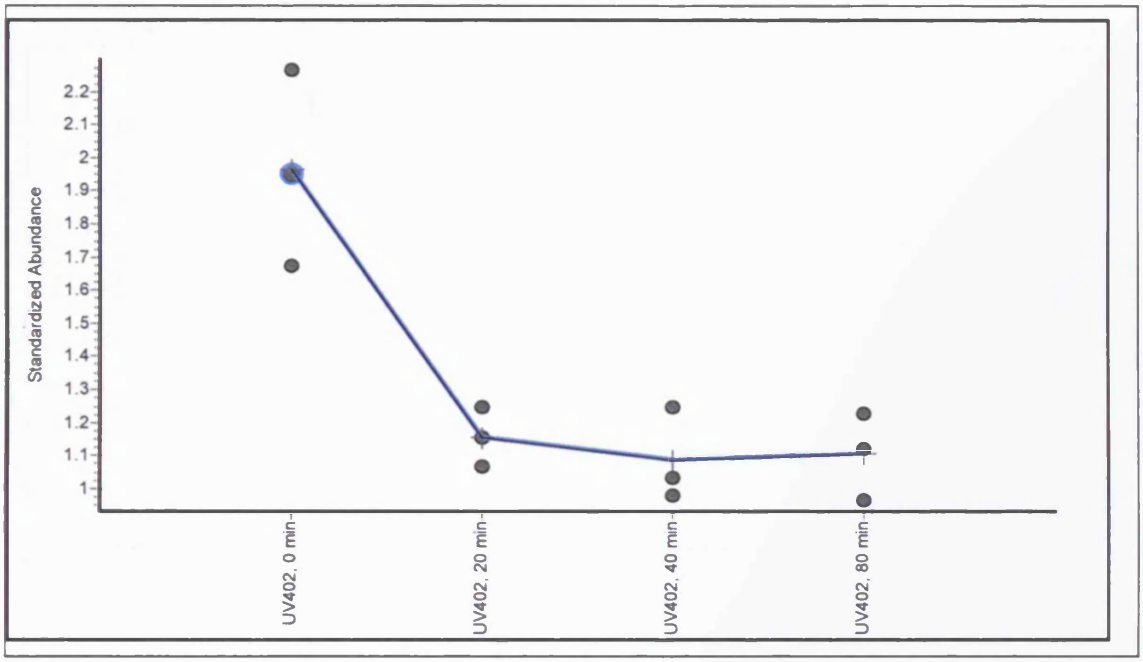
Standardized Abundance
2.2
2.1
2
1.9
1.8
1.7
1.6
1.5
1.4
1.3
1.2
1.1
1
UV402, 0 min
UV402, 20 min
UV402, 40 min
UV402, 80 min

C. ALB protein (448)

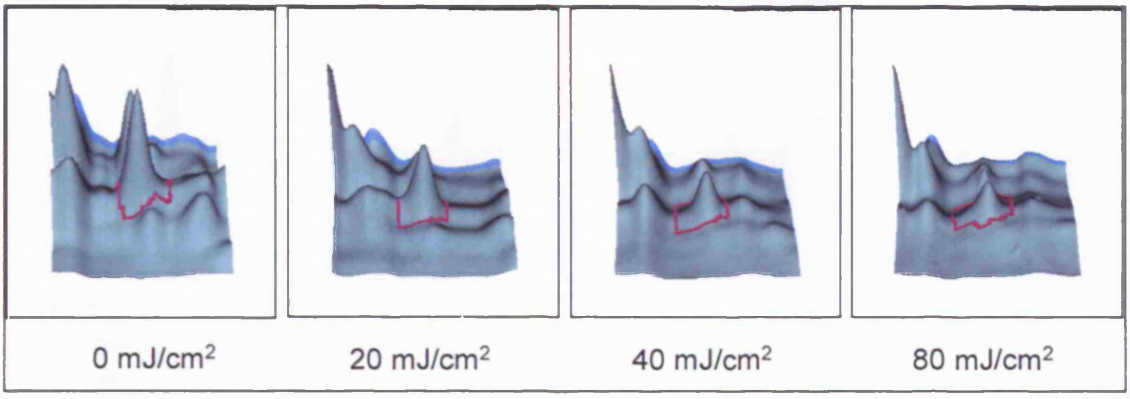

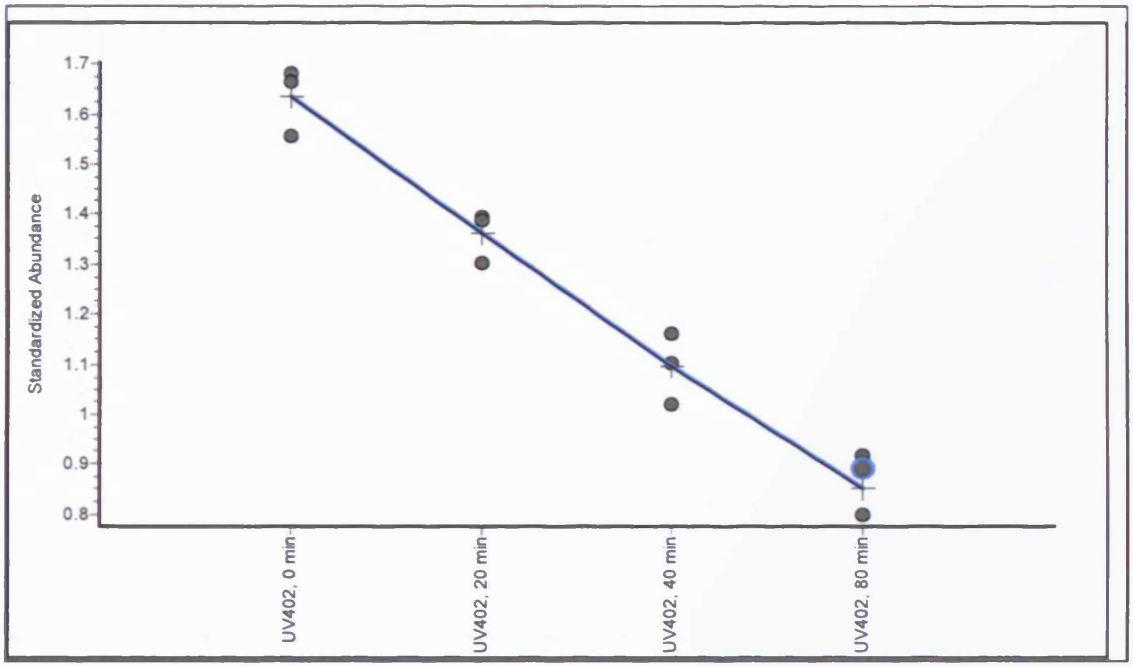

D. Serum Amyloid P (907)

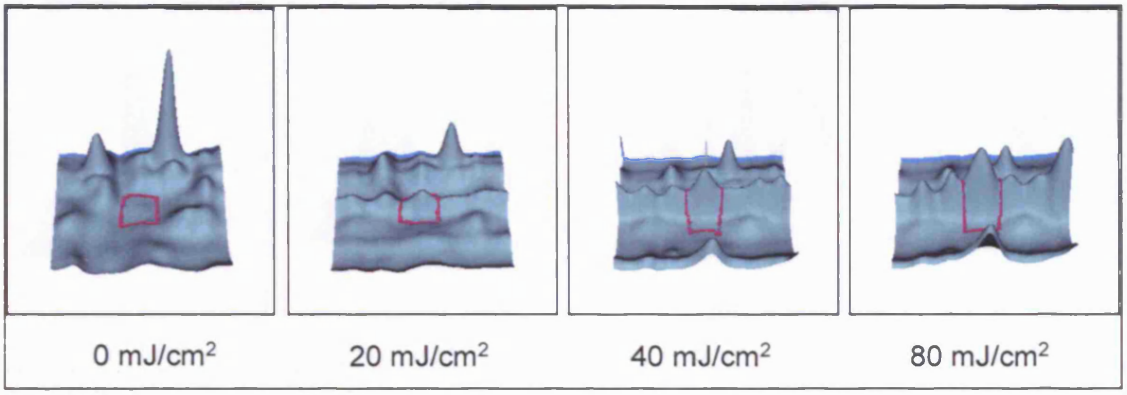

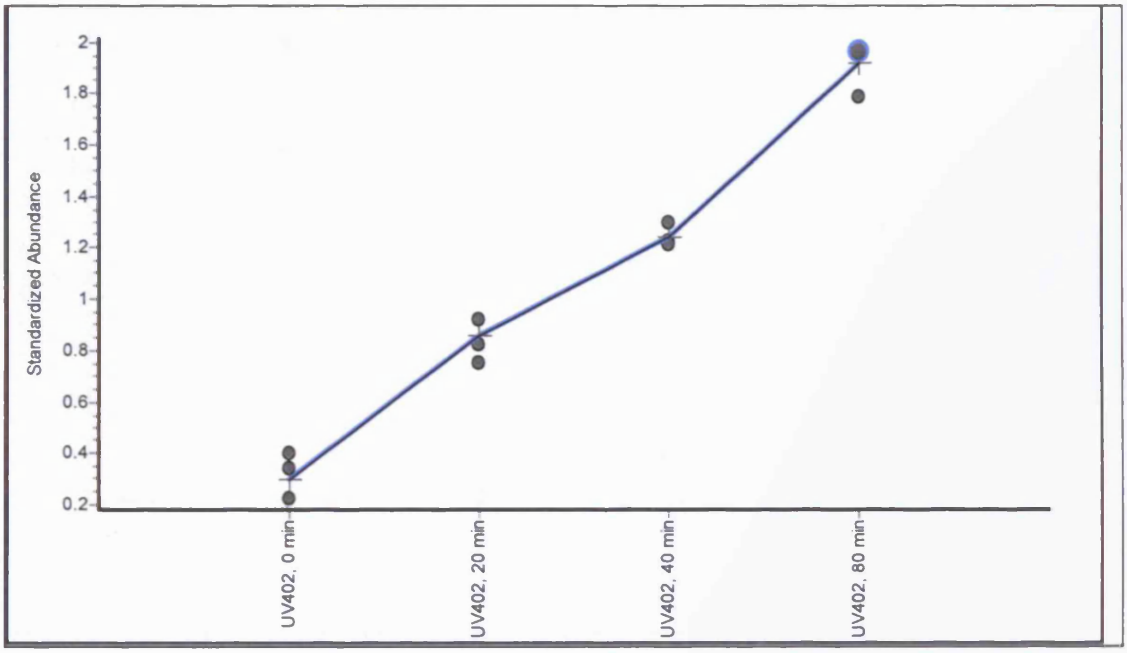

E. Complement C4 (437)

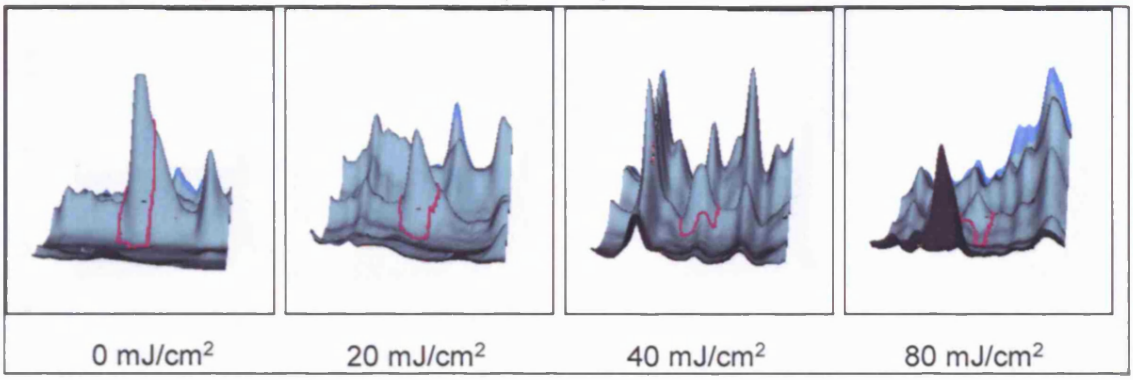

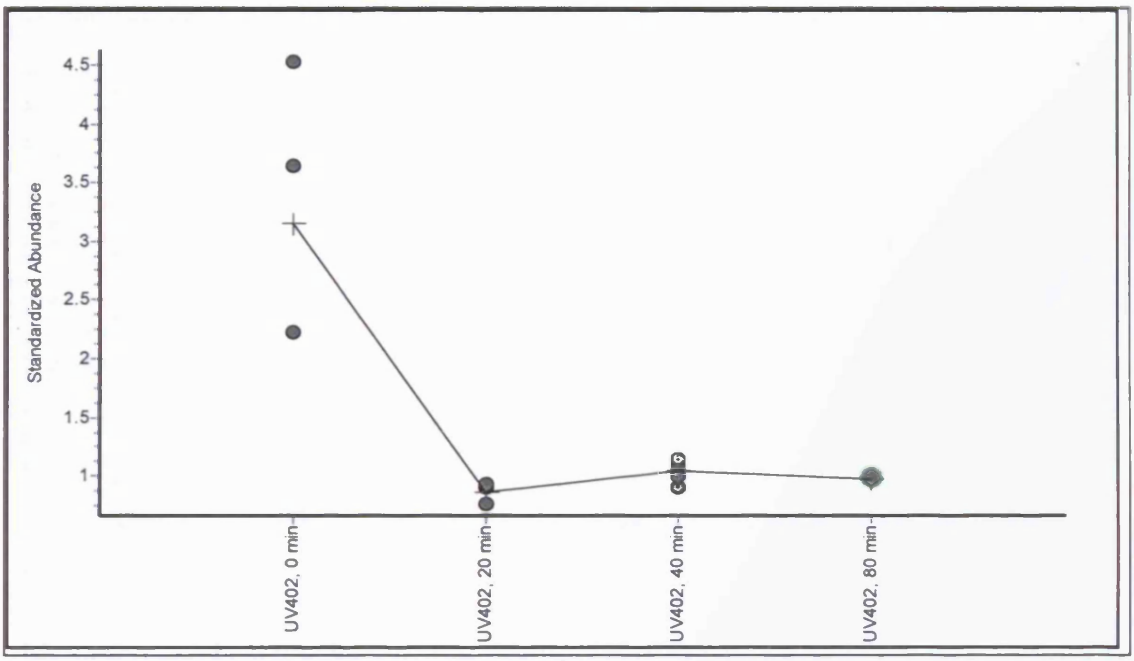

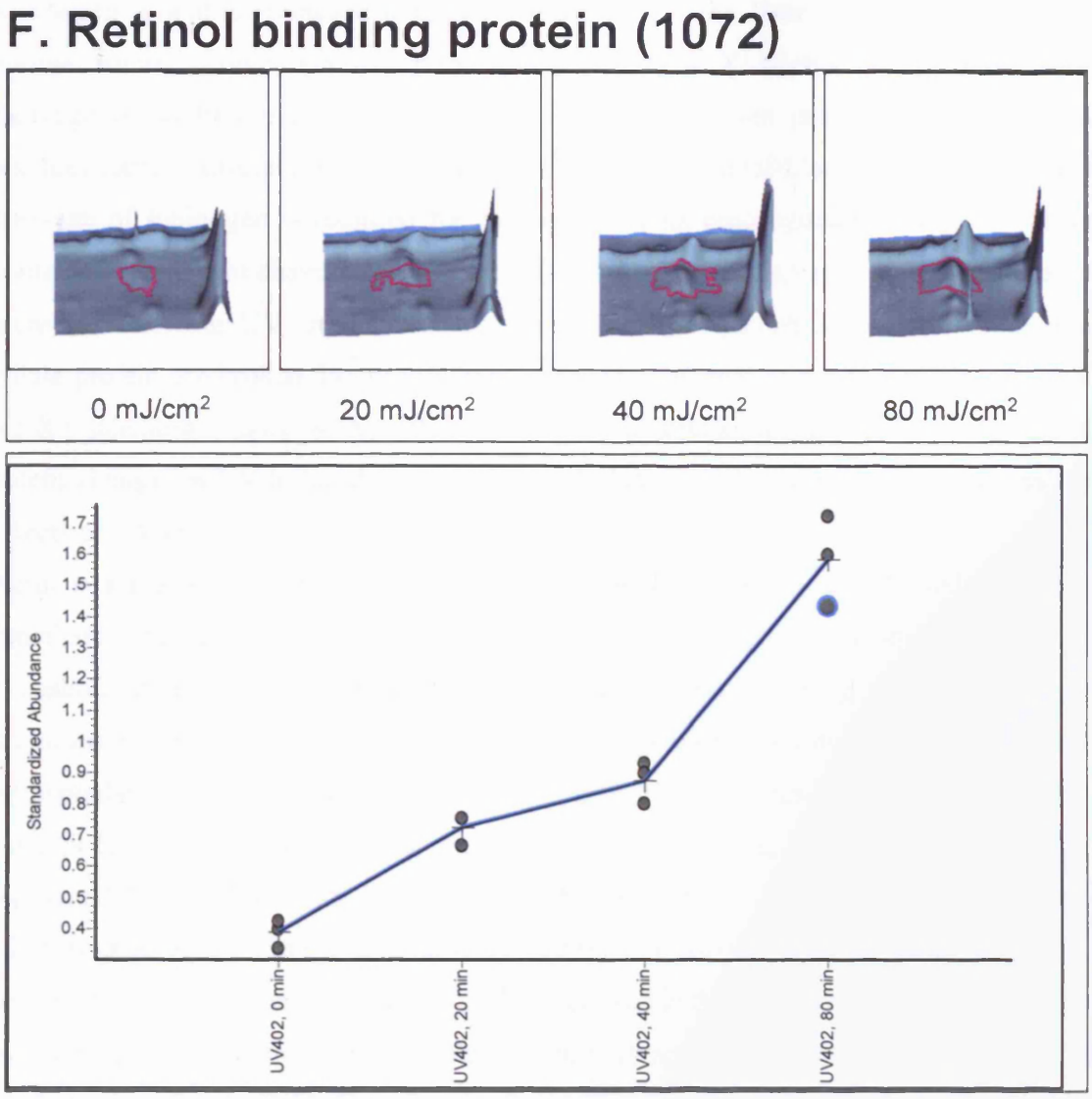

(Figure 6-5) Examples of protein isoforms identified by MALDI-TOF-MS displaying UV-induced thiol labelling changes. Proteins (Kininogen precursor **(A)**, Actin **(B)**, ALB protein **(C)**, Serum Amyloid P component **(D)**, Complement C4 **(E)** and Retinol binding protein **(F)**) display UV-induced differential labelling in plasma fractions and were identified from gels by MALDI-TOF-MS. Examples of 3D-images of spots are shown for the untreated (0 mJ/cm^2) and treated (20, 40 and 80 mJ/cm^2) samples. Graphs were derived from DeCyder image analysis where the standardised abundance is the ratio of the volume of a test gel feature versus the volume of the corresponding standard gel feature. Triplicate data points are shown for spots from the untreated and treated samples with lines joining the average values. MS searches are shown in Appendix G.

Kininogen is a thiol protease inhibitor synthesised in the liver and secreted into the plasma, where it complexes with prekallikrein and factor XI (Renne et al., 2002). After cleavage by kallikrein or factor XIIa, the mature kininogen protein comprising 626 residues forms a disulphide-linked two subunit protein (Shariat-Madar et al., 2002). This cleavage of kininogen is required for expression of its procoagulant activity, which is contained in the light chain. Here, ICy labelling of kininogen displayed a dose-responsive increase following UV irradiation, suggesting that the disulphide bridges within the whole protein are broken due to UV irradiation, thus increasing the free thiols available for ICy labelling (Figure 6-5A). This is the first time that kininogen has been found as a potential target of UV-induced damage, although further studies are required to assess the effects of UV on its function.

Actin is a major component of eukaryotic cells with mainly contractile and structural functions. The 2D-DIGE results showed a decrease in labelling of actin following UV exposure. It is the major constitutent of the cytoskeleton, forming filaments that are regulated by many intracellular signalling pathways and that interact with numerous intracellular proteins (Pollard and Cooper, 1986). Some studies have also shown that actin is found on the cell surface, in the extracellular matrix, and in serum and other biological fluids (Rohr and Mannherz, 1978;Owen et al., 1978;Thorstensson et al., 1982;Accinni et al., 1983;Moroianu et al., 1993). Normally, actin is released into the serum as a consequence of cell death and/or necrosis and is cleared from the circulation by the vitamin D-binding protein (Goldschmidt-Clermont et al., 1986). Monomeric actin binds to the vitamin D-binding protein through actin's C-terminal region although the intracellular cleavage of actin results in fragments that do not bind and therefore are not cleared as rapidly from the serum (Goldschmidt-Clermont *et al.*, 1986). There are no reports of the direct modification of serum actin by UV irradiation and so the results of the study here appear to be novel. Nevertheless, there is one report indicating that one of the major targets of UV-induced alterations intracellularly is the actin molecule (Maekawa et al., 1996) suggesting that serum actin could possibly be modified in a similar way. Since actin contains an odd number of cysteine residues, this implies that at least one free thiol exists that could be accessible for UV-induced modification. Such a

modification may explain the decrease in cysteine labelling after UV irradiation (Figure 6-5B).

Serum albumin is one of the major serum transport proteins which include serum albumin, fetoprotein, vitamin D-binding protein and afamin (Schoentgen et al., 1986;Haefliger et al., 1989;Lichenstein et al., 1994). Albumin is the most abundant protein in serum. It binds water, cations, fatty acids, hormones, bilirubin and drugs and regulates the osmotic pressure of blood (Minton, 1995). Recent studies indicate that UV-irradiation of a BSA solution in the presence of cysteine can alter the protein secondary structure of BSA. Moreover, UV irradiation also induced changes in albumin's binding ability (Samoilova et al., 1987). These reports suggest that the cysteine residues on albumin can be modified by UV irradiation and may induce changes in the physiological function of the protein. The result from this work indicates that the serum albumin protein exhibits a UV-C dose-dependent reduction in cysteine labelling suggesting that the free thiol in this protein has been oxidised (Figure 6-5C). The observation of peroxide-induced oxidation of human serum albumin shown in Figure 3-11 supports such a mechanism and may explain the thiol reactivity changes seen under UV irradiation.

Amyloid P component (AP) was first discovered as a glycoprotein present in all amyloid deposits in all types of amyloidosis, and was later found to be identical to the normal circulating plasma glycoprotein, serum amyloid P component (SAP) (de Haas, 1999). SAP belongs to the family of pentraxins, a superfamily of plasma proteins characterised by their pentameric assembly and calcium-dependent ligand binding. It has been reported to bind to glycosaminoglycans, especially heparin, heparin sulfate and dermatan sulfate, to mannose terminated glycans, and to glycans with preterminal galactose residues (Emsley et al., 1994c). In addition, native SAP is apparently the only protein from serum that shows calcium-dependent binding to DNA and chromatin at physiological pH and ionic strength (Pepys et al., 1994;Emsley et al., 1994b). SAP also plays an important role in pathogen defence in serum and has been shown to bind to lipopolysaccharide (LPS) which is the major component of the outer membrane of Gram-negative bacteria (Preston et al., 1996;de Haas et al., 1998). A structural study showed that native SAP contains two cysteines which are linked by an intramolecular disulphide bond (Thompson and Enfield, 1978;Emsley et al., 1994a). Since serum amyloid P component was identified in the

plasma fractions as a protein whose reactive thiol content was increased by UV irradiation (Figure 6-5D). This implies that UV-C exposure breaks the intramolecular disulphide bond and increase the content of available cysteines for ICy labelling.

Components of the complement system form a large family of glycoproteins that have important functions in the immune response and host defence (Goldman et al., 1982). They are proteolytically activated by cleavage at specific sites to form A- and B-fragments (Ogata et al., 1989). The proteins are highly hydrophilic, with a mainly alpha-helical structure held together by disulphide bridges (Gennaro et al., 1986). In this study, UV irradiation resulted in a significant reduction in the labelling of complement C4 protein (Figure 6-5E). Previous work by Livden et al. showed that complement C4 levels were significantly reduced under UV treatment for 4 weeks and it is tempting to speculate that the reduced labelling of complement C4 could be caused by the degradation of the protein in response to UV treatment.

Finally, Serum Retinol Binding Protein (RBP) is the major retinol transporter in plasma, binding a single all-trans-retinol molecule as its physiological ligand. RBP is synthesised in hepatic parenchymal cells, where the apoprotein is loaded with retinol. Subsequently, the retinol-RBP complex is released into plasma and associates with transthyretin forming the main transporting complex (Wolf, 1992). 85-90% of plasma RBP carries bound retinol (Blaner, 1989). RBP-mediated retinol transport facilitates the transfer of insoluble retinol from storage sites to peripheral tissues, with the synthesis of RBP regulating retinol release from the liver and controlling the specificity of its uptake by target cells (Newcomer, 1995a). In addition, it has been shown that RBP protects bound retinol from oxidation (Newcomer, 1995b). RBP-target-cell interaction is important for its biological function: RBP is recognised by a cell-surface receptor, releasing retinol, and losing its affinity for transthyretin. The resulting apo-RBP is filtered by the kidney, reabsorbed and catabolised (Wolf, 1992;Sundaram et al., 1998). Interestingly, the amino acid sequence of RBP contains 6 cysteines which form 3 disulphide bonds without any free thiols in the native protein (Rask et al., 1987). In addition, the substitution of these cysteines with serines induces decreased affinity for retinol and disturbs the 3D structure of the protein (Reznik et al., 2003). As with kininogen and serum amyloid P, the ICy dye labelling of RBP progressively increased with increasing UV doses (Figure 6-5F),

consistent with the generation of free thiol groups. Again, a likely explanation is that the disulphide bridges within RBP are broken due to UV irradiation, thus, increasing the free thiol content for ICy dye labelling.

6.3 Conclusions

In this chapter, UV-treated human plasma fractions provided by Baxter Healthcare were subjected to cysteine 2D-DIGE and MALDI-TOF-MS analysis. The aim was to investigate the effect of UV-C on plasma proteins particularly its effect on thiol oxidation and may be useful for understanding the possible drawbacks of UV disinfection of serum products. By means of cysteine 2D-DIGE, 29 protein features out of 1461 were confidently identified as UV-induced changes due to alterations in thiol reactivity or protein content of the samples. Seventeen gel features were aligned to coomassie blue stained gels and accurately picked for in-gel digestion and MALDI-TOF-MS identification and 13 of these were identified with confidence. The changes observed were classified into two groups, those displaying increased ICy dye labelling and those with decreased labelling. None of the changes were biphasic. Two serum transport proteins, serum amyloid P component (SAP) and retinol binding protein (RBP), and the coagulant-related factor, kininogen were found to display dose-dependent increases in labelling. One of the possible mechanisms for this could be the UV-induced breakage of disulphide bonds and exposure of pairs of free cysteine thiols for ICy dye labelling. Structural studies of SAP and RBP support this hypothesis as all of the cysteines in the two native proteins form disulphide bonds. The only mechanism for ICy dye labelling to take place therefore is the reduction of the disulphide bonds to generate free available thiols. As the formation/breakage of disulphide bonds may adversely alter the biological activity of proteins, the evaluation of the modifications of serum amyloid P, retinol binding protein and kininogen must be considered in preparations of blood derived products.

In contrast, the serum carrier protein ALB, the cytoskeleton protein actin, the host defense protein complement C4 and the coagulant factor prethrombin 2 all showed decreased ICy dye labelling with UV-treatment. Possible mechanisms to explain this are that the proteins could be degraded by UV as reported by Livden et al. (Livden et al.,

1987) or available free thiols are modified by UV-induced ROS to form the sulfenic, sulfinic or sulfonic forms of cysteines (Schafer *et al.*, 2001) which would both reduce labelling. These modifications might also exert the irreversible loss of protein activity and need to be evaluated before preparing UV-irradiated blood products for therapeutic use.

In this 2D-DIGE study, numerous SAP isoforms were identified in a charge train with all isoforms showing increase ICy dye labelling with increasing UV dose. This charge train might be caused by poor focusing or by labelling of multiple isoforms of SAP. As SAP contains only 2 cysteines, the ICy labelled protein would not generate more than 2 shifted isoforms indicating the formation of the charge train is not only due to labelling-induced p*I* shifts, but also contributed by uncharacterised isoforms of SAP. It is worth mentioning that a lysine 2D-DIGE analysis was also carried out to compare changes in protein abundance between untreated and UV-treated (80 mJ/cm^2) samples. This analysis revealed two consistent differences in repeat experiments, where the abundance of two protein isoforms was increased by an average of 2.75 and 10.1 fold, respectively. These isoforms represented very low-abundance species and could not be identified by MALDI-TOF-MS. Importantly, they ran at very different p*I*s and molecular weight than the isoforms displaying differential ICy labelling and are therefore unlikely to represent any of the isoforms identified here. These data suggest that UV induces specific changes in the thiol chemistry of proteins rather than changes in the abundance of the whole proteins or their degraded products. There are two hypotheses to explain the UV-C-induced reduction of disulphide bonds. One of these is that UV-C generates ROS to reduce the disulphide bond (Figure 6-6A). The other hypothesis is the disulphide bond absorbs the energy directly from UV-C and then the reduction event occurs (Figure 6-6B). The wavelength of UV-C ranges from 200 nm to 280 nm which overlaps with the absorbance spectra of DNA and RNA, but has little effect on protein (Chin et al., 1995). Therefore, a ROS mediated disulphide bond reduction model is the preferred mechanism.

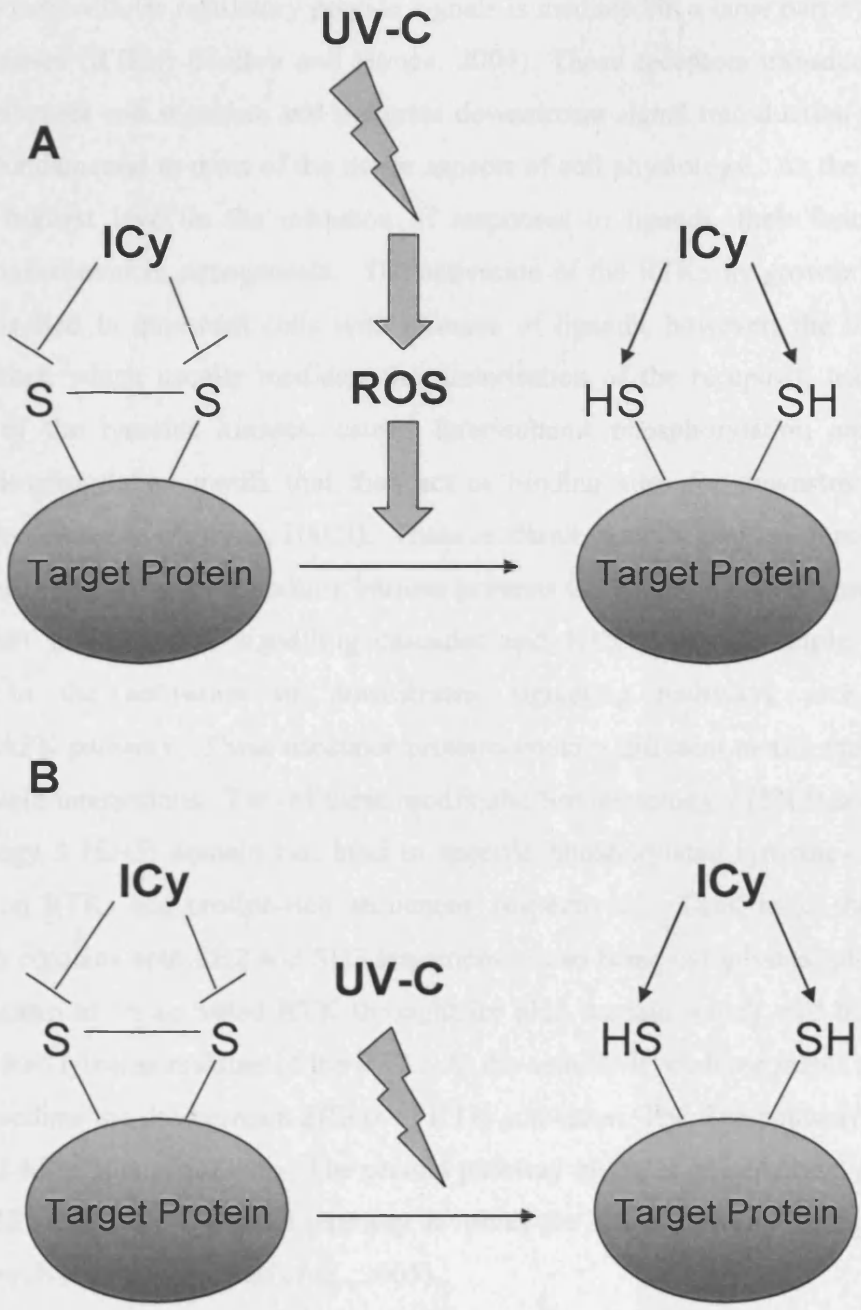

(Figure 6-6) Possible mechanisms for UV induced ICy dye labelling. (A) Indirect UV-C induces the breakage of disulphide bond due to the formation of ROS. (B) Direct UV-C induces the breakage of disulphide bond.

Chapter 7-DISCUSSION AND FUTURE PROSPECTS

The control of cell differentiation, proliferation, apoptosis, growth and migration in response to extracellular regulatory peptide signals is mediated in a large part by receptor tyrosine kinases (RTKs) (Holbro and Hynes, 2004). These receptors transduce signals across membranes and stimulate and integrate downstream signal transduction pathways which are fundamental to most of the major aspects of cell physiology. As the receptors are at the highest level in the initiation of responses to ligands, their functions are frequently taken over in oncogenesis. The activation of the RTKs by growth factors is tightly controlled in quiescent cells with absence of ligands, however, the binding of growth factors, which usually mediates the dimerisation of the receptors, leads to the activation of the tyrosine kinases, causes inter-subunit phosphorylation and creates tyrosine phosphorylation motifs that then act as binding sites for downstream signal mediators (reviewed in (Arteaga, 2002)). These mediator proteins play an important role in intracellular signalling by recruiting various proteins to specific locations, providing a link between molecules of signalling cascades and RTKs. For example, Grb2 is important in the activation of downstream signalling pathways such as the Ras/Raf/MAPK pathway. These mediator proteins contain different motifs that mediate protein-protein interactions. Two of these motifs, the Src homology 2 (SH2) domain and Src homology 3 (SH3) domain can bind to specific phoshorylated tyrosine-containing sequences on RTKs and proline-rich sequences, respectively. Thus, as in the case of Grb2 which contains both SH2 and SH3 sequences, it can bring cytoplasmic proteins via its SH3 domain to an activated RTK throught its SH2 domain which will bind to the phosphorylated tyrosine residues of the RTK. At the cellular level, three major signalling pathways mediate the downstream effects of RTK activation. The first pathway involves the Ras-Raf-MAP kinase pathway. The second pathway involves phosphatidylinositol 3-kinase (PI3K) and Akt. The third pathway involves the stress-activated protein kinase pathway, involving Jak/Stat (Bell *et al.*, 2005).

Because of the critical roles of RTKs in cellular signalling processes, their catalytic activity is under tight control. This is achieved by several mechanisms, which can be briefly summarised as follows: the phosphorylation state of a RTK can be controlled by

the activation of opposing signals such as protein tyrosine phosphtases (Hunter, 1995). Ligand-binding can lead to removal of receptors from the cell surface by endocytosis (Waterman and Yarden, 2001) and RTKs can be degraded following ubiquitination (Shtiegman and Yarden, 2003).

The critical position of the receptor at the top of the signal transduction cascade, means that alterations in expression levels, mutations of the receptor itself or loss of receptor - modifying enzymes, can lead to altered cellular functions and can therefore drive deregulated cell growth and contribute to the process of transformation (review in (Nicholson *et al.*, 2001)). Indeed, many oncogenes, which were discovered because of their altered function or expression in cancers or because they were related to viral oncogenes encode RTKs (Baserga, 1994). The era of genomics has extended the definition of those RTKs through gene sequencing projects and many RTKs are now known to be mutated or overexpressed in human cancers (Blume-Jensen and Hunter, 2001;Cox et al., 2005). The deregulation of the RTKs can also be caused by increased stimulation of RTKs through autocrine growth factor loops (Deuel et al., 1983;Sizeland and Burgess, 1992). Recent reports also indicate the increased RTK activity can be mediated by deletion or point mutation of the RTKs (Paez et al., 2004;Mason et al., 2004;Singh et al., 2005). For example, v-erbB, the oncogenic counterpart of EGFR, transduced as the viral oncogene of avian erythroblastosis virus. The mechanism of v-ErbB activation involves deletion of its ligand-binding domain, resulting in a truncated receptor (Downward et al., 1984). Another example is the neu transforming gene, the rat homologue of ErbB-2/HER2, which was identified as having a specific mutation in its transmembrane domain that was found to be responsible for its oncogenic potential and the constitutive activation of the kinase (Bargmann and Weinberg, 1988). These investigations suggest that these RTKs would be potential targets for human cancer therapy and according to the mechanism of RTK activation, many possible strategies can be used for therapeutic purpose. These include the design of antagonists for preventing ligands binding to RTKs (Sebti and Hamilton, 2000), the design of antibodies against RTKs (Glennie and Johnson, 2000), the design of kinase inhibitors for RTKs (Garrett and Workman, 1999), the design of inhibitors for preventing adaptor protein signalling (Garbay et al., 2000) and the design of inhibitors for preventing receptor dimerisation

(Berezov et al., 2002a) For example, the humanised monoclonal anti-ErbB-2 antibody Trastuzumab (Herceptin) can bind to the extracellular domain of ErbB-2 and lead to down-regulation of ErbB-2 by inducing receptor internalisation (Kumar et al., 1991) whilst small molecule EGFR tyrosine kinase inhibitors such as Gefitinib have been developed for non-small cell lung carcinoma therapy (Wakeling et al., 1996). Moreover, peptides of 12-30 amino acids which were derived from the potential extracellular dimerisation surface of ErbB receptors can inhibit ErbB-2 dimerisation and growth of cells overexpressing these receptors (Berezov et al., 2002b). However, the development of cancers is not only due to simple mutations or overexpression, but also the contribution of the deregulation of many biomolecules. The additional molecular abnormalities might reduce the therapeutic effect. Thus, combined treatment with different target-specific agents is necessary.

Proteomic technologies provide a powerful tool for the detailed comparison of proteins from cells under different growth conditions and have been applied to evaluate the effect of cancer therapies. For example, a proteomic method combining SDS-PAGE, chromatography and mass spectrometry has been used to profile the cellular targets affected by the action of the EGFR kinase inhibitor gefitinib and the results generated can help rational design of drugs (Brehmer et al., 2005). In addition, the ErbB receptor families have been intensively pursued as therapeutic targets owing to the large number of cancer patients whose tumours show aberrant ErbB family expression. Indeed, the ErbB-2 receptor has been shown to be overexpressed in 25 to 30% of invasive breast cancers and provides a useful marker for therapy. This is the reason why the model cell lines HB4a and its ErbB-2 overexpressing partner, C3.6 cells, were used to study cancer cell signalling in this thesis. Thus, proteomic techniques which can analyse the global changes of gene products and signalling molecules on a large scale are powerful tools to explore cancer-related signalling and to identify potential therapeutic candidates.

Studies on ErbB-2 have mostly focused on its proliferative and anti-apoptotic signalling capabilities which have been shown to promote tumourigenesis. However, there is very little information about the relationship between ErbB-2 signalling and cellular ROS, which can be induced by growth factor stimulation and may play a secondary messenger role in normal and cancer cells. With this in mind, another purpose of this study was to

examine the effects of ErbB-2 overexpression on the cellular response to oxidative stress. This study was thus aimed at elucidating the effects of ErbB-2 overexpression and H_2O_2-induced oxidative stress on protein levels and post-translational modifications using a combination of proteomic and biochemical analysis.

Several techniques have been used for proteomic differential expression studies, involving gel-based and non-gel based approaches (see Introduction). In this study, the recently developed technique of 2D-DIGE analysis was employed. This protein tagging and detection method uses a panel of matched fluorescent dyes to compare different samples on the same 2D gel, thus providing increased experimental reproducibility and accuracy for statistical analysis of differential protein expression between biological samples. In addition, given the wider linear dynamic range of fluorescence detection, this technique provides a better strategy for carrying out global expression profiling compared to conventional methods. The original 2D-DIGE methodology uses three N-hydroxysuccinimidyl (NHS) ester-derivatives of the cyanine dyes (NHS-Cy2, -Cy3 and -Cy5) for covalent labelling of protein primary amino groups (i. e. lysine ε-amino and N-terminal α-amino groups). In this procedure, differentially labelled samples are mixed and separated on the same 2D gels generating directly super-imposable 2DE images for quantitative analysis (Unlu *et al.*, 1997b). In 2D-DIGE expression profiling, one dye (e.g. Cy2) is used to label an internal standard pool of all samples which is run on every gel against the Cy3 and Cy5 labelled test samples (Gharbi *et al.*, 2002;Alban *et al.*, 2003). The fluorescence signal from each protein feature (Cy3 or Cy5 labelled) is then compared with the co-migrating standard feature (Cy2 labelled) on each gel to give a standardised abundance ratio that can be averaged across replicate samples and compared between different samples to allow identification of significant changes. NHS-Cy dye lysine labelling is typically carried out under conditions that limit modification to an estimated 3-5% of total protein (minimal labelling). This low stoichiometry is essential to avoid sample insolubility and heterogeneous multiple labelling in the molecular weight dimension. Overlabelling of lysine may also block tryptic cleavage sites, hindering the downstream identification of labelled proteins by mass spectrometry.

In order to improve the sensitivity of the NHS-Cy dye minimal labelling technique, labelling of a less prevalent amino acid at higher stoichiometry would be required. Such

an amino acid is cysteine which can be labelled through alkylation of its thiol group. To this end, a pair of iodoacetylated derivatives of the fluorescent cyanine dye was synthesised by our collaborator Dr. Piers Gaffney (LICR and now at Imperial College London). These reagents are charge- and size-matched, making it possible to carry out accurate protein expression profiling based on cysteinyl thiol labelling 2D-DIGE. In addition, cysteinyl thiols are targets of stress-induced oxidative modification, then these reagents were used to monitor such modifications, based on the fact that the iodoacetyl dyes would no longer react with oxidised thiol groups. Thus, the cysteine labelling dyes developed and described in this thesis were used to monitor changes in the redox status of protein thiols in response to specific stimuli, such as oxidants (Chapter 4), growth factors (Chapter 5) or UV irradiation (Chapter 6), as well as to examine changes in protein expression.

Initially, protein labelling using the ICy dyes was characterised and optimised for use in 2D-DIGE analysis (Chapter 3). These experiments showed that the ICy labelling is rapid under non-denaturing or denaturing conditions and that the protein solubility at high stoichiometry is better than with lysine labelling. The sensitivity of the ICy labelling is higher than the corresponding silver and CCB stains, though only 50% of the ICy-labelled protein features could be aligned to post-stained silver or CCB features. This difference is partly attributed to non free thiol-containing proteins which can not be detected by cysteine labelling strategy or proteins that silver-stain/ CCB stain poorly. Study of the dye to protein ratio optimum for labelling showed that 80 pmol of dye per μg of total cell lysate, which was chosen for 2D-DIGE experiments, gave a reasonably high sensitivity of labelling without compromising sample solubility or resulting in heterogeneous labelling and formation of over-complex spot patterns. Moreover, different thiols appeared to display different labelling reactivities although labelling was specific for free thiol groups. This could be caused by imcompletely denaturation of proteins or by the adjacent peptide sequences that interfere the dye accessibility. Apparent dye bias was observed in a small group of labelled proteins over 25-30 kDa molecular weight range. One hypothesis for this could be that SDS could interact differently with the two differentially labelled protein pools and affect their migration in gels. However, this could be overcome by using the internal standard labelling strategy.

Importantly, ICy dye labelling was compatible with MS analysis used to identify the differentially labelled proteins of interest. Thus, an optimised workflow was established for the analysis of protein expression profiles and redox-dependent thiol modifications.

Compared to the conventional NHS-lysine labelling strategy of 2D-DIGE, a drawback for the ICy dyes used here is the potential p*I* shift of ICy-labelled proteins caused by the positive charge on the dyes. Although such shifts were not formerly proved, this charge difference may lead to the loss of accurate experimental p*I* information which can help in the validation of MS search results. In addition, given the likely sub- stoichiometric labelling, dye-dependent shifts are likely to dilute the total amount of protein available for MS-identification and could partly explain why the "hit" rate for identification of differentially ICy labelled proteins was rather low. Since ICy dye labelling under non-reducing conditions is not completely dependent on protein amount, but rather reveals the total amount of free thiol groups that are affected by changes in thiol reactivity, a validation step such as immunoblotting or lysine-labelling 2D-DIGE is required to discriminate the labelling differences caused by altered thiol reactivity versus altered protein expression.

During the course of this work, a study based on the use of a pair of maleimide Cy dyes for cysteine 2D-DIGE labelling was reported by Shaw et al (Shaw et al., 2003). These dyes were recently commercialized by GE Helthcare for cysteine thiol "saturation" labelling of denatured and reduced samples. The evaluation of this labelling strategy showed improved sensitivity and dynamic range for the technique over the commercial minimal labelling method based on lysine labelling dyes (Shaw *et al.*, 2003). This analytical strategy was recently applied in two separate studies to identify proteomic changes in rare samples; between laser micro-dissected normal intestinal epithelium and adenoma (Kondo et al., 2003) and between differentially sorted murine bone marrow cell populations displaying distinct chemotactic responses (Evans et al., 2004). Comparison of the ICy dye labelling strategy used in this study with that for the maleimide Cy dyes revealed some similar findings, including increased sensitivity of detection of thiol-containing proteins, increased protein precipitation at high labelling ratios, altered 2DE spot patterns compared with minimal lysine labelling, a similar dynamic range of detection (~5000) and some apparent dye bias. However, there are notable differences

between the two strategies. The maleimide dyes were used for labelling of all cysteine-containing proteins in pre-reduced samples for sensitive expression profiling, whereas the focus here was to label non-reduced samples with a view to following redox-dependent thiol-reactivity. This is likely to affect the reactivity and extent of labelling. As such, we opted to use a lower dye to protein ratio and did not see the appreciable sample losses due to precipitation that was reported by Shaw et al (Shaw *et al.*, 2003). The labelling of fully reduced samples for ICy dye 2D-DIGE has yet to be explored. It is also worth noting that the maleimide dyes are sulphonated to give them a net neutral charge, and so they have the advantage that they should not alter the p*I* of labelled proteins, unlike the ICy dyes, where potential p*I* shifts will add complexity to the analysis. The other significant difference is that the current study used iodoacetyl derivatives of Cy3 and Cy5 as opposed to maleimides, on the basis of their expected greater reactivity. This should allow efficient labelling at lower temperatures, thereby reducing the risk of protein modification by the breakdown products of urea in the lysis buffer.

Although sample solubility is a problem when high stoichiometric labelling of either cysteine or lysine is carried out, we show that there is a distinct analytical advantage to be gained from labelling the lower-occurrence cysteine residues. This advantage was evident for example, in the reduction of heterogeneous labelling and the ability to monitor redox-dependent thiol modifications simultaneously. It is worth noting that our recent calculations predict that around 95% of all human open reading frames encode a cysteine-containing protein (R. Jacobs, unpublished data). Although a proportion of these would not be accessible to alkylation, our data showed significant labelling of free thiols in denatured, non-reduced lysates, with around 5% of the detectable proteins found to be susceptible to changes in labelling in response to oxidative stress. Since free/reactive thiol groups play important roles in enzyme catalysis and protein function, their redox modification is likely to alter protein function or oxidant-dependent signal transduction. Given the importance of oxidative stress in human disease, further studies should be undertaken to assess the functional significance of these modifications and to assess their role in cytoprotection, induced cellular damage and signalling.

In this thesis, the cysteine-labelling 2D-DIGE strategy was used to study the effects of H_2O_2 and ErbB-2 overexpression in a model cell system consisting of immortalised

HMLECs and to relate these changes to the early stages of breast cancer progression and the response to oxidative stress. These cell lines are an appropriate cell type to use, since most breast cancers arise from the luminal epithelium. In addition, the C3.6 cells were shown to overexpress surface levels of ErbB-2 similar to those observed in certain breast cancers (Harris *et al.*, 1999). The intracellular signalling pathways triggered by hydrogen peroxide were first examined. In agreement with previous studies (Caselli et al., 1998;Kwon *et al.*, 2004), cellular phospho-tyrosine levels were increased in both the HB4a and C3.6 cells after hydrogen peroxide treatment supporting the notion that H_2O_2 inhibits the activity of protein tyrosine phosphatases (PTP) by oxidising the free thiol cysteines of their active sites. Interestingly, more proteins were tyrosine phosphorylated and to a greater degree in the HB4a cells versus the C3.6 cells, indicating that ErbB-2 overexpression can affect the response to cellular oxidative stress. A model of the signalling role of H_2O_2 in growth factor stimulated cells is shown in Figure 7-1. The concentrations of free thiols in HB4a and C3.6 cells were reduced by 45% and 23%, respectively, after hydrogen peroxide treatment for 2 min, then recovered to ~80 % of the basal level after 20 min in both cell lines. This implies that C3.6 cells have a higher tolerance for peroxide and a more efficient mechanism for its removal which is somehow dependent upon ErbB-2 overexpression. In support of this, HB4a cells activated more rapid and stronger signalling responses, such as p38 activation, than the C3.6 cells. Thus, the C3.6 defence mechanisms would appear to act upstream of these signalling events and could remove H_2O_2 before these signalling events are activated. Cells were further compared by cysteine 2D-DIGE and fifty-one proteins with significant differential labelling were identified by MALDI-TOF-MS. It is important to note that all proteins identified contain at least one free cysteine thiol, validating the labelling specificity. Those identified proteins that were differentially labelled or expressed in response to hydrogen peroxide fell into three main functional groups that included molecular chaperones, cellular redox regulators and metabolic enzymes. The experimental strategy used also allowed simultaneous detection of proteins that were correlated with ErbB-2 overexpression in luminal epithelial cells. These ErbB-2 overexpression-related proteins included cytoskeletal proteins, molecular chaperones, redox regulatory proteins and

proliferation regulatory proteins. Importantly, some of the identified targets were differentially regulated by both H_2O_2 treatment and ErbB-2 overexpression.

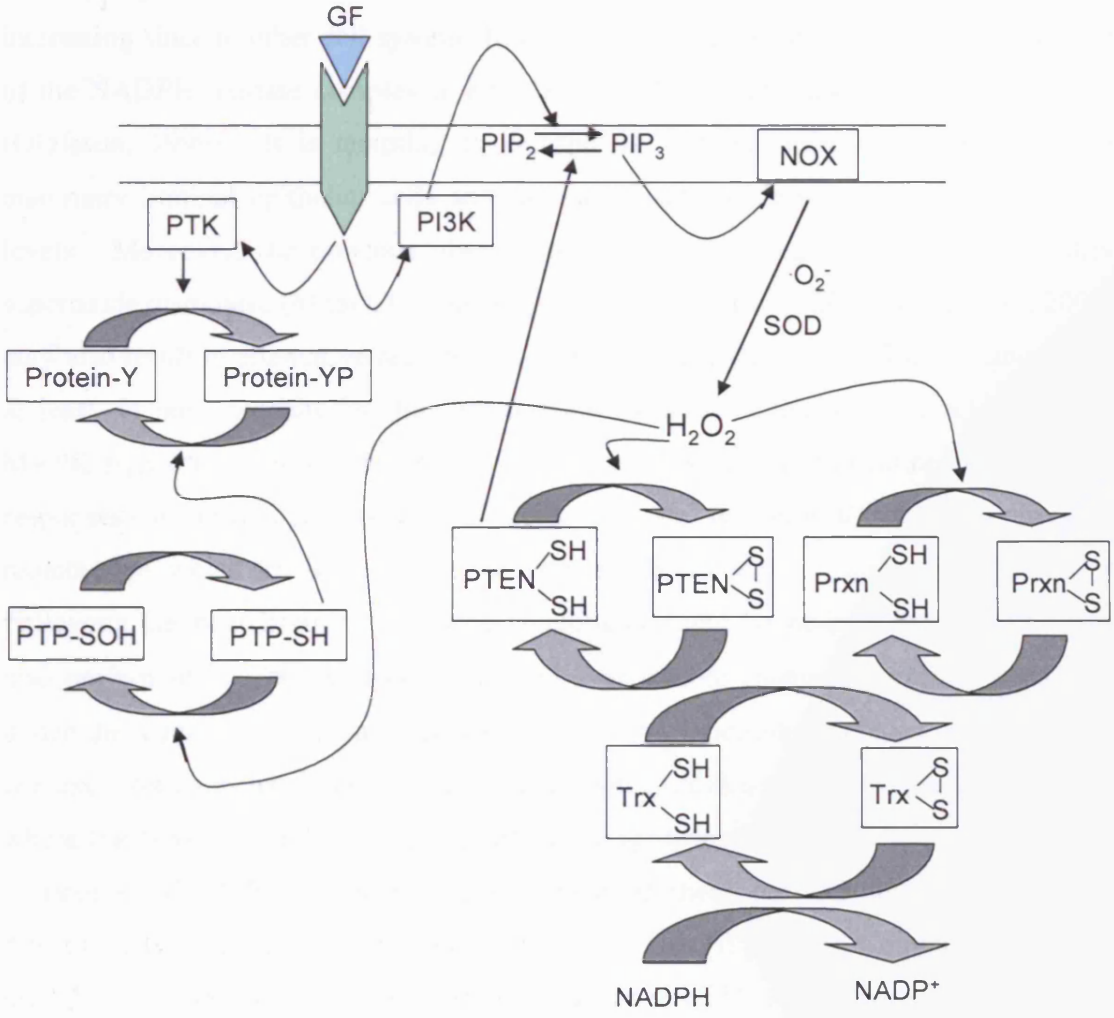

(Figure 7-1) Mechanisms for the production, signalling and removal of H_2O_2 in growth factor-stimulated cells. Stimulation of cells with a growth factor induces the activation of PI3K which catalyses the conversion of PIP_2 to PIP_3. PIP_3 can activate the NADPH oxidase (NOX) complex, which results in the production of O_2^- that can be converted to H_2O_2 through the action of SODs. The H_2O_2 mediates the inactivation of PTPs, PTEN and Prxs by modification of their active site cysteines to form Cys-SOH or intra-/inter-molecules disulphides. The oxidised PTEN and Prxs are regenerated by the cellular thioredoxin system.

The results from this study support the concept that ErbB-2 overexpression has diverse effects on the response of cells to oxidative stress through the regulated expression and activity of redox-sensitive enzymes and also through changes in stress-inducible proteins. The up-regulation of RhoGDI1 in the ErbB-2 overexpressing cells is particularly interesting since in other cell systems Rho-GDI has been shown to modulate recruitment of the NADPH oxidase complex to Rho-family GTPases for superoxide ion generation (Olofsson, 1999). It is tempting to extrapolate that this interaction also occurs in mammary luminal epithelial cells and may alter superoxide ion production and H_2O_2 levels. Moreover, the previous observation of the down-regulation of mitochondrial superoxide dismutase (MnSOD) in the C3.6 cells (Gharbi *et al.*, 2002;White et al., 2004), may also result in alternative regulation of intracellular H_2O_2 levels. These changes may at least, in part, account for the altered H_2O_2-inducible activation of Erk1/2 and p38 MAPK signalling in this cell system, which in turn has direct implications on the stress responses of normal versus tumour cells and the response to chemotherapy and radiotherapy which are likely to alter the redox status of cells.

Following the identification of cysteine-labelling changes, lysine-labelling 2D-DIGE was also performed to identify H_2O_2- and ErbB-2-dependent changes in protein expression under the same conditions and to compare the two labelling strategies in a biological context. As expected, there was an overlap with previous work from our labortatory where the HB4a and C3.6 cell proteomes were compared by lysine labelling 2D-DIGE (Gharbi *et al.*, 2002). In both cases, most of these proteins displayed the same directionality of up- or down-regulation in C3.6 versus HB4a cells. Comparison between the ICy and NHS-Cy dye analysis technologies revealed 11 individual gene products that were common to both methods and most of these displayed similar changes in labelling. This data confirms that the ICy dyes could detect changes in the abundance for these proteins, whilst the identification of unique gene products by each method shows the usefulness of applying both labelling strategies in better defining the proteomic changes associated with peroxide stress and ErbB-2 overexpression. Despite this, it is still difficult to discern the relative contributions of changes in protein abundance versus changes in thiol reactivity using the ICy dye labelling method alone and therefore, other

strategies are needed to discriminate between the two. Toward this end, 1D and 2D immunoblotting were applied. In most cases, changes in abundance were not detected, indicating the labelling changes were due to thiol modifications that block (e.g. formation of sulphinic acid or disulphide bonds) or enhance labelling (formation of free thiols or breakage of disulphide bonds). On the other hand, the proteins with changes both in abundance and in labelling mean that their gene expression are regulated by H_2O_2 or ErbB-2 overexpression.

Of the protein isoforms identified by both labelling methods, peroxiredoxins 1, 2 and 6 were identified as doublet spots with differing p*I*s by lysine labelling. Notably, the more basic spots in these doublets were all shown to be down-regulated after peroxide treatment, whilst the more acidic spots were up-regulated. A similar observation has been reported (Wagner *et al.*, 2002;Rabilloud *et al.*, 2002b) and was found to be due to oxidation of the active site cysteine thiols of these proteins. Such shifts provide an explanation for the observed differential labelling by the ICy dyes. Figure 7-2 explains a possible model for p*I* shift-induced differential labelling. Briefly, hydrogen peroxide oxidises a specific free thiol cysteine of a multi-cysteine protein and induces the acidic-shift of the protein. When ICy labelling is performed, the remaining free thiols of the p*I* shifted protein and the original protein are both labelled resulting in the increased detection of the shifted isoform and decreased detection of the original isoform due to changes in abundance. This model is made more valid by the fact that Prxns 1, 2, and 6 also possess free thiols in addition to the reactive site thiol, which is the presumed target of H_2O_2-dependent oxidation. Elongation factor 2 and enolase alpha also existed as multiple isoforms, where the more acidic isoforms were up-regulated by peroxide treatment, suggesting that they may also be oxidised and shifted in p*I*. These modifications may affect protein activity and warrant further investigation. It should be noted, however, that the dyes may also shift labelled proteins to more basic isoforms, thus, complicating the pattern of detected isoforms, although such dye-induced shifts were not formally proven.

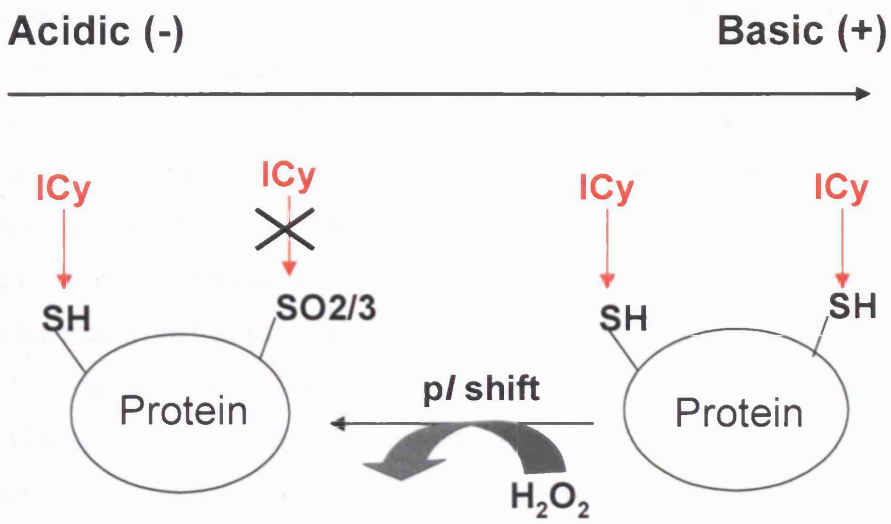

(Figure 7-2) A possible model for p*I* shift induced differential ICy dye labelling.

The data from 2D-DIGE protein expression profiling of the model human luminal epithelial cell system presented here was compared to other published proteomic studies of breast and other cancers and some correlations in the datasets were observed. Several of the identified proteins have been shown to be differentially regulated in various human cancers and could therefore play important roles in the processes associated with human luminal epithelial cell transformation. For example, Hsp27 showed a significant increase in abundance in the C3.6 cells compared to the HB4a cells. This chaperone protein has been implicated in various cellular processes including stress response and apoptosis and has been reported to be overexpressed in various human cancers (Sarto et al., 2000a) including breast ductal carcinoma (Wulfkuhle et al., 2002). L-plastin is a member of the plastin family of actin-bundling proteins. Although it was thought to be specific to heamopoietic cell lineages, it has been found overexpressed in malignant human solid tumours (Lin et al., 1993;Park et al., 1994). L-plastin is known to regulate cell adhesion and motility (Otsuka et al., 2001) and its deregulated expression has been correlated with cancer invasion and metastasis (Zheng et al., 1999). Indeed, cancer cells transfected with an antisense L-plastin gene were shown to display suppression of *in vivo* tumour invasion in nude mice. Since L-plastin upregulation was observed in the C3.6 cells, it may thus

contribute to ErbB-2-dependent tumour invasion. Cytokeratin17 which is overexpressed in squamous cell carcinomas has been shown to be a highly sensitive and specific immunohistochemical marker for premalignant and malignant transformation in the larynx (Cohen-Kerem et al., 2004). The observation of increased cytokeratin 17 in the ErbB-2 overexpressing cells again supports the notion that it may be involved in ErbB-2-dependent malignancy. Thus, the current study using 2D-DIGE can be used for the identification of important putative protein targets that have potential regulatory roles in ErbB-2-dependent cell transformation. The proteomic approach undertaken here has provided crucial preliminary information regarding the effects of ErbB-2 overexpression in a cellular model, giving rise to many interesting hypotheses which should be followed up on and which could provide new insights into the molecular mechanisms associated with cancer progression.

Although ICy3/5 labelling could be used to specifically and sensitively detect free thiol groups in proteins and investigate redox regulations in cells, it appeared that some low-abundance, differentially expressed/labelled proteins were not amenable to mass spectrometric identification due to insufficient material. Thus, in the future, enrichment strategies should be employed to try and identify these proteins. This could include the uses of zoom gels or sub-cellular fractionation to increase the loading and analysis of proteome subsets. However, proteins could also be labelled with affinity-tagged cysteine dyes, to enable enrichment of only labelled protein prior to 2DE. Our laboratory has recently synthesised such dyes containing a biotin group on the opposite arm to the iodoacetamide group and they should allow for recovery of purified labelled protein using immobilised streptavidin with improved recovery through the use of a cleavable linker (Figure 7-3). Conditions are currently being optimised in our laboratory for the use of these reagents for 2D-DIGE and subsequent protein identification by mass spectrometry.

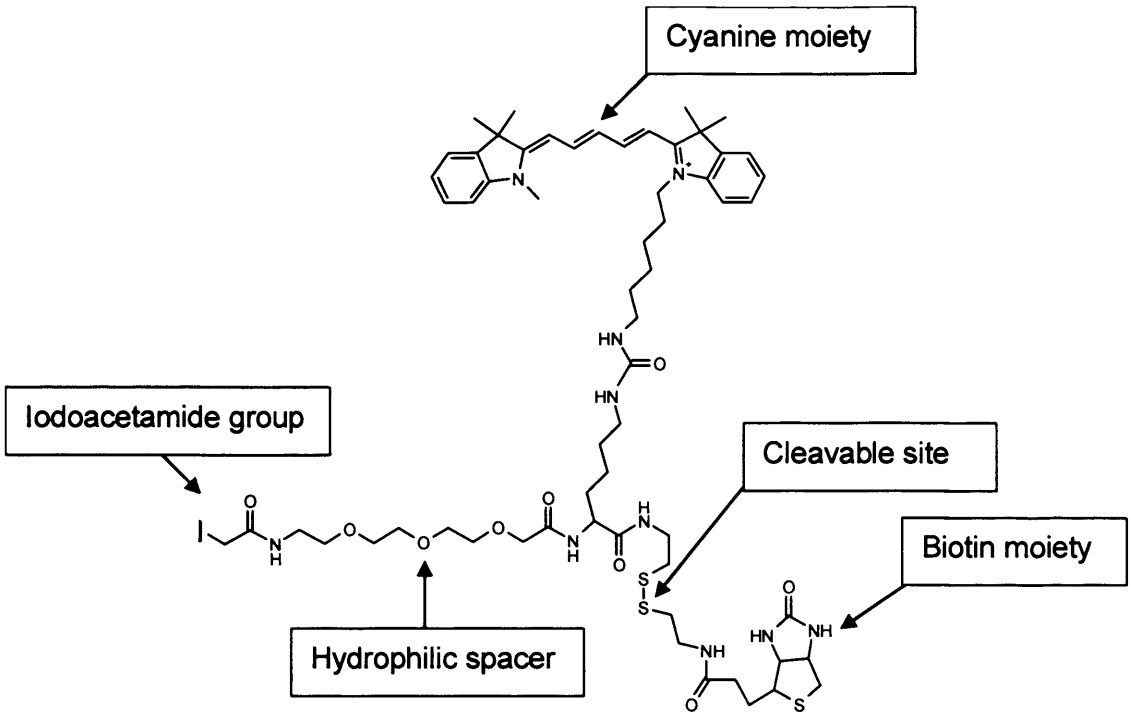

(Figure 7-3) The structure of an affinity-tagged cleavable cysteine label (IBCCy3).

In general, the 2D-DIGE analysis in this thesis represents a new technique to help understand ErbB-2 dependent cellular transformation and how ErbB-2 affects redox responses. However, further work beyond the scope of this study should be carried out to characterise how the identified changes affect cell behaviour, cellular signalling or cell morphology. For example, one question would be whether oxidation of RanGTPase affects nucleo-cytoplasmic transport. This could be achieved by proteins known to be transported by Ran using immunofluorescence. Others experiments would use RNAi-mediated knockdown to alter the expression of specific proteins of interest (Cullen, 2002;Famulok and Verma, 2002). This strategy could be applied to this model cell system to examine the effects of particular proteins on cell proliferation and survival in the absence or prescence of oxidative stress. As an inverse strategy, overexpression of the proteins of interest (such as peroxiredoxin 6) could also be tested for effects on cell proliferation and survival, following exposure to oxidative stress.

One of the important issues in redox studies is to look for the breakage or formation of disulphide bonds. Whilst the ICy dye strategy used here must be detecting such events,

an alternative reverse labelling strategy could be applied to more directly assess disulphide formation/breakage. Basically, protein samples from ROS treated cells would be harvested under anaerobic conditions in lysis buffer containing an alkylating agent such as iodoacetic acid (IAA). Those cellular proteins that had not encountered ROS in the cell will become irreversibly alkylated on their free thiol groups by IAA. In contrast, any protein in which free thiol cysteines have been oxidised in response to the ROS stimulation will be resistant to alkylation. Following reduction with DTT, all of the reversible ROS-modified proteins will now possess free thiols for labelling. This technique has been used to study the reversible oxidation and inactivation of proteins including protein tyrosine phosphatases (Meng et al., 2002;Baty et al., 2002). An advantage of this methodology is that it was suitable for conducting in-gel protein activity assays to test the effect of oxidation of PTP activity. Thus, the ICy dyes could be used for this reverse labelling strategy in the future.

The usefulness of the ICy dye labelling strategy was further tested by applying it to examine EGF-induced changes in thiol labelling. Native and denatured protein labelling were both performed to study potential EGF-induced thiol accessibility and reactivity changes of proteins. There were few significant changes observed in these experiments, suggesting that alterations in the accessibility of cysteinyl thiols and the redox modification of protein thiols do occur, however, the dissociation/association of protein complexes or the redox regulation of cellular cysteines is not the dominant mechanism of regulation following EGF treatment. Instead, EGF stimulation predominately induces downstream signalling or regulates cell functions by mechanisms such as phosphorylation of mediators through kinase action. Nevertheless, the importance of the EGF signalling related dissociation/association of protein complexes and redox regulation cannot be neglected. Notably, Prxn-6 was identified as being differentially labelled under both native condition and denaturing condition suggesting that the changes in thiol reactivity of the Prxn-6 are caused by covalent modification (redox reaction) rather than by cysteine accessibility. Furthermore, this redox modification of Prxn-6 could be that EGF stimulates the generation of low concentrations of intracellular H_2O_2 which oxidises the active site cysteine of Prxn-6 in cells (see Chapter 5).

In a different application, ICy 2D-DIGE was used to investigate UV-C induced changes in thiol reactivity in human plasma fractions. Although UV-C irradiation did not induce significant effects on the blood clotting functions of the fractions (data from Baxter Healthcare), it did indeed induce thiol reactivity changes in the purified plasma proteins in this study. The possible mechanisms for these could involve UV induced breakage of disulphide bonds or direct modification of free thiols by UV-C induced ROS. Future studies would aim to identify the nature of these modifications, try to assess how they affect protein function and find out why those identified proteins are more easily modified by UV-C than the other proteins. More important than evaluation of loss of bio-reactivity or change of the structure of these proteins is the question of whether the potential toxicity of these modified proteins presents a danger to patients.

In summary, cysteine-labelling 2D-DIGE using the ICy dyes has been optimised and evaluated for differential proteomics in this thesis. Using MS, their application has been shown in the identification of targets of cellular oxidative stress (Chapter 4), to study growth factor-induced thiol reactivity (Chapter 5) and to determine UV-C-induced thiol reactivity changes (Chapter 6). In future, cysteine-labelling 2D-DIGE could be applied to study other systems and diseases where oxidative stress is thought to play a role. For example, this system could be applied to study ischemic reperfusion-injury in cardiac cells (Ambrosio et al., 1992;Molyneux et al., 2002;Leducq et al., 2003) or to study protein targets of radiation (χ-ray/γ-ray)-induced intracellular oxidative stress that cause DNA damage and apoptosis (Nakano and Shinohara, 1994;Risom et al., 2003). In conclusion, the cysteine-labelling 2D-DIGE provides an MS-compatible and reproducible technique for identifying significant differences in the expression and redox modification of free thiol-containing proteins in multiple biological samples. This was achieved by labelling cysteine thiol groups with a matched pair of fluorescent alkylating agents.

REFERENCES

Accinni,L., Natali,P.G., Silvestrini,M., and De Martino,C. (1983). Actin in the extracellular matrix of smooth muscle cells. An immunoelectron microscopic study. *Connect. Tissue Res.*, **11,** 69-78.

Adra,C.N., Manor,D., Ko,J.L., Zhu,S., Horiuchi,T., Van Aelst,L., Cerione,R.A., and Lim,B. (1997). RhoGDIgamma: a GDP-dissociation inhibitor for Rho proteins with preferential expression in brain and pancreas. *Proc. Natl. Acad. Sci. U. S. A,* **94,** 4279-4284.

Aebersold,R. and Mann,M. (2003). Mass spectrometry-based proteomics. *Nature,* **422,** 198-207.

Alban,A., David,S.O., Bjorkesten,L., Andersson,C., Sloge,E., Lewis,S., and Currie,I. (2003). A novel experimental design for comparative two-dimensional gel analysis: two-dimensional difference gel electrophoresis incorporating a pooled internal standard. *Proteomics.*, **3,** 36-44.

Allen,R.G. and Tresini,M. (2000). Oxidative stress and gene regulation. *Free Radic. Biol. Med.*, **28,** 463-499.

Ambrosio,G., Santoro,G., Tritto,I., Elia,P.P., Duilio,C., Basso,A., Scognamiglio,A., and Chiariello,M. (1992). Effects of ischemia and reperfusion on cardiac tolerance to oxidative stress. *Am. J. Physiol,* **262,** H23-H30.

Amstad,P., Crawford,D., Muehlematter,D., Zbinden,I., Larsson,R., and Cerutti,P. (1990). Oxidants stress induces the proto-oncogenes, C-fos and C-myc in mouse epidermal cells. *Bull. Cancer,* **77,** 501-502.

Arscott,L.D., Veine,D.M., and Williams,C.H., Jr. (2000). Mixed disulfide with glutathione as an intermediate in the reaction catalyzed by glutathione reductase from yeast and as a major form of the enzyme in the cell. *Biochemistry,* **39,** 4711-4721.

Arteaga,C.L. (2002). Overview of epidermal growth factor receptor biology and its role as a therapeutic target in human neoplasia. *Semin. Oncol.*, **29,** 3-9.

Aslan,M. and Ozben,T. (2003). Oxidants in receptor tyrosine kinase signal transduction pathways. *Antioxid. Redox. Signal.*, **5,** 781-788.

Babior,B.M. (1999). NADPH oxidase: an update. *Blood,* **93,** 1464-1476.

Bae,Y.S., Kang,S.W., Seo,M.S., Baines,I.C., Tekle,E., Chock,P.B., and Rhee,S.G. (1997). Epidermal growth factor (EGF)-induced generation of hydrogen peroxide. Role in EGF receptor-mediated tyrosine phosphorylation. *J Biol Chem,* **272,** 217-21.

Bae,Y.S., Sung,J.Y., Kim,O.S., Kim,Y.J., Hur,K.C., Kazlauskas,A., and Rhee,S.G. (2000). Platelet-derived growth factor-induced H(2)O(2) production requires the activation of phosphatidylinositol 3-kinase. *J Biol Chem,* **275,** 10527-31.

Bange,J., Zwick,E., and Ullrich,A. (2001). Molecular targets for breast cancer therapy and prevention. *Nat. Med.,* **7,** 548-552.

Bardel,J., Louwagie,M., Jaquinod,M., Jourdain,A., Luche,S., Rabilloud,T., Macherel,D., Garin,J., and Bourguignon,J. (2002). A survey of the plant mitochondrial proteome in relation to development. *Proteomics.,* **2,** 880-898.

Bardos,J.I. and Ashcroft,M. (2004). Hypoxia-inducible factor-1 and oncogenic signalling. *Bioessays,* **26,** 262-269.

Bargmann,C.I. and Weinberg,R.A. (1988). Oncogenic activation of the neu-encoded receptor protein by point mutation and deletion. *EMBO J.,* **7,** 2043-2052.

Barnouin,K., Dubuisson,M.L., Child,E.S., Fernandez De Mattos,S., Glassford,J., Medema,R.H., Mann,D.J., and Lam,E.W. (2002). H2O2 induces a transient multi-phase cell cycle arrest in mouse fibroblasts through modulating cyclin D and p21Cip1 expression. *J Biol Chem,* **4,** 4.

Barrett,W.C., DeGnore,J.P., Keng,Y.F., Zhang,Z.Y., Yim,M.B., and Chock,P.B. (1999). Roles of superoxide radical anion in signal transduction mediated by reversible regulation of protein-tyrosine phosphatase 1B. *J Biol Chem,* **274,** 34543-6.

Bartek,J., Bartkova,J., Kyprianou,N., Lalani,E.N., Staskova,Z., Shearer,M., Chang,S., and Taylor-Papadimitriou,J. (1991). Efficient immortalization of luminal epithelial cells from human mammary gland by introduction of simian virus 40 large tumor antigen with a recombinant retrovirus. *Proc. Natl. Acad. Sci. U. S. A,* **88,** 3520-3524.

Baselga,J. (2001). The EGFR as a target for anticancer therapy--focus on cetuximab. *Eur. J. Cancer,* **37 Suppl 4,** S16-S22.

Baserga,R. (1994). Oncogenes and the strategy of growth factors. *Cell,* **79,** 927-930.

Baty,J.W., Hampton,M.B., and Winterbourn,C.C. (2002). Detection of oxidant sensitive thiol proteins by fluorescence labeling and two-dimensional electrophoresis. *Proteomics,* **2,** 1261-6.

Baulida,J., Kraus,M.H., Alimandi,M., Di Fiore,P.P., and Carpenter,G. (1996). All ErbB receptors other than the epidermal growth factor receptor are endocytosis impaired. *J. Biol. Chem.,* **271,** 5251-5257.

Beckman,J.S. (1996). Oxidative damage and tyrosine nitration from peroxynitrite. *Chem. Res. Toxicol.,* **9,** 836-844.

Behrend,L., Henderson,G., and Zwacka,R.M. (2003). Reactive oxygen species in oncogenic transformation. *Biochem. Soc. Trans.*, **31,** 1441-1444.

Bell,H.S. and Ryan,K.M. (2005). Intracellular signalling and cancer: complex pathways lead to multiple targets. *Eur. J. Cancer,* **41,** 206-215.

Bell,L.A. and Ryan,K.M. (2004). Life and death decisions by E2F-1. *Cell Death. Differ.*, **11,** 137-142.

Benvenuti,S., Cramer,R., Bruce,J., Waterfield,M.D., and Jat,P.S. (2002). Identification of novel candidates for replicative senescence by functional proteomics. *Oncogene,* **21,** 4403-4413.

Berezov,A., Chen,J., Liu,Q., Zhang,H.T., Greene,M.I., and Murali,R. (2002a). Disabling receptor ensembles with rationally designed interface peptidomimetics. *J. Biol. Chem.*, **277,** 28330-28339.

Berezov,A., Chen,J., Liu,Q., Zhang,H.T., Greene,M.I., and Murali,R. (2002b). Disabling receptor ensembles with rationally designed interface peptidomimetics. *J. Biol. Chem.*, **277,** 28330-28339.

Berggren,K.N., Chernokalskaya,E., Lopez,M.F., Beechem,J.M., and Patton,W.F. (2001). Comparison of three different fluorescent visualization strategies for detecting Escherichia coli ATP synthase subunits after sodium dodecyl sulfate-polyacrylamide gel electrophoresis. *Proteomics.*, **1,** 54-65.

Berggren,K.N., Schulenberg,B., Lopez,M.F., Steinberg,T.H., Bogdanova,A., Smejkal,G., Wang,A., and Patton,W.F. (2002). An improved formulation of SYPRO Ruby protein gel stain: comparison with the original formulation and with a ruthenium II tris (bathophenanthroline disulfonate) formulation. *Proteomics.*, **2,** 486-498.

Biemann,K. (1990). Appendix 5. Nomenclature for peptide fragment ions (positive ions). *Methods Enzymol.*, **193,** 886-887.

Biemann,K. and Scoble,H.A. (1987). Characterization by tandem mass spectrometry of structural modifications in proteins. *Science,* **237,** 992-998.

Birge,R.B., Bartolone,J.B., Cohen,S.D., Khairallah,E.A., and Smolin,L.A. (1991). A comparison of proteins S-thiolated by glutathione to those arylated by acetaminophen. *Biochem. Pharmacol.*, **42 Suppl,** S197-S207.

Bishop,A.L. and Hall,A. (2000). Rho GTPases and their effector proteins. *Biochem. J.*, **348 Pt 2,** 241-255.

Bjellqvist,B., Ek,K., Righetti,P.G., Gianazza,E., Gorg,A., Westermeier,R., and Postel,W. (1982). Isoelectric focusing in immobilized pH gradients: principle, methodology and some applications. *J. Biochem. Biophys. Methods,* **6,** 317-339.

Blagoev,B., Kratchmarova,I., Ong,S.E., Nielsen,M., Foster,L.J., and Mann,M. (2003). A proteomics strategy to elucidate functional protein-protein interactions applied to EGF signaling. *Nat. Biotechnol.*, **21,** 315-318.

Blanc,A., Pandey,N.R., and Srivastava,A.K. (2003). Synchronous activation of ERK 1/2, p38mapk and PKB/Akt signaling by H2O2 in vascular smooth muscle cells: potential involvement in vascular disease (review). *Int. J. Mol. Med.*, **11,** 229-234.

Blaner,W.S. (1989). Retinol-binding protein: the serum transport protein for vitamin A. *Endocr. Rev.*, **10,** 308-316.

Blume-Jensen,P. and Hunter,T. (2001). Oncogenic kinase signalling. *Nature,* **411,** 355-365.

Bokoch,G.M. (2000). Regulation of cell function by Rho family GTPases. *Immunol. Res.*, **21,** 139-148.

Boveris,A. and Chance,B. (1973). The mitochondrial generation of hydrogen peroxide. General properties and effect of hyperbaric oxygen. *Biochem. J.*, **134,** 707-716.

Brehmer,D., Greff,Z., Godl,K., Blencke,S., Kurtenbach,A., Weber,M., Muller,S., Klebl,B., Cotten,M., Keri,G., Wissing,J., and Daub,H. (2005). Cellular targets of gefitinib. *Cancer Res.*, **65,** 379-382.

Brigelius,R., Muckel,C., Akerboom,T.P., and Sies,H. (1983). Identification and quantitation of glutathione in hepatic protein mixed disulfides and its relationship to glutathione disulfide. *Biochem. Pharmacol.*, **32,** 2529-2534.

Brocklehurst,K., Kierstan,M., and Little,G. (1972). The reaction of papain with Ellman's reagent (5,5'-dithiobis- (2-nitrobenzoate) dianion). *Biochem. J.*, **128,** 811-816.

Butterfield,D.A. and Kanski,J. (2001). Brain protein oxidation in age-related neurodegenerative disorders that are associated with aggregated proteins. *Mech. Ageing Dev.*, **122,** 945-962.

Cantley,L.C., Auger,K.R., Carpenter,C., Duckworth,B., Graziani,A., Kapeller,R., and Soltoff,S. (1991). Oncogenes and signal transduction. *Cell,* **64,** 281-302.

Caplan,J.F., Filipenko,N.R., Fitzpatrick,S.L., and Waisman,D.M. (2004). Regulation of annexin A2 by reversible glutathionylation. *J. Biol. Chem.*, **279,** 7740-7750.

Caselli,A., Marzocchini,R., Camici,G., Manao,G., Moneti,G., Pieraccini,G., and Ramponi,G. (1998). The inactivation mechanism of low molecular weight phosphotyrosine- protein phosphatase by H2O2. *J Biol Chem,* **273,** 32554-60.

Castellanos-Serra,L., Proenza,W., Huerta,V., Moritz,R.L., and Simpson,R.J. (1999). Proteome analysis of polyacrylamide gel-separated proteins visualized by reversible negative staining using imidazole-zinc salts. *Electrophoresis,* **20,** 732-737.

Chae,H.Z., Chung,S.J., and Rhee,S.G. (1994). Thioredoxin-dependent peroxide reductase from yeast. *J. Biol. Chem.*, **269,** 27670-27678.

Chan,R., Hardy,W.R., Laing,M.A., Hardy,S.E., and Muller,W.J. (2002). The catalytic activity of the ErbB-2 receptor tyrosine kinase is essential for embryonic development. *Mol. Cell Biol.*, **22,** 1073-1078.

Chen,G., Gharib,T.G., Huang,C.C., Thomas,D.G., Shedden,K.A., Taylor,J.M., Kardia,S.L., Misek,D.E., Giordano,T.J., Iannettoni,M.D., Orringer,M.B., Hanash,S.M., and Beer,D.G. (2002). Proteomic analysis of lung adenocarcinoma: identification of a highly expressed set of proteins in tumors. *Clin. Cancer Res.*, **8,** 2298-2305.

Chin,S., Williams,B., Gottlieb,P., Margolis-Nunno,H., Ben Hur,E., Hamman,J., Jin,R., Dubovi,E., and Horowitz,B. (1995). Virucidal short wavelength ultraviolet light treatment of plasma and factor VIII concentrate: protection of proteins by antioxidants. *Blood,* **86,** 4331-4336.

Choi,H.J., Kang,S.W., Yang,C.H., Rhee,S.G., and Ryu,S.E. (1998). Crystal structure of a novel human peroxidase enzyme at 2.0 A resolution. *Nat. Struct. Biol.*, **5,** 400-406.

Ciardiello,F. (2000). Epidermal growth factor receptor tyrosine kinase inhibitors as anticancer agents. *Drugs,* **60 Suppl 1,** 25-32.

Cohen-Kerem,R., Madah,W., Sabo,E., Rahat,M.A., Greenberg,E., and Elmalah,I. (2004). Cytokeratin-17 as a potential marker for squamous cell carcinoma of the larynx. *Ann. Otol. Rhinol. Laryngol.*, **113,** 821-827.

Connolly,T. and Gilmore,R. (1989). The signal recognition particle receptor mediates the GTP-dependent displacement of SRP from the signal sequence of the nascent polypeptide. *Cell,* **57,** 599-610.

Cooper,J.W., Wang,Y., and Lee,C.S. (2004). Recent advances in capillary separations for proteomics. *Electrophoresis,* **25,** 3913-3926.

Corthals,G.L., Wasinger,V.C., Hochstrasser,D.F., and Sanchez,J.C. (2000). The dynamic range of protein expression: a challenge for proteomic research. *Electrophoresis,* **21,** 1104-1115.

Cotgreave,I.A. and Gerdes,R.G. (1998). Recent trends in glutathione biochemistry--glutathione-protein interactions: a molecular link between oxidative stress and cell proliferation? *Biochem. Biophys. Res. Commun.*, **242,** 1-9.

Cox,C., Bignell,G., Greenman,C., Stabenau,A., Warren,W., Stephens,P., Davies,H., Watt,S., Teague,J., Edkins,S., Birney,E., Easton,D.F., Wooster,R., Futreal,P.A., and Stratton,M.R. (2005). A survey of homozygous deletions in human cancer genomes. *Proc. Natl. Acad. Sci. U. S. A,* **102,** 4542-4547.

Cross,A.R. and Jones,O.T. (1991). Enzymic mechanisms of superoxide production. *Biochim. Biophys. Acta,* **1057,** 281-298.

Cullen,B.R. (2002). RNA interference: antiviral defense and genetic tool. *Nat. Immunol.,* **3,** 597-599.

Curtin,J.F., Donovan,M., and Cotter,T.G. (2002). Regulation and measurement of oxidative stress in apoptosis. *J. Immunol. Methods,* **265,** 49-72.

Daban,J.R. (2001). Fluorescent labeling of proteins with nile red and 2-methoxy-2,4-diphenyl-3(2H)-furanone: physicochemical basis and application to the rapid staining of sodium dodecyl sulfate polyacrylamide gels and Western blots. *Electrophoresis,* **22,** 874-880.

Daban,J.R., Bartolome,S., and Samso,M. (1991). Use of the hydrophobic probe Nile red for the fluorescent staining of protein bands in sodium dodecyl sulfate-polyacrylamide gels. *Anal. Biochem.,* **199,** 169-174.

Dalle-Donne,I., Rossi,R., Milzani,A., Di Simplicio,P., and Colombo,R. (2001). The actin cytoskeleton response to oxidants: from small heat shock protein phosphorylation to changes in the redox state of actin itself. *Free Radic. Biol. Med.,* **31,** 1624-1632.

de Haas,C.J. (1999). New insights into the role of serum amyloid P component, a novel lipopolysaccharide-binding protein. *FEMS Immunol. Med. Microbiol.,* **26,** 197-202.

de Haas,C.J., van der Tol,M.E., Van Kessel,K.P., Verhoef,J., and Van Strijp,J.A. (1998). A synthetic lipopolysaccharide-binding peptide based on amino acids 27-39 of serum amyloid P component inhibits lipopolysaccharide-induced responses in human blood. *J. Immunol.,* **161,** 3607-3615.

Declercq,J.P., Evrard,C., Clippe,A., Stricht,D.V., Bernard,A., and Knoops,B. (2001). Crystal structure of human peroxiredoxin 5, a novel type of mammalian peroxiredoxin at 1.5 A resolution. *J. Mol. Biol.,* **311,** 751-759.

Delaunay,A., Pflieger,D., Barrault,M.B., Vinh,J., and Toledano,M.B. (2002). A thiol peroxidase is an H2O2 receptor and redox-transducer in gene activation. *Cell,* **111,** 471-481.

Denu,J.M. and Tanner,K.G. (1998). Specific and reversible inactivation of protein tyrosine phosphatases by hydrogen peroxide: evidence for a sulfenic acid intermediate and implications for redox regulation. *Biochemistry,* **37,** 5633-42.

DerMardirossian,C., Schnelzer,A., and Bokoch,G.M. (2004). Phosphorylation of RhoGDI by Pak1 mediates dissociation of Rac GTPase. *Mol. Cell,* **15,** 117-127.

Deuel,T.F., Huang,J.S., Huang,S.S., Stroobant,P., and Waterfield,M.D. (1983). Expression of a platelet-derived growth factor-like protein in simian sarcoma virus transformed cells. *Science,* **221,** 1348-1350.

Di-Poi,N., Faure,J., Grizot,S., Molnar,G., Pick,E., and Dagher,M.C. (2001). Mechanism of NADPH oxidase activation by the Rac/Rho-GDI complex. *Biochemistry,* **40,** 10014-22.

Downward,J., Yarden,Y., Mayes,E., Scrace,G., Totty,N., Stockwell,P., Ullrich,A., Schlessinger,J., and Waterfield,M.D. (1984). Close similarity of epidermal growth factor receptor and v-erb-B oncogene protein sequences. *Nature,* **307,** 521-527.

Dyson,N., Howley,P.M., Munger,K., and Harlow,E. (1989). The human papilloma virus-16 E7 oncoprotein is able to bind to the retinoblastoma gene product. *Science,* **243,** 934-937.

El'chaninov,V.V. and Fedorovich,I.B. (1990). [The mechanism of photodamage of eye structures. IV. Changes in the reactivity of crystalline SH-groups during UV irradiation]. *Biokhimiia.,* **55,** 1304-1308.

Emsley,J., White,H.E., O'Hara,B.P., Oliva,G., Srinivasan,N., Tickle,I.J., Blundell,T.L., Pepys,M.B., and Wood,S.P. (1994b). Structure of pentameric human serum amyloid P component. *Nature,* **367,** 338-345.

Emsley,J., White,H.E., O'Hara,B.P., Oliva,G., Srinivasan,N., Tickle,I.J., Blundell,T.L., Pepys,M.B., and Wood,S.P. (1994a). Structure of pentameric human serum amyloid P component. *Nature,* **367,** 338-345.

Emsley,J., White,H.E., O'Hara,B.P., Oliva,G., Srinivasan,N., Tickle,I.J., Blundell,T.L., Pepys,M.B., and Wood,S.P. (1994c). Structure of pentameric human serum amyloid P component. *Nature,* **367,** 338-345.

Ennion,S.J. and Evans,R.J. (2002). Conserved cysteine residues in the extracellular loop of the human P2X(1) receptor form disulfide bonds and are involved in receptor trafficking to the cell surface. *Mol. Pharmacol.,* **61,** 303-311.

Essex,D.W., Li,M., Miller,A., and Feinman,R.D. (2001). Protein disulfide isomerase and sulfhydryl-dependent pathways in platelet activation. *Biochemistry,* **40,** 6070-6075.

Evans,C.A., Tonge,R., Blinco,D., Pierce,A., Shaw,J., Lu,Y., Hamzah,H.G., Gray,A., Downes,C.P., Gaskell,S.J., Spooncer,E., and Whetton,A.D. (2004). Comparative proteomics of primitive hematopoietic cell populations reveals differences in expression of proteins regulating motility. *Blood,* **103,** 3751-3759.

Famulok,M. and Verma,S. (2002). In vivo-applied functional RNAs as tools in proteomics and genomics research. *Trends Biotechnol.,* **20,** 462-466.

Fenn,J.B., Mann,M., Meng,C.K., Wong,S.F., and Whitehouse,C.M. (1989). Electrospray ionization for mass spectrometry of large biomolecules. *Science,* **246,** 64-71.

Fialkow,L., Chan,C.K., Rotin,D., Grinstein,S., and Downey,G.P. (1994). Activation of the mitogen-activated protein kinase signaling pathway in neutrophils. Role of oxidants. *J. Biol. Chem.*, **269,** 31234-31242.

Finkel,T. (2000). Redox-dependent signal transduction. *FEBS Lett,* **476,** 52-4.

Fleet,A., Ashworth,R., Kubista,H., Edwards,H., Bolsover,S., Mobbs,P., and Moss,S.E. (1999). Inhibition of EGF-dependent calcium influx by annexin VI is splice form-specific. *Biochem. Biophys. Res. Commun.*, **260,** 540-546.

Floyd,R.A. (1990). The role of 8-hydroxyguanine in carcinogenesis. *Carcinogenesis,* **11,** 1447-50.

Fratelli,M., Demol,H., Puype,M., Casagrande,S., Eberini,I., Salmona,M., Bonetto,V., Mengozzi,M., Duffieux,F., Miclet,E., Bachi,A., Vandekerckhove,J., Gianazza,E., and Ghezzi,P. (2002). Identification by redox proteomics of glutathionylated proteins in oxidatively stressed human T lymphocytes. *Proc Natl Acad Sci U S A,* **99,** 3505-10.

Fukuda,R., Hirota,K., Fan,F., Jung,Y.D., Ellis,L.M., and Semenza,G.L. (2002). Insulin-like growth factor 1 induces hypoxia-inducible factor 1-mediated vascular endothelial growth factor expression, which is dependent on MAP kinase and phosphatidylinositol 3-kinase signaling in colon cancer cells. *J. Biol. Chem.*, **277,** 38205-38211.

Galvani,M., Rovatti,L., Hamdan,M., Herbert,B., and Righetti,P.G. (2001). Protein alkylation in the presence/absence of thiourea in proteome analysis: a matrix assisted laser desorption/ionization-time of flight-mass spectrometry investigation. *Electrophoresis,* **22,** 2066-2074.

Gamaley,I.A. and Klyubin,I.V. (1999). Roles of reactive oxygen species: signaling and regulation of cellular functions. *Int. Rev. Cytol.*, **188,** 203-255.

Garant,M.J., Kole,S., Maksimova,E.M., and Bernier,M. (1999). Reversible change in thiol redox status of the insulin receptor alpha-subunit in intact cells. *Biochemistry,* **38,** 5896-5904.

Garbay,C., Liu,W.Q., Vidal,M., and Roques,B.P. (2000). Inhibitors of Ras signal transduction as antitumor agents. *Biochem. Pharmacol.*, **60,** 1165-1169.

Garg,T.K. and Chang,J.Y. (2003). Oxidative stress causes ERK phosphorylation and cell death in cultured retinal pigment epithelium: prevention of cell death by AG126 and 15-deoxy-delta 12, 14-PGJ2. *BMC. Ophthalmol.*, **3,** 5.

Garrett,M.D. and Workman,P. (1999). Discovering novel chemotherapeutic drugs for the third millennium. *Eur. J. Cancer,* **35,** 2010-2030.

Gennaro,R., Simonic,T., Negri,A., Mottola,C., Secchi,C., Ronchi,S., and Romeo,D. (1986). C5a fragment of bovine complement. Purification, bioassays, amino-acid sequence and other structural studies. *Eur. J. Biochem.*, **155,** 77-86.

Gergel',D. and Cederbaum,A.I. (1997). Interaction of nitric oxide with 2-thio-5-nitrobenzoic acid: implications for the determination of free sulfhydryl groups by Ellman's reagent. *Arch. Biochem. Biophys.*, **347,** 282-288.

Gharahdaghi,F., Weinberg,C.R., Meagher,D.A., Imai,B.S., and Mische,S.M. (1999). Mass spectrometric identification of proteins from silver-stained polyacrylamide gel: a method for the removal of silver ions to enhance sensitivity. *Electrophoresis,* **20,** 601-605.

Gharbi,S., Gaffney,P., Yang,A., Zvelebil,M.J., Cramer,R., Waterfield,M.D., and Timms,J.F. (2002). Evaluation of Two-dimensional Differential Gel Electrophoresis for Proteomic Expression Analysis of a Model Breast Cancer Cell System. *Mol Cell Proteomics,* **1,** 91-8.

Ghezzi,P. and Bonetto,V. (2003). Redox proteomics: identification of oxidatively modified proteins. *Proteomics,* **3,** 1145-53.

Glennie,M.J. and Johnson,P.W. (2000). Clinical trials of antibody therapy. *Immunol. Today,* **21,** 403-410.

Goldman,J.N., Bangalore,S., O'Rourke,K.S., and Goldman,M.B. (1982). Immune regulation of complement components in vivo. *Cell Immunol.*, **70,** 109-117.

Goldschmidt-Clermont,P.J., Allen,R.C., Nel,A.E., Emerson,D.L., Day,J.R., and Galbraith,R.M. (1986). Gc (vitamin D-binding protein) binds the 33.5 K tryptic fragment of actin. *Life Sci.*, **38,** 735-742.

Gonzalez-Pacheco,F.R., Caramelo,C., Castilla,M.A., Deudero,J.J., Arias,J., Yague,S., Jimenez,S., Bragado,R., and Alvarez-Arroyo,M.V. (2002). Mechanism of vascular smooth muscle cells activation by hydrogen peroxide: role of phospholipase C gamma. *Nephrol. Dial. Transplant.*, **17,** 392-398.

Gorg,A., Obermaier,C., Boguth,G., Harder,A., Scheibe,B., Wildgruber,R., and Weiss,W. (2000a). The current state of two-dimensional electrophoresis with immobilized pH gradients. *Electrophoresis,* **21,** 1037-1053.

Gorg,A., Obermaier,C., Boguth,G., Harder,A., Scheibe,B., Wildgruber,R., and Weiss,W. (2000b). The current state of two-dimensional electrophoresis with immobilized pH gradients. *Electrophoresis,* **21,** 1037-1053.

Gorg,A., Obermaier,C., Boguth,G., and Weiss,W. (1999). Recent developments in two-dimensional gel electrophoresis with immobilized pH gradients: wide pH gradients up to pH 12, longer separation distances and simplified procedures. *Electrophoresis,* **20,** 712-717.

Grammer,J.C., Cremo,C.R., and Yount,R.G. (1988). UV-induced vanadate-dependent modification and cleavage of skeletal myosin subfragment 1 heavy chain. 1. Evidence for active site modification. *Biochemistry,* **27,** 8408-8415.

Graus-Porta,D., Beerli,R.R., Daly,J.M., and Hynes,N.E. (1997). ErbB-2, the preferred heterodimerization partner of all ErbB receptors, is a mediator of lateral signaling. *EMBO J.*, **16,** 1647-1655.

Guy,P.M., Platko,J.V., Cantley,L.C., Cerione,R.A., and Carraway,K.L., III (1994). Insect cell-expressed p180erbB3 possesses an impaired tyrosine kinase activity. *Proc. Natl. Acad. Sci. U. S. A,* **91,** 8132-8136.

Guyton,K.Z., Liu,Y., Gorospe,M., Xu,Q., and Holbrook,N.J. (1996b). Activation of mitogen-activated protein kinase by H2O2. Role in cell survival following oxidant injury. *J. Biol. Chem.*, **271,** 4138-4142.

Guyton,K.Z., Liu,Y., Gorospe,M., Xu,Q., and Holbrook,N.J. (1996a). Activation of mitogen-activated protein kinase by H2O2. Role in cell survival following oxidant injury. *J Biol Chem,* **271,** 4138-42.

Gygi,S.P., Rist,B., and Aebersold,R. (2000). Measuring gene expression by quantitative proteome analysis. *Curr Opin Biotechnol,* **11,** 396-401.

Haefliger,D.N., Moskaitis,J.E., Schoenberg,D.R., and Wahli,W. (1989). Amphibian albumins as members of the albumin, alpha-fetoprotein, vitamin D-binding protein multigene family. *J. Mol. Evol.*, **29,** 344-354.

Haj,F.G., Markova,B., Klaman,L.D., Bohmer,F.D., and Neel,B.G. (2003). Regulation of receptor tyrosine kinase signaling by protein tyrosine phosphatase-1B. *J. Biol. Chem.*, **278,** 739-744.

Hamann,M., Zhang,T., Hendrich,S., and Thomas,J.A. (2002). Quantitation of protein sulfinic and sulfonic acid, irreversibly oxidized protein cysteine sites in cellular proteins. *Methods Enzymol,* **348,** 146-56.

Hanahan,D. and Weinberg,R.A. (2000). The hallmarks of cancer. *Cell,* **100,** 57-70.

Hanash,S.M., Strahler,J.R., Neel,J.V., Hailat,N., Melhem,R., Keim,D., Zhu,X.X., Wagner,D., Gage,D.A., and Watson,J.T. (1991). Highly resolving two-dimensional gels for protein sequencing. *Proc. Natl. Acad. Sci. U. S. A,* **88,** 5709-5713.

Hare,J.F. and Lee,E. (1989). Metabolic behavior of cell surface biotinylated proteins. *Biochemistry,* **28,** 574-580.

Harris,A.L. (2002). Hypoxia--a key regulatory factor in tumour growth. *Nat. Rev. Cancer,* **2,** 38-47.

Harris,R.A., Eichholtz,T.J., Hiles,I.D., Page,M.J., and O'Hare,M.J. (1999). New model of ErbB-2 over-expression in human mammary luminal epithelial cells. *Int J Cancer,* **80,** 477-84.

Harrison,R. (2002). Structure and function of xanthine oxidoreductase: where are we now? *Free Radic. Biol. Med.,* **33,** 774-797.

Hartman,B.K. and Udenfriend,S. (1969). A method for immediate visualization of proteins in acrylamide gels and its use for preparation of antibodies to enzymes. *Anal. Biochem.,* **30,** 391-394.

Hayes,M.J. and Moss,S.E. (2004). Annexins and disease. *Biochem. Biophys. Res. Commun.,* **322,** 1166-1170.

Henzel,W.J., Billeci,T.M., Stults,J.T., Wong,S.C., Grimley,C., and Watanabe,C. (1993). Identifying proteins from two-dimensional gels by molecular mass searching of peptide fragments in protein sequence databases. *Proc. Natl. Acad. Sci. U. S. A,* **90,** 5011-5015.

Herbert,B. (1999). Advances in protein solubilisation for two-dimensional electrophoresis. *Electrophoresis,* **20,** 660-663.

Hiran,T.S., Moulton,P.J., and Hancock,J.T. (1997). Detection of superoxide and NADPH oxidase in porcine articular chondrocytes. *Free Radic. Biol. Med.,* **23,** 736-743.

Hirotsu,S., Abe,Y., Okada,K., Nagahara,N., Hori,H., Nishino,T., and Hakoshima,T. (1999). Crystal structure of a multifunctional 2-Cys peroxiredoxin heme-binding protein 23 kDa/proliferation-associated gene product. *Proc. Natl. Acad. Sci. U. S. A,* **96,** 12333-12338.

Holbro,T. and Hynes,N.E. (2004). ErbB receptors: directing key signaling networks throughout life. *Annu. Rev. Pharmacol. Toxicol.,* **44,** 195-217.

Holmgren,A. (1989b). Thioredoxin and glutaredoxin systems. *J. Biol. Chem.,* **264,** 13963-13966.

Holmgren,A. (1989a). Thioredoxin and glutaredoxin systems. *J. Biol. Chem.,* **264,** 13963-13966.

Horowitz,P.M. and Bowman,S. (1987). Ion-enhanced fluorescence staining of sodium dodecyl sulfate-polyacrylamide gels using bis(8-p-toluidino-1-naphthalenesulfonate). *Anal. Biochem.,* **165,** 430-434.

Hung,C.C., Ichimura,T., Stevens,J.L., and Bonventre,J.V. (2003). Protection of renal epithelial cells against oxidative injury by endoplasmic reticulum stress preconditioning is mediated by ERK1/2 activation. *J. Biol. Chem.,* **278,** 29317-29326.

Hunt,D.F., Shabanowitz,J., Yates,J.R., III, Zhu,N.Z., Russell,D.H., and Castro,M.E. (1987). Tandem quadrupole Fourier-transform mass spectrometry of oligopeptides and small proteins. *Proc. Natl. Acad. Sci. U. S. A,* **84,** 620-623.

Hunter,T. (1995). Protein kinases and phosphatases: the yin and yang of protein phosphorylation and signaling. *Cell,* **80,** 225-236.

Hunter,T. (2000). Signaling--2000 and beyond. *Cell,* **100,** 113-127.

Inoguchi,T., Sonta,T., Tsubouchi,H., Etoh,T., Kakimoto,M., Sonoda,N., Sato,N., Sekiguchi,N., Kobayashi,K., Sumimoto,H., Utsumi,H., and Nawata,H. (2003). Protein kinase C-dependent increase in reactive oxygen species (ROS) production in vascular tissues of diabetes: role of vascular NAD(P)H oxidase. *J. Am. Soc. Nephrol.,* **14,** S227-S232.

Ishikawa,Y., Yokoo,T., and Kitamura,M. (1997). c-Jun/AP-1, but not NF-kappa B, is a mediator for oxidant-initiated apoptosis in glomerular mesangial cells. *Biochem. Biophys. Res. Commun.,* **240,** 496-501.

Jackson,A.L. and Loeb,L.A. (2001). The contribution of endogenous sources of DNA damage to the multiple mutations in cancer. *Mutat. Res.,* **477,** 7-21.

Jaffrey,S.R., Erdjument-Bromage,H., Ferris,C.D., Tempst,P., and Snyder,S.H. (2001a). Protein S-nitrosylation: a physiological signal for neuronal nitric oxide. *Nat. Cell Biol.,* **3,** 193-197.

Jaffrey,S.R., Erdjument-Bromage,H., Ferris,C.D., Tempst,P., and Snyder,S.H. (2001b). Protein S-nitrosylation: a physiological signal for neuronal nitric oxide. *Nat. Cell Biol.,* **3,** 193-197.

James,P., Quadroni,M., Carafoli,E., and Gonnet,G. (1993). Protein identification by mass profile fingerprinting. *Biochem. Biophys. Res. Commun.,* **195,** 58-64.

Jat,P.S. and Sharp,P.A. (1989). Cell lines established by a temperature-sensitive simian virus 40 large-T-antigen gene are growth restricted at the nonpermissive temperature. *Mol. Cell Biol.,* **9,** 1672-1681.

Jha,K.K., Banga,S., Palejwala,V., and Ozer,H.L. (1998). SV40-Mediated immortalization. *Exp Cell Res,* **245,** 1-7.

Jiang,B.H., Agani,F., Passaniti,A., and Semenza,G.L. (1997). V-SRC induces expression of hypoxia-inducible factor 1 (HIF-1) and transcription of genes encoding vascular endothelial growth factor and enolase 1: involvement of HIF-1 in tumor progression. *Cancer Res.,* **57,** 5328-5335.

Johnson,N.L., Gardner,A.M., Diener,K.M., Lange-Carter,C.A., Gleavy,J., Jarpe,M.B., Minden,A., Karin,M., Zon,L.I., and Johnson,G.L. (1996). Signal transduction pathways regulated by mitogen-activated/extracellular response kinase kinase kinase induce cell death. *J. Biol. Chem.,* **271,** 3229-3237.

Jones,S.A., O'Donnell,V.B., Wood,J.D., Broughton,J.P., Hughes,E.J., and Jones,O.T. (1996). Expression of phagocyte NADPH oxidase components in human endothelial cells. *Am. J. Physiol,* **271,** H1626-H1634.

Kamata,H. and Hirata,H. (1999). Redox regulation of cellular signalling. *Cell Signal.*, **11,** 1-14.

Karas,M. and Hillenkamp,F. (1988). Laser desorption ionization of proteins with molecular masses exceeding 10,000 daltons. *Anal. Chem.*, **60,** 2299-2301.

Kashiba-Iwatsuki,M., Kitoh,K., Kasahara,E., Yu,H., Nisikawa,M., Matsuo,M., and Inoue,M. (1997). Ascorbic acid and reducing agents regulate the fates and functions of S-nitrosothiols. *J. Biochem. (Tokyo),* **122,** 1208-1214.

Kenrick,K.G. and Margolis,J. (1970). Isoelectric focusing and gradient gel electrophoresis: a two-dimensional technique. *Anal. Biochem.*, **33,** 204-207.

Kim,H.H., Vijapurkar,U., Hellyer,N.J., Bravo,D., and Koland,J.G. (1998). Signal transduction by epidermal growth factor and heregulin via the kinase-deficient ErbB3 protein. *Biochem. J.*, **334 (Pt 1),** 189-195.

Kim,H.S., Manevich,Y., Feinstein,S.I., Pak,J.H., Ho,Y.S., and Fisher,A.B. (2003a). Induction of 1-cys peroxiredoxin expression by oxidative stress in lung epithelial cells. *Am. J. Physiol Lung Cell Mol. Physiol,* **285,** L363-L369.

Kim,J.R., Kwon,K.S., Yoon,H.W., Lee,S.R., and Rhee,S.G. (2002). Oxidation of proteinaceous cysteine residues by dopamine-derived H2O2 in PC12 cells. *Arch Biochem Biophys,* **397,** 414-23.

Kim,J.R., Yoon,H.W., Kwon,K.S., Lee,S.R., and Rhee,S.G. (2000). Identification of proteins containing cysteine residues that are sensitive to oxidation by hydrogen peroxide at neutral pH. *Anal. Biochem.*, **283,** 214-221.

Kim,M.H., Chung,J., Yang,J.W., Chung,S.M., Kwag,N.H., and Yoo,J.S. (2003b). Hydrogen peroxide-induced cell death in a human retinal pigment epithelial cell line, ARPE-19. *Korean J. Ophthalmol.*, **17,** 19-28.

Klatt,P. and Lamas,S. (2000). Regulation of protein function by S-glutathiolation in response to oxidative and nitrosative stress. *Eur. J. Biochem.*, **267,** 4928-4944.

Klatt,P., Pineda,M.E., Perez-Sala,D., and Lamas,S. (2000). Novel application of S-nitrosoglutathione-Sepharose to identify proteins that are potential targets for S-nitrosoglutathione-induced mixed-disulphide formation. *Biochem. J.*, **349,** 567-578.

Klose,J. (1999). Large-gel 2-D electrophoresis. *Methods Mol. Biol.*, **112,** 147-172.

Klose,J. and Spielmann,H. (1975). Gel isoelectric focusing of mouse lactate dehydrogenase: heterogeneity of the isoenzymes A4 and X4. *Biochem. Genet.*, **13,** 707-720.

Kondo,T., Seike,M., Mori,Y., Fujii,K., Yamada,T., and Hirohashi,S. (2003). Application of sensitive fluorescent dyes in linkage of laser microdissection and two-dimensional gel electrophoresis as a cancer proteomic study tool. *Proteomics.*, **3,** 1758-1766.

Kosower,N.S. and Kosower,E.M. (1978). The glutathione status of cells. *Int. Rev. Cytol.*, **54,** 109-160.

Kubbutat,M.H., Jones,S.N., and Vousden,K.H. (1997). Regulation of p53 stability by Mdm2. *Nature,* **387,** 299-303.

Kumar,R., Shepard,H.M., and Mendelsohn,J. (1991). Regulation of phosphorylation of the c-erbB-2/HER2 gene product by a monoclonal antibody and serum growth factor(s) in human mammary carcinoma cells. *Mol. Cell Biol.*, **11,** 979-986.

Kurth,J., Waldmann,R., Heith,J., Mausbach,K., and Burian,R. (1999). Efficient inactivation of viruses and mycoplasma in animal sera using UVC irradiation. *Dev. Biol. Stand.*, **99,** 111-118.

Kwon,J., Lee,S.R., Yang,K.S., Ahn,Y., Kim,Y.J., Stadtman,E.R., and Rhee,S.G. (2004). Reversible oxidation and inactivation of the tumor suppressor PTEN in cells stimulated with peptide growth factors. *Proc. Natl. Acad. Sci. U. S. A,* **101,** 16419-16424.

Lam,E.W. and Reprecht,A. (1994). Radiolucent entity of the anterior maxilla. *Iowa Dent. J.,* **80,** 17-18.

Land,H., Parada,L.F., and Weinberg,R.A. (1983). Tumorigenic conversion of primary embryo fibroblasts requires at least two cooperating oncogenes. *Nature,* **304,** 596-602.

Lander,H.M., Ogiste,J.S., Teng,K.K., and Novogrodsky,A. (1995). p21ras as a common signaling target of reactive free radicals and cellular redox stress. *J. Biol. Chem.*, **270,** 21195-21198.

Lane,H.A., Beuvink,I., Motoyama,A.B., Daly,J.M., Neve,R.M., and Hynes,N.E. (2000). ErbB2 potentiates breast tumor proliferation through modulation of p27(Kip1)-Cdk2 complex formation: receptor overexpression does not determine growth dependency. *Mol. Cell Biol.*, **20,** 3210-3223.

Laughner,E., Taghavi,P., Chiles,K., Mahon,P.C., and Semenza,G.L. (2001). HER2 (neu) signaling increases the rate of hypoxia-inducible factor 1alpha (HIF-1alpha) synthesis: novel mechanism for HIF-1-mediated vascular endothelial growth factor expression. *Mol. Cell Biol.*, **21,** 3995-4004.

Lazennec,G., Bresson,D., Lucas,A., Chauveau,C., and Vignon,F. (2001). ER beta inhibits proliferation and invasion of breast cancer cells. *Endocrinology,* **142,** 4120-4130.

Leducq,N., Bono,F., Sulpice,T., Vin,V., Janiak,P., Fur,G.L., O'Connor,S.E., and Herbert,J.M. (2003). Role of peripheral benzodiazepine receptors in mitochondrial,

cellular, and cardiac damage induced by oxidative stress and ischemia-reperfusion. *J. Pharmacol. Exp. Ther.*, **306,** 828-837.

Lee,A.S. (2001). The glucose-regulated proteins: stress induction and clinical applications. *Trends Biochem Sci,* **26,** 504-10.

Lee,K. and Esselman,W.J. (2002). Inhibition of PTPs by H(2)O(2) regulates the activation of distinct MAPK pathways. *Free Radic. Biol. Med.*, **33,** 1121-1132.

Lee,K.F., Simon,H., Chen,H., Bates,B., Hung,M.C., and Hauser,C. (1995). Requirement for neuregulin receptor erbB2 in neural and cardiac development. *Nature,* **378,** 394-398.

Lee,S.R., Kwon,K.S., Kim,S.R., and Rhee,S.G. (1998). Reversible inactivation of protein-tyrosine phosphatase 1B in A431 cells stimulated with epidermal growth factor. *J Biol Chem,* **273,** 15366-72.

Lee,S.R., Yang,K.S., Kwon,J., Lee,C., Jeong,W., and Rhee,S.G. (2002). Reversible inactivation of the tumor suppressor PTEN by H2O2. *J. Biol. Chem.*, **277,** 20336-20342.

Lee,Z.W., Kweon,S.M., Kim,S.J., Kim,J.H., Cheong,C., Park,Y.M., and Ha,K.S. (2000). The essential role of H2O2 in the regulation of intracellular Ca2+ by epidermal growth factor in rat-2 fibroblasts. *Cell Signal.*, **12,** 91-98.

Lenferink,A.E., Busse,D., Flanagan,W.M., Yakes,F.M., and Arteaga,C.L. (2001). ErbB2/neu kinase modulates cellular p27(Kip1) and cyclin D1 through multiple signaling pathways. *Cancer Res,* **61,** 6583-91.

Levine,R.L., Garland,D., Oliver,C.N., Amici,A., Climent,I., Lenz,A.G., Ahn,B.W., Shaltiel,S., and Stadtman,E.R. (1990). Determination of carbonyl content in oxidatively modified proteins. *Methods Enzymol.*, **186,** 464-478.

Levkowitz,G., Waterman,H., Ettenberg,S.A., Katz,M., Tsygankov,A.Y., Alroy,I., Lavi,S., Iwai,K., Reiss,Y., Ciechanover,A., Lipkowitz,S., and Yarden,Y. (1999). Ubiquitin ligase activity and tyrosine phosphorylation underlie suppression of growth factor signaling by c-Cbl/Sli-1. *Mol. Cell,* **4,** 1029-1040.

Levkowitz,G., Waterman,H., Zamir,E., Kam,Z., Oved,S., Langdon,W.Y., Beguinot,L., Geiger,B., and Yarden,Y. (1998). c-Cbl/Sli-1 regulates endocytic sorting and ubiquitination of the epidermal growth factor receptor. *Genes Dev.*, **12,** 3663-3674.

Lewis,T.S., Hunt,J.B., Aveline,L.D., Jonscher,K.R., Louie,D.F., Yeh,J.M., Nahreini,T.S., Resing,K.A., and Ahn,N.G. (2000). Identification of novel MAP kinase pathway signaling targets by functional proteomics and mass spectrometry. *Mol Cell,* **6,** 1343-54.

Libermann,T.A., Nusbaum,H.R., Razon,N., Kris,R., Lax,I., Soreq,H., Whittle,N., Waterfield,M.D., Ullrich,A., and Schlessinger,J. (1985). Amplification, enhanced expression and possible rearrangement of EGF receptor gene in primary human brain tumours of glial origin. *Nature,* **313,** 144-147.

Lichenstein,H.S., Lyons,D.E., Wurfel,M.M., Johnson,D.A., McGinley,M.D., Leidli,J.C., Trollinger,D.B., Mayer,J.P., Wright,S.D., and Zukowski,M.M. (1994). Afamin is a new member of the albumin, alpha-fetoprotein, and vitamin D-binding protein gene family. *J. Biol. Chem.*, **269,** 18149-18154.

Lin,C.S., Chen,Z.P., Park,T., Ghosh,K., and Leavitt,J. (1993). Characterization of the human L-plastin gene promoter in normal and neoplastic cells. *J. Biol. Chem.*, **268,** 2793-2801.

Lin,T.K., Hughes,G., Muratovska,A., Blaikie,F.H., Brookes,P.S., Darley-Usmar,V., Smith,R.A., and Murphy,M.P. (2002). Specific modification of mitochondrial protein thiols in response to oxidative stress: a proteomics approach. *J. Biol. Chem.*, **277,** 17048-17056.

Lind,C., Gerdes,R., Hamnell,Y., Schuppe-Koistinen,I., von Lowenhielm,H.B., Holmgren,A., and Cotgreave,I.A. (2002). Identification of S-glutathionylated cellular proteins during oxidative stress and constitutive metabolism by affinity purification and proteomic analysis. *Arch. Biochem. Biophys.*, **406,** 229-240.

Lindberg,L.E., Hedjazifar,S., and Baeckstrom,D. (2002). c-erbB2-induced disruption of matrix adhesion and morphogenesis reveals a novel role for protein kinase B as a negative regulator of alpha(2)beta(1) integrin function. *Mol. Biol. Cell,* **13,** 2894-2908.

Liu,R., Oberley,T.D., and Oberley,L.W. (1997). Transfection and expression of MnSOD cDNA decreases tumor malignancy of human oral squamous carcinoma SCC-25 cells. *Hum. Gene Ther.*, **8,** 585-595.

Livden,J.K., Bjerke,J.R., Degre,M., and Matre,R. (1987). Effect of UV radiation on interferon, immunoglobulins and complement components in serum from healthy individuals. *Photodermatol.*, **4,** 296-301.

Lopez,M.F., Berggren,K., Chernokalskaya,E., Lazarev,A., Robinson,M., and Patton,W.F. (2000). A comparison of silver stain and SYPRO Ruby Protein Gel Stain with respect to protein detection in two-dimensional gels and identification by peptide mass profiling. *Electrophoresis,* **21,** 3673-3683.

Maehama,T., Taylor,G.S., and Dixon,J.E. (2001). PTEN and myotubularin: novel phosphoinositide phosphatases. *Annu. Rev. Biochem.*, **70,** 247-279.

Maekawa,T.L., Takahashi,T.A., Fujihara,M., Akasaka,J., Fujikawa,S., Minami,M., and Sekiguchi,S. (1996). Effects of ultraviolet B irradiation on cell-cell interaction; implication of morphological changes and actin filaments in irradiated cells. *Clin. Exp. Immunol.*, **105,** 389-396.

Manevich,Y., Sweitzer,T., Pak,J.H., Feinstein,S.I., Muzykantov,V., and Fisher,A.B. (2002). 1-Cys peroxiredoxin overexpression protects cells against phospholipid peroxidation-mediated membrane damage. *Proc. Natl. Acad. Sci. U. S. A,* **99,** 11599-11604.

Mann,M., Hojrup,P., and Roepstorff,P. (1993). Use of mass spectrometric molecular weight information to identify proteins in sequence databases. *Biol. Mass Spectrom.*, **22,** 338-345.

Manna,S.K., Zhang,H.J., Yan,T., Oberley,L.W., and Aggarwal,B.B. (1998). Overexpression of manganese superoxide dismutase suppresses tumor necrosis factor-induced apoptosis and activation of nuclear transcription factor-kappaB and activated protein-1. *J Biol Chem,* **273,** 13245-54.

Marshall,C.J. (1996). Ras effectors. *Curr. Opin. Cell Biol.*, **8,** 197-204.

Mason,J.M., Morrison,D.J., Bassit,B., Dimri,M., Band,H., Licht,J.D., and Gross,I. (2004). Tyrosine phosphorylation of Sprouty proteins regulates their ability to inhibit growth factor signaling: a dual feedback loop. *Mol. Biol. Cell,* **15,** 2176-2188.

McClung,J.K., Jupe,E.R., Liu,X.T., and Dell'Orco,R.T. (1995). Prohibitin: potential role in senescence, development, and tumor suppression. *Exp Gerontol,* **30,** 99-124.

Meier,B., Cross,A.R., Hancock,J.T., Kaup,F.J., and Jones,O.T. (1991). Identification of a superoxide-generating NADPH oxidase system in human fibroblasts. *Biochem. J.*, **275 (Pt 1),** 241-245.

Meister,A. (1994). Glutathione, ascorbate, and cellular protection. *Cancer Res.*, **54,** 1969s-1975s.

Meng,T.C., Fukada,T., and Tonks,N.K. (2002). Reversible oxidation and inactivation of protein tyrosine phosphatases in vivo. *Mol Cell,* **9,** 387-99.

Mikoshiba,K. (1997). The InsP3 receptor and intracellular Ca2+ signaling. *Curr. Opin. Neurobiol.*, **7,** 339-345.

Minton,A.P. (1995). A molecular model for the dependence of the osmotic pressure of bovine serum albumin upon concentration and pH. *Biophys. Chem.*, **57,** 65-70.

Mitsui,A., Hirakawa,T., and Yodoi,J. (1992). Reactive oxygen-reducing and protein-refolding activities of adult T cell leukemia-derived factor/human thioredoxin. *Biochem. Biophys. Res. Commun.*, **186,** 1220-1226.

Molyneux,C.A., Glyn,M.C., and Ward,B.J. (2002). Oxidative stress and cardiac microvascular structure in ischemia and reperfusion: the protective effect of antioxidant vitamins. *Microvasc. Res.*, **64,** 265-277.

Moran,L.K., Gutteridge,J.M., and Quinlan,G.J. (2001). Thiols in cellular redox signalling and control. *Curr. Med. Chem.*, **8,** 763-772.

Moroianu,J., Fett,J.W., Riordan,J.F., and Vallee,B.L. (1993). Actin is a surface component of calf pulmonary artery endothelial cells in culture. *Proc. Natl. Acad. Sci. U. S. A,* **90,** 3815-3819.

Moss,S.E. and Morgan,R.O. (2004). The annexins. *Genome Biol.*, **5,** 219.

Moulton,P.J., Hiran,T.S., Goldring,M.B., and Hancock,J.T. (1997). Detection of protein and mRNA of various components of the NADPH oxidase complex in an immortalized human chondrocyte line. *Br. J. Rheumatol.*, **36,** 522-529.

Mujumdar,R.B., Ernst,L.A., Mujumdar,S.R., Lewis,C.J., and Waggoner,A.S. (1993). Cyanine dye labeling reagents: sulfoindocyanine succinimidyl esters. *Bioconjug. Chem.*, **4,** 105-111.

Mujumdar,R.B., Ernst,L.A., Mujumdar,S.R., and Waggoner,A.S. (1989). Cyanine dye labeling reagents containing isothiocyanate groups. *Cytometry,* **10,** 11-19.

Mukhopadhyay-Sardar,S., Rana,M.P., and Chatterjee,M. (2000). Antioxidant associated chemoprevention by selenomethionine in murine tumor model. *Mol. Cell Biochem.*, **206,** 17-25.

Musonda,C.A. and Chipman,J.K. (1998). Quercetin inhibits hydrogen peroxide (H2O2)-induced NF-kappaB DNA binding activity and DNA damage in HepG2 cells. *Carcinogenesis,* **19,** 1583-9.

Myrset,A.H., Bostad,A., Jamin,N., Lirsac,P.N., Toma,F., and Gabrielsen,O.S. (1993). DNA and redox state induced conformational changes in the DNA-binding domain of the Myb oncoprotein. *EMBO J.*, **12,** 4625-4633.

Nakamura,H., Nakamura,K., and Yodoi,J. (1997). Redox regulation of cellular activation. *Annu. Rev. Immunol.*, **15,** 351-369.

Nakano,H. and Shinohara,K. (1994). X-ray-induced cell death: apoptosis and necrosis. *Radiat. Res.*, **140,** 1-9.

Neuhoff,V., Arold,N., Taube,D., and Ehrhardt,W. (1988). Improved staining of proteins in polyacrylamide gels including isoelectric focusing gels with clear background at nanogram sensitivity using Coomassie Brilliant Blue G-250 and R-250. *Electrophoresis,* **9,** 255-262.

Neumann,C.A., Krause,D.S., Carman,C.V., Das,S., Dubey,D.P., Abraham,J.L., Bronson,R.T., Fujiwara,Y., Orkin,S.H., and Van Etten,R.A. (2003). Essential role for the peroxiredoxin Prdx1 in erythrocyte antioxidant defence and tumour suppression. *Nature,* **424,** 561-565.

Neve,R.M., Holbro,T., and Hynes,N.E. (2002). Distinct roles for phosphoinositide 3-kinase, mitogen-activated protein kinase and p38 MAPK in mediating cell cycle progression of breast cancer cells. *Oncogene,* **21,** 4567-4576.

Newcomer,M.E. (1995b). Retinoid-binding proteins: structural determinants important for function. *FASEB J.*, **9,** 229-239.

Newcomer,M.E. (1995a). Retinoid-binding proteins: structural determinants important for function. *FASEB J.*, **9**, 229-239.

Nicholson,R.I., Gee,J.M., and Harper,M.E. (2001). EGFR and cancer prognosis. *Eur. J. Cancer*, **37 Suppl 4**, S9-15.

Nikitovic,D. and Holmgren,A. (1996). S-nitrosoglutathione is cleaved by the thioredoxin system with liberation of glutathione and redox regulating nitric oxide. *J. Biol. Chem.*, **271**, 19180-19185.

Nishida,M., Maruyama,Y., Tanaka,R., Kontani,K., Nagao,T., and Kurose,H. (2000). G alpha(i) and G alpha(o) are target proteins of reactive oxygen species. *Nature*, **408**, 492-5.

Nishinaka,T. and Yabe-Nishimura,C. (2001). EGF receptor-ERK pathway is the major signaling pathway that mediates upregulation of aldose reductase expression under oxidative stress. *Free Radic. Biol. Med.*, **31**, 205-216.

Noh,D.Y., Ahn,S.J., Lee,R.A., Kim,S.W., Park,I.A., and Chae,H.Z. (2001). Overexpression of peroxiredoxin in human breast cancer. *Anticancer Res.*, **21**, 2085-2090.

Nose,K., Shibanuma,M., Kikuchi,K., Kageyama,H., Sakiyama,S., and Kuroki,T. (1991). Transcriptional activation of early-response genes by hydrogen peroxide in a mouse osteoblastic cell line. *Eur. J. Biochem.*, **201**, 99-106.

O'Farrell,P.H. (1975). High resolution two-dimensional electrophoresis of proteins. *J. Biol. Chem.*, **250**, 4007-4021.

Oberley,L.W. and Oberley,T.D. (1988). Role of antioxidant enzymes in cell immortalization and transformation. *Mol. Cell Biochem.*, **84**, 147-153.

Ogata,R.T., Rosa,P.A., and Zepf,N.E. (1989). Sequence of the gene for murine complement component C4. *J. Biol. Chem.*, **264**, 16565-16572.

Olayioye,M.A., Badache,A., Daly,J.M., and Hynes,N.E. (2001). An essential role for Src kinase in ErbB receptor signaling through the MAPK pathway. *Exp. Cell Res.*, **267**, 81-87.

Olayioye,M.A., Neve,R.M., Lane,H.A., and Hynes,N.E. (2000a). The ErbB signaling network: receptor heterodimerization in development and cancer. *Embo J*, **19**, 3159-67.

Olayioye,M.A., Neve,R.M., Lane,H.A., and Hynes,N.E. (2000b). The ErbB signaling network: receptor heterodimerization in development and cancer. *EMBO J.*, **19**, 3159-3167.

Olofsson,B. (1999). Rho guanine dissociation inhibitors: pivotal molecules in cellular signalling. *Cell Signal.*, **11**, 545-554.

Ong,S.E., Blagoev,B., Kratchmarova,I., Kristensen,D.B., Steen,H., Pandey,A., and Mann,M. (2002). Stable isotope labeling by amino acids in cell culture, SILAC, as a simple and accurate approach to expression proteomics. *Mol. Cell Proteomics.*, **1,** 376-386.

Ortiz,M.L., Calero,M., Fernandez,P.C., Patron,C.F., Castellanos,L., and Mendez,E. (1992). Imidazole-SDS-Zn reverse staining of proteins in gels containing or not SDS and microsequence of individual unmodified electroblotted proteins. *FEBS Lett.*, **296,** 300-304.

Ostman,A. and Bohmer,F.D. (2001). Regulation of receptor tyrosine kinase signaling by protein tyrosine phosphatases. *Trends Cell Biol.*, **11,** 258-266.

Otsuka,M., Kato,M., Yoshikawa,T., Chen,H., Brown,E.J., Masuho,Y., Omata,M., and Seki,N. (2001). Differential expression of the L-plastin gene in human colorectal cancer progression and metastasis. *Biochem. Biophys. Res. Commun.*, **289,** 876-881.

Overholser,J.P., Prewett,M.C., Hooper,A.T., Waksal,H.W., and Hicklin,D.J. (2000). Epidermal growth factor receptor blockade by antibody IMC-C225 inhibits growth of a human pancreatic carcinoma xenograft in nude mice. *Cancer,* **89,** 74-82.

Owen,M.J., Auger,J., Barber,B.H., Edwards,A.J., Walsh,F.S., and Crumpton,M.J. (1978). Actin may be present on the lymphocyte surface. *Proc. Natl. Acad. Sci. U. S. A,* **75,** 4484-4488.

Paez,J.G., Janne,P.A., Lee,J.C., Tracy,S., Greulich,H., Gabriel,S., Herman,P., Kaye,F.J., Lindeman,N., Boggon,T.J., Naoki,K., Sasaki,H., Fujii,Y., Eck,M.J., Sellers,W.R., Johnson,B.E., and Meyerson,M. (2004). EGFR mutations in lung cancer: correlation with clinical response to gefitinib therapy. *Science,* **304,** 1497-1500.

Park,H.S., Lee,S.H., Park,D., Lee,J.S., Ryu,S.H., Lee,W.J., Rhee,S.G., and Bae,Y.S. (2004). Sequential activation of phosphatidylinositol 3-kinase, beta Pix, Rac1, and Nox1 in growth factor-induced production of H2O2. *Mol. Cell Biol.*, **24,** 4384-4394.

Park,T., Chen,Z.P., and Leavitt,J. (1994). Activation of the leukocyte plastin gene occurs in most human cancer cells. *Cancer Res.*, **54,** 1775-1781.

Patton,W.F. (2000). A thousand points of light: the application of fluorescence detection technologies to two-dimensional gel electrophoresis and proteomics. *Electrophoresis,* **21,** 1123-1144.

Patton,W.F. and Beechem,J.M. (2002). Rainbow's end: the quest for multiplexed fluorescence quantitative analysis in proteomics. *Curr Opin Chem Biol,* **6,** 63-9.

Pawson,T. (1995). Protein modules and signalling networks. *Nature,* **373,** 573-580.

Pelaia,G., Cuda,G., Vatrella,A., Gallelli,L., Fratto,D., Gioffre,V., D'Agostino,B., Caputi,M., Maselli,R., Rossi,F., Costanzo,F.S., and Marsico,S.A. (2004). Effects of

hydrogen peroxide on MAPK activation, IL-8 production and cell viability in primary cultures of human bronchial epithelial cells. *J. Cell Biochem.*, **93,** 142-152.

Peles,E. and Yarden,Y. (1993). Neu and its ligands: from an oncogene to neural factors. *Bioessays,* **15,** 815-824.

Pepys,M.B., Booth,S.E., Tennent,G.A., Butler,P.J., and Williams,D.G. (1994). Binding of pentraxins to different nuclear structures: C-reactive protein binds to small nuclear ribonucleoprotein particles, serum amyloid P component binds to chromatin and nucleoli. *Clin. Exp. Immunol.*, **97,** 152-157.

Pina,B., Aragay,A.M., Suau,P., and Daban,J.R. (1985). Fluorescent properties of histone-1-anilinonaphthalene 8-sulfonate complexes in the presence of denaturant agents: application to the rapid staining of histones in urea and Triton-urea-polyacrylamide gels. *Anal. Biochem.*, **146,** 431-433.

Poli,G., Leonarduzzi,G., Biasi,F., and Chiarpotto,E. (2004). Oxidative stress and cell signalling. *Curr. Med. Chem.*, **11,** 1163-1182.

Pollard,T.D. and Cooper,J.A. (1986). Actin and actin-binding proteins. A critical evaluation of mechanisms and functions. *Annu. Rev. Biochem.*, **55,** 987-1035.

Preston,A., Mandrell,R.E., Gibson,B.W., and Apicella,M.A. (1996). The lipooligosaccharides of pathogenic gram-negative bacteria. *Crit Rev. Microbiol.*, **22,** 139-180.

Price,M.O., Atkinson,S.J., Knaus,U.G., and Dinauer,M.C. (2002). Rac activation induces NADPH oxidase activity in transgenic COSphox cells, and the level of superoxide production is exchange factor- dependent. *J Biol Chem,* **277,** 19220-8.

Puto,L.A., Pestonjamasp,K., King,C.C., and Bokoch,G.M. (2003). p21-activated kinase 1 (PAK1) interacts with the Grb2 adapter protein to couple to growth factor signaling. *J. Biol. Chem.*, **278,** 9388-9393.

Quimby,B.B. and Dasso,M. (2003). The small GTPase Ran: interpreting the signs. *Curr. Opin. Cell Biol.*, **15,** 338-344.

Rabilloud,T. (1998). Use of thiourea to increase the solubility of membrane proteins in two-dimensional electrophoresis. *Electrophoresis,* **19,** 758-760.

Rabilloud,T. (2000). Detecting proteins separated by 2-D gel electrophoresis. *Anal. Chem.*, **72,** 48A-55A.

Rabilloud,T., Blisnick,T., Heller,M., Luche,S., Aebersold,R., Lunardi,J., and Braun-Breton,C. (1999). Analysis of membrane proteins by two-dimensional electrophoresis: comparison of the proteins extracted from normal or Plasmodium falciparum-infected erythrocyte ghosts. *Electrophoresis,* **20,** 3603-3610.

Rabilloud,T., Heller,M., Gasnier,F., Luche,S., Rey,C., Aebersold,R., Benahmed,M., Louisot,P., and Lunardi,J. (2002b). Proteomics analysis of cellular response to oxidative stress. Evidence for in vivo overoxidation of peroxiredoxins at their active site. *J. Biol. Chem.*, **277**, 19396-19401.

Rabilloud,T., Heller,M., Gasnier,F., Luche,S., Rey,C., Aebersold,R., Benahmed,M., Louisot,P., and Lunardi,J. (2002a). Proteomics analysis of cellular response to oxidative stress. Evidence for in vivo overoxidation of peroxiredoxins at their active site. *J Biol Chem*, **277**, 19396-401.

Rabilloud,T., Valette,C., and Lawrence,J.J. (1994a). Sample application by in-gel rehydration improves the resolution of two-dimensional electrophoresis with immobilized pH gradients in the first dimension. *Electrophoresis*, **15**, 1552-1558.

Rabilloud,T., Vuillard,L., Gilly,C., and Lawrence,J.J. (1994b). Silver-staining of proteins in polyacrylamide gels: a general overview. *Cell Mol. Biol. (Noisy. -le-grand)*, **40**, 57-75.

Radeke,H.H., Cross,A.R., Hancock,J.T., Jones,O.T., Nakamura,M., Kaever,V., and Resch,K. (1991). Functional expression of NADPH oxidase components (alpha- and beta-subunits of cytochrome b558 and 45-kDa flavoprotein) by intrinsic human glomerular mesangial cells. *J. Biol. Chem.*, **266**, 21025-21029.

Rahman,I., Marwick,J., and Kirkham,P. (2004). Redox modulation of chromatin remodeling: impact on histone acetylation and deacetylation, NF-kappaB and pro-inflammatory gene expression. *Biochem. Pharmacol.*, **68**, 1255-1267.

Rao,G.N., Glasgow,W.C., Eling,T.E., and Runge,M.S. (1996). Role of hydroperoxyeicosatetraenoic acids in oxidative stress-induced activating protein 1 (AP-1) activity. *J. Biol. Chem.*, **271**, 27760-27764.

Rask,L., Anundi,H., Fohlman,J., and Peterson,P.A. (1987). The complete amino acid sequence of human serum retinol-binding protein. *Ups. J. Med. Sci.*, **92**, 115-146.

Ravi,R., Mookerjee,B., Bhujwalla,Z.M., Sutter,C.H., Artemov,D., Zeng,Q., Dillehay,L.E., Madan,A., Semenza,G.L., and Bedi,A. (2000). Regulation of tumor angiogenesis by p53-induced degradation of hypoxia-inducible factor 1alpha. *Genes Dev.*, **14**, 34-44.

Renne,T., Gailani,D., Meijers,J.C., and Muller-Esterl,W. (2002). Characterization of the H-kininogen-binding site on factor XI: a comparison of factor XI and plasma prekallikrein. *J. Biol. Chem.*, **277**, 4892-4899.

Reznik,G.O., Yu,Y., Tarr,G.E., and Cantor,C.R. (2003). Native disulfide bonds in plasma retinol-binding protein are not essential for all-trans-retinol-binding activity. *J. Proteome. Res.*, **2**, 243-248.

Rhee,S.G., Chang,T.S., Bae,Y.S., Lee,S.R., and Kang,S.W. (2003). Cellular regulation by hydrogen peroxide. *J. Am. Soc. Nephrol.*, **14**, S211-S215.

Richard,D.E., Berra,E., Gothie,E., Roux,D., and Pouyssegur,J. (1999). p42/p44 mitogen-activated protein kinases phosphorylate hypoxia-inducible factor 1alpha (HIF-1alpha) and enhance the transcriptional activity of HIF-1. *J. Biol. Chem.*, **274,** 32631-32637.

Riddles,P.W., Blakeley,R.L., and Zerner,B. (1979). Ellman's reagent: 5,5'-dithiobis(2-nitrobenzoic acid)--a reexamination. *Anal. Biochem.*, **94,** 75-81.

Riener,C.K., Kada,G., and Gruber,H.J. (2002). Quick measurement of protein sulfhydryls with Ellman's reagent and with 4,4'-dithiodipyridine. *Anal. Bioanal. Chem.*, **373,** 266-276.

Riese,D.J.2. and Stern,D.F. (1998). Specificity within the EGF family/ErbB receptor family signaling network. *Bioessays,* **20,** 41-8.

Risom,L., Moller,P., Vogel,U., Kristjansen,P.E., and Loft,S. (2003). X-ray-induced oxidative stress: DNA damage and gene expression of HO-1, ERCC1 and OGG1 in mouse lung. *Free Radic. Res.*, **37,** 957-966.

Rohr,G. and Mannherz,H.G. (1978). Isolation and characterization of secretory actin . DNAase I complex from rat pancreatic juice. *Eur. J. Biochem.*, **89,** 151-157.

Rokutan,K., Thomas,J.A., and Johnston,R.B., Jr. (1991). Phagocytosis and stimulation of the respiratory burst by phorbol diester initiate S-thiolation of specific proteins in macrophages. *J. Immunol.*, **147,** 260-264.

Rollet-Labelle,E., Grange,M.J., Elbim,C., Marquetty,C., Gougerot-Pocidalo,M.A., and Pasquier,C. (1998). Hydroxyl radical as a potential intracellular mediator of polymorphonuclear neutrophil apoptosis. *Free Radic Biol Med,* **24,** 563-72.

Rothhut,B. (1997). Participation of annexins in protein phosphorylation. *Cell Mol. Life Sci.*, **53,** 522-526.

Ruffels,J., Griffin,M., and Dickenson,J.M. (2004). Activation of ERK1/2, JNK and PKB by hydrogen peroxide in human SH-SY5Y neuroblastoma cells: role of ERK1/2 in H2O2-induced cell death. *Eur. J. Pharmacol.*, **483,** 163-173.

Ryan,K.M., Phillips,A.C., and Vousden,K.H. (2001). Regulation and function of the p53 tumor suppressor protein. *Curr. Opin. Cell Biol.*, **13,** 332-337.

Samoilova,K.A., Vasil'eva,Z.F., Shtil'bans,V.I., Obolenskaia,K.D., and Shalygina,N.N. (1987). [Change in the binding capacity of human serum albumin following its exposure to therapeutic doses of UV radiation]. *Biull. Eksp. Biol. Med.*, **104,** 676-678.

Sarto,C., Binz,P.A., and Mocarelli,P. (2000a). Heat shock proteins in human cancer. *Electrophoresis,* **21,** 1218-1226.

Sarto,C., Binz,P.A., and Mocarelli,P. (2000b). Heat shock proteins in human cancer. *Electrophoresis,* **21,** 1218-26.

SBARRA,A.J. and KARNOVSKY,M.L. (1959). The biochemical basis of phagocytosis. I. Metabolic changes during the ingestion of particles by polymorphonuclear leukocytes. *J. Biol. Chem.*, **234,** 1355-1362.

Schafer,F.Q. and Buettner,G.R. (2001). Redox environment of the cell as viewed through the redox state of the glutathione disulfide/glutathione couple. *Free Radic. Biol. Med.*, **30,** 1191-1212.

Scheele,G.A. (1975). Two-dimensional gel analysis of soluble proteins. Charaterization of guinea pig exocrine pancreatic proteins. *J. Biol. Chem.*, **250,** 5375-5385.

Scheffner,M., Werness,B.A., Huibregtse,J.M., Levine,A.J., and Howley,P.M. (1990). The E6 oncoprotein encoded by human papillomavirus types 16 and 18 promotes the degradation of p53. *Cell,* **63,** 1129-1136.

Scheler,C., Lamer,S., Pan,Z., Li,X.P., Salnikow,J., and Jungblut,P. (1998). Peptide mass fingerprint sequence coverage from differently stained proteins on two-dimensional electrophoresis patterns by matrix assisted laser desorption/ionization-mass spectrometry (MALDI-MS). *Electrophoresis,* **19,** 918-927.

Schirmer,E.C. and Gerace,L. (2002). Organellar proteomics: the prizes and pitfalls of opening the nuclear envelope. *Genome Biol.*, **3,** REVIEWS1008.

Schlessinger,J. (2000). Cell signaling by receptor tyrosine kinases. *Cell,* **103,** 211-225.

Schoentgen,F., Metz-Boutigue,M.H., Jolles,J., Constans,J., and Jolles,P. (1986). Complete amino acid sequence of human vitamin D-binding protein (group-specific component): evidence of a three-fold internal homology as in serum albumin and alpha-fetoprotein. *Biochim. Biophys. Acta,* **871,** 189-198.

Schreck,R., Rieber,P., and Baeuerle,P.A. (1991). Reactive oxygen intermediates as apparently widely used messengers in the activation of the NF-kappa B transcription factor and HIV-1. *EMBO J.*, **10,** 2247-2258.

Sebti,S.M. and Hamilton,A.D. (2000). Design of growth factor antagonists with antiangiogenic and antitumor properties. *Oncogene,* **19,** 6566-6573.

Shariat-Madar,Z., Mahdi,F., and Schmaier,A.H. (2002). Assembly and activation of the plasma kallikrein/kinin system: a new interpretation. *Int. Immunopharmacol.*, **2,** 1841-1849.

Shaw,J., Rowlinson,R., Nickson,J., Stone,T., Sweet,A., Williams,K., and Tonge,R. (2003). Evaluation of saturation labelling two-dimensional difference gel electrophoresis fluorescent dyes. *Proteomics,* **3,** 1181-95.

Shen,C. and Nathan,C. (2002). Nonredundant antioxidant defense by multiple two-cysteine peroxiredoxins in human prostate cancer cells. *Mol. Med.*, **8,** 95-102.

Shenton,D. and Grant,C.M. (2003). Protein S-thiolation targets glycolysis and protein synthesis in response to oxidative stress in the yeast Saccharomyces cerevisiae. *Biochem. J.*, **374,** 513-519.

Sherr,C.J. and McCormick,F. (2002). The RB and p53 pathways in cancer. *Cancer Cell,* **2,** 103-112.

Shevchenko,A., Wilm,M., Vorm,O., and Mann,M. (1996). Mass spectrometric sequencing of proteins silver-stained polyacrylamide gels. *Anal Chem,* **68,** 850-8.

Shoelson,S.E. (1997). SH2 and PTB domain interactions in tyrosine kinase signal transduction. *Curr. Opin. Chem. Biol.*, **1,** 227-234.

Shtiegman,K. and Yarden,Y. (2003). The role of ubiquitylation in signaling by growth factors: implications to cancer. *Semin. Cancer Biol.*, **13,** 29-40.

Simon,A.R., Rai,U., Fanburg,B.L., and Cochran,B.H. (1998). Activation of the JAK-STAT pathway by reactive oxygen species. *Am. J. Physiol,* **275,** C1640-C1652.

Singh,A.J., Meyer,R.D., Band,H., and Rahimi,N. (2005). The Carboxyl Terminus of VEGFR-2 Is Required for PKC-mediated Down-Regulation. *Mol. Biol. Cell,* **16,** 2106-2118.

Sizeland,A.M. and Burgess,A.W. (1992). Anti-sense transforming growth factor alpha oligonucleotides inhibit autocrine stimulated proliferation of a colon carcinoma cell line. *Mol. Biol. Cell,* **3,** 1235-1243.

Slamon,D.J., Clark,G.M., Wong,S.G., Levin,W.J., Ullrich,A., and McGuire,W.L. (1987). Human breast cancer: correlation of relapse and survival with amplification of the HER-2/neu oncogene. *Science,* **235,** 177-182.

Smolka,M.B., Zhou,H., Purkayastha,S., and Aebersold,R. (2001). Optimization of the isotope-coded affinity tag-labeling procedure for quantitative proteome analysis. *Anal Biochem,* **297,** 25-31.

Songyang,Z., Shoelson,S.E., Chaudhuri,M., Gish,G., Pawson,T., Haser,W.G., King,F., Roberts,T., Ratnofsky,S., and Lechleider,R.J. (1993). SH2 domains recognize specific phosphopeptide sequences. *Cell,* **72,** 767-778.

Sorkin,A. and Waters,C.M. (1993). Endocytosis of growth factor receptors. *Bioessays,* **15,** 375-382.

Sorkina,T., Huang,F., Beguinot,L., and Sorkin,A. (2002). Effect of tyrosine kinase inhibitors on clathrin-coated pit recruitment and internalization of epidermal growth factor receptor. *J. Biol. Chem.*, **277,** 27433-27441.

Srivastava,S.K., Ramana,K.V., Chandra,D., Srivastava,S., and Bhatnagar,A. (2003). Regulation of aldose reductase and the polyol pathway activity by nitric oxide. *Chem. Biol. Interact.*, **143-144,** 333-340.

Stadtman,E.R. and Berlett,B.S. (1997). Reactive oxygen-mediated protein oxidation in aging and disease. *Chem. Res. Toxicol.*, **10,** 485-494.

Stamps,A.C., Davies,S.C., Burman,J., and O'Hare,M.J. (1994). Analysis of proviral integration in human mammary epithelial cell lines immortalized by retroviral infection with a temperature-sensitive SV40 T-antigen construct. *Int J Cancer,* **57,** 865-74.

Steinbeck,M.J., Appel,W.H., Jr., Verhoeven,A.J., and Karnovsky,M.J. (1994). NADPH-oxidase expression and in situ production of superoxide by osteoclasts actively resorbing bone. *J. Cell Biol.*, **126,** 765-772.

Steinberg,T.H., Jones,L.J., Haugland,R.P., and Singer,V.L. (1996). SYPRO orange and SYPRO red protein gel stains: one-step fluorescent staining of denaturing gels for detection of nanogram levels of protein. *Anal. Biochem.*, **239,** 223-237.

Steinberg,T.H., Lauber,W.M., Berggren,K., Kemper,C., Yue,S., and Patton,W.F. (2000). Fluorescence detection of proteins in sodium dodecyl sulfate-polyacrylamide gels using environmentally benign, nonfixative, saline solution. *Electrophoresis,* **21,** 497-508.

Su,L.F., Knoblauch,R., and Garabedian,M.J. (2001). Rho GTPases as modulators of the estrogen receptor transcriptional response. *J. Biol. Chem.*, **276,** 3231-3237.

Sulis,M.L. and Parsons,R. (2003). PTEN: from pathology to biology. *Trends Cell Biol.*, **13,** 478-483.

Sullivan,D.M., Wehr,N.B., Fergusson,M.M., Levine,R.L., and Finkel,T. (2000). Identification of oxidant-sensitive proteins: TNF-alpha induces protein glutathiolation. *Biochemistry,* **39,** 11121-11128.

Sullivan,S.G., Chiu,D.T., Errasfa,M., Wang,J.M., Qi,J.S., and Stern,A. (1994). Effects of H2O2 on protein tyrosine phosphatase activity in HER14 cells. *Free Radic. Biol. Med.*, **16,** 399-403.

Sundaram,M., Sivaprasadarao,A., DeSousa,M.M., and Findlay,J.B. (1998). The transfer of retinol from serum retinol-binding protein to cellular retinol-binding protein is mediated by a membrane receptor. *J. Biol. Chem.*, **273,** 3336-3342.

Takai,Y., Kaibuchi,K., Kikuchi,A., Sasaki,T., and Shirataki,H. (1993). Regulators of small GTPases. *Ciba Found. Symp.*, **176,** 128-138.

Tanaka,K., Pracyk,J.B., Takeda,K., Yu,Z.X., Ferrans,V.J., Deshpande,S.S., Ozaki,M., Hwang,P.M., Lowenstein,C.J., Irani,K., and Finkel,T. (1998). Expression of Id1 results in apoptosis of cardiac myocytes through a redox-dependent mechanism. *J Biol Chem,* **273,** 25922-8.

Thompson,A.R. and Enfield,D.L. (1978). Human plasma P component: isolation and characterization. *Biochemistry,* **17,** 4304-4311.

Thorstensson,R., Utter,G., and Norberg,R. (1982). Further characterization of the Ca2+-dependent F-actin-depolymerizing protein of human serum. *Eur. J. Biochem.,* **126,** 11-16.

Timms,J.F., White,S.L., O'Hare,M.J., and Waterfield,M.D. (2002). Effects of ErbB-2 overexpression on mitogenic signalling and cell cycle progression in human breast luminal epithelial cells. *Oncogene,* **21,** 6573-6586.

Tonge,R., Shaw,J., Middleton,B., Rowlinson,R., Rayner,S., Young,J., Pognan,F., Hawkins,E., Currie,I., and Davison,M. (2001). Validation and development of fluorescence two-dimensional differential gel electrophoresis proteomics technology. *Proteomics,* **1,** 377-96.

Torres,M. and Forman,H.J. (2003). Redox signaling and the MAP kinase pathways. *Biofactors,* **17,** 287-296.

Tzahar,E., Waterman,H., Chen,X., Levkowitz,G., Karunagaran,D., Lavi,S., Ratzkin,B.J., and Yarden,Y. (1996). A hierarchical network of interreceptor interactions determines signal transduction by Neu differentiation factor/neuregulin and epidermal growth factor. *Mol. Cell Biol.,* **16,** 5276-5287.

Ullrich,A., Coussens,L., Hayflick,J.S., Dull,T.J., Gray,A., Tam,A.W., Lee,J., Yarden,Y., Libermann,T.A., and Schlessinger,J. (1984). Human epidermal growth factor receptor cDNA sequence and aberrant expression of the amplified gene in A431 epidermoid carcinoma cells. *Nature,* **309,** 418-425.

Unlu,M., Morgan,M.E., and Minden,J.S. (1997a). Difference gel electrophoresis: a single gel method for detecting changes in protein extracts. *Electrophoresis,* **18,** 2071-7.

Unlu,M., Morgan,M.E., and Minden,J.S. (1997b). Difference gel electrophoresis: a single gel method for detecting changes in protein extracts. *Electrophoresis,* **18,** 2071-7.

Van Aelst,L. and D'Souza-Schorey,C. (1997). Rho GTPases and signaling networks. *Genes Dev.,* **11,** 2295-2322.

Vanhaesebroeck,B., Leevers,S.J., Panayotou,G., and Waterfield,M.D. (1997). Phosphoinositide 3-kinases: a conserved family of signal transducers. *Trends Biochem. Sci.,* **22,** 267-272.

Veal,E.A., Findlay,V.J., Day,A.M., Bozonet,S.M., Evans,J.M., Quinn,J., and Morgan,B.A. (2004). A 2-Cys peroxiredoxin regulates peroxide-induced oxidation and activation of a stress-activated MAP kinase. *Mol. Cell,* **15,** 129-139.

Vercoutter-Edouart,A.S., Lemoine,J., Le,B., X, Louis,H., Boilly,B., Nurcombe,V., Revillion,F., Peyrat,J.P., and Hondermarck,H. (2001). Proteomic analysis reveals that 14-3-3sigma is down-regulated in human breast cancer cells. *Cancer Res.,* **61,** 76-80.

Verheij,M., Bose,R., Lin,X.H., Yao,B., Jarvis,W.D., Grant,S., Birrer,M.J., Szabo,E., Zon,L.I., Kyriakis,J.M., Haimovitz-Friedman,A., Fuks,Z., and Kolesnick,R.N. (1996). Requirement for ceramide-initiated SAPK/JNK signalling in stress-induced apoptosis. *Nature,* **380,** 75-79.

Wagner,E., Luche,S., Penna,L., Chevallet,M., van Dorsselaer,A., Leize-Wagner,E., and Rabilloud,T. (2002). A method for detection of overoxidation of cysteines: peroxiredoxins are oxidized in vivo at the active-site cysteine during oxidative stress. *Biochem. J.,* **366,** 777-785.

Wainwright,M. (2002a). Pathogen inactivation in blood products. *Curr. Med. Chem.,* **9,** 127-143.

Wainwright,M. (2002b). Pathogen inactivation in blood products. *Curr. Med. Chem.,* **9,** 127-143.

Wakeling,A.E., Barker,A.J., Davies,D.H., Brown,D.S., Green,L.R., Cartlidge,S.A., and Woodburn,J.R. (1996). Specific inhibition of epidermal growth factor receptor tyrosine kinase by 4-anilinoquinazolines. *Breast Cancer Res. Treat.,* **38,** 67-73.

Wang,J., Boja,E.S., Tan,W., Tekle,E., Fales,H.M., English,S., Mieyal,J.J., and Chock,P.B. (2001). Reversible glutathionylation regulates actin polymerization in A431 cells. *J. Biol. Chem.,* **276,** 47763-47766.

Wang,S.C. and Hung,M.C. (2001). HER2 overexpression and cancer targeting. *Semin. Oncol.,* **28,** 115-124.

Washburn,M.P., Wolters,D., and Yates,J.R.3. (2001). Large-scale analysis of the yeast proteome by multidimensional protein identification technology. *Nat Biotechnol,* **19,** 242-7.

Wasylyk,C. and Wasylyk,B. (1993). Oncogenic conversion of Ets affects redox regulation in-vivo and in-vitro. *Nucleic Acids Res.,* **21,** 523-529.

Waterman,H. and Yarden,Y. (2001). Molecular mechanisms underlying endocytosis and sorting of ErbB receptor tyrosine kinases. *FEBS Lett.,* **490,** 142-152.

Weiss,A. and Schlessinger,J. (1998). Switching signals on or off by receptor dimerization. *Cell,* **94,** 277-280.

Westbrook,J.A., Yan,J.X., Wait,R., Welson,S.Y., and Dunn,M.J. (2001a). Zooming-in on the proteome: very narrow-range immobilised pH gradients reveal more protein species and isoforms. *Electrophoresis,* **22,** 2865-2871.

Westbrook,J.A., Yan,J.X., Wait,R., Welson,S.Y., and Dunn,M.J. (2001b). Zooming-in on the proteome: very narrow-range immobilised pH gradients reveal more protein species and isoforms. *Electrophoresis,* **22,** 2865-2871.

White,S.L., Gharbi,S., Bertani,M.F., Chan,H.L., Waterfield,M.D., and Timms,J.F. (2004). Cellular responses to ErbB-2 overexpression in human mammary luminal epithelial cells: comparison of mRNA and protein expression. *Br. J. Cancer,* **90,** 173-181.

Whitehouse,C.M., Dreyer,R.N., Yamashita,M., and Fenn,J.B. (1985). Electrospray interface for liquid chromatographs and mass spectrometers. *Anal. Chem.,* **57,** 675-679.

Wilkins,M.R., Sanchez,J.C., Gooley,A.A., Appel,R.D., Humphery-Smith,I., Hochstrasser,D.F., and Williams,K.L. (1996). Progress with proteome projects: why all proteins expressed by a genome should be identified and how to do it. *Biotechnol. Genet. Eng Rev.,* **13,** 19-50.

Willett,W.S. and Copley,S.D. (1996). Identification and localization of a stable sulfenic acid in peroxide- treated tetrachlorohydroquinone dehalogenase using electrospray mass spectrometry. *Chem Biol,* **3,** 851-7.

Williamson,J.R., Chang,K., Frangos,M., Hasan,K.S., Ido,Y., Kawamura,T., Nyengaard,J.R., van den,E.M., Kilo,C., and Tilton,R.G. (1993). Hyperglycemic pseudohypoxia and diabetic complications. *Diabetes,* **42,** 801-813.

Wilm,M., Shevchenko,A., Houthaeve,T., Breit,S., Schweigerer,L., Fotsis,T., and Mann,M. (1996). Femtomole sequencing of proteins from polyacrylamide gels by nano-electrospray mass spectrometry. *Nature,* **379,** 466-469.

Wolf,G. (1992). Cellular retinol-binding protein functions in the regulation of retinoid metabolism. *Nutr. Rev.,* **50,** 197-199.

Wood,Z.A., Schroder,E., Robin Harris,J., and Poole,L.B. (2003). Structure, mechanism and regulation of peroxiredoxins. *Trends Biochem Sci,* **28,** 32-40.

Wu,Y., Kwon,K.S., and Rhee,S.G. (1998). Probing cellular protein targets of H2O2 with fluorescein-conjugated iodoacetamide and antibodies to fluorescein. *FEBS Lett.,* **440,** 111-115.

Wulfkuhle,J.D., Sgroi,D.C., Krutzsch,H., McLean,K., McGarvey,K., Knowlton,M., Chen,S., Shu,H., Sahin,A., Kurek,R., Wallwiener,D., Merino,M.J., Petricoin,E.F., III, Zhao,Y., and Steeg,P.S. (2002). Proteomics of human breast ductal carcinoma in situ. *Cancer Res.,* **62,** 6740-6749.

Yabe-Nishimura,C. (1998). Aldose reductase in glucose toxicity: a potential target for the prevention of diabetic complications. *Pharmacol. Rev.,* **50,** 21-33.

Yamamoto,K. and Sekine,T. (1978). Fluorescent tracer method for protein SH groups. III. Use of N-(7-dimethylamino-4-methylcoumarinyl) maleimide as a tracer of cysteine-containing peptides. *Anal. Biochem.,* **90,** 300-308.

Yan,J.X., Wait,R., Berkelman,T., Harry,R.A., Westbrook,J.A., Wheeler,C.H., and Dunn,M.J. (2000). A modified silver staining protocol for visualization of proteins

compatible with matrix-assisted laser desorption/ionization and electrospray ionization-mass spectrometry. *Electrophoresis,* **21,** 3666-3672.

Yano,H., Wong,J.H., Lee,Y.M., Cho,M.J., and Buchanan,B.B. (2001). A strategy for the identification of proteins targeted by thioredoxin. *Proc. Natl. Acad. Sci. U. S. A,* **98,** 4794-4799.

Yarden,Y. and Sliwkowski,M.X. (2001). Untangling the ErbB signalling network. *Nat Rev Mol Cell Biol,* **2,** 127-37.

Yates,J.R., III, Speicher,S., Griffin,P.R., and Hunkapiller,T. (1993). Peptide mass maps: a highly informative approach to protein identification. *Anal. Biochem.,* **214,** 397-408.

Ye,Y.Z., Strong,M., Huang,Z.Q., and Beckman,J.S. (1996). Antibodies that recognize nitrotyrosine. *Methods Enzymol.,* **269,** 201-209.

Yeh,J.I., Claiborne,A., and Hol,W.G. (1996). Structure of the native cysteine-sulfenic acid redox center of enterococcal NADH peroxidase refined at 2.8 A resolution. *Biochemistry,* **35,** 9951-7.

Yin,Y., Terauchi,Y., Solomon,G.G., Aizawa,S., Rangarajan,P.N., Yazaki,Y., Kadowaki,T., and Barrett,J.C. (1998). Involvement of p85 in p53-dependent apoptotic response to oxidative stress. *Nature,* **391,** 707-710.

Young,T.W., Mei,F.C., Yang,G., Thompson-Lanza,J.A., Liu,J., and Cheng,X. (2004). Activation of antioxidant pathways in ras-mediated oncogenic transformation of human surface ovarian epithelial cells revealed by functional proteomics and mass spectrometry. *Cancer Res.,* **64,** 4577-4584.

Zahler,W.L. and Cleland,W.W. (1968). A specific and sensitive assay for disulfides. *J. Biol. Chem.,* **243,** 716-719.

Zhang,Z., Leonard,S.S., Huang,C., Vallyathan,V., Castranova,V., and Shi,X. (2003). Role of reactive oxygen species and MAPKs in vanadate-induced G(2)/M phase arrest. *Free Radic. Biol. Med.,* **34,** 1333-1342.

Zheng,J., Rudra-Ganguly,N., Powell,W.C., and Roy-Burman,P. (1999). Suppression of prostate carcinoma cell invasion by expression of antisense L-plastin gene. *Am. J. Pathol.,* **155,** 115-122.

Zhong,W., Oberley,L.W., Oberley,T.D., Yan,T., Domann,F.E., and St Clair,D.K. (1996). Inhibition of cell growth and sensitization to oxidative damage by overexpression of manganese superoxide dismutase in rat glioma cells. *Cell Growth Differ.,* **7,** 1175-1186.

Zwick,E., Bange,J., and Ullrich,A. (2002). Receptor tyrosine kinases as targets for anticancer drugs. *Trends Mol. Med.,* **8,** 17-23.

Appendix A--Synthesis of Cy dyes

The following describes the synthese of NHS-Cy3/5 & ICy3/5 dyes which was carried out by Dr. Piers Gaffney (Imperial College London).

NHS ester-derivatives of the fluorescent cyanine dyes Cy3 and Cy5 (NHS-Cy3 and NHS-Cy5) for lysine labelling were synthesized in-house following a modified version of the published protocol (Unlu et al., 1997a), and are structurally identical to the commercially available NHS-Cy dyes. Briefly, Cy carboxylic acids were prepared from the reactions of **1** and **2** (Figure 1A), and these converted to the corresponding NHS-Cy reagents. To optimise yields and ensure compound purity, each of the reported intermediates for NHS-Cy preparation was purified before commencing the next step, instead of carrying through crude material. However, in our hands, the published preparation of **1b** gave poor and variable yields; an alternative preparation, that has worked reliably for several phenylimido indoline Cy3 and Cy5 precursors, is described for **1a**. Also, in our hands, the published preparation of **2** gave material significantly contaminated with 1-[6-hexanoyl(6-hexanoic acid)]-2-methylene-3,3-dimethyl indolinium bromide. We have overcome this by alkylating 2,3,3-trimethyl indolenine with a 6-bromohexanoate silyl ester. The iodoacetyl versions of Cy3 and Cy5 (ICy3 and ICy5) were synthesised via the illustrated route starting with the reaction of 1 and 3 (Fig. 1A) and their structures are shown in Fig. 1B. All Cy dyes were made as stock solutions in anhydrous 99.8% *N,N*-dimethylformamide and stored at -20 °C.

All reverse phase (RP) chromatography used 100 ml silanised silica, Merck (cat. no. 1.07719). Normal phase thin layer chromatography (TLC) was run on glass-backed silica gel 60 F_{254}, Merck (cat. no. 1.05715) and RP thin layer chromatography (RPTLC) was run on glass-backed silica gel 60 F_{254}s, Merck (cat. no. 1.15388).

2-[4-(Phenylimido)butenylidene]-1, 3, 3-trimethyl indoline, 1a

2-Methylene-1, 3, 3-trimethyl indoline (0.177 ml, 1.0 mmol) and malonaldehyde dianil hydrochloride (0.354 g, 1. 5 mmol) were dissolved in DMF (1 ml) and to this was added TFA (0.084 ml, 1.1 mmol). The mixture was heated at 90 °C for 4.5 h then cooled to RT. The reaction was diluted with water (50 ml, plus a little dil. HCl) and applied directly to

a RP column. The column was first eluted with a gradient of MeCN - H_2O, containing 1% sat. $NaHCO_3$, then MeOH; the product, contaminated with dianil, eluted at the end of the gradient. The appropriate fractions were combined and the organic solvents evaporated under reduced pressure. The aqueous residue was acidified and re-chromatographed on a RP column eluted with a gradient of MeCN - H_2O, containing 0.5% 4M HCl; the product eluted at 35 - 50% MeCN. The appropriate fractions were combined, neutralised with $NaHCO_3$ and the organic solvents evaporated under reduced pressure. Brine was added to the resultant aqueous solution and the product extracted into $CHCl_3$ (4 x 30 ml). The combined organic layers were dried (Na_2SO_4) and evaporated to dryness to give the *title compound* as a deep orange/yellow gum (**1a**, 0.185 g, 61%). RPTLC, MeCN - H_2O - AcOH (75 : 14. 9 : 0. 1) R_f 0. 27.

1-(6-Hexanoic acid)-2-methylene-3, 3-dimethyl indolinium bromide, 2

First 6-bromo-*tert*-butyl dimethylsilyl hexanoate was prepared: 6-bromohexanoic acid (7. 941 g, 40.7 mmol) was taken up in THF (100 ml) to which was added Et_3N (6.81 ml, 1.2 eq.). Dropwise addition of *tert*-butyl dimethylsilyl chloride (6.136 g, 40.7 mmol) followed, with vigorous stirring, and the reaction continued for 1 h. The suspension was then filtered, rinsing the salts with dry ether, and the filtrate evaporated to dryness to give crude 6-bromo-*tert*-butyl dimethylsilyl hexanoate (12.781 g) which was used without further purification. 2, 3, 3-Trimethyl indolenine (2. 258 g, 14. 2 mmol) was dissolved in 6-bromo-*tert*-butyl dimethylsilyl hexanoate (6.574 g, 21.3 mmol, 1.5 eq.) and the mixture stirred at 100 °C overnight. The next day the reaction was allowed to cool when lightly coloured crystals formed in the dark red gummy mother liquor. The mixture was mobilised by the addition of a little DCM (*ca.* 5 ml) then diluted by the gradual addition of EtOAc (100 ml) with constant swirling. The solids were filtered off, rinsing with more EtOAc, to give the *title compound* as a pale pink powder (**2**, 0.777 g). The filtrate was evaporated to dryness and taken up in MeOH (20 ml) to which was added TFA (0.163 ml, *ca.* 0.1 per silyl ester). After 1 h the solvent was stripped off and the EtOAc precipitation repeated to give a second crop of the *title compound* (**2**, 0.755 g, total *ca.* 30%).

1-(6-Azidohexyl)-2-methylene-3, 3-dimethyl indoline, 3

2, 3, 3-Trimethyl indoleneine (3.20 ml, 20 mmol) was dissolved in 1, 2-dichlorobenzene (40 ml) and to this was added 1, 6-dibromohexane (9.24 ml, 60 mmol). The stirred reaction was heated at 110 °C overnight and the next day the solvent was stripped off *in vacuo* (oil pump, oil bath 60 °C) to leave a dark lilac oil. This residue was dissolved in $CHCl_3$ (100 ml), washed with dilute hydrobromic acid (20 ml 48% HBr + 180 ml water) and the aqueous layer was extracted with further $CHCl_3$ (2 x 50 ml). The combined organic layers were dried ($MgSO_4$) and evaporated to dryness leaving a dark oil (8.00 g). To the residue were added DCM (100 ml) then silanised silica (100 ml) and the solvent stripped off *in vacuo*. The silica was placed in a large sinter funnel and washed with H_2O - MeCN - AcOH (500 ml, 74 : 25 : 1 v/v/v). The filtrate was concentrated on a rotary evaporator, basified with Na_2CO_3 (aq.), then saturated with NaCl. This was extracted into $CHCl_3$ (4 x 50 ml), dried ($MgSO_4$) and the solvent evaporated to give crude 1-(6-bromohexyl)-2-methylene-3, 3-dimethyl indoline (3.71 g) which was used without further purification.

The crude bromide was dissolved in DMF. To this solution was added NaN_3 (2.28 g, 3 eq.) and the reaction was stirred vigorously for 2 days at RT. The solution was then diluted with water (200 ml), buffered with a little $NaHCO_3$ (aq.), then saturated with NaCl. The turbid solution was extracted with EtOAc (200 ml) and the organic layer was washed with $NaHCO_3$ (aq.) then brine. The aqueous layers were combined and extracted with further EtOAc (100 ml). This organic layer was also washed with $NaHCO_3$ (aq.) then brine. The combined organic layers were washed with water, containing a little $NaHCO_3$ (3 x 100 ml), and finally brine. This was dried ($MgSO_4$) and the solvent evaporated to give the crude *title compound* (**3**, 3.272 g, *ca.* 57%). The neat oil decomposes significantly overnight, even at -20 °C.; it may be stored for months in the fridge in acidified chloroform (3 g in 50 ml $CHCl_3$ plus 2 ml AcOH).

***N*-(6-Azidohexyl)-*N'*-methyl Cy5 chloride, 4a, and *N*-(6-azidohexyl)-*N'*-propyl Cy3 chloride, 4b**

1-(6-Azidohexyl)-2-methylene-3, 3-dimethyl indoline (**3**, 0.376 g, 1.32 mmol) and 2-[4-(phenylimido)butenylidene]-1, 3, 3-trimethyl indoline (**1a**, 0.401 g, 1.33 mmol) were

dissolved in acetic anhydride (2.5 ml). After stirring for 30 min the solvent was evaporated under high vacuum and the residue applied to a RP column. This was eluted with a gradient of MeCN - H_2O, containing 1% AcOH; the product eluted in 60 - 70% MeCN. The appropriate fractions were combined and the solvent evaporated at reduced pressure. The residue was taken up in $CHCl_3$ and washed with a mixture of brine and $NaHCO_3$ (aq.). The aqueous layers were washed with further $CHCl_3$ (3 or 4 times), until the colour was almost completely extracted, the combined organic layers were dried (Na_2SO_4) and evaporated to dryness to give *N-(6-azidohexyl)-N'-methyl Cy5 chloride* (**4a**, 0.538 g, 77%). TLC, pre-dip plate, MeOH - $CHCl_3$ - AcOH (10 : 89.9 : 0.1) R_f 0.37; RPTLC, MeCN - H_2O - AcOH (80 : 19.9 : 0.1) R_f 0. 27. Similarly, 1-(6-azidohexyl)-2-methylene-3, 3-dimethyl indoline (**3**, 0.381 g, 1.34 mmol) and 2-[2-(phenylimido)ethylidene]-1-propyl-3, 3-dimethyl indoline (**1b**, 0.418 g, 1.37 mmol) were reacted in actetic anhydride (2.5 ml). After RP chromatography and extraction, this gave *N*-(6-azidohexyl)-*N'*-propyl Cy3 chloride (**4b**, 0.533 g, 73%). TLC, pre-dip plate, MeOH - $CHCl_3$ - AcOH (10 : 89.9 : 0.1) R_f 0. 15; RPTLC, MeCN - H_2O - AcOH (70 : 29. 9 : 0.1) R_f 0.15.

N-(6-Aminohexyl)-N'-methyl Cy5 iodide, 5a, and N-(6-aminohexyl)-N'-propyl Cy3 iodide, 5b

N-(6-Azidohexyl)-*N'*-methyl Cy5 chloride (**4a**, 0.264 g, 0.50 mmol) was dissolved in THF (4 ml). To this solution was added triphenyl phosphine (0.199 g, 0.76 mmol) then water (1 ml) and the reaction was stirred overnight in the dark. The following day the solvent was stripped off and the residue was applied to a RP column. This was eluted with a gradient of MeCN - H_2O, containing 1% AcOH; the product eluted in 30 - 50% MeCN. The appropriate fractions were combined and the solvent evaporated at reduced pressure. The residue was taken up in $CHCl_3$ and washed with a mixture of KI (50% aq.) and a little $NaHCO_3$. The aqueous layers were washed with further $CHCl_3$ (2 or 3 times), until the colour was almost completely extracted, the combined organic layers were dried (Na_2SO_4) and evaporated to dryness to give *N-(6-aminohexyl)-N'-methyl Cy5 iodide* (**5a**, 0.214 g, 72%). TLC, pre-dip plate, MeOH - $CHCl_3$ - AcOH (10 : 89. 9 : 0.1) R_f 0.07. Similarly, *N*-(6-azidohexyl)-*N'*-propyl Cy3 chloride (**4b**, 0.261 g, 0.49 mmol) was reacted

with triphenyl phosphine (0.196 g, 0.75 mmol) in THF (4 ml) and water (1 ml). After RP chromatography and extraction, this gave *N-(6-aminohexyl)-N'-propyl Cy3 iodide* (**5b**, 0.291 g, 99%). TLC, pre-dip plate, MeOH - $CHCl_3$ - AcOH (10 : 89.9 : 0.1) R_f base-line.

N-(6-Iodoacetamidohexyl)-N'-methyl Cy5 iodide, 6a, and N-(6-iodoacetamidohexyl)-N'-propyl Cy3 iodide, 6b

N-(6-Aminohexyl)-*N'*-methyl Cy5 iodide (**5a**, 0.150 g, 0.25 mmol) was evaporated from dry MeCN (3 x 2 ml), the residue was taken up in DCM (0.75 ml) and to this was added iodoacetic anhydride (0.099 g, 0.31 mmol, 1.2 eq.). The reaction was stirred for 2 h then the solvent was evaporated. The residue was taken up in $CHCl_3$ and washed with KI (50% aq.), containing a little $NaHCO_3$, dried (Na_2SO_4) and evaporated to dryness. This material (0.210 g) was triturated with EtOAc and evaporated to dryness to give the crude product (0.188 g). This material is contaminated with iodoacetic acid/anhydride: crude product (0.072 g) was applied to a RP column which was eluted with a gradient of MeCN - H_2O, containing 0.5% KI (50% aq.) and 10 drops/100ml dil. H_2SO_4 (20% aq.); the product eluted in 65 - 70% MeCN. The appropriate fractions were combined and the MeCN evaporated under reduced pressure. The aqueous solution was extracted with $CHCl_3$ (4 x 20 ml), the combined extracts dried (Na_2SO_4) and evaporated to dryness to give pure *N-(6-iodoacetamidohexyl)-N'-methyl Cy5 iodide* (**6a**, 0.052 g). TLC, pre-dip plate, MeOH - $CHCl_3$ - AcOH (10 : 89. 9 : 0.1) 0.23. Similarly, *N*-(6-Aminohexyl)-*N'*-propyl Cy3 iodide (**5b**, 0.163 g, 0.27 mmol) was reacted with iodoacetic anhydride (0.110 g, 0.31 mmol, 1.2 eq.) in DCM (0.5 ml). Initial work-up gave the crude product (0.211 g). After RP chromatography (0.056g) of this material gave the pure *N-(6-iodoacetamidohexyl)-N'-propyl Cy3 iodide* (**6b**, 0.046 g). TLC, pre-dip plate, MeOH - $CHCl_3$ - AcOH (10 : 89.9 : 0.1) 0.15.

A

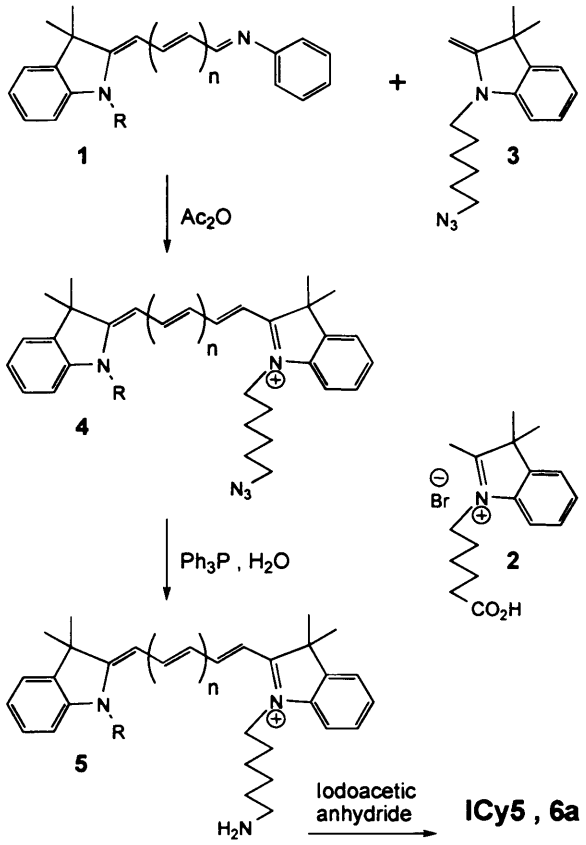

B

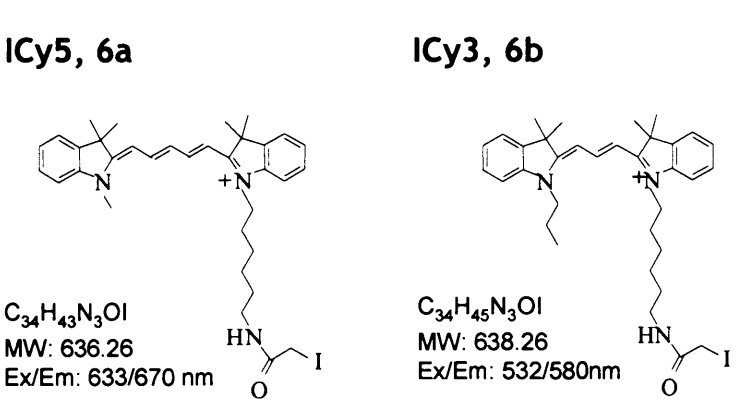

(Appendix A) Synthesis and structure of the iodoacetyl cyanine dyes. (A) Scheme for synthesis of ICy3 and ICy5. (B) ICy5 and ICy3 (compounds 6a and 6b respectively from the synthetic scheme) showing chemical formulas, molecular weights and the excitation/emission wavelengths used for detection.

Appendix B--Quantitative determination of free thiol content in standard proteins and in total cell lysates

Free thiol groups can be determined with Ellman's reagent (Zahler and Cleland, 1968). Aliphatic sulphydryls can cleave the disulphide-bridge of DTNB (5, 5'-dithiobis (2-nitrobenzoic acid)). The resulting TNB^{2-} (2-nitro-5-thiobenzoate) anion has a bright yellow colour, whilst DTNB has a faint yellowish colour. Thus, TNB^{2-} has a distinct spectrometric property for detection. The advantages of this reagent are that it is water-soluble, it may be used at neutral pH with few side reactions and its reaction with thiols is fast. The reagent has been used not only in the study of thiol chemistry, but also for the analysis of biological samples and in enzymology for many years (Brocklehurst et al., 1972;Gergel' and Cederbaum, 1997;Riener et al., 2002). According to the examination of ICy cysteine-labelling of standard proteins presented in Figure 3-4 of this thesis, the fluorescence intensities of the ICy-labelled standards did not correlate with the number of free thiols on the proteins, even though they were present at equimolar amounts. Therefore, Ellman's tests were performed to determine the free thiol number in each standard protein. The results showed that 0.61, 1.67 and 0.53 mol/mol of free thiols were present in BSA (1 free thiol), Ova (4 free thiols) and α-Crys (1 free thiol), respectively Figure Appendix B1). This suggests that these standard proteins were all partially oxidised before performing the labelling test. However, these values alone cannot explain the variable fluorescence intensities between these labelled standards. Thus, it would appear that labelling does not depend upon thiol content alone, but also on the reactivity and/or accessibility of specific thiol groups.

In sections (3.2.4) and (4.2), Ellman's reactions were also applied for determining the average free thiol number per protein molecule from human luminal epithelial cells. For this, 200 μg of cell lysate was diluted to 900 μl with sodium phosphate buffer and an absorbance (412nm) of 0.4 units was obtained for the HB4a lysate using the Ellman's reagent (Figure Appendix B2). It is important to note that the absorbance was linear over a whole range of different lysate amounts. According to the equation ([SH] = [A412 (sample)-A412 (reference)] / 13650), 27 nmols of thiol groups were present in this sample. The average molecular weight of a human protein, was then calculated to be 48

kDa, by averaging the predicted molecular weights of all known human sequences in the SwissProt/ TrEMBL & NCBI databases accessed using the international protein index (IPI) (calculated by Richard Jacob, LICR, UCL). Thus, 200 μg of cell lysate is approximately equal to 4.2 nmol of protein molecules and so there were 6.4 moles free thiol/ mol of protein.

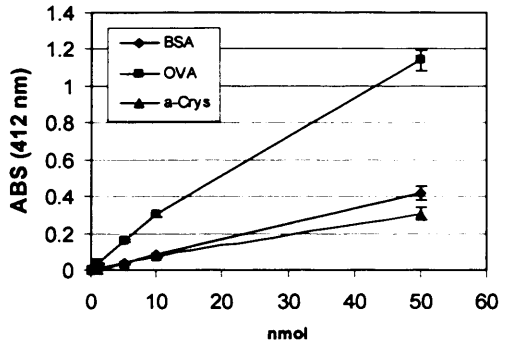

(Figure Appendix B1) Quantitative determination of free thiol content in standard proteins (BSA, OVA and α-Crys). 100 μl of standard proteins (BSA, OVA and α-Crys) were prepared at the indicated molar amounts and diluted with 100 μl of 0.01 M DTNB (Ellman's reagent) and 2800 μl of 0.1 M sodium phosphate buffer (pH 8.0). The mixture was incubated in the dark for 15 min and then the absorbance measured at 412 nm in a 1 cm cuvette. A reference solution was prepared containing 100 μl of 0.01 M DTNB and 2900 μl of 0.1 M sodium phosphate buffer (pH 8.0) and the absorbance measured. The concentration of sulphydryl groups was calculated using the following equation; [SH] = [A412 (sample)-A412 (reference)] / 13650.

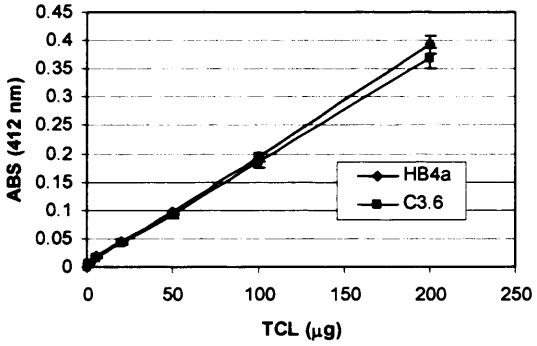

(Figure Appendix B2) Quantitative determination of free thiols (Ellman test). **(A)** HB4a and C3.6 cell lysates were freshly prepared in ICy lysis buffer and the protein concentration determined. The indicated amounts of total protein in 100 μl were then diluted with 2900 μl of 0.1 M sodium phosphate buffer (pH 8.0) containing DTNB (Ellman's reagent) at a final concentration of 0. 33 mM. Samples were mixed well, and incubated in the dark at room temperature prior to measurement of the absorbance at 412 nm.

Appendix C--Spectra, MOWSE scores, matched peptide and sequence coverage of identified proteins (Table 4-1)

Spot 769 Bip Protein

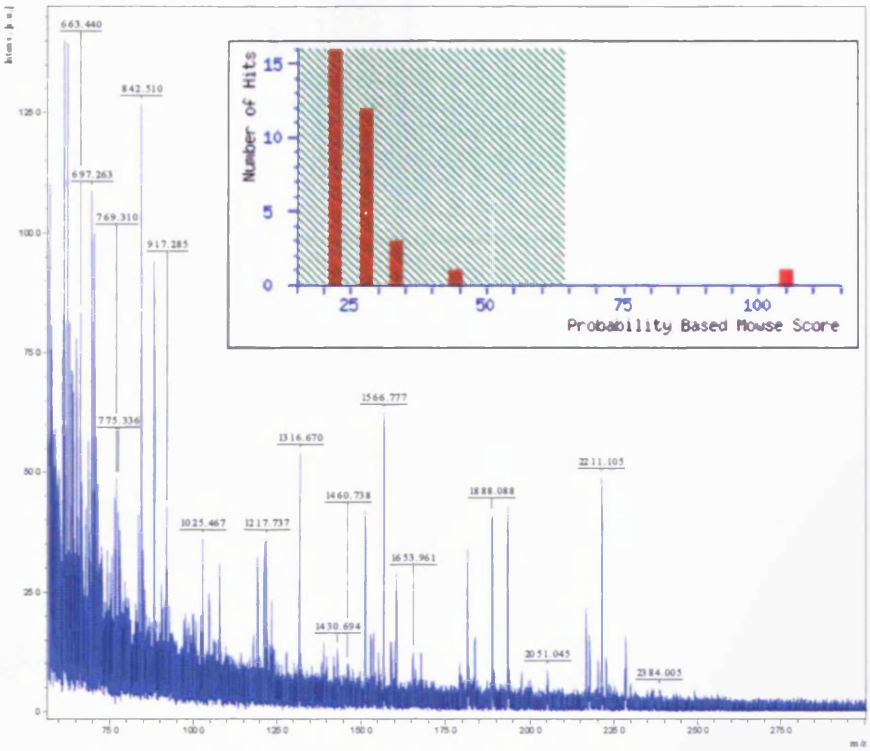

Start - End	Observed	Mr(expt)	Mr(calc)	Delta	Miss	Sequence
50 - 68	1230.68	1227.68	1227.63	0.03	0	R.VEILAADQGSR.I
61 - 76	1566.78	1565.77	1565.77	-0.00	0	R.ITPSYVAFTPEGER.L
102 - 113	1430.69	1429.69	1429.68	0.00	0	R.TWNDPSVQQDIK.F
124 - 138	1684.90	1683.89	1683.86	0.03	0	R.TKPYIQVDIGGGQTK.T
139 - 152	1536.83	1535.82	1535.79	0.03	0	R.TFAPEEISAMVLTK.M
139 - 152	1552.80	1551.79	1551.79	0.00	0	R.TFAPEEISAMVLTK.M Oxidation (M)
153 - 163	1240.63	1239.63	1239.63	0.01	1	K.MKETAAAYLGK.K
164 - 197	1233.62	1232.61	1232.62	-0.01	0	K.DAGTIAGLNVMR.I Oxidation (M)
208 - 216	997.51	996.51	996.51	-0.00	0	R.ALSSQHQAR.I
207 - 226	2165.01	2164.01	2163.98	0.03	0	R.IEIESFYEGEDFSETLTR.A
225 - 236	1512.81	1511.80	1511.74	0.06	1	R.AKPEELMMDLFR.S
225 - 236	1528.76	1527.76	1527.74	0.02	1	R.AKPEELMMDLFR.S Oxidation (M)
354 - 367	1660.74	1659.73	1659.75	-0.02	0	R.SDIDETVLVGGSTR.I
448 - 464	1836.86	1835.85	1835.93	-0.07	0	R.SQIPSTASDNQPTVTIK.V
463 - 474	1191.63	1190.62	1190.63	-0.01	0	K.VTIKDNKQLTK.D
475 - 492	1934.01	1933.00	1933.01	-0.00	0	K.DNKLLGTFDLTGIPPAPR.G
522 - 532	1316.67	1315.66	1315.66	-0.02	1	R.KMITITNDQNR.L
597 - 606	637.36	636.35	636.38	-0.03	0	K.KTDEEL.A

```
   1 MKLSLVAAML LLLSAARAEE EDKKEDVGTV VGIDLGTTYS CVGVFKNGRV
  51 EIIANDQGNR ITPSYVAFTP EGERLIGDAA KNQLTSNPEN TVFDAKRLIG
 101 RTWNDPSVQQ DIKFLPFKVV EKKTKPYIQV DIGGGQTKTF APEEISAMVL
 151 TKMKETAEAY LGKKVTHAVV TVPAYFNDAQ RQATKDAGTI AGLNVMRIIN
 201 EPTAAAIAYG LDKREGEKNI LVFDLGGGTF DVSLLTIDNG VFEVVATNGD
 251 THLGGEDFDQ RVMEHFIKLY KKKTGKDVRK DNRAVQKLRR EVEKAKRALS
 301 SQHQARIEIE SFYEGEDFSE TLTRAKFEEL NMDLFRSTMK PVQKVLEDSD
 351 LKKSDIDEIV LVGGSTRIPK IQQLVKEFFN GKEPSRGINP DEAVAYGAAV
 401 QAGVLSGDQD TGDLVLLDVC PLTLGIETVG GVMTKLIPRN TVVPTKKSQI
 451 FSTASDNQPT VTIKVYEGER PLTKDNKLLG TFDLTGIPPA PRGVPQIEVT
 501 FEIDVNGILR VTAEDKGTGN KNKITITNDQ NRLTPEEIER MVNDAEKFAE
 551 EDKKLKERID TRNELESYAY SLKNQIGDKE KLGGKLSSED KETMEKAVEE
 601 KIEWLESHQD ADIEDFKAKK KELEEIVQPI ISKLYGSAGP PPTGEEDTAE
 651 KDEL
```

Spot 1123 Chaperonin containing TCP1-α

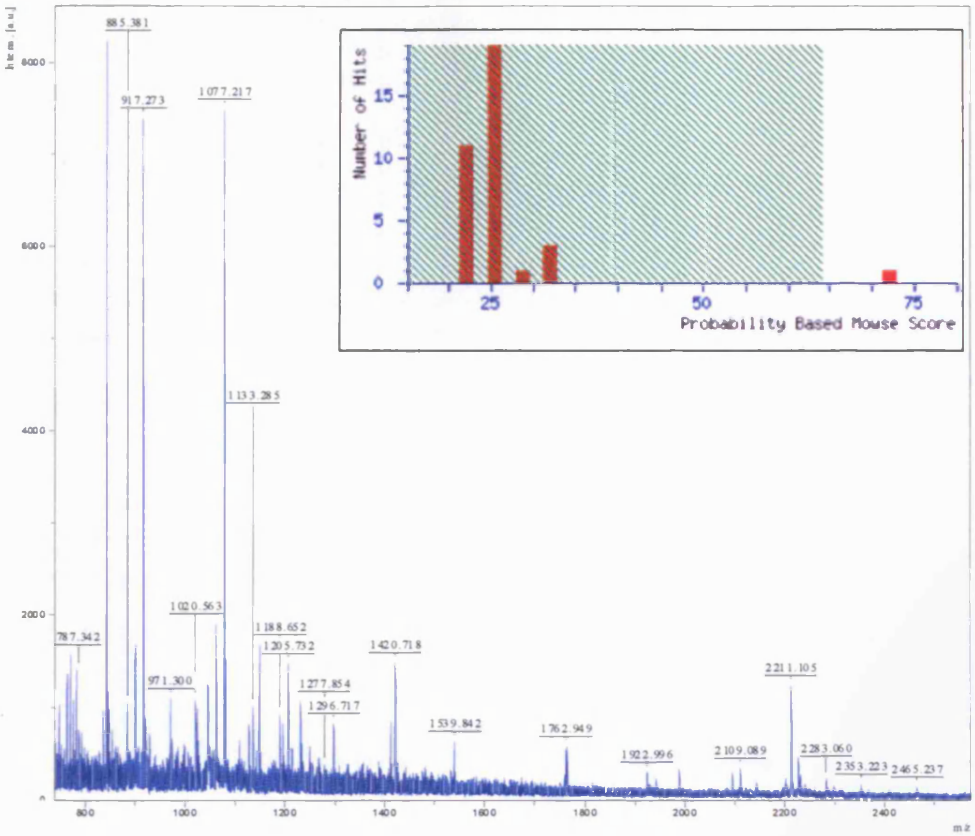

Start - End	Observed	Mr(expt)	Mr(calc)	Delta	Miss	Sequence
64 - 73	1106.65	1105.65	1105.61	0.03	0	K.LLEVEKPAAK.V
85 - 102	1814.94	1813.93	1814.00	-0.07	0	K.EVGDGTTSVVIIAAELLK.H
112 - 122	1229.70	1228.69	1228.66	0.03	0	K.IMPTSVISGYR.L
131 - 145	1762.95	1761.94	1761.89	0.05	0	R.YIHENLIVNTDELGR.D
190 - 199	1146.64	1145.63	1145.64	-0.01	0	R.YPVNSVNILK.A
234 - 243	1194.65	1193.64	1193.61	0.03	0	K.IACLDFSLQK.T
248 - 264	1923.00	1921.99	1922.08	-0.09	1	K.LGVQVVITDPEKLDQIR.Q
444 - 466	2353.22	2352.22	2352.29	-0.07	0	R.SLLVIPNTLAVNAAQDSTDLVAK.L
469 - 480	1411.74	1410.73	1410.66	0.07	0	R.AFNNEAQVNPER.K
469 - 481	1539.84	1538.83	1538.76	0.08	1	R.AFNNEAQVNPERK.N
500 - 510	1188.65	1187.64	1187.65	-0.01	0	K.QAGVFEPTIVK.V
516 - 526	1205.73	1204.73	1204.68	0.04	0	K.FATEAAITILR.I

```
  1 MEGPLSVFGD RSTGETIRSQ NVMAAASIAN IVKSSLGPVG LDKMLVDDIG
 51 DVTITNDGAT ILKLLEVEHP AAKVLCELAD LQDKEVGDGT TSVVIIAAEL
101 LKNADELVKQ KIHPTSVISG YRLACKEAVR YIMENLIVNT DELGRDCLIN
151 AAKTSMSSKI IGINGDFFAN MVVDAVLAIK YTDIRGQPRY PVNSVNILKA
201 HGRSQMESML ISGYALNCVV GSQGMPKRIV NAKIACLDFS LQKTKMKLGV
251 QVVITDPEKL DQIRQRESDI TKERIQKILA TGANVILTTG GIDDMCLKYF
301 VEAGAMAVRR VLKRDLKRIA KASGATILST LANLEGEETF EAAMLGQAEE
351 VVQERICDDE LILIKNTKAR TSASIILRGA NDFMCDEMER SLHDALCVVK
401 RVLESKSVVP GGGAVEAALS IYLENYATSM GSREQLAIAE FARSLLVIPN
451 TLAVNAAQDS TDLVAKLRAF HNEAQVNPER KNLKWIGLDL SNGKPRDNKQ
501 AGVFEPTIVK VKSLKFATEA AITILRIDDL IKLHPESKDD KHGSYEDAVH
551 SGALND
```

Spot 1242 Chaperonin containing TCP1-β

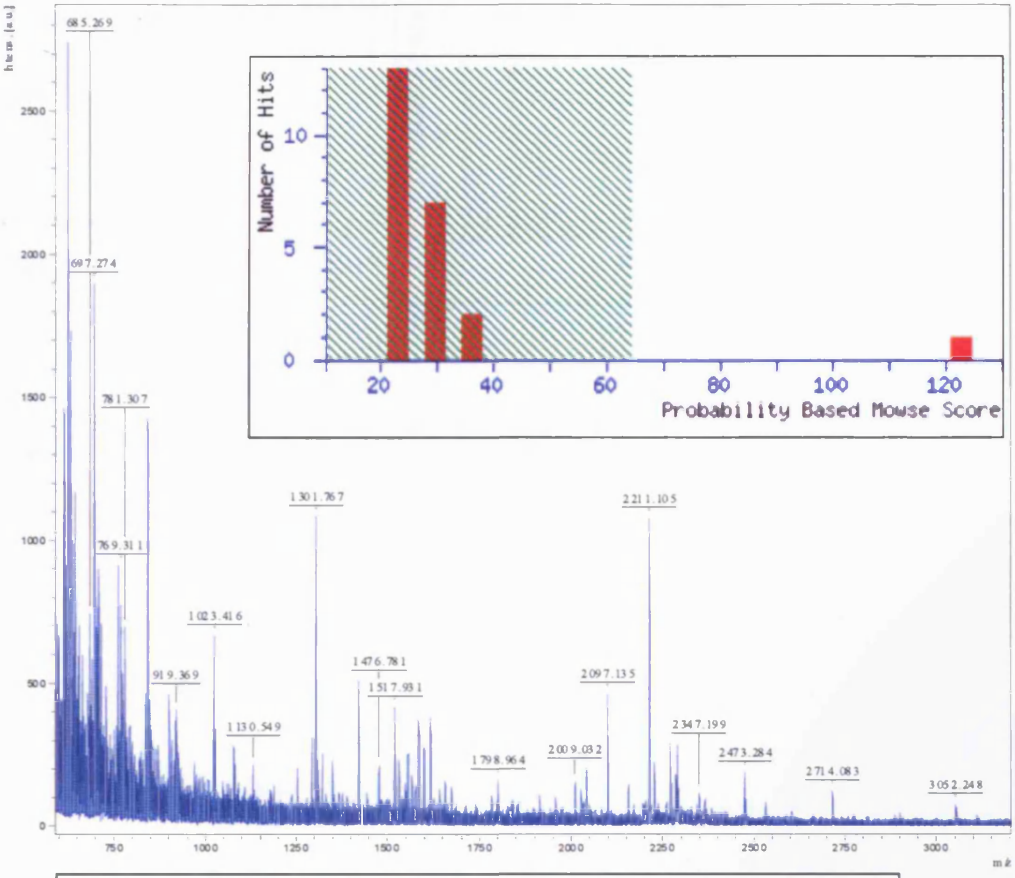

Start - End	Observed	Mr(expt)	Mr(calc)	Delta	Miss	Sequence
25 - 39	1517.93	1516.92	1516.89	0.04	0	R.LTSFIGAIAIGDLVK.S
72 - 88	1798.96	1797.96	1797.94	0.02	1	K.NIGVDNPAARVLVDMSR.V
89 - 118	2288.16	2287.16	2287.15	0.00	0	R.VQDDEVGDGTTSVTVLAAELLR.E
119 - 138	1419.76	1418.75	1418.81	-0.07	1	K.EIMPQTIIAGWR.E
120 - 130	1291.73	1290.72	1290.72	0.00	0	K.IMPQTIIAGWR.E
134 - 169	1781.97	1780.96	1780.91	0.04	1	R.FRQDLMNIAGTTLSSK.L
181 - 188	870.54	869.54	869.53	0.00	0	K.LAVEAVLR.L
191 - 202	1251.70	1250.70	1250.70	-0.00	0	K.GSGNLEAIHIIK.E
204 - 222	2041.07	2040.06	2040.04	0.02	1	K.LGGSLADSYLDEGFLLDKK.I
204 - 292	1130.55	1129.54	1129.55	-0.00	0	K.HSIHCFIHR.Q
322 - 341	2097.14	2096.13	2096.12	0.01	0	R.LALVTGGEIASTFDHPELVK.L
350 - 375	1956.10	1955.09	1955.07	0.02	0	K.LIHFSGVALGEACTIVLR.G
388 - 401	1554.81	1553.80	1553.82	-0.02	0	R.SLHDALCVLAQTVK.D
388 - 404	1912.99	1911.99	1911.98	0.00	1	R.SLHDALCVLAQTVKDSR.T
444 - 465	2347.20	2346.19	2346.19	0.00	0	R.HLPTIIADMAGTDSADLVAQLR.A
444 - 465	2363.11	2362.10	2362.18	-0.09	0	R.HLPTIIADMAGTDSADLVAQLR.A Oxidation (M)
466 - 488	1546.67	1545.66	1545.68	-0.02	0	R.AANSEGNTTAGLDMR.E Oxidation (M)
481 - 499	2009.03	2008.03	2008.02	0.01	0	R.EGTIGDMAILGITESFQVK.R
501 - 515	1502.98	1501.97	1501.91	0.07	0	R.QVLLSAAEAAEVILR.V

```
  1 ASLSLAPVNI FKAGADEERA ETARLTSFIG AIAIGDLVKS TLGPKGMDKI
 51 LLSSGRDASL MVTNDGATIL KNIGVDNPAA KVLVDMSRVQ DDEVGDGTTS
101 VTVLAAELLR EAESLIAKKI HPQTIIAGWR EATKAAREAL LSSAVDHGSD
151 EVKFRQDLMN IAGTTLSSKL LTHHKDHFTK LAVEAVLRLK GSGNLEAIHI
201 IKKLGGSLAD SYLDEGFLLD KKIGVNQPKR IENAKILIAN TGMDTDKIKI
251 FGSRVRVDST AKVAEIEHAE KEKMKEKVER ILKHGINCFI NRQLIYNYPE
301 QLFGAAGVMA IEHADFAGVE RLALVTGGEI ASTFDHPELV KLGSCKLIEE
351 VMIGEDKLIH FSGVALGEAC TIVLRGATQQ ILDEAERSLH DALCVLAQTV
401 KDSRTVYGGG CSEMLMAHAV TQLANRTPGK EAVAMESYAK ALRMLPTIIA
451 DNAGYDSADL VAQLRAAHSE GNTTAGLDMR EGTIGDMAIL GITESFQVKR
501 QVLLSAAEAA EVILRVDNII KAAPRKRVPD HHPC
```

Spot 1206 Chaperonin containing TCP1-β

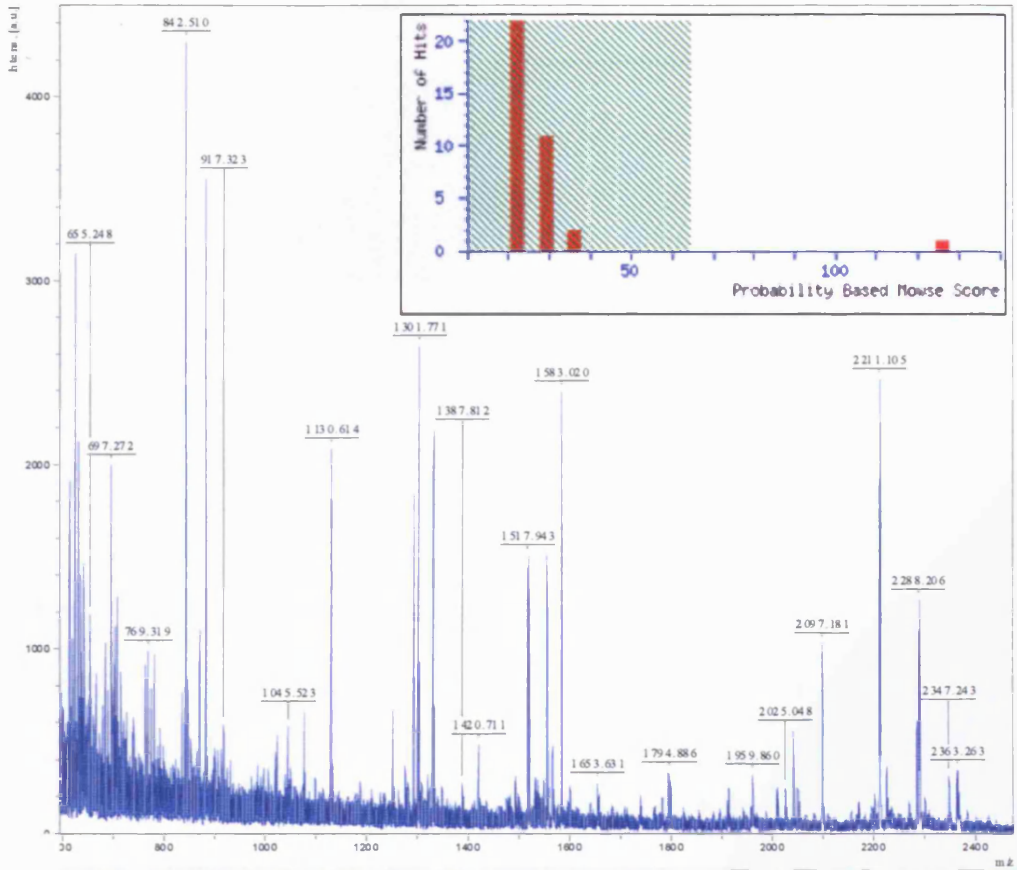

Start - End	Observed	Mr(expt)	Mr(calc)	Delta	Miss	Sequence
13 - 24	1275.55	1274.54	1274.59	-0.05	1	K.AGADEERAETAR.L
25 - 39	1517.94	1516.94	1516.89	0.05	0	R.LTSFIGAIAIGDLVK.S
57 - 71	1548.76	1547.75	1547.79	-0.03	0	R.DASLMVTMDGATILK.M
57 - 71	1564.76	1563.75	1563.78	-0.03	0	R.DASLMVTMDGATILK.M Oxidation (M)
89 - 110	2288.21	2287.20	2287.15	0.04	0	R.VQDDEVGDGTTSVTVLAAELLR.E
120 - 130	1291.78	1290.78	1290.72	0.06	0	K.IKPQTIIAGWR.E
181 - 188	870.57	869.56	869.53	0.03	0	K.LAVEAVLR.L
189 - 202	1492.84	1491.83	1491.88	-0.05	1	R.LKGSGMLEAIMIIK.K
191 - 202	1251.75	1250.74	1250.70	0.04	0	K.GSGMLEAIMIIK.K
204 - 221	1912.89	1911.89	1911.95	-0.06	0	K.LGGSLADSYLDEGFLLDK.K
204 - 222	2041.07	2040.07	2040.04	0.03	1	K.LGGSLADSYLDEGFLLDKK.I
263 - 273	1282.64	1281.63	1281.66	-0.03	1	K.VAEIEMAEKEK.M
322 - 341	2097.18	2096.17	2096.12	0.06	0	R.LALVTGGEIASTFDHPELVK.L
376 - 387	1330.69	1329.68	1329.65	0.03	0	R.GATQQILDEAER.S
388 - 401	1554.84	1553.83	1553.82	0.01	0	R.SLMDALCVLAQTVK.D
444 - 465	2347.24	2346.24	2346.19	0.05	0	R.MLPTIIADNAGYDSADLVAQLR.A
444 - 465	2363.26	2362.26	2362.18	0.07	0	R.MLPTIIADNAGYDSADLVAQLR.A Oxidation (M)
466 - 480	1538.65	1529.64	1529.69	-0.05	0	R.AAMSEGMTTAGLDMR.E
481 - 499	2009.10	2008.09	2008.02	0.07	0	R.EGTIGDMAILGITESFQVK.R
481 - 499	2025.05	2024.04	2024.01	0.03	0	R.EGTIGDMAILGITESFQVK.R Oxidation (M)

```
  1 ASLSLAPVNI FKAGADEERA ETARLTSFIG AIAIGDLVKS TLGPKGMDKI
 51 LLSSGRDASL MVTMDGATIL KNIGVDNPAA KVLVDMSRVQ DDEVGDGTTS
101 VTVLAAELLR EAESLIAKKI HPQTIIAGWR EATKAAREAL LSSAVDHGSD
151 EVKFRQDLMN IAGTTLSSKL LTHHKDHFTK LAVEAVLRLK GSGNLEAIHI
201 IKKLGGSLAD SYLDEGFLLD KKIGVNQPKR IENAKILIAN TGMDTDKIKI
251 FGSRVRVDST AKVAEIEMAE KEKMKEKVER ILKHGINCFI NRQLIYNYPE
301 QLFGAAGVMA IEHADFAGVE RLALVTGGEI ASTFDHPELV KLGSCKLIEE
351 VMIGEDKLIH FSGVALGEAC TIVLRGATQQ ILDEAERSLH DALCVLAQTV
401 KDSRTVYGGG CSEMLMAHAV TQLANRTPGK EAVAMESYAK ALRMLPTIIA
451 DNAGYDSADL VAQLRAAMSE GNTTAGLDMR EGTIGDMAIL GITESFQVKR
501 QVLLSAAEAA EVILRVDNII KAAPRKRVPD HHPC
```

Spot 1110 Chaperonin containing TCP1-γ

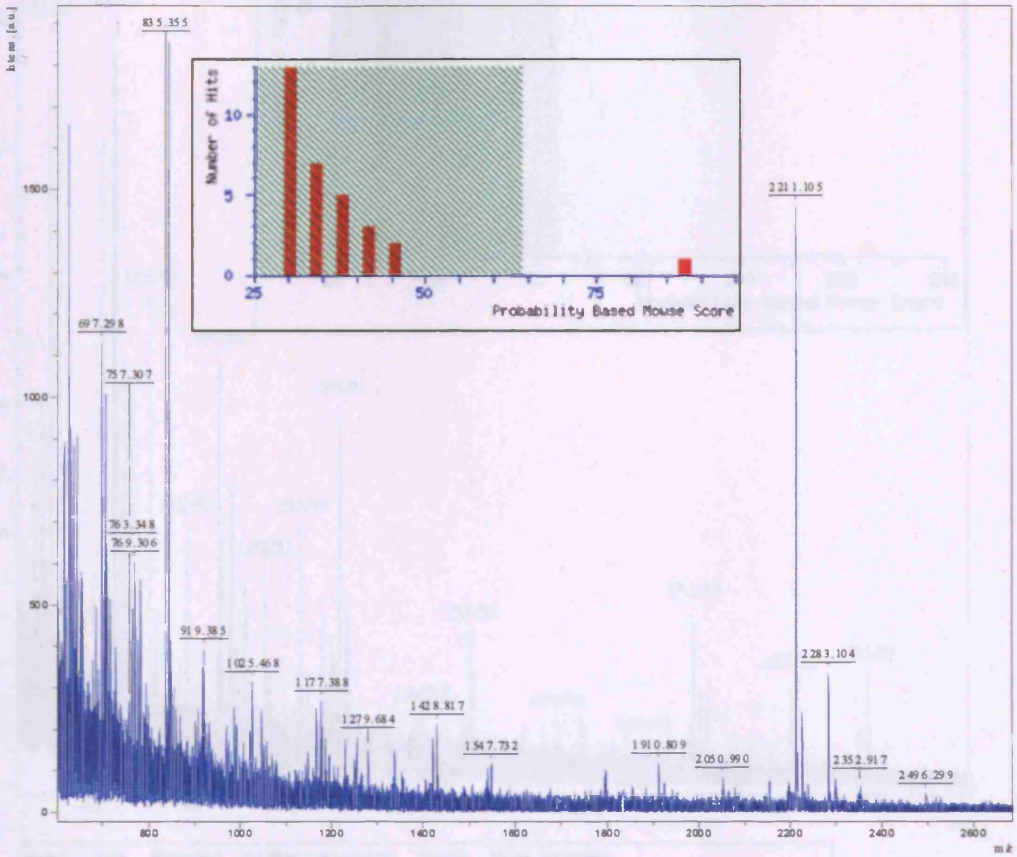

Start - End	Observed	Mr(expt)	Mr(calc)	Delta	Miss	Sequence
31 - 31	1129.54	1128.53	1128.63	-0.09	1	R.KVQSGNINAA.K
69 - 78	1128.58	1119.58	1119.68	-0.11	0	R.EIQVQMPAAK.S
69 - 85	1952.97	1951.96	1952.01	-0.06	1	R.EIQVQMPAAKSNIEISR.T Oxidation (M)
79 - 85	835.36	834.35	834.43	-0.08	0	K.SNIEISR.T
129 - 138	1106.59	1105.59	1105.57	0.02	0	K.ALDNMISTLK.K
129 - 139	1234.67	1233.67	1233.66	0.00	1	K.ALDNMISTLKK.I
168 - 181	1547.73	1546.73	1546.78	-0.06	0	R.VSSLACNIALDAVK.M
204 - 216	1428.82	1427.81	1427.74	0.07	0	K.IPGGIIEDSCVLR.G
230 - 240	1279.68	1278.68	1278.71	-0.03	0	R.IVLLDSSLEYK.K
230 - 266	2025.82	2024.82	2024.93	-0.11	1	K.GESQTDIEITREEDFTR.I
295 - 306	1403.73	1402.72	1402.70	0.02	0	K.GISDLAQNTLNR.A
295 - 306	1419.70	1418.70	1418.70	-0.00	0	K.GISDLAQNTLNR.A Oxidation (M)
331 - 353	2496.30	2495.29	2495.32	-0.03	1	R.IVSRPEELREDDVGTGAGLLEIK.K
355 - 370	1949.05	1948.04	1947.89	0.15	1	K.IGDEYTFTITDCKDPK.A
428 - 438	1337.60	1336.59	1336.62	-0.03	0	K.AMTQVEQMPYR.A
428 - 438	1353.59	1352.58	1352.62	-0.04	0	K.AMTQVEQMPYR.A Oxidation (M)
439 - 449	1166.72	1165.71	1165.68	0.03	0	R.AVAQALEVIPR.T
450 - 461	1333.63	1332.63	1332.68	-0.06	0	R.TLIQHCGASTIR.L
492 - 502	1254.67	1253.66	1253.70	-0.04	0	K.ELGIWEPLAVK.L
508 - 518	1185.64	1184.63	1184.71	-0.08	0	K.TAVETAVLLLR.I

```
  1 MMGHRPVLVL SQNTKRESGR KVQSGNINAA KTIADIIRTC LGPKSMMKML
 51 LDPMGGIVMT NDGNAILREI QVQMPAAKSN IEISRTQDEE VGDGTTSVII
101 LAGEMLSVAE HFLEQQMHPT VVISAYRKAL DDMISTLKKI SIPVDISDSD
151 MMLNIINSSI TTKAISRWSS LACNIALDAV KMVQFEENGR KEIDIKKYAR
201 VEKIPGGIIE DSCVLRGVMI NKDVTHPRMR RYIKNPRIVL LDSSLEYKKG
251 ESQTDIEITR EEDFTRILQM EEEYIQQLCE DIIQLKPDVV ITEKGISDLA
301 QMYLMRANIT AIRRVRKTDN NRIARACGAR IVSRPEELRE DDVGTGAGLL
351 EIKKIGDEYF TFITDCKDPK ACTILLRGAS KEILSEVERN LQDAMQVCRN
401 VLLDPQLVPG GGASEMAVAH ALTEKSKAMT GVEQMPYRAV AQALEVIPRT
451 LIQHCGASTI RLLTSLRAKH TQENCETWGV NGETGTLVDM KELGIWEPLA
501 VKLQTYKTAV ETAVLLLRID DIVSGHKKKG DDQSRQGGAP DAGQE
```

Spot 1144 Chaperonin containing TCP1-ζ

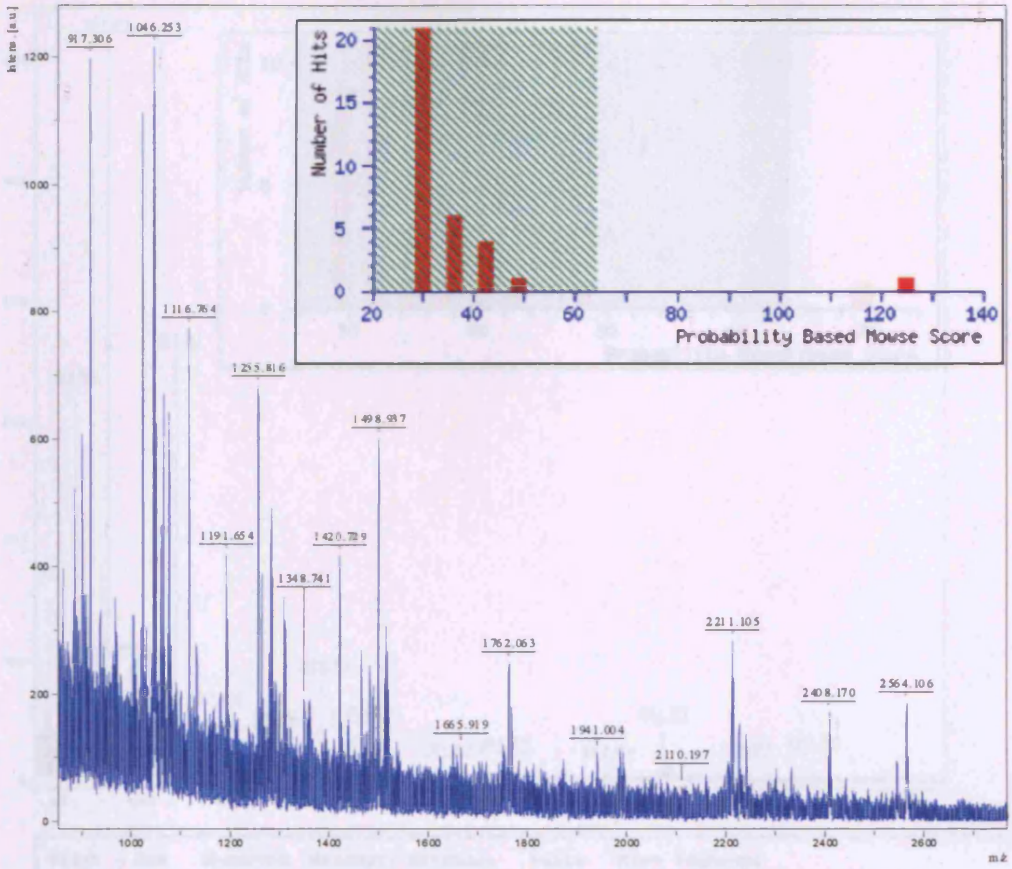

Start - End	Observed	Mr(expt)	Mr(calc)	Delta	Miss	Sequence
14 - 26	1255.82	1254.81	1254.78	0.10	0	R.AQAALAVNISAAR.G
27 - 33	800.43	799.42	799.46	-0.03	0	R.GLQDVLR.T
44 - 56	1348.74	1347.73	1347.74	-0.01	1	K.MLVSGAGDIKLTK.D Oxidation (M)
78 - 102	2544.43	2543.42	2543.33	0.09	0	K.VATAQDDITGDGTTSNVLIIGELLK.Q
128 - 136	1076.64	1075.63	1075.59	0.04	0	K.ALQFLEEVK.V
158 - 178	2286.28	2285.27	2285.23	0.05	0	K.VHAELADVLTEAVVDSILAIK.K
179 - 195	2110.20	2109.19	2109.02	0.17	1	K.KQDEPIDLFMIEIMEMK.H
240 - 249	1191.65	1190.65	1190.56	0.09	0	K.TEVNSGFFYK.S
240 - 254	1763.89	1762.88	1762.82	0.07	1	K.TEVNSGFFYKSAEER.E
271 - 276	743.47	742.46	742.50	-0.03	1	K.KIIELK.R
279 - 293	1665.92	1664.91	1664.87	0.09	1	K.VCGDSDKGFVVINQK.G
286 - 293	904.51	903.51	903.52	-0.01	0	K.GFVVINQK.G
294 - 305	1262.75	1261.74	1261.66	0.09	0	K.GIDPFSLDALSK.E
306 - 312	757.42	756.42	756.45	-0.03	0	K.EGIVALR.D
317 - 321	705.38	704.29	704.34	-0.05	1	R.RMMER.L
317 - 321	721.27	720.26	720.33	-0.07	1	R.RMMER.L Oxidation (M)
358 - 363	784.36	783.35	783.42	-0.06	0	K.FYFIEK.C
380 - 386	840.49	839.48	839.49	-0.01	0	K.MTLTQIK.D
391 - 397	758.42	757.41	757.44	-0.04	1	R.DGLRAVK.N
431 - 447	1768.13	1767.12	1767.03	0.09	0	R.AQLGVQAFADALLIIPK.V
448 - 463	1762.06	1761.06	1760.93	0.12	0	K.VLAQNSGFDLQETLVK.I

```
  1 AVKTLNPKAE VARAQAALAV NISAARGLQD VLRTNLGPKG TMKMLVSGAG
 51 DIKLTKDGNV LLHEMQIQHP TASLIAKVAT AQDDITGDGT TSNVLIIGEL
101 LKQADLYISE GLHPRIITEG FEAAKEKALQ FLEEVKVSRE MDRETLIDVA
151 RTSLRTKVHA ELADVLTEAV VDSILAIKKQ DEPIDLFMIE IMEMKHKSET
201 DTSLIRGLVL DHGARHPDMK KRVEDACILT CNVSLEYEKT EVNSGFFYKS
251 AEEREKLVKA ERKFIEDRVK KIIELKRKVC GDSDKGFVVI NQKGIDPFSL
301 DALSKEGIVA LRRAKRRNME RLTLACGGVA LNSFDDLSPD CLGHAGLVYE
351 YTLGEEKFTF IEKCNNPRSV TLLIKGPNKH TLTQIKDAVR DGLRAVKNAI
401 DDGCVVPGAG AVEVAMAEAL IKHKPSVKGR AQLGVQAFAD ALLIIPKVLA
451 QNSGFDLQET LVKIQAEHSE SGQLVGVDLN TGEPMVAAEV GVWDNYCVKK
501 QLLHSCTVIA TNILLVDEIM RAGMSSLKG
```

Spot 1143 Cytokeratin 10

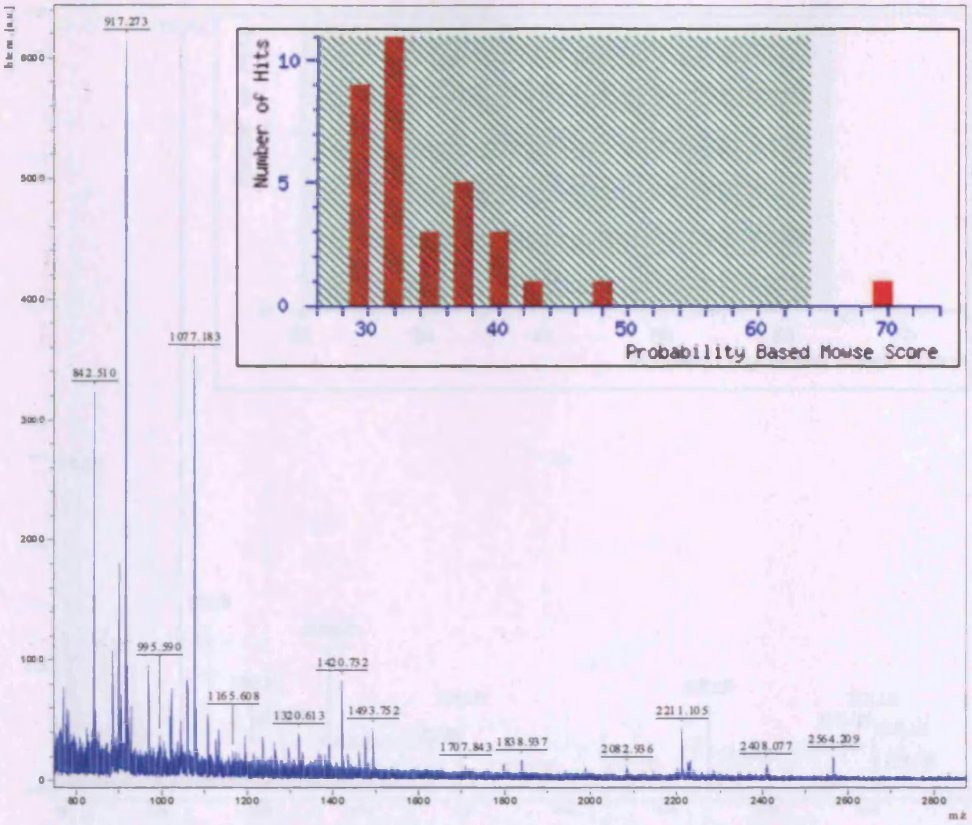

Start - End	Observed	Mr(expt)	Mr(calc)	Delta	Miss	Sequence
41 - 59	1707.84	1706.84	1706.76	0.07	0	K.GSLGGGFSSGGFSGGSFSR.G
60 - 86	2342.99	2341.98	2341.98	0.01	0	R.GSSGGGCFGGSSGGYGGLGGFGGGSFR.G
166 - 177	1381.69	1380.69	1380.64	0.05	0	R.ALEESNYELEGK.I
178 - 184	995.59	994.58	994.51	0.07	1	K.IKEWYEK.M
208 - 228	2367.47	2366.46	2366.26	0.21	0	K.MQILMLTTDNANILLQIDNAR.L
236 - 245	1234.68	1233.67	1233.67	-0.00	1	R.LKYENEVALR.Q
323 - 333	1365.73	1364.72	1364.63	0.09	0	R.SQYEQLAEQNR.K
323 - 334	1493.75	1492.74	1492.73	0.02	1	R.SQYEQLAEQNRK.D
371 - 386	1797.00	1796.00	1796.00	-0.01	0	R.NVQALEIELQSQLALK.Q
387 - 399	1390.78	1389.77	1389.67	0.10	0	K.QSLEASLAETEGR.Y
423 - 439	2082.94	2081.93	2081.96	-0.03	0	R.AETECQNTEYQQLLDIK.I
440 - 450	1434.73	1433.72	1433.76	-0.04	1	K.IRLENEIQTYR.S
442 - 450	1165.61	1164.60	1164.58	0.02	0	R.LENEIQTYR.S

```
  1 MSVRYSSSKH YSSSRSGGGG GGGGCGGGGG VSSLRISSSK GSLGGGFSSG
 51 GFSGGSFSRG SSGGGCFGGS SGGYGGLGGF GGGSFRGSYG SSSFGGSYGG
101 SFGGGSFGGG SFGGGSFGGG GFGGGGFGGG FGGGFGGDGG LLSGNEKVTM
151 QNLNDRLASY LDKVRALEES NYELEGKIKE WYEKHGNSHQ GEPRDYSKYY
201 KTIDDLKNQI LMLTTDNANI LLQIDNARLA ADDFRLKYEN EVALRQSVEA
251 DINGLRRVLD ELTLTKADLE MQIESLTEEL AYLKKNHEEE MKDLRNVSTG
301 DVNVEMNAAP GVDLTQLLNN MRSQYEQLAE QNRKDAEAWF NEKSKELTTE
351 IDNNIEQISS YKSEITELRR NVQALEIELQ SQLALKQSLE ASLAETEGRY
401 CVQLSQIQAQ ISALEEQLQQ IRAETECQNT EYQQLLDIKI RLENEIQTYR
451 SLLEGEGSSG GGGRGGGSFG GGYGGGSSGG GSSGGGYGGG HGGSSGGGYG
501 GGSSGGGSSG GGYGGGSSSG GHGGSSSGGY GGGSSGGGGG GYGGGSSGGG
551 SSSGGGYGGG SSSGGHKSSS SGSVGESSSK GPRY
```

Spot 2276 Glutathione S-transferase π

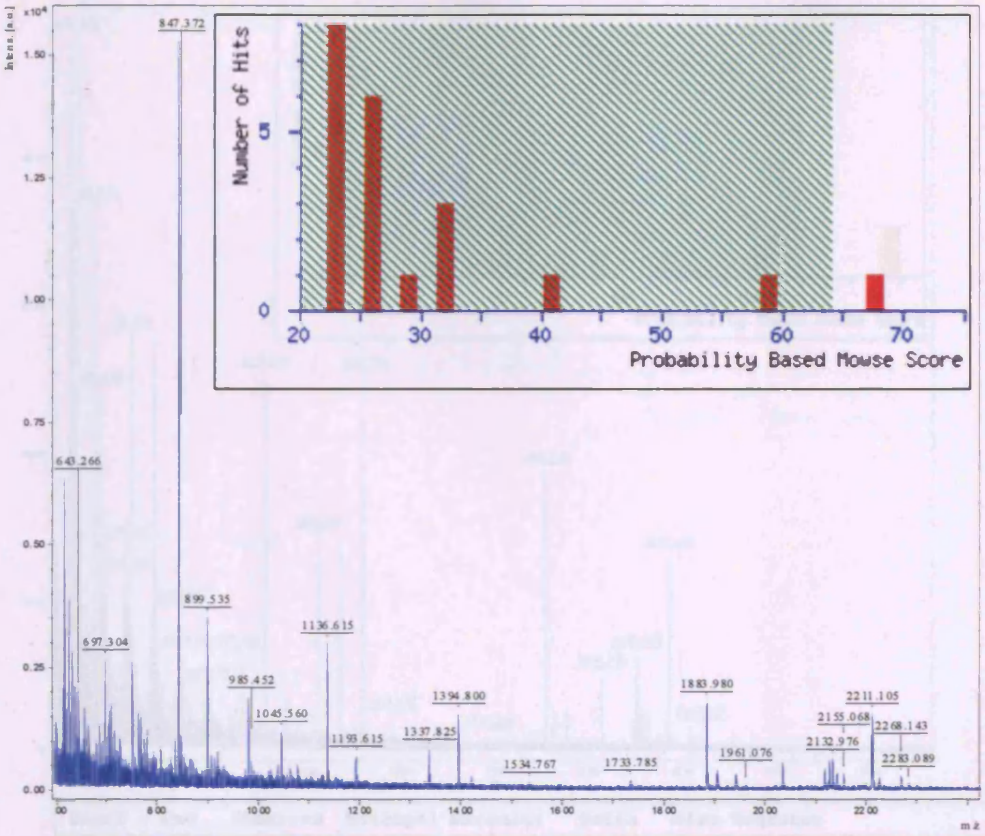

Start - End	Observed	Mr(expt)	Mr(calc)	Delta	Miss	Sequence	
29 - 43	1733.78	1732.78	1732.85	-0.07	0	K.EEVVTVETWQEGSLK.A	
44 - 53	1136.61	1135.61	1135.57	0.04	0	K.ASCLYGQLPK.F	
54 - 69	1883.98	1882.97	1882.94	0.03	0	K.FQDGDLTLYQSNTILR.H	
74 - 80	751.42	750.42	750.43	-0.01	0	R.TLGLYGK.D	
81 - 99	2117.01	2116.00	2115.97	0.03	0	K.DQQEAALVDMVNDGVEDLR.C	
81 - 99	2132.98	2131.97	2131.97	-0.00	0	K.DQQEAALVDMVNDGVEDLR.C	Oxidation (M)
102 - 114	1534.77	1533.76	1533.77	-0.01	0	K.YISLIYTNYEAGK.D	
102 - 119	2155.07	2154.06	2154.05	0.01	1	K.YISLIYTNYEAGKDDYVK.A	
120 - 139	2126.25	2125.25	2125.15	0.09	0	K.ALPGQLKPFETLLSQNQGGK.T	
190 - 207	1903.99	1902.98	1902.98	-0.00	0	K.AFLASPEYVNLPINGNGK.Q	

```
  1 PYTVVYFPVR GRCAALRMLL ADQGQSWKEE VVTVETWQEG SLKASCLYGQ
 51 LPKFQDGDLT LYQSNTILRH LGRTLGLYGK DQQEAALVDM VNDGVEDLRC
101 KYISLIYTNY EAGKDDYVKA LPGQLKPFET LLSQNQGGKT FIVGDQISFA
151 DYNLLDLLLI HEVLAPGCLD AFPLLSAYVG RLSARPKLKA FLASPEYVNL
201 PINGNGKQ
```

Spot 2253 Glutathione S-transferase π

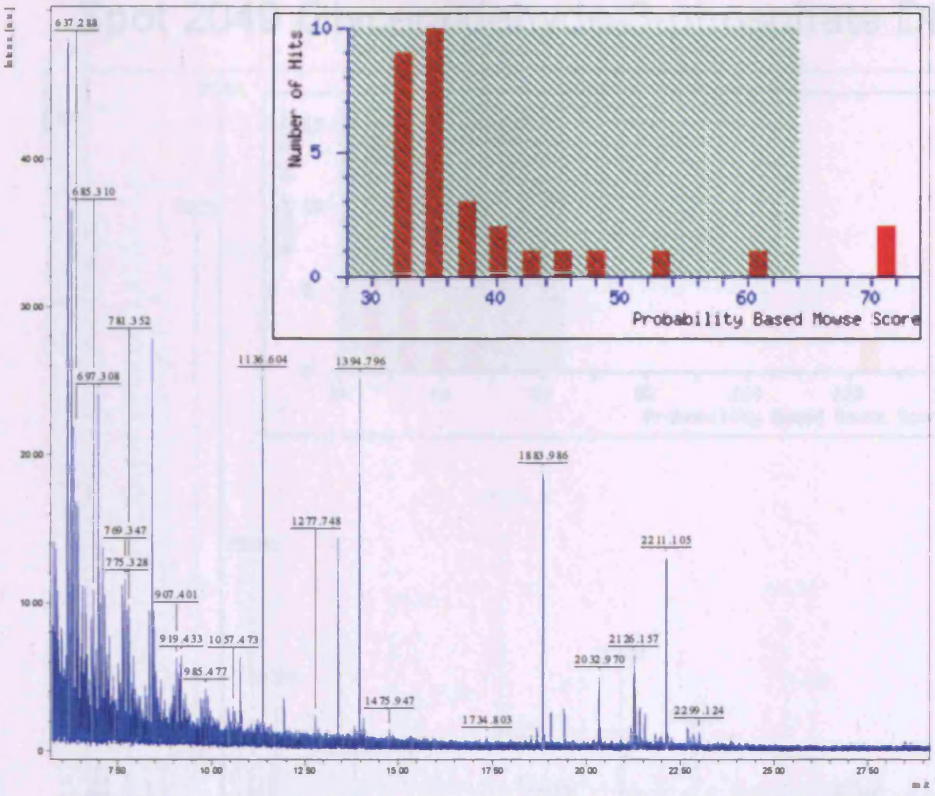

Start - End	Observed	Mr(expt)	Mr(calc)	Delta	Miss	Sequence
1 - 11	1337.78	1336.78	1336.72	0.06	0	-.PPYTVVYFPVR.G
55 - 70	1883.99	1882.98	1882.94	0.04	0	K.FQDGDLTLYQSNTILR.M
75 - 100	2849.21	2848.21	2848.39	-0.18	1	R.TLGLYGKDQQEAALVDMVNDGVEDLR.C
82 - 100	2117.07	2116.06	2115.97	0.09	0	K.DQQEAALVDMVNDGVEDLR.C
101 - 115	1765.78	1764.78	1764.88	-0.10	1	R.CKYISLIYTNYEAGK.D
103 - 120	2155.02	2154.01	2154.05	-0.04	1	K.YISLIYTNYEAGKDDYVK.A
121 - 140	2126.16	2125.15	2125.15	-0.00	0	K.ALPGQLKPFETLLSQNQGGK.T
191 - 208	1904.01	1903.01	1902.98	0.02	0	K.AFLASPEYVNLPINGNGK.Q
191 - 209	2032.12	2031.11	2031.04	0.07	1	K.AFLASPEYVNLPINGNGKQ.-

```
  1 PPYTVVYFPV RGRCAALRML LADQGQSWKE EVVTVETWQE GSLKASCLYG
 51 QLPKFQDGDL TLYQSNTILR HLGRTLGLYG KDQQEAALVD MVNDGVEDLR
101 CKYISLIYTN YEAGKDDYVK ALPGQLKPFE TLLSQNQGGK TFIVGDQISF
151 ADYNLLDLLL IHEVLAPGCL DAFPLLSAYV GRLSARPKLK AFLASPEYVN
201 LPINGNGKQ
```

Spot 2049 Glyceraldehyde-3-phosphate DH

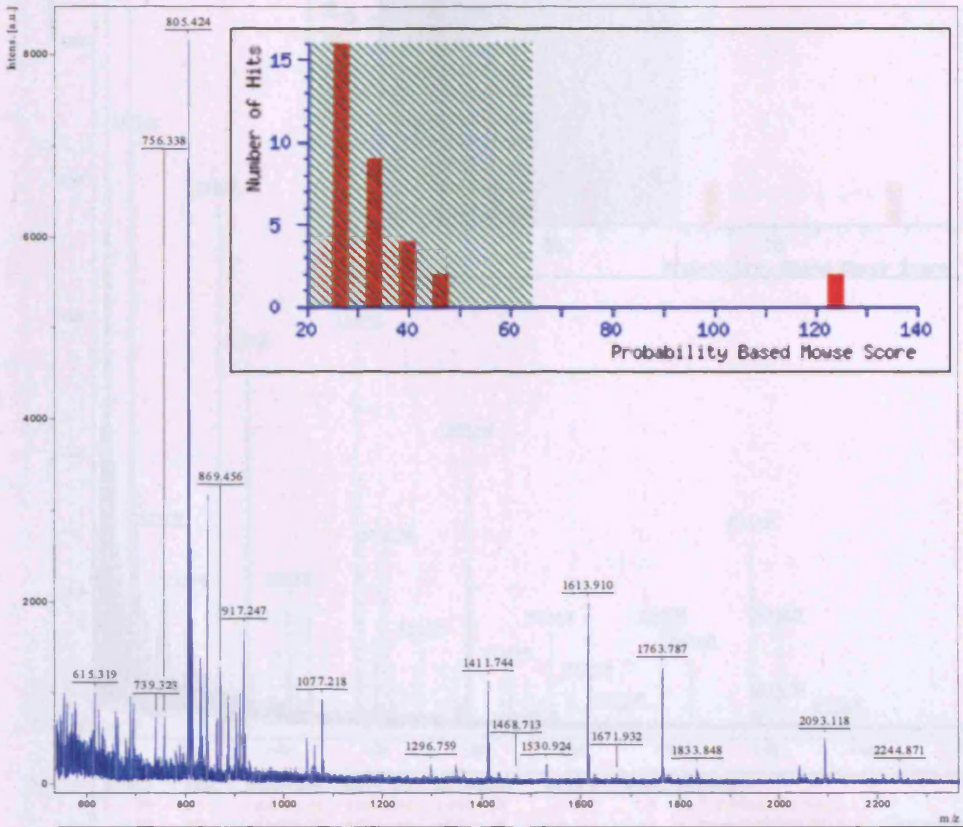

Start - End	Observed	Mr(expt)	Mr(calc)	Delta	Miss	Sequence
6 - 13	805.42	804.42	804.42	-0.01	0	K.VGVNGFGR.I
21 - 27	694.30	693.29	693.34	-0.05	0	R.AAFNSGK.V
56 - 61	688.32	687.31	687.37	-0.06	0	K.FHGTVK.A
67 - 80	1613.91	1612.90	1612.89	0.01	0	K.LVINGNPITIFQER.D
67 - 84	2041.11	2040.10	2040.10	-0.00	1	K.LVINGNPITIFQERDPSK.I
108 - 117	909.44	908.43	908.48	-0.05	0	K.AGAMLQQGAK.R
140 - 145	739.32	738.32	738.35	-0.04	0	K.YDNSLK.I
146 - 162	1833.85	1832.84	1832.91	-0.07	0	K.IISNASCTTNCLAPLAK.V
201 - 215	1411.74	1410.74	1410.78	-0.05	0	R.GALQNIIPASTGAAK.A
220 - 227	869.46	868.45	868.50	-0.05	0	K.VIPELNGK.L
228 - 234	811.38	810.38	810.41	-0.03	0	K.LTGMAFR.V Oxidation (M)
235 - 248	1530.92	1529.92	1529.79	0.13	0	R.VPTANVSVVDLTCR.L
255 - 260	781.35	780.34	780.40	-0.06	1	K.YDDIKK.V
264 - 271	829.40	828.39	828.43	-0.04	0	K.QASEGPLK.G
310 - 323	1763.79	1762.78	1762.80	-0.02	0	K.LISWYDNEFGYSNR.V

```
  1 MGKVKVGVNG FGRIGRLVTR AAFNSGKVDI VAINDPFIDL NYMVYMFQYD
 51 STHGKFHGTV KAENGKLVIN GNPITIFQER DPSKIKWGDA GAEYVVESTG
101 VFTTMEKAGA HLQGGAKRVI ISAPSADAPM FVMGVNHEKY DNSLKIISNA
151 SCTTNCLAPL AKVIHDNFGI VEGLMTTVHA ITATQKTVDG PSGKLWRDGR
201 GALQNIIPAS TGAAKAVGKV IPELNGKLTG MAFRVPTANV SVVDLTCRLE
251 KPAKYDDIKK VVKQASEGPL KGILGYTEHQ VVSSDFNSDT HSSTFDAGAG
301 IALNDHFVKL ISWYDNEFGY SNRVVDLMAH MASKE
```

Spot 1088 HSP-73

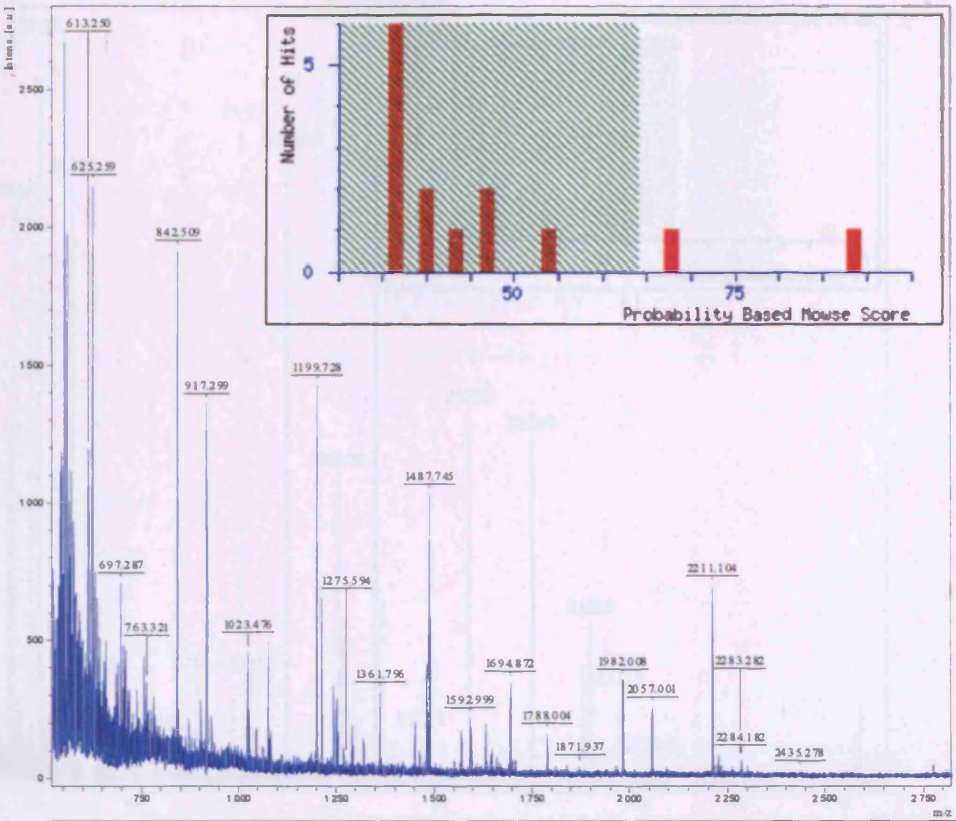

Start - End	Observed	Mr(expt)	Mr(calc)	Delta	Miss	Sequence
37 - 49	1487.74	1486.74	1486.69	0.04	0	R.TTPSYVAFTDTER.L
57 - 71	1665.76	1664.75	1664.78	-0.03	0	K.MQVAMDPTNTVFDAK.R Oxidation (M)
113 - 126	1632.82	1631.82	1631.78	0.04	0	K.SFXPEEVSSMVLTK.M Oxidation (M)
127 - 137	1268.68	1267.67	1267.65	0.02	1	K.MKKIAEAYLGK.Y Oxidation (M)
138 - 155	1902.01	1901.00	1900.99	0.01	0	K.TVTHAVVTVPAYFNDSQR.Q
160 - 171	1199.73	1198.72	1198.67	0.05	0	K.DAGTIAGLNVLR.I
172 - 187	1659.93	1658.92	1658.89	0.04	0	R.IINEPTAAAIAYGLDK.K
172 - 188	1788.00	1787.00	1786.98	0.01	1	R.IINEPTAAAIAYGLDKK.V
221 - 236	1691.74	1690.74	1690.72	0.02	0	K.STAGDTHLGGEDFDNR.M
237 - 246	1251.66	1250.65	1250.61	0.04	0	R.MVNHFIAEFK.R Oxidation (M)
252 - 257	705.35	704.34	704.33	0.01	0	K.DISENK.R
265 - 271	835.39	834.38	834.40	-0.02	1	R.TACERAK.R
308 - 311	1480.79	1479.78	1479.75	0.04	1	R.ARFEELNADLFR.G
302 - 311	1253.67	1252.67	1252.61	0.06	0	R.FEELNADLFR.G
326 - 342	1838.06	1837.05	1837.01	0.04	1	K.LDKSQIHDIVLVGGSTR.I
346 - 357	1450.77	1449.76	1449.80	-0.03	1	K.IQKLLQDFFNGK.E
349 - 357	1081.55	1080.55	1080.56	-0.02	0	K.LLQDFFNGK.E
362 - 384	2260.19	2259.18	2259.14	0.04	0	K.SINPDEAVAYGAAVQAAILSGDK.S
424 - 447	2774.56	2773.55	2773.32	0.23	0	K.QTQTFTTYSDNQPGVLIQVYEGER.A
494 - 500	763.32	762.31	762.39	-0.07	1	K.STGKENK.I
540 - 550	1319.60	1318.59	1318.59	0.00	0	K.NSLESYAFNMK.A Oxidation (M)

```
  1 MSKGPAVGID LGTTYSCVGV FQHGKVEIIA NDQGNRTTPS YVAFTDTERL
 51 IGDAAKNQVA MNPTNTVFDA KRLIGRRFDD AVVQSDMKHW PFMVVNDAGR
101 PKVQVEYKGE TKSFYPEEVS SMVLTKMKEI AEAYLGKTVT NAVVTVPAYF
151 NDSQRQATKD AGTIAGLNVL RIINEPTAAA IAYGLDKKVG AERNVLIFDL
201 GGGTFDVSIL TIEDGIFEVK STAGDTHLGG EDFDNRMVNH FIAEFKRKHK
251 KDISENKRAV RRLRTACERA KRTLSSSTQA SIEIDSLYEG IDFYTSITRA
301 RFEELNADLF RGTLDPVEKA LRDAKLDKSQ IHDIVLVGGS TRIPKIQKLL
351 QDFFNGKELN KSINPDEAVA YGAAVQAAIL SGDKSENVQD LLLLDVTPLS
401 LGIETAGGVM TVLIKRNTTI PTKQTQTFTT YSDNQPGVLI QVYEGERAMT
451 KDNNLLGKFE LTGIPPAPRG VPQIEVTFDI DANGILNVSA VDKSTGKENK
501 ITITNDKGRL SKEDIERMVQ EAEKYKAEDE KQRDKVSSKN SLESYAFNMK
551 ATVEDEKLQG KINDEDKQKI LDKCNEIINW LDKNQTAEKE EFEHQQKELE
601 KVCNPIITKL YQSAGGMPGG MPGGFPGGGA PPSGGASSGP TIEEVD
```

Spot 2482 Peptidyl-prolyl cis-trans isomerase A

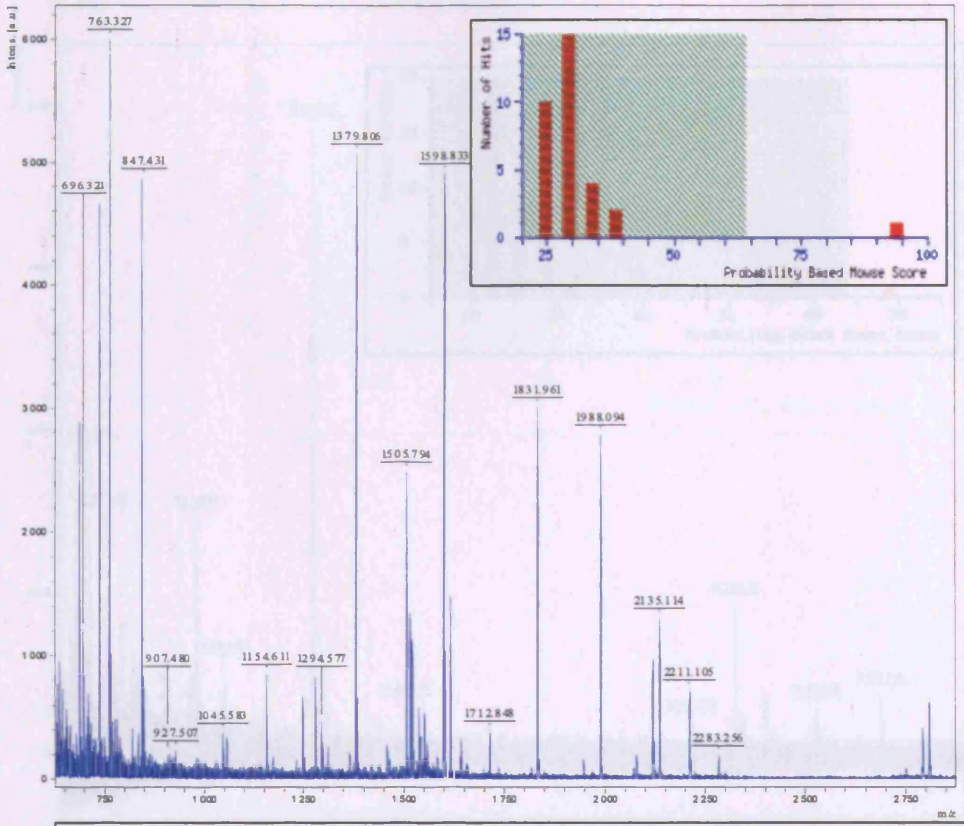

Start - End	Observed	Mr(expt)	Mr(calc)	Delta	Miss	Sequence
1 - 18	1946.06	1945.05	1944.99	0.06	0	-.VNPTVFFDIAVDGEPLGR.V
19 - 38	1379.81	1378.80	1378.75	0.05	1	R.VSFELFADKVPK.T
31 - 36	737.34	736.33	736.35	-0.02	0	K.TAENFR.A
49 - 54	763.33	762.32	762.32	-0.00	0	K.GSCFHR.I
55 - 68	1614.82	1613.81	1613.73	0.08	0	R.IIPGFMCQGGDFTR.H Oxidation (M)
76 - 90	1831.96	1830.95	1830.90	0.05	1	K.SIYGEKFEDENFILK.H
82 - 90	1154.61	1153.60	1153.57	0.04	0	K.FEDENFILK.H
118 - 130	1515.84	1514.83	1514.79	0.04	1	K.TEWLDGKHVVFGK.V
131 - 143	1505.79	1504.79	1504.74	0.05	1	K.VKEGMNIVEAMER.F
131 - 143	1521.76	1520.75	1520.73	0.02	1	K.VKEGMNIVEAMER.F Oxidation (M)
131 - 143	1537.74	1536.73	1536.73	0.00	1	K.VKEGMNIVEAMER.F 2 Oxidation (M)
133 - 143	1278.64	1277.63	1277.57	0.05	0	K.EGMNIVEAMER.F
133 - 143	1294.58	1293.57	1293.57	0.00	0	K.EGMNIVEAMER.F Oxidation (M)
133 - 143	1310.54	1309.54	1309.56	-0.03	0	K.EGMNIVEAMER.F 2 Oxidation (M)
154 - 164	1247.64	1246.63	1246.62	0.01	1	K.KITIADCGQLE.-

```
  1 VNPTVFFDIA VDGEPLGRVS FELFADKVPK TAENFRALST GEKGFGYKGS
 51 CFHRIIPGFM CQGGDFTRHN GTGGKSIYGE KFEDENFILK HTGPGILSMA
101 NAGPNTNGSQ FFICTAKTEW LDGKHVVFGK VKEGMNIVEA MERFGSRNGK
151 TSKKITIADC GQLE
```

Spot 1536 Peroxiredoxin 1

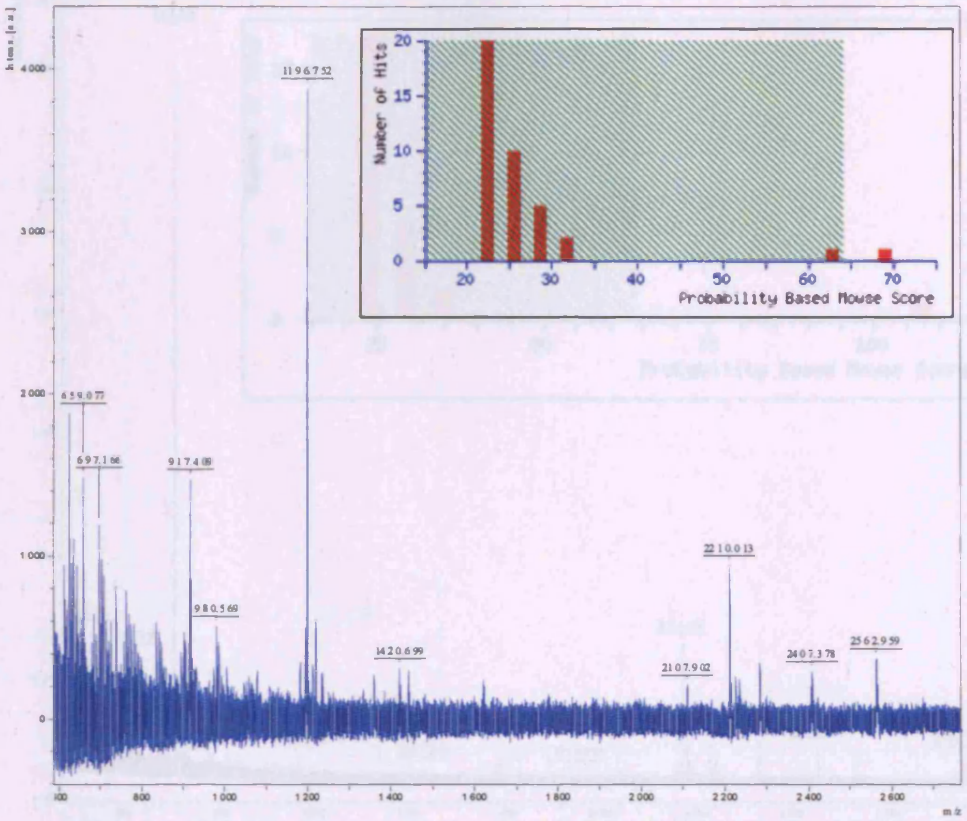

Start - End	Observed	Mr(expt)	Mr(calc)	Delta	Miss	Sequence
8 - 16	980.60	979.59	979.52	0.06	0	K.IGMPAPNFK.A
121 - 128	894.47	893.47	893.42	0.04	0	K.ADEGISFR.G
129 - 136	920.48	919.47	919.50	-0.03	0	R.GLFIIDDK.G
129 - 140	1359.92	1358.92	1358.79	0.13	1	R.GLFIIDDKGILR.Q
152 - 158	819.36	818.35	818.41	-0.06	0	R.SVDETLR.L
152 - 168	1996.99	1995.99	1996.03	-0.04	1	R.SVDETLRLVQAFQFTDK.H
169 - 190	2407.38	2406.38	2406.16	0.21	0	K.HGEVCPAGWKPGSDTIKPDVQK.S

```
  1 MSSGNAKIGH PAPNFKATAV MPDGQFKDIS LSDYKGKYVV FFFYPLDFTF
 51 VCPTEIIAFS DRAEEFKKLN CQVIGASVDS HFCHLAWVNT PKKQGGLGPM
101 NIPLVSDPKR TIAQDYGVLK ADEGISFRGL FIIDDKGILR QITVNDLPVG
151 RSVDETLRLV QAFQFTDKHG EVCPAGWKPG SDTIKPDVQK SKEYFSKQK
```

Spot 1603 Peroxiredoxin 2

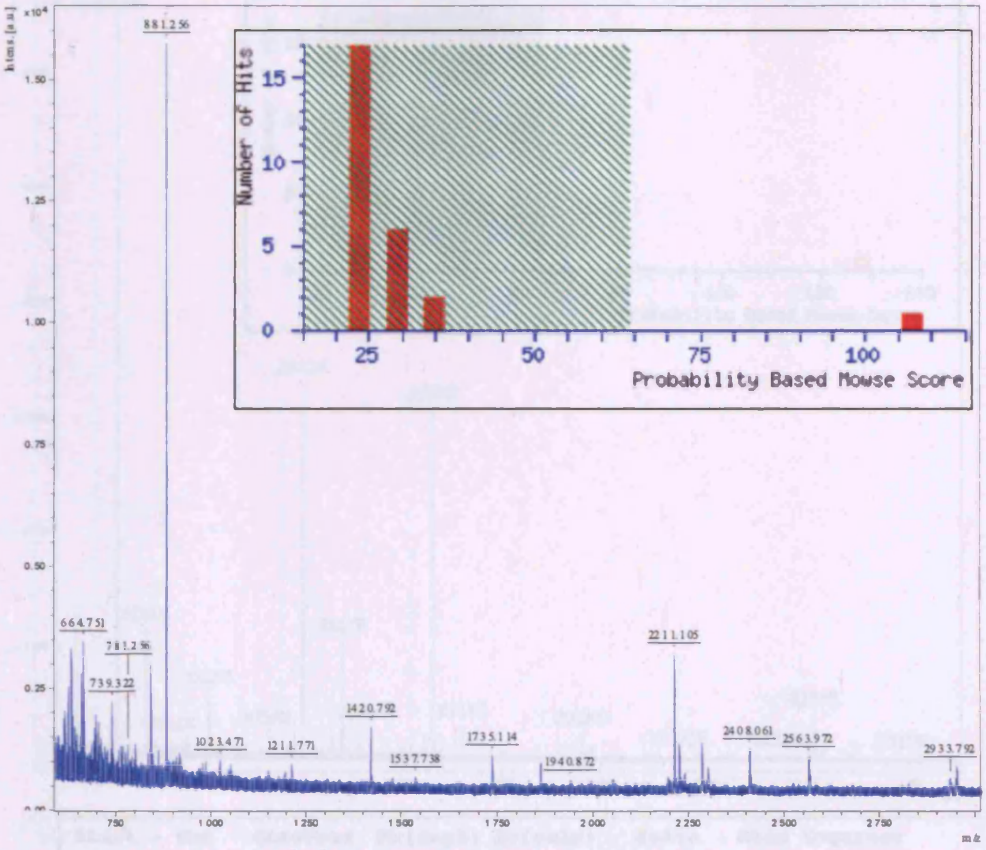

Start - End	Observed	Mr(expt)	Mr(calc)	Delta	Miss	Sequence
1 - 7	706.30	705.29	705.32	-0.03	0	-.MASGNAR.I
8 - 16	972.64	971.63	971.54	0.09	0	R.IGKPAPDFK.A
17 - 26	978.55	977.54	977.52	0.02	0	K.ATAVVDGAFK.E
17 - 29	1334.75	1333.74	1333.72	0.01	1	K.ATAVVDGAFKEVK.L
110 - 119	1179.74	1178.73	1178.63	0.10	1	R.RLSEDYGVLK.T
111 - 119	1023.47	1022.46	1022.53	-0.06	0	R.LSEDYGVLK.T
120 - 127	924.49	923.48	923.43	0.04	0	K.TDEGIAYR.G
128 - 135	862.42	861.41	861.50	-0.08	0	R.GLFIIDGK.G
140 - 150	1211.77	1210.76	1210.67	0.10	0	R.QITVNDLPVGR.S

```
  1 MASGNARIGK PAPDFKATAV VDGAFKEVKL SDYKGKYVVL FFYPLDFTFV
 51 CPTEIIAFSN RAEDFRKLGC EVLGVSVDSQ FNHLAWINTP RKEGGLGPLN
101 IPLLGDVTRR LSEDYGVLKT DEGIAYRGLF IIDGKGVLRQ ITVNDLPVGR
151 SVDEALRLVQ AFQYTDEHGE VCPAGWKPGS DTIKPNVDDS KEYFSKHN
```

Spot 2274 Peroxiredoxin 3

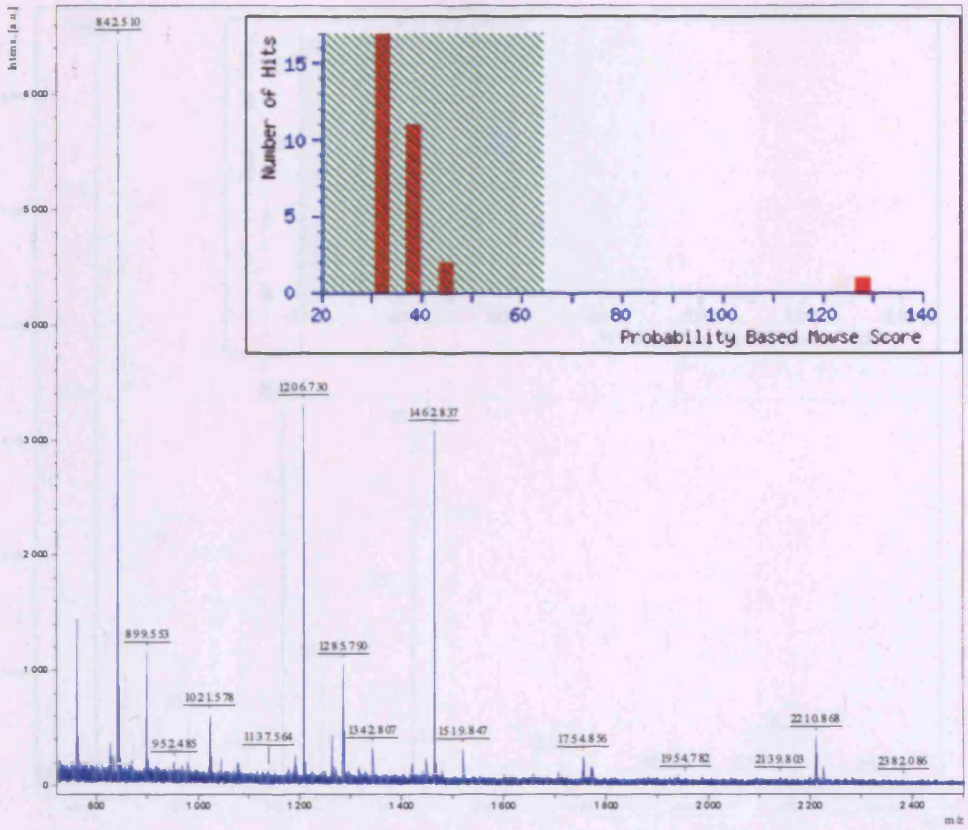

Start - End	Observed	Mr(expt)	Mr(calc)	Delta	Miss	Sequence
1 - 7	706.30	705.29	705.32	-0.03	0	-.MASGNAR.I
8 - 16	972.64	971.63	971.54	0.09	0	R.IGKPAPDFK.A
17 - 26	978.55	977.54	977.52	0.02	0	K.ATAVVDGAFK.E
17 - 29	1334.75	1333.74	1333.72	0.01	1	K.ATAVVDGAFKEVK.L
110 - 119	1179.74	1178.73	1178.63	0.10	1	R.RLSEDYGVLK.T
111 - 119	1023.47	1022.46	1022.53	-0.06	0	R.LSEDYGVLK.T
120 - 127	924.49	923.48	923.43	0.04	0	K.TDEGIAYR.G
128 - 135	862.42	861.41	861.50	-0.08	0	R.GLFIIDGK.G
140 - 150	1211.77	1210.76	1210.67	0.10	0	R.QITVNDLPVGR.S

```
  1 MASGNARIGK PAPDFKATAV VDGAFKEVKL SDYKGKYVVL FFYPLDFTFV
 51 CPTEIIAFSN RAEDFRKLGC EVLGVSVDSQ FNHLAWINTP RKEGGLGPLN
101 IPLLGDVTRR LSEDYGVLKT DEGIAYRGLF IIDGKGVLRQ ITVNDLPVGR
151 SVDEALRLVQ AFQYTDEHGE VCPAGWKPGS DTIKPNVDDS KEYFSKHN
```

Spot 2510 Peroxiredoxin 5

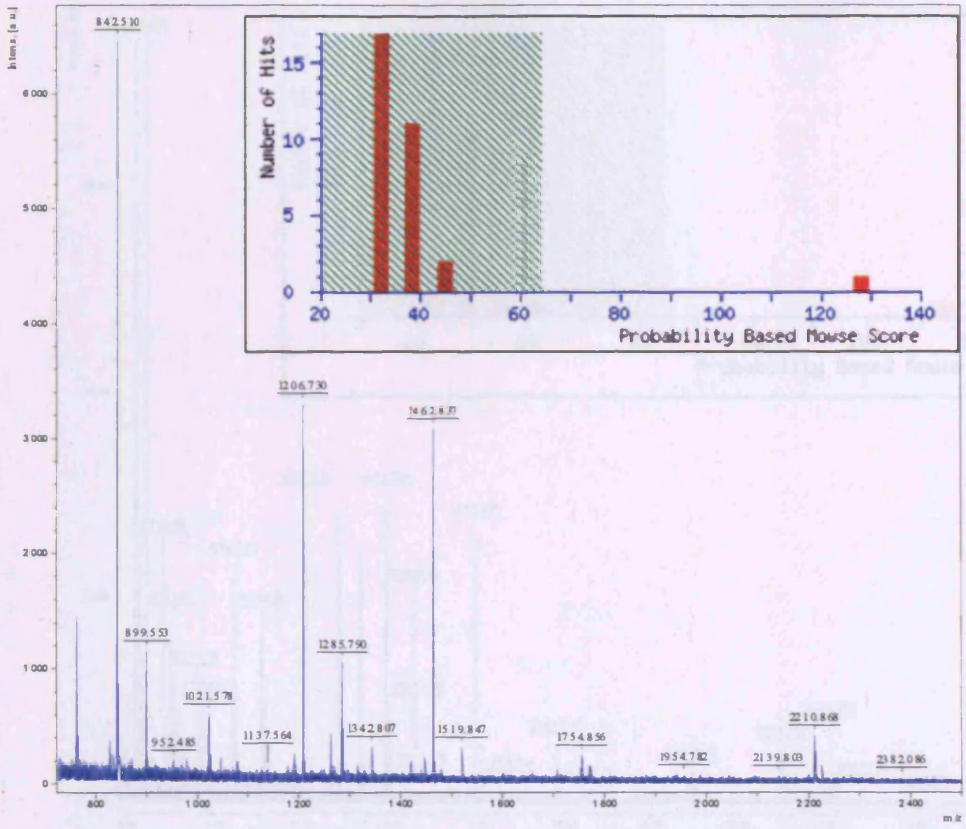

Start - End	Observed	Mr(expt)	Mr(calc)	Delta	Miss	Sequence	
1 - 10	1057.55	1056.54	1056.62	-0.08	1	-.MAAAVGRLLR.A	
74 - 83	1021.58	1020.57	1020.52	0.05	0	K.GTAVVNGEFK.D	
74 - 91	1954.78	1953.77	1953.97	-0.19	1	K.GTAVVNGEFKDLSLDDFK.G	
84 - 91	952.49	951.48	951.45	0.02	0	K.DLSLDDFK.G	
84 - 93	1137.56	1136.56	1136.57	-0.01	1	K.DLSLDDFKGK.Y	
150 - 166	1753.84	1752.83	1752.92	-0.09	0	K.NGGLGHMNIALLSDLTK.Q	
150 - 166	1769.93	1768.92	1768.91	0.01	0	K.NGGLGHMNIALLSDLTK.Q	Oxidation (M)
171 - 184	1462.84	1461.83	1461.78	0.05	0	R.DYGVLLEGSGLALR.G	
185 - 196	1285.79	1284.78	1284.74	0.04	0	R.GLFIIDPNGVIK.M	
197 - 207	1206.73	1205.72	1205.65	0.07	0	K.MLSVNDLPVGR.S	
208 - 214	833.43	832.43	832.43	-0.00	0	R.SVEETLR.L	
249 - 253	714.32	713.31	713.34	-0.02	0	K.EYFQK.V	

```
  1 MAAAVGRLLR ASVARHVSAI PWGISATAAL RPAACGRTSL TNLLCSGSSQ
 51 AKLFSTSSSC HAPAVTQHAP YFKGTAVVNG EFKDLSLDDF KGKYLVLFFY
101 PLDFTFVCPT EIVAFSDKAN EFHDVNCEVV AVSVDSHFSH LAWINTPRKN
151 GGLGHMNIAL LSDLTKQISR DYGVLLEGSG LALRGLFIID PNGVIKHLSV
201 NDLPVGRSVE ETLRLVKAFQ YVETHGEVCP ANWTPDSPTI KPSPAASKEY
251 FQKVNQ
```

Spot 2195 Peroxiredoxin 6

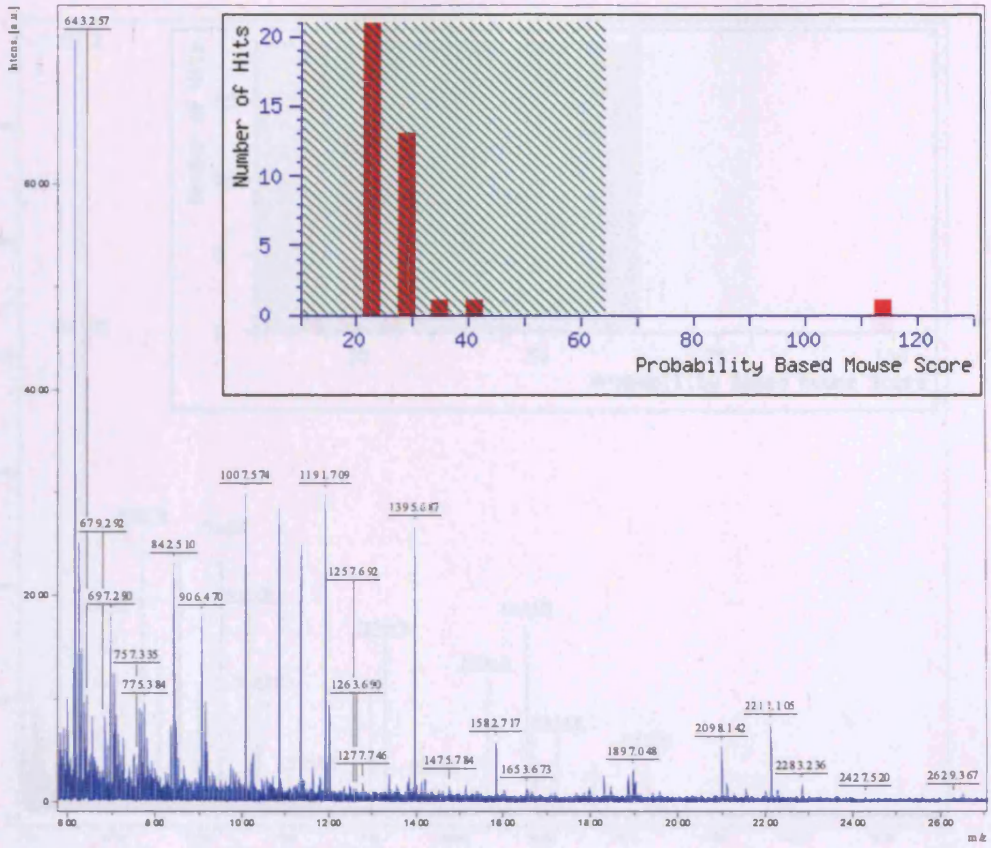

Start - End	Observed	Mr(expt)	Mr(calc)	Delta	Miss	Sequence	
1 - 21	2098.14	2097.14	2097.09	0.05	0	-.PGGLLLGDVAPNFEANTTVGR.I	
41 - 52	1395.69	1394.68	1394.65	0.03	0	R.DFTPVCTTELGR.A	
53 - 62	1045.58	1044.58	1044.60	-0.02	1	R.AAKLAPEFAK.R	
67 - 83	1897.05	1896.04	1896.00	0.04	0	K.LIALSIDSVEDHLAWSK.D	
84 - 96	1582.72	1581.71	1581.66	0.05	0	K.DINAYNCEEPTEK.L	
97 - 105	1005.61	1004.61	1004.59	0.02	0	K.LPFPIIDDR.N	
108 - 121	1512.82	1511.82	1511.83	-0.01	0	R.ELAILLGMLDPAEK.D	
108 - 124	1885.01	1884.00	1883.99	0.01	1	R.ELAILLGMLDPAEKDEK.G	
108 - 124	1900.93	1899.92	1899.99	-0.07	1	R.ELAILLGMLDPAEKDEK.G	Oxidation [M]
132 - 148	1007.57	1006.57	1006.55	0.02	0	R.VVFVFGPDK.K	
132 - 141	1135.68	1134.67	1134.64	0.03	1	R.VVFVFGPDKK.L	
144 - 154	1191.71	1190.70	1190.67	0.04	0	K.LSILYPATTGR.N	
155 - 161	906.47	905.46	905.46	0.00	0	R.NPDEILR.V	
162 - 172	1200.75	1199.75	1199.71	0.03	0	R.VVISLQLTAEK.R	
162 - 173	1356.80	1355.79	1355.81	-0.02	1	R.VVISLQLTAEKR.V	
174 - 181	915.47	914.47	914.49	-0.02	0	R.VATPVDWK.D	
182 - 198	1829.90	1828.89	1828.88	0.01	0	K.DGDSVMVLPTIPEEEAK.K	
182 - 198	1845.84	1844.84	1844.87	-0.04	0	K.DGDSVMVLPTIPEEEAK.K	Oxidation [M]
182 - 199	1957.94	1956.93	1956.97	-0.04	1	K.DGDSVMVLPTIPEEEAKK.L	

```
  1 PGGLLLGDVA PNFEANTTVG RIRFHDFLGD SWGILFSHPR DFTPVCTTEL
 51 GRAAKLAPEF AKRNVKLIAL SIDSVEDHLA WSKDINAYNC EEPTEKLPFP
101 IIDDRNRELA ILLGMLDPAE KDEKGMPVTA RVVFVFGPDK KLKLSILYPA
151 TTGRNFDEIL RVVISLQLTA EKRVATPVDW KDGDSVMVLP TIPEEEAKKL
201 FPKGVFTKEL PSGKKYLRYT PQP
```

Spot 2228 Peroxiredoxin 6

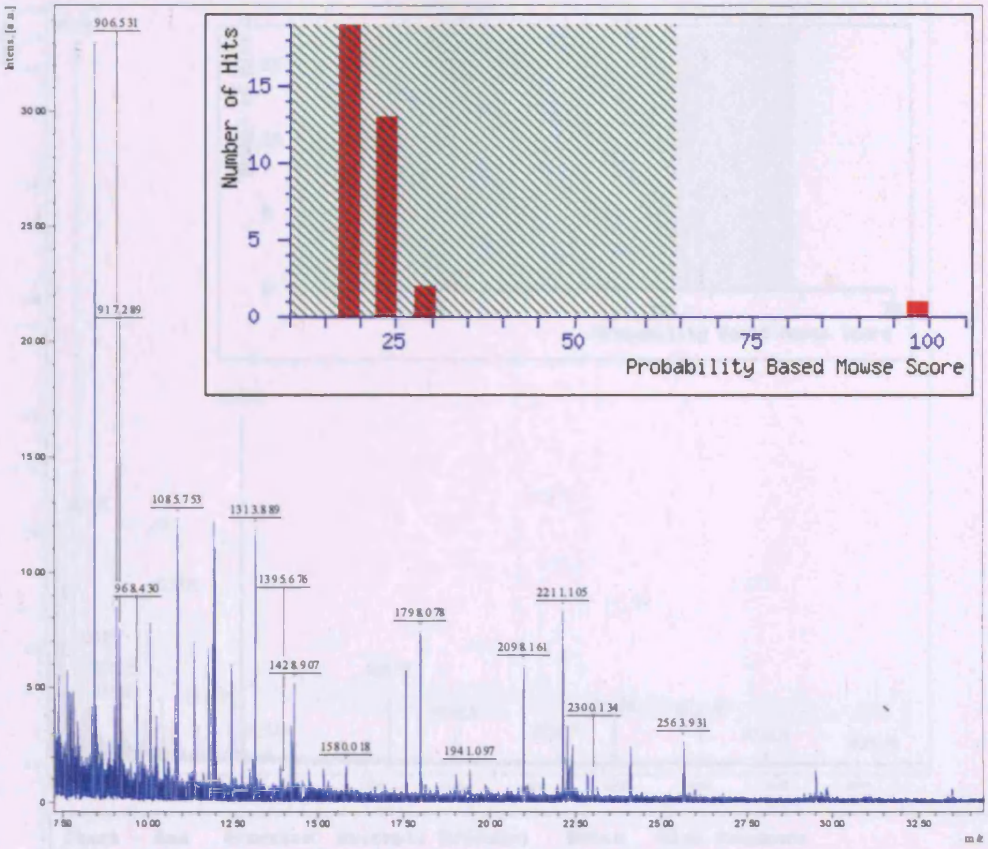

Start - End	Observed	Mr(expt)	Mr(calc)	Delta	Miss	Sequence
1 - 21	2098.16	2097.15	2097.89	0.87	0	-.PGGLLLGDVAPNFEANTTVGR.I
22 - 40	2300.13	2299.13	2299.16	-0.84	1	R.IRPHDFLGDSWGILFSHPR.D
41 - 52	1395.68	1394.67	1394.65	0.82	0	R.DFTPVCTTELGR.A
41 - 55	1665.88	1664.88	1664.82	0.86	1	R.DFTPVCTTELGRAAK.L
67 - 83	1897.04	1896.03	1896.00	0.03	0	K.LIALSIDSVEDHLAWSK.D
106 - 121	1799.01	1798.00	1797.97	0.04	1	R.NRELAILLGMLDPAEK.D Oxidation (M)
108 - 121	1528.87	1527.86	1527.82	0.84	0	R.ELAILLGMLDPAEK.D Oxidation (M)
132 - 140	1007.61	1006.60	1006.55	0.85	0	R.VVFVFGPDK.K
162 - 172	1200.71	1199.70	1199.71	-0.81	0	R.VVISLQLTAEK.R
182 - 198	1845.87	1844.86	1844.87	-0.81	0	K.DGDSVMVLPTIPEEEAK.K Oxidation (M)

```
  1 PGGLLLGDVA PNFEANTTVG RIRFHDFLGD SWGILFSHPR DFTPVCTTEL
 51 GRAAKLAPEF AKRNVKLIAL SIDSVEDHLA WSKDINAYNC EEPTEKLPFP
101 IIDDRNRELA ILLGMLDPAE KDEKGMPVTA RVVFVFGPDK KLKLSILYPA
151 TTGRNFDEIL RVVISLQLTA EKRVATPVDW KDGDSVMVLP TIPEEEAKKL
201 FPKGVFTKEL PSGKKYLRYT PQP
```

Spot 2157 Prohibitin

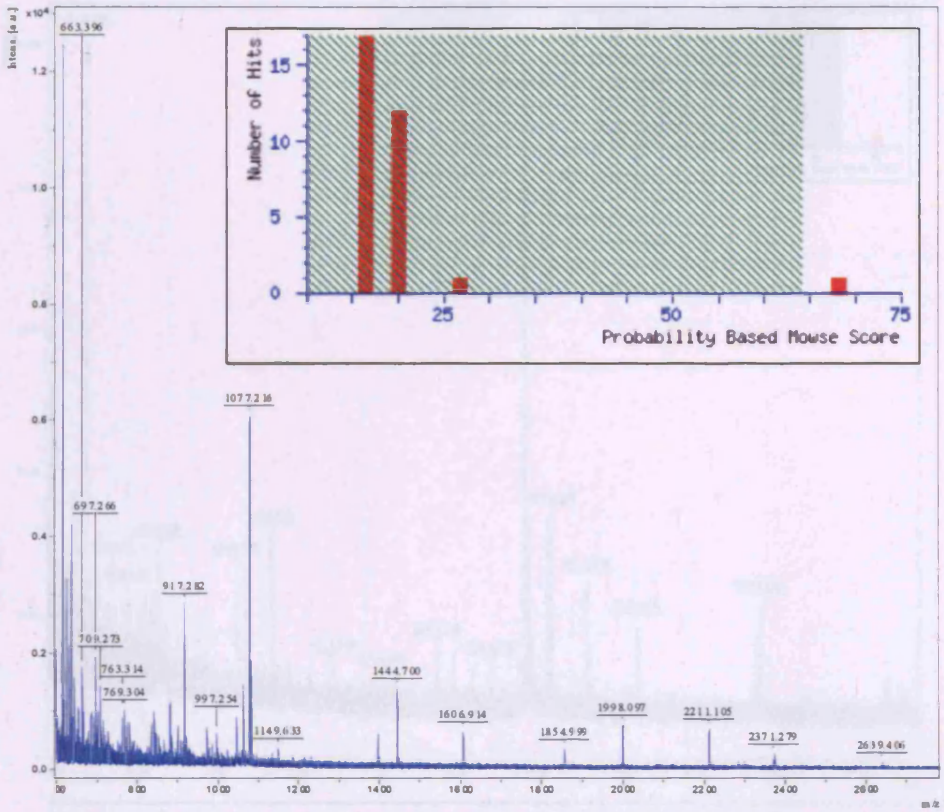

Start - End	Observed	Mr(expt)	Mr(calc)	Delta	Miss	Sequence
12 - 35	2371.28	2370.27	2370.24	0.03	0	K.FGLALAVAGGVVNSALYNVDAGHR.A
94 - 105	1396.89	1395.89	1395.84	0.05	0	R.ILFRPVASQLPR.I
106 - 117	1444.70	1443.69	1443.65	0.04	0	R.IFTSIGEDYDER.V
106 - 128	2639.41	2638.40	2638.37	0.02	1	R.IFTSIGEDYDERVLPSITTEILK.S
134 - 143	1149.63	1148.63	1148.58	0.04	0	R.FDAGELITQR.E
220 - 239	1998.10	1997.09	1997.08	0.01	0	K.AAELIANSLATAGDGLIELR.K
240 - 253	1606.91	1605.91	1605.84	0.07	1	R.KLEAAEDIAYQLSR.S
256 - 272	1855.00	1853.99	1854.03	-0.03	0	R.NITYLPAGQSVLLQLPQ.-

```
  1 MAAKVFESIG KFGLALAVAG GVVNSALYNV DAGHRAVIFD RFRGVQDIVV
 51 GEGTHFLIPW VQKPIIFDCR SRPRNVPVIT GSKDLQNVNI TLRILFRPVA
101 SQLPRIFTSI GEDYDERVLP SITTEILKSV VARFDAGELI TQRELVSRQV
151 SDDLTERAAT FGLILDDVSL THLTFGKEFT EAVEAKQVAQ QEAERARFVV
201 EKAEQQKKAA IISAEGDSKA AELIANSLAT AGDGLIELRK LEAAEDIAYQ
251 LSRSRNITYL PAGQSVLLQL PQ
```

Spot 1563 Proteasome β2 subunit

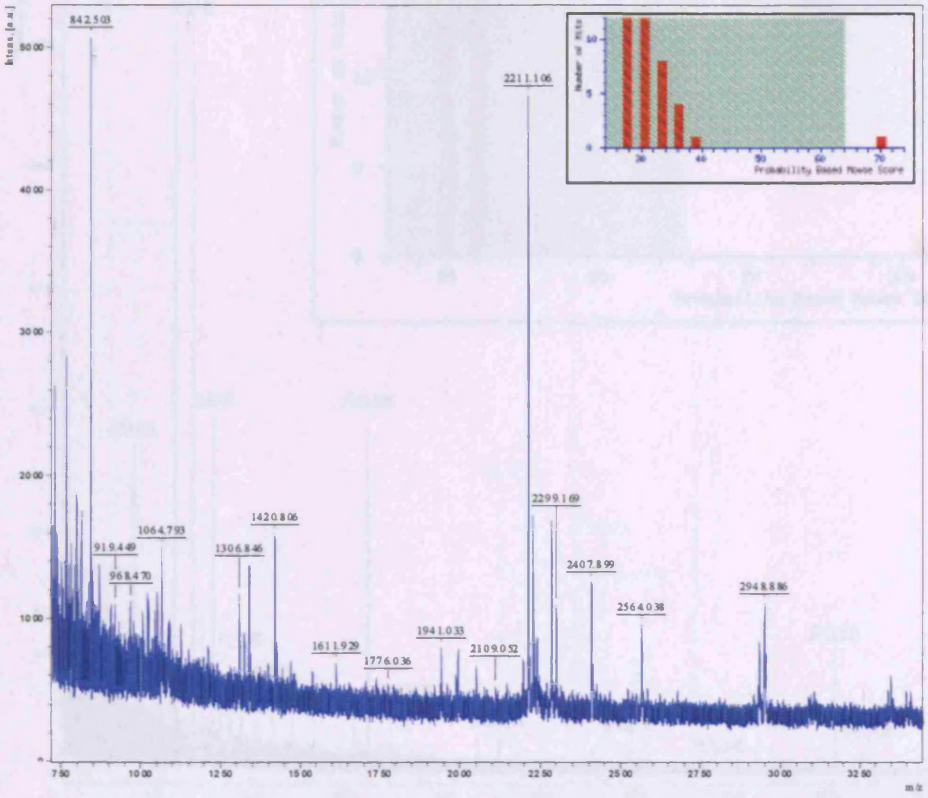

Start - End	Observed	Mr(expt)	Mr(calc)	Delta	Miss	Sequence	
1 - 19	2155.07	2154.06	2154.07	-0.01	0	-.MEYLIGIQGPDYVLVASDR.V	Oxidation (M)
69 - 85	1898.81	1897.81	1897.91	-0.10	1	K.MRNGYELSPTAAANFTR.R	
71 - 85	1611.93	1610.92	1610.77	0.15	0	R.NGYELSPTAAANFTR.R	
146 - 153	1000.58	999.57	999.50	0.07	0	R.YYTPTISR.E	
154 - 161	985.50	984.49	984.57	-0.08	1	R.ERAVELLR.K	
163 - 169	919.45	918.44	918.45	-0.01	0	K.CLEELQK.R	
171 - 181	1306.85	1305.84	1305.74	0.09	0	R.FILNLPTFSVR.I	
171 - 185	1776.04	1775.03	1775.03	-0.01	1	R.FILNLPTFSVRIIDK.N	

```
  1 MEYLIGIQGP DYVLVASDRV AASNIVQMKD DHDKMFKMSE KILLLCVGEA
 51 GDTVQFAEYI QKNVQLYKMR NGYELSPTAA ANFTRRNLAD CLRSRTPYHV
101 NLLLAGYDEH EGPALYYMDY LAALAKAPFA AHGYGAFLTL SILDRYYTPT
151 ISRERAVELL RKCLEELQKR FILNLPTFSV RIIDKNGIHD LDNISFPKQG
201 S
```

Spot 2271 RAN small GTPase

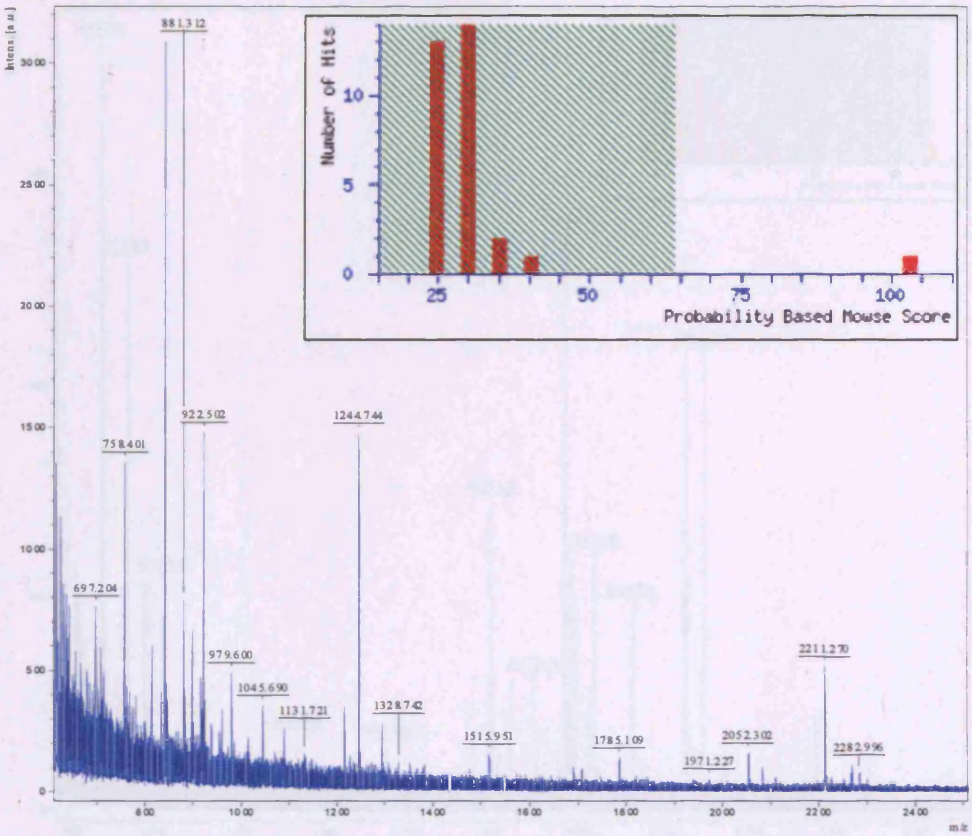

Start - End	Observed	Mr(expt)	Mr(calc)	Delta	Miss	Sequence	
13 - 23	1015.58	1014.57	1014.57	0.00	0	K.LVLVGDGGTGK.T	
38 - 37	960.51	959.50	959.47	0.03	0	R.MLIGEFEK.K	
38 - 38	1088.61	1087.60	1087.57	0.03	1	R.MLIGEFEKK.Y	
39 - 56	2052.30	2051.29	2051.10	0.20	0	K.YVATLGVEVHPLVFHTNR.G	
57 - 71	1689.98	1688.98	1688.85	0.13	1	R.GPIKFNVWDTAGQEK.F	
77 - 95	2267.10	2266.09	2266.04	0.05	0	R.DGYYIQAQCAIIMFDVTSR.V	Oxidation (M)
100 - 106	922.50	921.49	921.46	0.04	0	K.NVPNWHR.D	
111 - 127	1971.23	1970.22	1970.03	0.19	1	R.VCENIPIVLCGNKVDIK.D	
135 - 140	758.40	757.39	757.42	-0.03	0	K.SIVFHR.K	
143 - 152	1214.70	1213.69	1213.60	0.09	0	K.NLQYYDISAK.S	

```
  1 MAAQGEPQVQ FKLVLVGDGG TGKTTFVKRH LTGEFEKKYV ATLGVEVHPL
 51 VFHTNRGPIK FNVWDTAGQE KFGGLRDGYY IQAQCAIIMF DVTSRVTYKN
101 VPNWHRDLVR VCENIPIVLC GNKVDIKDRK VKAKSIVFHR KKNLQYYDIS
151 AKSNYNFEKP FLWLARKLIG DPNLEFVAMP ALAPPEVVMD PALAAQYEHD
201 LEVAQTTALP DEDDDL
```

Spot 2141 Signal recognition particle receptor β

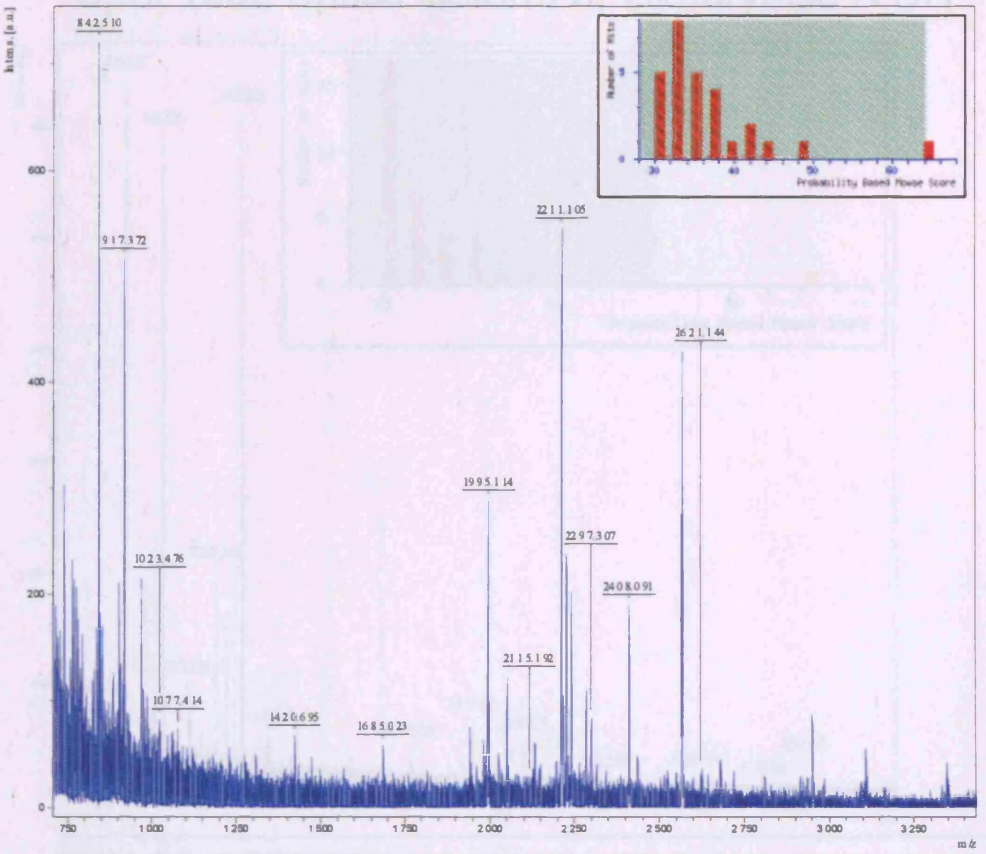

Start - End	Observed	Mr(expt)	Mr(calc)	Delta	Miss	Sequence
8 - 27	2851.22	2850.21	2850.02	0.19	1	R.RVADGGGAGGTFQPYLDTLR.Q
8 - 27	2851.16	2850.15	2850.02	0.13	1	R.RVADGGGAGGTFQPYLDTLR.Q
84 - 90	835.49	834.48	834.50	-0.02	0	R.LLTGLYR.D
151 - 170	2297.31	2296.30	2296.20	0.10	1	R.EVKDVAEFLYQVLIDSMGLK.N
151 - 170	2313.16	2312.15	2312.20	-0.05	1	R.EVKDVAEFLYQVLIDSMGLK.N Oxidation (M)
154 - 170	1940.95	1939.95	1940.00	-0.05	0	K.DVAEFLYQVLIDSMGLK.N
182 - 188	776.34	775.33	775.39	-0.06	0	K.QDIAMAK.S
192 - 199	999.60	998.59	998.58	0.02	0	K.LIQQQLEK.E
200 - 205	745.42	744.41	744.41	0.00	0	K.ELNTLR.V
206 - 227	2145.25	2144.24	2144.11	0.13	1	R.VTRSAAPSTLDSSSTAPAQLGK.K
206 - 227	2144.96	2143.96	2144.11	-0.15	1	R.VTRSAAPSTLDSSSTAPAQLGK.K

```
  1 MASADSRRVA DGGGAGGTFQ PYLDTLRQEL QQTDPTLLSV VVAVLAVLLT
 51 LVFWKLIRSR RSSQRAVLLV GLCDSGKTLL FVRLLTGLYR DTQTSITDSC
101 AVYRVNNNRG NSLTLIDLPG HESLRLQFLE RFKSSARAIV FVVDSAAFQR
151 EVKDVAEFLY QVLIDSMGLK NTPSFLIACN KQDIAMAKSA KLIQQQLEKE
201 LNTLRVTRSA APSTLDSSST APAQLGKKGK EFEFSQLPLK VEFLECSAKG
251 GRGDVGSADI QDLEKWLAKI A
```

Spot 1302 Splice isoform of Glutaryl-Co A DH

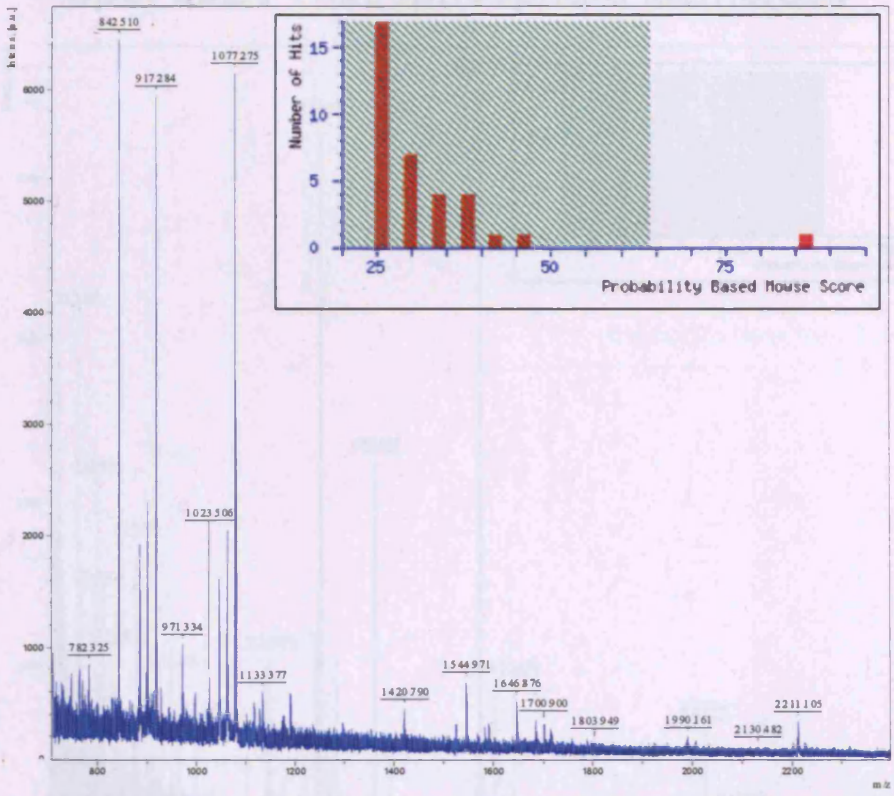

Start - End	Observed	Mr(expt)	Mr(calc)	Delta	Miss	Sequence
1 - 9	988.56	987.55	987.56	-0.01	1	-.MALRGVSVR.L
5 - 13	986.65	985.65	985.60	0.04	1	R.GVSVRLLSR.G
79 - 88	1196.76	1195.75	1195.72	0.03	1	R.LMPRILLANR.N
79 - 88	1212.72	1211.71	1211.72	-0.01	1	R.LMPRILLANR.N Oxidation (M)
95 - 111	1802.04	1801.03	1800.95	0.08	0	R.EIISEMGELGVLGPTIK.G Oxidation (M)
112 - 128	1700.90	1699.89	1699.84	0.06	0	K.GYGCAGVSSVAYGLLAR.E
112 - 132	2227.97	2226.96	2227.11	-0.14	1	K.GYGCAGVSSVAYGLLARELER.V
203 - 210	883.39	882.38	882.44	-0.06	0	K.SYTLNGTK.T
211 - 227	2007.09	2006.08	2006.01	0.07	0	K.TWITNSPMADLFVVWAR.C
211 - 227	2023.06	2022.05	2022.00	0.05	0	K.TWITNSPMADLFVVWAR.C Oxidation (M)
228 - 234	909.28	908.27	908.35	-0.08	0	R.CEDGCIR.G
235 - 243	1050.53	1049.53	1049.57	-0.04	1	R.GFLLEKGMR.G
235 - 243	1066.61	1065.60	1065.56	0.04	1	R.GFLLEKGMR.G Oxidation (M)
241 - 249	944.47	943.46	943.50	-0.04	1	K.GMRGLSAPR.I
295 - 313	2108.18	2107.17	2107.03	0.14	0	R.YGIAWGVLGASEFCLHTAR.Q
329 - 335	871.56	870.55	870.53	0.02	1	R.NQLIQKK.L
336 - 355	2225.23	2224.23	2224.17	0.06	0	K.LADMLTEITLGLHACLQLGR.L

```
  1 MALRGVSVRL LSRGPGLHVL RTWVSSAAQT EKAGRTQSQL AKSSRPEFDW
 51 QDPLVLEEQL TTDEILIRDT FRTYCQERLM PRILLANRNE VFHREIISEM
101 GELGVLGPTI KGYGCAGVSS VAYGLLAREL ERVDSGYRSA MSVQSSLVMH
151 PIYAYGSEEQ RQKYLPQLAK GELLGCFGLT EPNSGSDPSS METRAHYNSS
201 NKSYTLNGTK TWITNSPMAD LFVVWARCED GCIRGFLLEK GMRGLSAPRI
251 QGKFSLRASA TGMIIMDGVE VPEENVLPGA SSLGGPFGCL NNARYGIAWG
301 VLGASEFCLH TARQYALDRM QFGVPLARNQ LIQKKLADML TEITLGLHAC
351 LQLGRLKDQD KAAPEMVSLL KRNNCGKALD IARQARDMLG GNGISDEYHV
401 IRHAMNLEAV NTYEGTHDIH ALILGRAITG IQAFTASK
```

Spot 2224 Triosephosphate isomerase

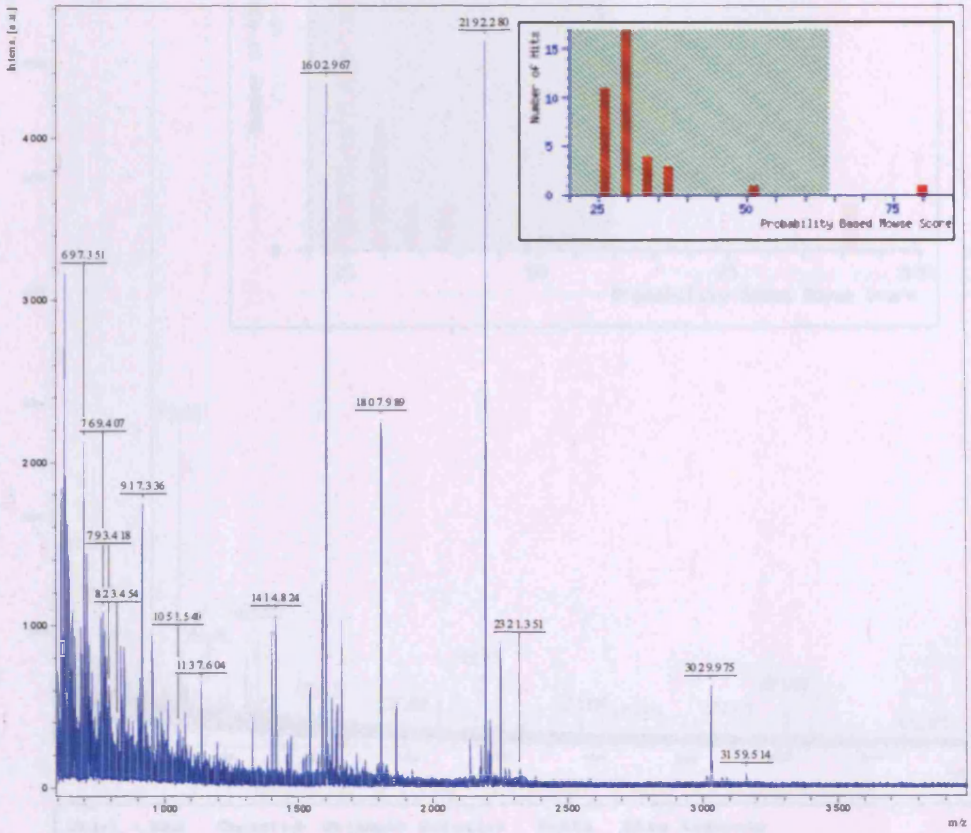

Start - End	Observed	Mr(expt)	Mr(calc)	Delta	Miss	Sequence	
6 - 13	954.52	953.51	953.48	0.04	0	K.FFVGGNWK.M	
18 - 32	1542.89	1541.88	1541.88	0.01	1	R.KQSLGELIGTLNAAK.V	
19 - 32	1414.82	1413.82	1413.78	0.03	0	K.QSLGELIGTLNAAK.V	
59 - 68	1137.60	1136.60	1136.56	0.03	0	K.IAVAAQNCYK.V	
69 - 84	1621.85	1620.84	1620.82	0.02	0	K.VTNGAFTGEISPGMIK.D	
69 - 84	1637.79	1636.79	1636.81	-0.03	0	K.VTNGAFTGEISPGMIK.D	Oxidation (M)
85 - 98	1586.79	1585.78	1585.73	0.05	0	K.DCGATWVVLGHSER.R	
99 - 112	1614.83	1613.82	1613.82	0.01	1	R.RHVFGESDELIGQK.V	
100 - 112	1458.77	1457.76	1457.71	0.05	0	R.HVFGESDELIGQK.V	
113 - 130	1807.99	1806.98	1806.97	0.02	0	K.VAHALAEGLGVIACIGEK.L	
142 - 148	850.50	849.49	849.46	0.03	0	K.VVFEQTK.V	
160 - 174	1602.97	1601.96	1601.88	0.08	0	K.VVLAYEPVWAIGTGK.T	

```
  1 APSRKFFVGG NWKMNGRKQS LGELIGTLNA AKVPADTEVV CAPPTAYIDF
 51 ARQKLDPKIA VAAQNCYKVT NGAFTGEISP GMIKDCGATW VVLGHSERRH
101 VFGESDELIG QKVAHALAEG LGVIACIGEK LDEREAGITE KVVFEQTKVI
151 ADNVKDWSKV VLAYEPVWAI GTGKTATPQQ AQEVHEKLRG WLKSNVSDAV
201 AQSTRIIYGG SVTGATCKEL ASQPDVDGFL VGGASLKPEF VDIINAKQ
```

Spot 2095 14-3-3 protein σ

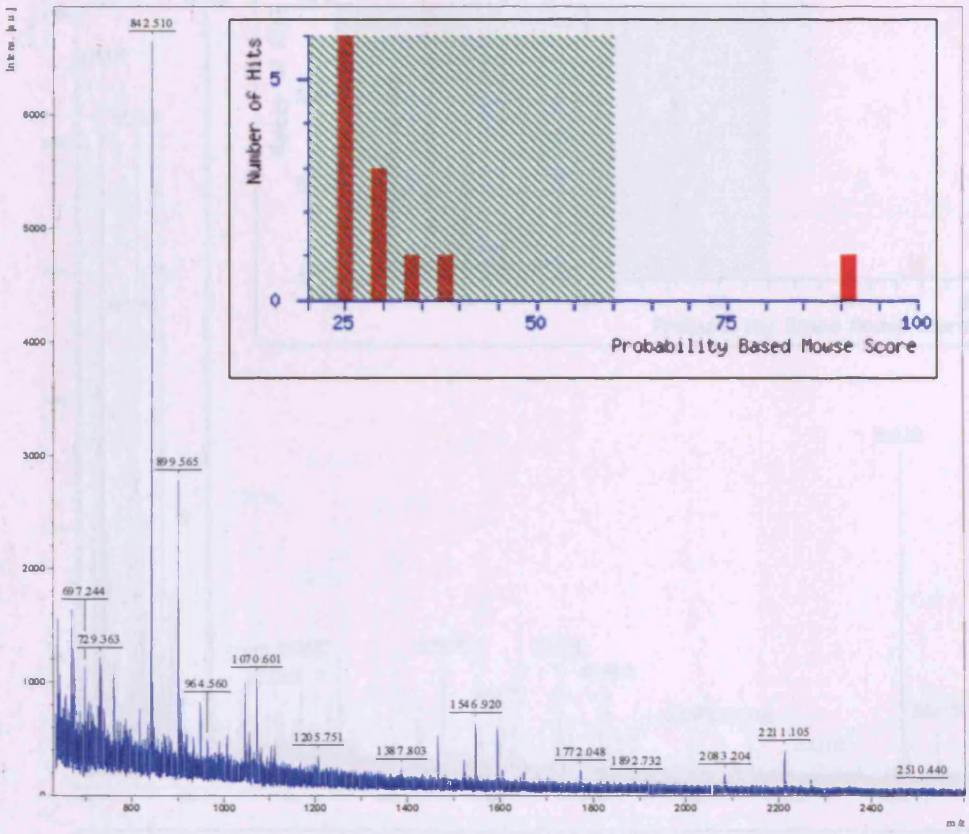

Start - End	Observed	Mr(expt)	Mr(calc)	Delta	Miss	Sequence
12 - 18	816.45	815.45	815.41	0.03	0	K.LAEQAER.Y
19 - 32	1605.87	1604.86	1604.72	0.14	1	R.YEDMAAFMKGAVEK.G Oxidation (M)
42 - 49	907.53	906.52	906.52	0.01	0	R.NLLSVAYK.M
50 - 56	729.36	728.36	728.39	-0.04	0	K.NVVGGQR.A
50 - 60	1213.70	1212.69	1212.65	0.04	1	K.NVVGGQRAAWR.V
57 - 68	1387.80	1386.80	1386.76	0.03	1	R.AAWRVLSSIEQK.S
61 - 68	903.56	902.55	902.51	0.04	0	R.VLSSIEQK.S
61 - 77	1892.73	1891.72	1891.90	-0.18	1	R.VLSSIEQKSNEEGSEEK.G
78 - 85	1005.49	1004.48	1004.50	-0.03	1	K.GPEVREYR.E
110 - 117	834.38	833.37	833.35	0.02	0	K.EAGDAESR.V
123 - 129	948.45	947.45	947.42	0.03	1	K.MKGDYYR.Y Oxidation (M)
149 - 160	1386.78	1385.77	1385.65	0.13	1	R.SAYQEAMDISKK.E Oxidation (M)
161 - 169	1054.59	1053.59	1053.53	0.06	0	K.EMPPTNPIR.L
161 - 169	1070.60	1069.59	1069.52	0.07	0	K.EMPPTNPIR.L Oxidation (M)
215 - 224	1205.75	1204.74	1204.65	0.10	0	K.DSTLIMQLLR.D Oxidation (M)

```
  1 MERASLIQKA KLAEQAERYE DMAAFMKGAV EKGEELSCEE RNLLSVAYKN
 51 VVGGQRAAWR VLSSIEQKSN EEGSEEKGPE VREYREKVET ELQGVCDTVL
101 GLLDSHLIKE AGDAESRVFY LKMKGDYYRY LAEVATGDDK KRIIDSARSA
151 YQEAMDISKK EMPPTNPIRL GLALNFSVFH YEIANSPEEA ISLAKTTFDE
201 AMADLHTLSE DSYKDSTLIM QLLRDNLTLW TADNAGEEGG EAPQEPQS
```

Spot 1207 Aldehyde dehydrogenase 6

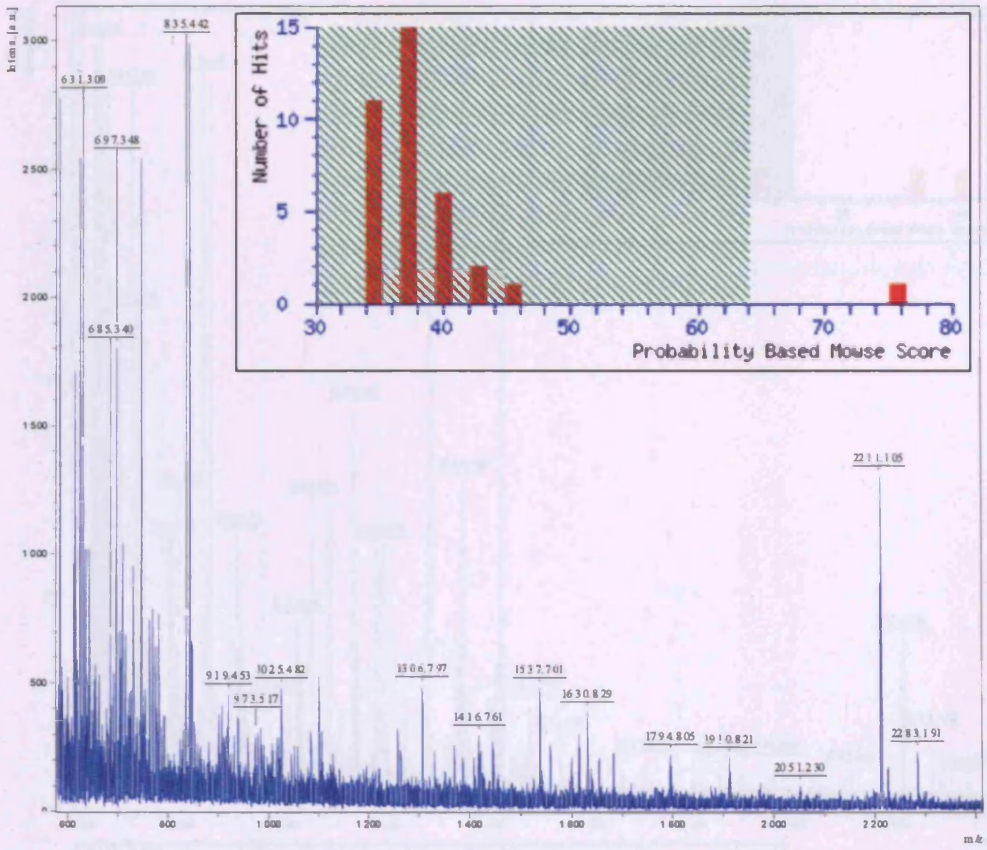

Start - End	Observed	Mr(expt)	Mr(calc)	Delta	Miss	Sequence
34 - 44	1416.76	1415.75	1415.68	0.07	0	K.IFINNEWHESK.S
99 - 109	1306.80	1305.79	1305.74	0.05	0	R.LLHQLADLVER.D
143 - 150	957.49	956.48	956.44	0.04	0	R.YFAGWADK.I
155 - 167	1537.70	1536.69	1536.72	-0.03	0	K.TIPTDDNVVCFTR.H
320 - 332	1630.83	1629.82	1629.80	0.02	0	R.VFVEEQVYSEFVR.R
340 - 350	1257.68	1256.67	1256.69	-0.02	1	K.KRPVGDPFDVK.T
341 - 350	1129.64	1128.63	1128.59	0.04	0	K.RPVGDPFDVK.T
407 - 421	1681.96	1680.96	1680.98	-0.03	1	R.IAKEEIFGPVQPILK.F
410 - 421	1369.88	1368.88	1368.77	0.11	0	K.EEIFGPVQPILK.F
424 - 431	973.52	972.51	972.56	-0.05	1	K.SIEEVIKR.A
432 - 446	1558.79	1557.79	1557.77	0.02	0	R.ANSTDYGLTAAVFTK.N
482 - 487	637.32	636.31	636.26	0.05	0	K.MSGNGR.E Oxidation (N)
488 - 501	1614.78	1613.77	1613.78	-0.01	0	R.ELGEYALAEYTEVK.T
507 - 512	643.31	642.31	642.33	-0.03	1	K.LGDKNP.-

```
  1 MATANGAVEN GQPDGKPPAL PRPIRNLEVK FTKIFINNEW HESKSGKKFA
 51 TCNPSTREQI CEVEEGDKPD VDKAVEAAQV AFQRGSPWRR LDALSRGRLL
101 HQLADLVERD RATLAALETM DTGKPFLHAF FIDLEGCIRT LRYFAGWADK
151 IQGKTIPTDD NVVCFTRHEP IGVCGAITPW NFPLLMLVWK LAPALCCGNT
201 MVLKPAEQTP LTALYLGSLI KEAGFPPGVV NIVPGFGPTV GAAISSHPQI
251 NKIAFTGSTE VGKLVKEAAS RSNLKRVTLE LGGKNPCIVC ADADLDLAVE
301 CAHQGVFFNQ GQCCTAASRV FVEEQVYSEF VRRSVEYAKK RPVGDPFDVK
351 TEQGPQIDQK QFDKILELIE SGKKEGAKLE CGGSAMEDKG LFIKPTVFSE
401 VTDNMRIAKE EIFGPVQPIL KFKSIEEVIK RANSTDYGLT AAVFTKNLDK
451 ALKLASALES GTVWINCYNA LYAQAPFGGF KMSGNGRELG EYALAEYTEV
501 KTVTIKLGDK NP
```

Spot 1183 Cytokeratin 6

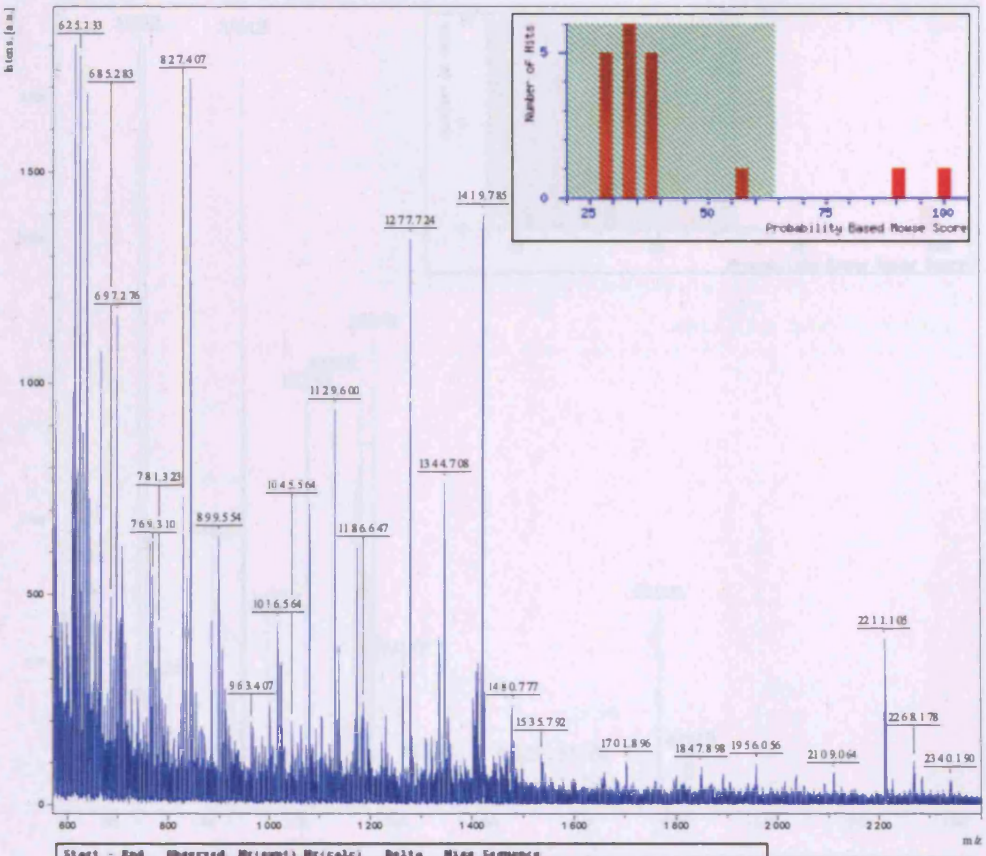

Start - End	Observed	Mr(expt)	Mr(calc)	Delta	Miss	Sequence
45 - 53	911.39	910.38	910.41	-0.04	0	R.SYTSGPGSR.I
54 - 61	670.42	669.42	669.42	-0.01	0	R.ISSSSFSR.V
62 - 68	766.35	765.35	765.38	-0.03	0	R.VGSSNFR.G
123 - 129	827.41	826.40	826.42	-0.02	0	K.FASFIDK.V
130 - 138	1161.63	1160.63	1160.63	-0.00	1	K.VKFLEQQNK.M
139 - 145	906.43	905.42	905.46	-0.04	0	R.FLEQQNK.M
171 - 179	1045.56	1044.56	1044.55	0.01	0	R.QLETLGQEK.L
180 - 197	2034.14	2033.13	2033.05	0.08	1	K.LKLEAELGNMQGLVEDFK.N
208 - 218	1352.72	1351.71	1351.67	0.04	0	R.TDNEARFVLIK.K
208 - 219	1480.78	1479.77	1479.76	0.01	1	R.TDNEARFVLIKK.D
208 - 219	1496.72	1495.72	1495.76	-0.04	1	R.TDNEARFVLIKK.D Oxidation (M)
235 - 246	1419.79	1418.78	1418.74	0.04	0	R.LEHLTDEIHFLR.Q
255 - 273	2180.06	2180.06	2180.01	0.05	0	R.ELQSQISDTSVVLSMDNSR.S
255 - 273	2196.01	2196.00	2196.00	0.00	0	R.ELQSQISDTSVVLSMDNSR.S Oxidation (M)
274 - 285	1320.71	1319.70	1319.66	0.04	0	R.SLNMDSIIAEVK.A
286 - 294	1079.52	1078.51	1078.52	-0.01	0	K.AQYEDIANR.S
338 - 346	1000.50	999.50	999.56	-0.03	0	R.IQAEIEGLK.G
338 - 362	1344.71	1343.70	1343.67	0.03	0	R.ASLEAAIADAEQR.G
338 - 368	1956.06	1955.05	1955.03	0.02	1	R.ASLEAAIADAEQRGELAIK.D
363 - 373	1129.60	1128.59	1128.61	-0.02	1	R.GELAIKDANAK.L
364 - 390	819.45	818.45	818.41	0.04	1	K.ANQMNAR.Q
364 - 390	835.37	834.36	834.40	-0.04	1	K.ANQMNAR.Q Oxidation (M)
394 - 407	1153.58	1152.57	1152.53	0.03	0	R.EYQELMNVK.L
394 - 407	1169.58	1168.49	1168.54	-0.05	0	R.EYQELMNVK.L Oxidation (M)
403 - 413	1297.72	1296.72	1296.70	0.01	0	K.LALDIEIATYR.K
403 - 414	1405.79	1404.79	1404.80	-0.01	1	K.LALDIEIATYRK.L
494 - 504	1173.69	1172.68	1172.63	0.06	0	K.LVSESSDVLPK.-

```
  1 FSAPSRISAV FGPPASTPAS TMSIRVTQKS YKVSTSGPRA FSSRSYTSGP
 51 GSRISSSSFS RVGSSNFRGG LGGGYGGASG MGGITAVTVN QSLLSPLVLE
101 VDPNIQAVRT QEKEQIKTLN NKFASFIDKV RFLEQQNKML ETKWSLLQQQ
151 KTARSNMDNM FESYINNLRR QLETLGQEKL KLEAELGNMQ GLVEDFKNKY
201 EDEINKRTEM ENEFVLIKKD VDEAYMNKVE LESRLEGLTD EINFLRQLYE
251 EEIRELQSQI SDTSVVLSMD NSRSLDMDSI IAEVKAQYED IANRSRAEAE
301 SMYQIKYEEL QSLAGKHGDD LRRTKTEISE MNRNISRLQA EIEGLKGQRA
351 SLEAAIADAE QRGELAIKDA NAKLSELEAA LQRAKQDMAR QLREYQELMN
401 VKLALDIEIA TYRKLLEGEE SRLESGMQNM SIHTKTTSGY AGGLSSAYGG
451 LTSPGLSYSL GSSFGSGAGS SSFSRTSSSR AVVVKKIETR DGKLVSESSD
501 VLPK
```

Spot 1277 Cytokeratin 7

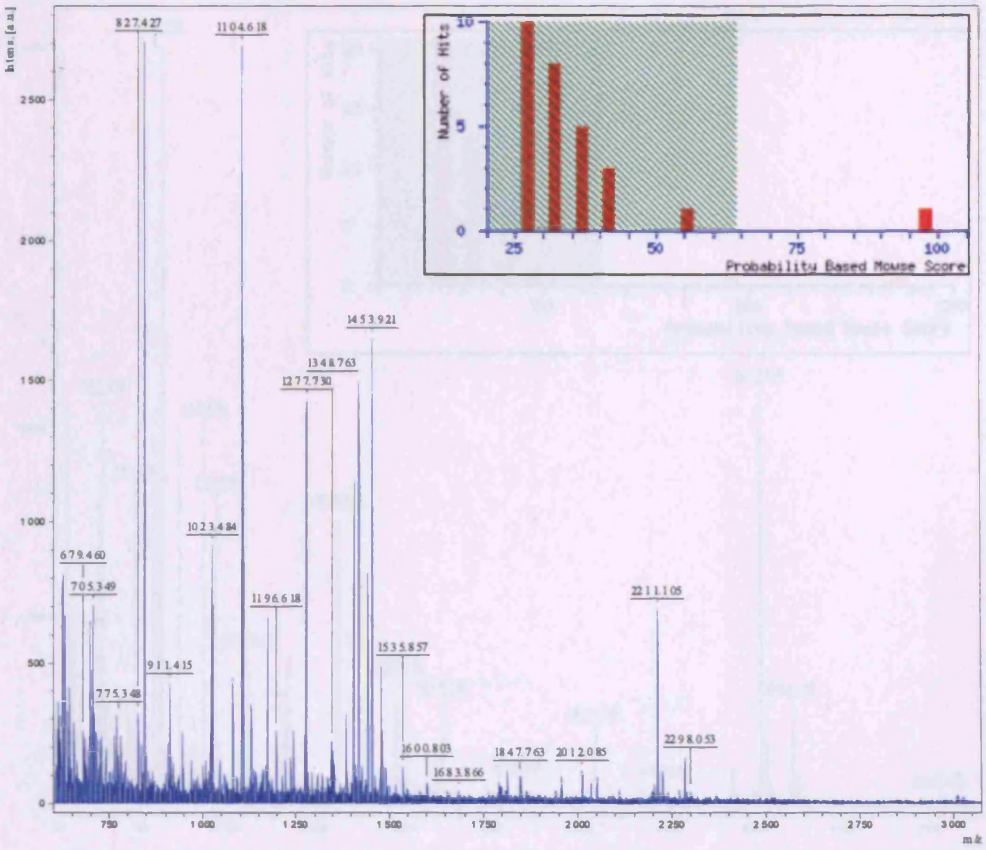

Start - End	Observed	Mr(expt)	Mr(calc)	Delta	Miss	Sequence
53 - 64	1104.62	1103.61	1103.57	0.04	0	R.SAYGGPVGAGIR.E
78 - 86	1014.56	1013.55	1013.51	0.04	0	R.LDADFSLQR.V
102 - 108	827.43	826.42	826.42	-0.00	0	K.FASFIDK.V
111 - 117	906.44	905.44	905.46	-0.03	0	R.FLEQQMK.L
111 - 122	1490.76	1489.75	1489.81	-0.06	1	R.FLEQQMKLLETK.W
123 - 130	1045.58	1044.58	1044.56	0.02	0	K.WYLLQEQK.S
137 - 149	1442.84	1441.83	1441.79	0.04	0	R.LPDIFEAQIAGLR.G
150 - 167	1953.97	1952.96	1953.03	-0.07	1	R.GQLEALQVDGGRLEAELR.S
168 - 177	1213.59	1212.58	1212.53	0.05	0	R.SMQDVVEDFK.N Oxidation (M)
180 - 190	1220.71	1219.70	1219.64	0.06	0	R.TAAENEFVVLK.K
180 - 199	1348.76	1347.76	1347.74	0.02	1	R.TAAENEFVVLKK.D
215 - 226	1418.73	1417.72	1417.72	0.00	0	K.VDALNDEINFLR.T
254 - 273	2239.02	2238.01	2238.11	-0.09	1	R.SLDLDGIIAEVKAQYEDMAK.C Oxidation (M)
332 - 348	1812.96	1811.95	1811.96	-0.01	1	K.LEAAIAEAEERGELALK.D
354 - 363	1186.62	1185.61	1185.60	0.01	0	K.QEELEAALQR.A
354 - 365	1385.76	1384.75	1384.73	0.02	1	K.QEELEAALQRAK.Q
364 - 378	835.39	834.38	834.40	-0.02	1	R.AKQDMAR.Q Oxidation (M)
374 - 382	1126.57	1125.57	1125.54	0.03	0	R.EYQELMSVK.L
374 - 382	1142.53	1141.53	1141.53	-0.01	0	R.EYQELMSVK.L Oxidation (M)
383 - 393	1277.73	1276.72	1276.70	0.02	0	K.LALDIEIATYR.K
383 - 394	1405.77	1404.76	1404.80	-0.04	1	K.LALDIEIATYRK.L

```
  1 MSIHFSSPVF TSRSAAFSGR GAQVRLSSAR PGGLGSSSLY GLGASRPRVA
 51 VRSAYGGPVG AGIREVTINQ SLLAPLRLDA DPSLQRVRQE ESEQIKTLNN
101 KFASFIDKVR FLEQQNKLLE TKWTLLQEQK SAKSSRLPDI FEAQIAGLRG
151 QLEALQVDGG RLEAELRSMQ DVVEDFKNKY EDEINRRTAA ENEFVVLKKD
201 VDAAYMSKVE LEAKVDALND EINFLRTLNE TELTELQSQI SDTSVVLSMD
251 NSRSLDLDGI IAEVKAQYEE MAKCSRAEAE AWYQTKFETL QAQAGKHGDD
301 LRNTRNEISE MNRAIQRLQA EIDNIKNQRA KLEAAIAEAE ERGELALKDA
351 RAKQEELEAA LQRAKQDMAR QLREYQELMS VKLALDIEIA TYRKLLEGEE
401 SRLAGDGVGA VNISVMNSTG GSSSGGGIGL TLGGTMGSNA LSFSSSAGPG
451 LLKAYSIRTA SASRRSARD
```

Spot 1307 Cytokeratin 13

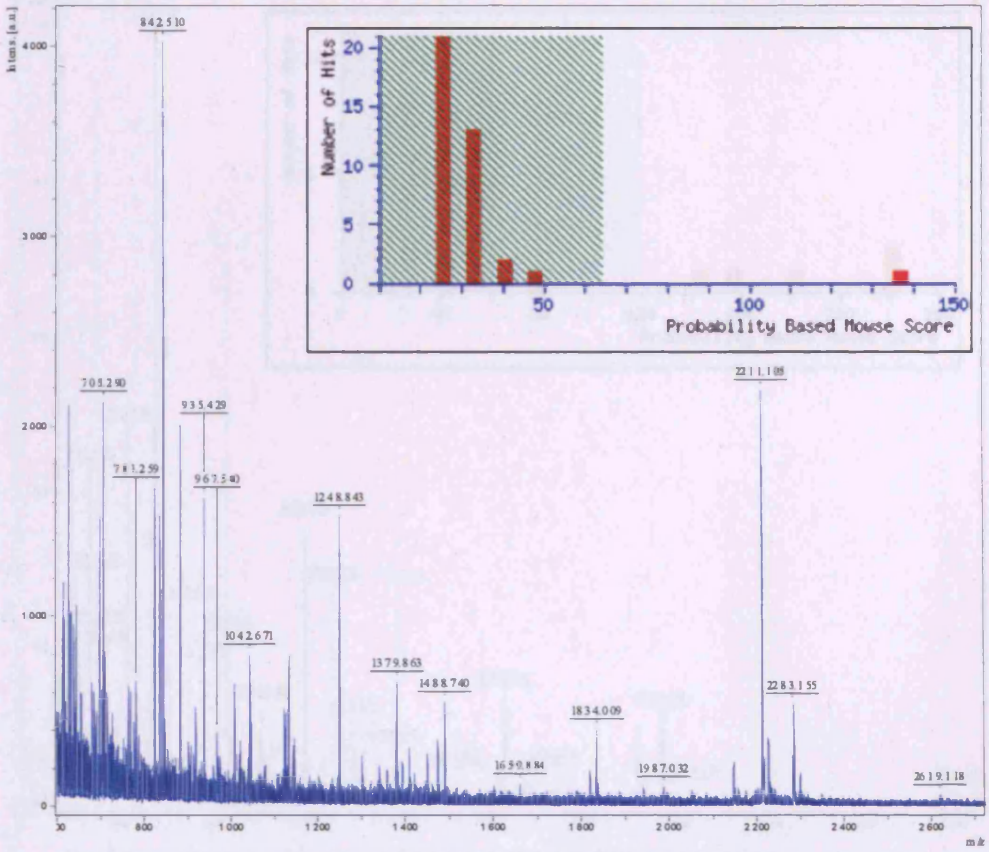

Start - End	Observed	Mr(expt)	Mr(calc)	Delta	Miss	Sequence
5 - 27	2147.02	2146.02	2145.95	0.07	0	R.LQSSSASYGGGFGGGSCQLGGGR.G
106 - 114	1120.65	1119.64	1119.53	0.11	0	K.ITMQNLMDR.L Oxidation (M)
115 - 121	823.43	822.42	822.45	-0.03	0	R.LASYLEK.V
124 - 135	1381.76	1380.76	1380.65	0.10	0	R.ALEEANADLEVK.I
136 - 142	967.54	966.53	966.54	-0.01	1	K.IRDWHLK.Q
143 - 150	871.45	870.45	870.42	0.03	0	K.QSPASPER.D
151 - 157	935.43	934.42	934.41	0.01	0	R.DYSPYYK.T
166 - 175	1144.69	1143.68	1143.62	0.05	0	K.ILTATIENNR.V
176 - 184	1042.67	1041.66	1041.58	0.08	0	R.VILEIDNAR.L
185 - 191	835.39	834.39	834.42	-0.04	0	R.LAVDDFR.I
223 - 240	2157.02	2156.01	2156.00	0.01	0	K.TDLEMQIESLNEELAYMK.K
249 - 272	2619.12	2618.11	2618.26	-0.15	0	K.EFSMQVVGQVNVEMDATPGIDLTR.V
291 - 299	1132.57	1131.56	1131.50	0.06	0	R.DAEEWFMAK.S
300 - 318	2052.06	2051.05	2051.02	0.03	1	K.SAELNKEVSTMTAMIQTSK.T
319 - 326	1017.53	1016.53	1016.56	-0.04	1	K.TEITELRR.T
327 - 342	1818.15	1817.14	1816.96	0.18	0	R.TLQGLEIELQSQLSMK.A
327 - 342	1834.01	1833.00	1832.96	0.05	0	R.TLQGLEIELQSQLSMK.A Oxidation (M)
379 - 389	1445.71	1444.70	1444.56	0.14	0	R.SEMECQNQEYK.N
396 - 406	1379.86	1378.86	1378.72	0.14	1	K.TRLEQEIATYR.S
398 - 406	1122.68	1121.67	1121.57	0.10	0	R.LEQEIATYR.S
416 - 429	1408.82	1407.81	1407.68	0.13	0	K.NIGFPSSAGSVSPR.S Oxidation (M)

```
  1 MSLRLQSSSA SYGGGFGGGS CQLGGGRGVS TCSTRFVSGG SAGGYGGGVS
 51 CGFGGGADSG FGGGYGGGLG GGYGGGLGGG FGGGFAGGFV DFGACDGGLL
101 TGNEKITMQN LNDRLASYLE KVRALEEANA DLEVKIRDWH LKQSPASPER
151 DYSPYYKTIE ELRDKILTAT IENNRVILEI DNARLAVDDF RLKYENELAL
201 RQSVEADING LRRVLDELTL SKTDLEMQIE SLNEELAYMK KNHEEEMKEF
251 SNQVVGQVNV ENDATPGIDL TRVLAEMREQ YEAMAERNRR DAEEWFMAKS
301 AELNKEVSTN TAMIQTSKTE ITELRRTLQG LEIELQSQLS MKAGLENTVA
351 ETECRYALQL QQIQGLISSI EAQLSELRSE MECQNQEYKM LLDIKTRLEQ
401 EIATYRSLLE GQDAKNIGFP SSAGSVSPRS TSVTTTSSAS VTTTSNASGR
451 RTSDVRRP
```

Spot 1298 Cytokeratin 13

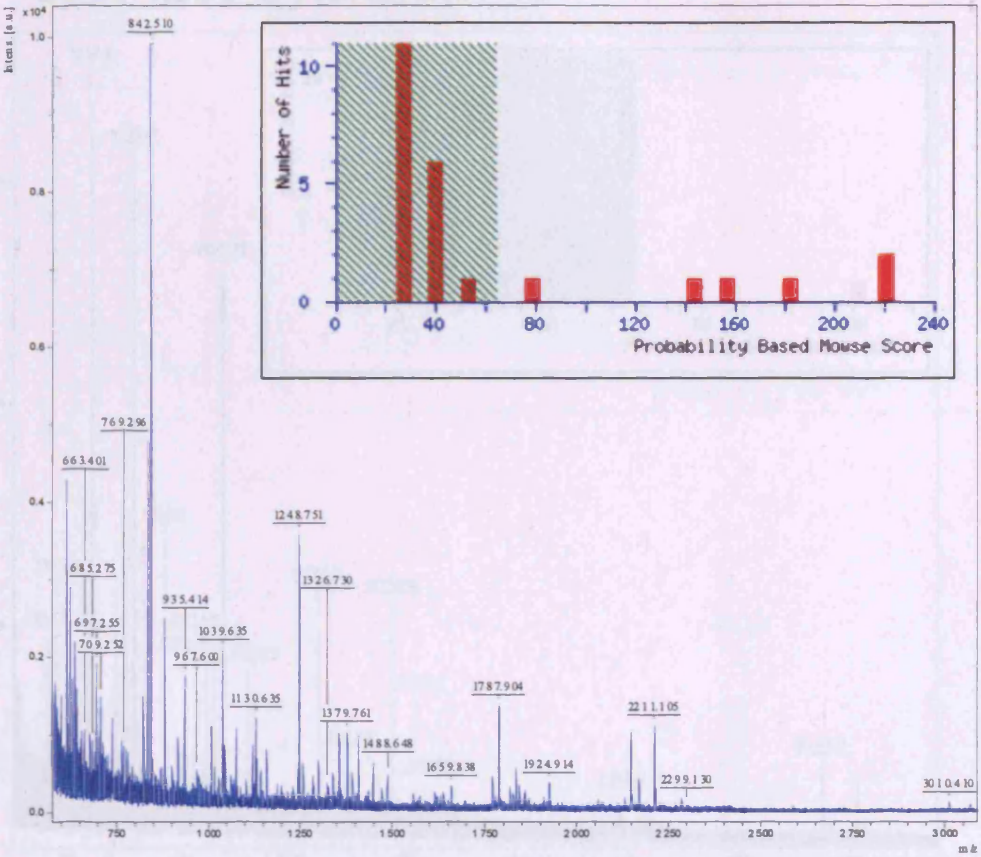

Start - End	Observed	Mr(expt)	Mr(calc)	Delta	Miss	Sequence
5 - 27	2146.99	2145.98	2145.95	0.03	0	R.LQSSSASTGGGFGGGSCQLGGGR.G
106 - 114	1120.59	1119.58	1119.53	0.04	0	K.ITMQMLNDR.L Oxidation (M)
106 - 121	1909.03	1908.02	1907.98	0.04	1	K.ITMQMLNDRLASYLEK.V
106 - 121	1924.91	1923.91	1923.97	-0.07	1	K.ITMQMLNDRLASYLEK.V Oxidation (M)
115 - 121	823.43	822.43	822.45	-0.02	0	R.LASYLEK.V
115 - 123	1078.65	1077.65	1077.62	0.03	1	R.LASYLEKVR.A
124 - 135	1301.63	1300.62	1300.65	-0.03	0	R.ALEEANADLEVK.I
143 - 157	1787.90	1786.90	1786.82	0.08	1	K.QSPASPERDTSPTIK.Y
151 - 157	935.41	934.41	934.41	-0.00	0	R.DTSPTIK.Y
166 - 184	2168.27	2167.26	2167.20	0.06	1	K.ILTATIENNSVILEIDNAR.L
176 - 184	1042.63	1041.62	1041.58	0.04	0	R.VILEIDNAR.L
185 - 191	835.42	834.42	834.42	-0.01	0	R.LAVDDFR.L
192 - 201	1248.75	1247.74	1247.69	0.06	1	R.LKTEMELALR.Q
194 - 201	1007.55	1006.54	1006.51	0.03	0	K.TEMELALR.Q
202 - 212	1201.67	1200.67	1200.61	0.06	0	R.QSVEADINGLR.R
202 - 213	1357.76	1356.75	1356.71	0.04	1	R.QSVEADINGLRR.V
214 - 222	1017.59	1016.58	1016.54	0.01	0	R.VLDELTLSK.T
223 - 237	1825.90	1824.89	1824.85	0.04	1	R.VLAEMREQYEAMAER.N
223 - 237	1841.91	1840.90	1840.84	0.06	1	R.VLAEMREQYEAMAER.N Oxidation (M)
223 - 237	1857.76	1856.76	1856.84	-0.08	1	R.VLAEMREQYEAMAER.N 2 Oxidation (M)
327 - 342	1833.97	1832.96	1832.96	0.00	0	R.TLQQLEIELQSQLSMK.A Oxidation (M)
343 - 355	1449.70	1448.69	1448.66	0.03	0	K.AGLENTVAETECR.Y
396 - 406	1379.76	1378.75	1378.72	0.03	1	K.TRLEQEIATYR.S
398 - 406	1122.60	1121.59	1121.57	0.02	0	R.LEQEIATYR.S
416 - 429	1392.76	1391.75	1391.69	0.06	0	K.MIGFPSSAGSVSPR.S
416 - 429	1408.71	1407.70	1407.68	0.02	0	K.MIGFPSSAGSVSPR.S Oxidation (M)

```
  1 MSLRLQSSSA SYGGGFGGGS CQLGGGRGVS TCSTRFVSGG SAGGYGGGVS
 51 CGFGGGADSG FGGGYGGGLG GGYGGGLGGG FGGGFAGGFV DFGACDGGLL
101 TGNEKITMQN LNDRLASYLE KVRALEEANA DLEVKIRDWH LKQSPASPER
151 DYSPYYKTIE ELRDKILTAT IENNRVILEI DNARLAVDDF RLKYENELAL
201 RQSVEADING LRRVLDELTL SKTDLEMQIE SLNEELAYMK KNHEEEMKEF
251 SNQVVGQVNV EMDATPGIDL TRVLAEMREQ YEAMAERNRR DAEEWFHAKS
301 AELNKEVSTN TAMIQTSKTE ITELRRTLQG LEIELQSQLS MKAGLENTVA
351 ETECRYALQL QQIQGLISSI EAQLSELRSE MECQNQEYKM LLDIKTRLEQ
401 EIATYRSLLE GQDAKMIGFP SSAGSVSPRS TSVTTTSSAS VTTTSNASGR
451 RTSDVRRP
```

Spot 1295 Cytokeratin 13

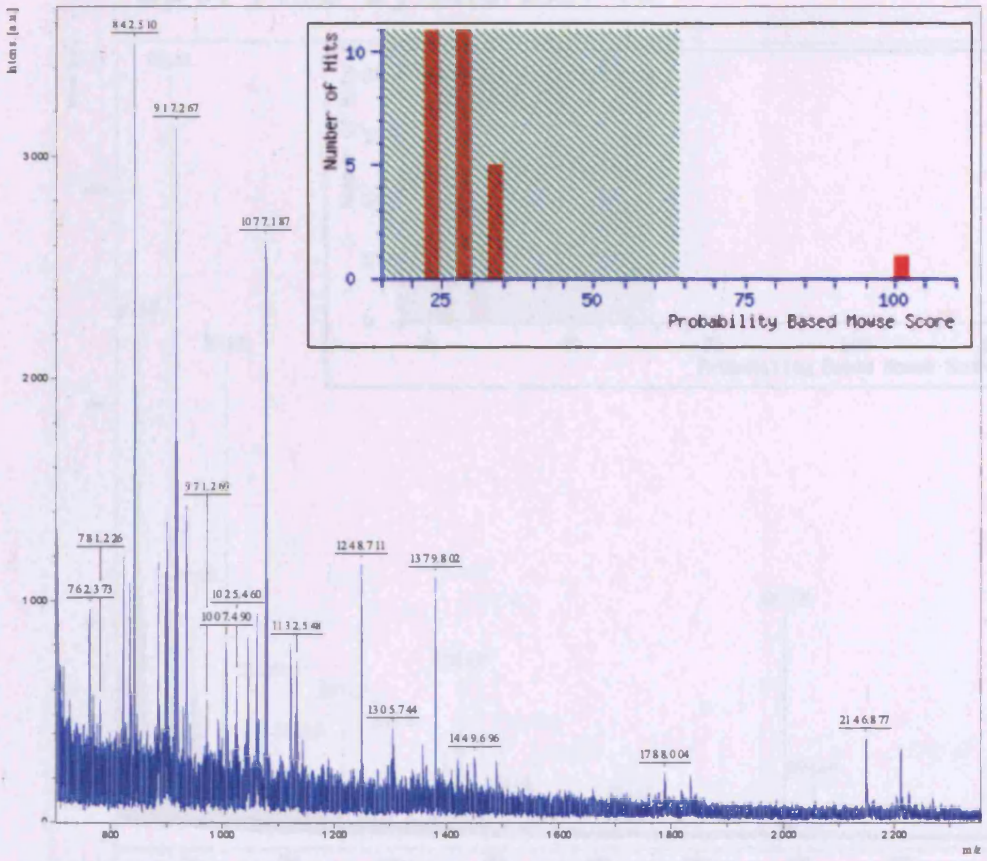

Start - End	Observed	Mr(expt)	Mr(calc)	Delta	Miss	Sequence	
5 - 27	2146.88	2145.87	2145.95	-0.08	0	R.LQSSSASYGGGFGGGSCQLGGGR.G	
124 - 135	1301.67	1300.66	1300.65	0.01	0	R.ALEEAMADLEVK.I	
151 - 157	935.40	934.39	934.41	-0.02	0	R.DYSPYYK.T	
176 - 184	1042.58	1041.58	1041.58	-0.01	0	R.VILEIDNAR.L	
185 - 191	835.43	834.43	834.42	0.00	0	R.LAVDDFR.L	
192 - 201	1248.71	1247.70	1247.69	0.02	1	R.LKYEMELALR.Q	
194 - 201	1007.49	1006.48	1006.51	-0.03	0	K.YEMELALR.Q	
202 - 213	1357.72	1356.71	1356.71	0.00	1	R.QSVEADINGLRR.V	
291 - 299	1132.55	1131.54	1131.50	0.04	0	R.DAEEWFNAK.S	
327 - 342	1817.97	1816.97	1816.96	0.01	0	R.TLQGLEIELQSQLSMK.A	
327 - 342	1834.00	1833.00	1832.96	0.04	0	R.TLQGLEIELQSQLSMK.A	Oxidation (M)
343 - 355	1449.70	1448.69	1448.66	0.03	0	K.AGLEMTVAETECR.Y	
398 - 406	1122.58	1121.58	1121.57	0.01	0	R.LEQEIATYR.S	
416 - 429	1408.74	1407.73	1407.68	0.05	0	K.MIGFPSSAGSVSPR.S	Oxidation (M)

```
  1 MSLRLQSSSA SYGGGFGGGS CQLGGGRGVS TCSTRFVSGG SAGGYGGGVS
 51 CGFGGGADSG FGGGYGGGLG GGYGGGLGGG FGGGFAGGFV DFGACDGGLL
101 TGNEKITMQN LNDRLASYLE KVRALEEANA DLEVKIRDWH LKQSPASPER
151 DYSPYYKTIE ELRDKILTAT IENNRVILEI DNARLAVDDF RLKYENELAL
201 RQSVEADING LRRVLDELTL SKTDLEMQIE SLNEELAYMK KNHEEEMKEF
251 SNQVVGQVNV EMDATPGIDL TRVLAEMREQ YEAMAERNRR DAEEWFMAKS
301 AELNKEVSTN TAMIQTSKTE ITELRRTLQG LEIELQSQLS MKAGLEMTVA
351 ETECRYALQL QQIQGLISSI EAQLSELRSE MECQNQEYKM LLDIKTRLEQ
401 EIATYRSLLE GQDAKMIGFP SSAGSVSPRS TSVTTTSSAS VTTTSNASGR
451 RTSDVRRP
```

Spot 1165 Cytokeratin 13

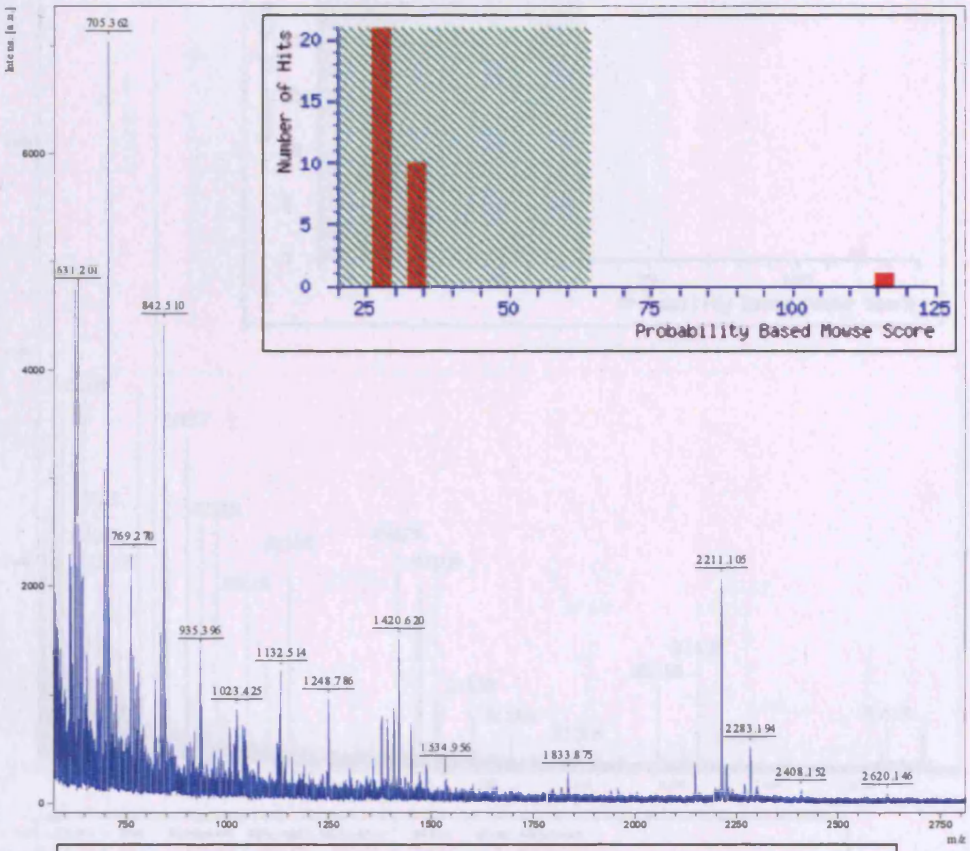

Start - End	Observed	Mr(expt)	Mr(calc)	Delta	Miss	Sequence
5 - 27	2146.99	2145.98	2145.95	0.03	0	R.LQSSSASTGGGFSGGSCQLGGGR.G
115 - 121	823.48	822.40	822.45	-0.05	0	R.LASYLER.V
124 - 135	1381.67	1380.66	1380.65	0.01	0	R.ALEEANADLEVK.I
136 - 142	967.46	966.45	966.54	-0.09	1	K.IRDWHLK.Q
151 - 157	935.40	934.39	934.41	-0.02	0	R.DYSPYYK.T
176 - 184	1042.63	1041.62	1041.58	0.04	0	R.VILEIDNAR.L
192 - 201	1248.79	1247.78	1247.69	0.09	1	R.LKYENELALR.Q
202 - 212	1201.56	1200.55	1200.61	-0.06	0	R.QSVEADINGLR.R
202 - 213	1357.69	1356.68	1356.71	-0.03	1	R.QSVEADINGLRR.V
214 - 222	1017.61	1016.60	1016.58	0.03	0	R.VLDELTLSK.T
279 - 287	1126.54	1125.53	1125.48	0.06	0	R.EQYEAMAER.N
291 - 299	1132.51	1131.51	1131.50	0.01	0	R.DAEEWFHAK.S
306 - 325	2268.24	2267.24	2267.13	0.11	1	K.EVSTNTAMIQTSKTEITELR.R Oxidation (M)
327 - 342	1817.86	1816.85	1816.96	-0.11	0	R.TLQGLEIELQSQLSMK.A
327 - 342	1833.88	1832.87	1832.96	-0.09	0	R.TLQGLEIELQSQLSMK.A Oxidation (M)
343 - 355	1449.78	1448.78	1448.66	0.12	0	K.AGLENTVAETECR.Y
396 - 406	1379.80	1378.80	1378.72	0.08	1	K.TRLEQEIATYR.S
398 - 406	1122.65	1121.64	1121.57	0.07	0	R.LEQEIATYR.S
416 - 429	1392.76	1391.75	1391.69	0.07	0	R.MIGFPSSAGSVSPR.S
416 - 429	1408.71	1407.70	1407.68	0.02	0	R.MIGFPSSAGSVSPR.S Oxidation (M)

```
  1 MSLRLQSSSA SYGGGFGGGS CQLGGGRGVS TCSTRFVSGG SAGGYGGGVS
 51 CGFGGGADSG FGGGYGGGLG GGYGGGLGGG FGGGFAGGFV DFGACDGGLL
101 TGNEKITMQN LNDRLASYLE KVRALEEANA DLEVKIRDWH LKQSPASPER
151 DYSPYYKTIE ELRDKILTAT IENNRVILEI DNARLAVDDF RLKYENELAL
201 RQSVEADING LRRVLDELTL SKTDLEMQIE SLNEELAYMK KNHEEEMKEF
251 SNQVVGQVNV EMDATPGIDL TRVLAEMREQ YEAMAERNRR DAEEWFHAKS
301 AELNKEVSTN TAMIQTSKTE ITELRRTLQG LEIELQSQLS MKAGLENTVA
351 ETECRYALQL QQIQGLISSI EAQLSELRSE MECQNQEYKM LLDIKTRLEQ
401 EIATYRSLLE GQDAKMIGFP SSAGSVSPRS TSVTTTSSAS VTTTSNASGR
451 RTSDVRRP
```

Spot 1303 Dihydrolipoamide DH

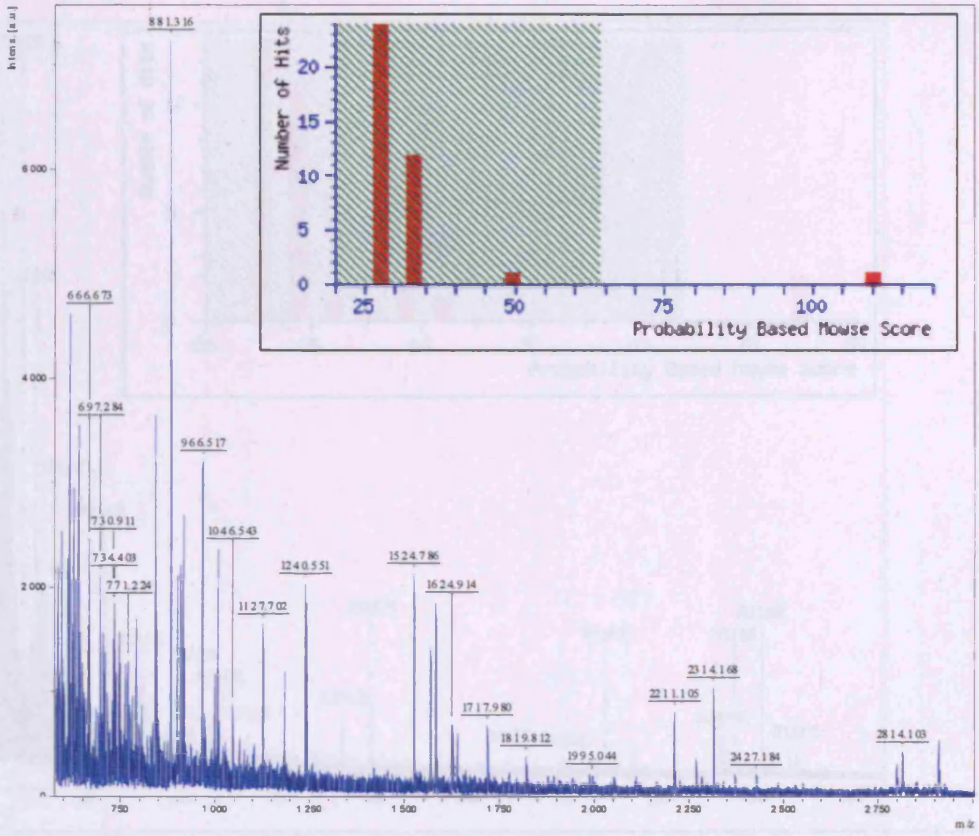

Start - End	Observed	Mr(expt)	Mr(calc)	Delta	Miss	Sequence
60 - 66	734.40	733.40	733.41	-0.02	0	K.AAQLGFK.T
67 - 72	749.34	748.34	748.38	-0.04	0	K.TVCIEK.H
73 - 89	1819.81	1818.80	1818.86	-0.06	0	K.HETLGGTCLNVGCIPSK.A
105 - 109	595.25	594.24	594.28	-0.04	0	K.DFASR.G
110 - 117	920.39	919.38	919.44	-0.06	0	R.GIEMSEVR.L
110 - 117	936.47	935.46	935.44	0.02	0	R.GIEMSEVR.L Oxidation (M)
133 - 143	1127.70	1126.69	1126.65	0.04	0	K.ALTGGIAHLFK.Q
147 - 155	972.44	971.43	971.52	-0.09	0	K.VVVGVGYGK.I
167 - 177	1104.59	1103.58	1103.55	0.04	0	K.ADGGTQVIDTK.H
216 - 234	1986.18	1985.17	1985.08	0.09	0	K.HNVIHAAGVIGVELGSVWQR.L Oxidation (M)
268 - 277	1046.54	1045.54	1045.60	-0.07	1	K.HFQRILQK.Q
285 - 300	1533.75	1532.74	1532.77	-0.03	1	K.SDGKIDVSIEAASGGK.A
289 - 300	1146.53	1145.53	1145.59	-0.07	0	K.IDVSIEAASGGK.A
301 - 315	1717.98	1716.97	1716.89	0.08	0	K.AEVITCDVLLVCIGR.R
316 - 320	648.37	647.36	647.38	-0.01	0	R.RPFTK.N
321 - 334	1567.84	1566.83	1566.83	0.01	0	K.NLGLEELGIELDPR.G
347 - 365	1979.00	1977.99	1978.07	-0.08	0	K.IPNIYAIGDVVAGPMLAHK.A
347 - 365	1995.84	1994.84	1994.87	-0.03	0	K.IPNIYAIGDVVAGPMLAHK.A Oxidation (M)
405 - 417	1581.80	1580.79	1580.76	0.04	1	K.SEEQLKEEGIEYK.V
421 - 428	909.48	908.47	908.45	0.02	0	K.FPPAANSR.A
483 - 495	1524.79	1523.78	1523.73	0.05	0	R.VCHAHPTLSEAFR.E
496 - 505	1007.53	1006.52	1006.51	0.01	0	R.EAHLAASFGK.S

```
  1 MQSWSRVYCS LAKRGHFNRI SHGLQGLSAV PLRTYADQPI DADVTVIGSG
 51 PGGYVAAIKA AQLGFKTVCI EKNETLGGTC LNVGCIPSKA LLNNSHYYHM
101 AHGKDFASRG IEMSEVRLNL DKMMEQKSTA VKALTGGIAH LFKQNKVVMV
151 NGYGKITGKN QVTATKADGG TQVIDTKNIL IATGSEVTPF PGITIDEDTI
201 VSSTGALSLK KVPEKMVVIG AGVIGVELGS VWQRLGADVT AVEFLGHVGG
251 VGIDMEISKN FQRILQKQGF KFKLNTKVTG ATKKSDGKID VSIEAASGGK
301 AEVITCDVLL VCIGRRPFTK NLGLEELGIE LDPRGRIPVN TRFQTKIPNI
351 YAIGDVVAGP MLAHKAEDEG IICVEGMAGG AVHIDYNCVP SVIYTHPEVA
401 WVGKSEEQLK EEGIEYKVGK FPFAANSRAK TNADTDGMVK ILGQKSTDRV
451 LGAHILGPGA GEMVNEAALA LEYGASCEDI ARVCHAHPTL SEAFREAHLA
501 ASFGKSINF
```

Spot 2262 Glutathione S-transferase π

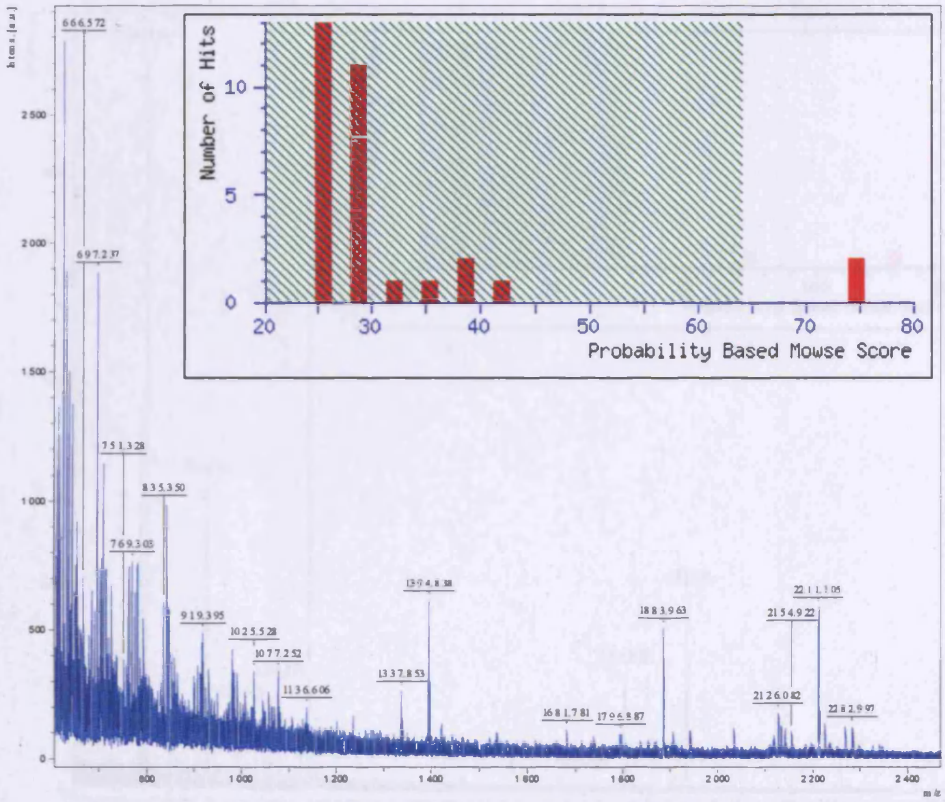

Start - End	Observed	Mr(expt)	Mr(calc)	Delta	Miss	Sequence	
1 - 14	1681.78	1680.77	1680.88	-0.11	1	-.MPPYTVVYFPVRGR.C	
2 - 12	1337.85	1336.85	1336.72	0.13	0	M.PPYTVVYFPVR.G	
31 - 45	1733.84	1732.84	1732.85	-0.02	0	K.EEVVTVETWQEGSLK.A	
46 - 55	1136.61	1135.60	1135.57	0.03	0	K.ASCLYGQLPK.F	
56 - 71	1883.96	1882.96	1882.94	0.01	0	K.FQDGDLTLYQSNTILR.H	
72 - 82	1214.64	1213.63	1213.69	-0.07	1	R.HLGRTLGLYGK.D	
83 - 101	2116.90	2115.89	2115.97	-0.08	0	K.DQQEAALVDMVNDGVEDLR.C	
83 - 101	2132.87	2131.86	2131.97	-0.11	0	K.DQQEAALVDMVNDGVEDLR.C	Oxidation (M)
104 - 121	2154.92	2153.91	2154.85	-0.14	1	K.YISLIYTNYEAGKDDYVK.A	
122 - 141	2126.08	2125.07	2125.15	-0.08	0	K.ALPGQLKPFETLLSQNQGGK.T	
192 - 209	1903.92	1902.91	1902.98	-0.08	0	K.AFLASPEYVNLPINGNGK.Q	

```
  1 MPPYTVVYFP VRGRCAALRM LLADQGQSWK EEVVTVETWQ EGSLKASCLY
 51 GQLPKFQDGD LTLYQSNTIL RHLGRTLGLY GKDQQEAALV DMVNDGVEDL
101 RCKYISLIYT NYEAGKDDYV KALPGQLKPF ETLLSQNQGG KTFIVGDQIS
151 FADYNLLDLL LIHEVLAPGC LDAFPLLSAY VGRLSARPKL KAFLASPEYV
201 NLPINGNGKQ
```

Spot 2182 HSP-27

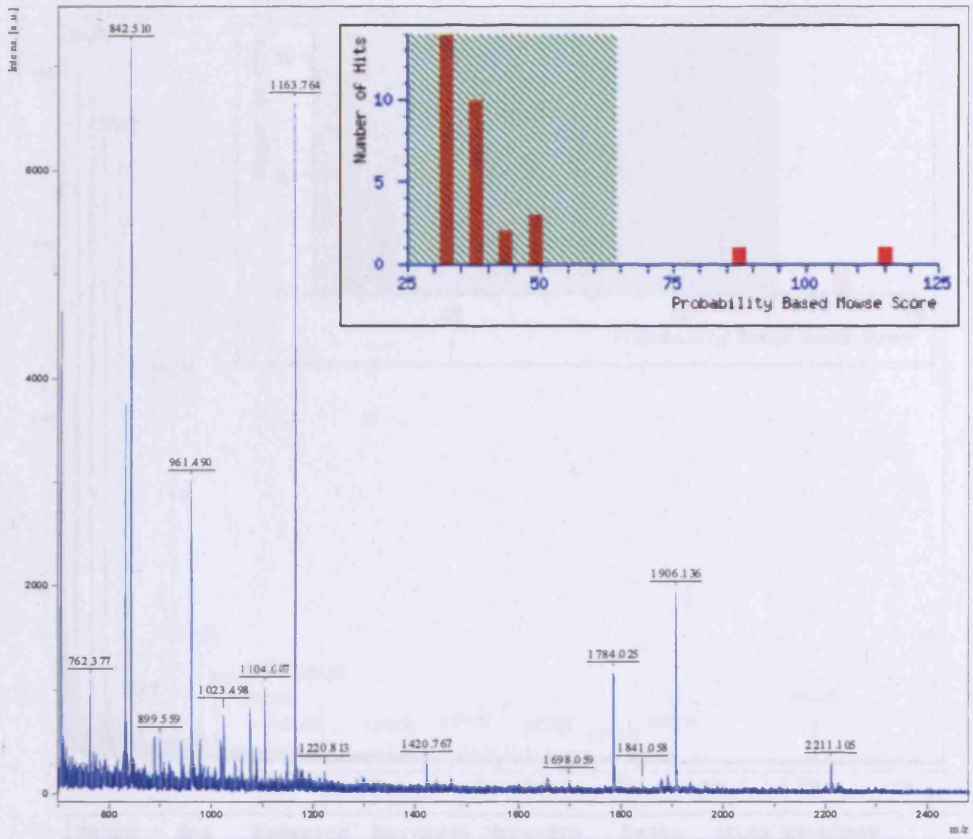

Start - End	Observed	Mr(expt)	Mr(calc)	Delta	Miss	Sequence
6 - 12	831.53	830.52	830.50	0.02	0	R.VPFSLLR.G
13 - 20	961.49	960.48	960.45	0.04	0	R.GPSWDPFR.D
21 - 27	960.49	959.48	959.42	0.06	0	R.DWYPHSR.L
80 - 89	1075.65	1074.64	1074.57	0.07	0	R.QLSSGVSEIR.H
97 - 112	1784.02	1783.02	1782.92	0.10	0	R.VSLDVNHFAPDELTVK.T
124 - 136	1655.79	1654.78	1654.74	0.03	1	K.HEERQDEHGYISR.C
128 - 136	1104.61	1103.60	1103.50	0.10	0	R.QDEHGYISR.C
172 - 188	1906.14	1905.13	1904.98	0.14	0	K.LATQSNEITIPVTFESR.A
189 - 198	941.52	940.51	940.50	0.01	0	R.AQLGGPEAAK.S

```
  1 MTERRVPFSL LRGPSWDPFR DWYPHSRLFD QAFGLPRLPE EWSQWLGGSS
 51 WPGYVRPLPP AAIESPAVAA PAYSRALSRQ LSSGVSEIRH TADRWRVSLD
101 VNHFAPDELT VKTKDGVVEI TGKHEERQDE HGYISRCFTR KYTLPPGVDP
151 TQVSSSLSPE GTLTVEAPMP KLATQSNEIT IPVTFESRAQ LGGPEAAKSD
201 ETAAK
```

Spot 2213 HSP-27

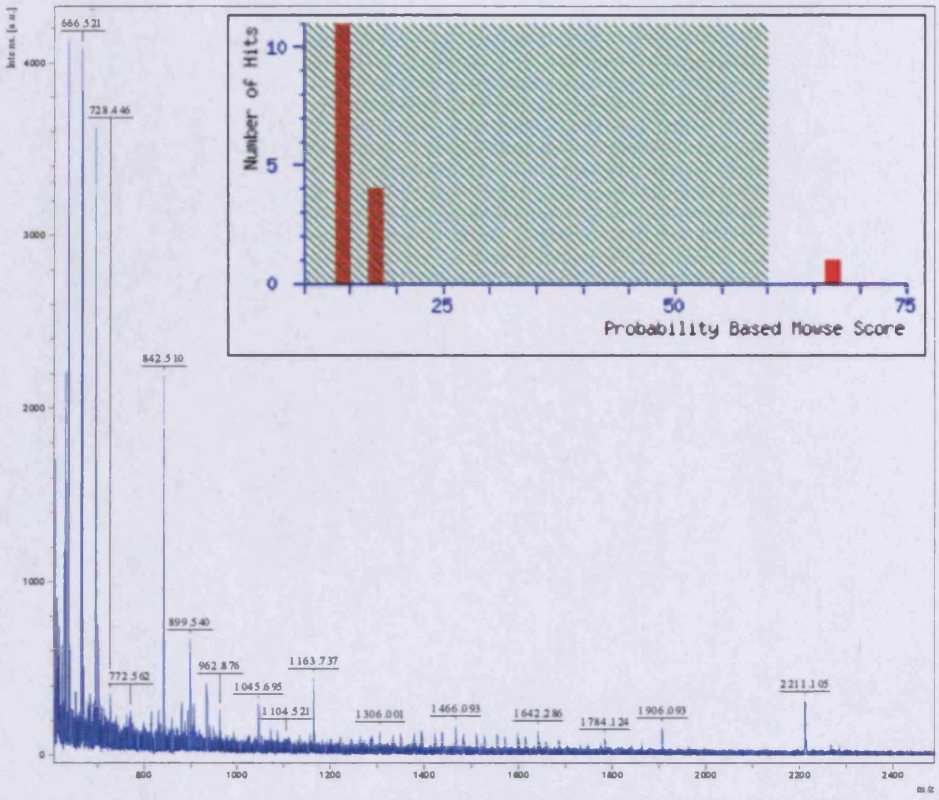

Start - End	Observed	Mr(expt)	Mr(calc)	Delta	Miss	Sequence
5 - 12	987.53	986.52	986.60	-0.08	1	R.RVPFSLLR.G
6 - 12	831.47	830.47	830.50	-0.04	0	R.VPFSLLR.G
6 - 20	1773.97	1772.96	1772.94	0.02	1	R.VPFSLLRGPSWDPFR.D
13 - 20	961.45	960.44	960.45	-0.00	0	R.GPSWDPFR.D
21 - 27	960.48	959.47	959.42	0.04	0	R.DWYPHSR.L
28 - 37	1163.74	1162.73	1162.61	0.12	0	R.LFDQAFGLPR.L
128 - 136	1104.52	1103.51	1103.50	0.01	0	R.QDEHGYISR.C
172 - 188	1906.09	1905.09	1904.98	0.10	0	K.LATQSNEITIPVTFESR.A
189 - 198	941.50	940.50	940.50	-0.00	0	R.AQLGGPEAAK.S

```
  1 MTERRVPFSL LRGPSWDPFR DWYPHSRLFD QAFGLPRLPE EWSQWLGGSS
 51 WPGYVRPLPP AAIESPAVAA PAYSRALSRQ LSSGVSEIRH TADRWRVSLD
101 VNHFAPDELT VKTKDGVVEI TGKHEERQDE HGYISRCFTR KYTLPPGVDP
151 TQVSSSLSPE GTLTVEAPMP KLATQSNEIT IPVTFESRAQ LGGPEAAKSD
201 ETAAK
```

Spot 1104 HSP-60

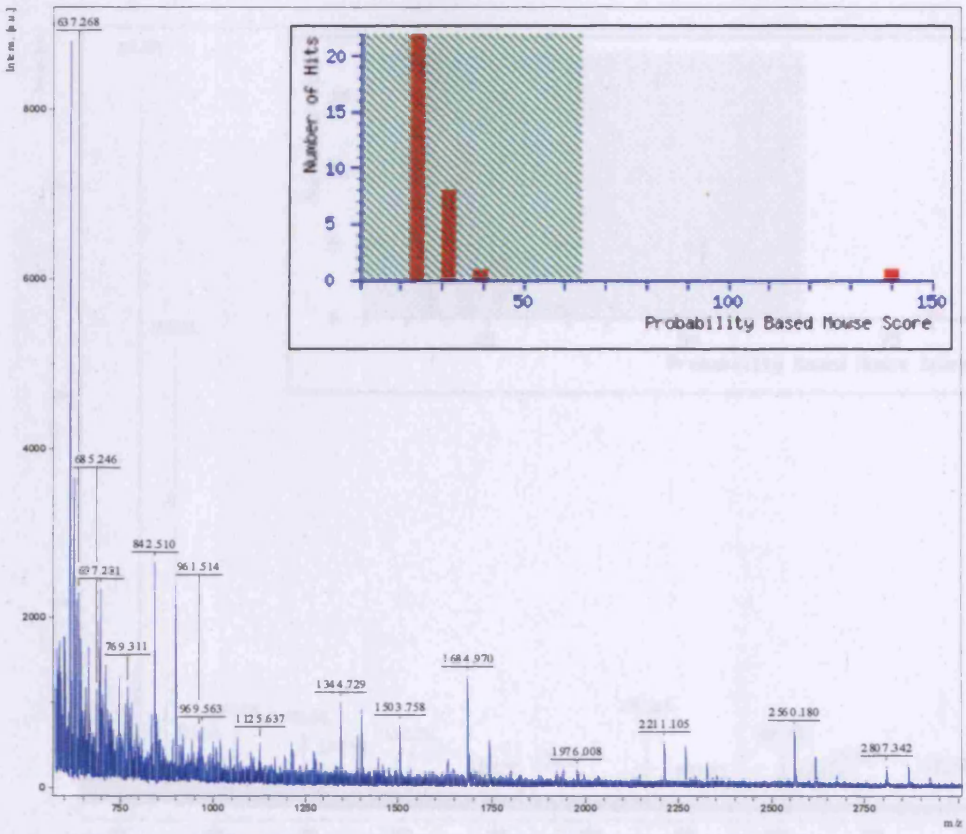

Start - End	Observed	Mr(expt)	Mr(calc)	Delta	Miss	Sequence
29 - 37	970.50	977.49	977.49	0.00	1	K.DVKFGADAR.A
38 - 58	2149.17	2144.16	2144.13	0.04	0	R.AIMLQGVDLLADAVAVTMGPK.G 2 Oxidation (M)
61 - 72	1344.73	1343.72	1343.71	0.01	0	R.TVIIEQSWGSPK.V
97 - 121	2560.18	2559.17	2559.24	-0.07	0	K.LVQDVAMTMGPAGDGTTTATVLAR.S
122 - 130	1008.51	1007.51	1007.53	-0.02	1	R.SIAKEGFEK.I
134 - 141	955.45	954.45	954.46	-0.01	0	K.GANPVEIR.R
206 - 218	1504.77	1503.76	1503.75	0.01	0	K.TLMDELEIIEGMK.F
206 - 221	1922.99	1921.99	1921.95	0.04	1	K.TLMDELEIIEGMKFDR.G
206 - 221	1938.98	1937.98	1937.94	-0.04	1	K.TLMDELEIIEGMKFDR.G Oxidation (M)
222 - 232	1388.73	1388.72	1388.78	0.02	0	R.GYISPYFINTSK.G
233 - 248	1919.13	1918.12	1918.06	0.06	0	K.ISSIQSIVPALEIANAHR.K
291 - 301	1153.72	1152.71	1152.76	-0.05	1	R.LEVSLQVVAVK.A
302 - 309	833.40	832.39	832.38	0.01	0	K.APGFGDNR.K
302 - 310	961.51	960.51	960.48	0.03	1	K.APGFGDNRK.N
345 - 352	844.52	843.51	843.51	0.00	0	K.VGEVIVTK.D
343 - 358	1638.88	1629.87	1629.88	0.07	1	K.VGEVIVTKDDAMLLK.G
343 - 359	1646.90	1645.89	1645.90	-0.01	1	K.VGEVIVTKDDAMLLK.G Oxidation (M)
360 - 376	843.48	842.47	842.50	-0.03	1	K.LMDNLAH.L
404 - 417	1233.64	1232.63	1232.59	0.04	0	K.VGGTSDVEVDEK.K
421 - 429	960.48	959.47	959.50	-0.03	0	R.VTDALNATR.A
430 - 446	1644.97	1643.96	1643.98	0.06	0	R.AAVEEGIVLGGGCALLR.C
463 - 470	941.41	940.40	940.41	-0.01	1	K.ISDIILKR.T
462 - 493	1215.64	1214.64	1214.63	-0.02	0	K.RAAVEEGLIVGR.I

```
  1 MLRLPTVFRQ MRPVSRVLAP HLTRAYAKDV KFGADARALM LQGVDLLADA
 51 VAVTMGPKGR TVIIEQSWGS PKVTKDGVTV AKSIDLKDKY KNIGAKLVQD
101 VANNTNEEAG DGTTTATVLA RSIAKEGFEK ISKGANPVEI RRGVMLAVDA
151 VIAELKKQSK PVTTPEEIAQ VATISANGDK EIGNIISDAM KKVGRKGVIT
201 VKDGKTLNDE LEIIEGMKFD RGYISPYFIN TSKGQKCEFQ DAYVLLSEKK
251 ISSIQSIVPA LEIANAHRKP LVIIAEDVDG EALSTLVLNR LKVGLQVVAV
301 KAPGFGDNRK NQLKDMAIAT GGAVFGEEGL TLNLEDVQPH DLGKVGEVIV
351 TKDDAMLLKG KGDKAQIEKR IQEIIEQLDV TTSEYEKEKL NERLAKLSDG
401 VAVLKVGGTS DVEVNEKKDR VTDALNATRA AVEEGIVLGG GCALLRCIPA
451 LDSLTPANED QKIGIEIIKR TLKIPAMTIA KNAGVEGSLI VEKIMQSSSE
501 VGYDAMAGDF VNMVEKGIID PTKVVRTALL DAAGVASLLT TAEVVVTEIP
551 KEEKDPGMGA MGGMGGGMGG GMF
```

Spot 1060 HSP-60

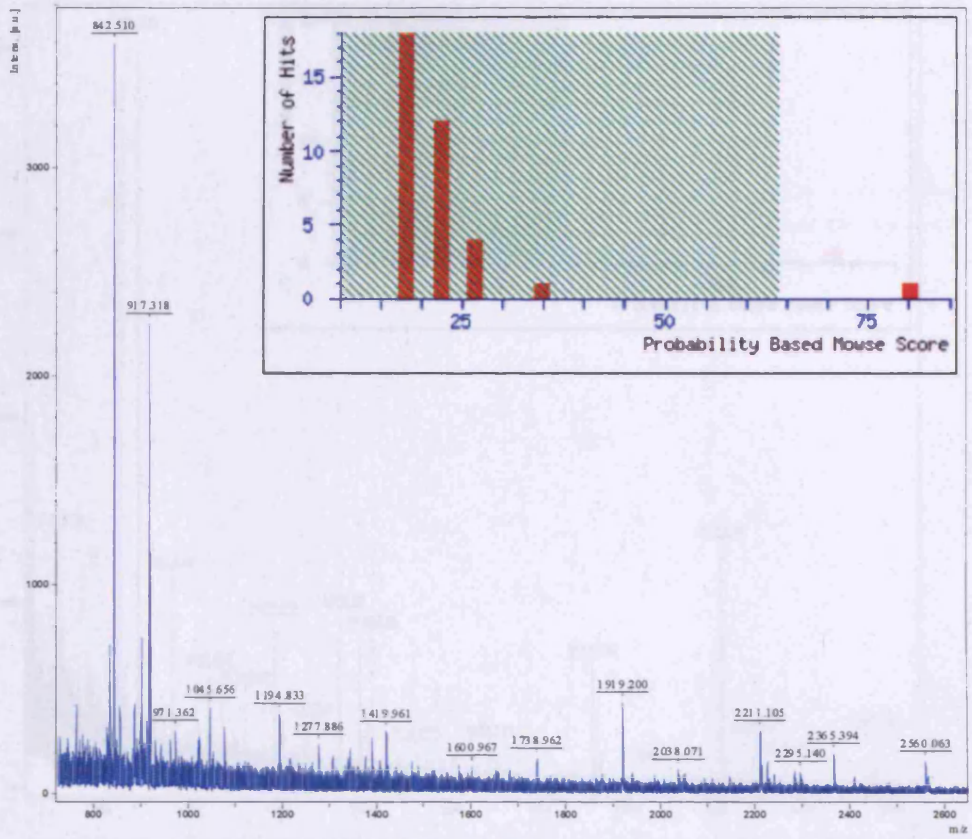

Start - End	Observed	Mr(expt)	Mr(calc)	Delta	Miss	Sequence
134 - 141	855.44	854.43	854.46	-0.03	0	K.GANPVEIR.R
142 - 156	1600.97	1599.96	1599.90	0.06	1	R.RGVMLAVDAVIAELK.K Oxidation (M)
206 - 221	1938.91	1937.91	1937.94	-0.03	1	K.TLNDELEIIEGMKFDR.G Oxidation (M)
237 - 249	1601.70	1600.69	1600.74	-0.05	0	K.CEFQDAYVLLSEK.K
269 - 290	2365.39	2364.39	2364.33	0.06	0	R.KPLVIIAEDVDGEALSTLVLNR.L
291 - 301	1153.75	1152.75	1152.76	-0.01	1	R.LKVGLQVVAVK.A
293 - 301	912.59	911.58	911.58	-0.00	0	K.VGLQVVAVK.A
302 - 309	833.38	832.37	832.38	-0.01	0	K.APGFGDNR.K
371 - 387	2038.07	2037.06	2037.02	0.05	0	R.IQEIIEQLDVTTSEYEK.E
371 - 389	2295.14	2294.13	2294.15	-0.02	1	R.IQEIIEQLDVTTSEYEKEK.L
390 - 396	843.51	842.50	842.50	0.01	1	K.LNERLAK.L
463 - 470	941.65	940.64	940.61	0.03	1	K.IGIEIIKR.T
474 - 481	844.50	843.49	843.49	0.01	0	K.IPAMTIAK.N

```
  1 MLRLPTVFRQ MRPVSRVLAP HLTRAYAKDV KFGADARALM LQGVDLLADA
 51 VAVTMGPKGR TVIIEQSWGS PKVTKDGVTV AKSIDLKDKY KNIGAKLVQD
101 VANNTNEEAG DGTTTATVLA RSIAKEGFEK ISKGANPVEI RRGVMLAVDA
151 VIAELKKQSK PVTTPEEIAQ VATISANGDK EIGNIISDAM KKVGRKGVIT
201 VKDGKTLNDE LEIIEGMKFD RGYISPYFIN TSKGQKCEFQ DAYVLLSEKK
251 ISSIQSIVPA LEIANAHRKP LVIIAEDVDG EALSTLVLNR LKVGLQVVAV
301 KAPGFGDNRK NQLKDMAIAT GGAVFGEEGL TLNLEDVQPH DLGKVGEVIV
351 TKDDAMLLKG KGDKAQIEKR IQEIIEQLDV TTSEYEKEKL NERLAKLSDG
401 VAVLKVGGTS DVEVNEKKDR VTDALNATRA AVEEGIVLGG GCALLRCIPA
451 LDSLTPANED QKIGIEIIKR TLKIPAMTIA KNAGVEGSLI VEKIMQSSSE
501 VGYDAMAGDF VNMVEKGIID PTKVVRTALL DAAGVASLLT TAEVVVTEIP
551 KEEKDPGMGA MGGMGGGMGG GMF
```

Spot 1082 HSP-60

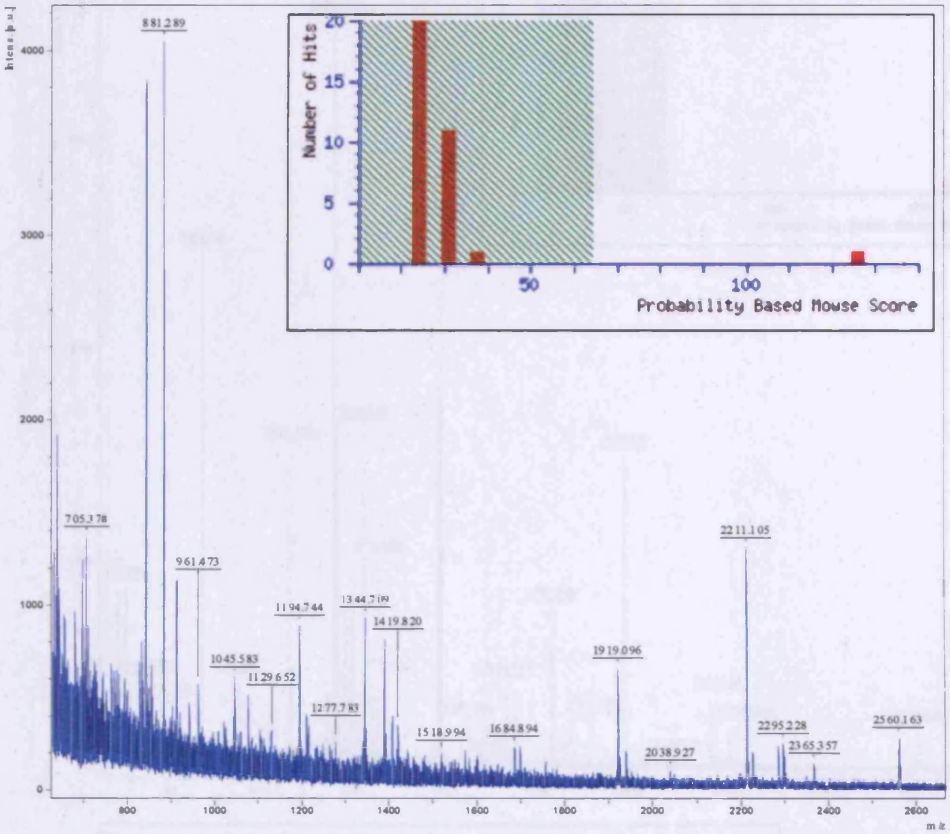

Start - End	Observed	Mr(expt)	Mr(calc)	Delta	Miss	Sequence
61 - 72	1344.71	1343.70	1343.71	-0.01	0	R.TVIIEQSWGSPK.V
97 - 121	2560.16	2559.16	2559.24	-0.09	0	K.LVQDVANNTNEEAGDGTTTATVLAR.S
134 - 141	855.44	854.43	854.46	-0.03	0	K.GANPVEIR.R
143 - 157	1572.96	1571.95	1571.90	0.05	1	R.GVMLAVDAVIAELKK.Q Oxidation (M)
206 - 221	1938.97	1937.96	1937.94	0.02	1	K.TLNDELEIIEGMKFDR.G Oxidation (M)
222 - 233	1389.74	1388.74	1388.70	0.04	0	R.GYISPYFINTSK.G
237 - 249	1601.81	1600.80	1600.74	0.06	0	K.CEFQDAYVLLSEK.K
251 - 268	1919.10	1918.09	1918.06	0.03	0	K.ISSIQSIVPALEIANAHR.K
269 - 290	2365.36	2364.35	2364.33	0.02	0	R.KPLVIIAEDVDGEALSTLVLNR.L
293 - 301	912.58	911.58	911.58	-0.00	0	K.VGLQVVAVK.A
302 - 309	833.40	832.39	832.38	0.01	0	K.APGFGDNR.K
302 - 310	961.47	960.47	960.48	-0.01	1	K.APGFGDNRK.N
371 - 389	2295.23	2294.22	2294.15	0.07	1	R.IQEIIEQLDVTTSEYEKEK.L
397 - 405	901.53	900.53	900.53	-0.00	0	K.LSDGVAVLK.V
430 - 446	1684.89	1683.89	1683.90	-0.01	0	R.AAVEEGIVLGGGCALLR.C
463 - 470	941.59	940.59	940.61	-0.02	1	K.IGIEIIKR.T
482 - 493	1215.60	1214.59	1214.65	-0.06	0	K.NAGVEGSLIVEK.I

```
  1 MLRLPTVFRQ MRPVSRVLAP HLTRAYAKDV KFGADARALM LQGVDLLADA
 51 VAVTMGPKGR TVIIEQSWGS PKVTKDGVTV AKSIDLKDKY KNIGAKLVQD
101 VANNTNEEAG DGTTTATVLA RSIAKEGFEK ISKGANPVEI RRGVMLAVDA
151 VIAELKKQSK PVTTPEEIAQ VATISANGDK EIGNIISDAM KKVGRKGVIT
201 VKDGKTLNDE LEIIEGMKFD RGYISPYFIN TSKGQKCEFQ DAYVLLSEKK
251 ISSIQSIVPA LEIANAHRKP LVIIAEDVDG EALSTLVLNR LKVGLQVVAV
301 KAPGFGDNRK NQLKDMAIAT GGAVFGEEGL TLNLEDVQPH DLGKVGEVIV
351 TKDDAMLLKG KGDKAQIEKR IQEIIEQLDV TTSEYEKEKL NERLAKLSDG
401 VAVLKVGGTS DVEVNEKKDR VTDALNATRA AVEEGIVLGG GCALLRCIPA
451 LDSLTPANED QKIGIEIIKR TLKIPAMTIA KNAGVEGSLI VEKIMQSSSE
501 VGYDAMAGDF VNMVEKGIID PTKVVRTALL DAAGVASLLT TAEVVVTEIP
551 KEEKDPGMGA MGGMGGGMGG GMF
```

Spot 996 HSP-70

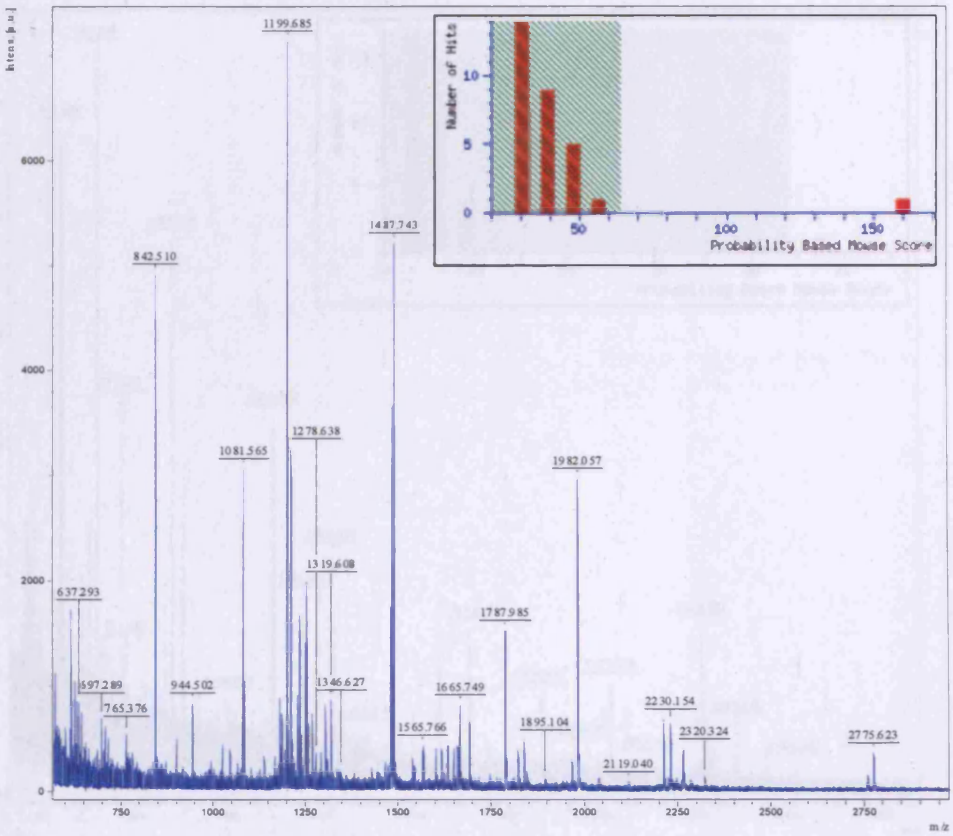

Start - End	Observed	Mr(expt)	Mr(calc)	Delta	Miss	Sequence
4 - 25	2263.10	2262.09	2262.11	-0.02	0	K.GPAVGIDLGTTYSCVGVFQHGKVEIIA.N
26 - 36	1228.65	1227.64	1227.62	0.02	0	K.NDQGNRTTPS.Y
37 - 49	1487.76	1486.74	1486.69	0.04	0	R.YVAFTDTERL.I
37 - 71	1649.76	1648.74	1648.79	-0.03	0	R.YVAFTDTERLIGDAAKNQVAMNPTNTVFDAKRLIGRRFDD.A
37 - 71	1665.75	1664.74	1664.78	-0.04	0	R.YVAFTDTERLIGDAAKNQVAMNPTNTVFDAKRLIGRRFDD.A Oxidation (M)
37 - 72	1021.87	1020.86	1020.88	-0.02	1	R.YVAFTDTERLIGDAAKNQVAMNPTNTVFDAKRLIGRRFDDA.V Oxidation (M)
183 - 192	1180.63	1179.62	1179.61	0.00	1	K.VQVEYKGETK.T
113 - 126	1616.81	1615.80	1615.78	0.02	0	K.SFYPEEVSSMVLTK.M
113 - 126	1632.76	1631.75	1631.78	-0.02	0	K.SFYPEEVSSMVLTK.M Oxidation (M)
127 - 137	1368.64	1367.63	1367.63	-0.01	1	K.MKEIAEAYLGK.T Oxidation (M)
130 - 155	1902.06	1901.05	1900.99	0.06	0	K.TVTNAVVTVPAYFNDSQRQ.A
168 - 171	1190.69	1190.68	1190.67	0.01	0	K.RAGVIAGLNVLR.I
172 - 187	1659.84	1658.84	1658.89	-0.05	0	R.IINEPTAAAIAYGLDKKV.G
172 - 188	1707.90	1706.90	1706.90	-0.01	1	R.IINEPTAAAIAYGLDKKVG.A
221 - 236	1691.77	1690.76	1690.79	-0.03	0	K.SVAGDTHLGGEDFDNRMVNH.F
237 - 240	1235.63	1234.64	1234.62	0.02	0	R.INEEPTAAIAYGLN.E
237 - 246	1251.63	1250.62	1250.61	0.01	0	R.INEEPTAAIAYGLN.E Oxidation (M)
300 - 311	1480.82	1479.81	1479.75	0.06	1	R.AAFDELRADLFR.G
326 - 343	1838.16	1837.09	1837.01	0.09	1	K.LDKSQIHDIVLVGGSTR.I
349 - 357	1081.57	1080.56	1080.56	-0.00	0	K.LLQDFFNGK.E
349 - 361	1565.77	1564.76	1564.82	-0.07	1	K.LLQDFFNGKELN.K
448 - 458	1304.69	1303.68	1303.63	-0.05	1	R.AMTKDNELLGK.F
540 - 550	1303.61	1302.61	1302.59	0.02	0	K.HSLESYAFNMK.A
540 - 550	1319.61	1318.60	1318.59	0.01	0	K.HSLESYAFNMK.A Oxidation (M)
584 - 597	1745.84	1744.84	1744.80	0.04	1	K.HQTAQEEFEHQQK.E
602 - 609	944.50	943.50	943.52	-0.02	0	K.VCNPIITK.L

```
  1 MSKGPAVGID LGTTYSCVGV FQHGKVEIIA NDQGNRTTPS YVAFTDTERL
 51 IGDAAKNQVA MNPTNTVFDA KRLIGRRFDD AVVQSDMKHW PFMVVNDAGR
101 PKVQVEYKGE TKSFYPEEVS SMVLTKMKEI AEAYLGKTVT NAVVTVPAYF
151 NDSQRQATKD AGTIAGLNVL RIINEPTAAA IAYGLDKKVG AERNVLIFDL
201 GGGTFDVSIL TIEDGIFEVK STAGDTHLGG EDFDNRMVNH FIAEFKRKHK
251 KDISENKRAV RRLRTACERA KRTLSSSTQA SIEIDSLYEG IDFYTSITRA
301 RFEELNADLF RGTLDPVEKA LRDAKLDKSQ IHDIVLVGGS TRIPKIQKLL
351 QDFFNGKELN KSINPDEAVA YGAAVQAAIL SGDKSENVQD LLLLDVTPLS
401 LGIETAGGVM TVLIKRNTTI PTKQTQTFTT YSDNQPGVLI QVYEGERAMT
451 KDNHLLGKFE LTGIPPAPRG VPQIEVTFDI DANGILNVSA VDKSTGKENK
501 ITITNDKGRL SKEDIERMVQ EAEKYKAEDE KQRDKVSSKN SLESYAFNMK
551 ATVEDEKLQG KINDEDKQKI LDKCNEIINW LDKNQTAEKE EFEHQQKELE
601 KVCNPIITKL YQSAGGMPGG MPGGFPGGGA PPSGGASSGP TIEEVD
```

Spot 1736 Maspin precusor

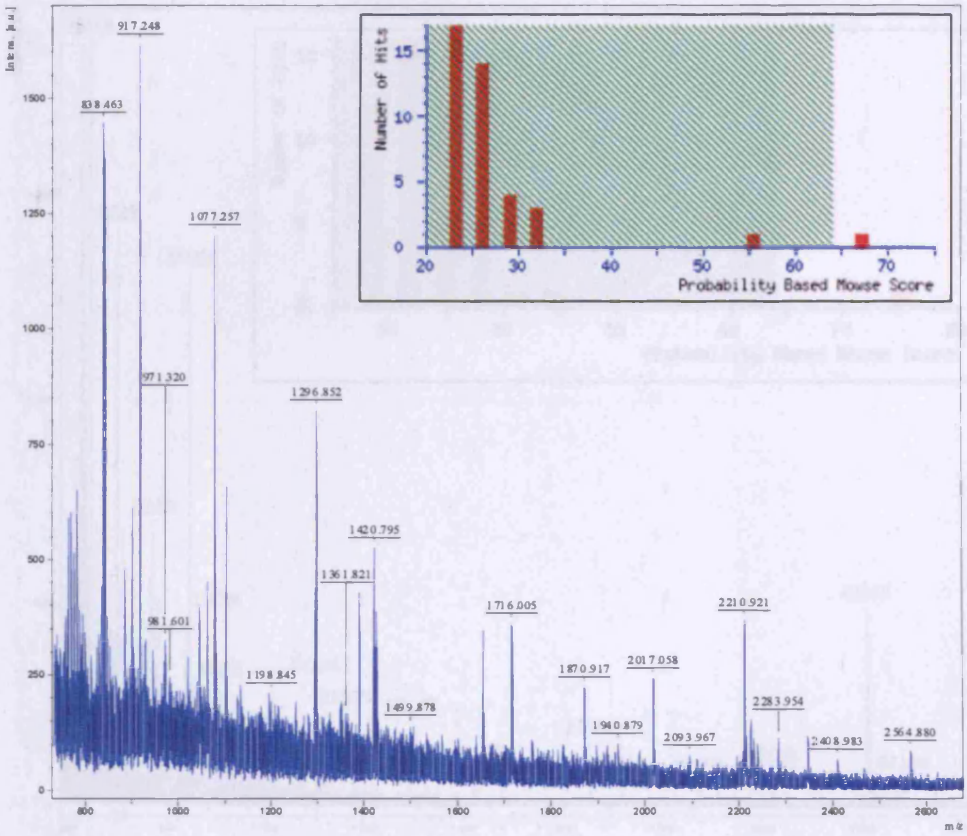

Start - End	Observed	Mr(expt)	Mr(calc)	Delta	Miss	Sequence
2 - 22	2239.99	2238.99	2239.09	-0.11	0	M.GQNSMDALQLANSAFAVDLFK.Q
53 - 69	1870.92	1869.91	1869.92	-0.01	0	K.GDTANEIGQVLHFENVK.D
70 - 84	1653.94	1652.93	1652.80	0.13	0	K.DVPFGFQTVTSDVNK.L
85 - 92	944.54	943.54	943.50	0.03	0	K.LSSFYSLK.L
143 - 163	2346.04	2345.04	2345.08	-0.04	0	K.DLTDGHFENILADNSVNDQTK.I
164 - 178	1739.01	1738.00	1737.96	0.04	1	K.ILVVNAAYFVGKWMK.K
221 - 229	1101.70	1100.69	1100.62	0.07	0	K.IIELPFQNK.H
230 - 239	1214.79	1213.79	1213.69	0.10	0	K.MLSMFILLPK.D Oxidation (M)
254 - 273	2222.87	2221.86	2222.03	-0.16	0	K.QLNSESLSQWTNPSTMANAK.V Oxidation (M)
300 - 316	1917.88	1916.87	1916.81	0.06	0	K.NIFSEDTSDFSGMSETK.G
300 - 316	1934.00	1932.99	1932.88	0.10	0	K.NIFSEDTSDFSGMSETK.G Oxidation (M)
327 - 345	2017.86	2016.85	2015.95	0.10	0	K.VCLEITEDGGDSIEVPGAR.I
351 - 364	1716.01	1715.00	1714.87	0.13	0	K.DELNADHPFIYIIR.H
370 - 376	838.46	837.46	837.47	-0.02	0	R.HIIFFGK.F

```
  1 MGQNSMDALQ LANSAFAVDL FKQLCEKEPL GNVLFSPICL STSLSLAQVG
 51 AKGDTANEIG QVLHFENVKD VPFGFQTVTS DVNKLSSFYS LKLIKRLYVD
101 KSLNLSTEFI SSTKRPYAKE LETVDFKDKL EETKGQINNS IKDLTDGHFE
151 NILADNSVND QTKILVVNAA YFVGKWMKKF PESETKECPF RLNKTDTKPV
201 QMMNMEATFC MGNIDSINCK IIELPFQNKH LSMFILLPKD VEDESTGLEK
251 IEKQLNSESL SQWTNPSTMA NAKVKLSIPK FKVEKMIDPK ACLENLGLKH
301 IFSEDTSDFS GMSETKGVAL SNVIHKVCLE ITEDGGDSIE VPGARILQHK
351 DELNADHPFI YIIRHNKTRN IIFFGKFCSP
```

Spot 1729 Maspin precusor

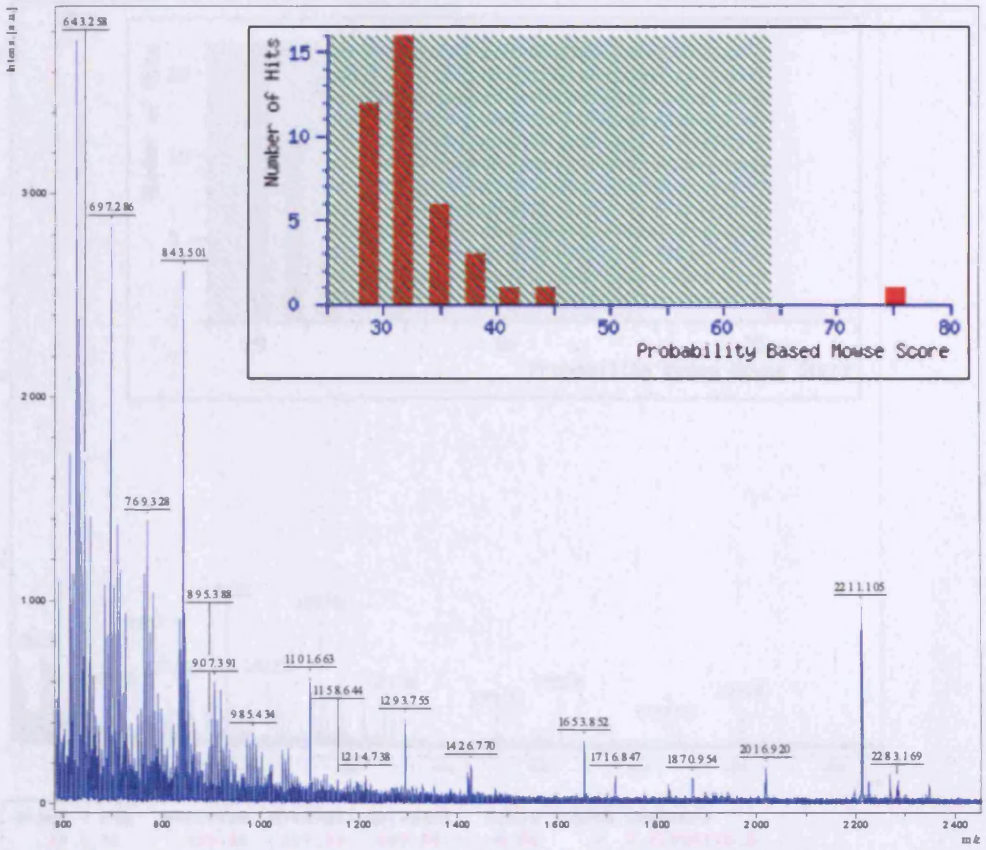

Start - End	Observed	Mr(expt)	Mr(calc)	Delta	Miss	Sequence
48 - 64	1870.95	1869.95	1869.92	0.03	0	K.GDTAMEIGQVLHFENVK.D
88 - 97	944.48	943.47	943.50	-0.03	0	K.LSSFYSLK.L
97 - 109	1426.77	1425.76	1425.74	0.03	0	K.SLHLSTEFISSTK.R
138 - 158	2346.15	2345.14	2345.08	0.06	0	K.DLTDGHFENILADHSVNDQTK.I
159 - 170	1293.76	1292.75	1292.75	-0.00	0	K.ILVVHAAYFVGK.W
159 - 173	1738.99	1737.99	1737.96	0.02	1	K.ILVVHAAYFVGKWMK.K
182 - 189	1063.48	1062.47	1062.53	-0.06	1	K.ECPFRLNK.T
216 - 224	1101.66	1100.66	1100.62	0.03	0	K.IIELPFQMK.H
225 - 234	1198.64	1197.64	1197.69	-0.06	0	K.HLSMFILLPK.D
225 - 234	1214.74	1213.73	1213.69	0.04	0	K.HLSMFILLPK.D Oxidation (M)
249 - 260	2222.98	2221.97	2222.03	-0.05	0	K.QLNSESLSQWTHPSTMANAK.V Oxidation (M)
295 - 311	1917.99	1916.98	1916.81	0.17	0	K.MIFSEDTSDFSGMSETK.G
295 - 311	1917.78	1916.77	1916.81	-0.04	0	K.MIFSEDTSDFSGMSETK.G
295 - 311	1933.88	1932.87	1932.80	0.06	0	K.MIFSEDTSDFSGMSETK.G Oxidation (M)
322 - 340	2016.92	2015.91	2015.95	-0.03	0	K.VCLEITEDGGDSIEVPGAR.I
346 - 359	1715.88	1714.87	1714.87	0.01	0	K.DELNADMPFIYIIR.H
365 - 371	838.47	837.46	837.47	-0.01	0	R.HIIPFGK.F
365 - 375	1329.66	1328.66	1328.66	-0.00	1	R.HIIPFGKFCSP.-

```
  1 MDALQLANSA FAVDLFKQLC EKEPLGNVLF SPICLSTSLS LAQVGAKGDT
 51 AMEIGQVLHF ENVKDIPFGF QTVTSDVNKL SSFYSLKLIK RLYVDKSLNL
101 STEFISSTKR PYAKELETVD FKDKLEETKG QINNSIKDLT DGHFENILAD
151 NSVNDQTKIL VVHAAYFVGK WMKKFPESET KECPFRLNKT DTKPVQMMNM
201 EATFCHGNID SINCKIIELP FQNKHLSMFI LLPKDVEDES TGLEKIEKQL
251 NSESLSQWTN PSTMANAKVK LSIPKFKVEK MIDPKACLEN LGLKHIFSED
301 TSDFSGMSET KGVALSNVIH KVCLEITEDG GDSIEVPGAR ILQHKDELNA
351 DHPFIYIIRH NKTRNIIFFG KFCSP
```

Spot 2507 Nucleoside diphosphate kinase A

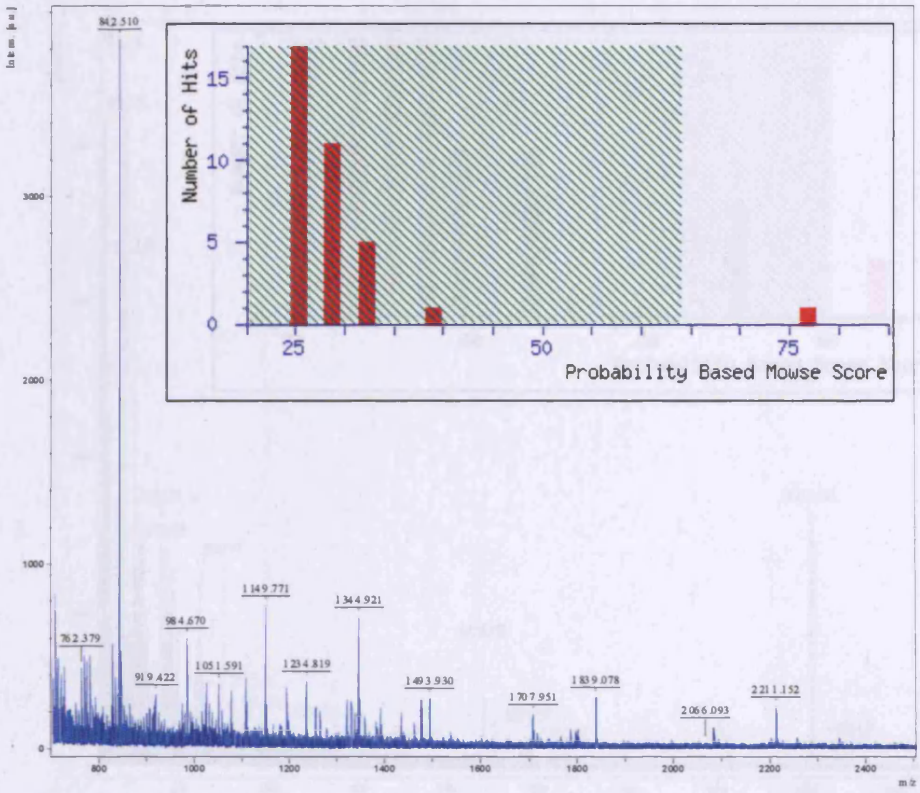

Start - End	Observed	Mr(expt)	Mr(calc)	Delta	Miss	Sequence
19 - 26	828.48	827.47	827.51	-0.04	0	R.GLVGEIIK.R
19 - 27	984.67	983.66	983.61	0.05	1	R.GLVGEIIKR.F
35 - 49	1707.95	1706.94	1706.93	0.02	1	R.LVGLKFMQASEDLLK.E Oxidation (M)
40 - 49	1197.68	1196.67	1196.57	0.09	0	K.FMQASEDLLK.E Oxidation (M)
40 - 56	2066.09	2065.09	2065.02	0.07	1	K.FMQASEDLLKEHYVDLK.D
67 - 85	2148.20	2147.19	2147.05	0.14	0	K.YDQSGPVVAMVWEGLNVVK.T 2 Oxidation (M)
89 - 105	1786.05	1785.04	1784.91	0.13	0	R.VMLGETNPADSKPGTIR.G
89 - 105	1802.07	1801.06	1800.90	0.16	0	R.VMLGETNPADSKPGTIR.G Oxidation (M)
106 - 114	1051.59	1050.58	1050.49	0.09	0	R.GDFCIQVGR.N

```
  1 MANCERTFIA IKPDGVQRGL VGEIIKRFEQ KGFRLVGLKF MQASEDLLKE
 51 HYVDLKDRPF FAGLVKYMHS GPVVAMVWEG LNVVKTGRVM LGETNPADSK
101 PGTIRGDFCI QVGRNIIHGS DSVESAEKEI GLWFHPEELV DYTSCAQNWI
151 YE
```

Spot 2248 Proteasome alpha 2 subunit

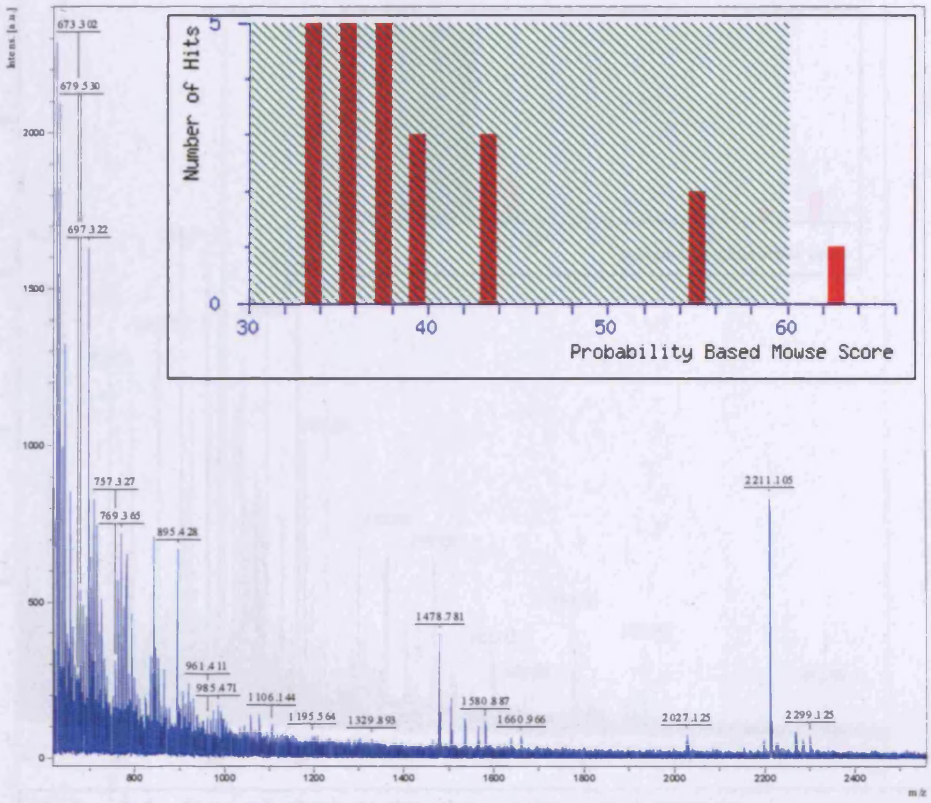

Start - End	Observed	Mr(expt)	Mr(calc)	Delta	Miss	Sequence
4 - 17	1478.78	1477.77	1477.71	0.07	0	R.GYSFSLTTFSPSGK.L
18 - 38	2027.13	2026.12	2026.15	-0.03	0	K.LVQIEYALAAVAGGAPSVGIK.A
53 - 59	895.43	894.42	894.44	-0.02	0	K.SILYDER.S
70 - 83	1564.75	1563.74	1563.75	-0.01	0	K.HIGLVYSGMGPDYR.V
171 - 175	637.31	636.30	636.35	-0.05	0	K.TFLEK.R
171 - 176	793.41	792.40	792.45	-0.05	1	K.TFLEKR.Y
219 - 226	943.54	942.53	942.55	-0.02	1	R.RLTPTEVK.D
220 - 226	787.38	786.37	786.45	-0.08	0	R.LTPTEVK.D
220 - 233	1504.83	1503.82	1503.82	0.00	1	R.LTPTEVKDYLAAIA.-

```
  1 AERGYSFSLT TFSPSGKLVQ IEYALAAVAG GAPSVGIKAA NGVVLATEKK
 51 QKSILYDERS VHKVEPITKH IGLVYSGMGP DYRVLVHRAR KLAQQYYLVY
101 QEPIPTAQLV QRVASVMQEY TQSGGVRPFG VSLLICGWNE GRPYLFQSDP
151 SGAYFAWKAT AMGKNYVNGK TFLEKRYNED LELEDAIHTA ILTLKESFEG
201 QMTEDNIEVG ICNEAGFRRL TPTEVKDYLA AIA
```

Spot 1204 Protein disulfide-isomerase A3 precusor

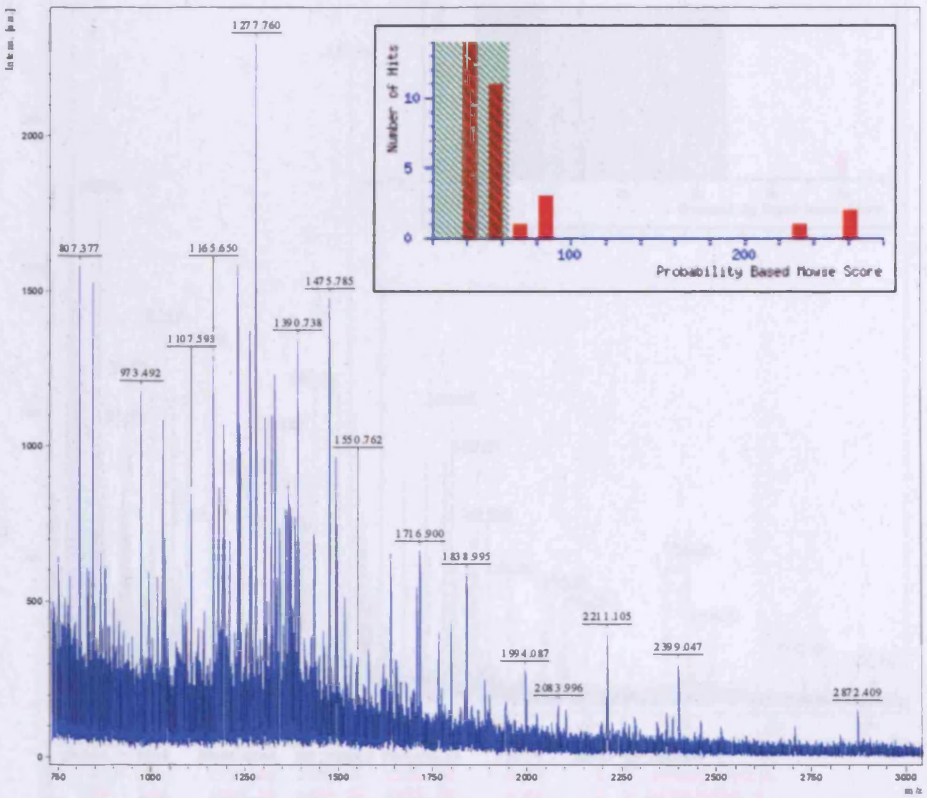

Start - End	Observed	Mr(expt)	Mr(calc)	Delta	Miss	Sequence	
21 - 38	1994.09	1993.08	1992.96	0.12	0	R.LVAASDVLELIDDNFESR.I	
63 - 73	1191.65	1190.64	1190.59	0.05	0	R.LAPEYEAAATR.L	
105 - 119	1652.83	1651.82	1651.76	0.07	1	K.IFRDGEEAGAYDGPR.T	
174 - 183	1179.66	1178.65	1178.58	0.07	1	K.AASNLRDNYR.F	
259 - 271	1619.82	1618.82	1618.78	0.04	0	K.DLLIAYYDVDYEK.N	
297 - 304	877.47	876.46	876.48	-0.02	0	K.LNFAVASR.K	
336 - 344	1172.60	1171.60	1171.53	0.06	0	K.FVMQEEFSR.D	
352 - 363	1515.87	1514.86	1514.75	0.11	1	R.FLQDYFDGMLKR.Y	
380 - 395	1833.04	1832.03	1831.90	0.13	0	K.VVVAENFDEIVNNENK.D	
434 - 448	1680.69	1679.68	1679.75	-0.06	0	K.NDATANDVPSPYEVR.G	Oxidation (M)
449 - 460	1341.71	1340.70	1340.68	0.02	0	R.GFPTIYFSPANK.K	
462 - 466	599.44	598.43	598.38	0.05	1	K.LNPKK.Y	
472 - 482	1370.82	1369.81	1369.69	0.12	0	R.ELSDFISYLQR.E	
483 - 496	1579.92	1578.91	1578.83	0.09	0	R.EATNPPVIQEEKPK.K	
483 - 497	1707.84	1706.83	1706.92	-0.09	1	R.EATNPPVIQEEKPKK.K	

```
  1 MRLRRLALFP GVALLLAAGR LVAASDVLEL TDDNFESRIS DTGSAGLMLV
 51 EFFAPWCGHC KRLAPEYEAA ATRLKGIVPL AKVDCTANTN TCNKYGVSGY
101 PTLKIFRDGE EAGAYDGPRT ADGIVSHLKK QAGPASVPLR TEEEFKKFIS
151 DKDASIVGFF DDSFSEAHSE FLKAASNLRD NYRFAHTNVE SLVNEYDDNG
201 EGIILFRPSH LTNKFEDKTV AYTEQKMTSG KIKKFIQENI FGICPHMTED
251 NKDLIQGKDL LIAYYDVDYE KNAKGSNYWR NRVMMVAKKF LDAGHKLNFA
301 VASRKTFSHE LSDFGLESTA GEIPVVAIRT AKGEKFVMQE EFSRDGKALE
351 RFLQDYFDGN LKRYLKSEPI PESNDGPVKV VVAENFDEIV NNENKDVLIE
401 FYAPWCGHCK NLEPKYKELG EKLSKDPNIV IAKMDATANE VPSPYEVRGF
451 PTIYFSPANK KLNPKKYEGG RELSDFISYL QREATNPPVI QEEKPKKKKK
501 AQEDL
```

Spot 1216 Protein disulfide-isomerase A3 precusor

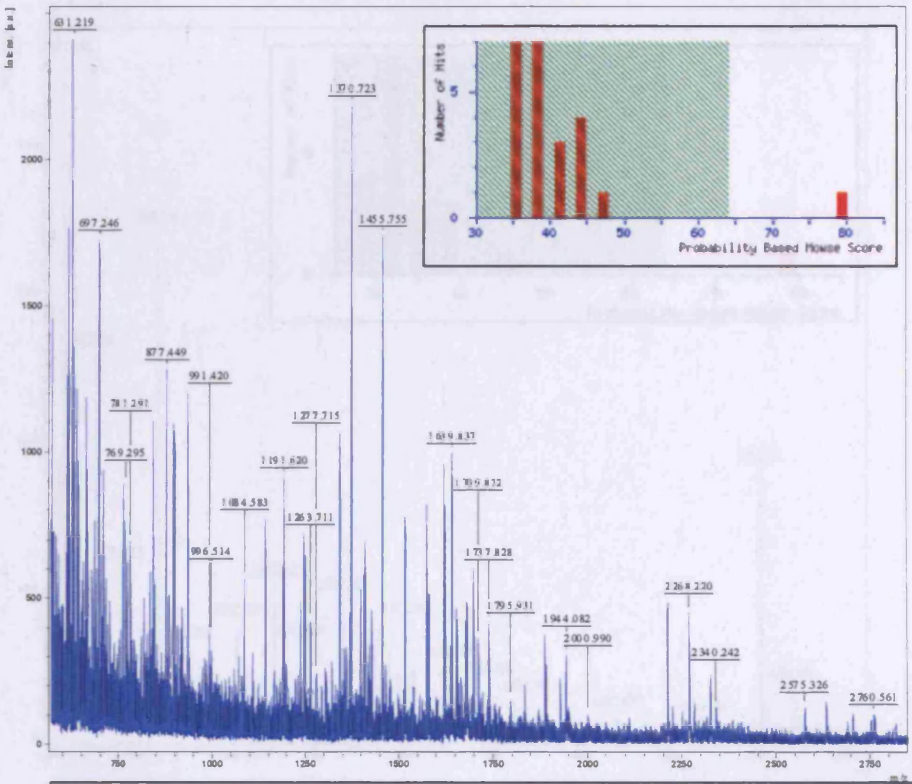

Start - End	Observed	Mr(expt)	Mr(calc)	Delta	Miss	Sequence
63 - 73	1191.62	1190.61	1190.59	0.02	0	R.LAPEYEAAATR.L
95 - 104	1084.58	1083.58	1083.56	0.02	0	K.YGVSGYPTLK.I
105 - 119	1652.82	1651.81	1651.76	0.05	1	K.IFRDGEEAGAYDGPR.T
108 - 119	1236.59	1235.58	1235.51	0.08	0	R.DGEEAGAYDGPR.T
213 - 226	1427.73	1426.72	1426.70	0.02	1	K.FEDKTVAYTEPK.M
297 - 304	877.45	876.44	876.48	-0.04	0	K.LMFAVASR.K
306 - 329	2575.33	2574.32	2574.30	0.02	0	K.TFSMELSDFGLESTAGEIPVVAIR.T
336 - 344	1172.48	1171.47	1171.53	-0.06	0	K.FVMQEEFSR.D
336 - 344	1188.56	1187.55	1187.53	0.02	0	K.FVMQEEFSR.D Oxidation (M)
352 - 362	1359.67	1358.67	1358.65	0.02	0	R.FLQDYFDGMLK.R
352 - 363	1515.78	1514.78	1514.75	0.03	1	R.FLQDYFDGMLKR.Y
367 - 379	1368.63	1367.63	1367.66	-0.03	0	K.SEPIPESMDGPVK.V
388 - 395	1833.01	1832.01	1831.90	0.11	0	K.VVVAEMFDEIVNNENK.D
434 - 448	1664.80	1663.79	1663.75	0.04	0	K.MDATAMDVPSPYEVR.G
434 - 448	1680.84	1679.84	1679.75	0.09	0	K.MDATAMDVPSPYEVR.G Oxidation (M)
449 - 460	1341.70	1340.69	1340.68	0.02	0	R.GFPTIYFSPAMK.K
472 - 482	1370.72	1369.72	1369.69	0.03	0	R.ELSDFISYLQR.E
483 - 496	1579.84	1578.84	1578.83	0.01	0	R.EATMPPVIQEEKPK.K

```
  1 MRLRRLALFP GVALLLAAAR LAAASDVLEL TDDNFESRIS DTGSAGLMLV
 51 EFFAPWCGHC KRLAPEYEAA ATRLKGIVPL AKVDCTANTN TCNKYGVSGY
101 PTLKIFRDGE EAGAYDGPRT ADGIVSHLKK QAGPASVPLR TEEEFKKFIS
151 DKDASIVGFF DDSFSEAHSE FLKAASNLRD NYRFAHTNVE SLVNEYDDNG
201 EGIILFRPSH LTNKFEDKTV AYTEPKMTSG KIKKFIQGNI FGICPHMTED
251 NKDLIQGKDL LIAYYDVDYE KNAKGSNYWR NRVMMVAKKF LDAGHKLNFA
301 VASRKTFSME LSDFGLESTA GEIPVVAIRT AKGEKFVMQE EFSRDGKALE
351 RFLQDYFDGN LKRYLKSEPI PESNDGPVKV VVAENFDEIV NNENKDVLIE
401 FYAPWCGHCK NLEPKYKELG EKLSKDPNIV IAKMDATAND VPSPYEVRGF
451 PTIYFSPAMK KLNPKKYEGG RELSDFISYL QREATNPPVI QEEKPKKKKK
501 AQEDL
```

Spot 1178 Protein disulfide-isomerase ER60 precusor

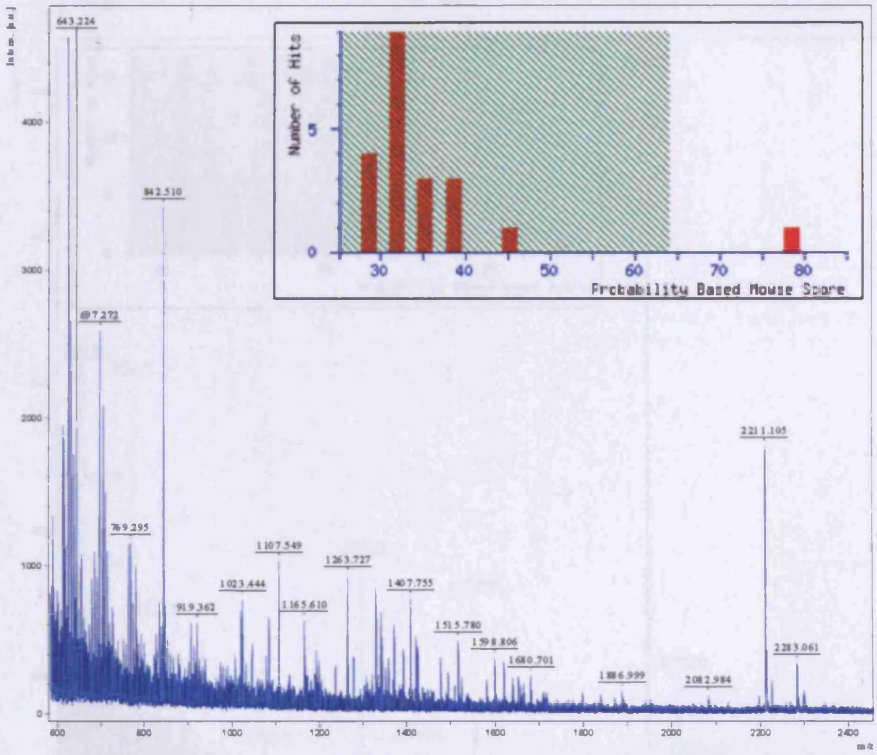

Start - End	Observed	Mr(expt)	Mr(calc)	Delta	Miss	Sequence	
63 - 73	1191.62	1190.61	1190.59	0.01	0	R.LAPEYEAAATR.L	
95 - 104	1084.57	1083.56	1083.56	0.00	0	K.YGVSGYPTLK.I	
105 - 119	1652.84	1651.83	1651.76	0.07	1	K.IFRDGEEAGAYDGPR.Y	
259 - 271	1619.79	1618.79	1618.78	0.01	0	K.DLLIAYYDVDYEK.N	
352 - 363	1515.78	1514.77	1514.75	0.02	1	R.FLQDYFDGNLKR.Y	
434 - 448	1664.83	1663.82	1663.75	0.07	0	K.NDATANDVPSPYEVR.G	
434 - 448	1680.70	1679.69	1679.75	-0.05	0	K.NDATANDVPSPYEVR.G	Oxidation (M)
449 - 460	1341.68	1340.67	1340.68	-0.00	0	R.GFPTIYFSPANK.K	
472 - 482	1370.70	1369.69	1369.69	0.00	0	R.ELSDFISYLQR.E	
483 - 496	1579.82	1578.81	1578.83	-0.01	0	R.EATMPPVIQEEKPK.K	

```
  1 MRLPRLALFP GVALLLAAAR LAAASDVLEL TDDNFESRIS DTGSAGLMLV
 51 EFFAPWCGHC KRLAPEYEAA ATRLKGIVPL AKVDCTANTN TCNKYGVSGY
101 PTLKIFRDGE EAGAYDGPRT ADGIVSHLKK QAGPASVPLR TEEEFKKFIS
151 DKDASIVGFF DDSFSEAHSE FLKAASNLRD NYRFAHTNVE SLVNEYDDNG
201 EGIILFRPSH LTNKFEDKTV AYTEPKMTSG KIKKFIQGNI FGICPHMTED
251 NKDLIQGKDL LIAYYDVDYE KNAKGSNYWR NRVMMVAKKF LDAGHKLNFA
301 VASRKTFSHE LSDFGLESTA GEIPVVAIRT AKGEKFVMQE EFSRDGKALE
351 RFLQDYFDGN LKRYLKSEPI PESNDGPVKV VVAENFDEIV NNENKDVLIE
401 FYAPWCGHCK NLEPKYKELG EKLSKDPNIV IAKMDATAND VPSPYEVRGF
451 PTIYFSPANK KLNPKKYEGG RELSDFISYL QREATMPPVI QEEKPKKKKK
501 AQEDL
```

Spot 2254 Rho-GDP-dissociation inhibitor 1

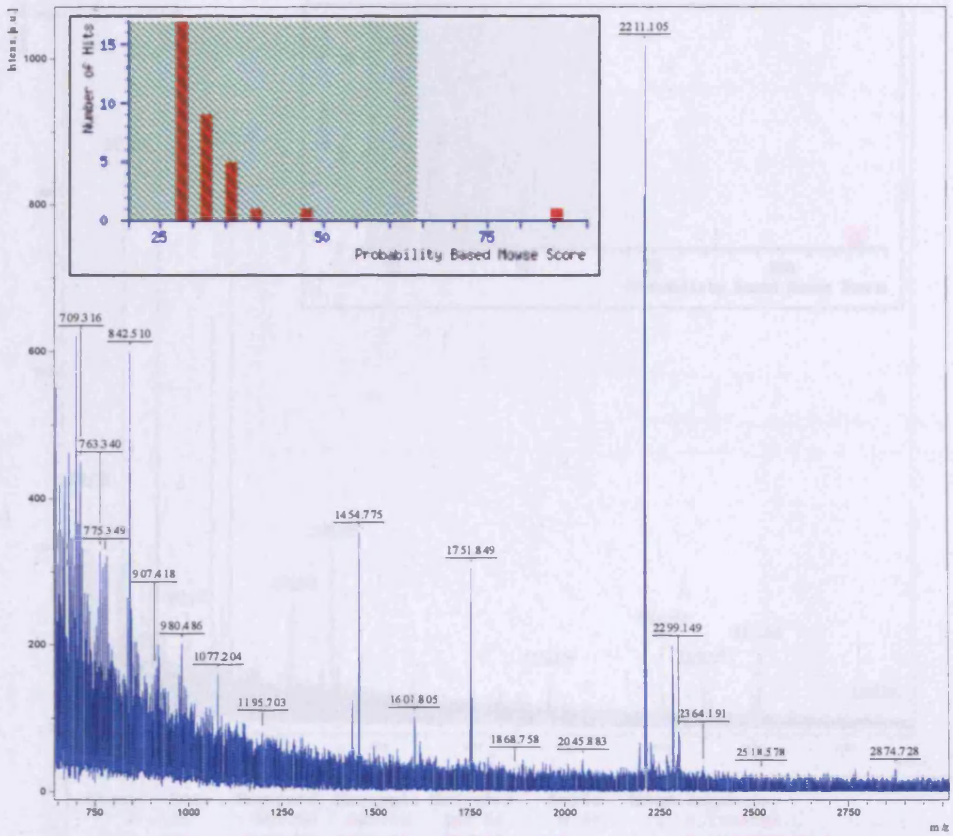

Start - End	Observed	Mr(expt)	Mr(calc)	Delta	Miss	Sequence
34 - 43	1202.72	1201.72	1201.62	0.10	0	K.SIQEIQELDK.D
100 - 111	1454.77	1453.77	1453.76	0.01	1	K.QSFVLKEGVEYR.I
118 - 127	1132.62	1131.61	1131.61	0.01	1	R.VMREIVSGMK.Y
118 - 127	1148.59	1147.58	1147.60	-0.02	1	R.VMREIVSGMK.Y Oxidation (M)
121 - 127	763.34	762.33	762.39	-0.06	0	R.EIVSGMK.Y
128 - 134	980.49	979.48	979.49	-0.01	0	K.YIGMTYR.K
139 - 152	1601.80	1600.80	1600.76	0.04	1	K.IDKTDYMVGSYGPR.A
139 - 152	1617.81	1616.81	1616.75	0.06	1	K.IDKTDYMVGSYGPR.A Oxidation (M)
142 - 152	1245.61	1244.60	1244.55	0.05	0	K.TDYMVGSYGPR.A
142 - 152	1261.58	1260.58	1260.54	0.03	0	K.TDYMVGSYGPR.A Oxidation (M)
153 - 167	1751.85	1750.84	1750.83	0.01	0	R.AEEYEFLTPVEEAPK.G
153 - 172	2296.09	2295.08	2295.11	-0.03	1	R.AEEYEFLTPVEEAPKGMLAR.G Oxidation (M)
181 - 199	2364.19	2363.18	2363.11	0.08	1	R.FTDDDKTDHLSWEWNLTIK.K

```
  1 MAEQEPTAEQ LAQIAAENEE DEHSVNYKPP AQKSIQEIQE LDKDDESLRK
 51 YKEALLGRVA VSADPNVPNV VVTGLTLVCS SAPGPLELDL TGDLESFKKQ
101 SFVLKEGVEY RIKISFRVNR EIVSGMKYIQ HTYRKGVKID KTDYMVGSYG
151 PRAEEYEFLT PVEEAPKGML ARGSYSIKSR FTDDDKTDHL SWEWNLTIKK
201 DWKD
```

Spot 2518 Ubiquitin-conjugating enzyme E2N

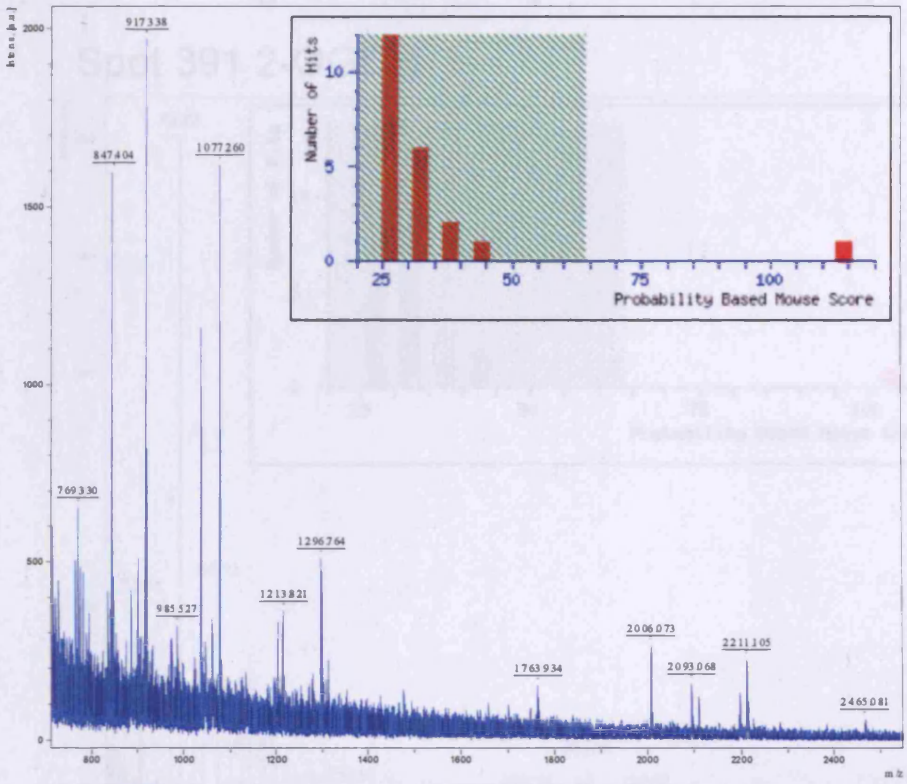

Start - End	Observed	Mr(expt)	Mr(calc)	Delta	Miss	Sequence
8 - 14	887.56	886.55	886.52	0.03	1	R.IIKETQR.L
15 - 24	1036.70	1035.69	1035.63	0.06	0	R.LLAEPVPGIK.A
15 - 33	2006.07	2005.07	2005.85	0.02	1	R.LLAEPVPGIKAEPDESNAR.Y
34 - 53	2196.24	2195.23	2195.07	0.16	0	R.YFNVVIAGPQDSPFEGGTFK.L
54 - 68	1763.93	1762.93	1762.89	0.04	0	K.LELFLPEEYPMAAPK.V Oxidation (M)
54 - 70	2019.05	2018.04	2018.85	-0.01	1	K.LELFLPEEYPMAAPKVR.F Oxidation (M)
75 - 82	985.53	984.52	984.50	0.02	0	K.IYKPNVDK.L
75 - 85	1311.83	1310.82	1310.71	0.12	1	K.IYKPNVDKLGR.I
86 - 92	874.54	873.53	873.50	0.03	0	R.ICLDILK.D
146 - 152	854.39	853.38	853.40	-0.02	0	R.LYAMDNI.- Oxidation (M)

```
  1 MAGLPRRIIK ETQRLLAEPV PGIKAEPDES NARYFHVVIA GPQDSPFEGG
 51 TFKLELFLPE EYPMAAPKVR FMTKIYHPNV DKLGRICLDI LKDKWSPALQ
101 IRTVLLSIQA LLSAPNPDDP LANDVAEQWK TNEAQAIETA RAWTRLYAMN
151 NI
```

Appendix D--Spectra, MOWSE scores, matched peptide and sequence coverage of identified proteins (Table 4-2)

Spot 391 2-OGDH

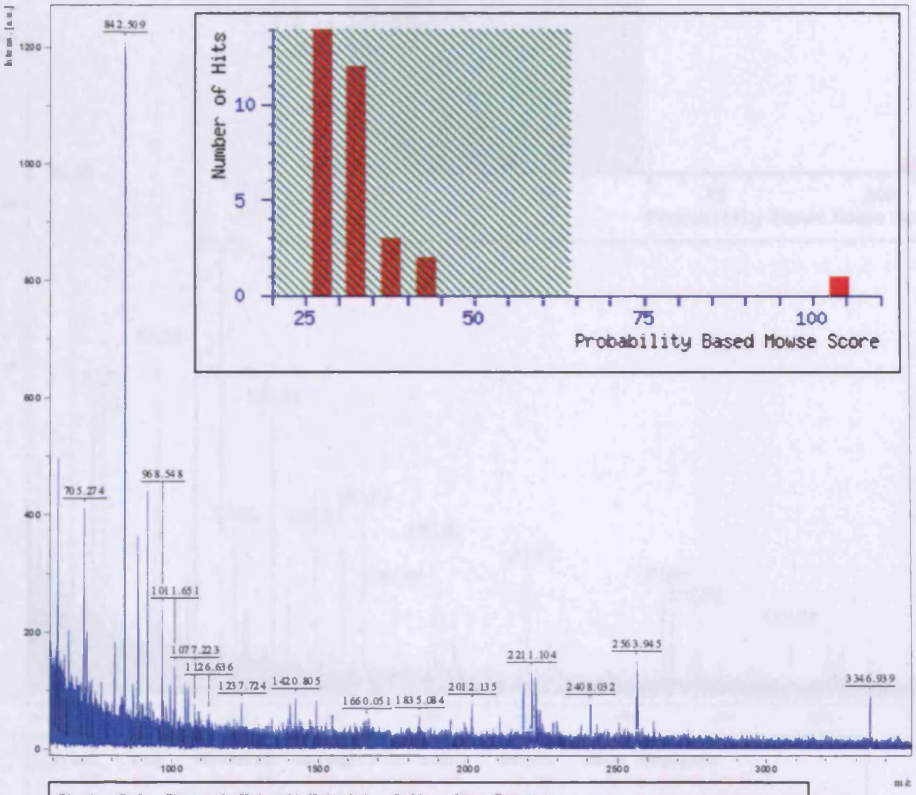

Start - End	Observed	Mr(expt)	Mr(calc)	Delta	Miss	Sequence
82 - 101	2012.14	2011.13	2011.01	0.12	0	R.HTHAGAPPGTAYQSPLPLSR.G
123 - 135	1492.93	1491.92	1491.84	0.08	0	K.LVEDMLAVQSLIR.A
172 - 184	1471.81	1470.81	1470.69	0.12	0	K.LGFYGLDESPLDK.V
185 - 204	2184.12	2183.12	2183.17	-0.06	0	K.VFHLPTTTFIGGQESALPLR.E
264 - 270	968.55	967.54	967.48	0.06	0	R.FEEFLQR.K
270 - 291	1545.96	1544.96	1544.83	0.13	0	R.PGLEGCEVLIPALK.Y
292 - 312	2378.16	2377.15	2377.14	0.01	1	K.TIDKSSEHGVDTVINGHPKR.G Oxidation (H)
313 - 323	1011.65	1010.64	1010.62	0.02	0	K.LNVLAIVIR.E
325 - 336	1543.71	1542.71	1542.70	0.00	0	K.ELEQIFCQFDSK.L
300 - 309	1237.72	1736.72	1236.62	0.10	0	K.DVVVDLVCYR.E
575 - 582	995.50	994.57	994.50	-0.01	1	K.DEKILMIK.H
845 - 851	806.59	805.58	805.54	0.04	0	R.QILLPER.E
852 - 860	1056.70	1055.77	1055.67	0.10	0	R.KPLIIFTPK.S
870 - 883	1667.89	1666.89	1666.74	0.15	0	R.SSFDEMLPGTHFQR.V Oxidation (M)
900 - 914	929.43	928.43	928.47	-0.04	0	K.VTYDLTR.E
930 - 943	1660.85	1659.84	1650.93	0.12	0	R.IEQLSPTPTDLLLK.E
948 - 961	1774.90	1773.89	1773.78	0.11	0	K.YPNAELANCQEEHK.H
962 - 972	1402.79	1401.78	1401.67	0.12	0	K.HQGYTDVVKPR.L
980 - 988	1047.65	1046.64	1046.57	0.08	0	R.AKPVVYAGR.H

Spot 1123 Cytokeratin 6A

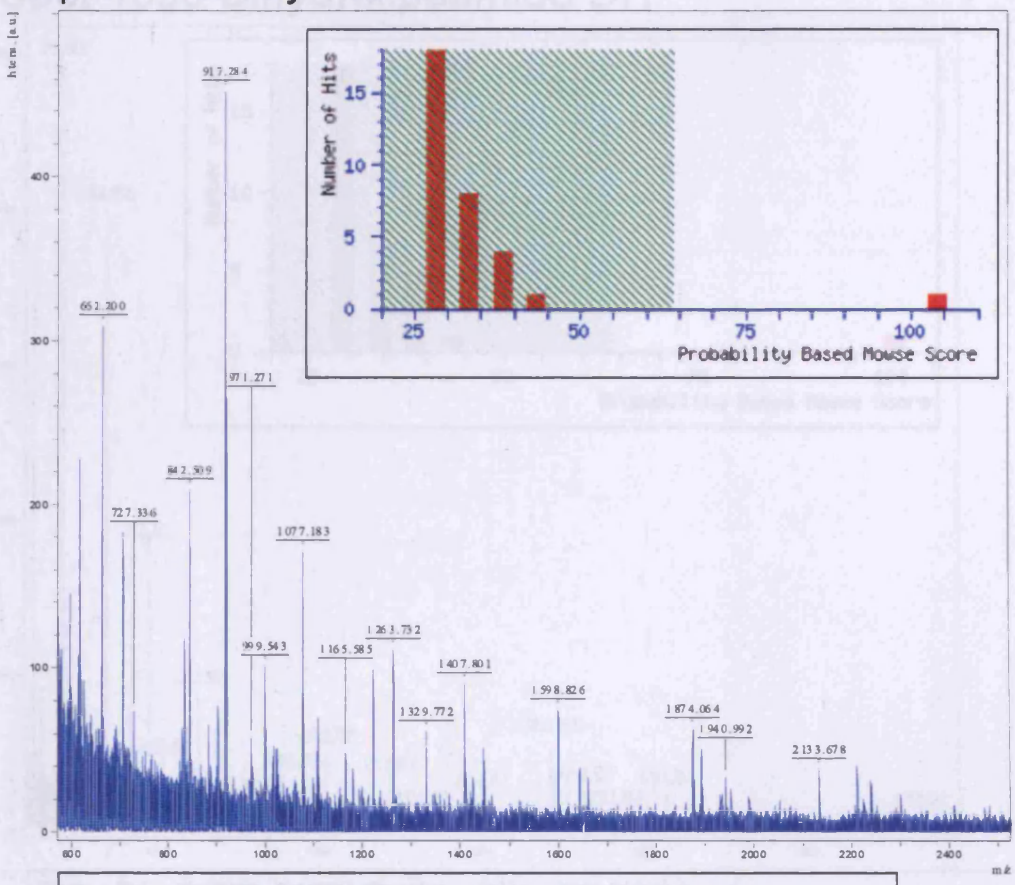

Start - End	Observed	Mr(expt)	Mr(calc)	Delta	Miss	Sequence
59 - 67	881.47	880.46	880.47	-0.00	0	R.SLYGLGGSK.R
69 - 85	1598.83	1597.82	1597.75	0.07	0	R.ISIGGGSCAISGGYGSR.A
173 - 179	827.43	826.42	826.42	0.00	0	K.FASFIDK.V
207 - 221	1891.02	1890.01	1889.96	0.05	0	R.QMLEPLFEQYINNLR.R
223 - 231	1016.51	1015.50	1015.53	-0.03	0	R.QLDSIVGER.G
240 - 249	1181.60	1180.59	1180.54	0.05	0	R.GMQDLVEDFK.N
260 - 270	1222.68	1221.67	1221.62	0.05	0	R.TAAENEFVTLK.K
287 - 298	1407.80	1406.79	1406.70	0.09	0	K.ADTLTDEINFLR.A
326 - 337	1329.77	1328.76	1328.72	0.05	0	R.NLDLDSIIAEVK.A
338 - 346	1107.58	1106.57	1106.54	0.04	0	K.AQYEEIAQR.S
359 - 368	1165.59	1164.58	1164.58	0.00	0	K.YEELQVTAGR.H
455 - 465	1263.73	1262.73	1262.69	0.04	0	K.LALDVEIATYR.K
533 - 549	1447.82	1446.82	1446.77	0.05	0	R.AIGGGLSSVGGGSSTIK.Y

```
  1 ASTSTTIRSH SSSRRGFSAN SARLPGVSRS GFSSVSVSRS RGSGGLGGAC
 51 GGAGFGSRSL YGLGGSKRIS IGGGSCAISG GYGSRAGGSY GFGGAGSGFG
101 FGGGAGIGFG LGGGAGLAGG FGGPGFPVCP PGGIQEVTVN QSLLTPLNLQ
151 IDPTIQRVRA EEREQIKTLN NKFASFIDKV RFLEQQNKVL ETKWTLLQEQ
201 GTKTVRQNLE PLFEQYINNL RRQLDSIVGE RGRLDSELRG MQDLVEDFKN
251 KYEDEINKRT AAENEFVTLK KDVDAAYMNK VELQAKADTL TDEINFLRAL
301 YDAELSQMQT HISDTSVVLS MDNNRNLDLD SIIAEVKAQY EEIAQRSRAE
351 AESWYQTKYE ELQVTAGRHG DDLRNTKQEI AEINRMIQRL RSEIDHVKKQ
401 CANLQAAIAD AEQRGEMALK DAKNKLEGLE DALQKAKQDL ARLLKEYQEL
451 MNVKLALDVE IATYRKLLEG EECRLNGEGV GQVNISVVQS TVSSGYGGAS
501 GVGSGLGLGG GSSYSYGSGL GVGGGFSSSS GRAIGGGLSS VGGGSSTIKY
551 TTTSSSSRKS YKH
```

Spot 1090 Dihydrolipoamide DH

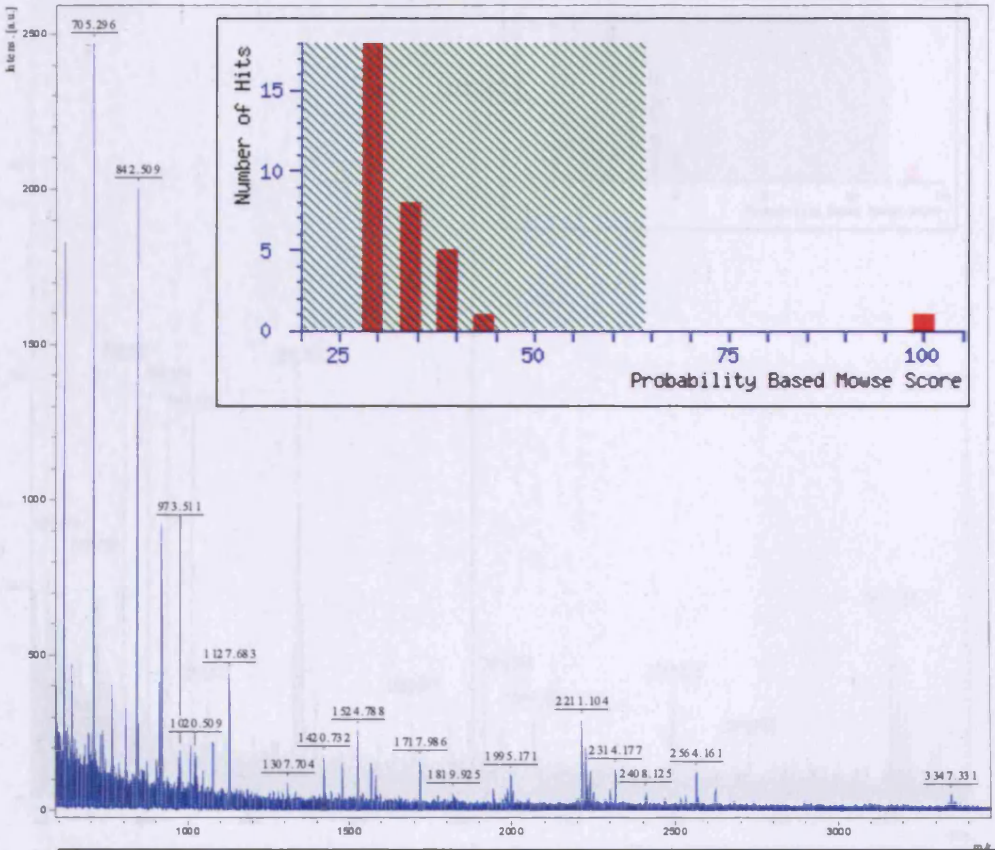

Start - End	Observed	Mr(expt)	Mr(calc)	Delta	Miss	Sequence
71 - 77	734.35	733.35	733.41	-0.07	0	K.AAQLGFK.T
84 - 100	1819.92	1818.92	1818.86	0.06	0	K.METLGGTCLNVGCIPSK.A
101 - 115	1771.87	1770.86	1770.83	0.04	0	K.ALLMMSMYYHMAHGK.D Oxidation (M)
144 - 154	1127.68	1126.68	1126.65	0.03	0	K.ALTGGIAMLFK.Q
227 - 245	1986.24	1985.23	1985.08	0.16	0	K.MVVIGAGVIGVELGSVWQR.L Oxidation (M)
246 - 270	2514.42	2513.42	2513.28	0.13	0	R.LGADVTAVEFLGHVGGVGIDMEISK.N
246 - 270	2530.38	2529.38	2529.28	0.02	0	R.LGADVTAVEFLGHVGGVGIDMEISK.N Oxidation (M)
312 - 326	1717.99	1716.98	1716.89	0.09	0	K.AEVITCDVLLVCIGR.R
332 - 345	1567.94	1566.93	1566.83	0.11	0	K.NLGLEELGIELDPR.G
358 - 376	1995.17	1994.16	1994.07	0.10	0	K.IPNIYAIGDVVAGPMLAHK.A Oxidation (M)
416 - 428	1581.88	1580.87	1580.76	0.12	1	K.SEEQLKEEGIEYK.V
432 - 439	909.46	908.46	908.45	0.01	0	K.FPFAANSR.A
494 - 506	1524.79	1523.78	1523.73	0.05	0	R.VCHAHPTLSEAFR.E
507 - 516	1007.54	1006.54	1006.51	0.03	0	R.EAMLAASFGK.S

```
  1 KYWRKGKYSG KMQSWSRVYC SLAKRGHFNR ISHGLQGLSA VPLRTYADQP
 51 IDADVTVIGS GPGGYVAAIK AAQLGFKTVC IEKNETLGGT CLNVGCIPSK
101 ALLMMSMYYH MAHGKDFASR GIEMSEVRLN LDKMMEQKST AVKALTGGIA
151 MLFKQNKVVH VNGYGKITGK NQVTATKADG GTQVIDTKNI LIATGSEVTP
201 FPGITIDEDT IVSSTGALSF KKVPEKMVVI GAGVIGVELG SVWQRLGADV
251 TAVEFLGHVG GVGIDMEISK NFQRILQKQG FKFKLNTKVT GATKKSDGKI
301 DVSIEAASGG KAEVITCDVL LVCIGRRPFT KNLGLEELGI ELDPRGRIPV
351 NTRFQTKIPN IYAIGDVVAG PMLAHKAEDE GIICVEGMAG GAVHIDYNCV
401 PSVIYTHPEV AWVGKSEEQL KEEGIEYKVG KFPFAANSRA KTNADTDGMV
451 KILGQKSTDR VLGAHILGPG AGEMVNEAAL ALEYGASCED IARVCHAHPT
501 LSEAFREANL AASFGKSINF
```

Spot 471 Elongation factor 2

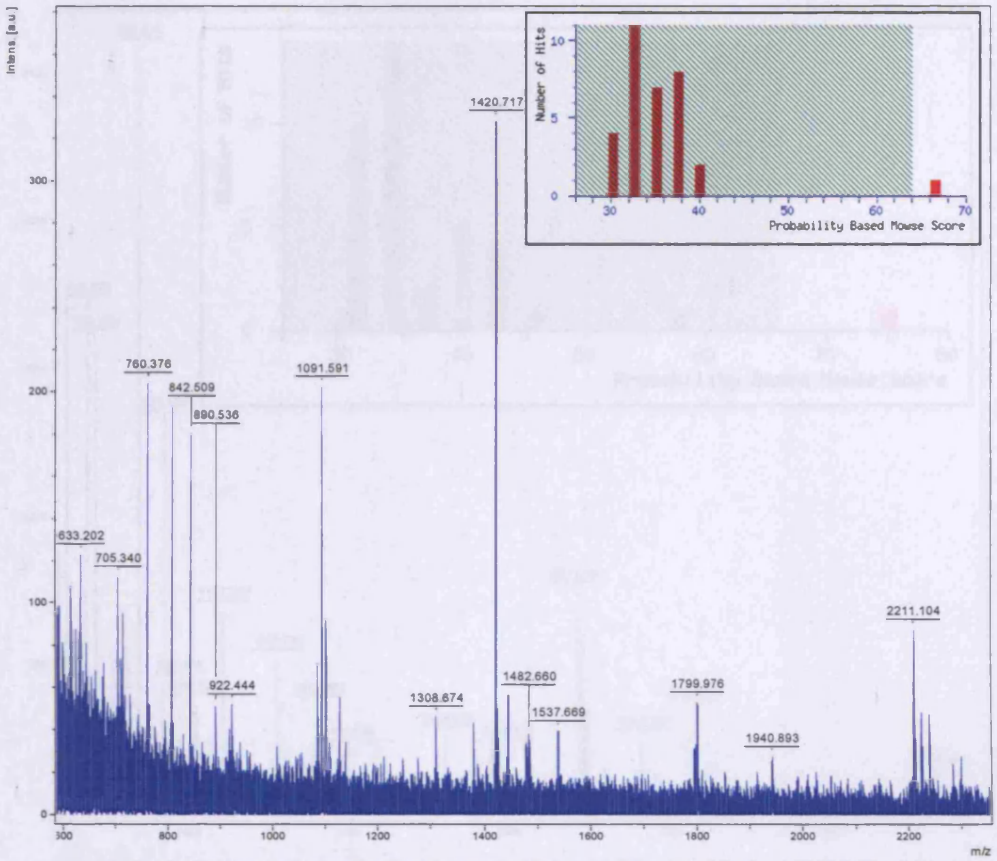

Start - End	Observed	Mr(expt)	Mr(calc)	Delta	Miss	Sequence
1 - 9	1091.59	1090.58	1090.58	0.01	0	-.VNFTVDQIR.A
299 - 307	1084.59	1083.58	1083.54	0.04	0	K.VFDAIMNFK.K
299 - 307	1100.54	1099.54	1099.54	-0.00	0	K.VFDAIMNFK.K Oxidation (M)
308 - 313	705.34	704.33	704.37	-0.04	1	K.KEETAK.L
409 - 414	760.38	759.37	759.37	-0.00	0	R.FYAFGR.V
415 - 425	1107.66	1106.65	1106.63	0.02	0	R.VFSGLVSTGLK.V
498 - 505	890.54	889.53	889.50	0.03	0	K.FSVSPVVR.V
572 - 579	922.44	921.44	921.46	-0.02	0	K.SDPVVSYR.E
638 - 646	1138.51	1137.50	1137.51	-0.01	0	K.YEWDVAEAR.K
676 - 687	1308.67	1307.67	1307.65	0.02	0	K.DSVVAGFQWATK.E
727 - 738	1378.66	1377.66	1377.71	-0.05	0	R.CLYASVLTAQPR.L
785 - 800	1799.98	1798.97	1798.89	0.08	0	K.AYLPVNESFGFTADLR.S
845 - 857	1444.78	1443.77	1443.76	0.01	1	K.EGIPALDNFLDKL.-

```
  1 VNFTVDQIRA IMDKKANIRN MSVIAHVDHG KSTLTDSLVC KAGIIASARA
 51 GETRFTDTRK DEQERCITIK STAISLFYEL SENDLNFIKQ SKDGAGFLIN
101 LIDSPGHVDF SSEVTAALRV TDGALVVVDC VSGVCVQTET VLRQAIAERI
151 KPVLMMNKMD RALLELQLEP EELYQTFQRI VENVNVIIST YGEGESGPMG
201 NIMIDPVLGT VGFGSGLHGW AFTLKQFAEM YVAKFAAKGE GQLGPAERAK
251 KVEDMMKKLW GDRYFDPANG KFSKSATSPE GKKLPRTFCQ LILDPIFKVF
301 DAIMNFKKEE TAKLIEKLDI KLDSEDKDKE GKPLLKAVMR RWLPAGDALL
351 QMITIHLPSP VTAQKYRCEL LYEGPPDDEA AMGIKSCDPK GPLMMYISKM
401 VPTSDKGRFY AFGRVFSGLV STGLKVRIMG PNYTPGKKED LYLKPIQRTI
451 LMMGRYVEPI EDVPCGNIVG LVGVDQFLVK TGTITTFEHA HNMRVMKFSV
501 SPVVRVAVEA KNPADLPKLV EGLKRLAKSD PMVQCIIEES GEHIIAGAGE
551 LHLEICLKDL EEDHACIPIK KSDPVVSYRE TVSEESNVLC LSKSPNKHNR
601 LYMKARPFPD GLAEDIDKGE VSARQELKQR ARYLAEKYEW DVAEARKIWC
651 FGPDGTGPNI LTDITKGVQY LNEIKDSVVA GFQWATKEGA LCEENMRGVR
701 FDVHDVTLHA DAIHRGGGQI IPTARRCLYA SVLTAQPRLM EPIYLVEIQC
751 PEQVVGGIYG VLNRKRGHVF EESQVAGTPM FVVKAYLPVN ESFGFTADLR
801 SNTGGQAFPQ CVFDHWQILP GDPFDNSSRP SQVVAETRKR KGLKEGIPAL
851 DNFLDKL
```

Spot 472 Elongation factor 2

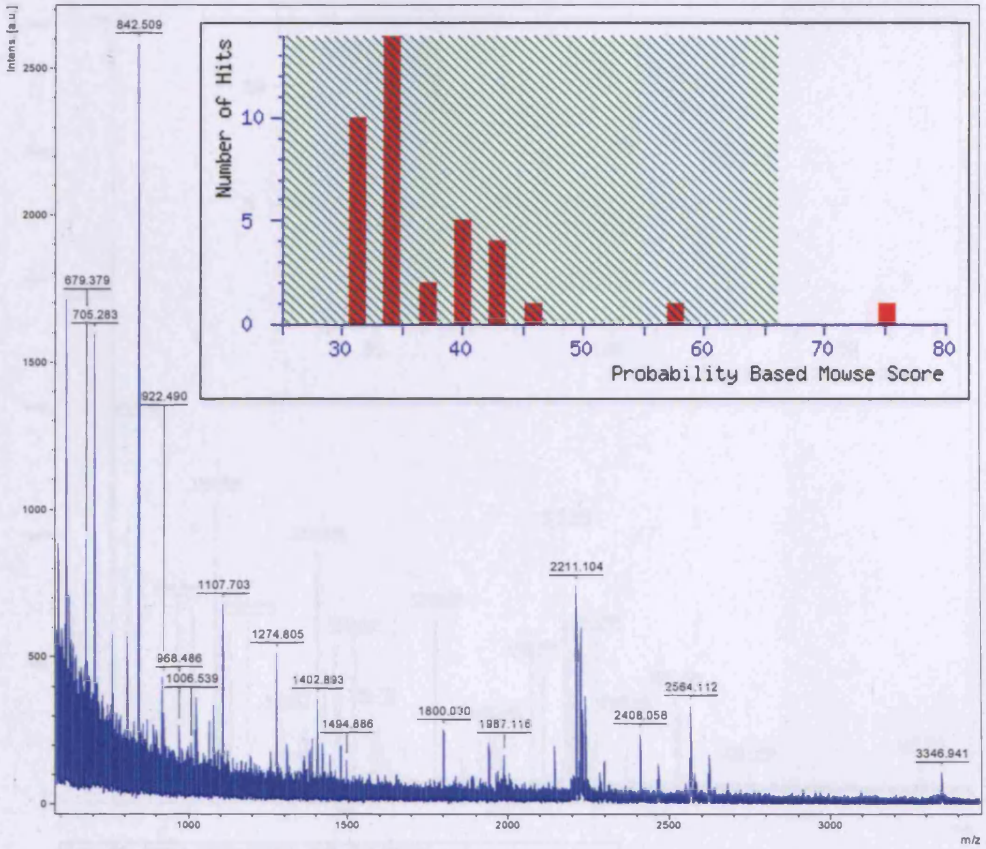

Start - End	Observed	Mr(expt)	Mr(calc)	Delta	Miss	Sequence
20 - 31	1307.72	1306.71	1306.65	0.07	0	R.NMSVIAHVDHGK.S
120 - 143	2576.18	2575.17	2575.30	-0.13	0	R.VTDGALVVVDCVSGVCVQTETVLR.Q
287 - 298	1494.89	1493.88	1493.80	0.08	0	R.TFCQLILDPIFK.V
299 - 307	1084.65	1083.64	1083.54	0.10	0	K.VFDAIMNFK.K
400 - 408	1006.54	1005.53	1005.49	0.04	1	K.MVPTSDKGR.F Oxidation (M)
409 - 414	760.37	759.36	759.37	-0.01	0	R.FYAFGR.V
415 - 425	1107.70	1106.70	1106.63	0.06	0	R.VFSGLVSTGLK.V
438 - 448	1402.89	1401.89	1401.80	0.09	1	K.KEDLYLKPIQR.T
439 - 448	1274.80	1273.80	1273.70	0.09	0	K.EDLYLKPIQR.T
498 - 505	890.53	889.52	889.50	0.02	0	K.FSVSPVVR.V
572 - 579	922.49	921.48	921.46	0.03	0	K.SDPVVSYR.E
605 - 624	2143.16	2142.15	2142.07	0.08	1	K.ARPFPDGLAEDIDKGEVSAR.Q
667 - 675	1063.63	1062.62	1062.57	0.05	0	K.GVQYLNEIK.D
727 - 738	1378.82	1377.81	1377.71	0.10	0	R.CLYASVLTAQPR.L
767 - 784	1962.01	1961.01	1960.97	0.03	0	R.GHVFEESQVAGTPMFVVK.A
785 - 800	1800.03	1799.02	1798.89	0.13	0	K.AYLPVNESFGFTADLR.S

```
  1 VNFTVDQIRA IMDKKANIRN MSVIAHVDHG KSTLTDSLVC KAGIIASARA
 51 GETRFTDTRK DEQERCITIK STAISLFYEL SENDLNFIKQ SKDGAGFLIN
101 LIDSPGHVDF SSEVTAALRV TDGALVVVDC VSGVCVQTET VLRQAIAERI
151 KPVLMMNKMD RALLELQLEP EELYQTFQRI VENVNVIIST YGEGESGPMG
201 NIMIDPVLGT VGFGSGLHGW AFTLKQFAEM YVAKFAAKGE GQLGPAERAK
251 KVEDMMKKLW GDRYFDPANG KFSKSATSPE GKKLPRTFCQ LILDPIFKVF
301 DAIMNFKKEE TAKLIEKLDI KLDSEDKDKE GKPLLKAVMR RWLPAGDALL
351 QMITIHLPSP VTAQKYRCEL LYEGPPDDEA AMGIKSCDPK GPLMMYISKM
401 VPTSDKGRFY AFGRVFSGLV STGLKVRIMG PNYTPGKKED LYLKPIQRTI
451 LMMGRYVEPI EDVPCGNIVG LVGVDQFLVK TGTITTFEHA HNMRVMKFSV
501 SPVVRVAVEA KNPADLPKLV EGLKRLAKSD PMVQCIIEES GEHIIAGAGE
551 LHLEICLKDL EEDHACIPIK KSDPVVSYRE TVSEESNVLC LSKSPNKHNR
601 LYMKARPFPD GLAEDIDKGE VSARQELKQR ARYLAEKYEW DVAEARKIWC
651 FGPDGTGPNI LTDITKGVQY LNEIKDSVVA GFQWATKEGA LCEENMRGVR
701 FDVHDVTLHA DAIHRGGGQI IPTARRCLYA SVLTAQPRLM EPIYLVEIQC
751 PEQVVGGIYG VLNRKRGMVF EESQVAGTPM FVVKAYLPVN ESFGFTADLR
801 SNTGGQAFPQ CVFDHWQILP GDPFDNSSRP SQVVAETRKR KGLKEGIPAL
851 DNFLDKL
```

Spot 476 Elongation factor 2

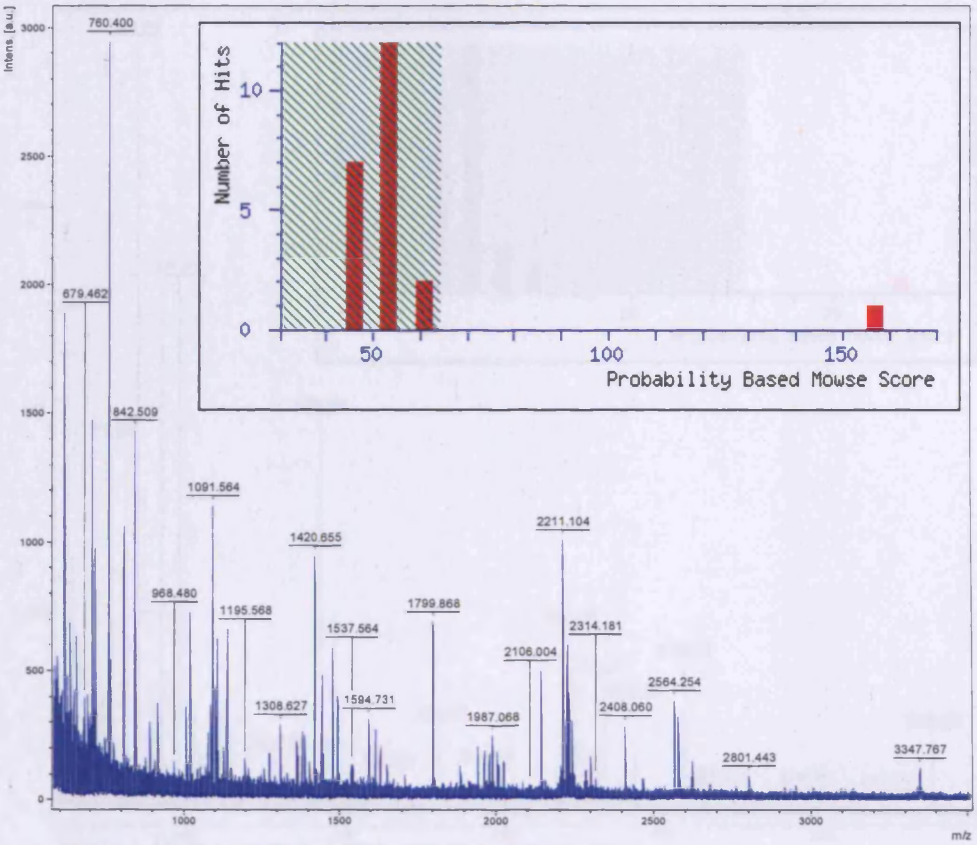

Start - End	Observed	Mr(expt)	Mr(calc)	Delta	Miss	Sequence
1 - 9	1091.56	1090.56	1090.58	-0.02	0	-.VNFTVDQIR.A
61 - 70	1291.63	1290.65	1290.62	0.02	1	K.DEQERCITIK.S
93 - 119	2801.44	2800.44	2800.40	0.03	0	K.DGAGFLINLIDSPGHVDFSSEVTAALR.V
162 - 179	2220.09	2219.09	2219.15	-0.06	0	R.ALLELQLEPEELYQTFQR.I
239 - 248	1013.46	1012.45	1012.49	-0.04	0	K.GEGQLGPAER.A
258 - 263	774.42	773.41	773.42	-0.01	1	K.KLWGDR.Y
259 - 263	646.31	645.30	645.32	-0.02	0	K.LWGDR.Y
287 - 298	1494.77	1493.76	1493.80	-0.03	0	R.TFCQLILDPIFK.V
287 - 307	2576.37	2575.36	2575.32	0.04	1	R.TFCQLILDPIFKVFDAIMNFK.K Oxidation (M)
299 - 307	1084.52	1083.52	1083.54	-0.02	0	K.VFDAIMNFK.K
299 - 307	1100.53	1099.52	1099.54	-0.02	0	K.VFDAIMNFK.K Oxidation (M)
308 - 313	705.35	704.34	704.37	-0.03	1	K.KEETAK.L
368 - 385	2023.87	2022.86	2022.89	-0.03	0	R.CELLYEGPPDDEAAMGIK.S Oxidation (M)
400 - 408	1006.48	1005.47	1005.49	-0.02	1	K.MVPTSDKGR.F Oxidation (M)
409 - 414	760.40	759.39	759.37	0.02	0	R.FYAFGR.V
415 - 425	1107.62	1106.62	1106.63	-0.02	0	R.VFSGLVSTGLK.V
438 - 448	1402.72	1401.71	1401.80	-0.09	1	K.KEDLYLKPIQR.T
439 - 448	1274.68	1273.67	1273.70	-0.03	0	K.EDLYLKPIQR.T
456 - 480	2759.52	2758.51	2758.43	0.09	0	R.YVEPIEDVPCGNIVGLVGVDQFLVK.T
481 - 494	1615.71	1614.70	1614.76	-0.06	0	K.TGTITTFEHAHNMR.V
481 - 494	1631.74	1630.73	1630.75	-0.02	0	K.TGTITTFEHAHNMR.V Oxidation (M)
498 - 505	890.49	889.49	889.50	-0.02	0	K.FSVSPVVR.V
580 - 593	1594.73	1593.72	1593.76	-0.03	0	R.ETVSEESNVLCLSK.S
605 - 618	1543.74	1542.73	1542.77	-0.04	0	K.ARPFPDGLAEDIDK.G
605 - 624	2143.12	2142.11	2142.07	0.04	1	K.ARPFPDGLAEDIDKGEVSAR.Q
638 - 646	1138.52	1137.51	1137.51	-0.00	0	K.YEWDVAEAR.K
676 - 687	1308.63	1307.62	1307.65	-0.03	0	K.DSVVAGFQWATK.E
727 - 738	1378.66	1377.65	1377.71	-0.06	0	R.CLYASVLTAQPR.L
767 - 784	1961.95	1960.94	1960.97	-0.03	0	R.GHVFEESQVAGTPMFVVK.A
767 - 784	1977.94	1976.94	1976.97	-0.03	0	R.GHVFEESQVAGTPMFVVK.A Oxidation (M)
785 - 800	1799.87	1798.86	1798.89	-0.03	0	K.AYLPVNESFGFTADLR.S
845 - 857	1444.74	1443.73	1443.76	-0.03	1	K.EGIPALDNFLDKL.-

```
  1 VNFTVDQIRA IMDKKANIRN MSVIAHVDHG KSTLTDSLVC KAGIIASARA
 51 GETRFTDTRK DEQERCITIK STAISLFYEL SENDLNFIKQ SKDGAGFLIN
101 LIDSPGHVDF SSEVTAALRV TDGALVVVDC VSGVCVQTET VLRQAIAERI
151 KPVLMMNKMD RALLELQLEP EELYQTFQRI VENVNVIIST YGEGESGPMG
201 NIMIDPVLGT VGFGSGLHGW AFTLKQFAEM YVAKFAAKGE GQLGPAERAK
251 KVEDMMKKLW GDRYFDPANG KFSKSATSPE GKKLPRTFCQ LILDPIFKVF
301 DAIMNFKKEE TAKLIEKLDI KLDSEDKDKE GKPLLKAVMR RWLPAGDALL
351 QMITIHLPSP VTAQKYRCEL LYEGPPDDEA AMGIKSCDPK GPLMMYISKM
401 VPTSDKGRFY AFGRVFSGLV STGLKVRIMG PNYTPGKKED LYLKPIQRTI
451 LMMGRYVEPI EDVPCGNIVG LVGVDQFLVK TGTITTFEHA HNMRVMKFSV
501 SPVVRVAVEA KNPADLPKLV EGLKRLAKSD PMVQCIIEES GEHIIAGAGE
551 LHLEICLKDL EEDHACIPIK KSDPVVSYRE TVSEESNVLC LSKSPNKHNR
601 LYMKARPFPD GLAEDIDKGE VSARQELKQR ARYLAEKYEW DVAEARKIWC
651 FGPDGTGPNI LTDITKGVQY LNEIKDSVVA GFQWATKEGA LCEENMRGVR
701 FDVHDVTLHA DAIHRGGGQI IPTARRCLYA SVLTAQPRLM EPIYLVEIQC
751 PEQVVGGIYG VLNRKRGHVF EESQVAGTPM FVVKAYLPVN ESFGFTADLR
801 SNTGGQAFPQ CVFDHWQILP GDPFDNSSRP SQVVAETRKR KGLKEGIPAL
851 DNFLDKL
```

Spot 468 Elongation factor 2

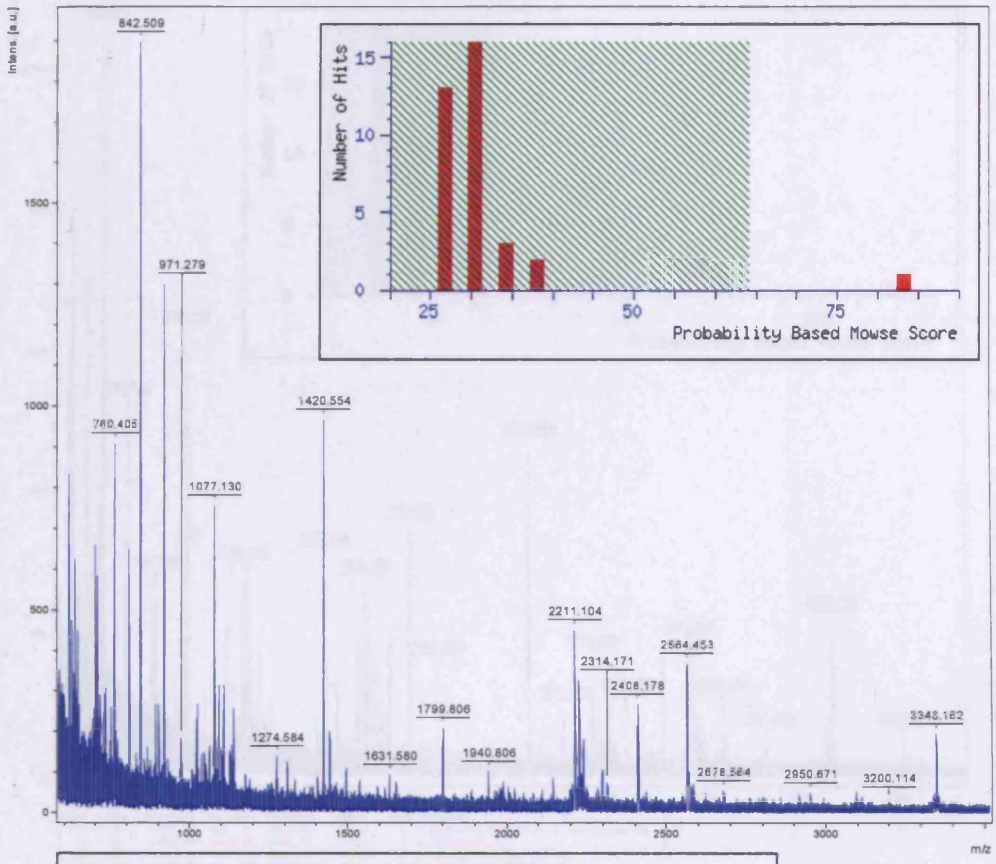

Start - End	Observed	Mr(expt)	Mr(calc)	Delta	Miss	Sequence
1 - 9	1091.50	1090.50	1090.58	-0.08	0	-.VMFTVDQIR.A
162 - 179	2220.14	2219.13	2219.15	-0.02	0	R.ALLELQLEPEELYQTFQR.I
287 - 298	1494.67	1493.66	1493.80	-0.14	0	R.TFCQLILDPIFK.V
287 - 307	2576.57	2575.56	2575.32	0.24	1	R.TFCQLILDPIFKVFDAIMMFK.M Oxidation (M)
299 - 307	1084.46	1083.45	1083.54	-0.09	0	K.VFDAIMMFK.M
299 - 307	1100.46	1099.45	1099.54	-0.09	0	K.VFDAIMMFK.M Oxidation (M)
308 - 313	705.38	704.37	704.37	0.00	1	K.KEETAK.L
368 - 385	2023.07	2022.06	2022.09	-0.03	0	R.CELLYEGPPDDEAAMGIK.S Oxidation (M)
400 - 408	1006.41	1005.41	1005.49	-0.09	1	K.MVPISDKGR.F Oxidation (M)
409 - 414	760.40	759.40	759.37	0.03	0	R.FYAFGR.V
415 - 425	1107.55	1106.54	1106.63	-0.10	0	R.VPSGLVSIGLK.V
426 - 437	1332.64	1331.63	1331.70	-0.07	1	K.VRIMGPNYTPGK.K
439 - 448	1274.58	1273.58	1273.70	-0.13	0	K.EDLYLKPIQR.T
439 - 455	2109.14	2108.13	2108.11	0.02	1	K.EDLYLKPIQRTILMMGR.Y 2 Oxidation (M)
481 - 494	1615.69	1614.68	1614.76	-0.07	0	K.TGTITTFEMAMDMR.V
498 - 505	890.45	889.44	889.50	-0.06	0	K.FSVSPVVR.V
605 - 624	2143.04	2142.03	2142.07	-0.04	1	K.ARPFPRGLAEDIDKGEVSAR.Q
638 - 646	1138.43	1137.44	1137.51	-0.07	0	K.YEVGVAEAR.K
667 - 675	1063.48	1062.47	1062.57	-0.10	0	K.GVQYLHEIK.D
676 - 687	1308.65	1307.64	1307.65	-0.01	0	K.DSVVAGFQWATK.E
767 - 784	1961.95	1960.94	1960.97	-0.03	0	R.GMVTEESQVAGTPMFVVK.A
767 - 784	1977.99	1976.98	1976.97	0.02	0	R.GMVTEESQVAGTPMFVVK.A Oxidation (M)
785 - 800	1799.81	1798.80	1798.89	-0.09	0	K.AYLPVMESFGFTADLR.S

```
  1 VMFTVDQIRA IMDKKANIRN MSVIAHVDHG KSTLTDSLVC KAGIIASARA
 51 GETRFTDTRK DEQERCITIK STAISLFYEL SENDLNFIKQ SKDGAGFLIN
101 LIDSPGHVDF SSEVTAALRV TDGALVVVDC VSGVCVQTET VLRQAIAERI
151 KPVLMMNKMD RALLELQLEP EELYQTFQRI VENVNVIIST YGEGESGPMG
201 NIMIDPVLGT VGFGSGLHGW AFTLKQFAEM YVAKFAAKGE GQLGPAERAK
251 KVEDMMKKLW GDRYFDPANG KFSKSATSPE GKKLPRTFCQ LILDPIFKVF
301 DAIMMFKKEE TAKLIEKLDI KLDSEDKDKE GKPLLKAVMR RWLPAGDALL
351 QMITIHLPSP VTAQKYRCEL LYEGPPDDEA AMGIKSCDPK GPLMMYISKM
401 VPTSDKGRFY AFGRVFSGLV STGLKVRIMG PNYTPGKKED LYLKPIQRTI
451 LMMGRYVEPI EDVPCGNIVG LVGVDQFLVK TGTITTFEMA HNMRVMKFSV
501 SPVVRVAVEA KNPADLPKLV EGLKRLAKSD PMVQCIIEES GEHIIAGAGE
551 LHLEICLKDL EEDHACIPIK KSDPVVSYRE TVSEESNVLC LSKSPNKHNR
601 LYMKARPFPD GLAEDIDKGE VSARQELKQR ARYLAEKYEW DVAEARKIWC
651 FGPDGTGPNI LTDITKGVQY LNEIKDSVVA GFQWATKEGA LCEENMRGVR
701 FDVHDVTLHA DAIHRGGGQI IPTARRCLYA SVLTAQPRLM EPIYLVEIQC
751 PEQVVGGIYG VLNRKRGHVF EESQVAGTPM FVVKAYLPVN ESFGFTADLR
801 SNTGGQAFPQ CVFDHWQILP GDPFDNSSRP SQVVAETRKR KGLKEGIPAL
851 DNFLDKL
```

Spot 487 Elongation factor 2

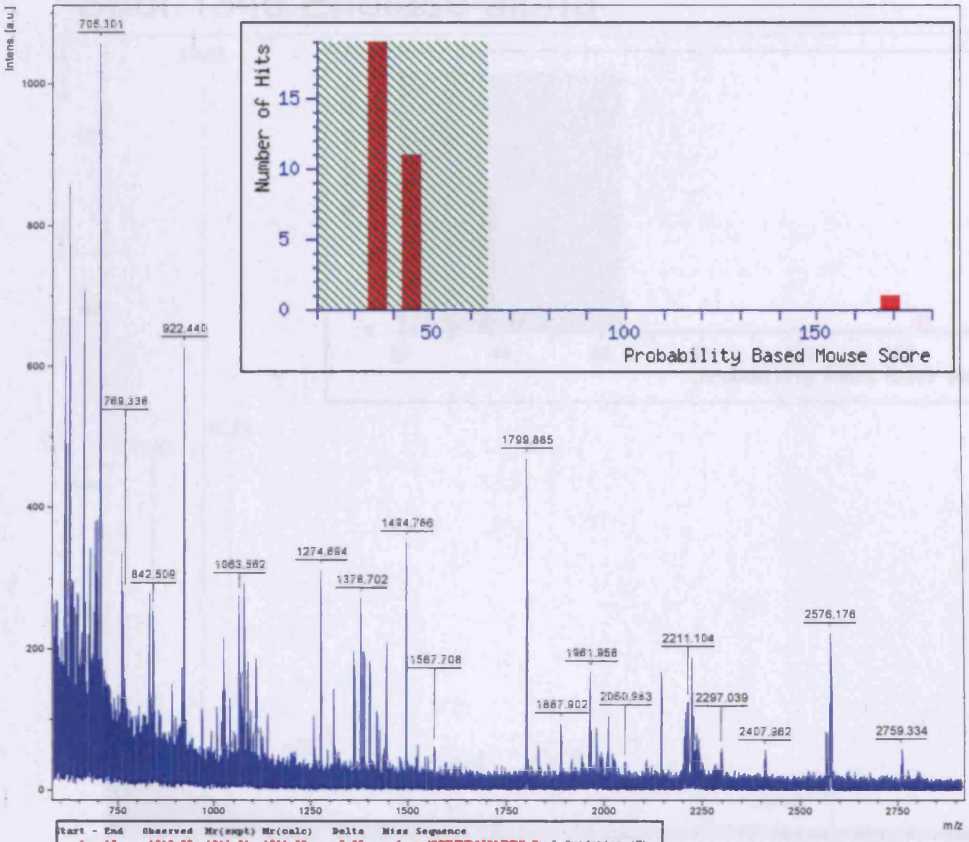

Start - End	Observed	Mr(expt)	Mr(calc)	Delta	Miss	Sequence
1 - 15	1812.92	1811.91	1811.89	0.02	1	-.MVNFTVDQIRAIMDKK.K 2 Oxidation (M)
2 - 16	1091.36	1090.35	1090.50	-0.02	0	M.VNFTVDQIR.A
72 - 90	2204.02	2203.01	2203.10	-0.09	0	K.SYAISLFYELSENDLNFIK.Q
121 - 144	2576.18	2575.17	2575.30	-0.13	0	R.VTDGALVVVDCVSGVCVQTETVLR.Q
163 - 180	2220.12	2219.11	2219.15	-0.04	0	R.ALLELQLEPEELYQTFQR.I
227 - 235	1086.52	1085.51	1085.52	-0.01	0	K.QFAEKVAK.F
227 - 235	1102.49	1101.48	1101.52	-0.04	0	K.QFAEKVAK.F Oxidation (M)
288 - 299	1494.81	1493.80	1493.80	0.00	0	R.TFCQLILDPIFK.V
288 - 299	1494.79	1493.78	1493.80	-0.02	0	R.TFCQLILDPIFK.V
300 - 308	1084.53	1083.53	1083.54	0.00	0	K.VFDAIDGFK.E
300 - 308	1100.53	1099.53	1099.54	0.01	0	K.VFDAIDGFK.E Oxidation (M)
392 - 400	1039.54	1038.53	1038.52	0.01	0	K.GPLMGYISK.M
392 - 400	1071.52	1070.51	1070.51	-0.01	0	K.GPLMGYISK.M 2 Oxidation (M)
410 - 415	760.36	759.35	759.37	-0.02	0	R.FYAFGR.V
416 - 426	1187.62	1186.61	1186.63	-0.02	0	R.VFSGLVSYGLR.V
429 - 438	1077.53	1076.53	1076.53	-0.01	0	R.IMGPMYTPGK.K
429 - 438	1093.51	1092.50	1092.53	-0.03	0	R.IMGPMYTPGK.K Oxidation (M)
439 - 449	1402.79	1401.78	1401.80	-0.02	1	K.KEDLYLKPIQR.Y
440 - 449	1274.69	1273.69	1273.70	-0.02	0	K.EDLYLKPIQR.Y
457 - 481	2759.33	2758.33	2758.43	-0.10	0	R.YVEPIEDVPCGNIVGLVGVDQFLVK.T
499 - 506	890.49	889.48	889.50	-0.02	1	R.FSVSPVVR.V
568 - 571	1439.73	1438.72	1438.68	0.03	0	K.DLEEDKACIPIK.K
568 - 572	1567.71	1566.70	1566.77	-0.07	1	K.DLEEDKACIPIKK.S
573 - 580	922.44	921.43	921.46	-0.02	0	K.SDPVVSYR.E
606 - 619	1543.73	1542.73	1542.77	-0.04	0	K.AAPIFDGLAEDIDK.G
606 - 623	2143.02	2142.02	2142.07	-0.05	1	K.AAPIFDGLAEDIDKGEVSAR.G
639 - 647	1138.58	1137.58	1137.51	-0.01	0	R.YEWDVAEAR.K
649 - 667	2184.86	2183.86	2184.03	-0.15	0	K.TNCFGFDGTGNTLTDITK.G
668 - 676	1063.56	1062.55	1062.57	-0.02	0	K.GWQYLEEIK.S
677 - 686	1308.64	1307.64	1307.65	-0.01	0	R.DSVVAGFQWATK.E
728 - 739	1378.70	1377.70	1377.71	-0.01	0	R.CLYASVLTAQPR.I
768 - 783	1961.96	1960.95	1960.97	-0.02	0	R.GNVTEESQVAGTPMFVVK.A
768 - 783	1977.91	1976.91	1976.97	-0.06	0	R.GNVTEESQVAGTPMFVVK.A Oxidation (M)
784 - 801	1799.88	1798.88	1798.89	-0.01	0	K.AYLFVMESFGFTADLR.S
846 - 850	1444.80	1443.79	1443.76	0.03	1	K.EGIPALDWFLDKL.-

```
  1 MVNFTVDQIR AIMDKKANIR NHSVIAHVDH GKSTLTDSLV CKAGIIASAR
 51 AGETRFTDTR KDEQERCITI KSTAISLFYE LSENDLNFIK QSKDGAGFLI
101 NLIDSPGHVD FSSEVTAALR VTDGALVVVD CVSGVCVQTE TVLRQAIAER
151 IKPVLMMNKM DRALLELQLE PEELYQTFQR IVENVNVIIS TYGEGESGPM
201 GNIMIDPVLG TVGFGSGLHG WAFTLKQFAE MYVAKFAAKG EGQLGPAERA
251 KKVEDMMKKL WGDRYFDPAN GKFSKSATSP EGKKLPRTFC QLILDPIFKV
301 FDAIMNFKKE ETAKLIEKLD IKLDSEDKDK EGKPLLKAVM RRWLPAGDAL
351 LQMITIHLPS PVTAQKYRCE LLYEGPPDDE AAMGIKSCDP KGPLMMYISK
401 MVPTSDKGRF YAFGRVFSGL VSTGLKVRIM GPNYTPGKKE DLYLKPIQRT
451 ILMMGRYVEP IEDVPCGNIV GLVGVDQFLV KTGTITTFEH AHNMRVMKFS
501 VSPVVRVAVE AKNPADLPKL VEGLKRLAKS DPMVQCIIEE SGEHIIAGAG
551 ELHLEICLKD LEEDHACIPI KKSDPVVSYR ETVSEESNVL CLSKSPNKEN
601 RLYMKARPFP DGLAEDIDKG EVSARQELKQ RARYLAEKYE WDVAEARKIW
651 CFGPDGTGPN ILTDITKGVQ YLNEIKDSVV AGFQWATKEG ALCEENMRGV
701 RFDVHDVTLH ADAIHRGGGQ IIPTARRCLY ASVLTAQPRL MEPIYLVEIQ
751 CPEQVVGGIY GVLNRKRGHV FEESQVAGTP MFVVKAYLPV MESFGFTADL
801 RSNTGGQAFP QCVFDHWQIL PGDPFDNSSR PSQVVAETRK RKGLKEGIPA
851 LDNFLDKL
```

Spot 1345 Enolase alpha

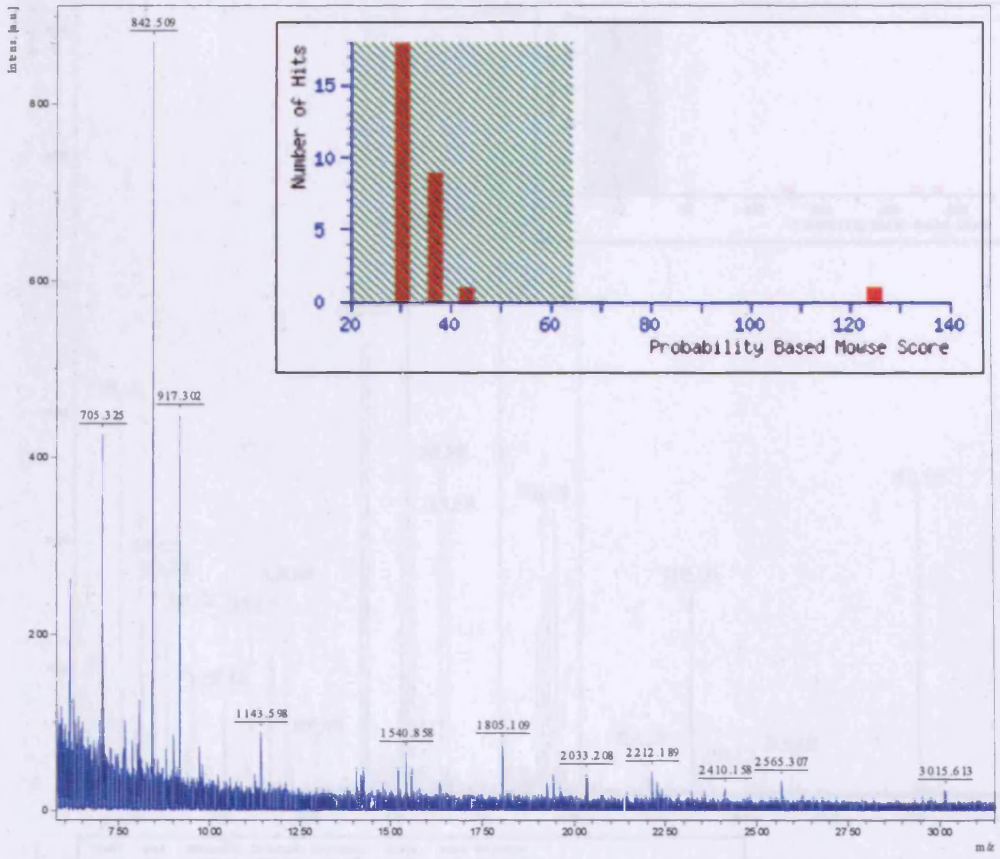

Start - End	Observed	Mr(expt)	Mr(calc)	Delta	Miss	Sequence
9 - 14	766.38	765.37	765.37	0.01	0	R.EIFDSR.G
15 - 27	1406.75	1405.75	1405.71	0.04	0	R.GNPTVEVDLFTSK.G
32 - 49	1805.11	1804.10	1803.94	0.17	0	R.AAVPSGASTGIYEALELR.D
71 - 79	899.56	898.55	898.55	0.00	0	K.TIAPALVSK.K
105 - 119	1519.94	1518.94	1518.82	0.11	0	K.FGANAILGVSLAVCK.A
162 - 178	1924.09	1923.08	1922.97	0.10	0	K.LAMQEFMILPVGAANFR.E Oxidation (M)
162 - 178	1940.13	1939.12	1938.97	0.15	0	K.LAMQEFMILPVGAANFR.E 2 Oxidation (M)
183 - 192	1143.60	1142.59	1142.61	-0.02	0	R.IGAEVYHNLK.N
202 - 220	1960.97	1959.96	1959.92	0.04	0	K.DATNVGDEGGFAPNILENK.E
239 - 252	1540.86	1539.85	1539.78	0.07	0	K.VVIGMDVAASEFFR.S
239 - 252	1556.82	1555.81	1555.77	0.04	0	K.VVIGMDVAASEFFR.S Oxidation (M)
256 - 261	800.36	799.35	799.38	-0.02	0	K.YDLDFK.S
269 - 280	1425.75	1424.74	1424.72	0.02	0	R.YISPDQLADLYK.S
306 - 325	2033.21	2032.20	2032.05	0.15	0	K.FTASAGIQVVGDDLTVTNPK.R
343 - 357	1633.97	1632.97	1632.81	0.15	0	K.VNQIGSVTESLQACK.L
406 - 411	806.49	805.49	805.44	0.04	0	K.YNQLLR.I

```
  1 SILKIHAREI FDSRGNPTVE VDLFTSKGLF RAAVPSGAST GIYEALELRD
 51 NDKTRYMGKG VSKAVEHINK TIAPALVSKK LNVTEQEKID KLMIEMDGTE
101 NKSKFGANAI LGVSLAVCKA GAVEKGVPLY RHIADLAGNS EVILPVPAFN
151 VINGGSHAGN KLAMQEFMIL PVGAANFREA MRIGAEVYHN LKNVIKEKYG
201 KDATNVGDEG GFAPNILENK EGLELLKTAI GKAGYTDKVV IGMDVAASEF
251 FRSGKYDLDF KSPDDPSRYI SPDQLADLYK SFIKDYPVVS IEDPFDQDDW
301 GAWQKFTASA GIQVVGDDLT VTNPKRIAKA VNEKSCNCLL LKVNQIGSVT
351 ESLQACKLAQ ANGWGVMVSH RSGETEDTFI ADLVVGLCTG QIKTGAPCRS
401 ERLAKYNQLL RIEEELGSKA KFAGRNFRNP LAK
```

Spot 863 L-plastin

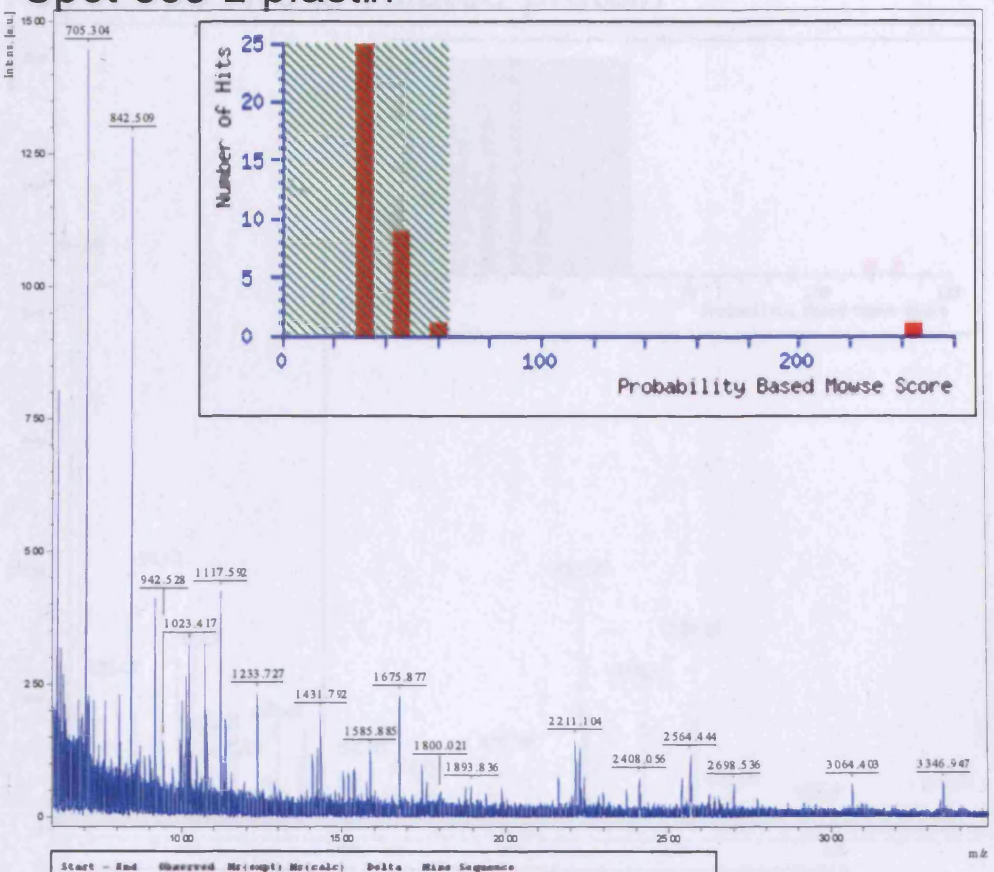

Start - End	Observed	Mr(expt)	Mr(calc)	Delta	Miss	Sequence
21 - 39	2161.04	2160.04	2160.00	0.03	0	R.VDTDGHGYIS FNELNDLFKA ACLPLPGYRV
40 - 49	1117.59	1116.58	1116.57	0.01	0	K.AACLPLPGYR.V
52 - 68	1877.00	1876.87	1876.85	0.03	0	R.EITEMLMATG DLDQDGRIS FDEFIKIFHG
52 - 68	1893.04	1892.83	1892.84	-0.01	0	R.EITEMLMATG DLDQDGRIS FDEFIKIFHG Oxidation (M)
69 - 76	998.54	997.53	997.51	0.02	0	R.LKSTDVAKTF.K
104 - 132	1154.64	1153.63	1153.58	0.04	0	K.YAFVNWLNK.A
104 - 141	2223.16	2224.16	2224.04	0.12	1	K.YAFVNWLNKALENDPDCR.N
166 - 178	1502.83	1501.82	1501.74	0.08	0	R.MIMLSVPDTIDER.T
166 - 178	1518.82	1517.82	1517.74	0.08	0	R.MIMLSVPDTIDER.T Oxidation (M)
234 - 244	1233.73	1232.72	1232.68	0.04	0	K.IGLPADIELSR.N
245 - 253	1012.63	1011.63	1011.61	0.01	0	R.NNALIALLR.E
264 - 272	1060.64	1060.63	1060.62	0.01	0	K.LSPDELLLR.W
286 - 294	994.55	993.54	993.51	0.03	0	R.IGHFSTDIK.D
290 - 309	1431.79	1430.78	1430.76	0.03	0	R.ATYDELIQWAFK.G
310 - 326	1743.90	1742.89	1742.85	0.04	0	K.GNETGVDAMVIDNSGLR.E
310 - 326	1759.88	1758.87	1758.85	0.02	0	K.GNETGVDAMVIDNSGLR.E Oxidation (M)
348 - 357	1135.63	1134.62	1134.60	0.02	0	R.GFVTATDVVR.G
362 - 373	1406.87	1404.86	1404.79	0.08	0	K.LNLAFIANLFNR.Y
374 - 395	2539.26	2538.26	2538.21	0.04	0	R.YPALNKPENQDIDWGALEGETREERTF.F
402 - 417	1907.71	1906.70	1906.63	0.06	0	R.NMDPSLGVNFR.V
413 - 432	2367.14	2366.13	2366.33	-0.08	0	R.VNNLYSNLSDALVIFQLYEK.I
433 - 441	1126.65	1125.64	1125.63	0.01	1	K.IKVPVDWAK.V
435 - 441	885.46	884.45	884.45	0.00	0	K.VPVDWAK.V
442 - 449	942.53	941.52	941.53	-0.01	0	R.VNEPTFK.I
456 - 468	1537.82	1536.81	1536.76	0.05	1	K.NLKEMCNEMELGK.N
473 - 488	1675.88	1674.87	1674.83	0.04	0	K.FSLVGIGGQDLNEGNR.T
482 - 515	1534.84	1533.84	1533.80	0.03	0	R.TLNLILEEIGGQGK.V
516 - 530	1800.82	1799.81	1799.92	-0.09	0	K.VNDDIIVNMVNETLR.E
539 - 547	862.51	861.50	861.47	0.03	0	K.SSSISSFK.D
548 - 570	2698.54	2697.53	2697.48	0.06	0	K.ISTSLPVLSGIRAIQPQSFNTDLLR.Y
585 - 591	811.44	810.43	810.41	0.03	0	K.YAISNAR.K
597 - 618	1585.88	1584.88	1584.84	0.04	0	R.VTNLPFDLVEVNPK.N

```
  1 MARGSVSDEE MNELREAFAK VDTDGHGYIS FNELNDLFKA ACLPLPGYRV
 51 REITEMLMAT GDLDQDGRIS FDEFIKIFHG LKSTDVAKTF RKAINKKEGI
101 CAIGGTSEQS SVGTQHSYSE EEKYAFVNWI NKALENDPDC RHVIPMNPNT
151 NDLFNAVGDG IVLCKMIMLS VPDTIDERTI NKKKLTPFTI QENLNLALNS
201 ASAIGCHVVN IGAEDLKEGK PYLVLGLLWQ VIKIGLFADI ELSRMEALIA
251 LLREGESLED LEKLSPEELL LRWANYHLEN AGCNKIGMFS TDIKDSKAYY
301 MLLEQVAPKG DEEGVPAVVI DMSGLREKDD IQRAECMLQQ AERLGCRQFV
351 TATDVVRGNP KLNLAFIANL FNRYPALNKP ENQDIDWGAL EGETREERTF
401 PMMMNSLGVM PRVNDLYSDL SDALVIFQLY EKIKVPVDWN KVNKPPYPKL
451 GGNMKKLENC NYAVELGKNQ AKFSLVGIGG QDLMEGNRTL TLALIWQLMR
501 RYTLNILEEI GGGQKVNDDI IVNMVNETLR EAEKSSSISS FKDPKISTSL
551 PVLDLIDAIQ PGSINYDLLK TENLNDDEKL NNAKYAISMA RKIGARVYAL
601 PEDLVEVNPK NVNTVFACLN GKGNKRV
```

Appendix J: Statistical treatment of DeCyder data in this thesis

Statistical analysis is an essential process what is used to determine the reliability of data obtained using DeCyder gel analysis. In general, to compare mean differences between two groups of data that have some correlations, one can run an independent samples student t-test. In contrast, when comparing means of 3 or more variables, the Analysis of variance (ANOVA) test is suitable for making this comparison and is used to replace multiple t-tests. In this thesis, although one or more than one triplicate test groups are being compared to triplicate control groups, the statistical analysis in was performed between two groups at a time (e.g. when comparing a hydrogen peroxide treated to non-treated HB4a cells) to test the significance. This strategy prevents the exclusion of some spots of interest that can happen when using ANOVA, where the differences are not consistent across all groups of conditions. For example, the identified proteins such as Lamin, flavin reductase, HSP-71 and peroxiredoxin 6 in Table 4-2 would be omitted in an ANOVA analysis used to look for H2O2 AND cell-line specific changes. Thus, the student t-test was chosen and applied in all 2D-DIGE experiments.

As Students t-test provides a method to make statistical comparisons of the means from two different groups, all protein identification tables in this thesis show a series of labelling/expression changes between two individual treatment comparisons (e.g. comparison of plasma fractions exposed to UV 80 mJ/cm^2 versus 0 mJ/cm^2; UV 40 mJ/cm^2 versus 0 mJ/cm^2; UV 20 mJ/cm^2 versus 0 mJ/cm^2 in Chapter 6). The experimental t-test values are calculated by using the following equations:

$$t_{exp} \text{ value} = \left| X_A - X_B \right| / S_{AB} \times (1/n_A + 1/n_B)^{1/2}$$

where X_A and X_B are the means of A and B groups, respectively; S_{AB} is the standard deviation of used values; n_A and n_B are the number of measurements in group A and group B, respectively.

The t_{exp} value can be compared with the t_{theo} (theoretical) value, which corresponds to the given degrees of freedom N ($N = n_A + n_B - 2$), and the confidence level chosen. Tables of t_{theo} values can be found in statistical textbooks. If $t_{exp} > t_{theo}$ then the H_o (null hypothesis

i.e. any differences, discrepancies, or suspiciously outlying results are purely due to random and not systematic errors) can be rejected. An erroneous rejection of H_o constitutes a type 1 error (i.e. false positive), whereas an erroneous acceptance of H_o constitutes a type 2 error (i.e. false negative).

All significance tests provide results within a predefined confidence level % (CL%). Confidence levels normally used are 90%, 95% and 99%, with 95% being the most popularly used value in biological analyses. A CL of 95% means that in the case of rejecting H_o, there is a 95% or more certainty that the result is true, i.e. a < 0.05 chance of a false positive. In addition, a CL of 95% is generally considered as a compromise between two types of errors due to decreasing CL to 90% significantly increase the type 1 error, while increasing CL to 99% obviously increases the type 2 error.

The *p*-value is the probability of a type 1 error happening and this value provides information for the user to judge the acceptance or the rejection of the null hypothesis H_o. For example, using a CL of 95% is the criteria for acceptance in one statistical analysis which means the probability of a type 1 error happening is 5% i.e. $p = 0.05$. While an experimental *p*-value of 0.09 means that H_o must be retained otherwise there is a higher risk of accepting a high probability of a type 1 error occuring.

All protein identification tables in this thesis which show expression/labelling changes as average ratios between two conditions include the *p*-value for those comparisons. Protein features were selected for identification where *p*-values were less than 0.05 and average fold-changes were > + or – 1.5 fold (except + or – 1.3 in the EGF stimulation experiments in Chapter 5). However, in a few cases (such as Lamin, flavin reductase, HSP-71 and peroxiredoxin 6 in Table 4-2), not all of the *p*-values of each comparison fulfilled the $p < 0.05$ criteria. For these cases, the average ratios of expression/labelling changes together with *p*-values are still listed in the tables.

PUBLICATIONS

1. **Chan,H.L.**, Gharbi,S.; Gaffney,P.; Cramer,R.; Waterfield,M.D.; Timms, J.F. Proteomic analysis of redox- and ErbB2-dependent changes in mammary luminal epithelial cells using cysteine- and lysine-labelling 2D-DIGE. ***Proteomics*** (2005) Vol. 5 in press

2. White,S.L.; Gharbi,S.; Bertani,M.F.; **Chan,H.L.**; Waterfield,M.D.; Timms,J.F. Cellular responses to ErbB-2 overexpression in human mammary luminal epithelial cells: comparison of mRNA and protein expression. ***Br. J. Cancer*** (2004) (90) Vol. 1, 173-181.

Proteomics 2005, *5*, 0000–0000 DOI 10.1002/pmic.200401300

REGULAR ARTICLE

Proteomic analysis of redox- and ErbB2-dependent changes in mammary luminal epithelial cells using cysteine- and lysine-labelling two-dimensional difference gel electrophoresis

Hong-Lin Chan[1], Severine Gharbi[1], Piers R. Gaffney[2], Rainer Cramer[1], Michael D. Waterfield[1] and John F. Timms[1]

British Journal of Cancer (2004) 90, 173–181

www.bjcancer.com

Cellular responses to ErbB-2 overexpression in human mammary luminal epithelial cells: comparison of mRNA and protein expression

SL White[1], S Gharbi[1], MF Bertani[1], H-L Chan[1], MD Waterfield[1] and JF Timms*[,1]